TABLE OF CONTENTS

1 Dialkylaminopyridine Chemistry

As part of the research into novel neutral non-metal electron donors that has been conducted within the Murphy group, the reaction of 2-dimethylaminopyridine (2-DMAP) **1.1** and 1,3-diiodopropane **1.2** was conducted. Unexpectedly, the reaction did not produce expected product **1.7**, but was observed to give products **1.4**, **1.5** and **1.6** (Scheme 1.1), thought to occur via superelectrophile disalt **1.3**. Investigation into the mechanism of this reaction and the subsequent discovery of superelectrophile disalt **1.3** will be discussed in Chapter 4. Chapter 1 provides an overview of the chemistry of dialkylaminopyridines, Chapter 2 reviews specific areas in the field of superelectrophiles and Chapter 7 looks at the [Fe]-hydrogenase, an intriguing enzyme with important links to superelectrophile chemistry. These reviews are designed to set my work in context. My results on the chemistry of the superelectrophiles synthesised in this work are discussed in Chapters 5, 6, 8 and 9.

SCHEME 1.1: Unusual reaction behaviour of 2-DMAP **1.1** and 1,3-diiodopropane **1.2**.

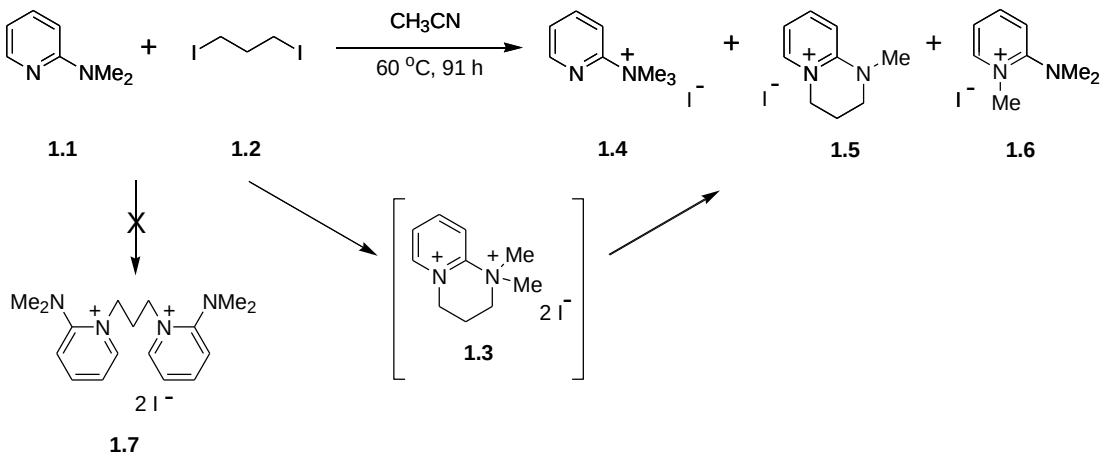

1.1 Introduction

The high power of 4-DMAP **1.8** as an acylation catalyst was first discovered in 1967 by Litvinenko and Kirichenko,[1] who found that replacing pyridine with 4-DMAP caused a 10^4 rate increase in the benzoylation of *m*-chloroaniline **1.10** (Scheme 1.2). Since then, the catalytic ability of 4-DMAP has been exploited in a variety of synthetically useful reactions.[2-3] Interestingly, 2-DMAP **1.1** does not share the same catalytic ability as its 4-DMAP analogue. In addition, 2-DMAP exhibits some unusual chemistry compared to 4-DMAP. This review looks at the development of dialkylaminopyridines as acylation catalysts (Section 1.2), the current state of thought regarding the mechanism of acylation using 4-DMAP (Section 1.3) and some other interesting chemistry performed by 4-DMAP (Sections 1.4 and 1.5). The unusual chemistry of 2-DMAP compared to 3-DMAP **1.9** and 4-DMAP will also be examined (Section 1.6).

SCHEME 1.2: Dialkylaminopyridines **1.1**, **1.8** and **1.9** and the benzoylation of *m*-chloroaniline **1.10** by 4-DMAP.

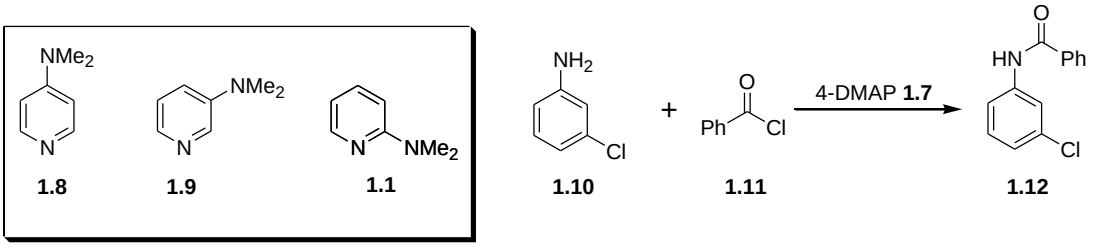

1.2 Dialkylaminopyridines as Acylation Catalysts

One of the major uses of 4-DMAP is in the acylation of sterically-hindered alcohols.[2-3] Independent of the discovery by Litvinenko and Kirichenko,[1] Steglich and Höfle[4] reported the superiority of 4-DMAP in the acylation of sterically-hindered alcohols 1-methylcyclohexanol **1.13** and *tert*-butyl alcohol **1.15** (Scheme 1.3).

SCHEME 1.3: Acylation of sterically-hindered alcohols **1.12** and **1.14**.

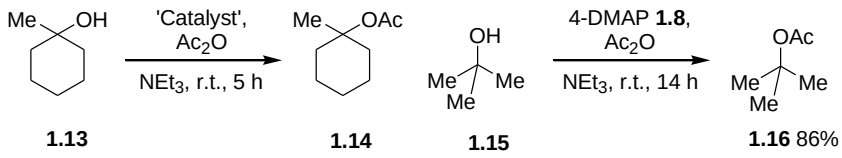

TABLE 1.1: Catalyst activity for acylation of **1.13** (Scheme 1.3).

'Catalyst'	**Yield 1.14 / %**
4-DMAP **1.8**	89
NMIM	15
Pyridine	<5

This improved catalytic activity was later quantified by Muruga and Scriven[5] in the acylation of **1.13** by 4-DMAP in comparison with pyridine and *N*-methylimidazole (NMIM) (Table 1.1).

SCHEME 1.4: Substituted pyridines investigated by Hassner *et al*.[6]

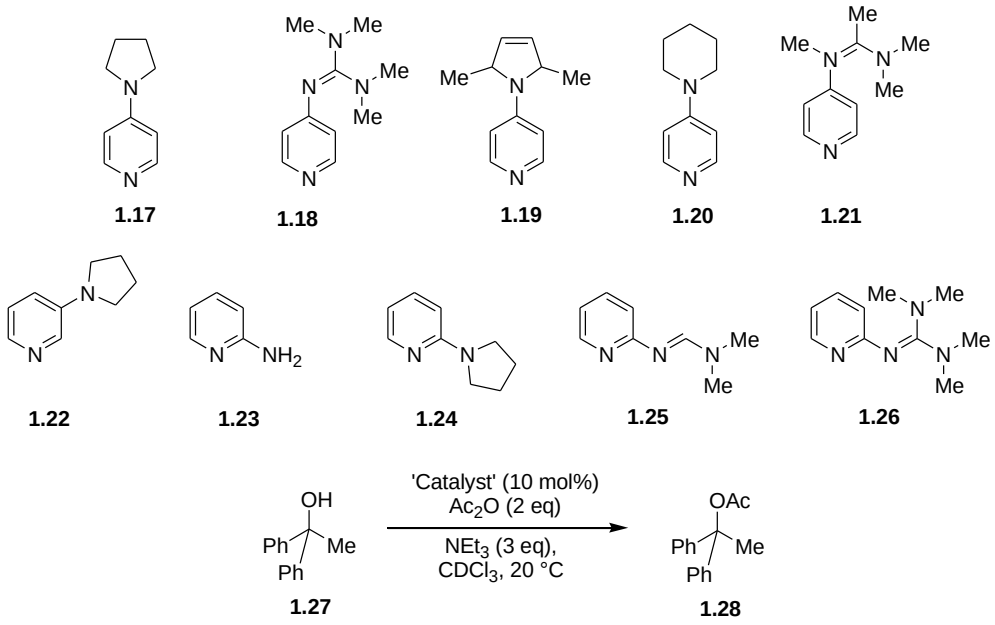

TABLE 1.2: Relative catalytic ability of substituted pyridines.

Catalyst	**Relative Rate**	**Catalyst**	**Relative Rate**
1.17	1.00	**1.19**	0.50
1.18	0.90	**1.20**	0.40
1.8	0.63	**1.21-1.26**	0.00

Hassner and co-workers[6] went on to investigate the structural requirements in substituted pyridines for catalytic activity in the acylation of sterically hindered alcohols. The various substituted pyridines (**1.8**, **1.17-1.26**, Scheme 1.4) were tested in the reaction of 1,1-diphenylethanol **1.27** with acetic anhydride in the presence of

triethylamine (Scheme 1.4, Table 1.2). 4-Pyrrolidinopyridine **1.17** (4-PPY) was discovered to be the most active acylation catalyst tested. Interestingly, 3-pyrrolidinopyridine **1.22**, 2-aminopyridine **1.23** and 2-aminopyridine derivatives **1.24-1.26** showed no catalytic activity in the acylation of **1.27**. The utility of 4-PPY **1.17** was demonstrated[6] in the reaction of other sterically hindered tertiary alcohols to give the corresponding acylated products (**1.29**-**1.31**, Scheme 1.5) in excellent 80-97 % yield.

SCHEME 1.5: Selected products of alcohol acylation using 4-PPY **1.17**.

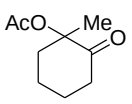

1.29 87%

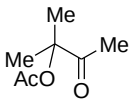

1.30 97%

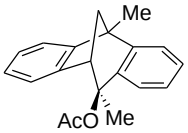

1.31 80%

Höfle *et al.*[7] reviewed a variety of interesting acylations of tertiary alcohols that highlighted the high catalytic activity of 4-DMAP and 4-PPY (Scheme 1.6, Table 1.3).

SCHEME 1.6: Acylation of alcohols reviewed by Höfle *et al.*[7]

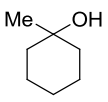

1.13

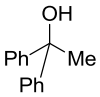

1.27

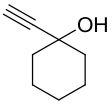

1.32

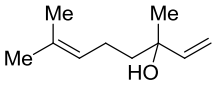

1.33

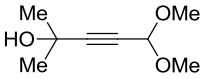

1.34

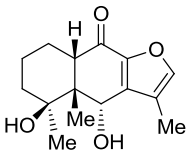

1.35

TABLE 1.3: Acylation results (Scheme 1.6).

Alcohol	Anhydride	Catalyst	Base	t / h	T / °C	Yield / %
1.13	Bz_2O	**1.8**	NEt_3	13	80	87
1.27	Ac_2O	**1.17**	NEt_3	40	r.t.	92
1.32	$(EtCO)_2O$	**1.8**	NEt_3	1	r.t.	94
1.33	Ac_2O	**1.8**	NEt_3	14	r.t.	80
1.34	Ac_2O	**1.8**	-	0.5	r.t.	92
1.35	Ac_2O	**1.8**	-	7	r.t.	95

Steglich *et al.*[8] later reported the application of a more efficient, conformationally-fixed 4-DMAP derivative. This was based on the study of the relative reactivities of 4,4-*bis*(dialkylamino)benzhydryl cations **1.36-1.38**, which showed a dramatic increase in stability when the nitrogen was part of a conformationally-fixed ring system (Scheme 1.7). Studies showed that cation **1.38** is ~120 times less electrophilic than cation **1.36**. Steglich *et al.*[8] proposed that conformational fixation of the dialkylamino group nitrogen would increase the catalytic ability of such a pyridine species. As a result of this, pyridine **1.39** was synthesised and tested in the acylation of 1-ethynylcyclohexanol **1.32** (Scheme 1.8). The rate of conversion was monitored by ^{1}H NMR spectroscopy, the results showing that conformationally-fixed pyridine **1.39** was, on average, ~6 times more reactive than 4-DMAP **1.7** and ~2.5 times more reactive than 4-PPY **1.17** (50 % acylation of alcohol **1.32** occurred in 20 min using **1.39**, 60 min for 4-PPY and 160 min for 4-DMAP).

SCHEME 1.7: Conformationally-fixed 4-dialkylaminopyridines. Rate determined from rate constants of each cation's reaction with the Danishefsky diene[9] at 20 °C.

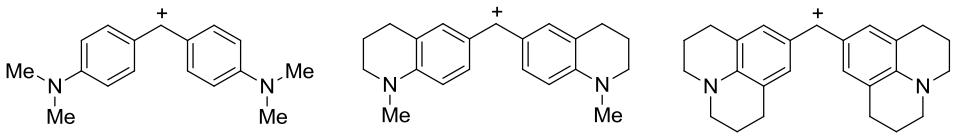

1.36 k_{rel} = 1 **1.37** k_{rel} = 1/11 **1.38** k_{rel} = 1/117

SCHEME 1.8: Conformationally-fixed 4-dialkylaminopyridines as acylation catalyst.

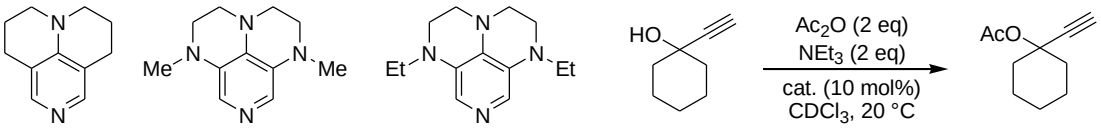

1.39 **1.40** **1.41** **1.32** **1.42**

Singh *et al.*[10] followed on from the work of Steglich *et al.*[8] in the synthesis of conformationally-fixed pyridines **1.40** and **1.41**. They reasoned that the presence of *meta*-nitrogens would provide greater stabilisation of the positive charge on the ring nitrogen and that conformational-fixing of the nitrogens would "lock" the nitrogen lone pair of electrons parallel to the π-system of the pyridine ring. The catalytic effectiveness of pyridines **1.39-1.41** were monitored by ^{1}H NMR spectroscopy in the acylation of alcohol **1.32**. The results showed that pyridine **1.41** gave a slight

improvement in acylation of alcohol **1.32** over pyridine **1.39** (~1-7 % improved conversion). Meanwhile, pyridine **1.40** showed slightly decreased catalytic ability compared to pyridine **1.39**. To date, pyridine **1.41** is the most powerful 4-dialkylaminopyridine derivative catalyst for the acylation of sterically-hindered alcohols.

1.3 Mechanism of Acylation

Hassner *et al*.[6] proposed the mechanism for acylation of alcohols using 4-dialkyl-aminopyridines as shown in Scheme 1.9. The mechanism consisted of initial formation of acetylpyridinium species **1.44**, which is stablised by conjugation with the 4-dialkylamino group. Attack by alcohol gives intermediate **1.45**, which breaks down to give acylated product **1.46** and recovery of 4-PPY **1.17**.

SCHEME 1.9: Mechanism of acylation proposed by Hassner *et al*.[6]

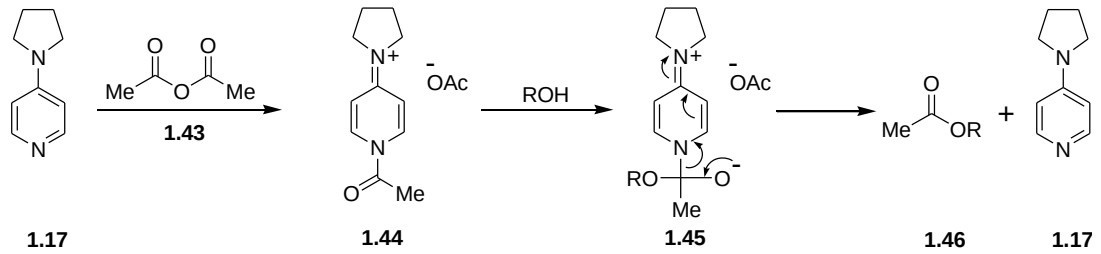

The authors suggested that the improved catalytic ability (over pyridine) was due to the donor ability of the 4-dialkylamino group helping to stabilise acetylpyridinium intermediate **1.44**. Acylation of 1,1-diphenylethanol **1.27** in a variety of different solvents was carried out (Table 1.4). It was found that the reaction occurred faster in non-polar solvents. This was unusual as it was thought that polar solvents, in which ionic intermediates **1.44** and **1.45** were more soluble, would aid the reaction. The beneficial effects of non-polar solvents were explained by their ability to aid the collapse of charged intermediate **1.45** to the neutral products,[6] although presumably the same factors would inhibit formation of acetylpyridinium **1.44**. The presence of an auxiliary base was shown to be necessary for complete acylation of alcohols. The acylation of *tert*-butanol **1.15** was found to proceed to 62 % conversion after 15 min, compared to 100 % conversion when 1 eq of triethylamine was added. In the absence

of an auxiliary base, the acetylation of *tert*-butanol **1.15** only proceeded to 90 % conversion after 10 days of reaction.

TABLE 1.4: Solvent effects on acylation of 1,1-diphenylethanol **1.27**.[a]

Solvent	**Yield of acylated product / %**
Et_2O	30
Hexane	75
CH_3CN	0
$PhNO_2$	0
DMF	0
Neat	92

[a] Acylation carried out using 4-PPY **1.17**, Ac_2O and NEt_3 in required solvent at r.t. for 24 h.

SCHEME 1.10: Catalytic ability of 2-substituted 4-PPY derivatives **1.47a-d**.

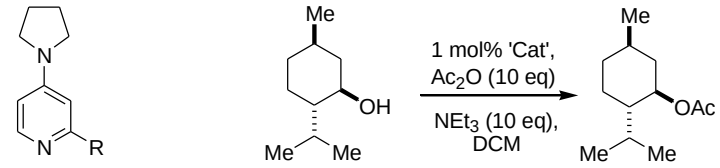

1.17 R = H
1.47 a R = Me
b R = Et
c R = ^{i}Pr
d R = ^{t}Bu

1.48 **1.49**

TABLE 1.5: Effect of 2-substitution on catalytic ability of 4-PPY **1.17**.

Catalyst	$\mathbf{k_{rel}}$
1.17	120.0
1.47a	4.0
1.47b	1.7
1.47c	1.0
1.47d	1.0

The pK_a of 4-DMAP **1.8** is higher than that of pyridine (9.70[11] versus 5.20[12]), so the increased catalytic effect of 4-DMAP could be argued to be simply due to its increased basicity compared to pyridine. However, the pK_a of triethylamine is 10.7,[7] but this reagent shows the same catalytic ability as pyridine. This suggests that the

mechanism of the reaction is not simply due to general base catalysis, but that the increase in activity of 4-DMAP is due to nucleophilic catalysis. The nucleophilic nature of the mechanism was shown by Sammakia and Hurley.[13] They tested the reactivity of a variety of 2-alkyl-4-PPY derivatives (**1.47a**-**d**) in the acylation of menthol **1.48** (Scheme 1.10, Table 1.5). The results showed that the rate of catalysis decreases with increasing bulk at the 2-position, despite having a marginal affect on the pK_a of the pyridine. This observation implied that the mechanism of 4-dialkylaminopyridines in the acylation of alcohols was nucleophilic, rather than due to general base catalysis.

Spivey and Arseniyadis[12] later proposed a mechanism that took into account the different rates in catalysis that occurred when using different anhydrides and by varying the auxiliary base. A simplified version of the mechanism is shown in Scheme 1.11.

SCHEME 1.11: Mechanism of acylation by Spivey and Arseniyadis.[12]

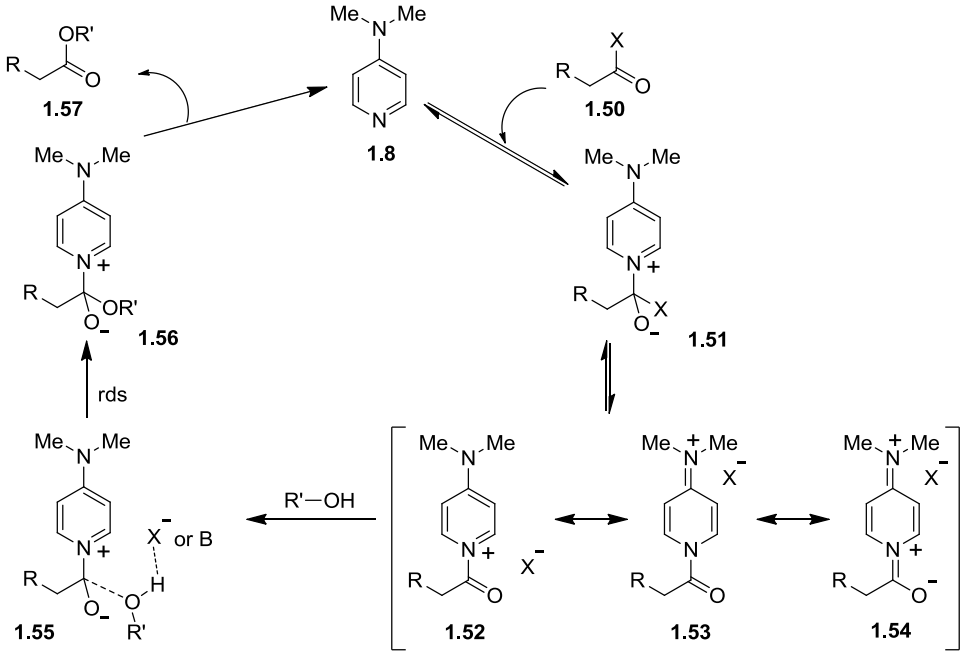

Reaction of 4-DMAP **1.7** and acyl species **1.50** results in reversible formation of tetrahedral intermediate **1.51**, which becomes *N*-acylpyridinium intermediate **1.52**. Salt **1.52** is stabilised by resonance structures **1.53** and **1.54**. Irreversible nucleophilic addition of alcohol gives **1.56**, through transition state **1.55** with loss of acid (HX or

HB) to give intermediate **1.56**, which breaks down to give acylated product **1.57** and regeneration of 4-DMAP **1.8**.

In order to increase the rate of the reaction, the equilibrium for the formation of *N*-acylpyridinium species such as **1.52** should be made more favourable. The equilibrium should be shifted in favour of formation of **1.52** for:

i. Pyridines that can stabilise the *N*-acylpyridinium ion **1.52**.
ii. Anions that have a high nucleofugacity (Cl > OAc).
iii. Polar solvents that can solvate the charge-separated salt more efficiently than the neutral starting materials or zwitterion **1.51**.

Despite these expectations, not all of the above statements hold true. In the case of (i) above, the assumption is correct. It has been shown that 4-dialkylaminopyridines that can better stabilise the positive charge in species **1.52** show increased catalytic ability relative to pyridine. For example, 4-PPY **1.17** with bulkier alkyl substituents on the amino group nitrogen shows increased catalytic ability over 4-DMAP. Conformationally-fixed pyridines **1.39**-**1.41** have the amino nitrogen lone pair of electrons fixed parallel to the π-system of the pyridine ring. This helps the stability of acylpyridinium salts such as **1.52** and leads to improved catalytic ability.

For point (ii), the opposite trend is true; reactions using acetic anhydride are faster than the corresponding reactions using acid chlorides. Variable temperature NMR experiments showed that a 1:1.5 mixture of 4-PPY:Ac_2O in $CDCl_3$ showed 5-10 % formation of acetylpyridinium acetate, whereas a 1:1.5 mixture of 4-PPY:AcCl showed ~100 % conversion to acetylpyridinium chloride.[7] Höfle *et al*.[7] studied the effect on acylation of 1-ethynylcyclohexanol **1.32** with 4-DMAP when using acetic anhydride over acetyl chloride (Scheme 1.12, Table 1.6). The results showed an almost three-fold rate increase in acylation when using acetic anhydride (X = OAc). Based on the variable temperature NMR experiments, it would be expected that using AcCl would show increased reaction rates due to increased concentrations of acetylpyridinium chloride over acetylpyridinium acetate (100 % versus 10 %).

In addition, the opposite trend is also observed for point (iii); acylation reactions proceed faster in non-polar solvents (shown in Table 1.4). Spivey and Arseniyadis[12]

attributed this trend to solvation and base catalysis effects for the acylpyridinium species. In polar solvents, the *N*-acetylpyridinium salts are well solvated, resulting in dissociated ions with low reactivity. In non-polar solvents, poor solvation of the *N*-acetylpyridinium salts means that they are present as highly reactive, tight ion pairs. In this instance, the ability of the anion to deprotonate the alcohol in the rds of the reaction is the important factor. In this case, the more basic acetate anion shows higher reactivity than the chloride anion.

SCHEME 1.12: Acylation reaction using different acylating reagents.

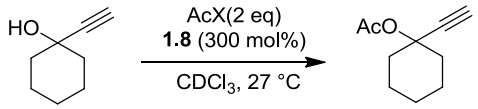

1.32 **1.42**

TABLE 1.6: Half-life ($t_{1/2}$) of acylation of **1.32** with different acylating reagents.

X	**$t_{1/2}$ / min**
OAc	7
Cl	20

This theory was reinforced by the work of Kattnig and Albert,[14] who found that when using insoluble potassium carbonate as an auxiliary base for the acylation of 2-propanol **1.58** using 4-DMAP, acylation using acetic anhydride occurred ~10 times faster than when using acetyl chloride (Scheme 1.13, Table 1.7, entries 1 and 2). However, when soluble auxiliary base pyridine was used the trend was dramatically reversed, so that acylation with acetyl chloride occurred ~700 times faster than with acetic anhydride (Table 1.7, entries 3 and 4).

SCHEME 1.13: Auxiliary base studies in acylation using 4-DMAP.

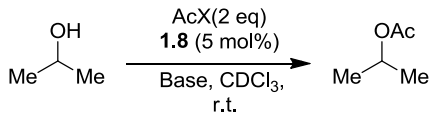

1.58 **1.59**

TABLE 1.7: Half-life of acylation of alcohol **1.58**.

Entry	X	Base	$t_{1/2}$ / min
1	OAc	K_2CO_3	18
2	Cl	K_2CO_3	200
3	OAc	Pyridine	120
4	Cl	Pyridine	<0.2

They concluded that when insoluble K_2CO_3 was used, deprotonation of the alcohol in the rds must rely solely on the *N*-acetylpyridinium counterion. In this case, the more basic acetate anion is more reactive than the chloride anion, hence the increase in the rate of reaction. When soluble pyridine is used, it can aid in the deprotonation step, meaning that the more abundant *N*-acetylpyridinium chloride reacts faster with 2-propanol **1.58**. This result was in contrast to the results observed by Höfle *et al.*[7] (Scheme 1.12, Table 1.6). Spivey and Arseniyadis[12] attributed this difference to the higher concentration of catalyst used in the reaction. In the case of Höfle *et al.*[7] (Scheme 1.12), 300 mol% of 4-DMAP **1.8** is used. In this instance, 4-DMAP acts as the auxiliary base in the reaction, hence the more reactive *N*-acetylpyridinium acetate shows increased activity over *N*-acetylpyridinium chloride.

SCHEME 1.14: Reaction for the computational study of acetylation using 4-DMAP **1.8**.

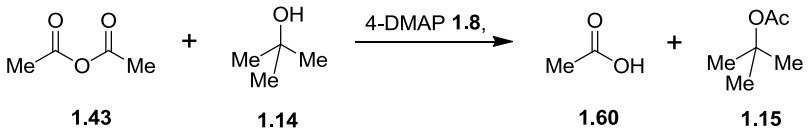

1.43 **1.14** **1.60** **1.15**

Xu *et al.*[15] studied the mechanism of the reaction of 4-DMAP **1.8** and acetic anhydride **1.43** in the acetylation of *tert*-butanol **1.14** (Scheme 1.14) using computational methods.[16] They found that a nucleophilic mechanism was more favourable than a base-catalysis mechanism. The calculated mechanism and energies for the nucleophilic pathway are shown in Scheme 1.15.

SCHEME 1.15: Calculated mechanism for acylation of *tert*-butanol **1.14**. Energies are in kJmol^{-1}.

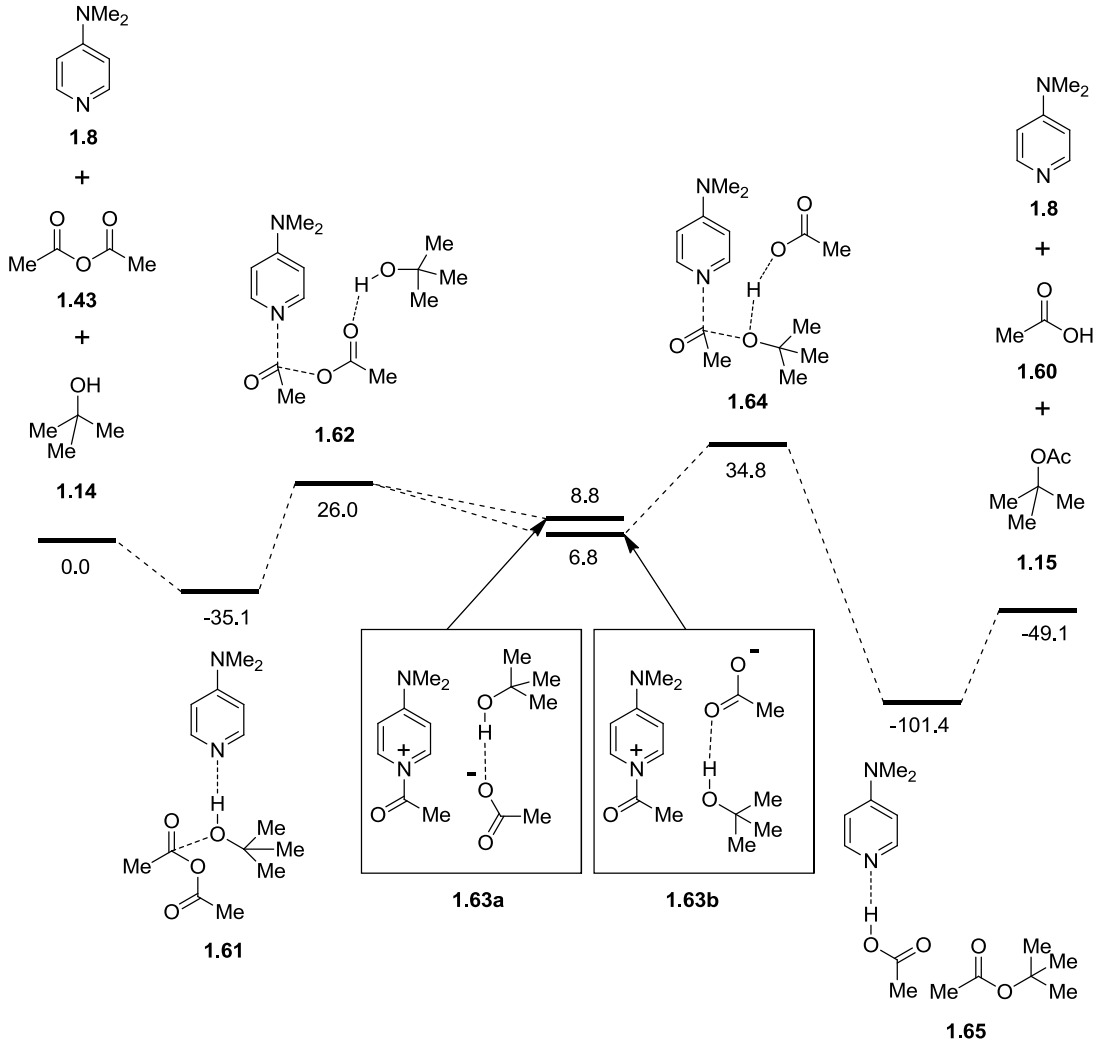

The reaction is initiated through formation of ternary complex **1.61**, which is favoured by 35.1 kJmol^{-1}. Expulsion of the acetate group is facilitated through formation of a hydrogen bond to the hydroxyl group of alcohol **1.14** through transition state **1.62** (26.0 kJmol^{-1}), eventually arriving at intermediate **1.63a** (8.8 kJmol^{-1}). Reorientation of the two components gives intermediate **1.63b**, which is 2 kJmol^{-1} more stable than **1.63a**. The orientation of **1.63b** allows alcohol **1.14** to attack the acetylpyridinium cation, the reactivity of the alcohol being enhanced by hydrogen-bonding to the acetate counterion. The reaction proceeds through transition state **1.64**, the rds of the reaction. This transition state shows the concerted formation and cleavage of four bonds; the C-N bond connecting the acetyl and pyridine ring nitrogen, the C-O ester bond in product **1.15**, the O-H bond in alcohol **1.14** and the

O-H bond in acetic acid **1.60**. Transition state **1.64** is 69.9 kJmol^{-1} above ternary complex **1.61** and 8.8 kJmol^{-1} above transition state **1.62**. Acyl transfer occurs to give complex **1.65**, which is stabilised by extensive hydrogen bonding (-101.4 kJmol^{-1}), which then breaks down to give acylated product **1.15**, acetic acid **1.60** and 4-DMAP **1.8** which is favourable by 49.1 kJmol^{-1}.

SCHEME 1.16: First transition state for base-catalysed acylation of **1.14**.

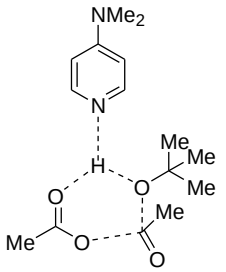

1.66

The same calculations were carried out using a base-catalysed mechanism. The first transition state takes the form **1.66** (Scheme 1.16) and was found to be 107.9 kJmol^{-1} less stable than ternary complex **1.61**, hence 46.8 kJmol^{-1} less stable than the first transition state for a nucleophilic mechanism, **1.62**. The calculations are in agreement with experimental evidence, where the rds of the reaction is the acyl transfer to the alcohol.

The effect of solvent was taken into account in the calculations and was found to be in agreement with experimental results. The mechanism was found to be more favourable in the order CCl_4 > $CHCl_3$ > DCM.

In the calculated nucleophilic mechanism (Scheme 1.15), the rds (**1.63b → 1.64**) does not have any dependence on the auxiliary base. In order to determine if this was the case, Xu *et al*.[15] studied the kinetics of the reaction of cyclohexanol **1.67** and acetic anhydride **1.43** (Scheme 1.17). Kinetic studies showed that the rate of reaction varied linearly with the concentration of 4-DMAP **1.8** and showed zero order dependence on the concentration of triethylamine. The reaction rate varied linearly with the concentration of cyclohexanol **1.67** and acetic anhydride **1.43**. The calculations and kinetic studies showed that the auxiliary base or 4-DMAP (as a base) are not involved in the acylation rds. This leaves the acetate counterion contained in the acetylpyridinium ion pair **1.63b** as the most likely base. The results

were consistent with the calculated mechanism in Scheme 1.15 and the proposed mechanism in Scheme 1.11.

SCHEME 1.17: Reaction for kinetic study of acylation of cyclohexanol **1.67**.

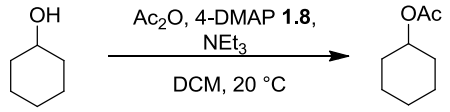

1.67 **1.68**

SCHEME 1.18: *N*-acetylpyridinium salts **1.69**-**1.72** and structure **1.73** (diagram representation of crystal structure of salt **1.70**).

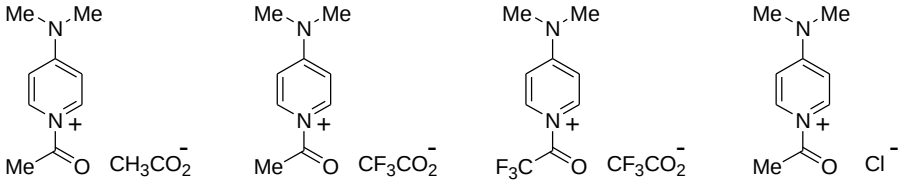

1.69 **1.70** **1.71** **1.72**

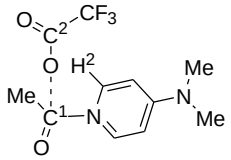

1.73

In order to study acetylpyridinium tight-ion pairs such as **1.52**, Lutz *et al.*[17] synthesised *N*-acetylpyridinium salts **1.69**-**1.72** (Scheme 1.18) and studied them by X-ray crystallography, NMR and IR studies. Salts **1.70**-**1.72** were crystallised for study.

For salt **1.70**, the crystal structure showed a close proximity of the oxygen of the counterion and the acyl carbon of 2.84 Å and an O-C^1-O bond angle of 95-96 °. Secondary H-bonding interactions with O-C(H^2) of 2.80 Å and C^2O-CF_3 of 2.80 Å were found. The results were similar for salt **1.71**. In comparison, salt **1.72** shows an acyl carbon-chloride distance of 3.37-3.93 Å and a Cl-C-O bond angle of 79-125°. Secondary bonding interactions of Cl-C(H^2) were found to be 3.2-4.9 Å and Cl-Me (acyl group) interactions were 2.9-4.4 Å. Solvent molecules (DCM) were shown to be incorporated into the crystal structure of **1.72**, indicating a loose association of the

chloride anion and the acetylpyridinium cation. Low-temperature NMR studies were carried out on salts **1.69**-**1.72**. From these, the barrier to rotation around the acyl carbon-pyridine nitrogen bond could be calculated as 9.3 ± 0.3 kcal.mol^{-1}. In addition, ^{1}H-^{19}F HOESY NMR studies of salt **1.70** showed close contact between the aromatic protons of the pyridine ring and the CF_3 group of the counterion, evidence of a tight-ion pair in solution. Low temperature IR studies on a 1:2 mixture of 4-DMAP and acetic anhydride in DCM showed a signal for salt **1.69** at 170 K. On increasing the temperature, the signal for **1.69** decreased to almost background level at 270 K. This indicates that the concentration of *N*-acetylpyridinium salts, such as **1.69**, is much lower at r.t. than previous NMR studies[7] suggest. Based on these results, Lutz *et al*.[17] proposed that the ability of the anion to guide the alcohol towards the reaction centre increases if it is anchored to the acylpyridinium salt. Additional hydrogen-bonding contacts to the pyridine ring aid this anchoring. This explains why acetylpyridinium acetate salts, with their close cation-anion interaction, are more reactive than the acetylpyridinium chloride equivalents.

Markey and Kelly[18] were able to synthesise remarkably stable acylpyridinium salt **1.75** from amine **1.74** and phosgene (Scheme 1.19). Unusually, ^{1}H NMR of salt **1.75** showed two singlet peaks at $\delta_H(CD_3OD)$ 3.45 and 3.52 ppm for the methyl protons on the 4-DMAP unit. Based on variable-temperature NMR studies, Markey and Kelly[18] calculated the barrier for rotation of the C-NMe_2 bond as 18.5 kcal.mol^{-1}, indicating substantial double-bond character.

Acylpyridinium salt **1.75** showed remarkable stability in methanol, with no reaction in methanol at 100 °C over 19 h. Reaction of **1.75** with water at 55 °C showed only 20 % conversion to carbamic acid **1.76** after 16 h, with subsequent loss of CO_2 to give amine **1.74**. Treatment of **1.75** with dimethylamine gave urea **1.77** after 3 h at r.t. However, urea **1.77** could be converted back to acylpyridinium salt **1.75** by dissolving in CD_3OD and removing the volatiles under vacuum.

SCHEME 1.19: Stable acylpyridinium salt **1.75**.

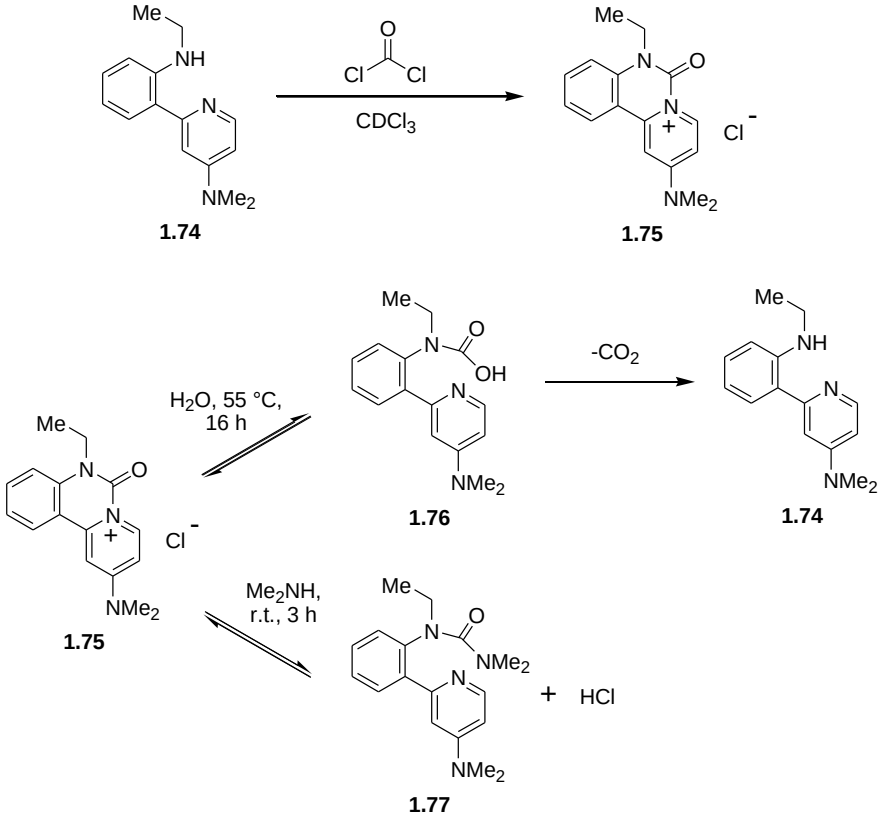

In summary, acylation of alcohols using 4-dialkylaminopyridines as catalysts occurs primarily via nucleophilic catalysis. The potent catalytic ability of 4-dialkylaminopyridines comes from the stabilisation of the *N*-acylpyridinium salts formed in the reaction, a factor which can be increased by increased alkyl substitution on the dialkylamino nitrogen (in the case of 4-PPY **1.17**) or by conformational fixation of the dialkylamino nitrogen (in the case of pyridines **1.39**-**1.41**). The reaction works best in non-polar solvents, where a tight-ion pair is formed as the reactive species. In this case, the basicity of the counterion influences the reactivity, the more basic anion helps in the deprotonation of the alcohol in the rds. Computational and kinetic studies agree with the proposed mechanism.

1.4 Further Reactions Involving 4-Dialkylaminopyridines

As well as the acylation of sterically-hindered alcohols, 4-dialkylaminopyridines can be used as catalysts for a variety of other synthetically useful reactions, a few of which will now be detailed.

1.4.1 The Baylis-Hillman Reaciton

The Baylis-Hillman reaction is the name commonly given to the base-catalysed reaction of aldehydes with acrylates at the C2 position.[5] The reaction is commonly catalysed by DABCO **1.84** or tributylphosphine. However, 4-DMAP has been shown to successfully catalyse reaction of 2-cyclohexenones with formaldehyde, a reaction that could not be catalysed by DABCO **1.84** (Scheme 1.21).[19] The mechanism is believed to occur via conjugate addition of 4-DMAP to the 2-cyclohexenone **1.85** to give intermediate **1.86**, which then undergoes reaction with the aldehyde to give product **1.87**. Some evidence for this mechanism was reported,[19] in that substitution of the *β*-position of the 2-cyclohexenones resulted in no reaction with aldehydes in the presence of 4-DMAP.

SCHEME 1.21: Baylis-Hillman Reaction.

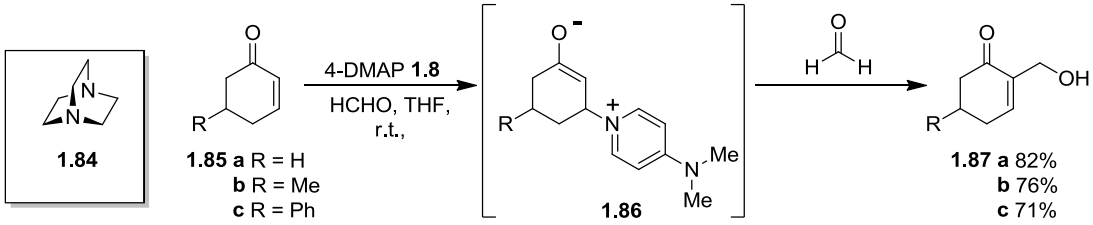

SCHEME 1.22: Formation of diadduct product using methyl vinyl ketone **1.89**.

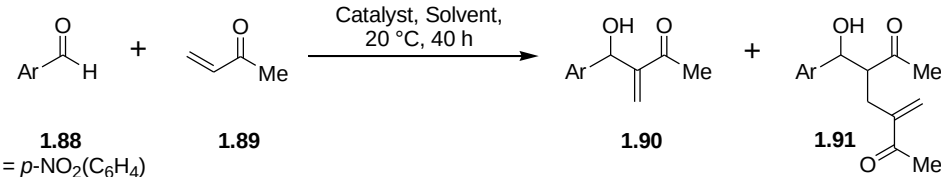

The use of 4-DMAP in the reaction of *p*-nitrobenzaldehyde **1.88** with methyl vinyl ketone **1.89** does not give the diadduct side-product **1.91** that can be formed when the reaction is carried out using DABCO **1.84** (Scheme 1.22, Table 1.8).[20] Only the normal Baylis-Hillman product **1.90** is formed in high yields.

TABLE 1.8: Catalyst effects on Baylis-Hillman reaction with **1.89**.

Entry	**Catalyst**	**Solvent**	**Yield / %**	
			1.90	**1.91**
1	DABCO **1.84**	DMSO	60	20
2	DABCO **1.84**	DMF	63	23
3	4-DMAP **1.8**	DMSO	85	0
4	4-DMAP **1.8**	DMF	83	0

1.4.2 The Dakin-West Reaction

The Dakin-West reaction is the name given to the conversion of an α-amino acid to the corresponding α-amino ketone (Scheme 1.23).[3] The reaction can be catalysed using 4-DMAP **1.7** under mild conditions in the presence of sensitive protecting groups.[21]

SCHEME 1.23: Dakin-West reaction of an α-amino acid.

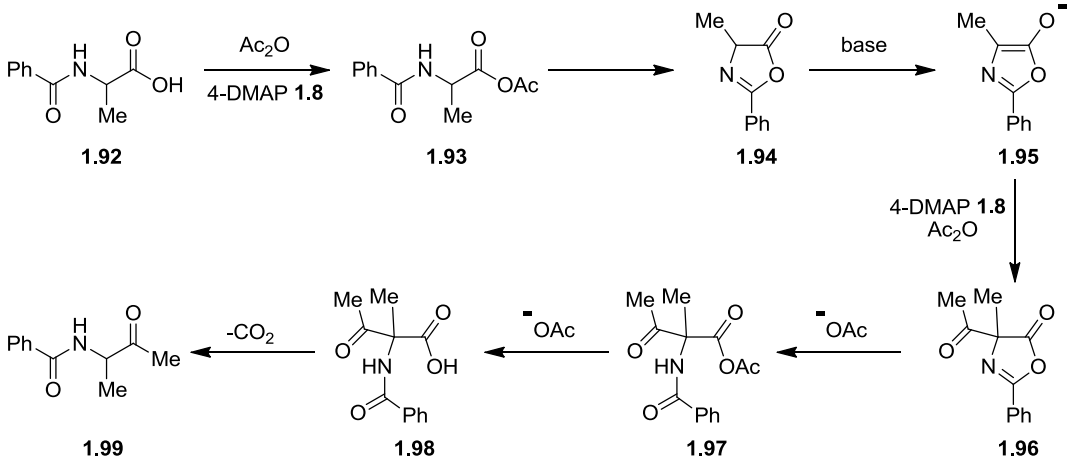

A similar type of reaction is the rearrangement of 5-acyloxyoxazole **1.100** to give 4-acyl-2-oxazolin-5-one **1.101** or 2-acyl-3-oxazoline **1.104** (which occurs when R^2 is an electron-withdrawing group) which is catalysed by 4-DMAP **1.8**.[7] The mechanism is shown in Scheme 1.24.

SCHEME 1.24: Rearrangement of 5-acyloxyoxazole **1.100**.

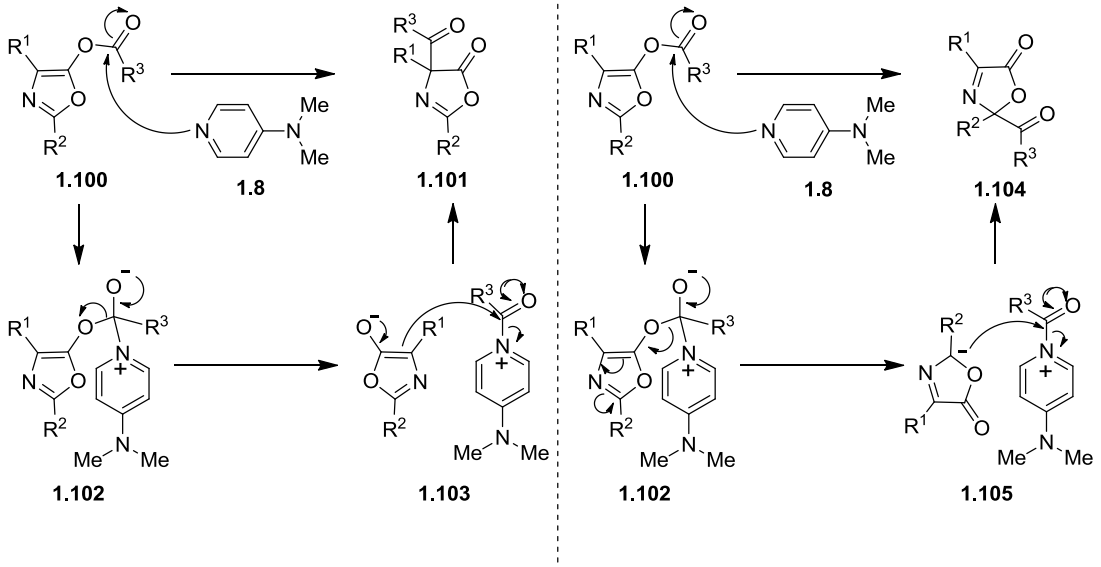

1.4.3 Miscellaneous Reactions

The use of 4-DMAP **1.8** as a reagent for the selective reaction of diols has been reported. Hernandez *et al*.[22] reported the synthesis of pyridinium salt **1.107**, which was shown to selectively tritylate primary alcohols over secondary alcohols (Scheme 1.25). In addition, salt **1.107** showed selective tritylation of primary amines (such as **1.110**) in the presence of hydroxyl groups.

Chaudhary and Hernandez[23] also reported the selective silylation of primary alcohols over secondary alcohols using 4-DMAP **1.8** and *tert*-butyldimethylsilyl chloride (TBS-Cl) (Scheme 1.26, Table 1.9).

SCHEME 1.25: Selective tritylations using pyridinium salt **1.107**.

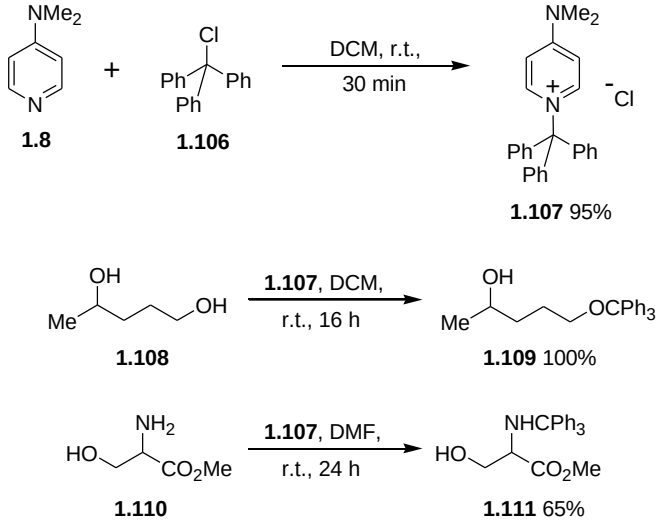

SCHEME 1.26: Selective silylation of primary alcohols.

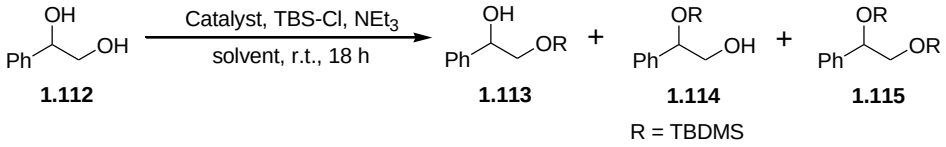

TABLE 1.9: Catalyst effects on silylation of alcohols.

Entry	**Catalyst**	**Solvent**	**GC-MS Yield / %**		
			1.113	**1.114**	**1.115**
1	DMAP (0.04 eq)	DCM	95	0	5
2	Imidazole (2.2 eq)	DMF	59	11	30

As well as the reaction with alcohols, 4-DMAP **1.8** can be used for the acylation of amines.[2] As with alcohols, the rate is greatly increased when using 4-DMAP **1.8** over pyridine or triethylamine (Scheme 1.27, Table 1.10).[7]

SCHEME 1.27: Acylation of amine **1.9** using different catalysts.

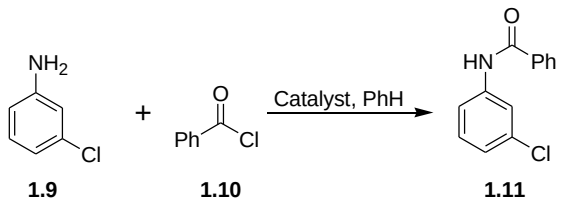

TABLE 1.10: Relative rates of acylation of amines.

Catalyst	**Relative Rate**
Pyridine	1.00
NEt_3	0.04
4-DMAP **1.8**	5900

4-DMAP **1.8** has been shown to be a powerful reagent for the synthesis of O^6-substituted guanines.[24] The previously used synthetic protocol involved the reaction of 2-amino-*N*,*N*,*N*-trimethyl-1*H*-purine-6-ammonium chloride **1.116** with the desired alcohol.

However, Schirrmacher *et al*.[24] found that for certain alcohols, the reaction resulted in poor yields or did not proceed at all for certain fluoropyridine alcohols (Scheme 1.28). When 4-DMAP was used with the required fluoropyridine alcohol, the O^6-substituted guanidines could be synthesised in higher yields (20-87 %). Interestingly, direct reaction of 4-DMAP **1.8** with **1.120** (the precursor of **1.116**), then subsequent reaction with the desired alcohol led to decreased yields for all the alcohols tested. It appears that the trimethylammonium group is necessary for good reaction with 4-DMAP, possibly due to increased polarisation of the C6 carbon in **1.116** over **1.120**.

SCHEME 1.28: Synthesis of O^6-substituted guanines.

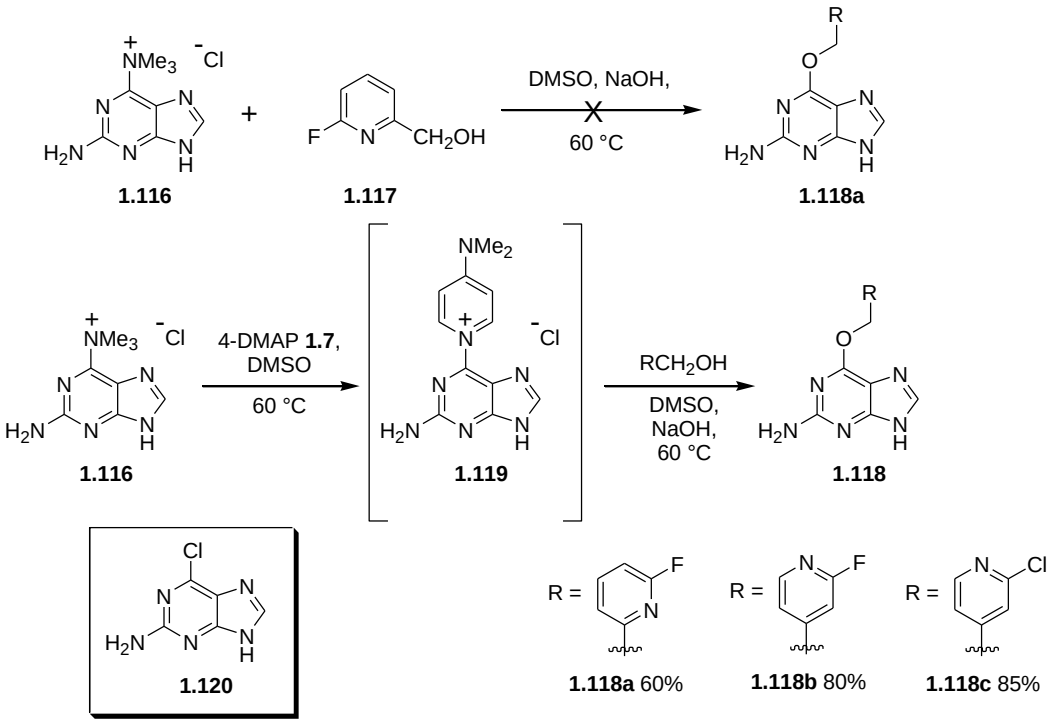

1.5 Chiral Analogues of 4-Dialkylaminopyridines

Chiral 4-dialkylaminopyridine analogues have found substantial use in synthesis in the past 15 years. The wide variety of catalysts synthesised and their uses are too large to cover in this review, though the use of chiral dialkylaminopyridine catalysts in asymmetric catalysis has been covered elsewhere.[25] This section will examine chiral dialkylaminopyridine derivatives as reagents for the kinetic resolution of alcohols, as this is where the first instance of an effective chiral 4-DMAP analogue was reported.[26]

1.5.1 4-DMAP derivatives with a Stereogenic Centre

The first chiral DMAP-based acyl transfer reagent was reported by Vedejs and Chen in 1996.[26] They synthesised 4-DMAP derivative **1.121** (Scheme 1.29), which is converted to the active reagent **1.123** upon reaction with chloroformate **1.122**. No reaction between **1.123** and secondary alcohols occurred at r.t., requiring the addition of a tertiary amine and a Lewis acid. Under the reaction conditions (Scheme 1.29, Table 1.11), kinetic resolution of secondary alcohols could be carried out in 20-44 % yield with ee's up to 87 % for the resolved alcohol **1.125**. The selectivity factor (s) is a measure of the efficiency of kinetic resolution by a catalyst. It is defined as [(rate of fast-reacting enantiomer)/(rate of slow-reacting enantiomer)], and generally for synthetically-useful reactions s ≥ 10. For **1.121**, s = 11-45 were observed.

SCHEME 1.29: Chiral 4-DMAP analogue **1.121**.

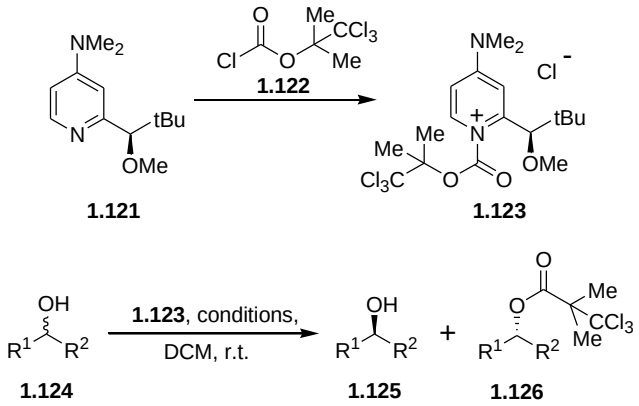

TABLE 1.11: Kinetic resolution of secondary alcohols by **1.123**.

Entry	**R^1**	**R^2**	**Cond.**	**t / h**	**Yield / %**	**ee 1.125 / %**	**ee 1.126 / %**	**s**
1	Me	Naphthyl	A	52	28	33	94	44
2			B	17	54	87	84	48
3	Ph	Et	A	62	20	22	89	22
4			B	40	39	ND	76	12
5	*o*-Me(C_6H_4)	Me	A	48	21	19	92	29
6			B	43	39	59	93	53

A- $ZnCl_2$ (1.0 eq), NEt_3 (1.5 eq). B- $MgBr_2$ (1.0 eq), 1,2,2,6,6-pentamethylpiperidine (1.5 eq).

Chiral reagent **1.121** could be recovered after aqueous work-up and reused without any loss of selectivity. However, **1.121** had to be used in stoichiometric amounts, most likely due to the steric constraints of 2-substitution of the 4-DMAP, as it has been previously shown that 2-substitution of the 4-dialkylaminopyridine inhibits nucleophilic catalysis (Scheme 1.9, Table 1.5).[13] Due to this limitation, substitution at the 3-position or the dialkylamino group has been subsequently employed for the synthesis of chirally-active catalysts.

Fuji *et al*.[27] reported 4-PPY derivative **1.127** as an effective catalyst for the kinetic resolution of secondary alcohols (Scheme 1.30). The chiral catalyst arises from reaction with the anhydride **1.28** to give the pyridinium cation **1.129**. Before reaction, **1.127** exists in an open (non π-stacking) conformation which is converted to a closed (π-stacking) conformation upon reaction with anhydride **1.128**, which was shown by NOE studies (**1.129**, Scheme 1.30). This closed conformation provides the stereochemical environment for the kinetic resolution. Fuji *et al*.[27] showed that secondary alcohols **1.130** could be resolved in 68-77 % conversion in 92 to >99 % ee (s = 5-12).

Connon *et al*.[28,29] reported 3-substituted 4-PPY catalyst **1.132** for the kinetic resolution of secondary alcohols (Scheme 1.31). Catalyst **1.132** gave yields of 68-78 % in 74-97 %ee (s = 6-30) for alcohols such as **1.133**.

SCHEME 1.30: Chiral 4-PPY catalyst **1.127** and resolution of alcohol **1.130**.

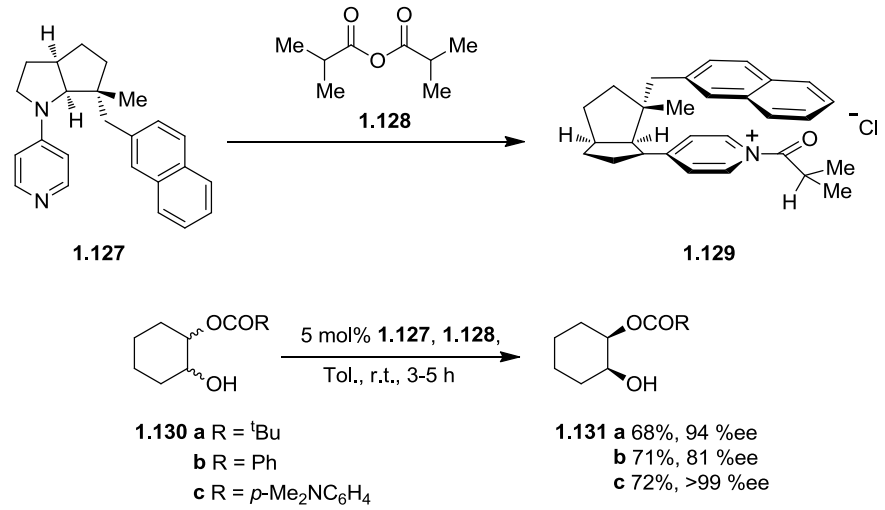

SCHEME 1.31: 3-Substituted 4-PPY catalyst **1.132**.

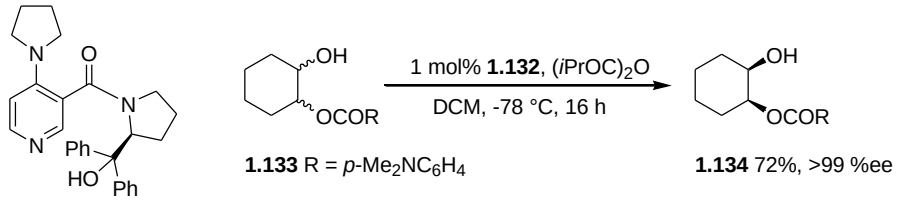

1.5.2 Catalysts with a Chiral Axis

In 1998, Spivey *et al.*[30] reported the synthesis of chiral 4-DMAP analogues that gained axial chirality from restricted rotation of an aryl-aryl bond substituted at the 3-position.

Catalysts **1.135** and **1.136** showed comparable reactivity to 4-DMAP **1.7** in the acylation of 1-methylcyclohexanol **1.12** (Scheme 1.32, Table 1.12), but showed low selectivities in the kinetic resolution of secondary alcohols.[31]

SCHEME 1.32: Axially-chiral catalysts **1.135** and **1.136**.

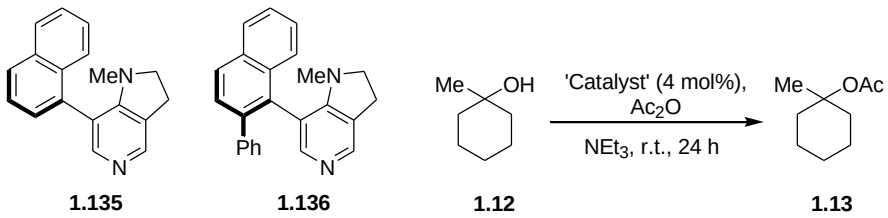

TABLE 1.12: Activity of different catalysts in acylation of **1.12**.[a]

Catalyst	Ratio 1.12:1.13
1.8	5:95
1.135	18:82
1.136	13:87

[a] Ac_2O (2.1 eq), NEt_3 (1.5 eq), catalyst (4 mol%), r.t.

They later synthesised catalyst **1.137** based on 4-diethylaminopyridine which showed s=10-25, with conversions of 18-51 % in up to 70 %ee (Scheme 1.33).[31] Catalyst **1.137** also showed improved selectivity in the kinetic resolution of singly acylated 1,2-diols **1.141**.[32]

SCHEME 1.33: Catalyst **1.137** for kinetic resolution.

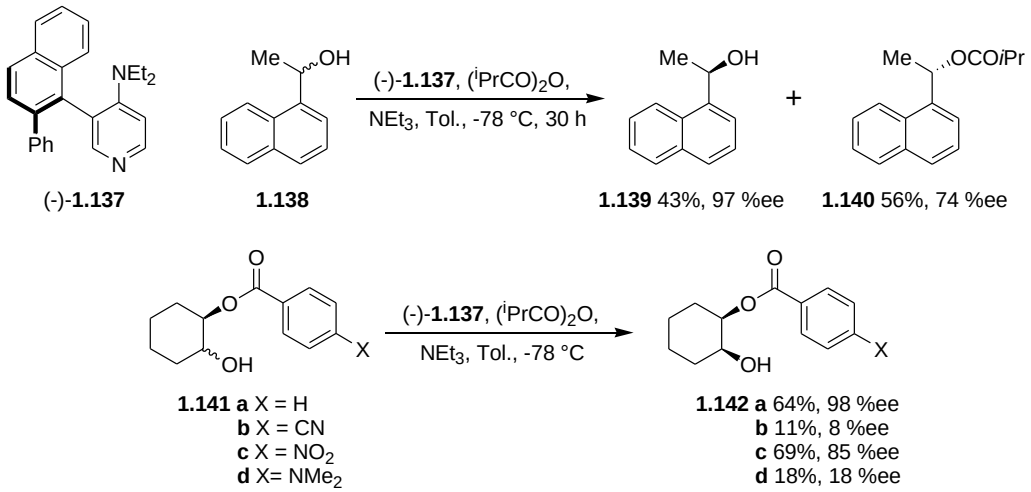

SCHEME 1.34: Dialkylamino catalysts **1.143a-d**.

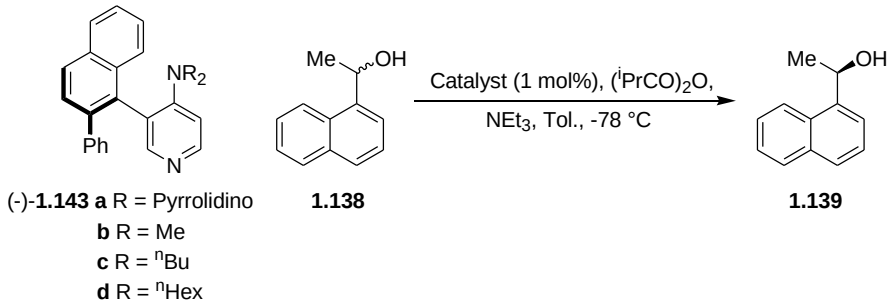

Spivey *et al.*[33] synthesised a variety of dialkylaminopyridine derivatives of catalyst **1.137** to see the effect of this group in the selectivity for the acylation of alcohol **1.138** (Scheme 1.34, Table 1.13). The *n*-butyl substituted catalyst **1.143c** showed the greatest selectivity in the kinetic resolution reaction studied. However, no correlation between alkyl group size and selectivity was observed.

TABLE 1.13: Selectivity of dialkylamino catalysts **1.143**.

Entry	Catalyst	Conversion	1.139 %ee	s
1	**1.143a**	70	68	3.5
2	**1.143b**	46	60	10
3	**1.137**	45	69	24
4	**1.143c**	59	99.9	31
5	**1.143d**[a]	37	54	9

[a] Reaction carried out at -93 °C.

They proposed structure **1.146** as a transition state for the kinetic resolution of secondary alcohols (Scheme 1.35).[32] Alcohol enantiomer **1.145** can react with acylated catalyst **1.137** due to the more favourable steric interactions between the small alkyl group (R_S) and the acyl group. Alcohol enantiomer **1.144** is disfavoured from reaction due to the bulkier R_L group having unfavourable interactions with the acyl group. The axially-chiral catalysts developed by Spivey *et al.*[30-33] represent a new type of chiral 4-DMAP analogue that has developed far from its first synthesis. However, in its current form (**1.137**) it shows good selectivity and product ee in a few specific examples, with most examples showing moderate selectivity and ee values.

SCHEME 1.35: Proposed transition state for reaction of catalyst **1.137**.

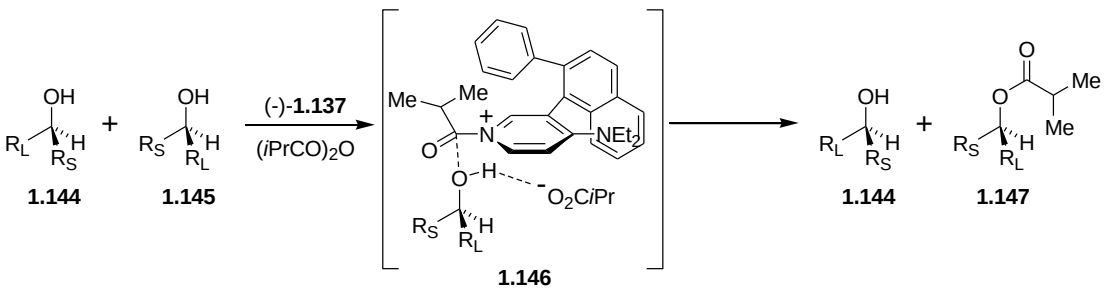

1.5.3 Catalysts with Planar Chirality

In 1996, Fu and Ruble[34] reported 4-DMAP based catalyst **1.149a** as an effective catalyst for the acylation of secondary alcohols. Catalyst **1.149a** achieved planar chirality by complexation to a metal and substitution at the 2-position of the pyridine ring. For acylation of alcohol **1.150**, catalyst **1.149a** showed a $t_{1/2}$ for acylation of < 3 min, compared to pyridine-based **1.148**, which showed a $t_{1/2}$ of ~ 50,000 min (Scheme 1.36).

SCHEME 1.36: Chiral catalyst **1.149** and acylation of alcohol **1.150**.

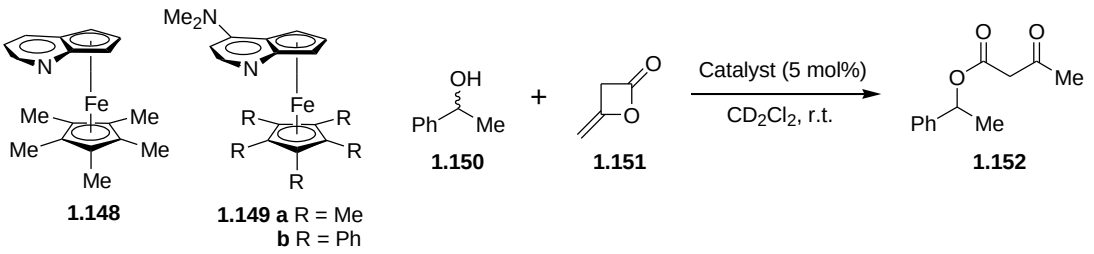

However, despite its high catalytic ability in the acylation of secondary alcohols, **1.149a** showed poor selectivity in the kinetic resolution of secondary alcohols.[35] Fu *et al*.[35] introduced additional steric bulk on the cyclopentadiene ring by replacing the Me groups with Ph groups to give catalyst **1.149b** (Scheme 1.36). As a result of this, catalyst **1.149b** showed high levels of selectivity in the kinetic resolution of secondary alcohols (s = 14-52)[35] as well as propargyl alcohols (s = 4-20)[36] (Scheme 1.37).

SCHEME 1.37: Kinetic resolution of secondary alcohols by **1.149b**.

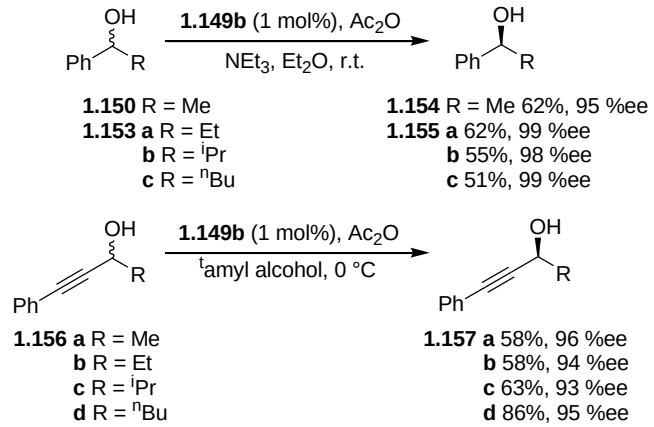

Fu *et al*.[36] were able to obtain a crystal structure of an acylated derivative of **1.149b** from the reaction of **1.149b** with AcCl, with subsequent counterion exchange using $AgSbF_6$ (**1.158**, Scheme 1.38). The crystal structure showed that the dimethylamino group, pyridine ring and acyl group were in the same plane. In addition, the bond lengths of the acylated 4-DMAP analogue **1.160** showed shortening of the Me_2N-C bond and C2-C3 bond of the pyridine ring compared to **1.159**. This indicated that a substantial contribution from resonance form **1.161** is likely to be found in the acylated catalyst.

SCHEME 1.38: Acylated catalyst **1.158** and bond lengths (Å).

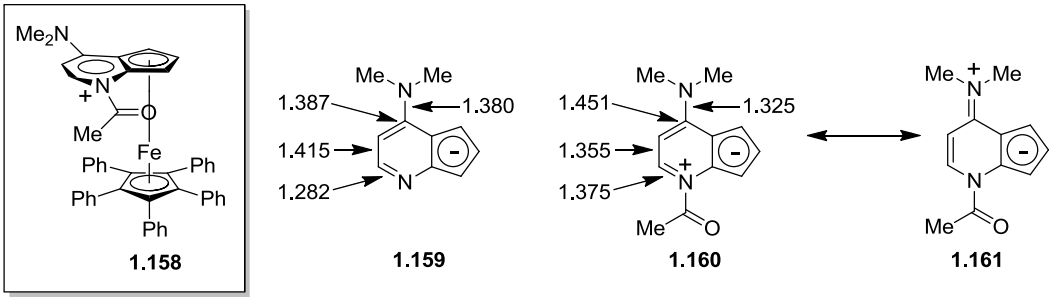

The 4-DMAP based catalysts developed by Fu *et al*.[34-36] represent the most potent chiral 4-dialkylaminopyridine catalysts for the kinetic resolution of secondary alcohols. Although very potent, these catalysts still require a metal to achieve chirality. As a result, highly potent organocatalysts based on 4-DMAP **1.7** for the kinetic resolution of secondary alcohols and other asymmetric reactions would be highly sought after. Perhaps in the future, such catalysts may be developed that show high levels of selectivity and that are commercially viable.

1.6 2-Dimethylaminopyridine

It has been shown that 2-dialkylaminopyridines do not share the same catalytic ability as 4-dialkylaminopyridines.[6] As a result of this, 2-DMAP **1.1** has not been as extensively studied in the literature as 4-DMAP **1.8** due to its limited synthetic utility. However, 2-DMAP does show some unusual chemical behaviour compared to 3-DMAP **1.9** and 4-DMAP, and this unusual behaviour has been documented by several groups.[37-43]

One of the first reported instances of the different methylation behaviour of 2-DMAP was by Tschitschibabin and Konowalowa,[37] who found that reaction of 2-DMAP and iodomethane at r.t. gave rise to the dimethylamino methylated product **1.4** only. Frampton *et al*.[38] also showed that for 2-DMAP, alkylation occurred preferentially on the dimethylamino nitrogen to give trimethylammonium species **1.4**. In contrast, methylation of 3-DMAP **1.9** and 4-DMAP **1.8** occurred to give the ring methylated products exclusively (to give **1.162** and **1.163** respectively (Scheme 1.39)). This reactivity was shown by NMR analysis, which showed singlets at $\delta_H(D_2O)$ 4.43 ppm and $\delta_H(D_2O)$ 3.16 ppm for aliphatic protons integrating to 3 and 6 protons respectively for species **1.163**, whereas trimethylpyridin-2-ylammonium iodide **1.4** showed a singlet at $\delta_H(D_2O)$ 3.86 ppm integrating to 9 protons.

SCHEME 1.39: Methylation of DMAPs **1.1**, **1.8** and **1.9**.

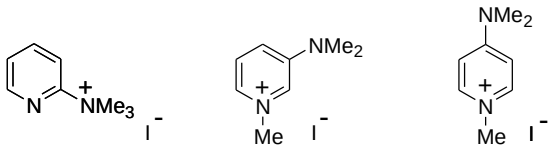

1.4 **1.162** **1.163**

In 1979, Barbieri *et al.*[39] studied the preferential protonation and methylation behaviour of dimethylaminopyridines. They showed experimentally that methylation of 2-DMAP occurred on the NMe_2 group preferentially, as opposed to 3- and 4-DMAP where methylation occurred exclusively on the ring nitrogen, in agreement with the results of Frampton *et al.*[38] Contrary to this, protonation of the dimethylaminopyridines (**1.1**, **1.8** and **1.9**) occurred exclusively on the ring nitrogen in all three cases.[39]

Semi-empirical CNDO/2 calculations on the conformational analysis of dimethylaminopyridines showed that the most stable conformation of 3- and 4-DMAP was when the dimethylamino group was co-planar with the pyridine ring (Scheme 1.40). For 4-DMAP, this conformation is consistent with delocalisation of the dimethylamino nitrogen lone pair of electrons which, through resonance, gives a partial negative charge on the ring nitrogen (**1.165**, Scheme 1.40), making it the preferential site of attack towards electrophiles. In the case of 2-DMAP, the most stable conformation was found to be when the dimethylamino group was rotated 15° out of the plane of the ring. This conformation indicates that the overlap between the lone pair of electrons on the dimethylamino nitrogen and the π-system of the pyridine ring is not as strong as for 3- and 4-DMAP.

SCHEME 1.40: Conformations of 4-DMAP and 2-DMAP and resonance of 4-DMAP.

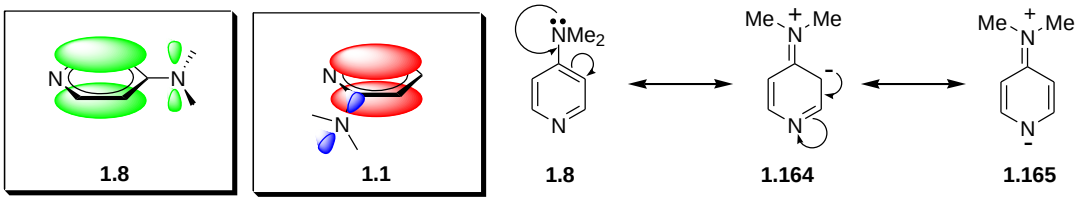

Barbieri *et al.*[39] also carried out charge density calculations on the dimethylaminopyridines. The charge density calculations (Table 1.14) show that for 2-DMAP and 4-DMAP the ring nitrogen has the most negative character, however, for 3-DMAP the most negative nitrogen belongs to the dimethylamino group. These calculations and results indicate that the experimentally observed methylation behaviour of the dimethylaminopyridines is not consistent purely with charge density considerations, as 2- and 4-DMAP would be expected to show alkylation on the ring nitrogen

preferentially, whereas 3-DMAP would alkylate on the dimethylamino nitrogen. In addition, the pK_a's of 2-DMAP, 3-DMAP and 4-DMAP are 6.94, 6.37 and 9.70 respectively.[11]

TABLE 1.14: Charge density calculations on dimethylaminopyridines.

Dimethylaminopyridine	**Calculated Charge Density**	
	Ring Nitrogen	**NMe_2 Nitrogen**
2-DMAP **1.1**	-0.1999	-0.1712
3-DMAP **1.9**	-0.1228	-0.1580
4-DMAP **1.8**	-0.1783	-0.1601

Calculations were then carried out on the relative energy of stabilisation of the different products of methylation and protonation (Scheme 1.41, Table 1.15).[39] They showed that protonation of the ring nitrogen was more stable for 2-, 3- and 4-DMAP. For the methylation of 3- and 4-DMAP, the product of the methylation of the ring nitrogen was the more stable product. For 2-DMAP, the product of ring nitrogen methylation was less stable by ~41 $kJmol^{-1}$. The gas phase calculations do not take into account any solvation effects from the dialkylaminopyridine salts in solution. However, the most stable calculated products are in very good agreement with experimental observations.

For protonation and methylation of 4-DMAP **1.8**, the experimental results are easily explained; the ring nitrogen of **1.8** shows the greatest negative character and the products from ring nitrogen protonation and methylation are calculated to be more stable than those using the dimethylamino nitrogen. For 3-DMAP **1.9**, the dimethylamino nitrogen is calculated to be the most basic. However, both protonation and methylation occur on the ring nitrogen, consistent with product stability calculations. A possible reason for this could be the increased steric strain upon protonation/methylation of the dimethylamino group compared to the ring nitrogen, albeit this effect would likely be small.

For 2-DMAP **1.1**, the situation is even more confusing. Charge density calculations show the ring nitrogen to be the more basic nitrogen. In addition, the products of

protonation and methylation are different. For 2-DMAP **1.1**, protonation occurs on the more basic ring nitrogen, consistent with product stability calculations. This indicates that the steric strain of the dimethylamino group in the 2-position is not sufficient to inhibit protonation on the ring nitrogen. However, for methylation of 2-DMAP, dimethylamino nitrogen methylated product **1.4** is preferentially (although not exclusively) formed. This indicates that even for a methyl group, the steric strain of the dimethylamino group in the 2-position is sufficient to hinder alkylation of the ring nitrogen, despite the possibility of resonance stabilisation of a ring-methylated 2-DMAP by the lone pair of electrons on the dimethylamino group (Scheme 1.42).

SCHEME 1.41: Proposed products for methylation and protonation of DMAP.

1.166 **1.167**

TABLE 1.15: Relative stabilities of protonated and methylated DMAP.

DMAP	**R**	**Rel. Stability of Product[a] / kJmol^{-1}**	
		1.166	**1.167**
2-DMAP **1.1**	H	-24.11	0
	Me	0	-41.01
3-DMAP **1.9**	H	-39.63	0
	Me	-63.36	0
4-DMAP **1.8**	H	-91.69	0
	Me	-146.61	0

[a] The energy of the less stable product was in each case arbitrarily set at 0 kJmol^{-1}.

SCHEME 1.42: Resonance stabilisation of ring-methylated 2-DMAP **1.6**.

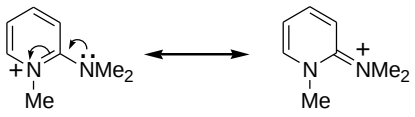

1.6 **1.168**

FIGURE 1.1: Ring-methylated 2-DMAP **1.6**.

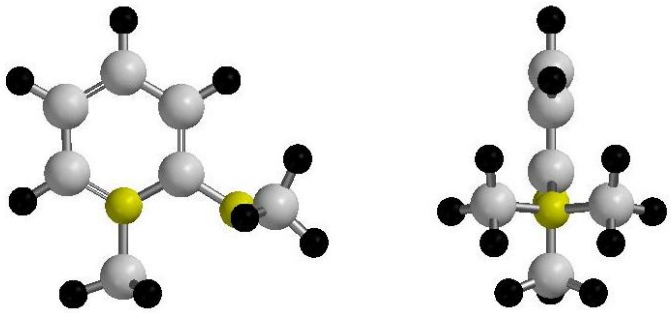

Indeed, our own calculations on the geometry of ring-methylated 2-DMAP **1.6** shows a highly-strained product (Figure 1.1). The equilibrium geometry of **1.6** was calculated on Spartan®[40] using Hartree-Fock calculations at 6-31G** level of theory.[41] As can be seen (Figure 1.1), methylation of the ring nitrogen in **1.6** causes the dimethylamino group to adopt a strained conformation, with the methyl carbons of the dimethylamino group lying at 90° to the plane of the pyridine ring. In addition to this, the dimethylamino group is forced to adopt a conformation between trigonal planar and tetrahedral, with C-N-C bond angles on the dimethylamino group at ~114°. The steric strain incurred by the methylation of the ring nitrogen causes a distortion of the dimethylamino group and rotation from 15° in 2-DMAP **1.1** to 57° for monocation **1.6**. Obviously the gas phase calculations again do not take into account any stabilising effects of solvent on the ring-methylated 2-DMAP **1.6**. However, it is reasonable to assume that even with solvation stabilisation, the steric hindrance of the dimethylamino group and the methyl on the ring nitrogen would still make this product unfavourable.

SCHEME 1.43: Methylation of 2-DMAP **1.1** using MeOTf and formation of 2-^{18}F-pyridine **1.172**.

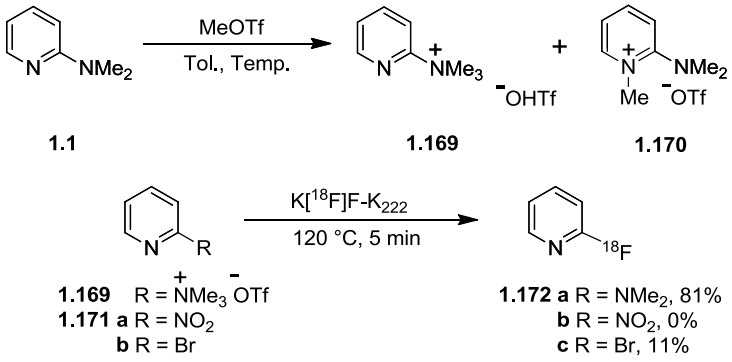

TABLE 1.16: Temperature effects on methylation of 2-DMAP **1.1**.

Entry	**Temperature / °C**	**Product Yield / %**	
		1.169	**1.170**
1	r.t.	35	-
2	80	-	30[a]

[a] Product obtained as an inseparable mixture of **1.169**:**1.170** (1:4 by ^{1}H NMR).

More recent work on the methylation of dimethylaminopyridines was conducted by Dollé *et al*.[42,43] They found that methylation of 2-DMAP **1.1** using methyl trifluoromethanesulfonate gave different products depending on the reaction temperature (Scheme 1.44, Table 1.16). It was found that at r.t., methylation of 2-DMAP gave trimethylpyridin-2-ylammonium trifluoromethanesulfonate **1.169** in 35 % yield. However, if the reaction temperature was increased to 80 °C, 2-dimethylamino-1-methylpyridinium trifluoromethanesulfonate **1.170** was formed as the major product (albeit as an inseparable mixture with **1.169**). They found that synthesis of 2-^{18}F-pyridine **1.172** occurred more successfully when using **1.169** rather than 2-nitropyridine **1.171a** or 2-bromopyridine **1.171b** (Scheme 1.43). A similar type of reactivity was shown in the reaction of 2-amino-*N*,*N*,*N*-trimethyl-1*H*-purine-6-ammonium chloride **1.116** with alcohols to form O^{6}-substituted guanines (Scheme 1.28).[24]

This review has examined the chemistry of popular acylation catalyst 4-DMAP **1.8**, including a look at its mechanism of reaction and the application of chiral analogues. In addition, this section has highlighted some of the unusual chemistry and reactivity of 2-DMAP **1.1**, a subject that will be explored in greater detail in later chapters.

2 Superelectrophiles

2.1 Introduction

Superelectrophiles are di- or polycation species that are more reactive than their parent monocations.[44,45] The concept was first proposed by Olah *et al*.[46] to explain the unusual reactivity between the acetyl cation **2.1** and 2-methylpropane **2.2** in superacids.

Superacids are highly ionising, low-nucleophilicity solvents. In some instances, they are capable of additional activation of electrophiles by further electrophilic interaction, such as coordination or solvation (protosolvation). Superacids are arbitrarily defined as acids stronger than 100 % H_2SO_4 or $AlCl_3$. They span the Hammett acidity (H_0) scale from -12 for 100 % H_2SO_4 to -25 in the case of some "magic acids".[47] Examples of superacid systems include FSO_3H, trifluoromethane-sulfonic acid (TfOH)-SbF_5, TfOH-$B(OTf)_3$, HF-SbF_5 and HF-BF_3.[45]

In 1993, Olah stated that "The overall concept and significance of these studies [superelectrophiles], however, has as yet aroused relatively little response or even interest in the broader chemical community. This is probably because our studies were considered of highly specialized nature involved generally in somewhat exotic superacidic media."[44] However, since this review, the concept of superelectrophilic activation has been expanded from superacid systems to have important consequences for reactions in organic synthesis and has even been proposed as a method of activation in enzymatic systems. The breadth of work now published on superelectrophiles is too large to review in great detail.

The remainder of this review will look at the first discovery of superelectrophilic activation (Section 2.2) and some different classes of superelectrophilic molecules (Sections 2.3-2.4). The final section will examine nitrogen heterocycle dications that have been reported in the literature, which have relevance to the work detailed here.

2.2 Superelectrophilic Activation

In 1973, Brouwer and Kiffin[48] reported that reaction of acetic acid **1.60** and 2-methylpropane **2.2** in HF-BF_3 resulted in hydride transfer from 2-methylpropane **2.2** to acetyl cation **2.1** to give acetaldehyde **2.3** and *tert*-butyl cation **2.4** (Scheme 2.1).

SCHEME 2.1: Proposed mechanism of the reaction of acetyl cation **2.1** and 2-methylpropane **2.2**.

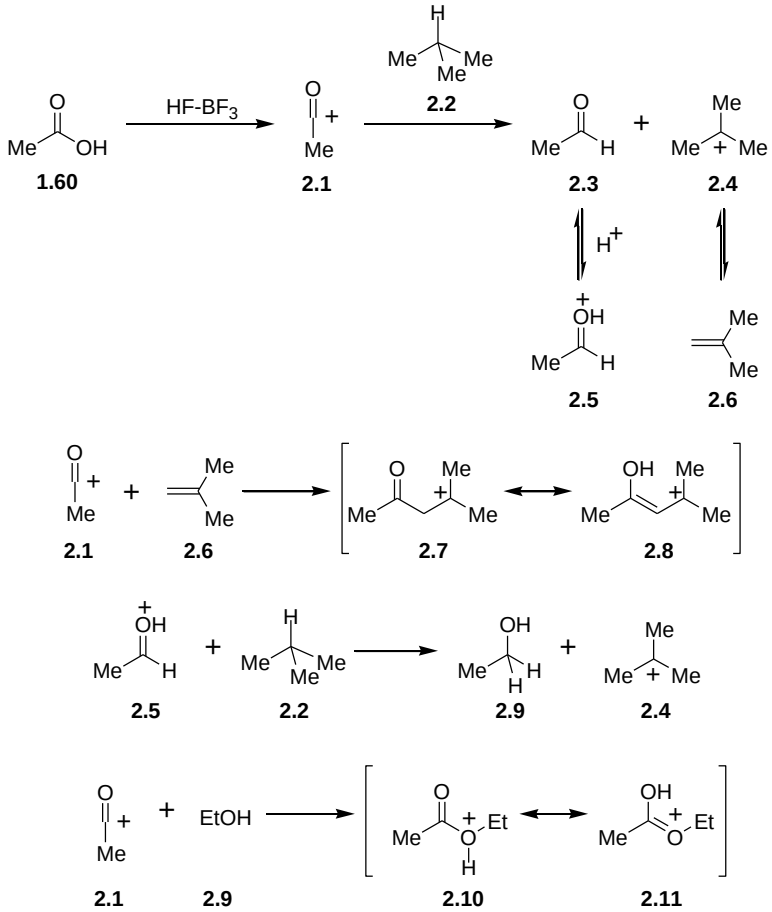

Acetaldehyde **2.3** and *tert*-butyl cation **2.4** could not be observed spectroscopically in the reaction, but their presence was inferred from the reaction products. The observed products in the reaction were protonated mesityl oxide **2.8** and protonated ethyl acetate **2.11**, produced in a ratio of 2:1. The proposed mechanism of the reaction is shown in Scheme 2.1. In the acid solution, acetaldehyde **2.3** is protonated to give **2.5**, and the *tert*-butyl cation **2.4** is converted to *iso*-butene **2.6**. Reaction of **2.1** and **2.6** gives protonated mesityl oxide **2.7**; its resonance form is shown as **2.8**. Protonated acetaldehyde **2.5** can abstract a hydride from 2-methylpropane **2.2** to give

ethanol **2.9** and *tert*-butyl cation **2.4**. Reaction of **2.1** with ethanol **2.9** gives protonated ethyl acetate **2.10** and its resonance form **2.11**. The rate of hydride transfer in HF-BF_3 was calculated as 3.0 x 10^{-5} $M^{-1}s^{-1}$. The authors also studied the reaction in the more acidic HF-SbF_5 (9:1) and the rate of hydride transfer was calculated as 2.0 x 10^{-5} $M^{-1}s^{-1}$. Brouwer and Kiffin stated that the hydride transfer from 2-methylpropane **2.2** to the acetyl cation **2.1** was practically the same in HF-BF_3 as in HF-SbF_5, despite the latter's higher acidity. From this they concluded that the transfer of hydride in the reaction wasn't helped by the protonation of the carbonyl group in the starting acid **1.60**.

SCHEME 2.2: Superelectrophilic activation of acetyl cation **2.1**.

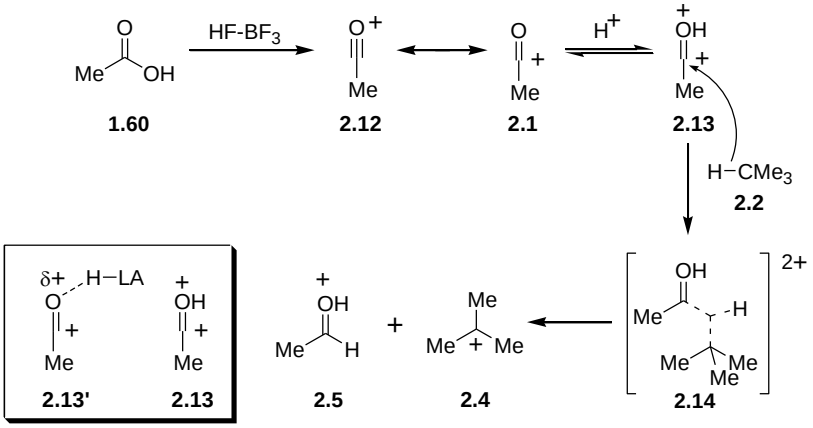

However, the reaction was later re-examined by Olah *et al*.[46] They reported that in aprotic solvents (including SO_2, SO_2ClF and AsF_3), no reaction between acetyl cation **2.1** and alkanes (including 2-methylpropane **2.2**) occurred. According to Brouwer and Kiffin,[48] the reaction of **2.1** and **2.2** did not require protonation of **1.60** (or **2.1**) to proceed. If this was the case, the reaction in aprotic media should have been successful. In order to explain this reactivity in superacid solvents, Olah *et al*.[46] proposed a mechanism of superelectrophilic activation (Scheme 2.2). Olah *et al*. postulated that the non-bonding electron pair on the oxygen of acetyl cation **2.1** can interact further with the superacidic solvent, leading to highly reactive superelectrophilic dication species **2.13**. In the limiting case, full protonation (protosolvation) of acetyl cation **2.1** could occur to give dication **2.13**. Alternatively, coordination of the superacid solvent to the acetyl cation could produce a superelectrophilic hydrogen bonded species such as **2.13′**. In either case, the

superelectrophilic **2.13** can abstract a hydride from 2-methylpropane **2.2**, via 3-centre-2-electron (3c-2e) bonded transition state **2.14**, to give *tert*-butyl cation **2.4** and protonated acetaldehyde **2.5**.

Superelectrophilic activation is brought about by protonation of acetyl cation **2.1**, which helps to polarise the C=O bond and increases the electrophilic activity of **2.1**. The reactivity of **2.1** is sufficiently increased that it can abstract a hydride from alkanes. However, dication superelectrophile **2.13** could not be observed by spectroscopy in the reaction, and its existence was postulated from the differing reactivity observed in superacid and aprotic solvents. The additional activation of **2.1** by superacidic solvation explains why no reaction between **2.1** and **2.2** occurs in aprotic media.

Similar behaviour is observed for the reaction of the nitronium ion in superacid solvents. Nitronium salts (NO_2BF_4 or NO_2PF_6) show no reactivity with methane in aprotic solvents. However, in the presence of fluorosulfonic acid or HF-BF_3, nitration occurs to give nitromethane **2.17** (Scheme 2.3). It was suggested that the reaction proceeds via protonation of the nitronium salt to give protonitronium ion **2.16′**, an example of superelectrophilic activation.

SCHEME 2.3: Proposed superelectrophilic activation of nitronium salts.

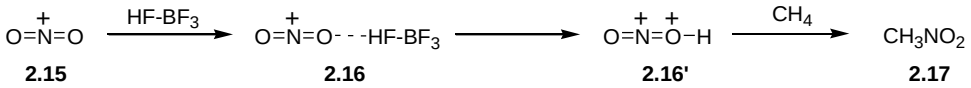

2.3 Superelectrophiles in Superacid

The most common types of superelectrophile reported are those that arise from further activation of cations in superacid. This section will examine some examples of superelectrophiles containing oxygen, carbon and nitrogen.

2.3.1 Oxygen Superelectrophiles

A variety of superelectrophiles containing oxygen as the cationic group have been reported.[44,45]

Olah *et al.*[49] observed H-D exchange for solutions of the hydroxonium ion in superacid solutions. A solution of $D_2{}^{17}O$ in HF-SbF_5 (1:1) was immediately protonated to form $HD_2{}^{17}O^+$ (as shown by ^{17}O NMR). Over 4 h, the ^{17}O spectrum

changed from $HD_2{}^{17}O^+$ to $H_3{}^{17}O^+$. Similarly, a solution of $H_2{}^{17}O$ in DF-SbF_5 was immediately deuterated to form $DH_2{}^{17}O^+$. Over 4.5 h, the ^{17}O spectrum changed from $DH_2{}^{17}O^+$ to $D_3{}^{17}O^+$. When the solution was made more acidic (HF-SbF_5 (2:1)), the rate of H-D transfer increased. Two mechanisms were proposed for the observed results (Scheme 2.4). In the first mechanism, dedeuteration of HD_2O^+ **2.18** occurs to give HDO **2.19**, which can be protonated to give DH_2O^+ **2.20**. This process occurs again to give H_3O^+ **2.22**. The second mechanism involves superelectrophilic activation of HD_2O^+ **2.18** to give $H_2D_2O^{2+}$ **2.23**. Dedeuteration gives DH_2O^+ **2.20**, which can subsequently undergo protonation and dedeuteration to form H_3O^+ **2.22**.

SCHEME 2.4: Mechanisms for H-D exchange in superacid.

Mechanism 1:

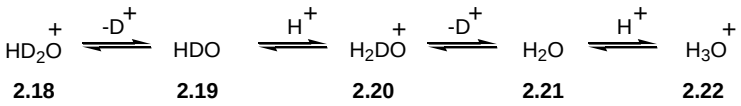

Mechanism 2:

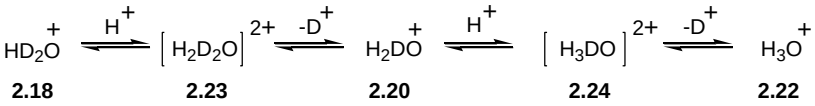

Using the less acidic "magic acid" (HSO_3F:SbF_5), no H-D exchange was observed. Olah *et al*.[49] proposed mechanism 1 (Scheme 2.4) would be disfavoured as the reaction occurs in highly acidic media where such a mechanism would be disfavoured and does not occur in less acidic solvents, where mechanism 1 would be favoured. Although the NMR studies could not prove which of the two mechanisms was valid, *ab initio*[49] calculations showed H_4O^{2+} to have a tetrahedral structure and to be kinetically stable. However, the same calculations showed the protonation of H_3O^+ to be unfavourable. In order to compensate for this result, Olah *et al*. stated that the gas phase calculations did not take into account solvation effects in the superacid solvent.

Alkyloxonium ions such as Meerwein salts (cations of the form Me_3O^+, Et_3O^+, with non-nucleophilic anions such as BF_4^-) are significantly stabilised by their alkyl substituents.[44] These salts are known to be excellent alkylating reagents for nucleophiles containing heteroatoms, but are not capable of C-alkylating aromatic or

aliphatic compounds.[44] However, in superacid, Meerwein salts can be activated to alkylate aromatic substrates. Methylation of toluene gives xylenes in the ratio of *ortho*:*meta*:*para* of ~60:10:30 using either $Me_3O.BF_4$ or $Me_3O.SbF_6$ in FSO_3H:SbF_5.[50] The superelectrophilic activation of Meerwein salts was presumed to be due to protonation to give a dicationic species such as R_3HO^{2+} as postulated for diprotonated water.[49]

2.3.2 Carbon Superelectrophiles

Several aliphatic and aromatic systems that show superelectrophilic character have also been reported.[45]

Hogeveen and Kwant[51] reported the formation of stable aliphatic dication species **2.26** (Scheme 2.5). Treatment of diol **2.25** with $FHSO_3$ at -60 °C led to formation of a product identified as dication **2.26**, which showed ^{1}H NMR signals of δ_H 1.96 (s, CH_3) and 2.65 (s, CH_3) ppm in a ratio of 5:1. ^{13}C NMR showed two signals at δ_C 22.5 and 126.6 ppm only. Both spectra were stable over the range of -140 to -40 °C. Dication **2.26** could also be obtained by treatment of cation **2.27** with $FHSO_3$ at -60 °C. The peak ratios of 5:1 for the methyl groups in the ^{1}H NMR were rationalised by a degenerate rearrangement of the bonds in **2.26** (Scheme 2.5, **2.28a-c**), making the five methyl groups on the cyclopentyl ring equivalent over the NMR timescale.

SCHEME 2.5: Aliphatic dication **2.26**.

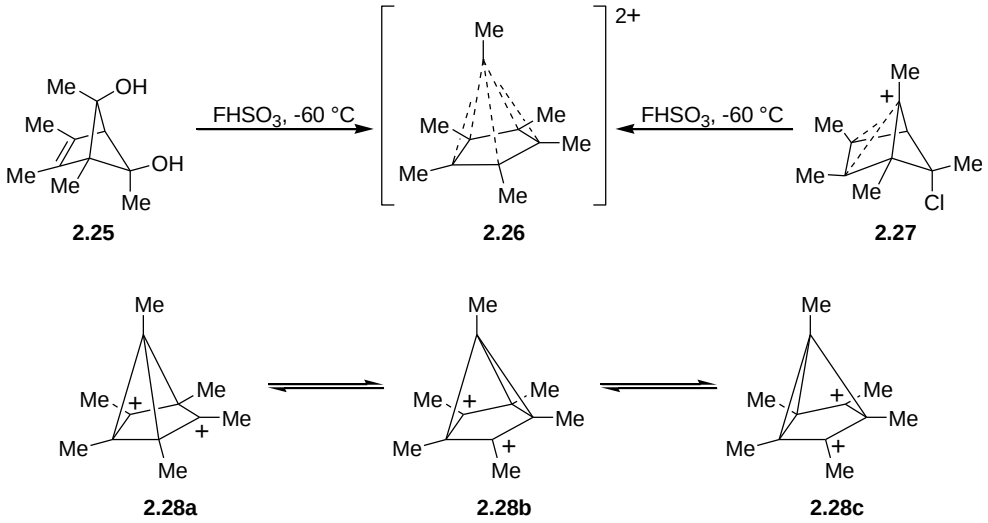

Olah *et al*.[52] studied the possibility of forming dication CH_6^{2+} by computational methods. The results showed that geometry **2.29** was the global energy minimum for CH_6^{2+} (Scheme 2.6). The structure consists of two 3c-2e bonds. Each bond has a long C-H bond length of 1.208 Å (*cf*. 1.123 Å in methane) and a H-C-H angle of 47.5°. In this geometry CH_6^{2+} could be regarded as diprotonated methane, where each proton adopts a stabilising 3c-2e bond, or as a dihydrogenated complex of CH_2^{2+}. The authors did not attempt to observe the CH_6^{2+} dication, but suggested that hydrogenation of CH_4^{2+} by mass-spectroscopic charge-stripping could be used as a means of experimental generation of CH_6^{2+}.

SCHEME 2.6: Calculated structure of CH_6^{2+} **2.29**.

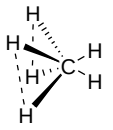

2.29

2.3.3 Nitrogen Superelectrophiles

Reaction of cinnamaldimine **2.30** with benzene in TfOH gives 3,3-diphenyl-propionaldehyde **2.31**, after aqueous work-up, in 39 % yield (Scheme 2.7).[53] The same reaction in trifluoroacetic acid (TFA) gives only cinnamaldehyde **2.32** after aqueous work-up.

SCHEME 2.7: Superelectrophilic activation of cinnamaldimine **2.30**.

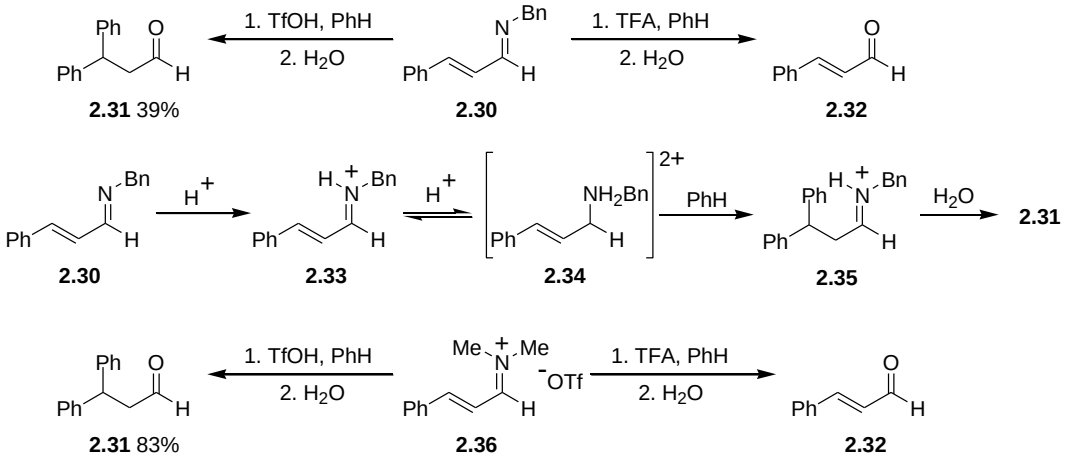

As TFA is acidic enough to protonate imine **2.30** (as shown by ^{1}H NMR spectroscopy), the authors proposed that formation of **2.31** must occur through

diprotonated superelectrophilic intermediate **2.34** (a representation of one of the resonance forms available). In addition, iminium salt **2.36** reacts with benzene in TfOH to give 3,3-diphenylpropionaldehyde **2.31** (83 %), after aqueous work-up. Again, the reaction in TFA gives only cinnamaldehyde **2.32** after aqueous work-up. A solution of **2.30** or **2.36** in CF_3SO_3D shows no incorporation of deuterium in the alkane or phenyl protons, indicating that additional protonation must occur on the nitrogen atom.

Similarly, nitro species **2.37** reacts with benzene in the presence of TfOH or HF to give phenylated oxime **2.38** (Scheme 2.8). However, the reaction in TFA does not proceed to give arylation. Again, a dicationic intermediate was proposed to explain the reactivity. The reaction does not occur with nitromethane in TfOH. From this the authors proposed that the dication intermediate is not of the form **2.43**, as an analogous intermediate could be formed by nitromethane in superacid. They surmised that the ester group must assist the formation of a superelectrophile intermediate, such as **2.40** or **2.40′** (Scheme 2.8).

SCHEME 2.8: Phenylation of nitro species **2.37**.

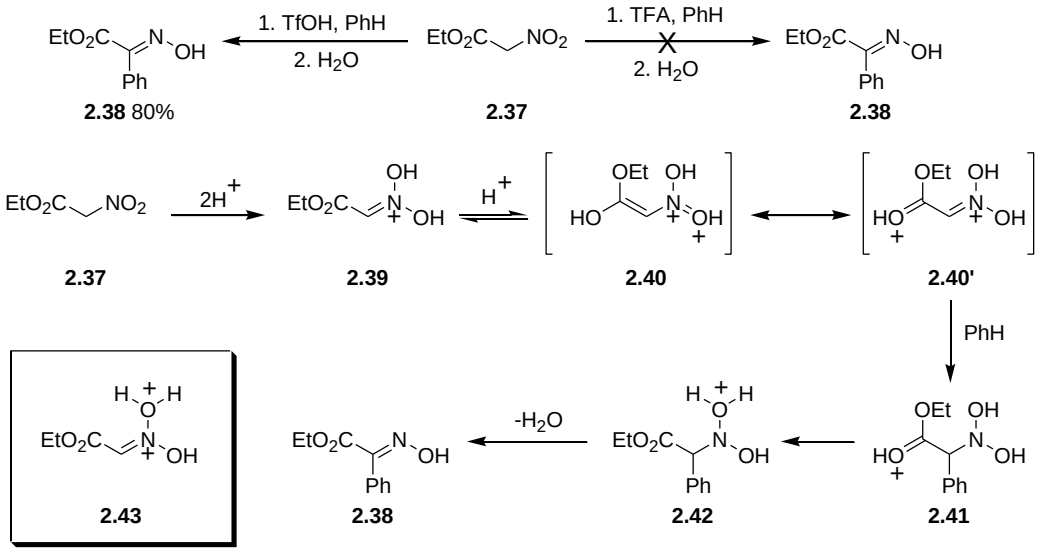

In superacid conditions, nitriles show high reactivity in the reaction with benzene. Yato *et al*.[54] showed that reaction of hydrogen cyanide and benzene did not occur in TfOH:TFA (~1:3). However, in superacid TfOH, the reaction proceeded to give benzaldehyde **2.46**, after aqueous work-up, in 44 % yield in 30 min (Scheme 2.9,

Table 2.1). In the more acidic TfOH:SbF_5 (1 %), the reaction yield increased to 65 % in 30 min, whereas in the highly acidic TfOH:SbF_5 (5 %) the reaction occurred instantaneously to give 92 % yield. In TfOH:TFA (~1:3), the system is acidic enough to protonate ~ 50 % of the nitrile present, but no reaction is observed. In more acidic systems the reaction rate increases, indicating that additional protonation of the nitrile might be necessary.

SCHEME 2.9: Superelectrophilic activation of nitriles.

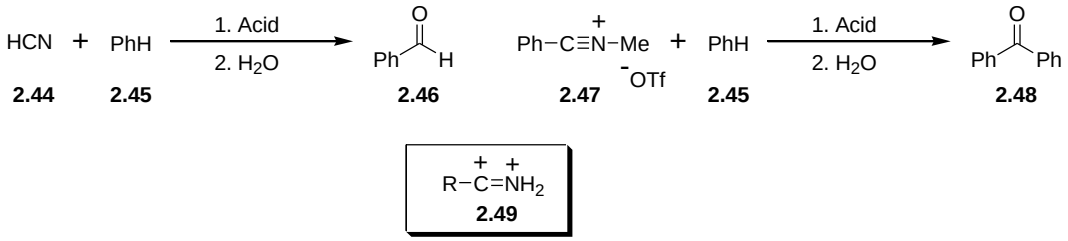

2.44 **2.45** **2.46** **2.47** **2.45** **2.48** **2.49**

TABLE 2.1: Acid effects on reaction of nitriles with benzene **2.45**.

Entry	**Acid**	**H_o**	**Product yield**	
			2.46	**2.48**
1	TFA:TfOH (3:1)	-10.6	0	0
2	TfOH	-13.7	44	3
3	TfOH:SbF_5 (1 %)	-16.8	65	-
4	TfOH:SbF_5 (5 %)	<-18	92	55

In order to investigate this assumption, Yato *et al.*[54] tested the reactivity of *N*-methylbenzonitrilium trifluoromethanesulfonate **2.47** with benzene in solutions of different acidity (Scheme 2.9, Table 2.1). In TfOH:TFA (~1:3) no reaction was observed and in TfOH, the reaction was sluggish (3 % **2.48** after 20 h). However, in highly acidic TfOH:SbF_5 (5 %), benzophenone **2.48** was isolated in 55 % yield. These results indicated that further protonation of nitrile salt **2.47** was necessary, as the reaction yield increased with increasing acidity. The authors proposed superelectrophilic dication intermediate **2.49** to explain the reactivity of the nitriles tested in the reaction with benzene **2.45**.

Yokoyama *et al.*[55] reported the superacid catalysed Pictet-Spengler cyclisation. This involves the intramolecular cyclisation of 2-arylethylamines such as **2.50** to give

1,2,3,4-tetrahydroisoquinolines such as **2.51** (Scheme 2.10). The proposed mechanism is shown in Scheme 2.10. Protonation of imine **2.50b** gives iminium salt **2.52**. Subsequent superacid activation gives dication intermediate **2.53**, which undergoes an intramolecular cyclisation reaction to give intermediate **2.54**. Rearomatisation gives intermediate **2.55** and, upon work-up, this intermediate is deprotonated to give 1,2,3,4-tetrahydroisoquinoline product **2.51b**.

SCHEME 2.10: Pictet-Spengler cyclisation of imine **2.50**.

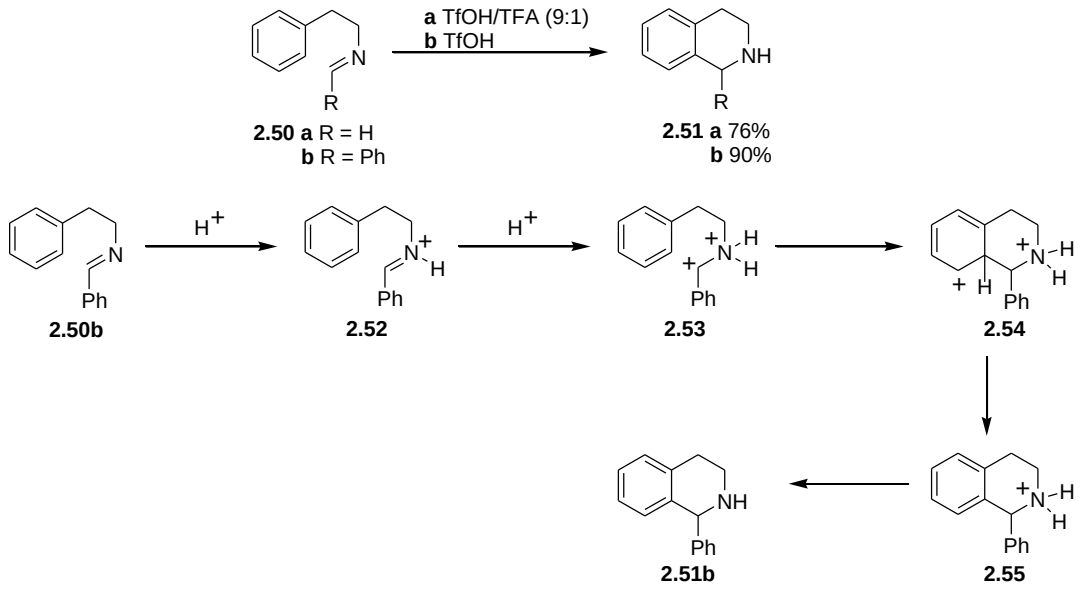

Kinetic studies under a variety of acidities [H_0 = -10.7-(-12.4)] showed first-order kinetics, with a linear relationship between the rate of intramolecular cyclisation and the acidity of the solution (the rate of cyclisation increasing with increasing acidity). The authors proposed that this correlation between reaction rate and acidity indicated the presence of dicationic superelectrophile intermediate **2.53** in the reaction mixture.

2.4 Superelectrophiles in Organic Synthesis

The use of superelectrophilic intermediates to explain unusual reactivity has normally been limited to reactions involving superacid activation, a medium rarely used in common synthetic reactions. However, recent work has highlighted the possibility of superelectrophilic intermediates under conventional reaction conditions.

Charette *et al*. have shown several synthetically useful transformations involving the reaction of amides with trifluoromethanesulfonic anhydride (Tf_2O) in the presence of pyridine.[56-61] They first reported the reaction in the preparation of bridged orthoesters from tertiary amides.[56] Treatment of amide **2.56** with Tf_2O and pyridine at low temperature (-40 °C), with subsequent reaction with triol **2.57**, led to formation of bridged orthoester **2.58** (Scheme 2.11).

SCHEME 2.11: Synthesis of bridged orthoester **2.58**.

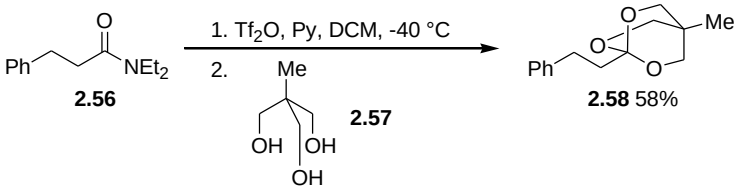

SCHEME 2.12: Proposed reaction of amide **2.56** with Tf_2O/Py.

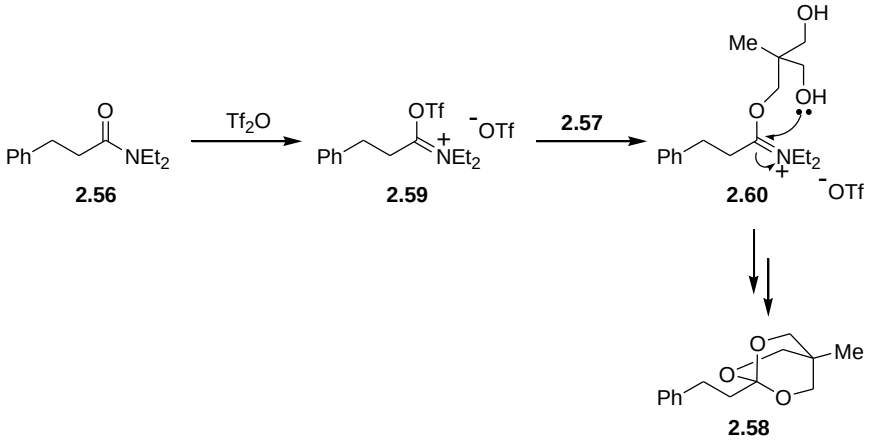

The mechanism was believed to proceed through the reaction of amide **2.56** with Tf_2O to give iminium salt **2.59**, which then reacts with triol **2.57** to give alkyl imino ester **2.60**. Subsequent cyclisation forms bridged orthoester **2.58** (Scheme 2.12). The role of the pyridine in the reaction was thought to be as an acid scavenger. Iminium salt **2.59** was not isolated or even observed in the reaction mixture.

Charette *et al*. used the reaction of amides with Tf_2O/pyridine and different nucleophiles for a variety of synthetic transformations including synthesis of thiazolines,[57] the conversion of amides to esters,[58] synthesis of thioamides and ^{18}O-

labelled amides[59] and synthesis of 2-substituted dihydropyridines[60] (examples of which are shown in Scheme 2.13).

SCHEME 2.13: Synthetic transformations using amides and Tf_2O/pyridine.

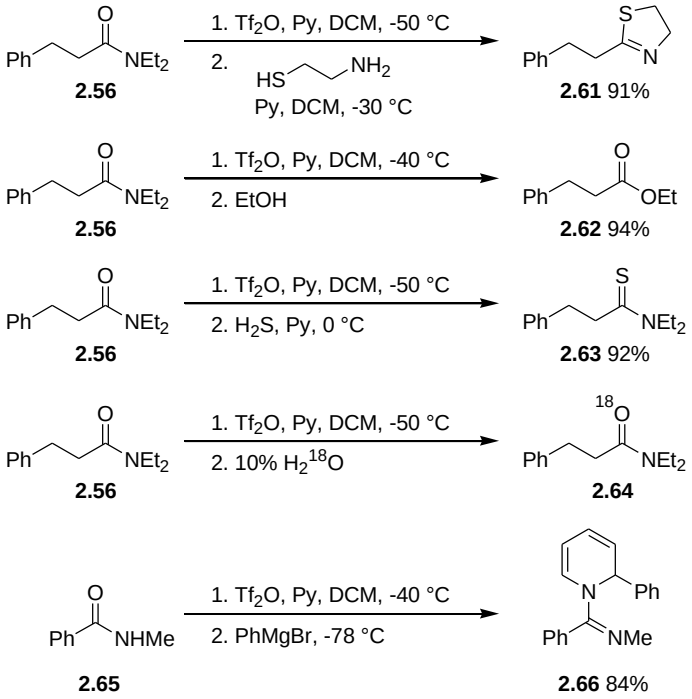

In 2001, Charette and Grenon[61] reported spectroscopic studies on the reaction of amides with Tf_2O and pyridine. Reaction of amide **2.67** with Tf_2O/Py indicated formation of pyridine salt **2.68** by ^1H NMR and ^{19}F NMR in a mixture of products (Scheme 2.14). When using tertiary amide **2.69**, formation of dicationic species **2.70** was proposed.

SCHEME 2.14: NMR studies on reaction of amides with Tf_2O/Py.

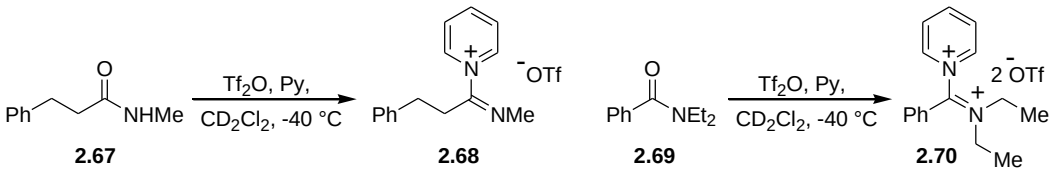

^1H NMR analysis of species **2.70** showed peaks consistent with the proposed product that were downfield of the peaks for **2.69**. The ^{19}F NMR showed a signal for the triflate anion (-79.8 ppm) and *N*-(trifluoromethylsulfonyl)pyridinium **2.72** (-75.9 ppm) only. No triflate salt such as **2.73** (Scheme 2.15) was observed. In a

competition reaction between amide **2.67** and pyridine in the reaction with Tf_2O, it was shown by ^{1}H and ^{19}F NMR that *N*-triflyl pyridinium **2.72** was formed exclusively. Based on these NMR studies, a mechanism for the reaction of amides with Tf_2O/Py was proposed (Scheme 2.15). Reaction of Tf_2O and pyridine **2.71** gives *N*-(trifluoromethylsulfonyl)pyridinium triflate **2.72**. This can transfer the triflyl group to amide **2.69** to give iminium salt **2.73**. Reaction with pyridine **2.71** gives superelectrophilic dication species **2.70**, which can undergo subsequent reaction with a nucleophile.

SCHEME 2.15: Proposed mechanism for formation of dication **2.70**.

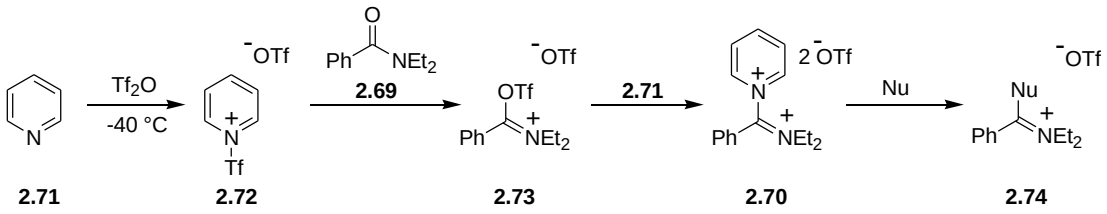

Based on these spectroscopic studies it appears that superelectrophilic dications such as **2.70** may be present as intermediates in the synthetic transformations shown in Schemes 2.11 and 2.12. If present, this could expand the scope for superelectrophilic activation from superacid media to conventional reaction conditions and solvents.

SCHEME 2.16: Reaction of amide **2.75** with Tf_2O/**2.77**.

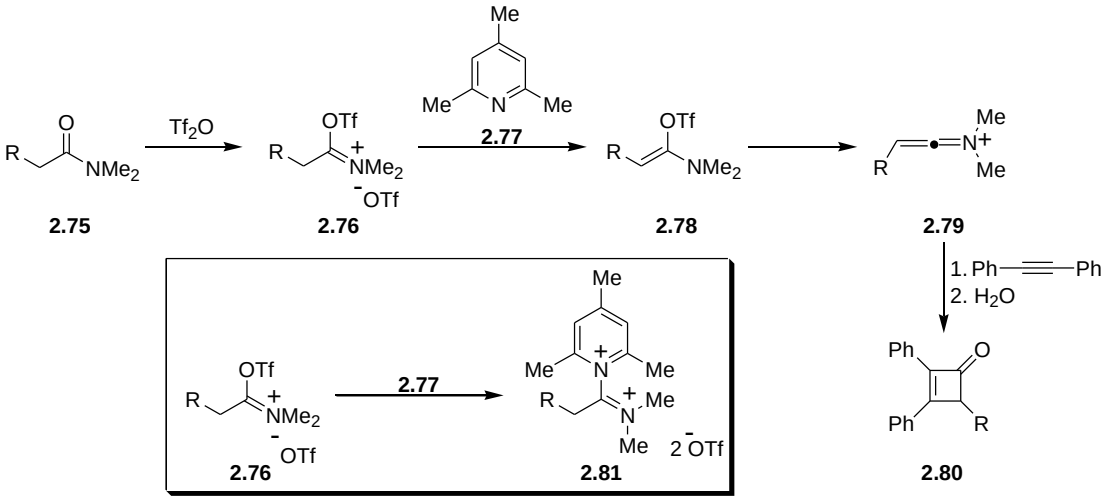

Before the work of Charette *et al*., the reaction of amides with Tf_2O and a nitrogen base was reported by Falmagne *et al*.[62] They reported that the reaction of amide **2.75**

with Tf_2O and collidine (2,4,6-trimethylpyridine) **2.77** gave rise to keteniminium salt **2.79**, via unobserved 1-dimethylaminoalkenyl intermediate **2.78**, which could be further reacted with alkynes to give cyclobutenone species **2.80** (Scheme 2.16). Intermediate **2.78** was proposed from the reaction of **2.75**, Tf_2O and collidine **2.77**. However, no spectroscopic evidence for **2.78** was observed. It is equally likely that the reaction of **2.76** with collidine **2.77** could proceed via superelectrophilic dication **2.81** (Scheme 2.16), although steric interactions may make this superelectrophilic intermediate unfavourable.

The synthesis of tetrazoles by the reaction of amides with Tf_2O in the presence of NaN_3 was also reported (Scheme 2.17).[63] No mechanism was proposed for the reaction, however, it is possible that the reaction proceeds via iminium salt **2.84**, which could undergo nucleophilic attack by NaN_3 (Scheme 2.17).

SCHEME 2.17: Synthesis of tetrazoles from amides.

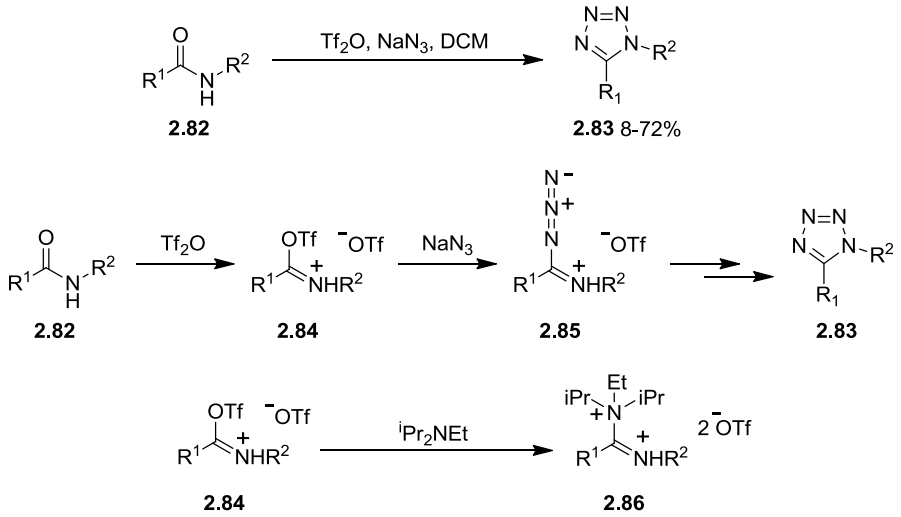

It was found that the presence of di-*iso*-propylethylamine accelerated the reaction. In some cases it gave the product tetrazole where no reaction occurred in its absence. It is entirely possible that reaction of **2.84** with di-*iso*-propylethylamine could form a superelectrophilic dication species such as **2.86** that shows greater reactivity than iminium salt **2.84**, allowing the reaction to occur.

A more recent example of potential superelectrophilic activation was reported by Movassaghi and Hill in the preparation of substituted pyrimidines.[64] They

synthesised pyrimidines such as **2.90** from amide **2.87** and nitriles using Tf_2O and 2-chloropyridine **2.89**. It was found that a large excess of 2-chloropyridine **2.89** inhibited the reaction, whereas an excess of nitrile was found to improve the yield. The proposed mechanism of the reaction is shown in Scheme 2.18. In this mechanism, reaction of amide **2.91** with Tf_2O gives iminium salt **2.96** as described previously, which undergoes nucleophilic attack by 2-chloropyridine **2.89** to give superelectrophilic intermediate **2.92**. The nitrile nucleophile **2.93** can then attack this superelectrophile to give intermediate **2.94** in equilibrium with dication **2.92**. Cyclisation of intermediate **2.94** gives pyrimidine **2.95**.

SCHEME 2.18: Synthesis of pyrimidines by superelectrophilic activation.

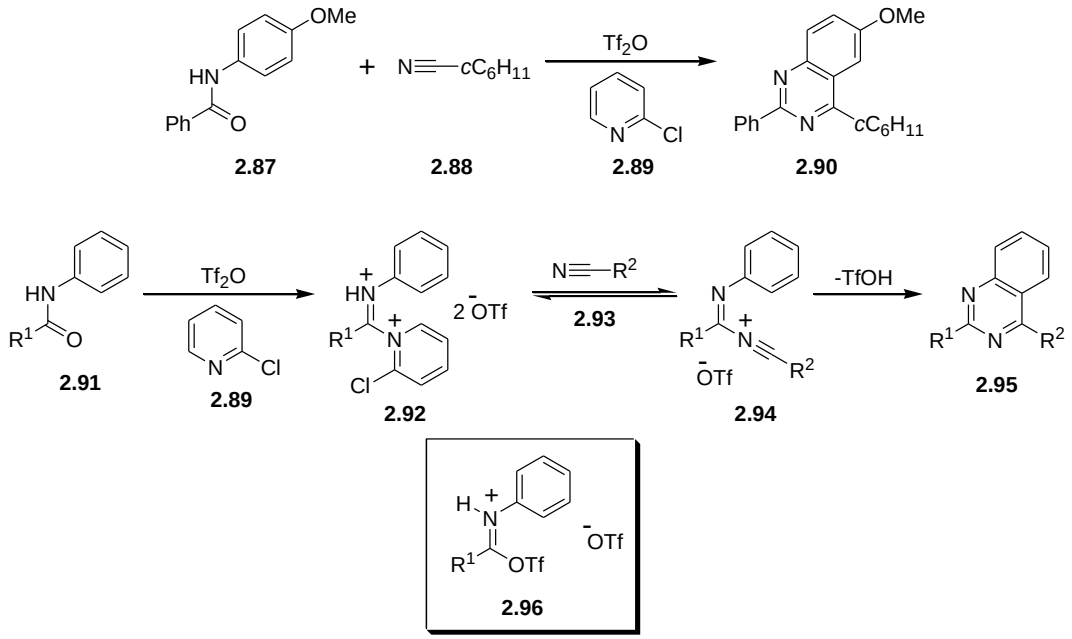

Some spectroscopic evidence was reported for formation of dication intermediate **2.92**. ^{19}F NMR showed a signal for the trifluoromethanesulfonate anion only, no evidence of an iminium triflate salt (such as **2.96**) was observed. React-IR monitoring of the reaction mixture showed consumption of **2.89** (1580 cm^{-1}) and a new absorbance at 1600 cm^{-1} on addition of amide **2.87** and Tf_2O. Addition of nitrile caused a decrease in the signal at 1600 cm^{-1} and generation of 2-chloropyridinium trifluoromethanesulfonate. In addition, the proposed mechanism agrees with experimental results; addition of 2-chloropyridine **2.89** forces the equilibrium **2.92**:**2.94** to the left, inhibiting the reaction. Addition of excess nitrile forces the equilibrium to the right, increasing the rate of reaction.

Previously, Movassaghi and Hill[65] had reported the synthesis of 3-azadienynes from amides using Tf_2O and 2-chloropyridine **2.89** (Scheme 2.19). The product 3-azadienynes were synthesised in yields of 63-97 % for a variety of substituted amides. No mechanism was given for the reaction, however, it can be assumed that the mechanism would be similar for the synthesis of pyrimidines shown above (Scheme 2.18).

SCHEME 2.19: Synthesis of 3-azadienynes from amides.

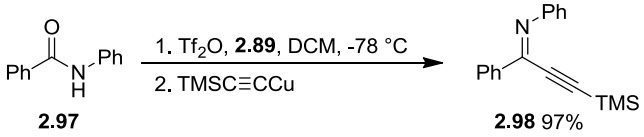

2.97 **2.98** 97%

Medley and Movassaghi[66] later reported the reaction of isoquinoline *N*-oxide and amides in the presence of Tf_2O/pyridine to form isoquinoline amides such as **2.101**. It was found that replacing 2-chloropyridine **2.86** with 2-fluoropyridine **2.102** led to a yield increase from 77 % to 99 %. The reaction showed moderate to excellent yields (25-100 %) for a variety of substituted amides in the reaction with isoquinoline, quinoline and pyridine *N*-oxides.

SCHEME 2.20: Synthesis of isoquinoline amide **2.94** using Tf_2O/pyridine.

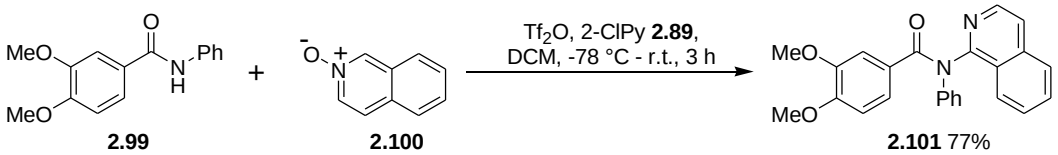

2.99 **2.100** **2.101** 77%

A mechanism was proposed that occurred via superelectrophile intermediate **2.103** (Scheme 2.21). Formation of intermediate **2.103** is believed to occur through an analogous mechanism as that described in Scheme 2.15. An equilibrium was thought to exist between superelectrophile intermediate **2.103** and pyridinium salt **2.105** (along with formation of nitrilium salt **2.104**). Reaction with isoquinoline *N*-oxide **2.100** would lead to intermediate **2.106**, which would subsequently lead to formation of intermediate **2.107**, which would break down to form amide product **2.108**.

The results of *in situ* IR and NMR studies were used to provide evidence for the proposed mechanism, again, no isolation of intermediates (superelectrophilic or otherwise) was reported. When 2-chloropyridine **2.89** was the tertiary amine source, IR studies showed that the equilibrium lay in favour of superelectrophile intermediate **2.103**, whereas, when 2-fluoropyridine **2.102** was used, IR studies showed that the equilibrium lay in favour of nitrilium salt **2.104** and pyridinium salt **2.105**.

SCHEME 2.21: Proposed mechanism for the formation of isoquinoline-substituted pyridines such as **2.108**.[66]

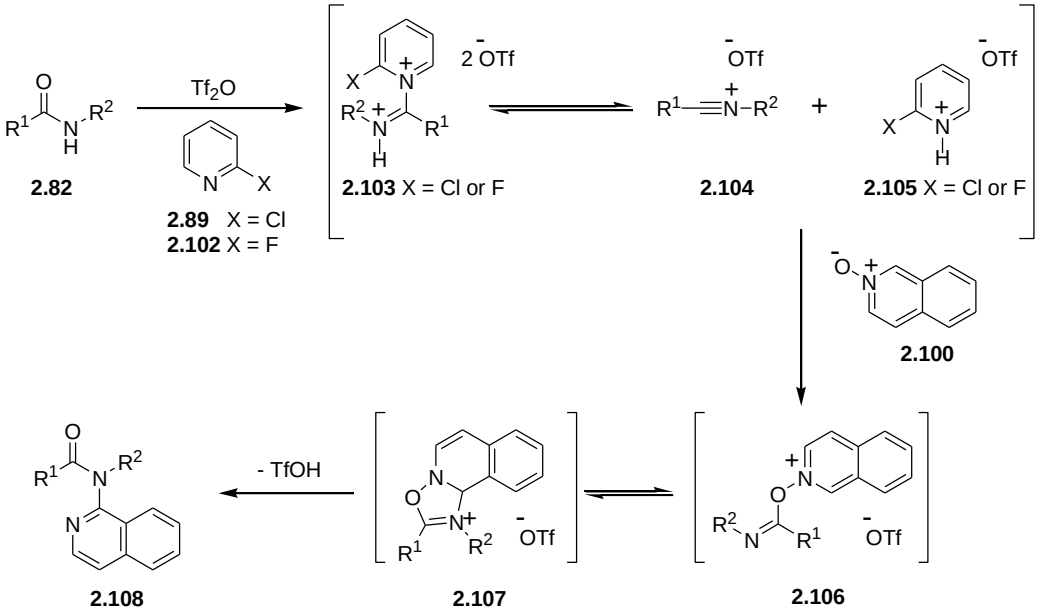

SCHEME 2.22: Deuterium-labelling study.[66]

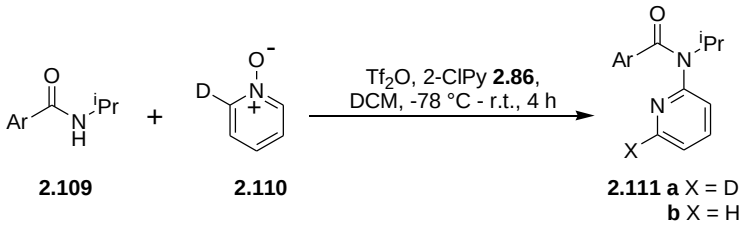

Formation of intermediate **2.107** was proposed due to NMR and deuterium labelling studies performed in the reaction (Scheme 2.22). Reaction of amide **2.109** and pyridine *N*-oxide **2.110** under the standard reaction conditions led to the formation of deuterated product **2.111a** and non-deuterated product **2.111b**, indicating loss of

hydrogen/deuterium from the pyridine ring of **2.110**, consistent with formation of intermediate **2.107**.[66]

In 2008, Cui *et al*.[67] reported the synthesis of indoles from the reaction of amides and ethyl diazoacetate **2.112** (EDA) using Tf_2O, 2-chloropyridine **2.89** and 2,6-dichloropyridine **2.113**, which was necessary for the reaction to occur.

SCHEME 2.23: Synthesis of indoles using amides, Tf_2O and pyridine.[67]

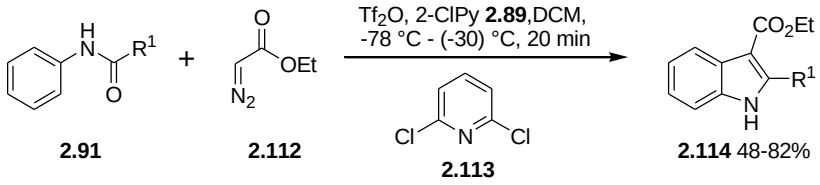

Again, the reaction was proposed to occur through formation of superelectrophile intermediates, namely **2.115** and **2.116** (Scheme 2.24). Reaction of amide **2.91** with Tf_2O and 2-chloropyridine **2.89** leads to formation of superelectrophile intermediate **2.115**. Exchange with 2,6-dichloropyridine **2.113** leads to formation of superelectrophile intermediate **2.116**, which then reacts with EDA **2.112** to eventually form indole **2.114** as shown in Scheme 2.24. No spectroscopic evidence was given for the proposed mechanism.

SCHEME 2.24: Proposed mechanism for synthesis of indoles via superelectrophile intermediates **2.115** and **2.116**.[67]

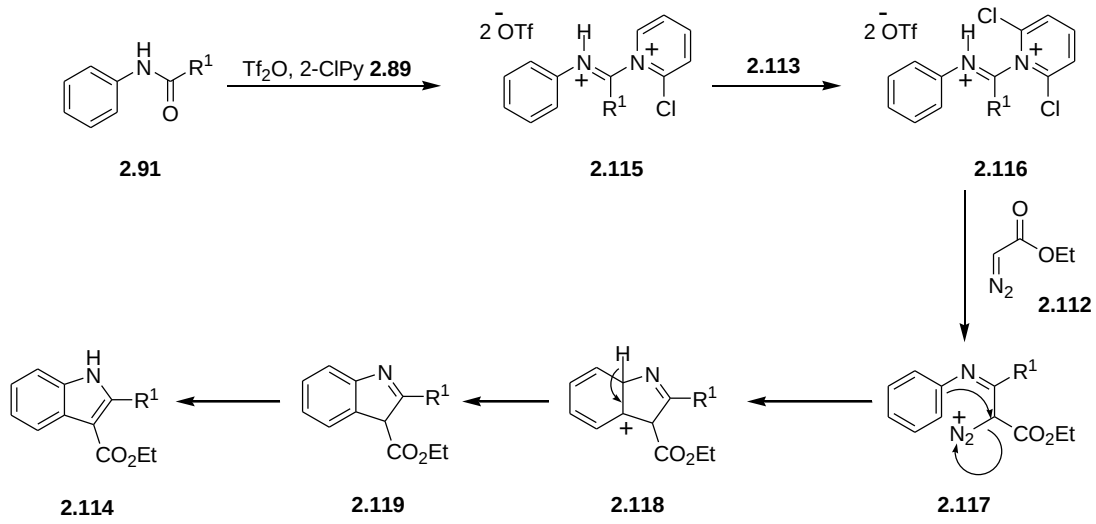

In an earlier work, Banwell *et al*.[68] reported the Tf_2O/4-DMAP **1.8** promoted cyclisation of amide substrates such as **2.120** to give cyclic product **2.121** (Scheme 2.25). The optimal reaction conditions were 5 eq Tf_2O and 3 eq of 4-DMAP **1.8** compared to amide **2.120**. In addition, a 1:1 mixture of Tf_2O:4-DMAP **1.8** did not allow the reaction to occur and Tf_2O on its own could not promote clean cyclisation.

SCHEME 2.25: Tf_2O/4-DMAP **1.8** promoted cyclisation of amide **2.120**.

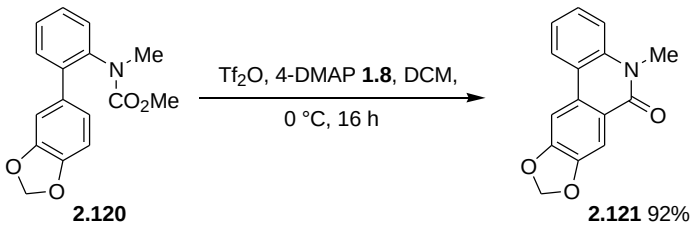

SCHEME 2.26: Proposed mechanisms for formation of product **2.121**.

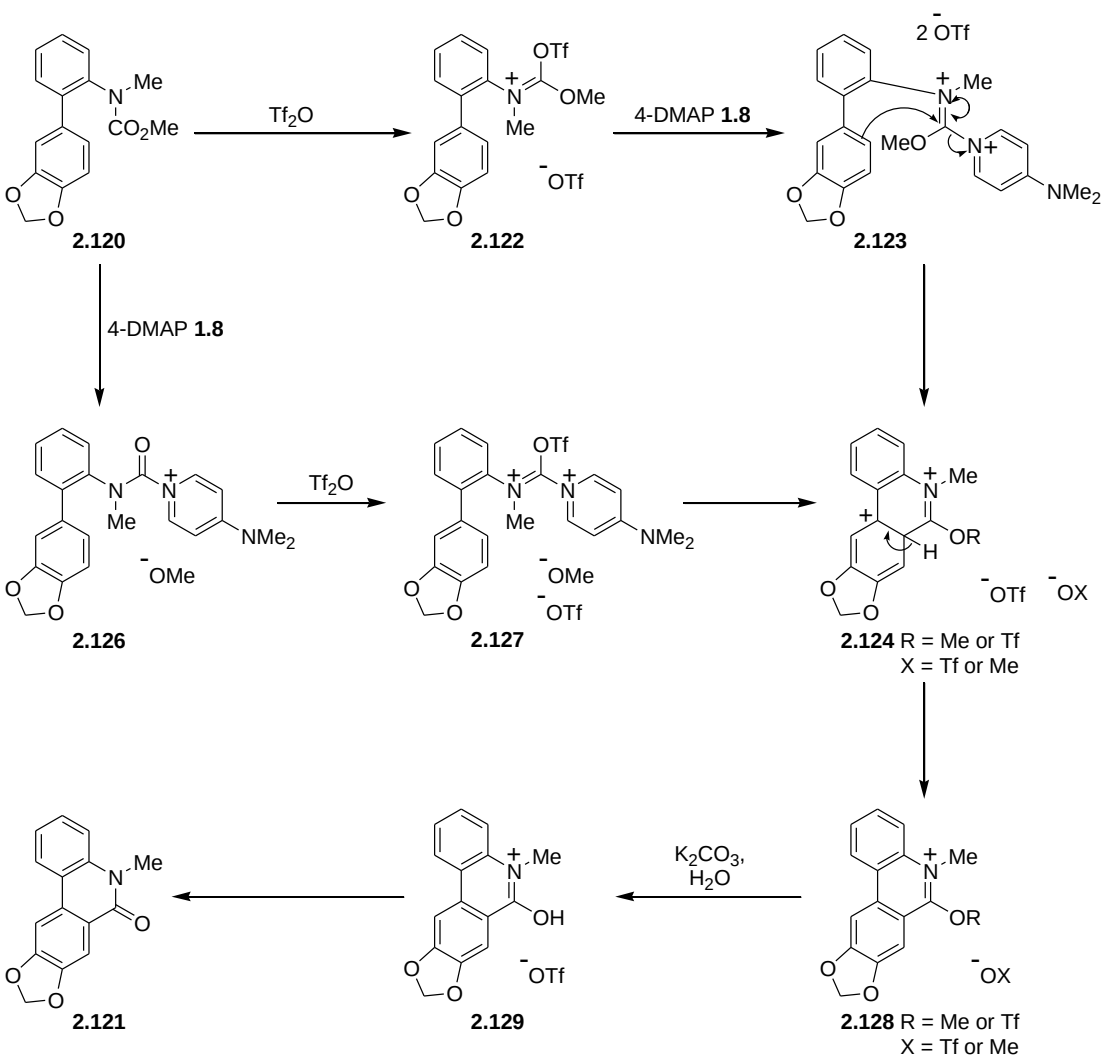

No mechanism was proposed for the cyclisation, but it is entirely plausible that the reaction mechanism could proceed through a superelectrophilic intermediate. The now proposed mechanisms are shown in Scheme 2.26. In the first proposed mechanism, reaction of the carbamate of **2.120** with Tf_2O gives rise to iminium triflate **2.122**. This can then react with 4-DMAP **1.8** to give rise to superelectrophilic intermediate **2.123**, which can then undergo cyclisation to give intermediate **2.124** (R = Me). Loss of a proton rearomatises the ring to give intermediate **2.128** (R = Me). Treatment with aqueous K_2CO_3 gives iminium enol intermediate **2.129**, which is deprotonated to give amide product **2.121**. Alternatively, starting carbamate **2.120** could first react with 4-DMAP **1.8** to give pyridinium salt **2.126**, with subsequent reaction with Tf_2O to give superelectrophilic intermediate **2.127**. Cylisation of **2.127** gives intermediate **2.124** (R = OTf), which proceeds as previously described to give cyclised product **2.121**.

SCHEME 2.27: Proposed superelectrophile intermediate **2.70**.[61]

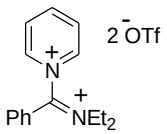

2.70

Superelectrophilic intermediates such as **2.70** (Scheme 2.27) have been proposed as reactive intermediates for a variety of reactions of amides with Tf_2O and tertiary nitrogen bases, however, little spectroscopic evidence exists to support existence of such superelectrophiles. Synthesis and isolation of these types of superelectrophile has never been achieved but would be an important step towards proving the mechanisms detailed above. In addition, such species may show high reactivity that could be exploited for synthetically useful transformations.

2.5 Nitrogen Heterocycle Dications

Although unusual, di- and polycations based on nitrogen heterocycles are not unknown. Various examples of alkylated heterocyclic systems have been reported.

One area of interest in the synthesis of nitrogen heterocycle dications is for use as oxidising agents. Summers *et al*.[69,70] reported the synthesis and reactivity of dialkylated naphthyridines **2.130** and **2.133** (Scheme 2.28). They reported that the dimethyl disalt analogue of **2.133** could not be synthesised using dimethyl sulfate. Reduction of **2.130** with Zn led to formation of radical cation **2.131**. Electrolytic reduction of dication **2.130** showed two symmetrical one-electron reductions at +0.02 and -0.33 V. Reaction of **2.130** with water led to formation of 2-hydroxynaphthyridine species **2.132**. Dication **2.133** was only stable at *p*H < 1.5. Attempts to reduce dication **2.133** with Zn were unsuccessful, but reaction with water gave 2-hydroxynaphthyridine species **2.134**.

SCHEME 2.28: Reactivity of dialkylated naphthyridines **2.130** and **2.133**.

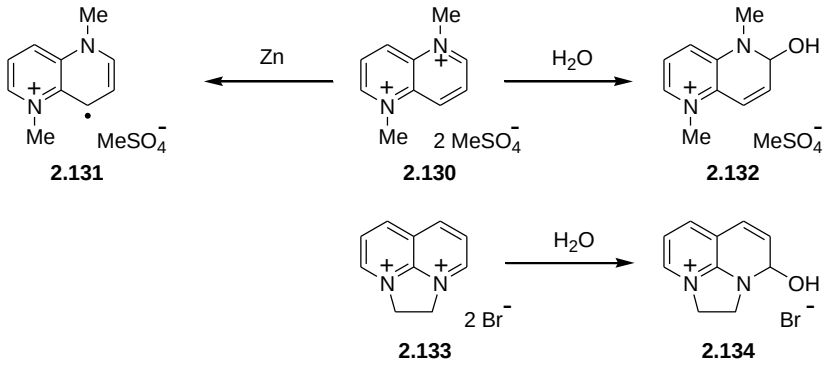

Later, Pokorny *et al*.[71] were able to synthesise dimethylated dication **2.135** from 1,8-naphthyridine and "magic methyl" (FSO_3Me). Reaction of **2.135** with CH_3OD led to formation of naphthyridinol cation **2.136** (Scheme 2.29). Attempts to reduce dication **2.135** were unsuccessful.

SCHEME 2.29: 1,8-Dimethylated naphthyridine **2.135**.

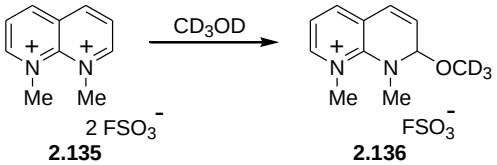

Curphey[72] and, Curphey and Prasad[73] reported the synthesis of a variety of nitrogen heterocycle dications **2.137**-**2.140** from Meerwein salts and the appropriate nitrogen heterocycle (Scheme 2.30). Only disalt **2.137** showed any evidence of reduction with

Zn, forming radical cation **2.141**, as shown by its e.s.r. spectrum. Pyrimidine disalt **2.138** also showed some interesting reactivity. Treatment of **2.138** with deuterated trifluoroacetic acid **2.142** showed H-D exchange in the 2- and 5-position over a long timescale (> 12 h). Deuteration in the 2-position was believed to occur through the formation of carbene **2.144** (Scheme 2.30).

SCHEME 2.30: Various nitrogen heterocycle dications.

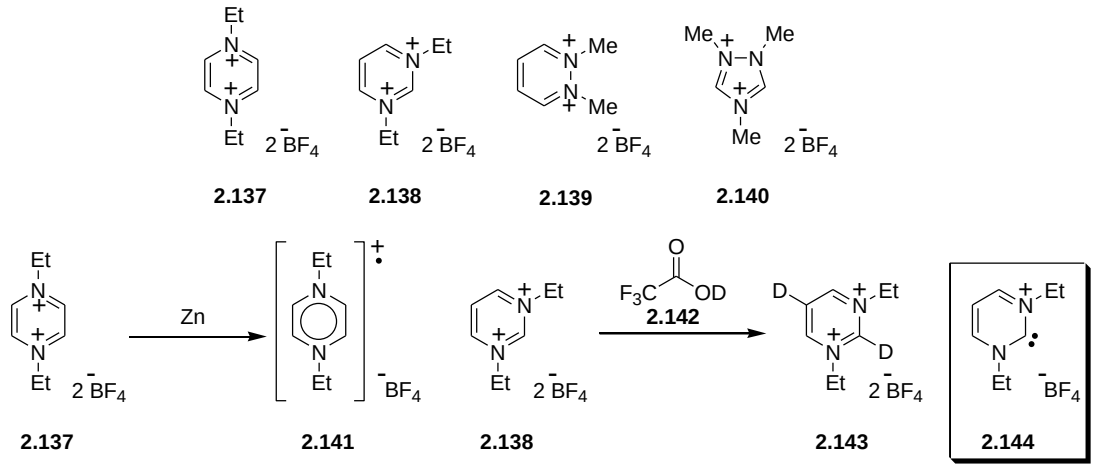

Another nitrogen heterocycle dication was reported by Katritzky *et al.*,[74] who synthesised disalt **2.146** from pyridinium salt **2.145** (Scheme 2.31). Attempts to reduce disalt **2.146** with sodium borohydride to obtain the corresponding dihydropyridine were unsuccessful.

SCHEME 2.31: Nitrogen heterocycle disalt **2.146**.

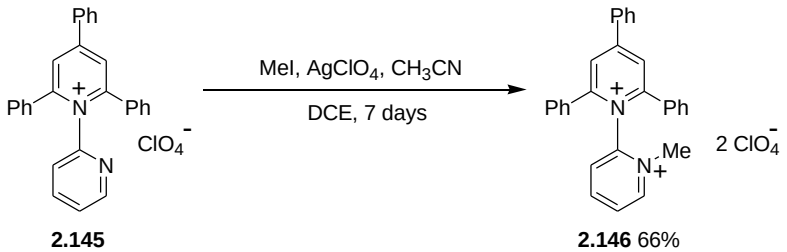

Examples of nitrogen heterocycle di- and polycations based on 4-DMAP **1.8** have been reported. Weiss and Roth[75] reported the synthesis of disalt **2.148** and trisalt **2.150** from the reaction of 4-DMAP **1.8** and phosgenes **2.147** and **2.149** (Scheme 2.32). Spectroscopic data (^{1}H NMR, ^{13}C NMR, IR) were reported for **2.148** and **2.150**, however, no details of the reactivity of the di- and trication was reported. For

trication **2.150**, a resonance form such as **2.151** may be a more suitable representation as this decreases the positive charge situated around the pyridine ring nitrogens and the phosgene nitrogen. A similar resonance structure may be more suitable for dication **2.148** also.

SCHEME 2.32: Di- and tricationsbased on 4-DMAP **1.8**.

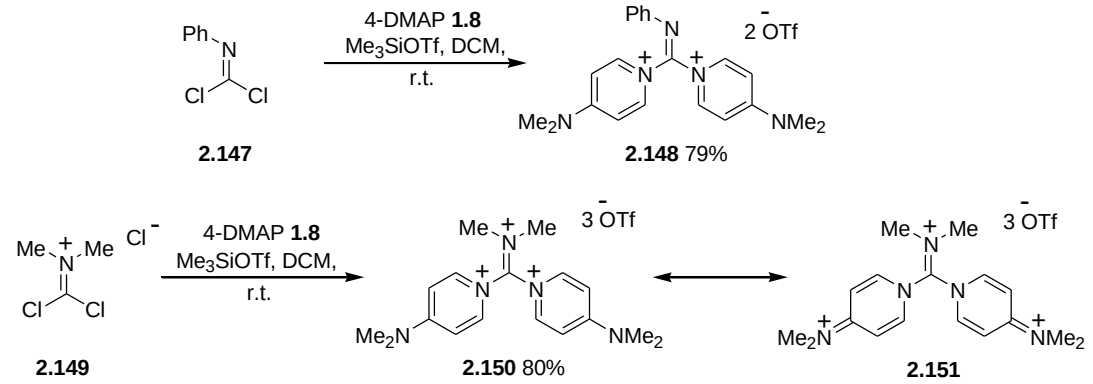

SCHEME 2.33: Proposed de-ethylation of disalt **2.138** and recovered mesomeric stabilisation from demethylation of disalt **1.3** to give salt **1.5**.

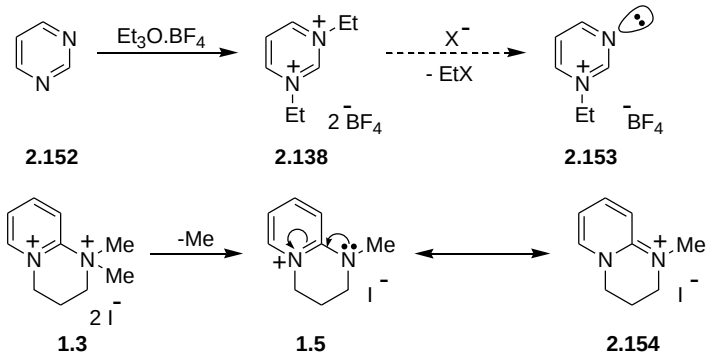

As can be seen, various disalt systems have been generated from nitrogen heterocycles. Most of the compounds listed were identified from ^{1}H NMR and elemental analysis; no mass spectrometry or crystallographic data have been used to show the dication peak or structure. In this thesis, the synthesis of disalt **1.3** will be addressed. Another distinguishing feature between the reported disalts and a dication species such as **1.3** that will be addressed in this thesis, is that none of the reported dications sacrifice mesomeric stabilisation. For example, synthesis of disalt **2.138** from pyrimidine **2.152** requires no sacrifice in mesomeric stabilisation as the lone pair of electrons on either nitrogen of pyrimidine **2.152** is not in the same plane as

the π-system of the pyrimidine ring. As a result of this, de-ethylation of **2.138** (to give monocation salt **2.153**) would not have the added driving force as seen for an amidinium disalt such as **1.3**, where demethylation of disalt **1.3** to give salt **1.5**, in which the lone pair of electrons on the newly demethylated nitrogen could stabilise the positive charge on the ring nitrogen (Scheme 2.33).

3 Previous Work

3.1 Super Electron Donor (SED) Reagents

Much of the previous work in the Murphy group has focused on the synthesis of novel neutral non-metal electron donors used for a variety of electron-transfer reactions, including the radical cyclisation of aryl halides.[76,77] These types of cyclisation have, until now, been routinely carried out using metals in low oxidation states,[78] electrochemical reduction at a metal electrode,[79] reduction by solvated electrons[80] and reduction by lithium naphthalenide.[81]

One of the first donors synthesised and investigated by the Murphy group was single-electron donor **3.5** (Scheme 3.1). This was synthesised from the reaction of benzimidazole **3.1** and 1,3-diiodopropane **1.2** to form precursor salt **3.2**. Treatment of salt **3.2** with base (either KHMDS or sodium hydride) gave donor species **3.5**, which was characterised by ^{1}H and ^{13}C NMR spectroscopy. Reaction of donor **3.5** with iodine gave disalt **3.6**, giving an indirect proof of formation of donor **3.5**.

SCHEME 3.1: Synthesis of electron-donor **3.5**.

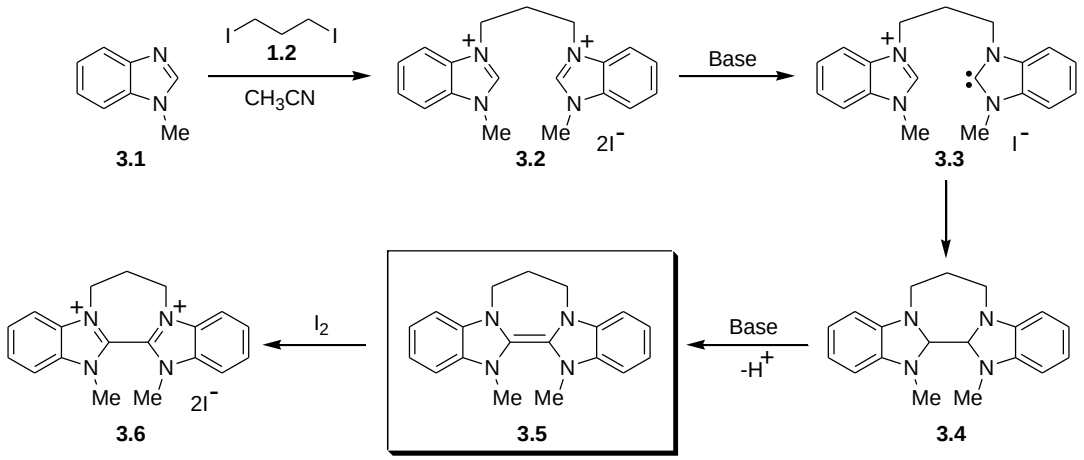

The utility of donor **3.5** was shown in the radical cyclisation of aryl iodides **3.7a-c**, aryl bromides **3.9a-c** and substrates **3.11a-b** and **3.13** (Scheme 3.2, Table 3.1).[76,77] The mechanism of the radical cyclisation is shown in Scheme 3.3. Electron transfer

from donor **3.5** to aryl iodide **3.7a** gives radical anion **3.15**. Loss of iodide gives radical species **3.16**, which undergoes intramolecular cyclisation, with subsequent hydrogen abstraction to give cyclised product **3.8a**.

SCHEME 3.2: Radical cylisation of aryl iodides using donor **3.5**.

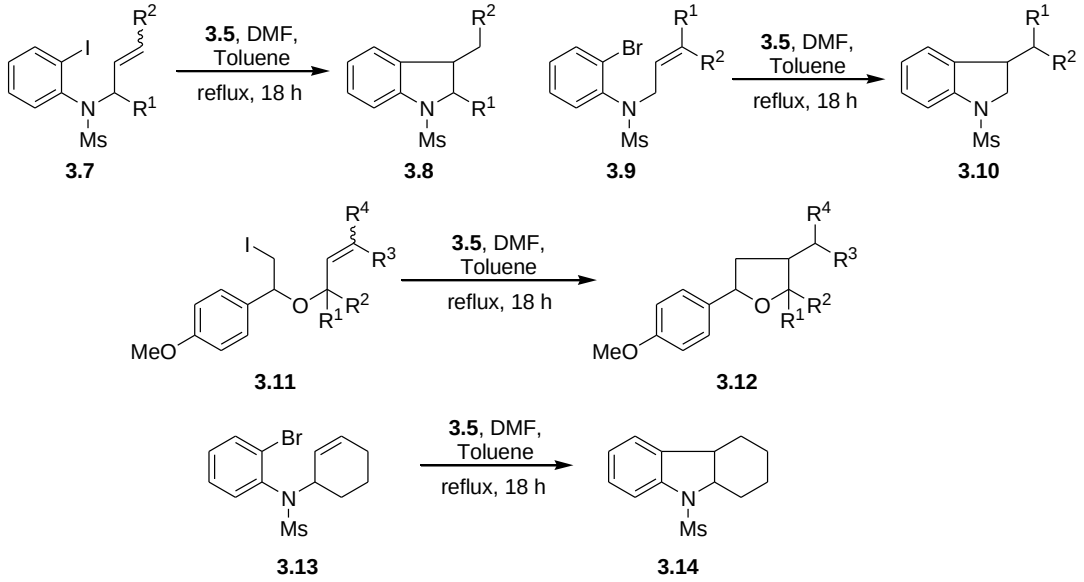

TABLE 3.1: Results of radical cyclisations using donor **3.5**.

Substrate	R^1	R^2	R^3	R^4	Product	Yield / %
3.7a	H	H	-	-	**3.8a**	80
3.7b	H	Me	-	-	**3.8b**	88
3.7c	H	H	-	-	**3.8c**	89
3.9a	H	H	-	-	**3.10a**	44
3.9b	Me	H	-	-	**3.10b**	59
3.9c	Me	Me	-	-	**3.10c**	57
3.11a	H	H	H	H	**3.12a**	83
3.11b	Me	Me	Me	Me	**3.12b**	88
3.13	-	-	-	-	**3.14**	53

More powerful neutral electron donor **3.20** was then synthesised from imidazole **3.18** and 1,3-diiodopropane **1.2** (Scheme 3.4). Donor **3.20** was shown to be an effective reagent for the reduction of activated sulfones and sulfonamides (Scheme 3.4).[82]

SCHEME 3.3: Mechanism of radical cyclisation of aryl iodides.

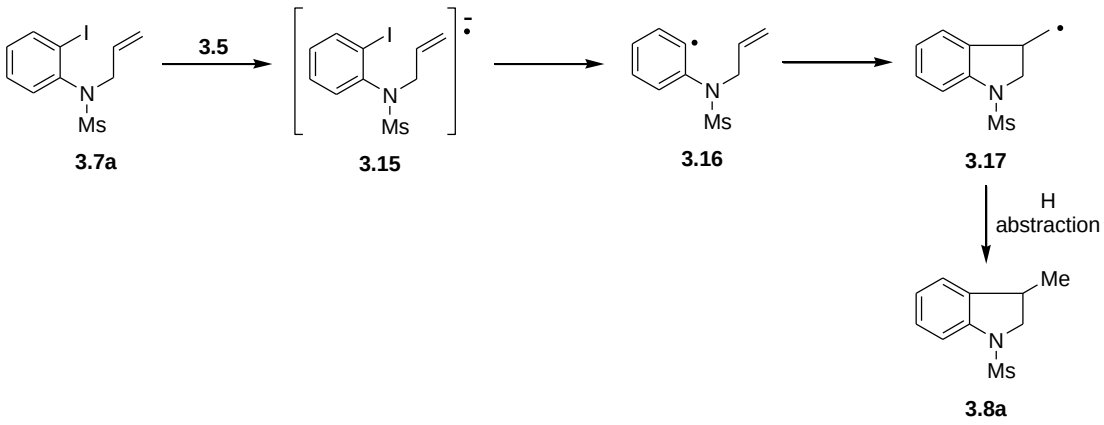

SCHEME 3.4: Synthesis of donor **3.20** and reduction of sulfones and sulfonamides.

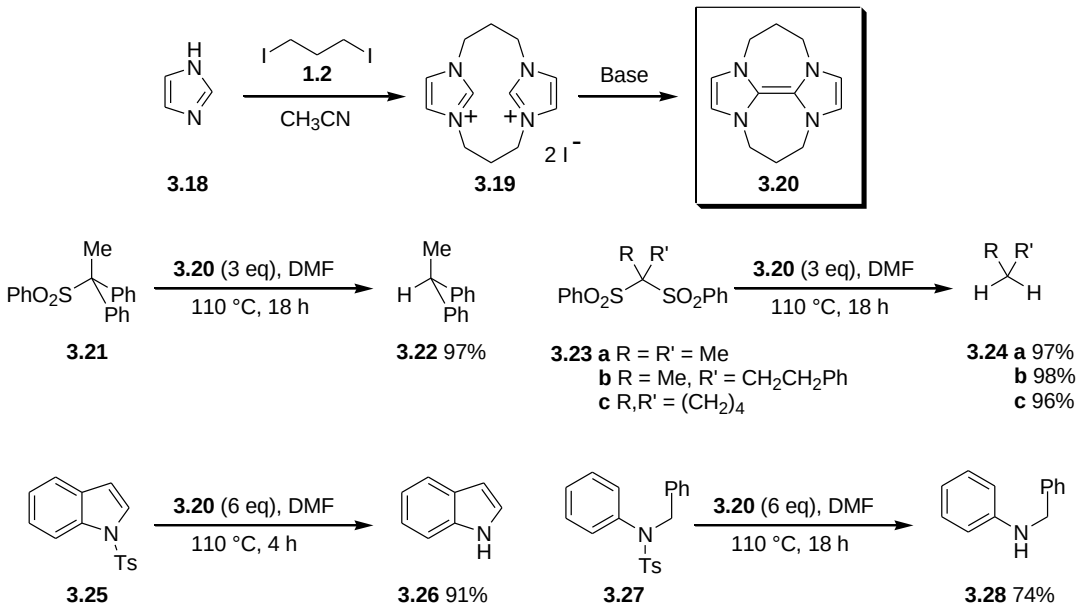

It was shown that donor **3.20** can transfer 2 electrons to an aryl halide substrate to form an aryl anion.[83] This was shown by the reaction of donor **3.20** with aryl iodide **3.29**. It was shown[83] that cyclisation of aryl iodide **3.29** to give ketone **3.30** could not be performed using an aryl radical; only an aryl anion would allow cyclisation to occur. Subsequently, donor **3.20** was able to form ketone **3.30** in 51 % yield (Scheme 3.5), whereas donor **3.5** gave only the reduced product **3.31**. Donor **3.20** was shown to be more powerful than donor **3.5** in the reduction of 9-bromophenanthrene **3.32** and 1-bromonaphthalene **3.34** (donor **3.5** gave only a 7 % yield of **3.33** in the reaction with **3.32** and showed no reaction with **3.34**). In addition, donor **3.20** was

shown to be an effective reagent for the reduction of chloroanthracenes **3.36** and **3.38**.[83]

SCHEME 3.5: Two-electron reduction of substrates by donor **3.20**.

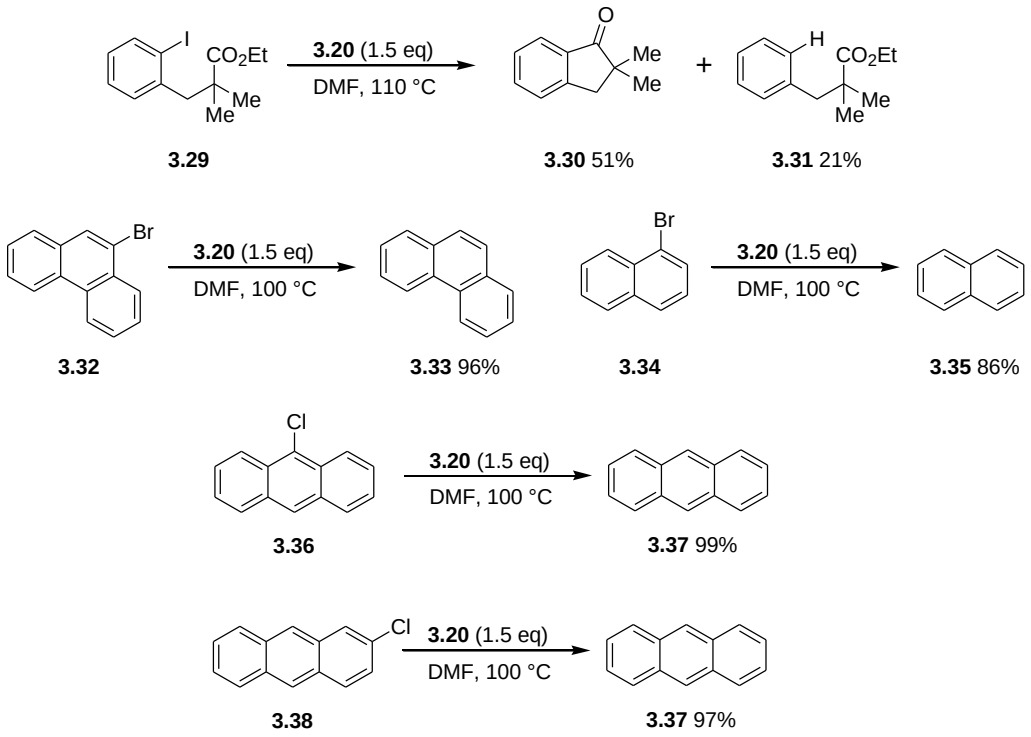

Further studies on the synthesis of a more powerful neutral non-metal electron donor led to the synthesis of 4-DMAP-derived donor **3.40**.[84] It was formed by the reaction of 4-DMAP **1.8** and 1,3-diiodopropane to give precursor salt **3.39**, which was treated with base to give donor **3.40** (Scheme 3.6).

SCHEME 3.6: Synthesis of 4-DMAP-derived donor **3.40**.

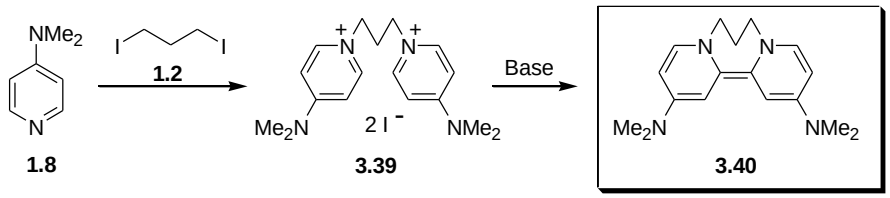

Donor **3.40** was also shown[84] to be capable of generating aryl anions from aryl halides and as such, proved to be a more effective electron donor than **3.20**, being able to effect the same types of reductions at r.t. compared to ≥ 100 °C for donor **3.20** (Scheme 3.7).

SCHEME 3.7: Reductions using donor **3.40**.

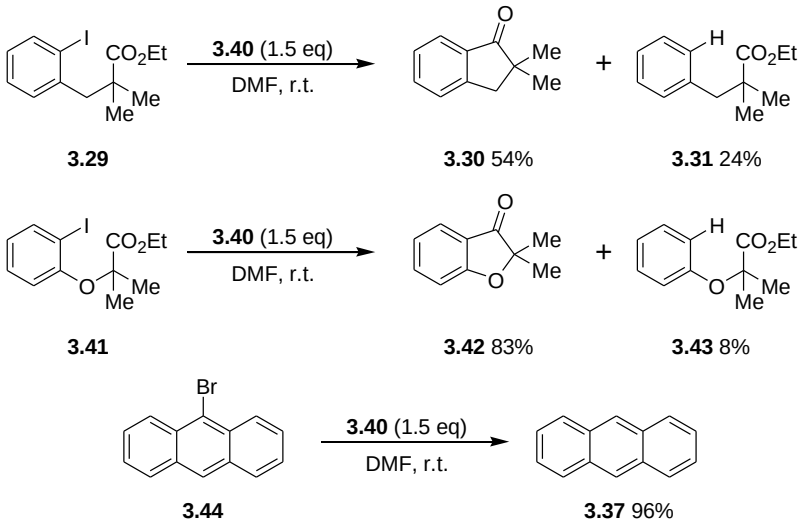

The utility of donor **3.40** was further shown by its ability to reduce sulfones,[84] Weinreb amides[85] and acyloin derivatives[86] (Scheme 3.8).

SCHEME 3.8: Synthetic utility of 4-DMAP-derived donor **3.40**.

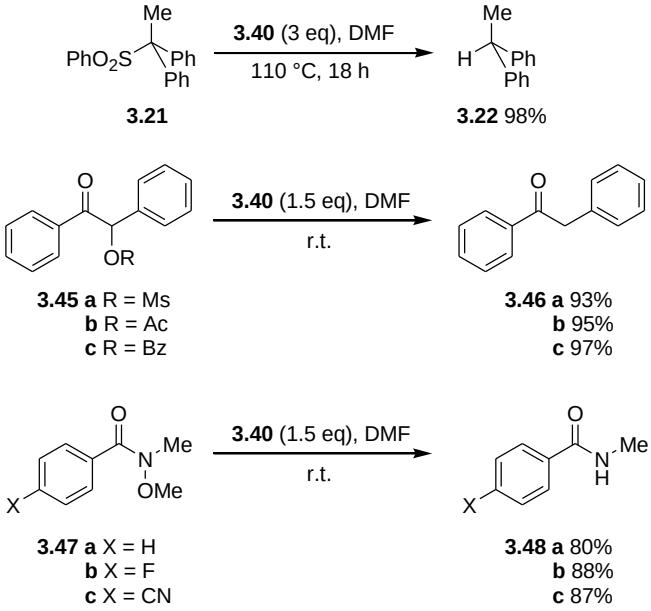

The next proposed step in the development of neutral non-metal electron donors was the planned synthesis of donor **3.49**. The proposed retrosynthetic route for its synthesis is shown in Scheme 3.9. It was hoped that addition of an *ortho*-dimethylamino group would help to futher stabilise the radical cation produced from electron-donation by donor **3.49**, thereby enhancing its reactivity. It was not known

what effect the group in the 2-position would have on the reaction of **3.51** and **1.2**; whether or not steric hindrance would prevent nucleophilic attack to form salt **3.50**. In order to test the effects, the reaction of 2-DMAP **1.1** and 1,3-diiodopropane **1.2** was investigated. However, the reaction did not proceed as expected, but gave rise to some very intriguing products that will be detailed in the next section.

SCHEME 3.9: Retrosynthetic analysis for synthesis of donor **3.49**.

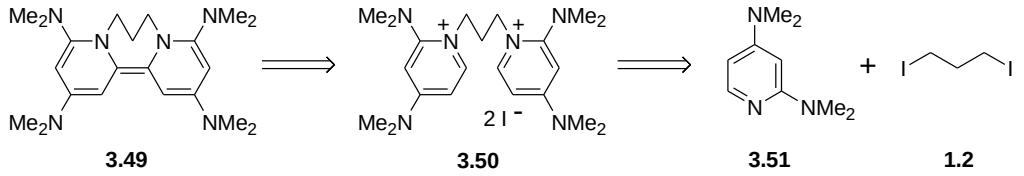

3.2 Reaction of 2-DMAP and 1,3-Diiodopropane

The initial work on this project was carried out within the Murphy group by Dr. Zhou.[87] The reaction of 2-DMAP **1.1** and 1,3-diiodopropane **1.2** did not proceed to give SED precursor salt **3.52** as expected. Instead, the reaction proceeded to give rise to products **1.4**-**1.6** (Scheme 3.10), identified by ^{1}H NMR and MS analysis of the crude reaction mixture.

SCHEME 3.10: Unusual reaction of 2-DMAP **1.1** and 1,3-diiodopropane **1.2**.

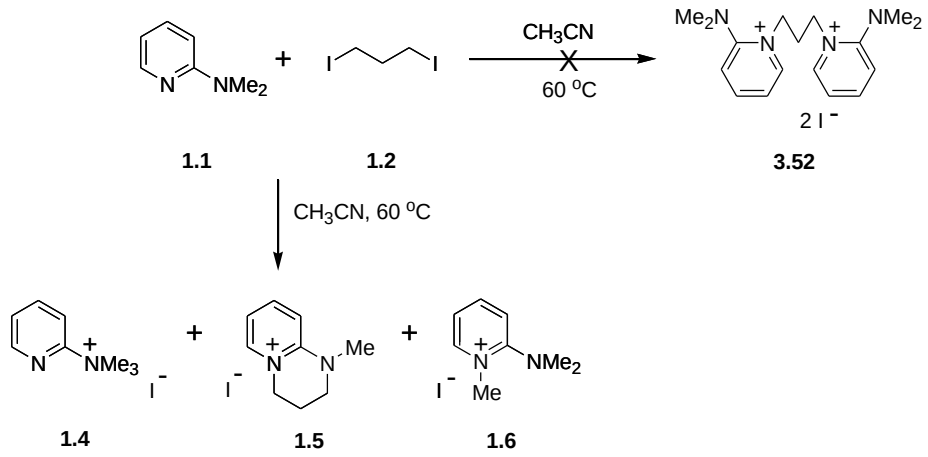

At this stage, the mechanism of formation of the products was not known. Two possible mechanisms for the formation of products **1.4**-**1.6** are shown in Scheme 3.11. In the first instance, reaction of 2-DMAP **1.1** with 1,3-diiodopropane **1.2** occurs with alkylation on the dimethylamino nitrogen to give ammonium species **3.53**. A

molecule of 2-DMAP **1.1** could then remove a methyl group from **3.53** to form **1.4** or **1.6**, from attack of the dimethylamino nitrogen or ring nitrogen respectively, and neutral species **3.54**. Intramolecular cyclisation of **3.54** gives the final product **1.5**. The second mechanism is initiated by reaction of 2-DMAP **1.1** with 1,3-diiodopropane **1.2** to form the ring-alkylated species **3.55**, which again could undergo demethylation by 2-DMAP **1.1** to form neutral species **3.56**. Subsequent intramolecular cyclisation gives product **1.5**.

SCHEME 3.11: Proposed mechanism of formation of products **1.4-1.6**.

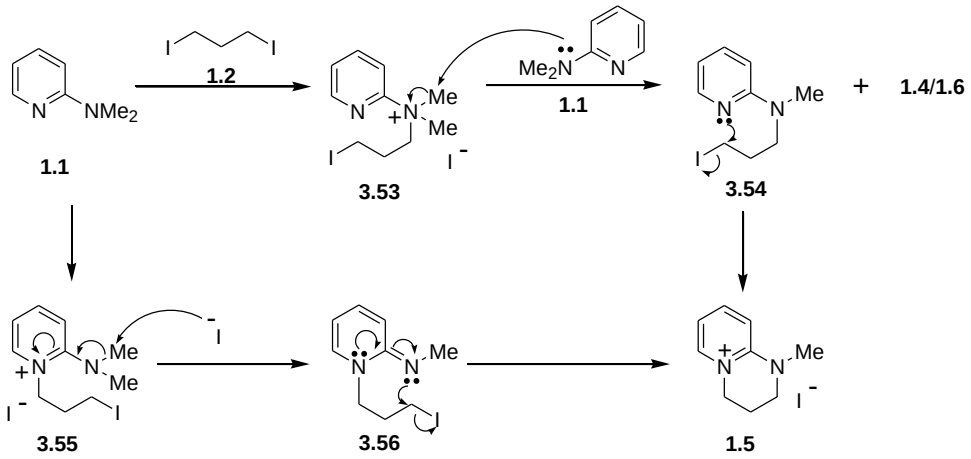

SCHEME 3.12: Proposed formation of 2-DMAP dication **1.3**.

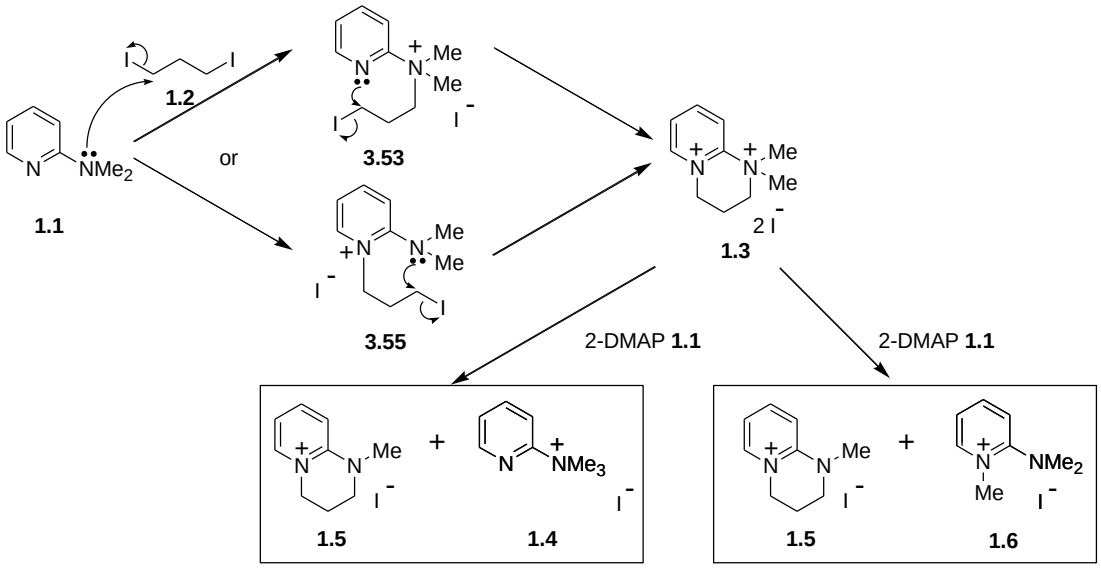

An alternative, more unusual mechanism is shown in Scheme 3.12. In this mechanism, reaction of the dimethylamino nitrogen of 2-DMAP **1.1** and 1,3-

diiodopropane **1.2** gives monocation **3.53** (or **3.55** if attack occurs using the ring nitrogen). Intramolecular cyclisation gives rise to 2-DMAP disalt **1.3**, which can be demethylated by another molecule of 2-DMAP **1.1**. Attack by the dimethylamino group of **1.1** on disalt **1.3** gives 2-DMAP salt **1.4** and salt **1.5**. Attack by the ring nitrogen of **1.1** gives rise to 2-DMAP salt **1.6** and salt **1.5**.

At this stage in the project there was no evidence for the formation of disalt species **1.3**, it was only one plausible mechanism for the formation of products **1.4**-**1.6**. The reaction of 2-DMAP **1.1** and 1,3-diiodopropane **1.2** was intriguing, as it demonstrated the possibility of 2-DMAP disalt **1.3** as a potential reagent for the transfer of a methyl group, as observed in the formation of methylated 2-DMAP **1.4** and **1.6**. In order to probe the utility of the reaction, 2-DMAP **1.1**, 1,3-diiodopropane **1.2** and 1-methylindole **3.57** were reacted to see if transfer of a methyl group from **1.3** to 1-methylindole **3.57** was possible (Scheme 3.13). However, no methylation of 1-methylindole **3.57** was detected.

SCHEME 3.13: Attempted methylation of 1-methylindole **3.57**.

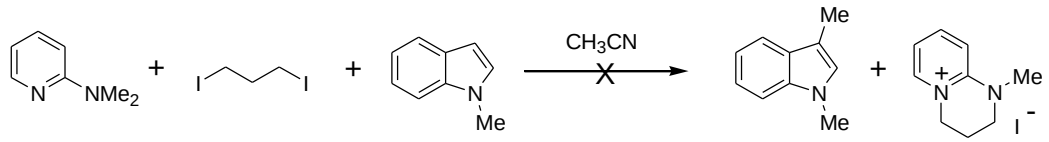

1.1 **1.2** **3.57** **3.58** **1.5**

Based on the result of the reactions detailed, a project was initiated to investigate the potential for the formation of 2-DMAP disalt **1.3**, and if successful, investigate the reactivity of such an unusual species.

4 Quest For a Dication

4.1 Project Aims

Based on the results of the reaction of 2-DMAP **1.1** and 1,3-diiodopropane **1.2** detailed in Chapter 3, the following project was initiated to investigate the potential for this unique and intriguing reaction in the synthesis and isolation of this potentially highly reactive superelectrophile intermediate and, if successful, to determine its reactivity. A set of reactions was proposed to investigate the feasibility of the proposed mechanism (Scheme 3.12). Prior to this project, a disalt species such as **1.3** had not been detected or isolated, so its existence in the reaction mixture has not been proven.

One aim of the project was to investigate the mechanism of the reaction. To do this, isolation and confirmation of the reaction products would need to be achieved. Also, the reactivity of 2-DMAP **1.1** with a variety of alkylating reagents was to be investigated in order to determine what factors influenced its reactivity, and therefore, would aid in determining the optimum reaction conditions. Of great importance would be proving the existence of, and isolating 2-DMAP disalt **1.3**. Isolation of this intriguing superelectrophile would provide evidence for the proposed mechanism for this unique reaction.

4.2 Reaction of 2-DMAP with 1,3-Diiodopropane

The reaction of 2-DMAP **1.1** with 1,3-diiodopropane **1.2** was repeated in an attempt to confirm the products formed during the reaction. The first reaction was carried out on a small scale (2 mmol 2-DMAP **1.1** and 1 mmol 1,3-diiodopropane **1.2**), heating overnight at 60 °C (Scheme 4.1). However, after 18 h of heating, the reaction gave only 26 mg of an inseparable mixture of compounds. The reaction was repeated on a larger scale, this time heating until no trace of 2-DMAP **1.1** was observed by TLC

and ^{1}H NMR spectroscopy. Using the larger scale and longer reaction time (91 h) allowed over 5 g of the product mixture to be collected after work-up.

SCHEME 4.1: Reaction of 2-DMAP **1.1** with 1,3-diiodopropane **1.2**.

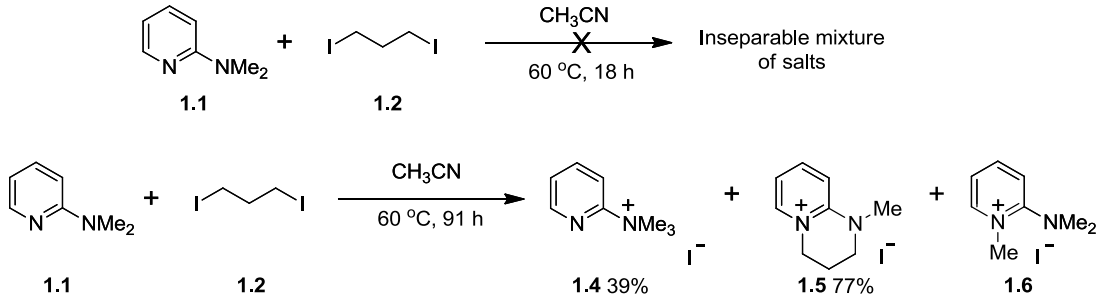

Recrystallisation of the orange solid from warm acetonitrile/diethyl ether gave trimethylpyridin-2-ylammonium iodide **1.4**, allowing its presence in the reaction mixture to be confirmed. Isolation of 1-methyl-1,2,3,4-tetrahydropyrido[1,2-α]pyrimidin-5-ylium iodide **1.5** was achieved by column chromatography using silica gel (CH_3CN/DCM 1:3), allowing salt **1.5** to be fully characterised for the first time. Unfortunately, 2-dimethylamino-1-methylpyridinium iodide **1.6** could not be isolated by recrystallisation or reverse-phase HPLC. This was not unexpected as previous attempts to separate **1.4** and **1.6** have also been reported, but all accounts were unable to separate these species.[37-43] The presence of **1.6** in the reaction mixture was shown by ^{1}H NMR analysis, with MS analysis being unable to conclusively confirm its presence due to **1.6** sharing the same *m*/*z* signal as **1.4**.

Trimethylpyridin-2-ylammonium iodide **1.4** shows characteristic downfield signals for the aromatic protons. These signals occur at approximately δ_H(d_6-DMSO) 8.7, 8.2, 8.1 and 7.7 ppm. These signals were found to be characteristic of trialkylpyridin-2-ylammonium species such as **1.4**, and as such allowed for easier identifications of products from ^{1}H NMR of the reaction mixture by looking for a downfield signal at δ_H(d_6-DMSO) ~8.7 ppm. 1-Methyl-1,2,3,4-tetrahydropyrido[1,2-α]pyrimidin-5-ylium iodide **1.5** was found to have characteristic proton signals at δ_H(d_6-DMSO) 8.0, 7.9, 7.2 and 6.9 ppm.

The difference in the chemical shifts of the dimethylamino- and ring-alkylated nitrogens can be explained as follows.[88] In a uniform magnetic field, electrons

surrounding the nucleus circulate, setting up a secondary magnetic field opposed to the applied magnetic field (Figure 4.1). As a result of this secondary field, nuclei in a region of high electron density experience a weaker magnetic field than those in a region of low electron density, so the higher density region nuclei require a higher field to be applied to bring them to resonance. High electron density shields the nucleus, causing resonance to occur at a relatively high field, causing an upfield shift in the chemical shift of the nucleus, resulting in the nucleus having lower δ_H values. Accordingly, low electron density at a nucleus causes resonance to occur at a relatively low field, causing a downfield shift in the chemical shift of the nucleus, resulting in high values of δ_H. This means that electron-donating groups move δ_H signals upfield (to lower ppm values) and electron-withdrawing groups move δ_H signals downfield (to higher ppm values).

FIGURE 4.1: Magnetic field influences on nuclei and ring systems

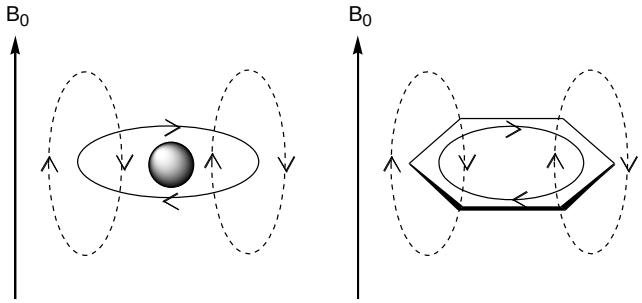

An important anisotropic effect is produced in the π-system of aromatic rings (Figure 4.1). The circulating electrons are called a ring-current and create a magnetic field opposed to the applied field at the centre of the ring, but reinforcing the applied field outside the ring. The induced field substantially deshields the hydrogen atoms attached to the aromatic ring.[88]

SCHEME 4.2: Resonance stabilisation of ring-alkylated 2-DMAP **4.1**.

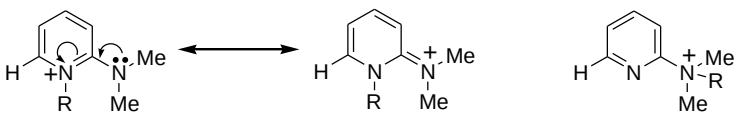

4.1a **4.1b** **4.2**

In the case of dimethylamino group nitrogen and pyridine nitrogen alkylation, the ring hydrogen that experiences the greatest downfield shift is the one on the carbon adjacent to the pyridine nitrogen as shown in **4.1a** and **4.2** (Scheme 4.2). The quaternisation of the nitrogen atoms in these species causes this hydrogen to have the characteristic chemical shift δ_H(d_6-DMSO) 8.4 ppm and δ_H(d_6-DMSO) 8.7 ppm for **4.1a** and **4.2** respectively. The downfield shift can be explained by the electron-withdrawing effects of the quaternised nitrogen atom in both cases, although the extent of the shift is different depending on which nitrogen is alkylated. In the case of pyridine nitrogen alkylation **4.1a**, resonance of the electrons in **4.1a** can be represented in the form **4.1b**, which decreases the electron-withdrawing effect of the alkylation, hence the shielding of the hydrogen atoms attached to the ring increases slightly compared to alkylation of pyridine, causing a decreased downfield shift in the aromatic protons. This type of resonance is not possible with alkylation of the dimethylamino nitrogen, as the lone pair of electrons in the ring nitrogen are not in the same plane as the π-system of the pyridine ring, so no overlap is possible. The electron-withdrawing effect of the pyridine-ring nitrogen and the additional inductive effect of the trialkylammonium group results in a greater deshielding of the hydrogen shown in **4.2**, causing a greater downfield shift compared to **4.1a** as observed.

4.3 Reaction of 2-DMAP with Different Alkylating Reagents

In order to provide evidence for the proposed mechanism and insight into optimisation of the reaction, the reactivity of 2-DMAP **1.1** with a variety of different alkylating reagents was investigated. The following section will detail the reactions conducted and discuss what insights can be drawn from these reactions.

4.3.1 Reaction of 2-DMAP with Iodoalkanes

The first reactions to be investigated were the reaction of 2-DMAP **1.1** with iodoalkanes of increasing chain length (iodomethane, iodoethane and 1-iodopropane). The aim of these reactions was to investigate both the rate of the reaction with increasing steric bulk and to examine product selectivity in terms of which nitrogen undergoes alkylation. The results are summarised in Scheme 4.3 and Table 4.1.

SCHEME 4.3: Reaction of 2-DMAP **1.1** with different iodoalkanes.

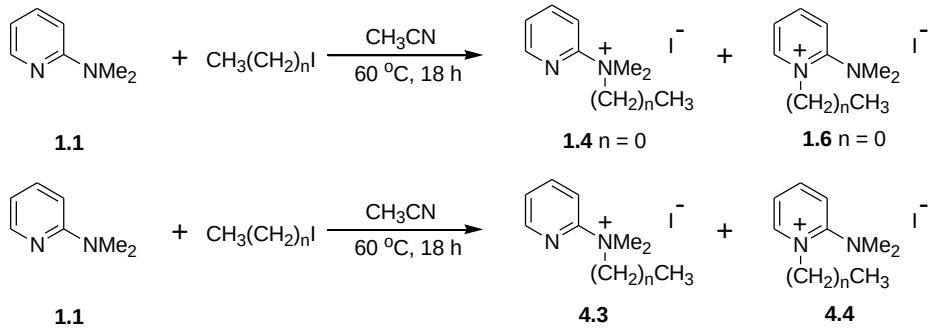

TABLE 4.1: Reaction of 2-DMAP **1.1** with different iodoalkanes.

Entry	**n**	**Recovered 2-DMAP / %**	**Isolated Yield**			
			Product	**Yield[a] / %**	**Product**	**Yield[b] / %**
1	0	25	**1.4**	68	**1.6**	0
2	1	75	**4.3a**	8	**4.4a**	0.1
3	2	87	**4.3b**	3	**4.4b**	0

[a] Sample isolated by recrystallisation. [b] Sample isolated by reverse-phase HPLC.

The reactions were carried out under the same conditions as the reaction of 2-DMAP **1.1** and 1,3-diiodopropane **1.2** for a more accurate comparison. The results of the reaction show two important issues; the inhibiting effect of increasing chain length and the selectivity in favour of the dimethylamino group nitrogen.

Reaction of 2-DMAP **1.1** with short-chain iodoalkanes occurs exclusively on the dimethylamino group nitrogen in the case of iodomethane and iodopropane (Table 4.1, entries 1 and 3 respectively) and preferentially in the case of iodoethane (Table 4.1, entry 2). This is in agreement with similar studies previously reported[37-43] and in stark contrast to 4-DMAP **1.7** which shows exclusive ring nitrogen alkylation due to the presence of the dimethylamino group in the 4-position (Scheme 1.41). The only evidence of ring alkylation was observed in the reaction with iodoethane.

Another important observation from these reactions is the extent to which the increasing chain length hinders the rate of the reaction. As the chain length increases, the amount of recovered starting material **1.1** increases and the yield of product isolated decreases. This can be explained by the disadvantageous steric interactions of the alkyl chain and the dimethylamino group, so that longer chain alkyl iodides react more slowly than short chain alkyl iodides. This effect is most pronounced in

going from iodomethane to iodoethane where there is approximately a 3.5-fold increase in starting material recovery (87 % and 25 % recovery of 2-DMAP **1.1** for EtI and MeI respectively). This shows that an increase in chain length of one carbon from iodomethane to iodoethane results in a significant decrease in reactivity with 2-DMAP **1.1**. When the alkyl chain is increased to 3 carbons, the reactivity of the alkylating reagent with 2-DMAP **1.1** decreases, but the effect is not as pronounced as going from MeI to EtI.

These results help to explain why the reaction of 2-DMAP **1.1** with 1,3-diiodopropane **1.2** takes several days to obtain only moderate yield of products, as preferential attack on the more hindered nitrogen by the bulky 1,3-diiodopropane **1.2** slows the rate of the reaction. Based on these results, it is likely that 1,3-diiodopropane **1.2** undergoes nucleophilic attack by the dimethylamino group nitrogen of 2-DMAP **1.1** in the first step of the reaction (Scheme 4.4). This leaves the other end of the alkyl chain in good position for attack by the lone pair of electrons on the ring nitrogen to form dication species **1.3**.

SCHEME 4.4: Revised mechanism for the reaction of 2-DMAP **1.1** and 1,3-diiodopropane **1.2**.

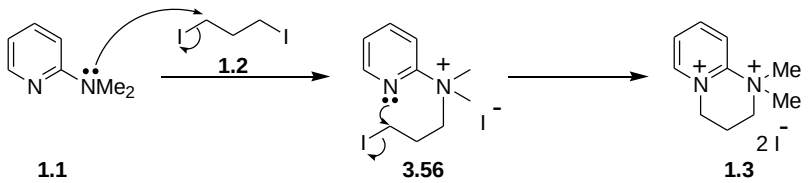

4.3.2 Reaction of 2-DMAP with Different Alkylating Reagents

In order to investigate the possibility of finding a more reactive bifunctional electrophile than 1,3-diiodopropane **1.2**, the reactions of 2-DMAP **1.1** with benzyl bromide **4.5** and with dimethyl sulfate **4.8** were examined; the results are shown in Scheme 4.5.

Reaction of 2-DMAP **1.1** and benzyl bromide **4.5** gave a complex mixture of products, which were not readily identified. Recrystallisation from ethanol yielded 7 mg of white crystals, which were identified as trimethylpyridin-2-ylammonium bromide **4.6**. Reverse-phase HPLC was used in an attempt to separate other reaction products, but was unsuccessful. Column chromatography on a portion of the ether-soluble part of the reaction mixture gave benzylmethylpyridin-2-ylamine **4.7** in 4 %

yield (which was extrapolated to 23 % for the whole reaction mixture). A possible mechanism for the formation of **4.6** and **4.7** is shown in Scheme 4.6. Alkylation of 2-DMAP **1.1** with benzyl bromide **4.5** gives rise to monocationic salt **4.11**. Demethylation of salt **4.11** by the dimethylamino nitrogen on 2-DMAP **1.1** leads to products **4.6** and **4.7** as observed.

SCHEME 4.5: Reaction of 2-DMAP **1.1** with various alkylating reagents.

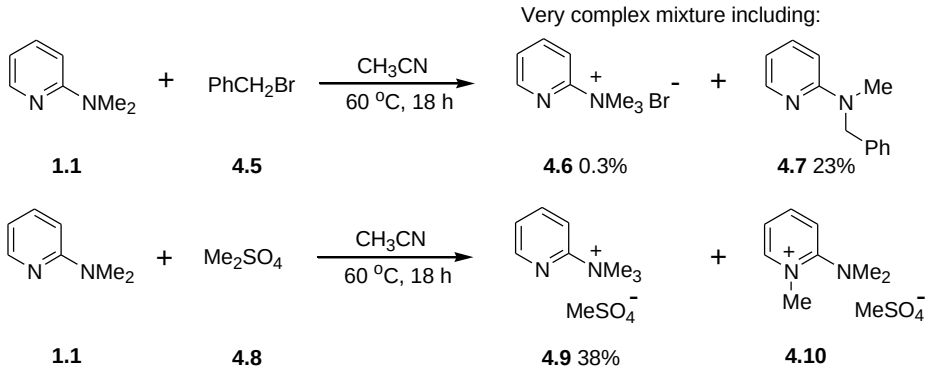

SCHEME 4.6: Mechanism for formation of **4.6** and **4.7**.

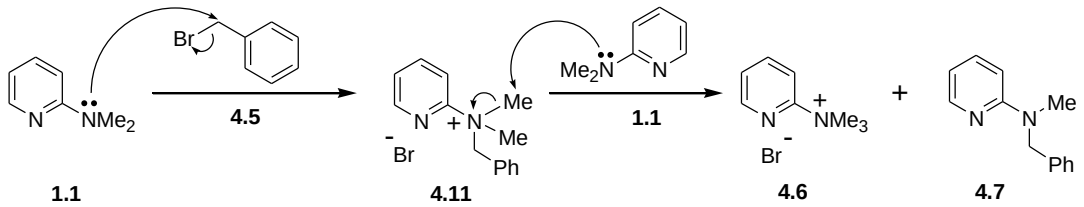

Reaction of 2-DMAP **1.1** with dimethyl sulfate **4.8** was a cleaner reaction that gave easily identifiable products. The reaction gave rise to a mixture of dimethylamino nitrogen methylated product **4.9** and ring nitrogen methylated product **4.10** in a ratio of 5:1 by ^{1}H NMR spectroscopy. Recrystallisation from ethanol gave trimethylpyridin-2-ylammonium methylsulfate **4.9** in 38 % yield. 2-Dimethylamino-1-methylpyridinium methylsulfate **4.10** could not be isolated from the reaction mixture. Preparative reverse-phase HPLC chromatography was not attempted as it was unable to separate analogous compounds **1.4** and **1.6** on an analytical scale (5 mg/mL).

In both reactions shown, there was no recovery of the 2-DMAP **1.1** starting material after 18 h of reaction, in contrast to the most reactive iodoalkane, which did not fully react with 2-DMAP **1.1**; reaction with iodomethane gave 25 % recovery of 2-DMAP

1.1 (Scheme 4.3, Table 4.1). This indicates that careful selection of the leaving group in a bifunctional electrophile may help in the formation of disalt species **1.3**, a factor that will be investigated in the next section.

Interestingly, the reaction of 2-DMAP **1.1** and benzyl bromide **4.5** provides some support for the mechanisms shown in Scheme 3.11 that do not proceed through a dication intermediate such as **1.3**. Formation of **4.6** in the reaction indicates transfer of a methyl group from one molecule of 2-DMAP **1.1** to another, possibly through a monocationic species such as **4.11**. Since the reaction of 2-DMAP **1.1** and benzyl bromide **4.5** is unlikely to result in the formation of a dication (resulting from benzylation of both the ring nitrogen and dimethylamino group nitrogen of 2-DMAP **1.1**), this indicates that a monocationic species (such as **4.11**) can be activated enough to transfer a methyl group to 2-DMAP **1.1**.

These reactions once again highlight the difficulty in the reaction of 2-DMAP with alkylating reagents where the alkyl groups are relatively bulky. A common feature of these reactions is the slow rate with which the alkylating reagents react with 2-DMAP and the difficulty in separating any products from the reaction.

4.4 Reaction of 2-DMAP with Bifunctional Electrophiles

The next section describes work that was conducted on attempts to discover a more reactive bifunctional electrophile than 1,3-diiodopropane **1.2**. The reason for this was that reaction of 2-DMAP with a more reactive bifunctional electrophile could lead to formation of a 2-DMAP disalt species such as **1.3**, and if the reaction were fast enough, it would prevent an excess of 2-DMAP being present in the reaction mixture that would be capable of demethylating **1.3** to form products **1.4-1.6** as previously observed.

Those bifunctional electrophiles chosen for the study were 1,3-*bis*-(4-toluenesulfonyloxy)propane **4.12**, 1,3-diiodopropane **1.2** with the addition of silver tetrafluoroborate and 1,3-*bis*-(trifluoromethanesulfonyloxy)propane **4.15** (Scheme 4.7).

1,3-*Bis*-(4-toluenesulfonyloxy)propane **4.12** was chosen as it was available within the research group. Silver tetrafluoroborate was chosen to trap any free iodide in the

reaction mixture formed during the reaction of **1.1** and **1.2**, preventing the potential of demethylation of disalt **1.3**. 1,3-*Bis*-(trifluoromethanesulfonyloxy)propane **4.15** was chosen as a highly reactive bifunctional electrophile; however, cheaper, more readily available bifunctional electrophiles were investigated first.

SCHEME 4.7: Proposed reactions for the formation of 2-DMAP disalt species.

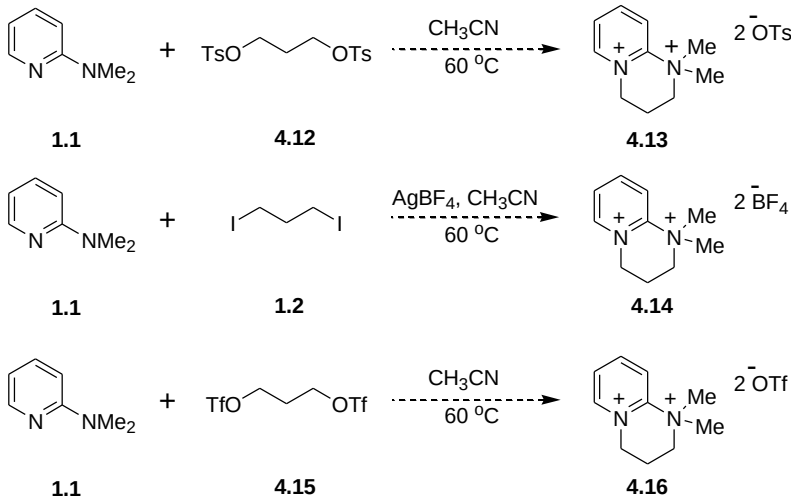

4.4.1 Reaction of 2-DMAP and 1,3-Bis-(4-toluenesulfonyloxy)propane

2-DMAP **1.1** and 1,3-*bis*-(4-toluenesulfonyloxy)propane **4.12** were reacted under the standard conditions in acetonitrile at 60 °C (Scheme 4.8). At 18 h, ^{1}H NMR showed no conversion of **1.1**, so the reaction temperature was increased to reflux. ^{1}H NMR analysis of the reaction mixture at various stages showed conversion of **1.1** to **4.17** and **4.18** by emergence of the characteristic aromatic signals for these products [$\delta_H(CD_3CN)$ 8.6-8.7 and 8.3-8.4 ppm respectively]. Table 4.2 shows the results of the NMR sampling.

The results in Table 4.2 show that conversion of **1.1** was very slow, requiring over 5 days for ~12 % conversion. Due to this slow rate of conversion, formation of **4.13** through reaction of **1.1** and **4.12** would not be feasible. Even if disalt **4.13** was formed in the reaction mixture, the high excess of **1.1** would most likely react to break down the dication species to products **4.17** and **4.18**.

SCHEME 4.8: Reaction of **1.1** and **4.12**.

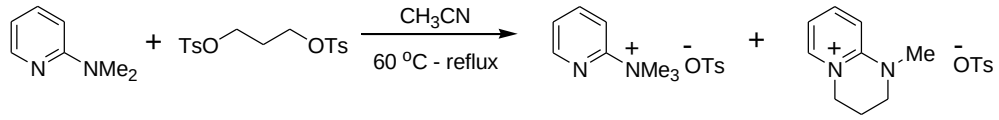

1.1 **4.12** **4.17** **4.18**

TABLE 4.2: Progress of reaction of **1.1** and **4.12**.

Sampling time / h	**T / °C**	**Wt. Sample removed / mg**	**Reaction mixture composition / % (Based on ^{1}H NMR (CD_3CN) integrations of given peaks)**		
			1.1 (δ_H 6.56 ppm)	**4.18 (δ_H 6.85 ppm)**	**4.17 (δ_H 8.65 ppm)**
18	60	5	100	0	0
46.5	reflux	4	100	0	0
139	reflux	3	88	8	4

4.4.2 Reaction of 2-DMAP and 1,3-Diiodopropane in the Presence of Silver Tetrafluoroborate

The next stage in the project was the reaction of 2-DMAP **1.1** and 1,3-diiodopropane **1.2**, but with silver tetrafluoroborate added in an attempt to increase the rate of the reaction. As well as the expected rate increase, the presence of silver tetrafluoroborate would aid in the trapping of iodide in the reaction mixture and prevent it from reaction with disalt species **4.14**; it is possible that removal of a methyl group from **4.14** could be performed by **1.1** or iodide. The reaction was also carried out in a low oxygen, low moisture glovebox to prevent any decomposition of products that could occur in air.

SCHEME 4.9: Reaction of **1.1** and **1.2** in presence of silver tetrafluoroborate.

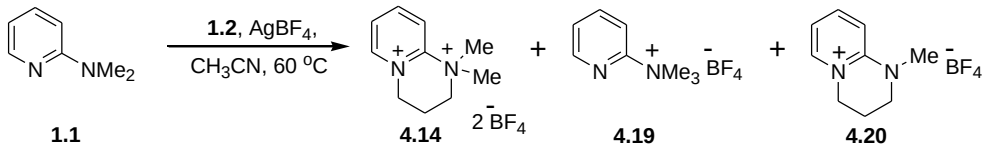

1.1 **4.14** **4.19** **4.20**

The reaction (Scheme 4.9) showed some very interesting results. ^{1}H NMR monitoring of the reaction at 5 h showed the emergence of a new aromatic multiplet at $\delta_H(CD_3CN)$ 8.74-8.79 ppm, further downfield than the signals observed for **1.4**

and **1.5** [$\delta_H(CD_3CN) \leq 8.6$ and ≤ 8.4 ppm respectively]. The new signal is consistent with a compound that is quaternised at both nitrogens, where the proton signal would be expected to be more downfield than either **1.4** or **1.5**. ^{1}H NMR of the reaction mixture at 23 h showed no evidence of the signal at $\delta_H(CD_3CN)$ 8.74-8.79 ppm, as well as increased ratios of **4.19** and **4.20**. This is consistent with synthesis of disalt **4.14** and conversion to the reaction products by reaction with 2-DMAP **1.1** as shown in Scheme 3.12.

In order to investigate the emergence of this new signal that could potentially be due to formation of **4.14**, the following NMR experiment was conducted; a solution of 1,3-diiodopropane **1.2** (0.05 mmol, 1.0 eq), 2-DMAP **1.1** (0.05 mmol, 1.0 eq) and silver tetrafluoroborate (0.104 mmol, 2.2 eq) in dry d_3-acetonitrile (1 mL) was prepared in a low oxygen, low moisture glovebox. The progress of the reaction was directly monitored by heating the reaction mixture to 60 °C in the NMR spectrometer and taking a 2 minute ^{1}H NMR scan every 15 minutes over a period of 15 h. The progress of the reaction was monitored by comparison of the ^{1}H integration peaks of the reaction products with the solvent peak for CD_3CN at δ_H 1.94 ppm, which remained constant throughout the reaction. Table 4.3 shows the product ratios for the integrations.

TABLE 4.3: Reaction progress monitored by ^{1}H NMR.

NMR Experiment Number	**Reaction Time**	**Ratio[a] of δ_H 8.76 ppm (4.14)**	**Ratio[a] of δ_H 8.56 ppm (4.19)**
2	15 min	0.63	0.44
5	1 h 6 min	1.17	0.83
6	1 h 23min	1.27	0.92
7	1 h 40 min	1.21	0.90
54	14 h 48 min	0.89	0.79

[a] Ratio with respect to residue of non-deuterated acetonitrile peak at δ_H 1.94 ppm taken as 1.000.

The results show the presence of the putative **4.14** in the initial spectrum recorded as well as throughout the 15 h NMR experiment timescale. Table 4.3 shows an increase in the concentration of '**4.14**' to a maximum at 1 h 23 min, which then decreases as

the reaction proceeds. This is consistent with the mechanism proposed (Scheme 3.12).

Based on the results of the ^{1}H NMR experiment, the reaction was repeated on a larger scale (0.5 mmol **1.1**) in a low oxygen, low moisture glovebox in an attempt to prove the existence of **4.14** by MS analysis. The reaction mixture was heated to 60 °C and a sample was removed at 1 h 23 min, believed to be the optimum time for sampling, for immediate MS analysis. MS analysis showed signals at *m*/*z* 188, 149, 137 and 123 as the peaks of interest, all singly charged species; unfortunately no doubly charged species was observed. The signals at *m*/*z* 149, 137 and 123 were attributed to **4.20**, **4.19** and **1.1** respectively (Scheme 4.9). The signal at *m*/*z* 188 was identified as the solvent-silver complex $[Ag(CH_3CN)_2]^+$, which was the peak of highest intensity in the spectrum. Attempts to separate the reaction products using LC-MS with dry acetonitrile were unsuccessful. In an attempt to remove excess silver ions from the reaction mixture, sodium chloride was added to the reaction mixture in excess and stirred for 1 h. A sample was filtered and MS analysis was repeated. The intensity of the signal at *m*/*z* 188 was significantly decreased, but no dication signal at *m*/*z* 82 was observed.

Although its presence could not be shown by MS analysis, some ^{1}H NMR spectroscopic evidence showed that a disalt species such as **4.14** could be formed in the reaction mixture.

4.4.3 Reaction of 2-DMAP and 1,3-Bis-(trifluoromethanesulfonyloxy)propane

The next stage in the project was the reaction of 2-DMAP **1.1**. with 1,3-*bis*-(trifluoromethanesulfonyloxy)propane **4.15**. It was hoped that the better leaving group, trifluoromethanesulfonate, would force the reaction to proceed faster than with *p*-toluenesulfonate or iodide, as well as avoiding the problems of dication identification that were observed when using silver tetrafluoroborate.

Synthesis of 1,3-*bis*-(trifluoromethanesulfonyloxy)propane **4.15** was easily achieved using the method described by Alder *et al*.[89] Reaction of 1,3-propanediol **4.21** with Tf_2O gave rise to **4.15** in 92 % yield (Scheme 4.10).

SCHEME 4.10: Synthesis of 1,3-*bis*-(trifluoromethanesulfonyloxy)propane **4.15**.

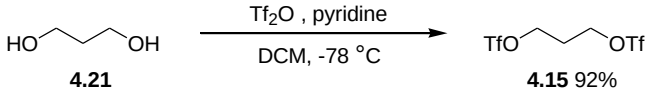

Reaction of **1.1** and ditriflate **4.15** was carried out in the glovebox in order to prevent decomposition of **4.16** by oxygen or water. Ditriflate **4.15** was used in excess (1.1 eq) to prevent attack on **4.16** by 2-DMAP **1.1** to form species **1.169**, **1.170** or **4.22**. The reaction was monitored by ^{1}H NMR spectroscopy and no trace of 2-DMAP **1.1** was observed in the reaction mixture after 4 h. The ^{1}H NMR spectrum showed evidence of **1.169** and **4.22**, as well as the new peaks at $\delta_H(CD_3CN)$ 8.79-8.83, which were thought to be due to **4.16**. Formation of ring nitrogen methylated product **1.170** could not be conclusively shown by ^{1}H NMR or MS analysis. The reaction is shown in Scheme 4.11.

SCHEME 4.11: Reaction of **1.1** and **4.15**.

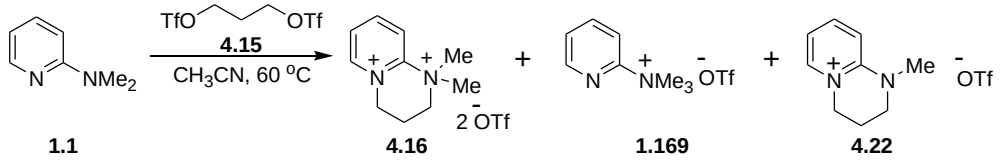

MS analysis of the reaction mixture showed signals at *m*/*z* 313, 149, 137, 123 and 82 M^{2+} as the peaks of interest. The signals at *m*/*z* 149, 137 and 123 were attributed to **4.22**, **1.169** and **1.1** respectively. The MS spectrum was also the first to show evidence of the formation of dication **4.16** in the reaction mixture; signals at *m*/*z* of 82.1 and 82.6 indicate the presence of a doubly charged species, which corresponds to the expected *m*/*z* for **4.16** $[M\text{-}2OTf]^{2+}$ (Figure 4.2). The signal at *m*/*z* 313 corresponds to $[M\text{-}OTf]^{+}$ for **4.16**.

In MS, the signal for a molecule (of molecular mass M) also shows a smaller peak at M+1 mass units. This signal is due to the presence of ^{13}C in the molecule. As ^{13}C has an abundance of 1.11 %,[90] the ratio of the M+1 signal to the M signal usually corresponds to the number of carbon atoms in the molecule multiplied by 1.1. For example, if a molecule of mass M has 10 carbon atoms, MS peaks at *m*/*z* of M and M+1 would be observed. The intensity ratio of M:M+1 would be 100:11 (~10:1), as

each carbon in the molecule could potentially be a ^{13}C. In a dicationic molecule, the presence of ^{13}C is still taken into account. If the molecule was singly charged, it would show peaks at M and M+1, however, as the 2+ charge results in a peak at M/2, the corresponding ^{13}C peak occurs at (M+1)/2 or (M/2)+0.5. Therefore, a mass separation of 0.5 mass units indicates the presence of a doubly charged species. Figure 4.3 shows a diagram illustrating this.

FIGURE 4.2: Dication signal attributed to dication **4.16**.

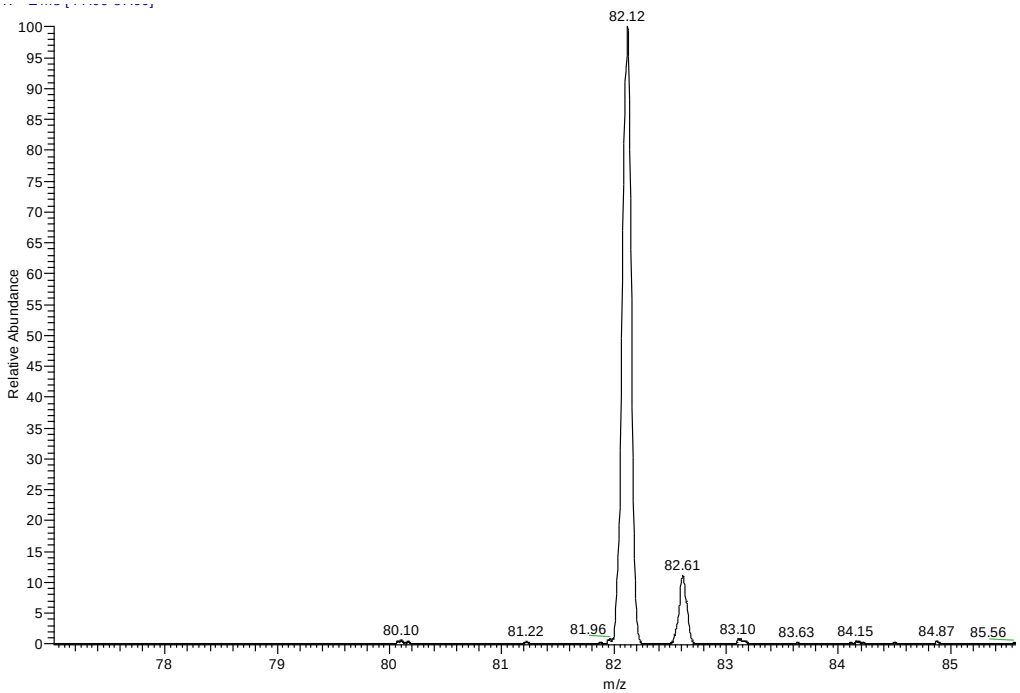

FIGURE 4.3: MS splitting patterns for cation and dication.

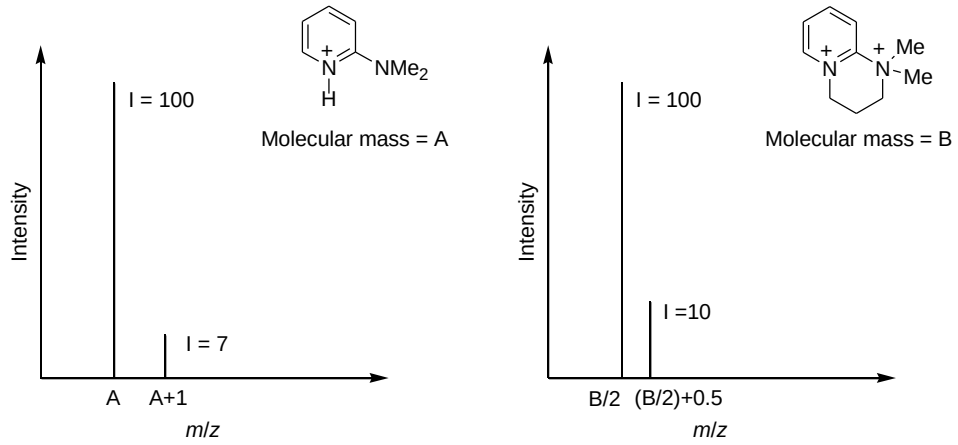

^{1}H NMR and MS evidence for the formation of 2-DMAP disalt **4.16** is proof that the reaction between 2-DMAP **1.1** and 1,3-diiodopropane **1.2** could proceed through the mechanism shown in Scheme 3.12 (reproduced below). Although this does not prove that the reaction proceeds exclusively through this mechanism (as opposed to alternative mechanisms shown in Scheme 3.11), it shows that a superelectrophilic dication species such as **1.3** can exist. As far as the author is aware, this type of 2-dialkylaminopyridine dication species has not previously been observed.

SCHEME 3.12: Proposed formation of 2-DMAP dication **1.3**.

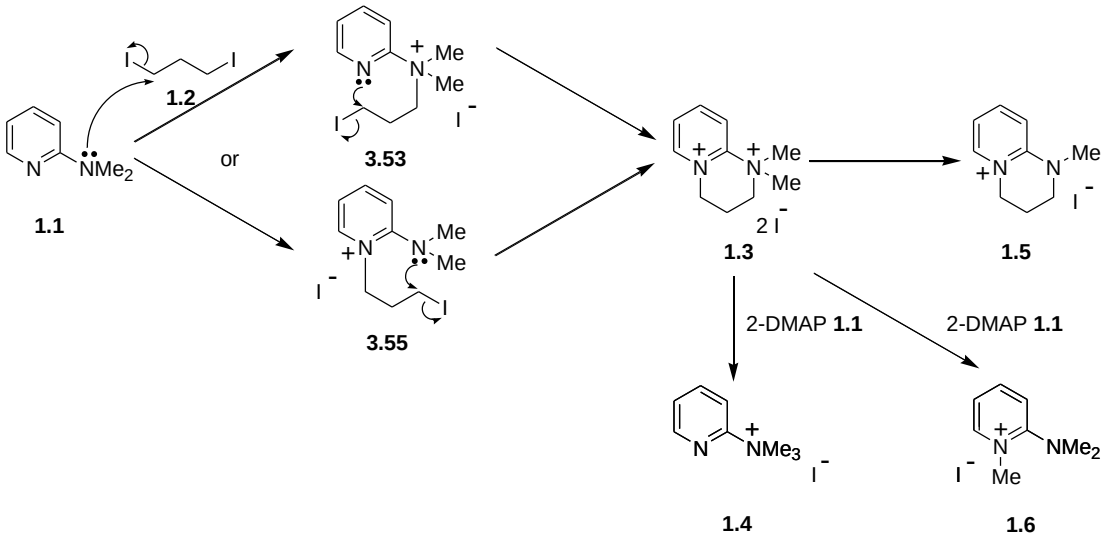

FIGURE 4.4: ^{1}H NMR (CD_3CN) of **4.16**

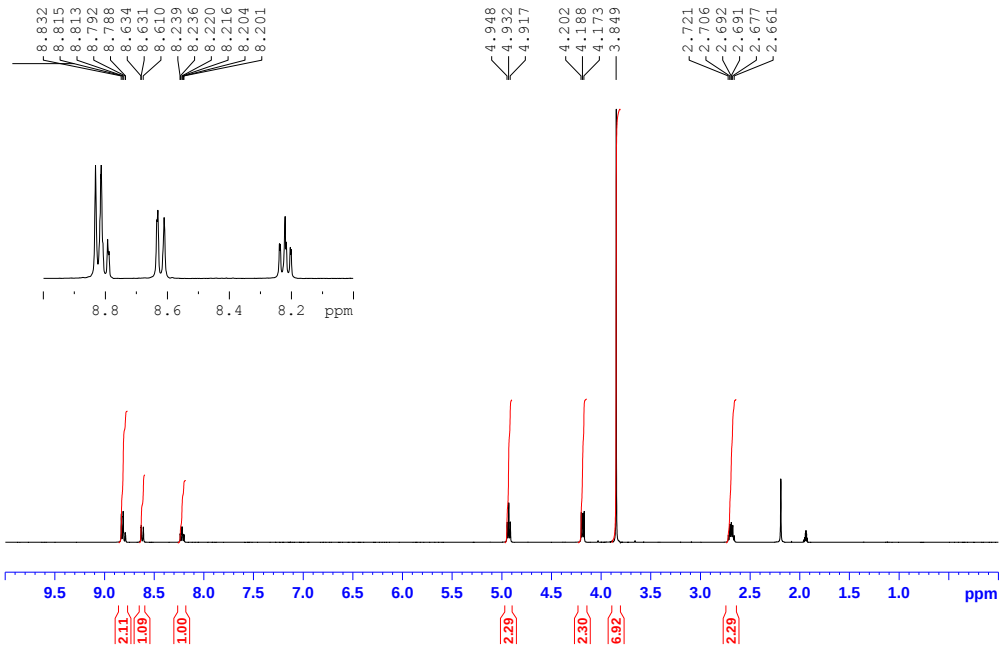

In order to synthesise 2-DMAP disalt **4.16** without decomposition to give **1.169** and **4.22**, the reaction was repeated using 1.5 eq of ditriflate **4.15**. This time the reaction was successful and **4.16** was isolated as a viscous red oil in 90 % yield at 0.5 mmol scale (Scheme 4.12). Formation of **4.16** was confirmed by ^{1}H NMR, ^{13}C NMR and MS analysis showing a dication peak at *m*/*z* 82 for $[M\text{-}2OTf]^{2+}$. Figure 4.4 shows the ^{1}H NMR (CD_3CN) spectrum for **4.16**. The NMR shows peaks for the aromatic, methyl and methylene protons of **4.16** which are downfield shifted compared to monocations **1.169** and **4.22**.

SCHEME 4.12: Isolation of 2-DMAP disalt **4.16**.

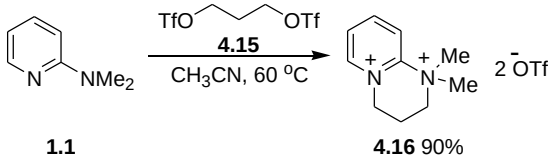

1.1 **4.16** 90%

4.5 Large-Scale Synthesis of 2-DMAP Disalt

At this stage, synthesis of 2-DMAP disalt **4.16** in a larger scale was attempted. Until this point, 2-DMAP disalt **4.16** was only ever synthesised in a 0.5 mmol scale and the product was a viscous red oil. Scale-up would allow more reactions to be carried out to investigate the reactivity of **4.16**. Scale-up of the reaction would also allow more disalt to be produced, with the possibility of recrystallisation of **4.16**. This would allow for easier handling and storage of **4.16**, as well as the possibility of obtaining a crystal structure.

4.5.1 Reaction of 2-DMAP and 1,3-Bis-(trifluoromethanesulfonyloxy)propane on a Larger Scale

In order to test the effects of scaling up the reaction, a 5-times scale-up was first performed (2.5 mmol **1.1** and 3.75 mmol of **4.15**). The reaction proceeded to give disalt **4.16**, but also led to the formation of a new product in almost 1:1 ratio with **4.16**. After spectroscopic investigation, the product was found to be ring-protonated 2-DMAP **4.23** (Scheme 4.13). This was indicated by the small, generally downfield, shift in the aromatic protons of 2-DMAP **1.1** from $\delta_H(CDCl_3)$ 6.47, 6.63, 7.36 and 8.13 ppm to $\delta_H(CDCl_3)$ 6.85, 7.01, 7.88 and 8.02 ppm in addition to a broad singlet at 10.01 ppm. MS analysis of the reaction mixture showed signals at *m*/*z* 313, 123

and 82, consistent with the formation of **4.16** and **4.23**. Also, IR analysis of the product shows a very broad signal at 3501 cm^{-1}, consistent with N-H hydrogen bonding. Formation of **4.23** is consistent with the studies of Barbieri *et al*.,[39] who found that protonation of 2-DMAP **1.1** occurred exclusively on the ring nitrogen.

SCHEME 4.13: Attempted large-scale synthesis of **4.16**.

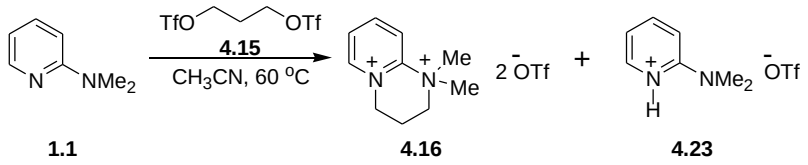

Two possible mechanisms for the formation of **4.23** are shown in Scheme 4.14. Reaction of alkyl triflates and nitriles is known to form nitrilium salts such as **4.26**.[91] Consequently, reaction of ditriflate **4.15** with two molecules of acetonitrile could result in the formation of nitrilium salt **4.27**. The pK_a of **4.27** would be expected to be decreased relative to the pK_a of acetonitrile, making removal of a proton by **1.1** possible to form ketenimine salt **4.28** and protonated 2-DMAP **4.23**. However, no evidence of the formation of ketenimine salt **4.28** was observed in the ^1H NMR of the reaction mixture. Another possible source of a proton could be from ditriflate **4.15**, as shown, resulting in the formation of **4.23** and **4.29**.

SCHEME 4.14: Possible sources of H for formation of **4.23**.

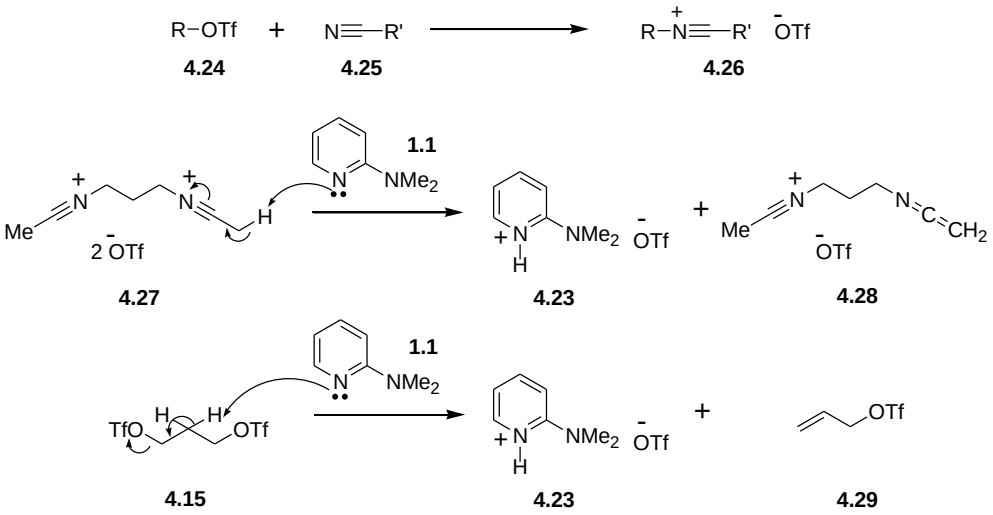

Regardless of how protonated 2-DMAP **4.23** was formed, its presence in the reaction mixture was problematic. Washing the reaction mixture with dry diethyl ether was

successful in removing **4.23**, although all traces of **4.23** could not be removed even after repeated washing over prolonged periods of time (~72 h). As protonated 2-DMAP **4.23** was present as a salt in the reaction mixture, attempts to purify 2-DMAP disalt **4.16** were made more difficult. In theory, addition of a base to the mixture and removal of the resulting neutral 2-DMAP **1.1** by washing with diethyl ether could remove **4.23**. However, the added base could react with 2-DMAP disalt **4.16** to make an even more complex mixture of products or the protonated base could also prove difficult to remove from the reaction mixture. As a result of this, a new protocol for the synthesis of disalt **4.16** was required.

4.5.2 Study of the Temperature-Dependent Formation of 2-DMAP Disalt and Protonated 2-DMAP

Formation of unwanted side-product **4.23** is believed to occur through attack of 2-DMAP **1.1** on **4.27**, itself formed from the reaction of ditriflate **4.15** and acetonitrile (Scheme 4.14). A search on the literature of the formation of nitrilium triflate salts such as **4.27** revealed the work of Booth *et al*.,[91] who showed that the formation of nitrilium salts, such as **4.26**, from the reaction of nitriles and alkyl trifluoromethanesulfonate reagents was helped by high temperatures.

Based on this, decreasing the temperature of the reaction between 2-DMAP **1.1** and ditriflate **4.15** should result in a decrease in the amount of protonated 2-DMAP **4.23** produced, by inhibiting the formation of species **4.27**. In order to determine the effect of temperature on the formation of **4.23**, the reaction between 2-DMAP **1.1** and ditriflate **4.15** in acetonitrile at different temperatures was investigated.

The same procedure was used for each reaction; 2-DMAP **1.1** (1.0 eq) was added dropwise to a solution of ditriflate **4.15** (1.5 eq) in acetonitrile at the required temperature (-78, -41, 0, r.t. or 60 °C) and stirred under argon. At 4 h, a sample of the reaction mixture was removed for ^{1}H NMR analysis to determine the ratio of **4.16** to **4.23** in the reaction mixture. For temperatures below r.t., the temperature was held for 6 h, then allowed to warm to r.t. overnight. At 23 h a further sample was taken for ^{1}H NMR analysis. At 23 h, stirring (and heating in the case of the reaction at 60 °C) was stopped and the solvent was removed *in vacuo*. The residue was then held under vacuum for at least 72 h to remove any residual solvent and a sample was removed

for ^{1}H NMR analysis. The results of the ^{1}H NMR analysis taken at each stage are shown in Table 4.4.

TABLE 4.4: Ratio of **4.23** to **4.16** at different reaction temperatures.

Entry	**T / °C**	**Ratio of 4.23:4.16 in reaction mixture[a]**		
		4 h	**23 h**	**Post work-up**
1	60	0.78[b]	0.87	-
2	r.t.	0.64	0.79	0.68
3	0	0.79	0.80[c]	0.94[c]
4	-41	0.03	0.28[c]	0.30[c]
5	-78	0.05	0.32[c]	0.32[c]

[a] Ratio taken by ^{1}H NMR comparison of peak at $\delta_H(CD_3CN)$ 6.8 ppm for **4.23** in comparison to ratio of 1.00 taken for **4.16** for peak at $\delta_H(CD_3CN)$ 8.2 ppm. [b] Sampling taken at 5.5 h. [c] Sampling occurred when reaction mixture at r.t.

Peaks at $\delta_H(CD_3CN)$ 6.8 ppm and $\delta_H(CD_3CN)$ 8.2 ppm were chosen to determine the ratios of **4.23** and **4.16** respectively. These two signals corresponded to the same proton signal in each product and were distinct enough so that overlap with other peaks in the spectrum was not a problem, helping to give more accurate comparison of the product ratios in the reaction mixture.

The results shown in Table 4.4 indicate that the formation of protonated 2-DMAP **4.23** is temperature-dependent and that at lower temperatures its formation is inhibited, most likely due to inhibiting the formation of **4.27**. Reaction at 60 °C and r.t. show roughly consistent ratios of **4.16** and **4.23** throughout the sampling period (Table 4.4, entries 1 and 2). Most encouraging are the results at -41 and -78 °C (Table 4.4, entries 4 and 5), which show very low ratios of **4.23** when sampled at their respective temperatures (~5 % contamination by **4.23**). However, as the reaction is allowed to warm to r.t., the concentration of **4.23** increases to ~30 % that of **4.16** at both temperatures. These results show the sensitivity of the reaction of 2-DMAP **1.1** and ditriflate **4.15** to temperature, where higher reaction temperatures results in an increase in the formation of protonated 2-DMAP side-product **4.23**.

The reactions leading to the formation of protonated 2-DMAP **4.23** still remain a mystery, however, the results of the temperature dependence reactions were very

promising, showing that formation of **4.23** could be decreased by carrying out the reaction at low temperatures. If formation of 2-DMAP disalt **4.16** was carried out at -41 °C and the excess ditriflate **4.15** and unwanted side-product **4.23** could be removed at this temperature, then it might be possible to isolate 2-DMAP disalt **4.16** in a pure form.

SCHEME 4.15: Isolation of 2-DMAP disalt **4.16**.

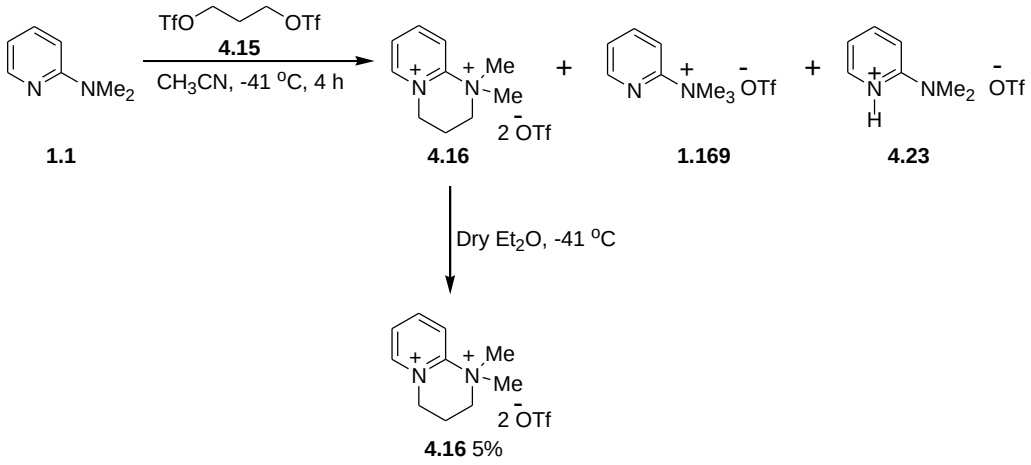

As a result of these findings, the following reaction was examined; 2-DMAP **1.1** and ditriflate **4.15** were reacted in a 1:1 ratio in dry acetonitrile at -41 °C (Scheme 4.15). The amount of ditriflate **4.15** was decreased in order to prevent excess formation of side-products such as **4.27**. The reaction was monitored by ^{1}H NMR spectroscopy and at 4 h showed formation of 2-DMAP disalt **4.16**, as well as traces of **4.23** and **1.169** (in ratios of 1.0:0.2:0.1 respectively by ^{1}H NMR). This result indicates that a higher number of equivalents of ditriflate **4.15** are required to prevent side-reactions between **4.16** and 2-DMAP **1.1** (most likely 1.1-1.5 eq). In an attempt to remove traces of contaminants, the reaction mixture was transferred to a flask containing a large excess of dry diethyl ether held at -41 °C. This caused the precipitation of a white solid, which was collected and identified as pure 2-DMAP disalt **4.16** (5 % yield). This reaction was a significant development in the progress of the project as it showed that 2-DMAP disalt **4.16** could be purified and isolated in a solid form, making its handling easier and providing the possibility of obtaining a crystal structure.

4.6 Development of an Efficient Synthesis of 2-DMAP Disalt

It was now known that 2-DMAP disalt **4.16** could be synthesised as a solid compound, and the challenge was now to develop an efficient and reliable synthetic protocol for its routine synthesis. One of the major problems inhibiting the synthesis of 2-DMAP disalt **4.16** was the formation of side-products such as protonated 2-DMAP **4.23**. As the formation of **4.23** was thought to be caused by a side-reaction of ditriflate **4.15** with acetonitrile, why not eliminate the problem by removing acetonitrile from the reaction?

The neat reaction of 2-DMAP **1.1** and ditriflate **4.15** was conducted. 2-DMAP **1.1** (0.5 mmol scale) was added dropwise to a tube containing an excess of ditriflate **4.15** (1.2 eq) under argon at 0 °C (Scheme 4.16). An excess of ditriflate **4.15** was used in order to prevent an excess of 2-DMAP **1.1** being present in the reaction mixture, in case it led to formation of side-products **1.169**, **1.170** and **4.22**. The reaction was carried out at 0 °C, rather than -41 or -78 °C where formation of **4.23** was inhibited, as ditriflate **4.15** froze at temperatures below 0 °C. Also, the removal of acetonitrile from the reaction mixture was expected to prevent the formation of **4.23**, so an increase in temperature would not be as detrimental as the same reaction in acetonitrile. Using the procedure detailed above, a white precipitate formed during the addition of 2-DMAP **1.1**. Recrystallisation of the solid from dry acetonitrile/diethyl ether gave 2-DMAP disalt **4.16** in 81 % yield as a white crystalline solid.

SCHEME 4.16: 2-DMAP disalt **4.16** using neat reaction conditions.

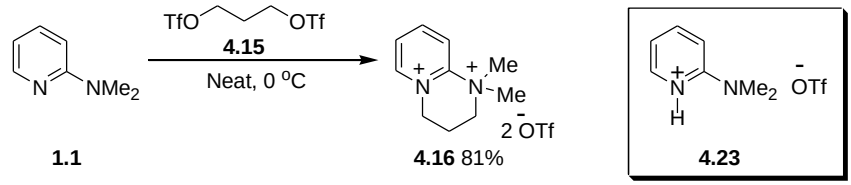

1.1 **4.16** 81% **4.23**

With a successful procedure for the formation of 2-DMAP disalt **4.16** achieved, a scale-up of the synthesis was required. Using the same procedure but in a larger scale (20 mmol of **1.1**) did not proceed as expected, giving a mixture of products (Scheme 4.17). 2-DMAP **1.1** was added dropwise to a flask containing ditriflate **4.15** and upon addition of approximately half the 2-DMAP, the solution turned from white to black

and ^{1}H NMR and MS analysis of the reaction products showed a mixture of **1.169**, **4.16** and **4.22**. The formation of the side-products was attributed to the 2-DMAP **1.1** being added too quickly, causing the reaction to overheat and promote the demethylation of **4.16** by **1.1** to form **1.169** and **4.22**.

In order to solve this problem, 2-DMAP **1.1** was added using a syringe pump to control its addition. Addition of 2-DMAP **1.1** (20 mmol scale) using a syringe pump at 1.27 mL.h^{-1} (for an addition time of ~2 h) to a flask containing ditriflate **4.15** at 0 °C led to formation of a white powder, which upon recrystallisation gave 2-DMAP disalt **4.16** in excellent 98 % yield (Scheme 4.17). This efficient and reliable procedure has been used several times for the synthesis of disalt **4.16**, consistently giving yields ≥ 80 %.

SCHEME 4.17: Large-scale synthesis of **4.16**.

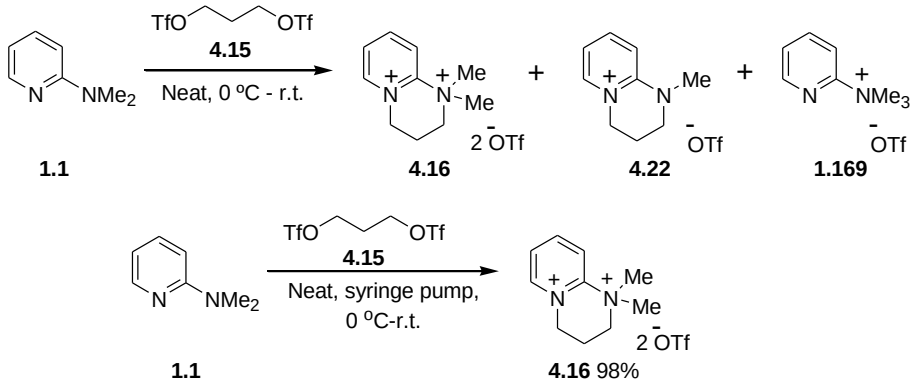

Recrystallisation of the reaction product gave crystals of high quality for X-ray crystallographic analysis. The resulting ORTEP diagrams are shown in Figure 4.5. The crystal structure was the final confirmation of the structure of **4.16**, which had already been fully characterised. The development of a successful procedure for the large-scale synthesis of 2-DMAP disalt **4.16** allowed enough material to be synthesised to begin to examine the reactivity of such an unusual superelectrophilic species. The results of these investigations are detailed in Chapters 5 and 8.

FIGURE 4.5: (a) ORTEP diagram of 2-DMAP disalt **4.16** cation. (b) ORTEP diagram of 2-DMAP disalt **4.16** (cation and two anions).

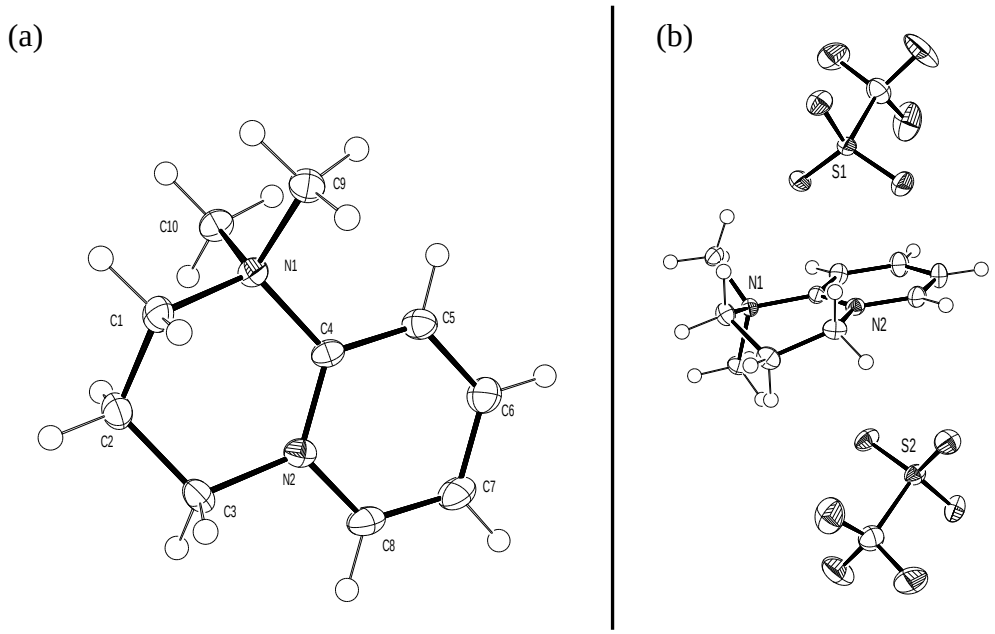

4.7 Dimethylaminopyrimidine Disalt

With the successful synthesis of 2-DMAP disalt **4.16**, development of another superelectrophile disalt was examined.[92] The next superelectrophile disalt to be envisioned was disalt **4.30** based on 2-dimethylaminopyrimidine **4.31** (Scheme 4.18).

SCHEME 4.18: Retrosynthetic analysis for disalt **4.30**.

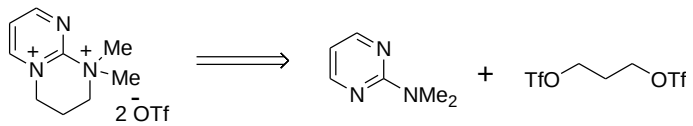

4.30 **4.31** **4.15**

SCHEME 4.19: Synthesis of 2-dimethylaminopyrimidine **4.31**.

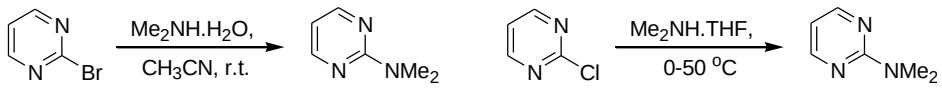

4.32 **4.31** 94% **4.33** **4.31** 72%

Synthesis of 2-dimethylaminopyrimidine **4.31** was readily achieved (in 94 % yield) by the reaction of 2-bromopyrimidine **4.32** with aqueous dimethylamine solution in acetonitrile (Scheme 4.19). An alternative synthesis using cheaper 2-chloro-

pyrimidine **4.33** involved heating **4.33** with dimethylamine solution (2.0 M in THF) at 50 °C for 18 h, giving **4.31** in 72 % yield (Scheme 4.19).

Reaction of 2-dimethylaminopyrimidine **4.31** and ditriflate **4.15** was carried out in a low oxygen, low moisture glovebox using a similar procedure to the synthesis of 2-DMAP disalt **4.16** (Scheme 4.20). 2-Dimethylaminopyrimidine **4.31** was added dropwise to a tube containing ditriflate **4.15** at r.t. in the glovebox and stirred until solidification of the reaction mixture occurred (~1.5 h). ^{1}H NMR of the resulting orange precipitate showed a mixture of two products. The major product showed three downfield aromatic protons at $\delta_H(CD_3CN)$ 8.37, 9.21 and 9.52 ppm as well as proton signals that closely matched the methyl and methylene proton signals of 2-DMAP disalt **4.16**. Based on these results, the proton signals for the major product were attributed to 2-dimethylaminopyrimidine disalt **4.30**. The minor product was later identified as 2-dimethylaminopyrimidine disalt hydrolysis product, hydroxypyrimidinium salt **4.34** (the identification of **4.34** and a mechanism for its formation will be discussed in greater detail in Chapter 5, as this product relates to the reaction of disalt **4.30** with different nucleophiles, in this case an oxygen nucleophile). In addition, MS analysis of the precipitate gave signals of *m*/*z* 332, 314, 182 and 83 M^{2+} consistent with hydroxypyrimidinium salt **4.34** (*m*/*z* 332 $[M\text{-}OTf]^+$, 182 $[M\text{-}H\text{-}2OTf]^+$) and 2-dimethylaminopyrimidine disalt **4.30** (*m*/*z* 314 $[M\text{-}OTf]^+$, 83 $[M\text{-}2OTf]^{2+}$).

SCHEME 4.20: Synthesis of 2-dimethylaminopyrimidine disalt **4.30**.

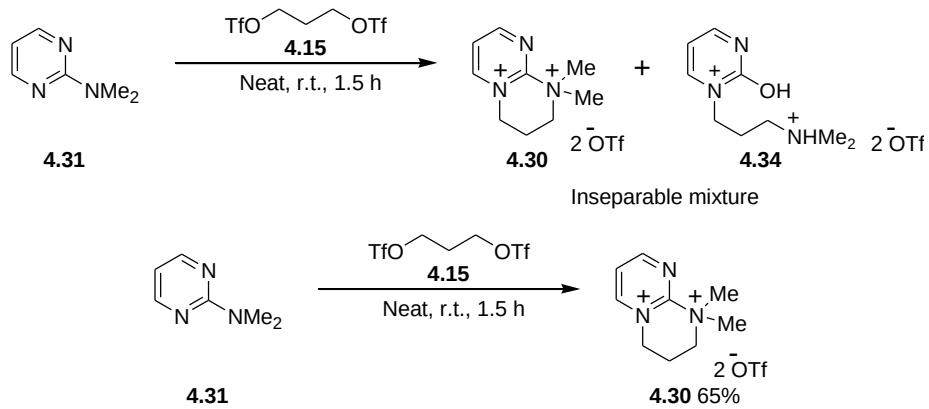

2-Dimethylaminopyrimidine disalt **4.30** could not be isolated from the reaction mixture, despite several attempts at recrystallisation and attempted syntheses of **4.30**.

The side-product **4.34** was due to hydrolysis of disalt **4.30**, so the use of dry reagents would help eliminate this hydrolysis product. Distillation of ditriflate **4.15** and 2-dimethylaminopyrimidine **4.31** was successful in preventing the formation of significant amounts of hydrolysis product **4.34**. This allowed 2-dimethylaminopyrimidine disalt **4.30** to be synthesised, with recrystallisation to give pure disalt **4.30** in 65 % yield.

Formation of disalt **4.30** was confirmed by spectroscopic analysis; ^{1}H NMR (Figure 4.6) and ^{13}C NMR analysis showed the expected product. MS analysis of the product showed a peak at *m*/*z* 82.6 and 83.1 (Figure 4.7), consistent with a dication of the correct mass for **4.30**. In addition, a crystal structure was obtained for disalt **4.30** showing the correct structure (Figure 4.8).

FIGURE 4.6: ^{1}H NMR spectrum for **4.30**.

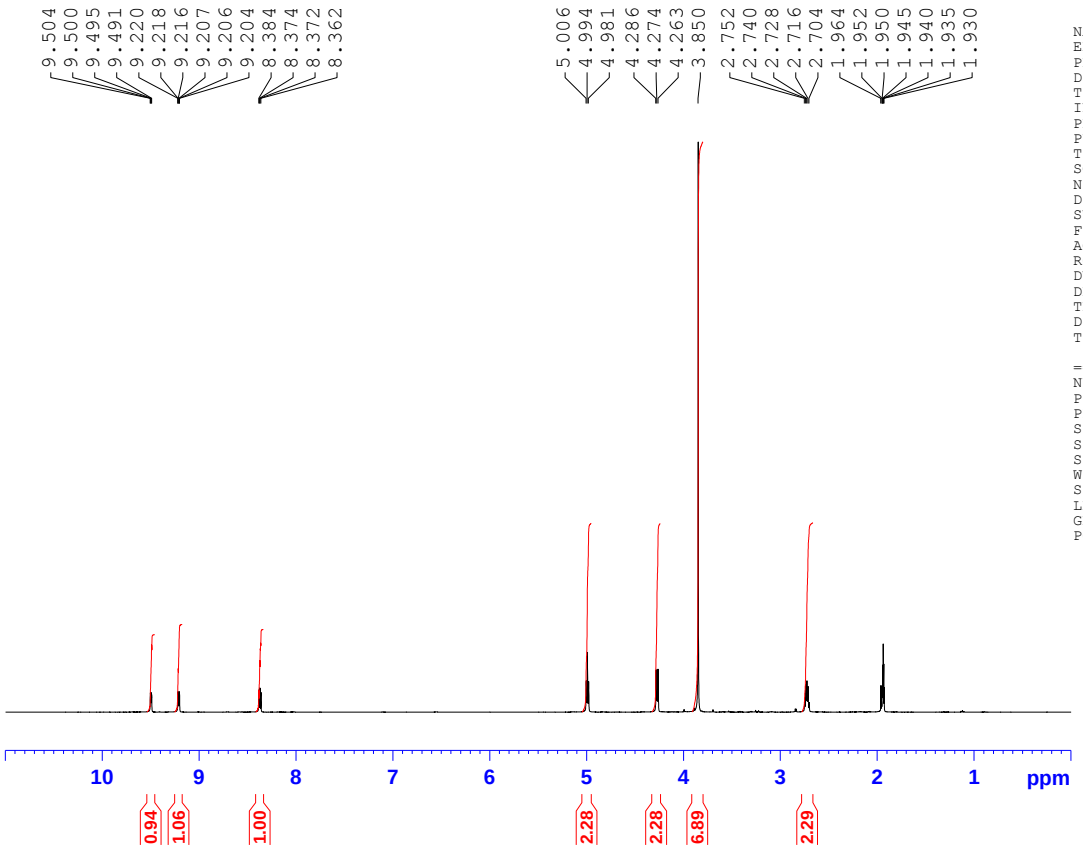

FIGURE 4.7: Dication signal for **4.30** in mass spectrum.

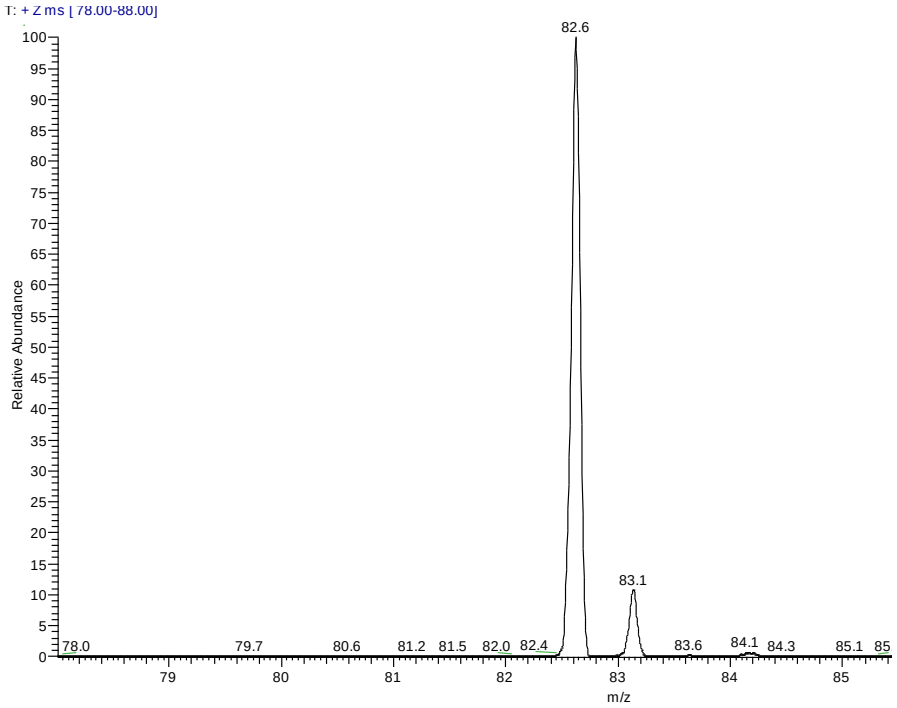

FIGURE 4.8: (a) ORTEP diagram for cation of disalt **4.30**. (b) ORTEP diagram for disalt **4.30** (cation and two anions).

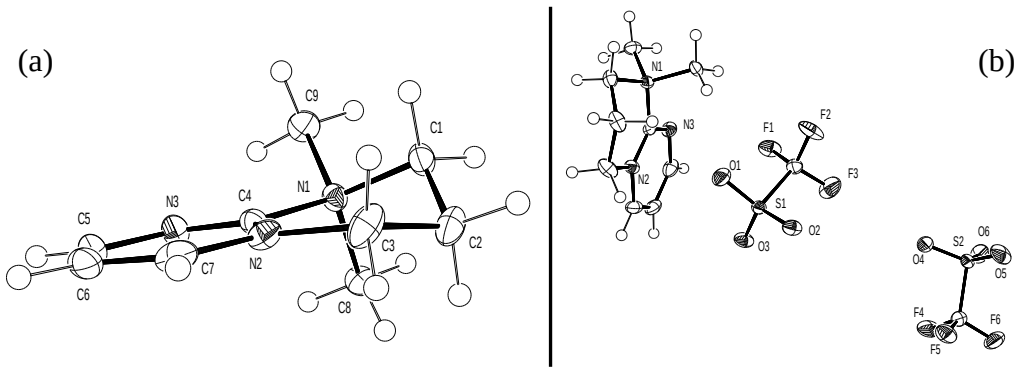

The reactivity of 2-DMAP **1.1** with a variety of electrophiles was examined. It was found that alkylation occurred preferentially on the dimethylamino nitrogen and that alkylation was hindered with increasing chain length for a series of iodoalkanes (iodomethane, iodoethane and 1-iodopropane). The reaction of 2-DMAP **1.1** with a variety of bifunctional electrophiles was also examined. 1,3-*Bis*-(4-toluenesulfonyloxy)propane **4.12** was found to react slowly with 2-DMAP **1.1**, meaning that a dication salt could not be isolated. Reaction of 2-DMAP **1.1** with 1,3-diiodopropane **1.2** in the presence of silver tetrafluoroborate showed the first

evidence of disalt **1.3**. Reaction with 1,3-*bis*-(trifluoromethanesulfonyloxy)propane **4.15** led to the synthesis of 2-DMAP disalt **4.16**. Low temperature and solvent-free conditions allowed disalt **4.16** to be synthesised in excellent yield.

Superelectrophile dication salts **4.16** and **4.30** have been successfully synthesised and fully characterised. The next chapter will examine the reactivity of these unusual and intriguing species with a variety of nucleophiles.

5 Probing Superelectrophile Reactivity

With superelectrophile disalts **4.16** and **4.30** synthesised, we were keen to explore the reactivity of these unusual species. The reactivity of 2-DMAP disalt **4.16** was first examined as it was easier to prepare and handle than disalt **4.30**. Towards this end, the reaction of 2-DMAP disalt **4.16** with 1-methylindole **3.57** and various other nucleophiles was examined.

5.1 Initial Studies with 1-Methylindole

The following reactions were carried out before the isolation of 2-DMAP disalt **4.16** as described in Section 4.5. These reactions are reported here due to some unusual reactivity that was observed that has relevance to later sections.

The first stage was the synthesis of 1,3-dimethyl-1*H*-indole **3.58** using 3-methylindole **5.1** (Scheme 5.1). The reason for this was to obtain a sample of **3.58** synthesised by alternative means for spectroscopic comparison in the reaction of 1-methylindole **3.57** and 2-DMAP disalt **4.16**. 3-Methylindole **5.1** was deprotonated using NaH, then methylated with iodomethane to provide 1,3-dimethyl-1*H*-indole **3.58** in 95 % yield.

SCHEME 5.1: Synthesis of 1,3-dimethyl-1*H*-indole **3.58** from 3-methylindole **5.1**.

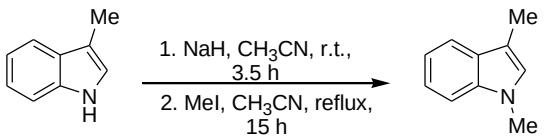

5.1 **3.58** 95%

Next came the reaction of 1-methylindole **3.57** and 2-DMAP disalt **4.16** obtained in 71 % purity (contaminated with **4.23**). After 89 h at reflux, 1,3-dimethyl-1*H*-indole **3.58** was isolated in 5 % yield by HPLC separation (Scheme 5.2). Although the yield was low, this reaction represented the first isolation of **3.58** and conclusive proof of

the ability of 2-DMAP disalt **4.16** to act as a reagent for the methylation of nitrogen heterocycles, another important breakthrough in the progress of the project. However, to make the reaction synthetically useful, the recovery of material from the reaction and the conversion of **3.57** to **3.58** would need to be greatly improved. The proposed mechanism of formation of **3.58** is shown in Scheme 5.3. 2-DMAP disalt **4.16** can be attacked by 1-methylindole **3.57** to form intermediate **5.2** and demethylated disalt species **4.22**. Loss of a proton from **5.2** restores the aromaticity to give 1,3-dimethyl-1*H*-indole **3.58**.

SCHEME 5.2: Synthesis of 1,3-dimethyl-1*H*-indole **3.58** using **4.16**.

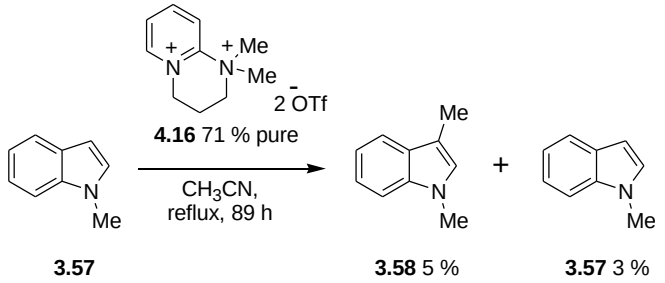

SCHEME 5.3: Proposed mechanism for formation of 1,3-dimethyl-1*H*-indole **3.58**.

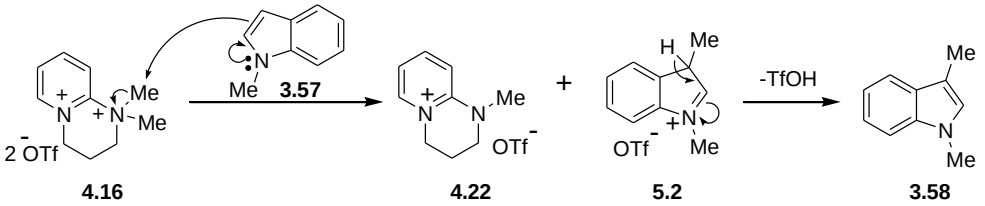

The reaction was repeated using different quantities of 2-DMAP disalt **4.16** (1-10 eq) at different temperatures (60 °C-reflux). However, no significant increases in mass recovery or product conversion was observed.[93]

The one-pot methylation of 1-methylindole **3.57** was then attempted (Scheme 5.4). This involved reaction of 2-DMAP **1.1** and ditriflate **4.15** in acetonitrile at 60 °C, then the addition of 1-methylindole **3.57** and increase of the reaction temperature to reflux. However, this did not lead to formation of **3.58**, but to isolation of ketone species **5.3** in 13 % yield. Formation of 1-(1-methyl-1*H*-indol-3-yl)ethanone **5.3** was confirmed by spectroscopic analysis; ^{13}C NMR analysis showed a peak at $\delta_C(CDCl_3)$ 193.9 ppm for the ketone carbon and ^{1}H NMR analysis showed a signal at $\delta_H(CDCl_3)$ 2.12 ppm integrating to 3 protons. IR analysis showed a peak at 1643 cm^{-1}, consistent

with a carbonyl and GC-MS analysis also confirmed its identity (RT 13.15 min, *m*/*z* 173). Though the presence of **5.3** was readily confirmed as a product in the reaction, its formation in the reaction mixture was not so readily explicable. The proposed mechanisms of formation are shown in Scheme 5.5.

SCHEME 5.4: Attempted one-pot methylation of 1-methylindole **3.57**.

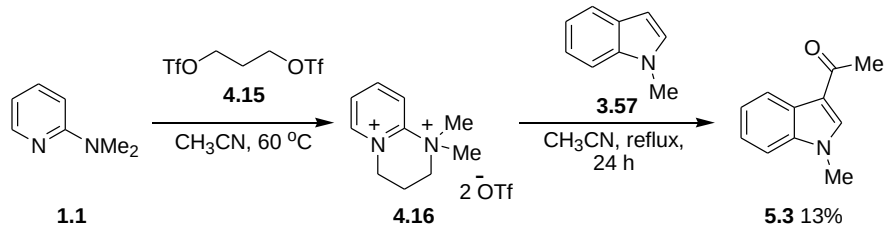

SCHEME 5.5: Proposed mechanisms for the formation of **5.3**.

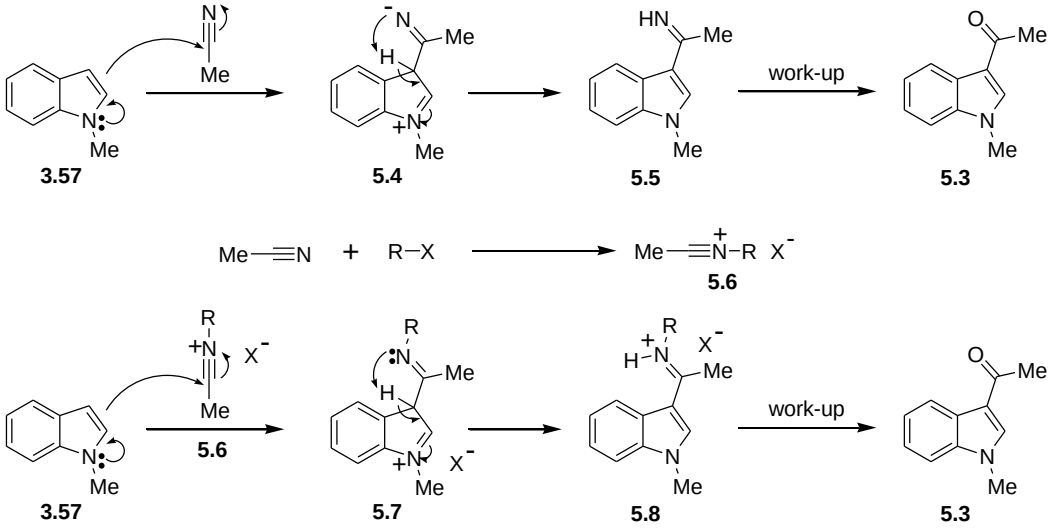

In the first proposed mechanism, 1-methylindole **3.57** might attack a molecule of acetonitrile to form charged intermediate **5.4**. Proton transfer to the nitrogen gives species **5.5**, which is converted to methyl ketone **5.3** on work-up. An alternative and more likely mechanism is also shown in Scheme 5.5. In this case, a molecule of acetonitrile is converted to nitrilium salt **5.6**, either by methylation by 2-DMAP disalt **4.16** or alkylation by ditriflate **4.15**. This charged species can then be attacked by 1-methylindole **3.57** to give intermediate **5.7**, which undergoes proton transfer to give iminium salt **5.8**. Upon work-up, this salt is hydrolysed to give methyl ketone **5.3**.

In order to investigate the proposed mechanisms, 1-methylindole **3.57** was refluxed in acetonitrile. No formation of ketone **5.3** was observed after 18 h, with recovery of

3.57 in 98 % yield. As expected no reaction of **3.57** with acetonitrile was observed, and so this excludes the first proposed mechanism (Scheme 5.5) as the mechanism of formation of **5.3**.

The reaction of 1-methylindole **3.57** with ditriflate **4.15** gave a more interesting result, i.e. formation of dication iminium salt **5.9** in 54 % yield (Scheme 5.6). Formation of **5.9** was confirmed by MS analysis which showed signals at *m*/*z* 535 $[M\text{-}OTf]^{+}$ and 193 $[M\text{-}2OTf]^{2+}$, with all other spectroscopic results confirming the formation of **5.9**. Iminium salt **5.9** is formed from the reaction of **4.15**, acetonitrile and **3.47** as shown in Scheme 5.6, in a similar mechanism to that shown in Scheme 5.5.

SCHEME 5.6: Formation of iminium disalt **5.9**.

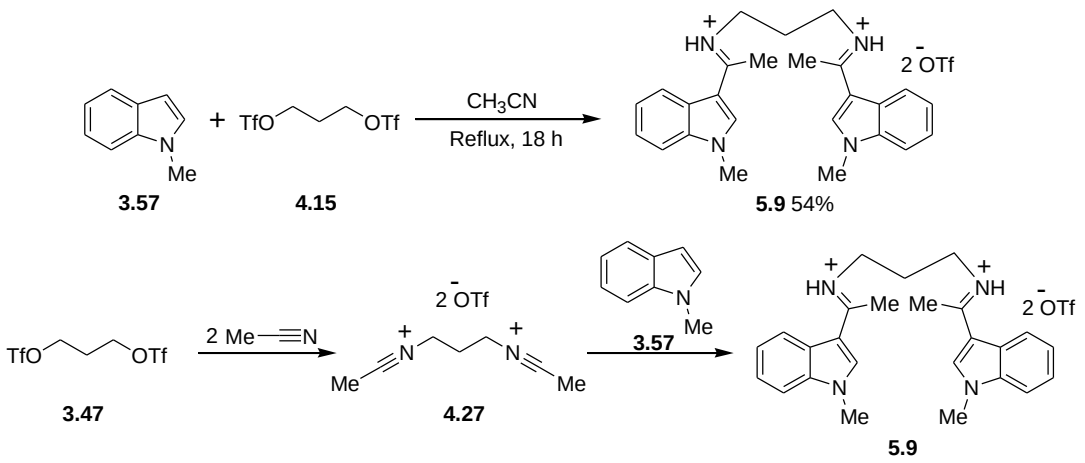

Subsequent hydrolysis of iminium disalt **5.9** with refluxing NaOH solution (2N) gave rise to methyl ketone **5.3** in 71 % yield (Scheme 5.7). Hydrolysis was first attempted at r.t., however, ^{1}H NMR analysis showed slow hydrolysis of iminium salt **5.9**, requiring the temperature to be increased.

SCHEME 5.7: Synthesis of ketone **5.3** using iminium salt **5.9**.

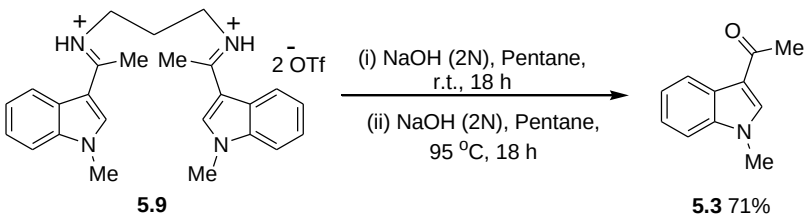

The formation of iminium salt **5.9** shows that reaction between ditriflate **4.15** and acetonitrile can occur. This reaction shows that the reaction of nitrilium salt **4.27** can occur, either with 1-methylindole **3.57** to form iminium salt **5.9** or possibly with 2-DMAP **1.1** to form a protonated species as described previously (Scheme 4.14), where the increased steric bulk of 2-DMAP **1.1** may prevent formation of an iminium salt using 2-DMAP **1.1**, resulting in deprotonation of **4.27** to give protonated 2-DMAP **4.23**.

5.2 Reaction of Pure 2-DMAP Disalt with 1-Methylindole

With the successful synthesis and isolation of 2-DMAP disalt **4.16** as a crystalline solid, the scope for testing its reactivity with a variety of nucleophiles was greatly expanded. One of the first efforts was in the development of **4.16** as a powerful reagent for the methylation of 1-methylindole.

Reaction of 1-methylindole **3.57** with 2-DMAP disalt **4.16** led to formation of 1,3-dimethyl-1*H*-indole **3.58** and 1-(1-methyl-1*H*-indol-3-yl)ethanone **5.3** (in a ratio of 5:1 by ^{1}H NMR, Scheme 5.8). Formation of 1,3-dimethyl-1*H*-indole **3.58** occurs as described previously (Scheme 5.3). A mechanism for the formation of **5.3** is also shown in Scheme 5.8. Methylation of acetonitrile by **4.16** produces nitrilium salt **5.10**, which can undergo attack by 1-methylindole **3.57** to give ketone **5.3** as previously shown (Scheme 5.5).

SCHEME 5.8: Proposed reaction of **4.16** and acetonitrile.

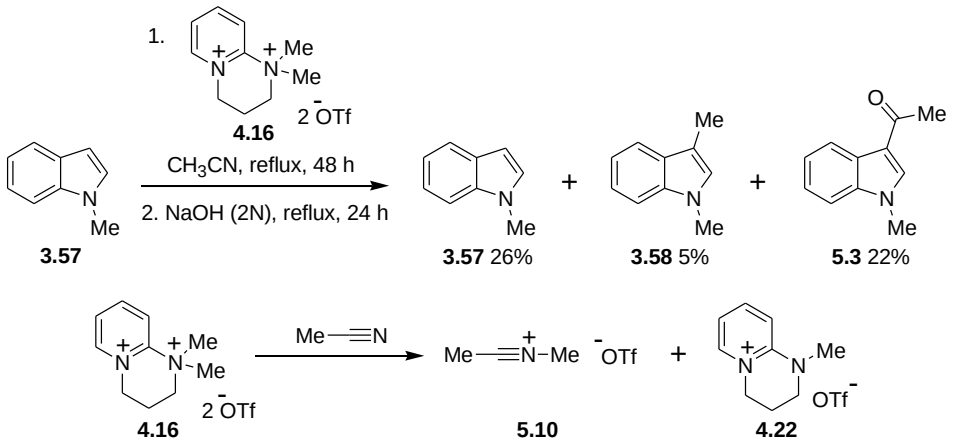

SCHEME 5.9: Reaction of **4.16** with nitriles.

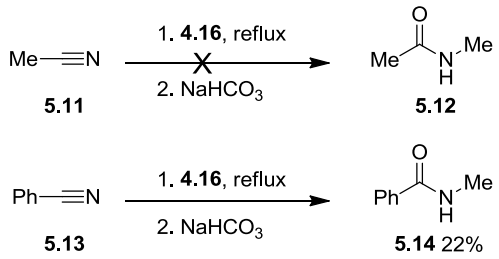

Disalt **4.16** was refluxed in an excess of acetonitrile for 18 h, then treated with saturated $NaHCO_3$ solution (Scheme 5.9). The expected product **5.12** would be formed from the methylation of acetonitrile to give nitrilium salt **5.10**, which would give amide **5.12** on hydrolysis. However, amide **5.12** was not isolated from the reaction mixture. When disalt **4.16** was refluxed in benzonitrile **5.13**, then treated with saturated $NaHCO_3$ solution (Scheme 5.9), expected amide product **5.14** was isolated in 22 % yield. Formation of **5.14** is believed to occur through methylation of benzonitrile to give a nitrilium salt, with subsequent hydrolysis to give amide **5.14**. Formation of **5.14** provides evidence that the methylation of nitriles may be achieved using disalt **4.16**, which could explain the formation of ketone **5.3** in the reaction with 1-methylindole **3.57** in acetonitrile (Scheme 5.8).

The formation of ketone **5.3** suggests that methylation of acetonitrile is being performed by 2-DMAP disalt **4.16**. However, it does highlight the difficulty in achieving the methylation of **3.57** in acetonitrile, as side-product formation from the reaction of **4.16** and the solvent poses a problem.

Removal of acetonitrile from the reaction mixture was the next logical step. 2-DMAP disalt **4.16** was reacted with an excess of 1-methylindole **3.57** (acting as solvent) at r.t. (Scheme 5.10). No reaction was observed at r.t. after 18 h, presumably due to solubility issues of the disalt in the organic indole, so the reaction mixture was heated to 60 °C. Again, after 24 h no reaction was observed, so the temperature was increased to 100 °C. This time ^{1}H NMR analysis showed evidence of reaction. GC-MS analysis of the reaction mixture showed evidence of formation of 1,3-dimethyl-1*H*-indole **3.58** and 1-methylindole dimer **5.15** as well as the presence of 1-methylindole **3.57**. Evidence of dimer species **5.15** was shown by a peak at RT 16.93

min, *m*/*z* 260. Identification of **5.15** by ^{1}H NMR analysis was hindered due to overlap with the proton signals of 1-methylindole **3.57**.

SCHEME 5.10: Neat reaction of **4.16** and **3.57**.

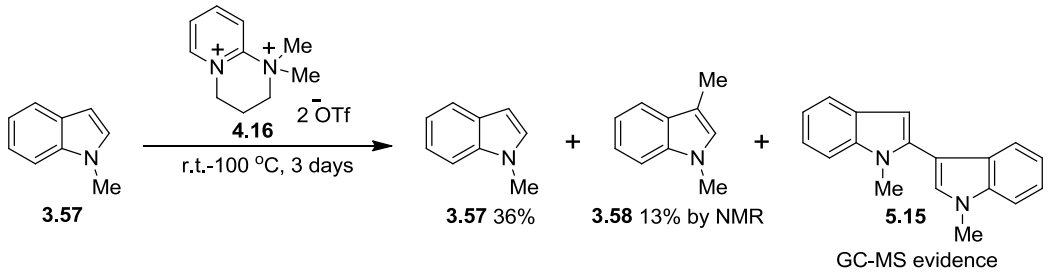

A proposed mechanism for the formation of dimer **5.15** is shown in Scheme 5.11. Methylation of 1-methylindole **3.57** by 2-DMAP disalt **4.16** gives rise to 1,3-dimethyl-1*H*-indole **3.58** and trifluoromethanesulfonic acid (TfOH) as shown previously (Scheme 5.3). The resulting acid can protonate **3.57** to form intermediate **5.16**. Subsequent attack by another molecule of 1-methylindole **3.57** gives rise to intermediate **5.17**. Exposure to air would rearomatise intermediate **5.17** to give dimer species **5.15**. The formation of dimer **5.15** was thought to be due to the excess of 1-methylindole **3.57** brought about by the use of neat conditions in the presence of acid. A solvent that the methylation reaction could occur in that would not react with 2-DMAP disalt **4.16** would be necessary for probing the reactivity of the superelectrophile dications.

SCHEME 5.11: Proposed mechanism for formation of dimer **5.15**.

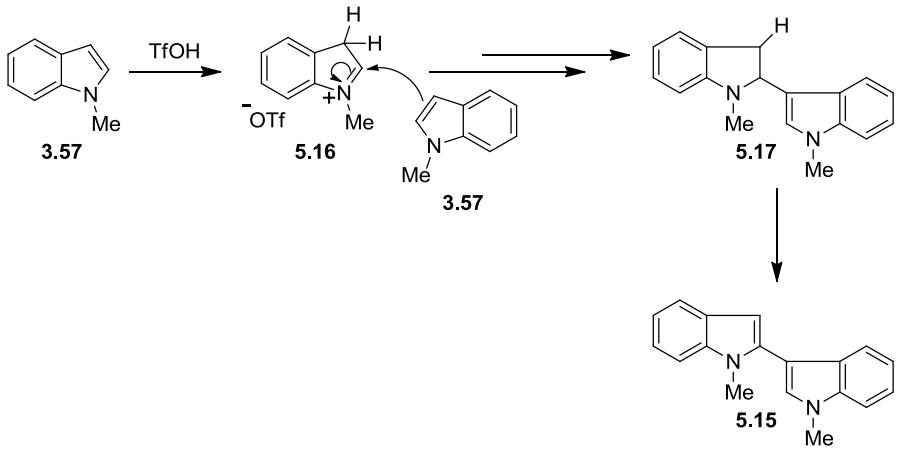

The use of acetonitrile as the reaction solvent was disadvantageous due to its reaction with **4.16**. In order to solve this problem, chlorobenzene was examined as a solvent in the reaction. Chlorobenzene was chosen as it was unlikely to undergo methylation by **4.16**, as chlorobenzene is known to be a poor substrate for Friedel-Crafts alkylation.[94]

In order to determine if reaction between **4.16** and chlorobenzene was possible, 2-DMAP disalt **4.16** was refluxed in dry chlorobenzene for 20 h. GC-MS analysis of the solution showed no evidence of methylation of chlorobenzene. With the inability of **4.16** to methylate chlorobenzene shown, the reaction of **4.16** with 1-methylindole **3.57** in chlorobenzene was examined (Scheme 5.12).

SCHEME 5.12: Reaction of **4.16** and **3.57** in chlorobenzene.

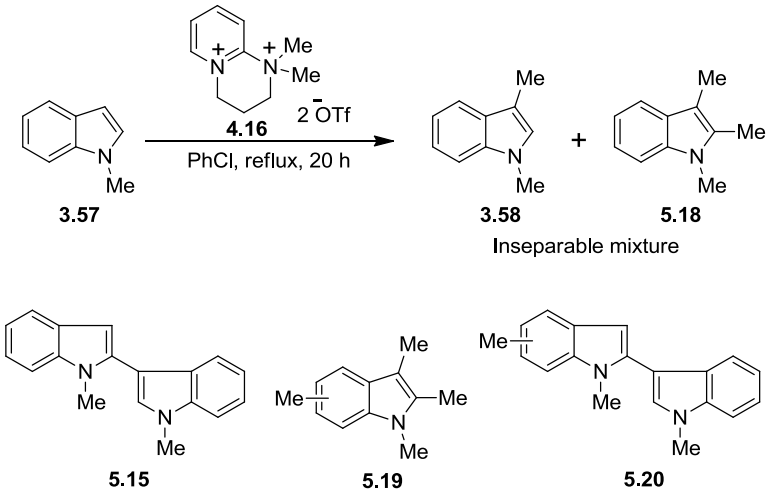

After 20 h refluxing in chorobenzene, GC-MS analysis of the reaction mixture showed peaks for 1,3-dimethyl-1*H*-indole **3.58** and 1,2,3-trimethyl-1*H*-indole **5.18** (RT 11.51 min *m*/*z* 159) as the major products and several peaks for minor products. These products were tentatively identified as 1-methylindole dimer **5.15** and polymethylated indoles **5.19** and **5.20** by their MS signals. Isolation of the reaction products gave 1,3-dimethyl-1*H*-indole **3.58** and 1,2,3-trimethyl-1*H*-indole **5.14** as an inseparable mixture (6 mg) in a ratio of ~3:1 by ^{1}H NMR.

In order to prevent the formation of dimer species **5.15**, the acid produced in the reaction would need to be removed. This produced the problem of finding a base that

could remove the acid, but would not react with disalt **4.16**. Use of a hindered tertiary nitrogen base would hopefully prevent demethylation of **4.16**. The first option considered was *N*,*N*-di-*iso*-propylethylamine **5.21**. However, reaction of 2-DMAP disalt **4.16** and *N*,*N*-di-*iso*-propylethylamine **5.21** led to demethylation of disalt **4.16** as shown by ^{1}H NMR and MS analysis. The next choice of hindered base was 2,6-di-*tert*-butylpyridine **5.23**. After refluxing in chlorobenzene for 18 h, only traces of methylated 2,6-di-*tert*-butylpyridine **5.24** were observed by MS analysis, and no evidence of **5.24** could be observed by ^{1}H NMR analysis of the reaction mixture (Scheme 5.13). This reaction showed that although disalt **4.16** could react with hindered base **5.23**, the reaction appeared to be very slow. In the presence of a more reactive substrate such as 1-methylindole **3.57**, the formation of **5.24** should not prove so significant as to preclude its use for trapping the acid formed in the reaction.

SCHEME 5.13: Reaction of disalt **4.16** with tertiary nitrogen hindered-nucleophiles.

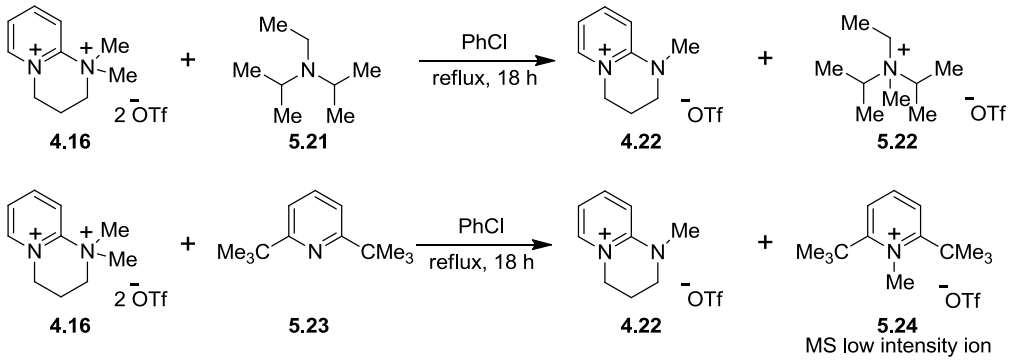

With a suitable solvent and base to prevent the formation of dimer **5.15**, the reaction of 2-DMAP disalt **4.16** and 1-methyindole **3.58** was carried out using a variety of conditions (Scheme 5.14, Table 5.1). Using 1 eq of disalt **4.16** led to a mixture of **3.57**:**3.58** in 88 % yield (yield based on 100 % conversion to 1-methylindole **3.58**) in a ratio of 70:30 by ^{1}H NMR (Table 5.1, entry 1). If 3 eq of disalt **4.16** was used, the ratio of products increased to 42:49:9 for **3.57**:**3.58**:**5.18** in a decreased yield of 82 % (Table 5.1, entry 2). When a decrease in solvent was used, the ratio of mono-methylated product **3.58** increased, but the total yield of product decreased (Table 5.1, entry 3).

SCHEME 5.14: Reaction of 2-DMAP disalt **4.16** and 1-methylindole **3.57**.

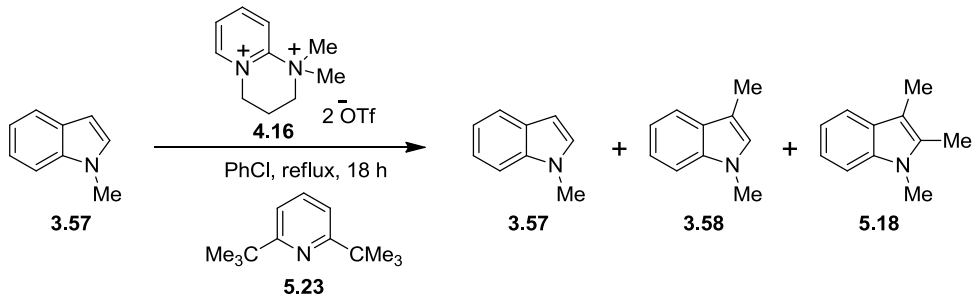

TABLE 5.1: Results for the reaction of 2-DMAP disalt **4.16** and 1-methylindole **3.57**.

Entry	**Eq of 4.16**	**Volume PhCl (mL)**	**Mass Recovery Organics[a] / %**	**^{1}H NMR Ratios / %**		
				3.57	**3.58**	**5.18**
1	1.0	5	88	70	30	-
2	3.0	20	82	42	49	9
3	3.0	15	72	39	54	7

[a]- Yield based on 1-methylindole **3.58** as product.T1's were not measured, so there may be errors in the integration of these signals.

The results showed that increasing the number of eq of **4.16** resulted in an increase of methylated products **3.58** and **5.18**. In addition, the amount of recovered material from the reaction decreased.

It has been shown that 2-DMAP disalt **4.16** can methylate 1-methylindole **3.57**. However, due to inherent problems with polymethylation and dimerisation of the indole, more suitable nucleophiles to probe the reactivity of **4.16** were sought.

5.3 Reaction with Different Nucleophiles

The reactivity of 2-DMAP disalt **4.16** with phosphorus-, nitrogen- and oxygen-nucleophiles was now investigated. We were keen to compare the reactivity of **4.16** to its monocation counterparts **1.169** and **1.170**, to see if the superelectrophile dication showed enhanced reactivity.

5.3.1 Synthesis of 2-DMAP Monocations

In order to examine the reactivity of dication **4.16** with respect to its monocation analogues, salts **1.169** and **1.170** would have to be synthesised. Reaction of 2-DMAP **1.1** and methyl trifluoromethanesulfonate led to the formation of trimethylpyridin-2-ylammonium trifluoromethanesulfonate **1.169**, which was recrystallised from the reaction mixture in 63 % yield (Scheme 5.15). 2-Dimethylamino-1-methyl-pyridinium trifluoromethanesulfonate **1.170** was also formed in the reaction, however, it could not be isolated from the reaction mixture.

The difficulty in the isolation of **1.170** from direct synthesis using 2-DMAP **1.1** required its synthesis from an indirect route. Methylation of 2-bromopyridine **1.171b** led to formation of pyridinium salt **5.25**. Reaction with dimethylamine solution led to exchange of the 2-bromo group with a 2-dimethylamino group to give monocation salt **1.170** (Scheme 5.15).

SCHEME 5.15: Synthesis of 2-DMAP monocations **1.169** and **1.170**.

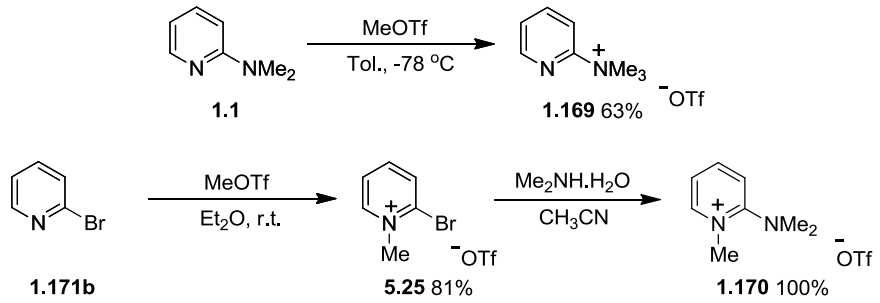

Comparison of the ^{1}H NMR aromatic proton signals of 2-DMAP disalt **4.16**, monocations **1.169** and **1.170** and 2-DMAP **1.1** shows some interesting features (Figure 5.1). All the aromatic protons in **4.16** show a significant downfield shift in comparison to the equivalent aromatic protons in **1.169** or **1.170**. For example, the signal for the furthest downfield aromatic proton for each salt comes at $\delta_H(CD_3CN)$ 8.81, 8.61 and 8.05 ppm for **4.16**, **1.169** and **1.170** respectively (Figure 5.1). Disalt **4.16** shows greater deshielding of the aromatic protons compared to monocation salts **1.169** and **1.170**, which is consistent with the increased positive charge present in this species.

FIGURE 5.1: ^{1}H NMR (CD_3CN) of aromatic protons of (a) **4.16**, (b) **1.169**, (c) **1.170**, (d) 2-DMAP **1.1**.

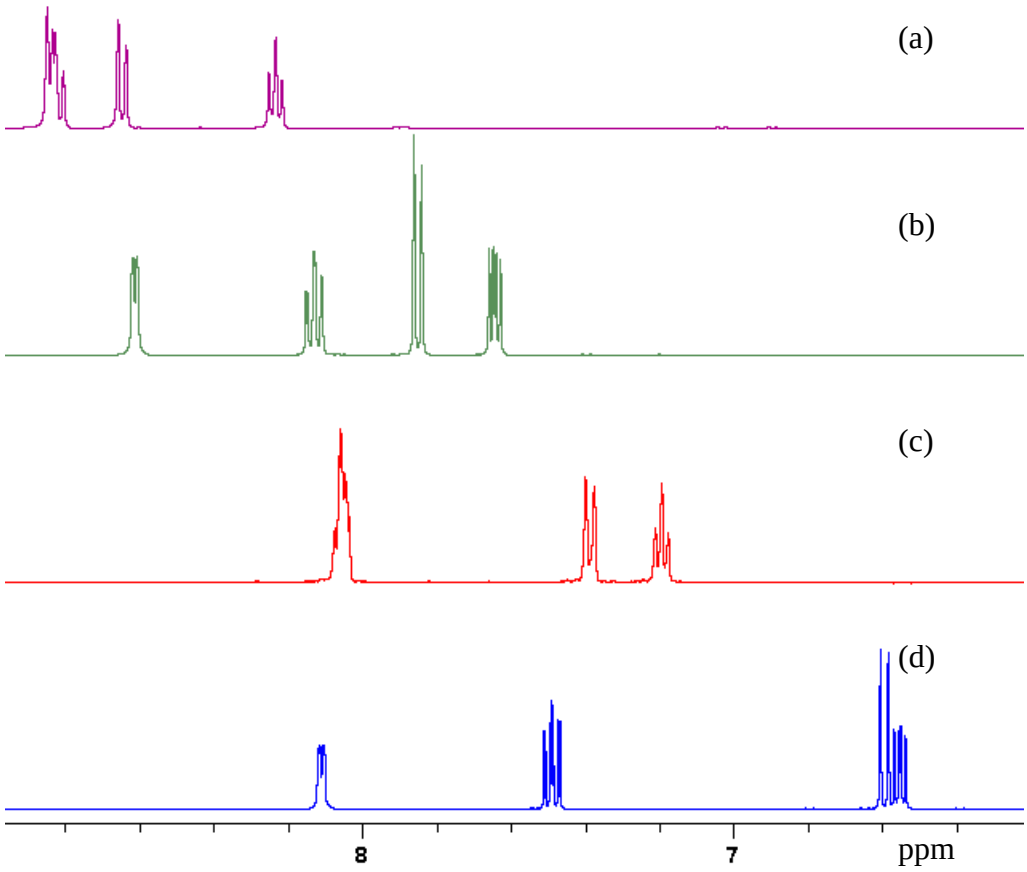

5.3.2 Reaction with Phosphorus Nucleophiles

With the three 2-DMAP salts synthesised, all three salts were reacted separately with triphenylphosphine **5.26** as a nucleophile in acetonitrile, or separately in chlorobenzene. In acetonitrile, 2-DMAP disalt **4.16** showed the highest reactivity with triphenylphosphine **5.26** (Scheme 5.16, Table 5.2, entry 1), with methylation to give **5.27** occurring in 97 % yield (demethylated dication **4.22** was also isolated in 95 % yield). Monocations **1.169** and **1.170** showed no reactivity with triphenylphosphine **5.26**, with no methylation being observed in acetonitrile (Table 5.2, entries 3 and 5). In chlorobenzene, the salts were reacted at reflux to ensure solubility of the salt in the solvent. In chlorobenzene, 2-DMAP disalt **4.16** again showed the highest reactivity with triphenylphosphine **5.26**, with methylated triphenylphosphine **5.28** isolated in 95 % yield (Table 5.2, entry 2). Monocation **1.169** exhibited some reactivity in chlorobenzene, with methylated

triphenylphosphine **5.28** isolated in 52 % yield (Table 5.2, entry 4). Monocation **1.170** showed no reactivity in chlorobenzene with 100 % recovery of triphenylphosphine **5.26**.

SCHEME 5.16: Reaction of 2-DMAP salts and triphenylphosphine **5.26**.

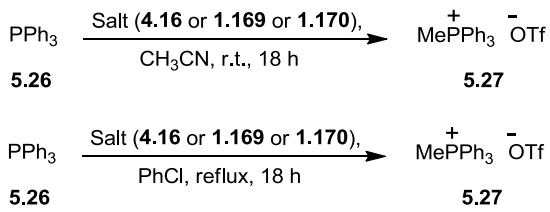

TABLE 5.2: Results of methylation of triphenylphosphine **5.22**.

Entry	**Salt**	**Solvent**	**T / °C**	**5.26 recovered / %**	**Salt Recovered (1.169 or 1.170) / %**	**Yield 5.27 / %**
1	**4.16**	CH_3CN	r.t.	0	0	97
2	**4.16**	PhCl	reflux	0	0	95
3	**1.169**	CH_3CN	r.t.	96	98	0
4	**1.169**	PhCl	reflux	29	29	52
5	**1.170**	CH_3CN	r.t.	90	84	0
6	**1.170**	PhCl	reflux	100	67	0

The results show that in acetonitrile, superelectrophile 2-DMAP disalt **4.16** showed significantly enhanced reactivity over its monocation counterparts **1.169** and **1.170**. In chlorobenzene, 2-DMAP disalt **4.16** showed greater reactivity than monocation **1.169**, with almost complete methylation of PPh_3 **5.26** with disalt **4.16**, compared to 52 % with monocation **1.169** after 18 h. Methyl transfer by monocation **1.169** showed different reactivity for this salt than usually observed for this species, where substitution of the NMe_3 group is more common (Scheme 1.28 and 1.44). 2-Dimethylamino-1-methylpyridinium trifluoromethanesulfonate **1.170** showed no ability to transfer a methyl group in acetonitrile or chlorobenzene. These results show that the superelectrophilic activation of **4.16**, resulting from the dipositive charge, leads to enhanced reactivity over singly-charged 2-DMAP salts **1.169** and **1.170**.

5.3.3 Reaction with Nitrogen Nucleophiles

With the enhanced reactivity of superelectrophile **4.16** over its monocation counterparts determined, we wished to compare its reactivity to commercially available methylating reagents iodomethane, dimethyl sulfate and methyl trifluoromethanesulfonate in the methylation of triethylamine **5.28** (Scheme 5.17).

SCHEME 5.17: Reaction of methylating reagents with triethylamine **5.28**.

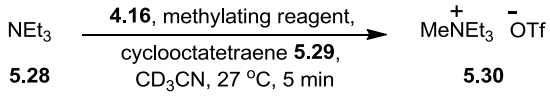

TABLE 5.3: Competitive methylation study of triethylamine **5.28** with disalts **4.16** and **4.30** at 27 °C in CD_3CN.

Entry	**Disalt Used**	**Methylating Reagent (MR)**	**Amount Remaining[a] / %**	
			Disalt	**MR**
1	**4.16**	MeI	0[b]	100[c]
2	**4.16**	Me_2SO_4	53[b]	59[d]
3	**4.16**	MeOTf	94[b]	0[e]
4	**4.30**	Me_2SO_4	23[f]	70[d]

[a] All proton signal integrations were taken relative to 1,3,5,7-cyclooctatetraene **5.29** $\delta_H(CD_3CN)$ 5.77 ppm set at 1.000. All experiments were carried out in CD_3CN. Amount remaining calculated from finishing proton integration as a percentage of starting proton integration. [b] Proton signal for Me groups at $\delta_H(CD_3CN)$ 3.84 ppm used. [c] Proton signal for Me group at $\delta_H(CD_3CN)$ 2.09 ppm used. [d] Proton signal for Me groups at $\delta_H(CD_3CN)$ 3.94 ppm used. [e] Proton signal for Me group at $\delta_H(CD_3CN)$ 4.27 ppm used. [f] Proton signal for Me groups at $\delta_H(CD_3CN)$ 3.85 ppm used.

Each individual methylating reagent and disalt **4.16** were reacted in a 1:1 competition reaction. Equimolar solutions of **4.16** (1 eq) and each separate commercial methylating reagent (1 eq) were treated with triethylamine **5.24** (1 eq). Using 1,3,5,7-cyclooctatetraene **5.29** as an internal non-reacting NMR standard, the quantities of each methylating reagent (**4.16**, iodomethane, dimethyl sulfate or MeOTf) before and after the reaction with triethylamine **5.28** in each competition reaction were determined by ^1H NMR analysis.

Triethylamine **5.28** was used as the reacting nucleophile as it was found that **5.28** reacted with 2-DMAP disalt **4.16** almost instantaneously in acetonitrile. Cyclooctatetraene **5.29** was used as a non-reacting NMR internal standard as it was shown that reaction between 2-DMAP disalt **4.16** and acetonitrile could occur (Scheme 5.8). The results of the competition reactions are shown in Table 5.3.

Figure 5.2 shows an example of the competition reaction between **4.16** and dimethyl sulfate. In red, the ^{1}H NMR spectrum shows the methylating reagents before the addition of triethylamine **5.28**. The spectrum in blue shows the ^{1}H NMR spectrum after the addition of triethylamine **5.28** with a decrease in the methyl signals of the two methylating reagents being observed.

FIGURE 5.2: ^{1}H NMR spectra for competition reaction between **4.16** and dimethyl sulfate.

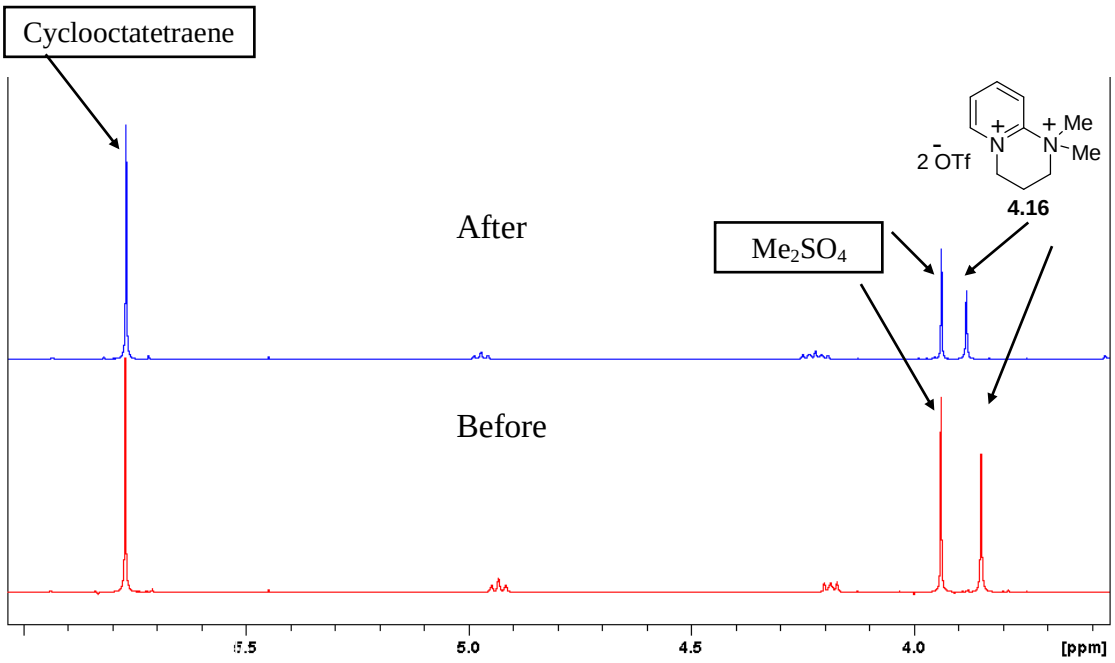

As can be seen from the results, disalt **4.16** was shown to be a far more powerful methylating reagent than iodomethane (Table 5.3, entry 1), with 100 % of iodomethane being present 5 min after the addition of triethylamine **5.28**. Disalt **4.16** even shows slightly higher reactivity than dimethyl sulfate (Table 5.3, entry 2), with 47 % and 41 % of **4.16** and dimethyl sulfate being consumed respectively. In the case of methyl trifluoromethanesulfonate (Tabel 5.3, entry 3), the high reactivity of this

potent methylating reagent is shown, with virtually no demethylation of disalt **4.16** observed.

To test the methylating ability of 2-dimethylaminopyrimidine disalt **4.30**, the competitive methylation of triethylamine **5.28** with dimethyl sulfate was examined. The results (Table 5.3, entry 4) showed that pyrimidine disalt **4.30** was a far more powerful methylating reagent than dimethyl sulfate with 23 % and 70 % of the methylating reagents remaining, respectively, after the addition of triethylamine **5.28**. Correspondingly, disalt **4.30** based on 2-dimethylaminopyrimidine **4.31** was shown to be a more powerful methylating reagent than 2-DMAP disalt **4.16**.

SCHEME 5.18: Reaction of 2-DMAP disalt **4.16** and *N*,*N*-di-*iso*-propylethylamine **5.21**.

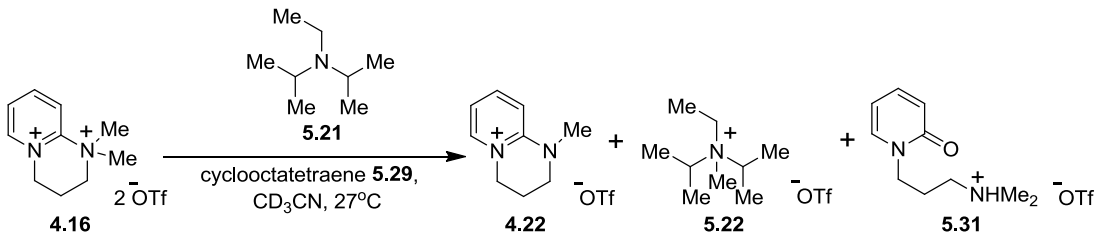

FIGURE 5.3: Plot of relative integral vs. time for reaction of disalt **4.16** and *N*,*N*-di*iso*propylamine **5.21**.

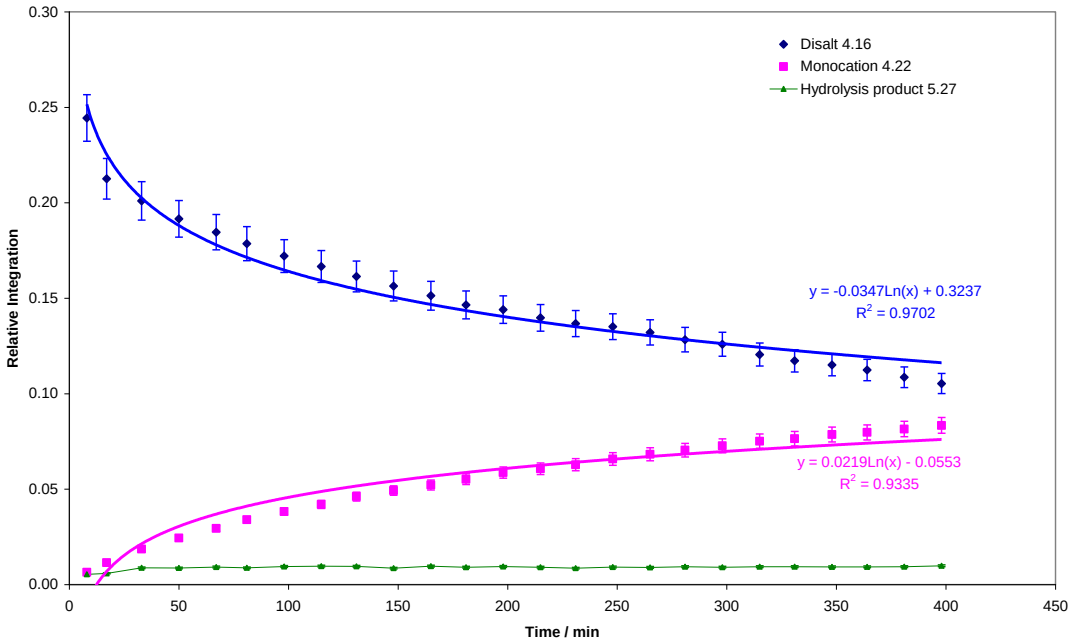

In order to determine the kinetics of reactivity of disalt **4.16**, its reaction with *N*,*N*-di-*iso*-propylethylamine **5.21** was followed by NMR. Reaction of **4.16** with **5.21** gave rise to monocation **4.22** and methylated product **5.22** (Scheme 5.18). The reaction also gave rise to hydrolysis product **5.31**, thought to occur by attack of adventitious water on disalt **4.16** (identification of and the mechanism of formation of **5.31** will be discussed in Section 5.3.4). Again, using 1,3,5,7-cyclooctatetraene **5.29** as an internal standard for the integrations, the relative proton intensities for disalt **4.16**, monocation **4.22** and hydrolysis product **5.29** were monitored (Figure 5.3).

For the second order reaction of reactants A and B to give product P (5.1), the rate equation is given by (5.2).[95]

$$A + B \longrightarrow P \qquad (5.1)$$

$$\frac{d[P]}{dt} = k[A][B] \qquad (5.2)$$

Integration of (5.2) is solved to give (5.3), where k is the rate constant and t is the time. A plot of $[1/([B]_0-[A]_0)]Ln([A]_0[B]/[B]_0[A])]$ with respect to time gives the rate constant for the reaction as the gradient of the straight line. However, in the case where $[A]_0=[B]_0$, this would result in unsolvable equation (5.4).

$$\left(\frac{1}{[B]_0 - [A]_0}\right)\ln\left(\frac{[A]_0[B]}{[A][B]_0}\right) = kt \qquad (5.3)$$

$$\left(\frac{1}{[B]_0 - [A]_0}\right) = \frac{1}{0} \qquad (5.4)$$

Under these circumstances, it is assumed that [A]=[B], so the rate equation (5.5) and integration (5.6) changes. In the form y = mx + c, (5.6) becomes (5.7). Therefore, a plot of 1/[A] against time gives a straight line of gradient k.

$$\frac{-d[A]}{dt} = k[A]^2 \qquad (5.5)$$

$$\frac{1}{[A]} - \frac{1}{[A]_0} = kt \qquad (5.6)$$

$$\frac{1}{[A]} = kt + \frac{1}{[A]_0} \qquad (5.7)$$

For the reaction of **4.16** and **5.21**, (5.5) must be used to determine the rate equation as the initial concentrations of **4.16** and **5.21** are the same. In the reaction, the equation is simplified by excluding the formation of hydrolysis product **5.31** from the rate equation. This is a reasonable assumption as the concentration of **5.31** remains approximately constant after the first few data points (Figure 5.3). When plotted as a second order reaction (Figure 5.4), a straight line was obtained giving a rate constant of 3 x 10^{-4} $M^{-1}s^{-1}$ at 27 °C.

FIGURE 5.4: 1st order kinetic plot for the reaction of **4.16** and **5.21** at 27 °C.

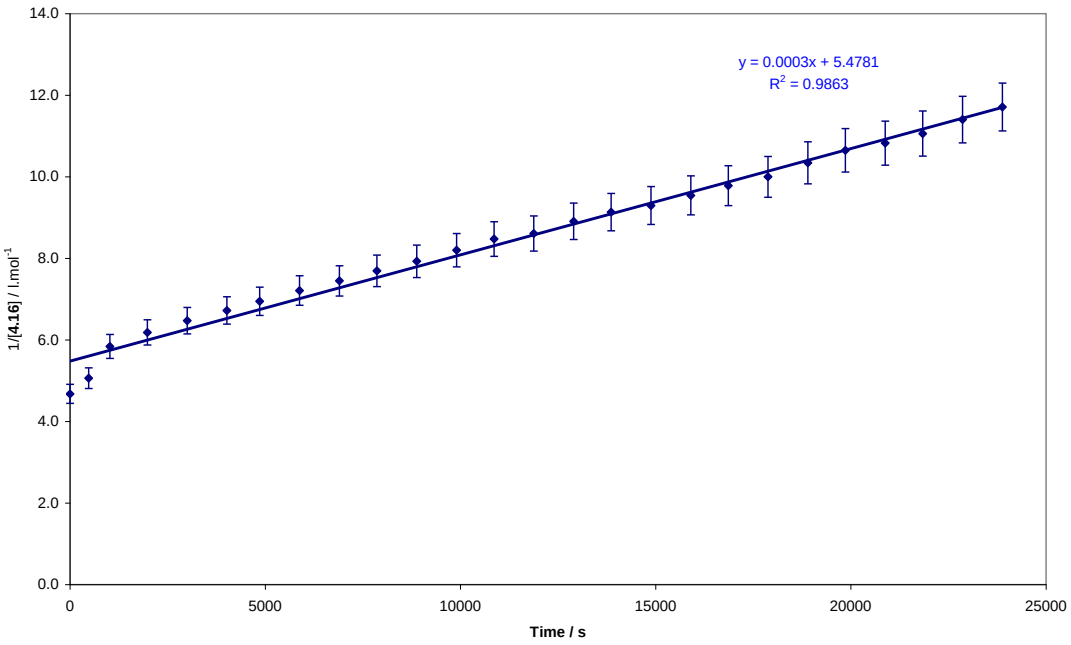

For a comparison with the kinetics of other methyl transfer reactions reported in the literature, Castejon and Wiberg measured the kinetics of the reaction of pyridine and bromomethane.[96] They calculated the rate constant to be 2.04 x 10^{-4} $M^{-1}s^{-1}$ in acetonitrile at 25 °C.

The high reactivity of superelectrophile disalts **4.16** and **4.30** in the reaction with nitrogen nucleophiles has been shown. The disalts have shown greater reactivity than dimethyl sulfate in the methylation of triethylamine **5.28**.

5.3.4 Reaction with Oxygen Nucleophiles

Hydrolysis of disalts **4.16** and **4.30** has been previously observed, indicating their reactivity with oxygen-nucleophiles.

In the reaction of 2-DMAP disalt **4.16** with *N*,*N*-di-*iso*-propylethylamine **5.21**, minor NMR peaks were observed that were not due to **4.22** or **5.18**. These peaks were attributed to formation of **5.31** (Scheme 5.19), a hydrolysis product of 2-DMAP disalt **4.16**. Pyridone **5.31** was identified by the upfield shift in its $C_{sp}{}^2$-H protons relative to 2-DMAP salts **4.16**, **1.169** or **1.170**, indicative of a neutral species and a ^{13}C NMR signal at δ_C(d_6-DMSO) 161.8 ppm resulting from the carbonyl carbon of the pyridone group. In addition, MS analysis showed a peak at *m*/*z* 181 $[M\text{-}OTf]^+$, consistent with the proposed hydrolysis product.

SCHEME 5.19: Hydrolysis of 2-DMAP disalt **4.16**.

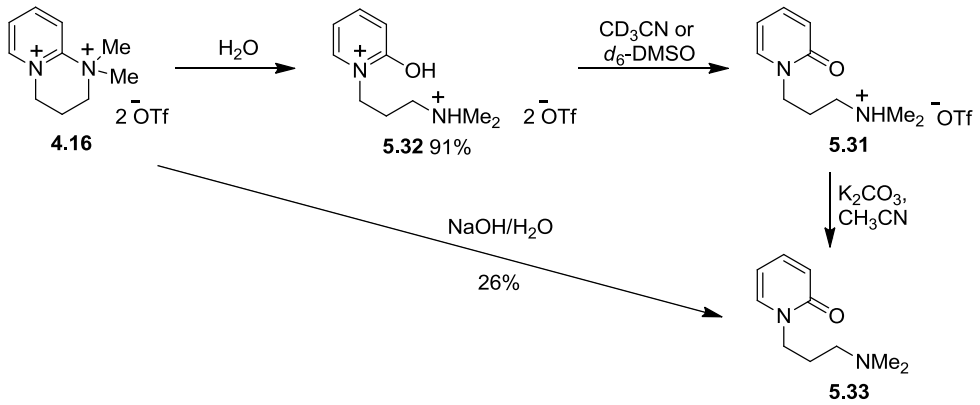

Formation of pyridone **5.31** in the kinetic study was believed to occur through the attack of adventitious water on disalt **4.16**. In order to test this theory, a sample of 2-DMAP disalt **4.16** was stirred in water (Scheme 5.19). Hydrolysis of 2-DMAP disalt **4.16** with water gave rise to hydroxypyridinium salt **5.32**. This was shown by the ^{13}C NMR signals for **5.32**, which were comparable to ring-methylated salt **1.169** (Table 5.4, entries 1 and 3 respectively).

SCHEME 5.20: Selected compounds for NMR comparison.

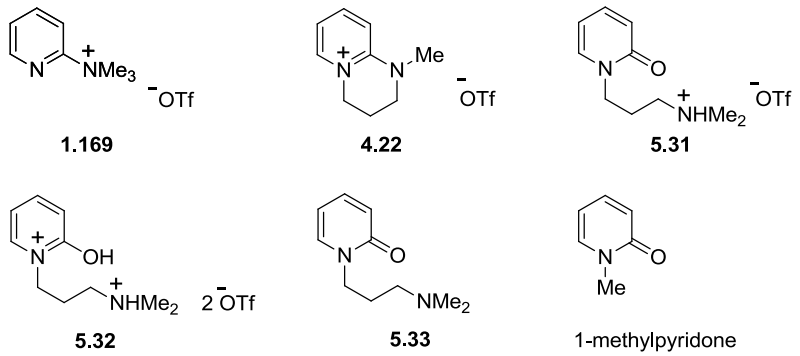

TABLE 5.4: NMR comparison of selected peaks of disalt hydrolysis products.

Entry	Compound	^{1}H NMR signals / ppm	^{13}C NMR signals / ppm
1	**1.169**	7.19, 7.39, 8.03-8.08[a]	117, 118, 143, 144, 159[a]
2	**5.31**	6.28, 6.46, 7.45, 7.68[b]	106, 120, 139, 140, 162[b]
3	**5.32**	7.35, 7.46, 8.15, 8.23[a]	116, 119, 142, 149, 161[a]
4	**5.33**	6.21, 6.36, 7.40, 7.64[b]	105, 120, 139, 140, 162[b]
5	1-methyl-pyridone	6.17, 6.54, 7.34, 7.35[c]	106, 120, 139, 140, 163[c]

[a] CD_3CN used as NMR solvent [b] d_6-DMSO used as NMR solvent [c] $CDCl_3$ used as NMR solvent.

Hydroxypyridinium salt **5.32** shows downfield ^{1}H NMR signals consistent with a ring-alkylated pyridinium compound. Comparison of the methylene protons in **5.32** with salt **4.22** shows similar ^{1}H NMR signals at $\delta_H(CD_3CN)$ 4.36, 3.17 and 2.25 ppm compared to $\delta_H(CD_3CN)$ 4.27, 3.55 and 2.15 ppm respectively. The slightly greater downfield shift in the methylene signal at ~ 2.2 ppm and splitting of the methyl signal to a doublet (J(H,H)= 5.2 Hz) in **5.32** suggests that the dimethylamino nitrogen is protonated. A broad singlet is observed at $\delta_H(CD_3CN)$ ~7.45 ppm, which could be due to either the proton of the OH group in the hydroxypryidinium ring or proton on the dimethylamino group nitrogen. A crystal structure was also obtained for hydroxypyridinium salt **5.32** (Figure 5.5), confirming the spectroscopically-determined structure.

Interestingly, over a period of several days in CD_3CN or instantly upon the addition of d_6-DMSO, hydroxypyridinium salt **5.32** is converted to pyridone salt **5.31**. This is shown by an upfield shift in the corresponding ring proton signals and ring carbon signals. Comparison of the NMR spectra of pyridone salt **5.31** and 1-methylpyridone[97] show very similar values for the relevant signals in the ^{1}H NMR and ^{13}C spectra (Table 5.4, entries 2 and 5 respectively).

FIGURE 5.5: (a) ORTEP diagram of pyridinol salt **5.32** cation. (b) ORTEP diagram of pyridinol salt **5.32** (cation and two anions).

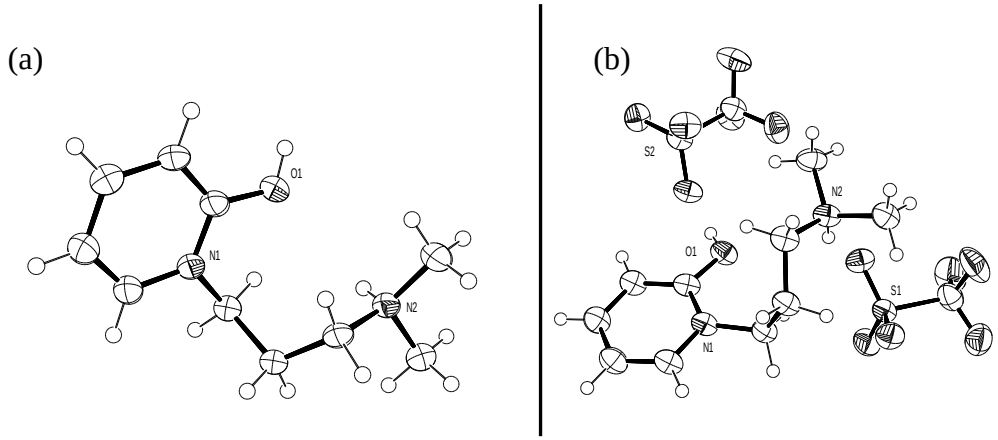

The proposed mechanisms for the formation of hydroxypyridinium **5.32** and pyridone **5.31** are shown in Scheme 5.21. Attack of water on disalt **4.16** gives rise to new disalt intermediate **5.30**. Proton transfer from oxygen to nitrogen leads to formation of hydroxypyridinium salt **5.32** as shown. This product can then be converted to pyridone salt **5.31** by loss of a proton.

As hydroxide ions may be present in the kinetic reaction, formed *in situ* from the reaction of traces of water and *N*,*N*-di-*iso*-propylethylamine **5.21**, a sample of **4.16** was also stirred in saturated NaOH solution (Scheme 5.18). Reaction of 2-DMAP disalt **4.16** with saturated sodium hydroxide solution led to the formation of pyridone **5.33**. The absence of the protonated nitrogen is shown by the upfield shift in the methyl and methylene protons of **5.33** compared to **5.31**. Pyridone **5.33** shows methylene protons at δ_H(d_6-DMSO) 1.79, 2.34 and 3.88 ppm compared to δ_H(d_6-DMSO) 2.04, 3.05 and 3.93 ppm for pyridone **5.31**. The methyl protons in **5.33** appear as a singlet at δ_H(d_6-DMSO) 2.24 ppm and as a doublet at δ_H(d_6-DMSO) 2.78

ppm (J(H,H)= 5.0 Hz) for pyridone salt **5.31**. Conversion of pyridone salt **5.31** to pyridone **5.33** was simply achieved by treating the former with base (Scheme 5.19). The mechanism of formation of **5.33** is shown in Scheme 5.20. For the reaction with hydroxide, direct attack in the 2-position by a hydroxide ion leads to formation of hydroxypyridinium salt **5.35** which would undergo immediate attack by hydroxide to give pyridone **5.33** (Scheme 5.21).

SCHEME 5.21: Mechanism of formation of hydrolysis products of **4.16**.

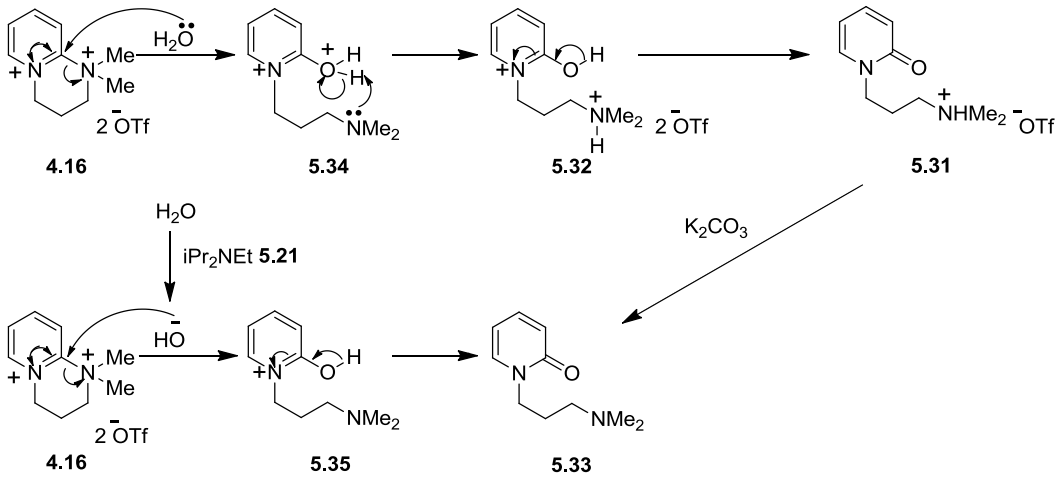

SCHEME 5.22: Hydrolysis of disalt **4.30**.

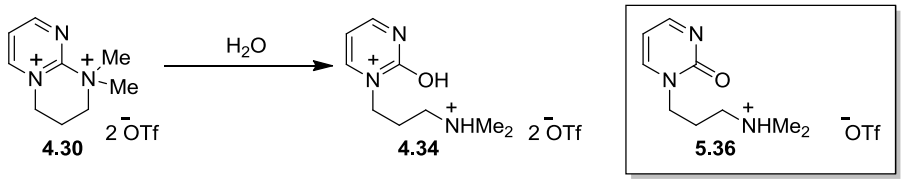

Unexpectedly, hydrolysis of 2-dimethylaminopyrimidine disalt **4.30** with water gave rise to hydroxypyrimidinium **4.34** rather than the corresponding pyrimidone **5.36** as in the case of 2-DMAP disalt **4.16** (Scheme 5.22). This is shown by the ^{1}H NMR signals for the aromatic protons of **4.34** at δ_H(d_6-DMSO) 6.91 and 8.83 ppm, further downfield than would be expected for a pyrimidone-type species. In addition, the ^{13}C NMR shows a peak at δ_C(d_6-DMSO) 149.6 ppm, further upfield than would be expected for a carbonyl carbon of a pyrimidone. No conversion of hydroxyl-pyrimidinium **4.34** to pyrimidone **5.36** is observed. Formation of **4.34** is envisioned to occur by a similar mechanism as for the formation of **5.31** (Scheme 5.21). Disalt

4.30 shows significantly enhanced reactivity towards oxygen nucleophiles relative to disalt **4.16**; disalt **4.30** is immediately converted to hydroxypyrimidinium **4.34** upon adding to undried d_6-DMSO, whereas disalt **4.16** takes several days to be fully hydrolysed in water.

It has been shown that 2-DMAP disalt **4.16** shows enhanced reactivity over its monocationic counterparts **1.169** and **1.170**, as per the definition of a superelectrophile. In addition, disalts **4.16** and **4.30** have shown greater reactivity than iodomethane and dimethyl sulfate in the methylation of triethylamine **5.28**. The reactivity towards oxygen nucleophiles has also been examined, with disalts **4.16** and **4.30** showing different products upon hydrolysis with water.

6 Polycation Superelectrophiles

With superelectrophile disalts **4.16** and **4.30** synthesised, our next aim was to develop more powerful superelectrophilic species based on the 2-DMAP unit. It was thought that a salt with additional cations in or around the heterocycle would make such a molecule less stable, and hence more reactive. Towards this end, a variety of polycationic molecules were envisioned as targets for synthesis (**6.1**-**6.3**, Scheme 6.1).

SCHEME 6.1: Targeted polycations for synthesis.

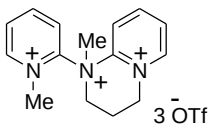

6.1

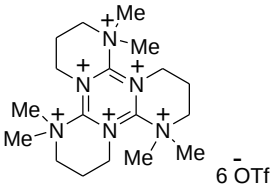

6.2

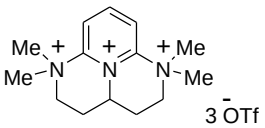

6.3

6.1 Dipyridinium Trication

The formation of trication **6.1** was devised as proceeding through reaction of 1,3-ditriflate **4.15** and pyridinium salt **6.4**, itself a coupling product of pyridinium salt **6.5** and 2-methylaminopyridine **6.6** (Scheme 6.2).

SCHEME 6.2: Retrosynthesis for trication **6.1**.

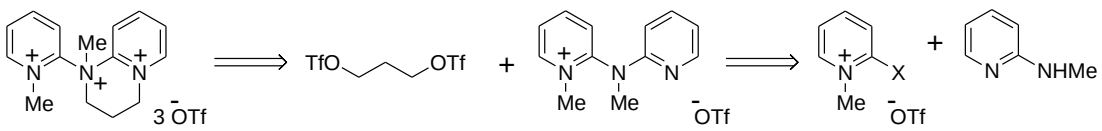

6.1 **4.15** **6.4** **6.5** **6.6**

The first stage was the synthesis of pyridinium salt **6.7**. This was achieved by the reaction of 2-bromopyridine **1.171b** and iodomethane. The resulting salt was isolated as a mixture of 2-bromo-1-methylpyridinium and 2-iodo-1-methylpyridinium as identified by ^{1}H and ^{13}C NMR (Scheme 6.3).

SCHEME 6.3: Synthesis of 2-halo-1-methylpyridinium **6.7**.

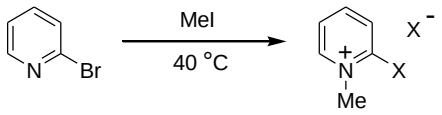

1.171b **6.7** X = I,Br

Reaction of pyridinium salt **6.7** with 2-methylaminopyridine **6.6** was first carried out in refluxing acetonitrile (Scheme 6.4). The reaction gave a mixture of products, with MS analysis showing a peak at *m*/*z* 200, consistent with the expected product $[M\text{-}X]^{+}$. Recrystallisation of the reaction mixture gave only 2-iodo-1-methylpyridinium iodide **6.8** in 12 % yield.

With direct substitution not effective, the next method of coupling was based on the work of Xiao *et al*.[98] and Buchwald *et al*.[99] in the Pd/BINAP-catalysed amination of aryl bromides. Pyridinium salt **6.7** and 2-methylaminopyridine **6.6** were reacted under the same palladium coupling conditions described (Scheme 6.4). ^{1}H NMR and MS analysis of the reaction mixture provided evidence of formation of the desired product. However, the product could not be isolated by recrystallisation or anion exchange.

SCHEME 6.4: Attempted coupling of pyridinium salt **6.7** by nucleophilic attack and palladium coupling.

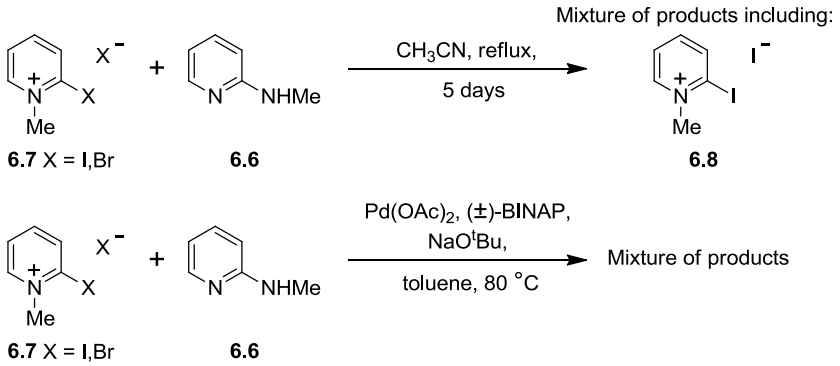

6.7 X = I,Br **6.6** **6.8**

6.7 X = I,Br **6.6**

At this stage, a better pyridinium salt than **6.7** was sought, as having only a single species would simplify analysis of the reaction mixture. Also, substitution of chloride by 2-methylaminopyridine **6.6** would be easier than for iodide or bromide. Towards this end, 2-chloro-1-methylpyridinium trifluoromethanesulfonate **6.10** was synthesised from 2-chloropyridine **6.9** (Scheme 6.5).[100] Reaction of pyridinium salt **6.10** with 2-methylaminopyridine **6.6** led to formation of pyridinium salt **6.4** and possible formation of pyridinium salt **6.11** (*m*/*z* = 263) (Scheme 6.6). The two salts could not be separated by recrystallisation. Pyridinium salt **6.11** could be formed by the demethylation of **6.4** by chloride present in the reaction mixture, then subsequent reaction with 2-chloro-1-methylpyridinium trifluoromethanesulfonate **6.10** to give a species such as **6.13**, with demethylation to give side-product **6.11** (Scheme 6.6).

SCHEME 6.5: Synthesis of pyridinium triflate **6.4**.

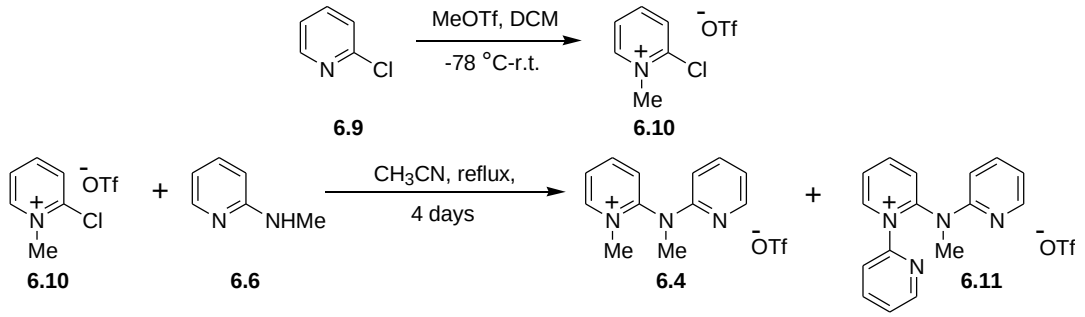

SCHEME 6.6: Proposed mechanism for formation of salt **6.11**.

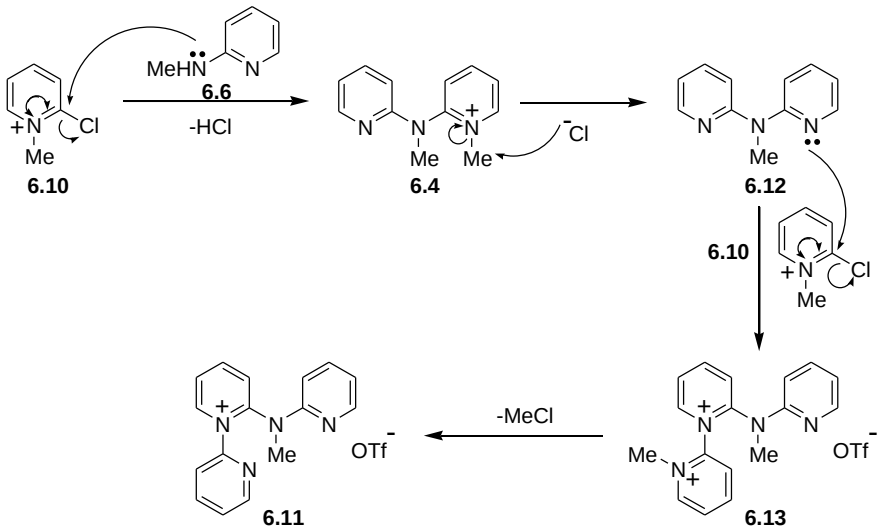

Formation of side-product **6.11** was obviously undesirable. Trapping of the chloride ions in the reaction mixture would hopefully prevent the formation of **6.11**. For this reason, the reaction was repeated in the presence of silver tetrafluoroborate to trap the free chloride produced (Scheme 6.7). After 5 days at reflux, the reaction mixture showed ~50 % conversion to product **6.4**, with no further conversion occurring after 6 days. This was attributed to protonation of the starting 2-methylaminopyridine **6.6** by HCl produced during the reaction. This protonated pyridine **6.14** would not undergo reaction with the pyridinium salt **6.10** to form the expected product. In order to prevent the reaction stopping due to protonation of the starting material, the reaction was repeated with the addition of proton sponge. This time the reaction was successful and pyridinium salt **6.4** was produced as the only product in 63 % yield (Scheme 6.7).

SCHEME 6.7: Synthesis and isolation of pyridinium salt **6.4**.

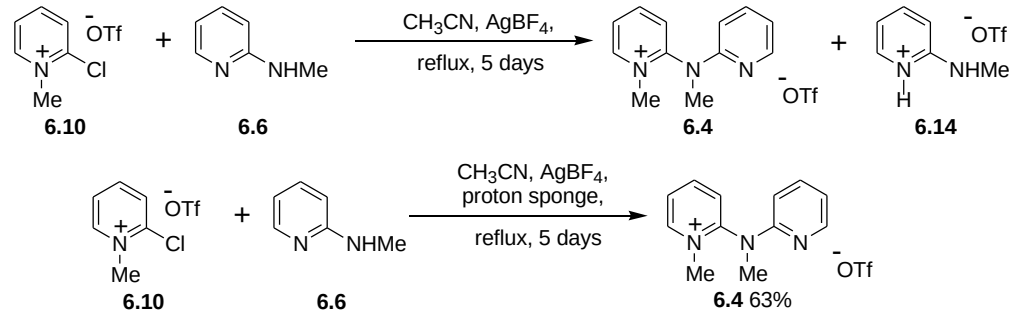

With pyridinium salt **6.4** in hand, synthesis of trisalt **6.1** was attempted (Scheme 6.8). Reaction of salt **6.4** with ditriflate **4.15** was carried out using analogous conditions for the synthesis of 2-DMAP disalt **4.16**. After stirring overnight at r.t., MS analysis of the reaction mixture showed starting material only. The reaction mixture was then heated to reflux for 5 h. Again, MS analysis of the reaction mixture showed only a signal at *m*/*z* = 200 for starting salt **6.4**. Despite several attempts to synthesise trication **6.1**, no spectroscopic evidence for the formation of **6.1** was observed. The unsuccessful reaction was attributed to the difficulty of adding another positive charge to an already cationic system.

SCHEME 6.8: Attempted synthesis of trication **6.1**.

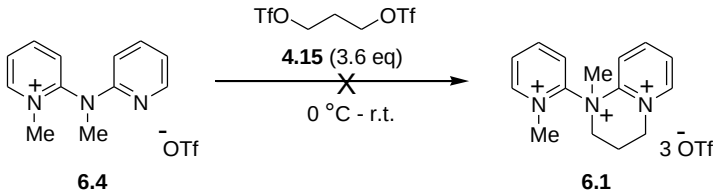

6.2 Hexacation Superelectrophile

Polycation **6.2** was to be synthesised from the reaction of ditriflate **4.15** and triazine **6.15** (Scheme 6.8).

SCHEME 6.8: Retrosynthetic synthesis for hexacation **6.2**.

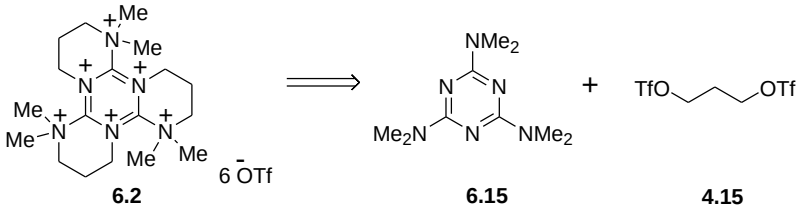

Based on the work of Arya and Dandia,[101] triazine **6.15** was readily synthesised from 2,4,6-trichloro-[1,3,5]-triazine **6.14** and dimethylamine using molecular sieves and microwave heating (Scheme 6.9).

SCHEME 6.9: Synthesis of triazine **6.14**.

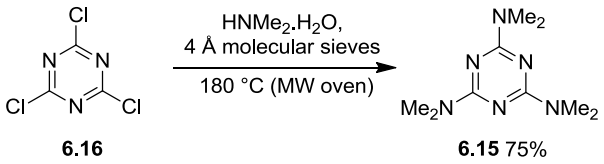

SCHEME 6.10: Synthesis of triazine disalt **6.17**.

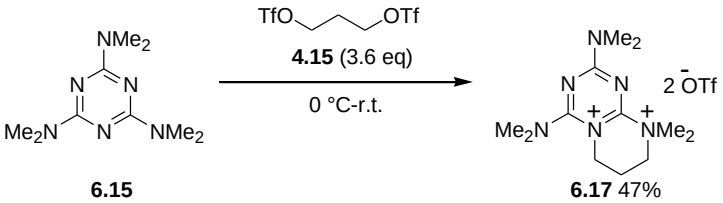

The first attempted synthesis of hexacation **6.2** was based on the method for synthesising 2-DMAP disalt **4.16**. Reaction of **6.15** with 3.6 eq of ditriflate **4.15** gave

disalt **6.17** as the only product (Scheme 6.10). ^{1}H and ^{13}C NMR analysis showed the appropriate peaks for disalt **6.17**. MS analysis did not show the dication peak for **6.17**, but did show a peak at *m*/*z* 401 $[M\text{-}OTf]^{+}$.

The reaction was then repeated, this time with the addition of amine **6.15** to 10 eq of ditriflate **4.15** at r.t. Unfortunately, the reaction proceeded again to give only disalt **6.17**. The reaction was repeated, with heating of the reaction mixture to 60 °C after addition of amine **6.15** at r.t. However, even after heating for 6 days, analysis of the reaction mixture by MS showed only peaks for amine **6.15** (*m*/*z* = 211) and dication **6.17** (*m*/*z* = 401 $[M\text{-}OTf]^{+}$).

At this stage, the further reaction of disalt **6.17** was investigated. A solution of disalt **6.17** and ditriflate **4.15** (5 eq) in dry acetonitrile was heated to reflux for 18 h (Scheme 6.11). MS analysis of the reaction mixture showed the major peak to be *m*/*z* 237, consistent with demethylated disalt **6.18** $[M\text{-}OTf]^{+}$, most likely formed by the attack of solvent on disalt **6.17**. No evidence of the addition of more than one ditriflate **4.15** to the triazine was observed. At this stage the synthesis of hexacation **6.2** was stopped, to investigate the synthesis of other polycation species.

SCHEME 6.11: Attempted synthesis of hexacation **6.2**.

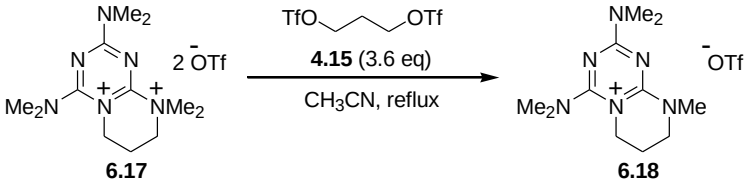

6.3 *N*,*N*,*N*′,*N*′-Tetramethylpyridine-2,6-diamine Trication

Trication **6.3** was based on 2-DMAP disalt **4.16** with an additional dimethylammonium group in the 6-position. In order to synthesise trication **6.3**, amine **6.19** and tritriflate **6.20** would need to be synthesised (Scheme 6.12).

SCHEME 6.12: Retrosynthetic scheme for trication **6.3**.

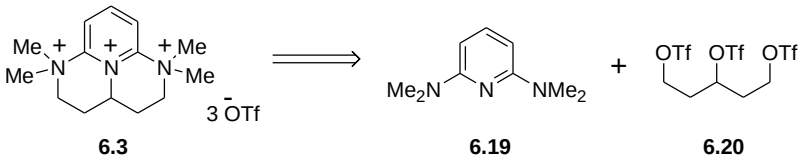

6.3 **6.19** **6.20**

6.3.1 Synthesis of N,N,N′,N′-Tetramethylpyridine-2,6-diamine

The first attempt at synthesis of *N,N,N′,N′*-tetramethylpyridine-2,6-diamine **6.19** was using the same procedure as in the synthesis of 2-dimethylaminopyrimidine **4.31** (Scheme 4.20). Reaction of 2,6-dibromopyridine **6.21** with dimethylamine solution (40% in H_2O) in acetonitrile led to an inseparable mixture of starting material **6.21** and 2-bromo-6-dimethylaminopyridine **6.22** (Scheme 6.13). No evidence of di-aminated product **6.19** was detected.

The next synthesis involved reaction of 2,6-dibromopyridine **6.21** using dimethylamine as a solvent. Dimethylamine was obtained by dropping dimethylamine solution (40% in H_2O) onto K_2CO_3 and condensing the evolved gas at -78 °C into a tube containing 2.6-dibromopyridine **6.21**. After heating to 60 °C for 18 h in a sealed tube, only 2-bromo-6-dimethylaminopyridine **6.22** was produced in 90 % yield (Scheme 6.13).

SCHEME 6.13: Attempted synthesis of amine **6.19**.

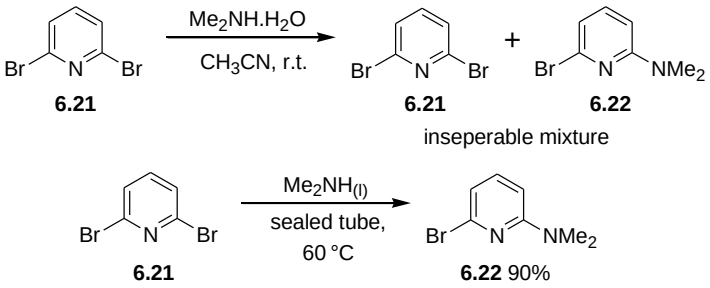

6.21 **6.21** **6.22**

6.21 **6.22** 90%

A search of the literature for the synthesis of 2-substituted pyridines provided a method of synthesis by Subat and König.[102] Reaction of 2,6-dibromopyridine **6.21** with dimethylamine solution (2.0 M in THF) in the presence of palladium (II) acetate and DPPF (Scheme 6.14) led to formation of 2-bromo-6-dimethylaminopyridine **6.22** and *N,N,N′,N′*-tetramethylpyridine-2-6-diamine **6.19** in a ratio of 1.0:0.1 respectively (by ^{1}H NMR). The reaction was repeated using condensed dimethylamine as the

amine source and this time gave the mono-aminated **6.22** and di-aminated **6.19** product in 48 % and 24 % yield respectively. Although amine **6.19** had been successfully synthesised, the low yield would prove problematic for large-scale synthesis. In an effort to improve the yield, the palladium reaction was repeated, this time using 2-bromo-6-dimethylaminopyridine **6.22** as the starting material, so that substitution of only one dimethylamino group was necessary. This time the reaction led to 35 % yield of the desired product **6.19** and recovery of 21 % of **6.22**. Even though the yields from the reaction were low, the procedure could be used to provide sufficient material for a synthesis of trication **6.3** to be attempted.

SCHEME 6.14: Synthesis of amine **6.19** by palladium catalysis.

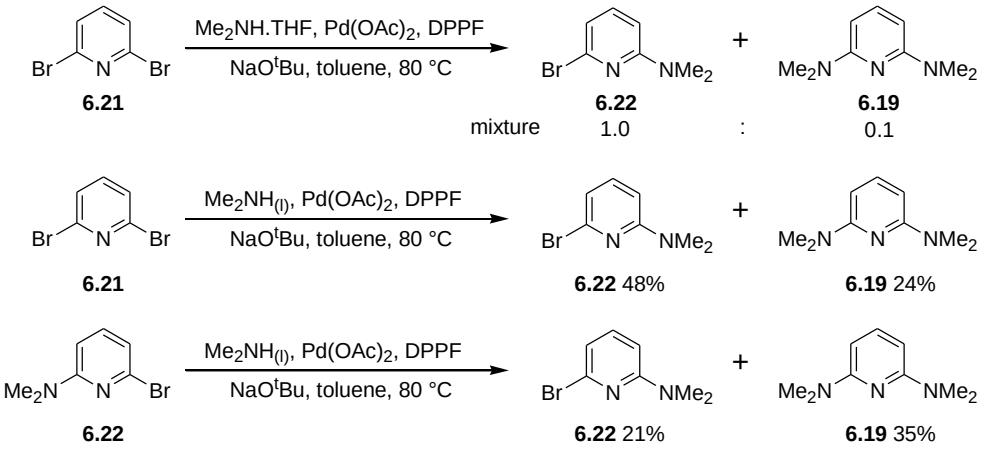

In order to use the palladium coupling synthesis described, larger quantities of mono-aminated product **6.22** were needed. However, attempts to make more 2-bromo-6-dimethylaminopyridine **6.22** led to a suprising, but fortuitous result. In an attempt to shorten the reaction time for the synthesis of 2-bromo-6-dimethylaminopyridine **6.22**, reaction of 2,6-dibromopyridine **6.21** with dimethylamine solution (40 % in H_2O) was carried out with microwave heating (Scheme 6.15). After 30 min heating at 120 °C, ^{1}H NMR analysis of the reaction mixture showed the presence of *N*,*N*,*N*′,*N*′-tetramethylpyridine-2,6-diamine **6.19**. Heating the reaction mixture to 150 °C for 3 h led to a 1:0.1 mixture of di-aminated **6.19** to mono-aminated product **6.22**. *N*,*N*,*N*′,*N*′-Tetramethylpyridine-2,6-diamine **6.19** was subsequently isolated in 53 % yield. Even though the reaction gave a moderate yield of the desired amine, the reaction conditions were simpler than the previous syntheses and gave almost 20 %

improvement in yield. With a reliable method for synthesis of amine **6.19**, attention was turned to the synthesis of tritriflate **6.20**.

SCHEME 6.15: Synthesis of amine **6.19** by microwave heating.

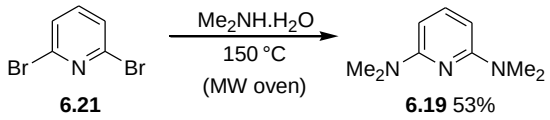

6.3.2 Synthesis of Tritriflate

With amine **6.19** available, attention was turned towards the synthesis of tritriflate **6.20**. It was thought that reaction of triol **6.23** with trifluoromethanesulfonic anhydride would yield tritriflate **6.20** in a similar fashion to synthesis of ditriflate **4.15**. Based on literature precedent,[103] dimethyl-3-oxopentane-1,5-dioate **6.24** was reduced with $LiAlH_4$. ^1H NMR analysis of the reaction mixture showed a complex mixture of products. MS analysis of the reaction mixture showed a peak at *m*/*z* 127, consistent with triol **6.23** complexed to lithium (Scheme 6.16). The resulting mixture could not be separated by column chromatography or distillation.

SCHEME 6.16: Attempted $LiAlH_4$ reduction of dioate **6.24**.

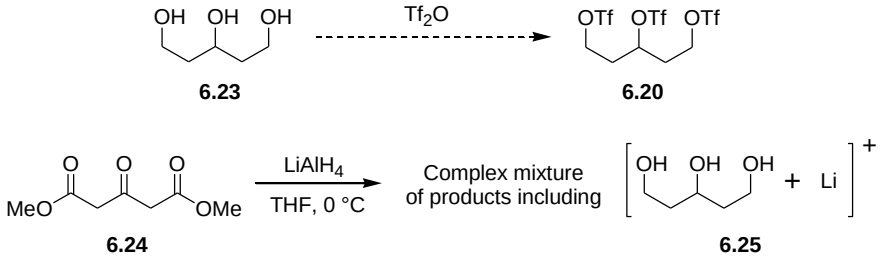

The next attempt at synthesising triol **6.23** was based on the work of Mori and Ikunaka.[104] It was thought that addition of a protecting group would aid in the isolation of the products. The synthetic route is shown in Scheme 6.17. Reduction of dimethyl-3-oxopentane-1,5-dioate **6.24** with $NaBH_4$ led to formation of alcohol **6.26**,[105] which was subsequently protected with the TBS protecting group to give **6.27**. However, reduction with $LiAlH_4$ again led to an inseparable mixture of products. MS analysis showed a peak at *m*/*z* 127, indicative of triol-lithium complex **6.25**, which could only result from the loss of the TBS protecting group.

SCHEME 6.17: Attempted synthesis of triol **6.23** using method by Mori and Ikunaka.[104]

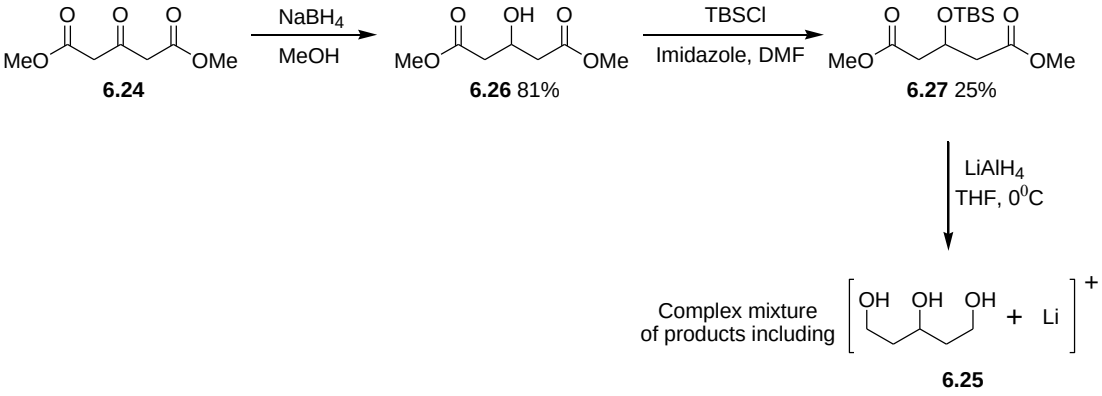

With difficulty in obtaining triol **6.23** starting from dimethyl-3-oxopentane-1,5-dioate **6.24**, the method of Parks *et al*.[106] was attempted. Diene **6.30** was synthesised from the Grignard reactions of allyl bromide **6.28** and ethyl formate **6.29** (Scheme 6.18). Ozonolysis of diene **6.30** and subsequent $NaBH_4$ reduction led to the formation of a complex mixture of products that could not be isolated.

SCHEME 6.18: Attempted synthesis of triol **6.23** via diene **6.30**.

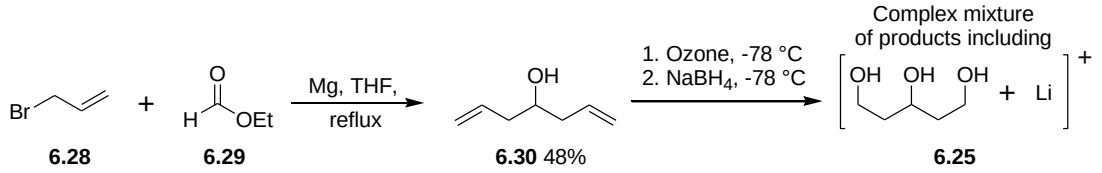

Simultaneous to the syntheses attempted above, successful synthesis of triol **6.23** was carried out by Dr. Roydhouse[107] within the Murphy group. This procedure is shown in Scheme 6.19. Previously synthesised alcohol **6.26** was converted to the acid **6.31** using potassium hydroxide. Reduction of the acid gave triol **6.23** (45 % over 2 steps), which was isolated by column chromatography. Reaction of alcohol **6.26** with potassium hydroxide gave acid **6.31** and dehydrated acid **6.32** as a side-product in a ratio of 85:15 respectively (by ^{1}H NMR). Variation of the reaction conditions could not prevent formation of this side-product, however, the side-product could fortunately be removed by column chromatography. With triol **6.23** in hand, synthesis of tritriflate **6.20** was readily achieved in 88 % yield using similar conditions to the synthesis of ditriflate **4.15**. The only modification to the procedure was an increase of the temperature from -78 to 0 °C. This was to increase the rate of

reaction between triol **6.23** and trifluoromethanesulfonic anhydride to prevent formation of a cyclic ether such as **6.35** (Scheme 6.20).

SCHEME 6.19: Synthesis of tritriflate **6.20**.

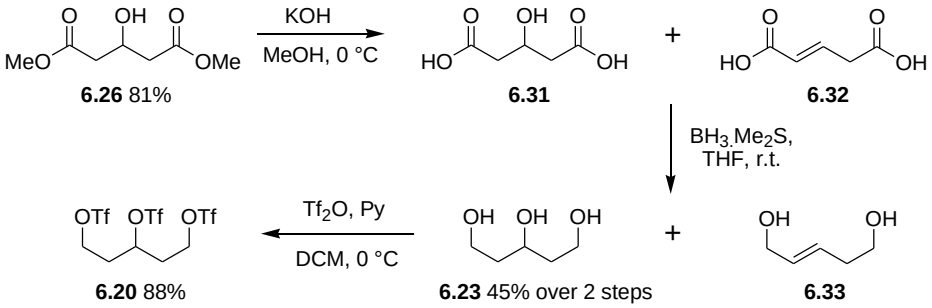

SCHEME 6.20: Proposed formation of cyclic ether side-product **6.35**.

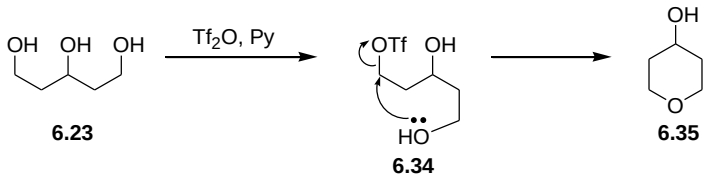

With tritriflate **6.20** and amine **6.19** readily available, attention was turned to the synthesis of trication **6.3**.

6.3.3 Attempted Synthesis of Trication

The proposed mechanism for the formation of trication **6.3** is shown in Scheme 6.21. This method relies on attack of one of the dimethylamino group nitrogens on one of the terminal triflate groups of tritriflate **6.20** to give salt **6.36**. Subsequent cyclisation of the remaining triflate groups first gives dication **6.37** and finally trication **6.3**. Attack on the terminal triflate group would be expected, as this is less hindered than the internal triflate group. However, if the preferential site of first methylation of amine **6.19** is on the ring nitrogen, this synthetic route would not be viable as cation **6.38** could not cyclise to form a trication.

Fortunately, reaction of amine **6.19** with iodomethane led to exclusive formation of the trimethylammonium salt **6.39**, which was isolated in 87 % yield (Scheme 6.22). The reaction showed that synthesis of trication **6.3** as shown in Scheme 6.21 is plausible, as the first methylation site is on one of the dimethylamino group

nitrogens. This result was not suprising given the behaviour of 2-DMAP **1.1** towards methylation.

SCHEME 6.21: Proposed synthesis of trication **6.3**.

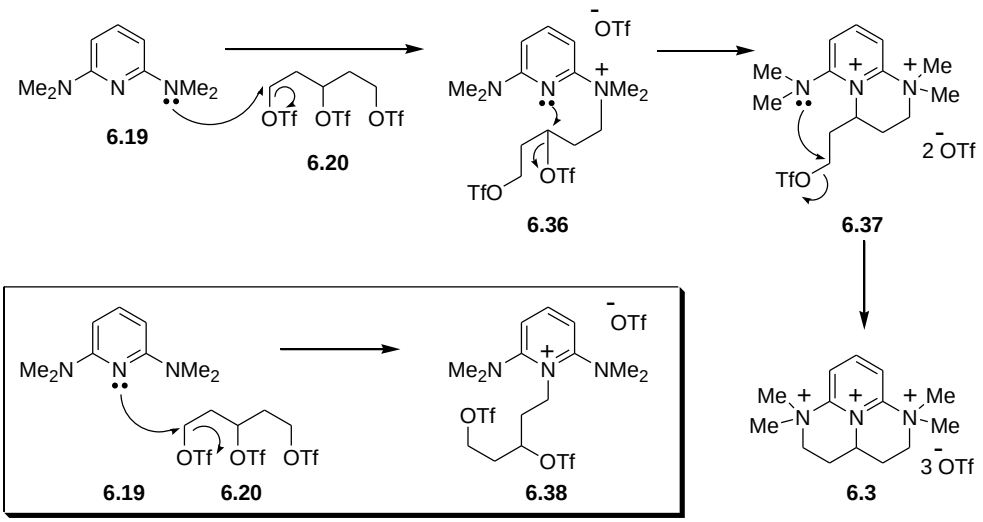

SCHEME 6.22: Methylation of *N*,*N*,*N*′,*N*′-tetramethylpyridine-2-6-diamine **6.19**.

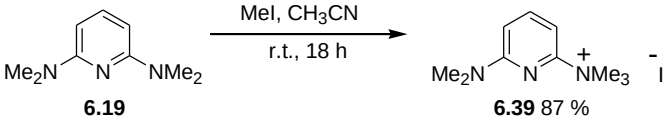

With formation of monocation **6.39**, the synthesis of the corresponding dication of *N*,*N*,*N*′,*N*′-tetramethylpyridine-2,6-diamine **6.19** was attempted. Reaction of *N*,*N*,*N*′,*N*′-tetramethylpyridine-2,6-diamine **6.19** with ditriflate **4.15** under the same conditions for formation of 2-DMAP disalt **4.16** led to formation of disalt **6.40** and dimer species **6.41** formed from the reaction of 2 eq of *N*,*N*,*N*′,*N*′-tetramethyl-pyridine-2,6-diamine **6.19** and ditriflate **4.15** (Scheme 6.23). Recrystallisation from dry acetonitrile/diethyl ether gave *N*,*N*,*N*′,*N*′-tetramethylpyridine-2,6-diamine disalt **6.40** in 23 % yield. Dimer **6.41** could not be isolated from the reaction mixture, but its presence was determined by ^{1}H NMR spectroscopy and MS analysis which showed peaks at *m*/*z* 162 $[M\text{-}2OTf]^{2+}$ and 475 $[M\text{-}OTf]^{+}$ consistent with formation of dimer **6.41**.

SCHEME 6.23: Formation of disalt **6.40**.

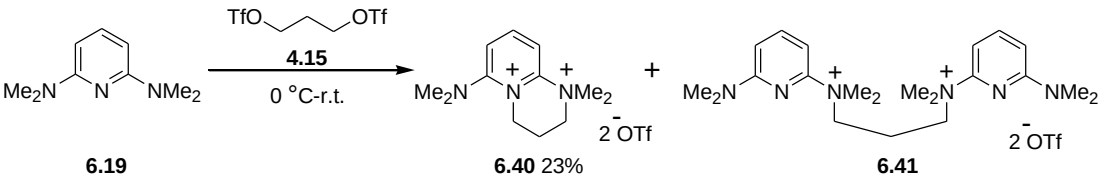

With superelectrophile disalt **6.40** synthesised, its reactivity, compared to dimethyl sulfate in a 1:1 competition reaction in the methylation of triethylamine **5.28**, was examined as described previously (Section 5.3.3). The results (Table 6.1) show that disalt **6.40** has poor reactivity in the methylation of triethylamine **5.28** compared to dimethyl sulfate, with only 8 % of disalt **6.40** being consumed in the reaction. Note, only a total of 77 % of methylating reagent (either disalt **6.40** or dimethyl sulfate) has been consumed in the competition reaction. This was attributed to the addition of a decreased volume of triethylamine **5.28** compared to previous competition reactions as a result of the small volume of nitrogen-nucleophile being used (0.007 mL).

TABLE 6.1: Competitive methylation study of triethylamine **5.28** with disalt **6.40** at 27 °C in CD_3CN.

Entry	**Disalt Used**	**Methylating Reagent (MR)**	**Amount Remaining[a] / %**	
			Disalt	**MR**
1	**6.40**	Me_2SO_4	92[b]	31[c]

[a] Proton signal integrations were taken relative to 1,3,5,7-cyclooctatetraene **5.29** $\delta_H(CD_3CN)$ 5.77 ppm set at 1.000. The experiment was carried out in CD_3CN. Amount remaining calculated from finishing proton integration as a percentage of starting proton integration. [b] Proton signal for Me groups at $\delta_H(CD_3CN)$ 3.73 ppm used. [c] Proton signal for Me groups at $\delta_H(CD_3CN)$ 3.94 ppm used.

This decreased reactivity was attributed to the resonance stabilisation of disalt **6.39** by the unquaternised *ortho*-dimethylamino group (Scheme 6.24). This resonance stabilisation serves to delocalise the positive charge on disalt **6.40** (such as in resonance form **6.42**) making the disalt less reactive.

SCHEME 6.24: Resonance stabilisation of disalt **6.40**.

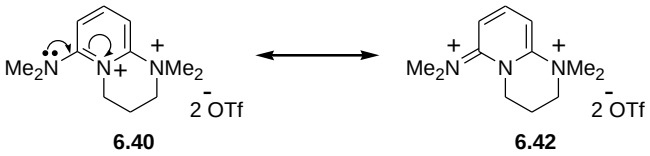

6.40 **6.42**

With monocationic salt **6.39** and disalt **6.40** synthesised, attention was turned to synthesis of trication **6.3**. Examination of the ^{1}H NMR spectrum for disalt **6.40** indicated that formation of trisalt **6.3** would likely result in an aromatic signal downfield of $\delta_H(CD_3CN)$ 8.09 ppm, indicative of the increased positive charge in tricationic **6.3** compared to dicationic **6.40**. In addition to this MS analysis would show a signal for *m*/*z* of 63.3 with a ^{13}C peak separation of one third of a mass unit for a trication.

The first reaction involved addition of a DCM solution of amine **6.19** to tritriflate **6.20** using a syringe pump (1.02 mL.h^{-1}) at 0 °C (Scheme 6.25). Analysis of the reaction mixture showed ^{1}H NMR peaks at $\delta_H(CD_3CN)$ 8.54 and 8.72 ppm and MS peaks at *m*/*z* 532, 382, 232 and 166. The downfield shift in the aromatic protons compared to disalt **6.40** could be indicative of the formation of trication **6.3**.

SCHEME 6.25: Attempted synthesis of trication **6.3**.

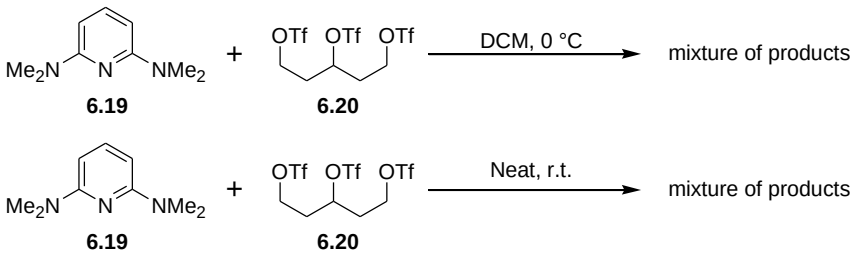

6.19 **6.20** **6.19** **6.20**

The MS peak at *m*/*z* 532 could be due to formation of trication **6.3** $[M\text{-}OTf]^+$, however, no trication peak at *m*/*z* 63.3 was observed. A more likely product would be monocation **6.43**, where attachment of only one triflate onto the amine. The peak at *m*/*z* 166 was attributed to starting amine **6.19** $[M+H]^+$. The peaks at *m*/*z* 382 and 232 could not be identified and the ^{1}H NMR spectrum was too complex to determine a structure. The structures of several plausible products from the reaction with their corresponding *m*/*z* peaks are shown in Scheme 6.26. As can be seen, the proposed

products do not match the corresponding MS peaks observed in the reaction mixture. Attempts to purify the reaction products by recrystallisation were unsuccessful.

SCHEME 6.26: Possible products from reaction of **6.19** and **6.20**.

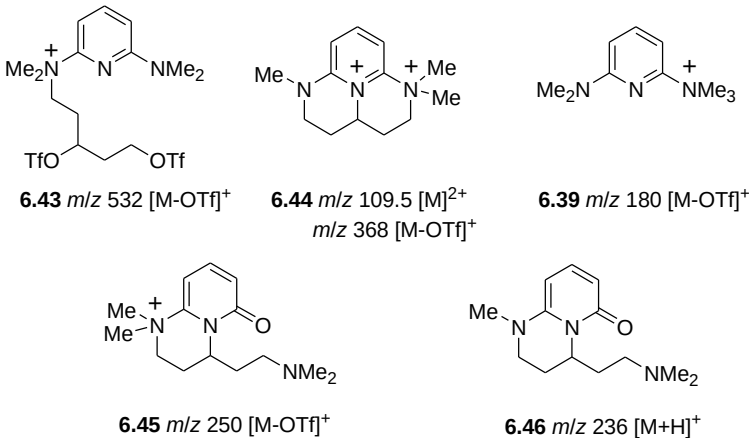

6.43 *m/z* 532 $[M\text{-}OTf]^+$ **6.44** *m/z* 109.5 $[M]^{2+}$ *m/z* 368 $[M\text{-}OTf]^+$ **6.39** *m/z* 180 $[M\text{-}OTf]^+$

6.45 *m/z* 250 $[M\text{-}OTf]^+$ **6.46** *m/z* 236 $[M+H]^+$

The reaction was then repeated without the use of solvent, at r.t. in the glovebox (Scheme 6.25). Again, analysis of the reaction mixture showed ^{1}H NMR peaks at $\delta_H(CD_3CN)$ 8.54 and 8.77 ppm and MS peaks at *m/z* 532, 382, 232 and 166. Attempts to purify the reaction products by recrystallisation were unsuccessful.

Next, the formation of trication **6.3** in diethyl ether was attempted. Various reaction conditions were attempted (Table 6.2). Slow addition of amine **6.19** in diethyl ether to tritriflate **6.20** led to formation of a white solid. MS analysis of the solid showed a peak at *m/z* 166, consistent with the starting amine **6.19** $[M+H]^+$ (Table 6.1, entry 1). Slower addition of amine **6.19** and longer reaction times led to MS signals at *m/z* 166 and 532, consistent with amine **6.19** and salt **6.43** (Table 6.2, entry 2). Increasing the number of equivalents of tritriflate **4.19** (from 1.1 to 3.0 eq) did not result in formation of trication **6.3** (Table 6.2, entry 3).

SCHEME 6.27: Attempted formation of trication **6.3** in diethyl ether.

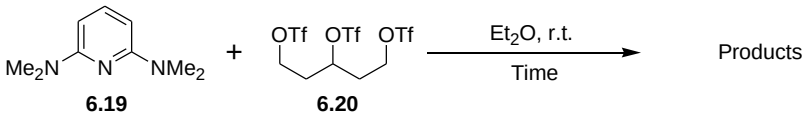

6.19 **6.20**

TABLE 6.2: Conditions for attempted synthesis of trication **6.3**.

Entry	Eq 6.20	Addition Speed / $mL.h^{-1}$	Time / h	MS Signals Observed
1	1.1	2.03	2	166
2	1.1	1.02	18	166, 532
3	3.0	0.508	18	166

Conditions for the formation of trication **6.3** from *N*,*N*,*N*′,*N*′-tetramethylpyridine-2,6-diamine **6.19** and tritriflate **6.20** could not be found. MS analysis of the reaction mixture mostly showed peaks for amine **6.19** and what was suspected to be salt **6.43**. This indicated that reaction of amine **6.19** with tritriflate **6.20** stopped after the reaction of **6.20** with one of the nitrogens of the dimethylamino group. The reason for this could be that trication **6.3** is too unstable to form, although it is not known why attachment at one nitrogen would not result in immediate cyclisation to form trication **6.3** (as shown in Scheme 6.21). In order for successful formation of a trication species, cyclisation of tritriflate **6.20** with the pyridine ring nitrogen would need to be promoted.

6.4 2,4,6-*Tris*-(dimethylamino)pyridine Trisalt Synthesis

With problems in the synthesis of trisalt **6.3**, the synthesis of new trisalt **6.47** was envisioned (Scheme 6.28). This trisalt was based on 2,4,6-*tris*-(dimethylamino)-pyridine **6.48**.

SCHEME 6.28: Retrosynthetic plan for trisalt **6.47**.

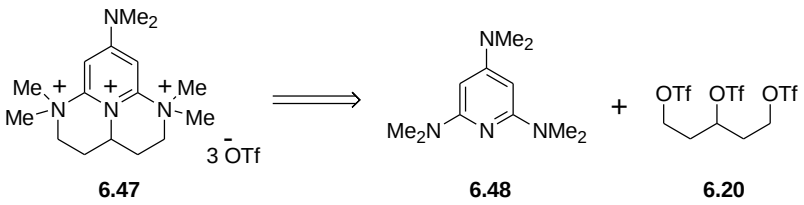

6.47 **6.48** **6.20**

6.4.1 Synthesis of 2,4,6-Tris-(dimethylamino)pyridine

Synthesis of 2,4,6-*tris*-(dimethylamino)pyridine **6.48** was carried out by Dr. Roydhouse within the group.[107] The first step in the synthesis involved the conversion of 4-DMAP **1.8** into 2,6-diiodo-4-(dimethylamino)pyridine **6.49** using the

procedure reported by Aucagne *et al*.[108] This led to formation of the diiodopyridine in 41 % yield (Scheme 6.29).

SCHEME 6.29: Synthesis of diiodopyridine **6.49**.

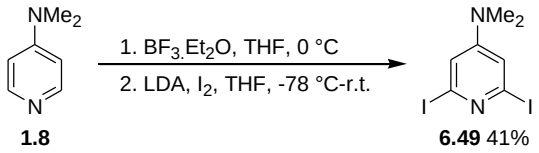

Based on the synthesis of *N*,*N*,*N*′,*N*′-tetramethylpyridine-2,6-diamine **6.19** using dimethylamine and microwave heating described previously (Scheme 6.15), the same conditions were used with 2,6-diiodo-4-(dimethylamino)pyridine **6.49**. Unfortunately, the reaction did not proceed to give 2,4,6-*tris*-(dimethylamino)-pyridine **6.48**. Synthesis of pyridine **6.48** was achieved based on work by Buchwald *et al*.[109] in the copper-ligand mediated amine substitution of iodopyridines. Ligand **6.50** was synthesised and used in the reaction to form 2,4,6-*tris*(dimethylamino)pyridine **6.48** in 95 % yield (Scheme 6.30).

SCHEME 6.30: Synthesis of 2,4,6-*tris*-(dimethylamino)pyridine **6.48**.

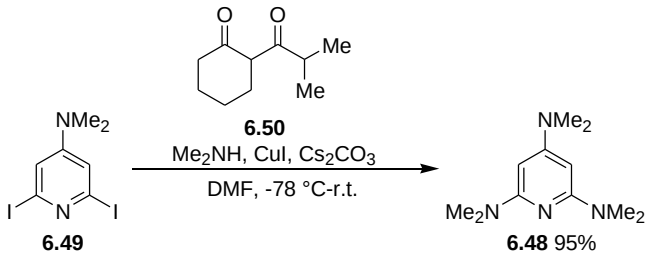

6.4.2 Synthesis and Reactivity of Trisalt

With amine **6.48** successfully synthesised, attention was turned to the synthesis of trisalt **6.47**. Fortunately, this was readily achieved by the addition of a solution of amine **6.48** in dry diethyl ether to tritriflate **6.20** at r.t. (Scheme 6.31). This resulted in the formation of an off-white solid, which was isolated and recrystallised in the glovebox to give 2,4,6-*tris*-(dimethylamino)pyridine trisalt **6.47** in 43 % yield.

SCHEME 6.31: Synthesis of 2,4,6-*tris*-(dimethylamino)pyridine trisalt **6.47**.

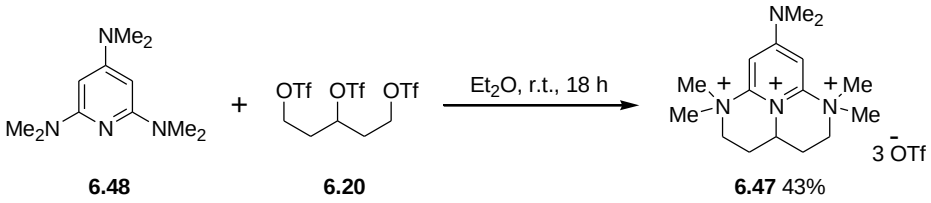

6.48 **6.20** **6.47** 43%

^{1}H NMR analysis of trisalt **6.47** showed the correct signals for the product (Figure 6.1 and 6.2). MS analysis of the trisalt gave the expected signal at *m*/*z* 575 $[M\text{-}OTf]^+$. In addition, crystal structure analysis of trisalt **6.47** gave the expected structure (Figure 6.3).

FIGURE 6.1: ^{1}H NMR spectrum of trisalt **6.47**.

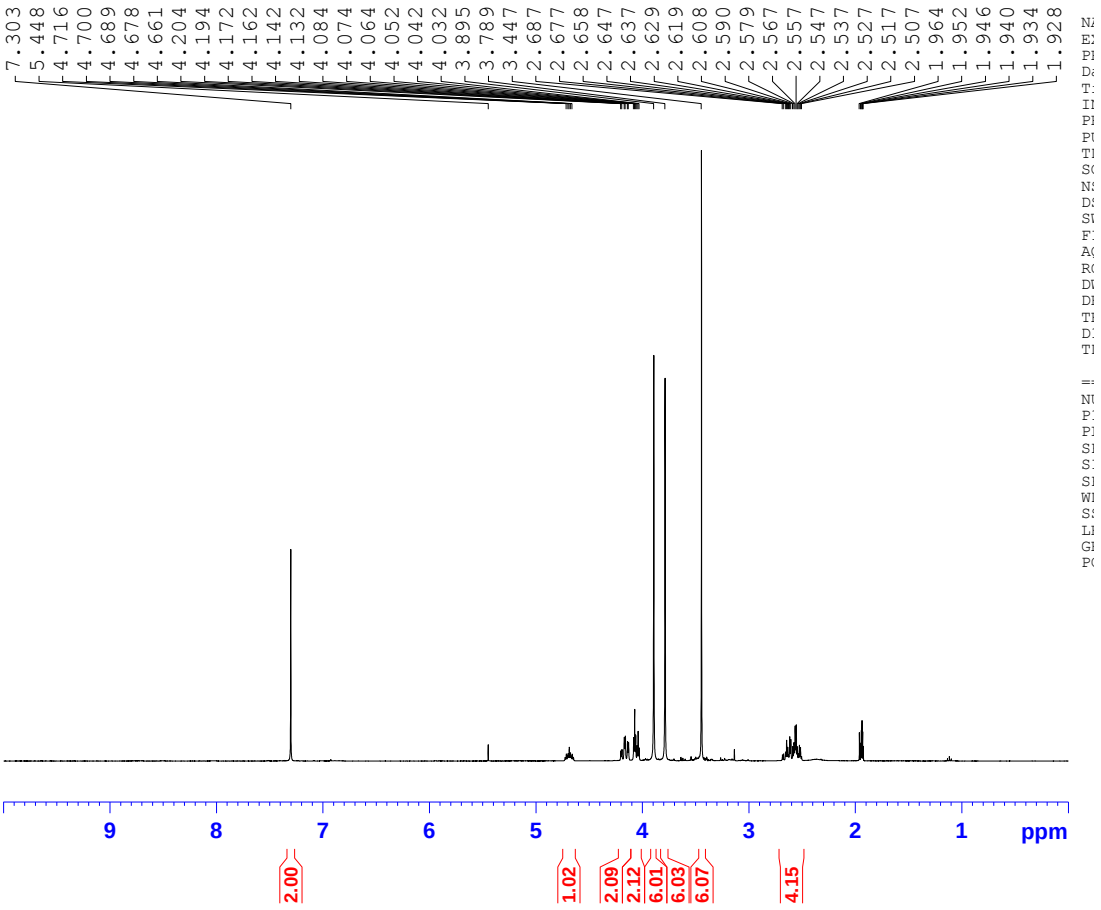

With trisalt **6.47** successfully synthesised, a 1:1 competition reaction with dimethyl sulfate in the methylation of triethylamine **5.28** was carried out. Due to signal overlap between trisalt **6.47** and triethylamine **5.28** in the ^{1}H NMR spectrum, the

integration of the methyl peaks for trisalt **6.47** could not be used to determine the reactivity. In this case, the integration of the aromatic peak for **6.47** at $\delta_H(CD_3CN)$ 7.30 ppm was used as this region of the spectrum was free from signal overlap.

TABLE 6.3: Competitive methylation study of triethylamine **5.28** with trisalt **6.47** at 27 °C in CD_3CN.

Entry	Trisalt Used	Methylating Reagent (MR)	Amount Remaining[a] / %	
			Disalt	MR
1	**6.47**	Me_2SO_4	52[b]	N.D.

[a] All proton signal integrations were taken relative to 1,3,5,7-cyclooctatetraene **5.29** $\delta_H(CD_3CN)$ 5.77 ppm set at 1.000. The experiment was carried out in CD_3CN. Amount remaining calculated from finishing proton integration as a percentage of starting proton integration. [b] Proton signal for aromatic proton at $\delta_H(CD_3CN)$ 7.30 ppm used.

FIGURE 6.2: Expansion (2.0-5.0 ppm) for ^{1}H NMR of **6.47**.

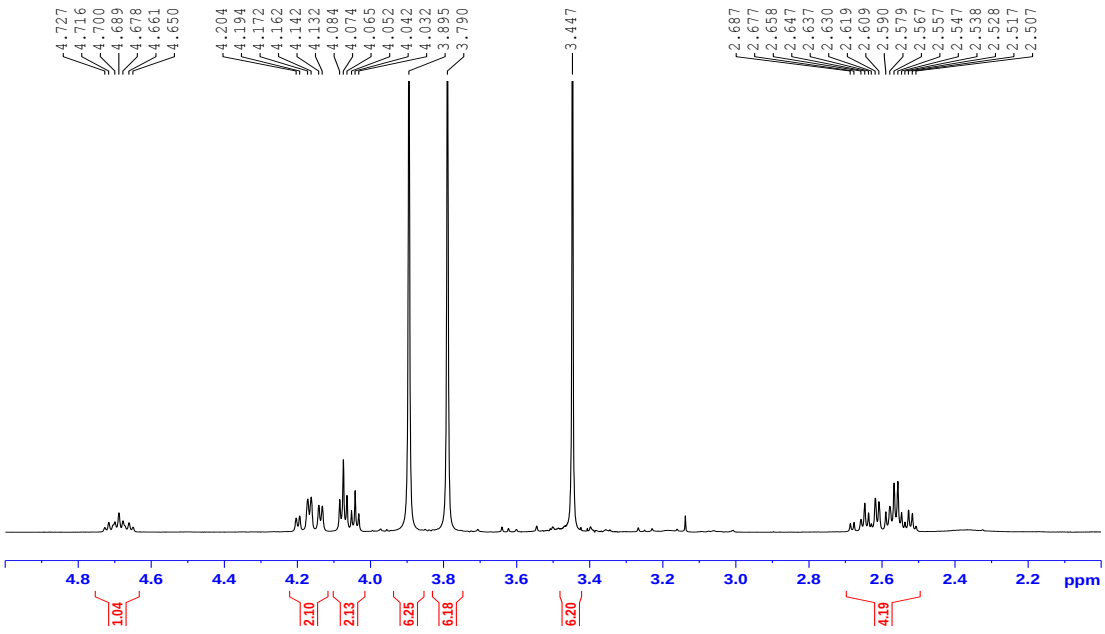

The results (Table 6.3) showed 52 % of trisalt **6.47** remaining after the reaction with triethylamine **5.28**. Assuming 100 % consumption of triethylamine **5.28**, this means that 52 % of dimethyl sulfate had been consumed in the reaction (48 % remaining). This indicates that trisalt **6.47** shows the same reactivity as dimethyl sulfate in the reaction with nitrogen-nucleophiles. It would be expected that a tricationic species such as **6.47** would display enhanced reactivity over a disalt species such as **4.16**.

However, the decreased reactivity of trisalt **6.47** relative to **4.16** can be explained by resonance stabilisation of trisalt **6.47** by the unquaternised dimethylamino group (Scheme 6.32).

FIGURE 6.3: (a) ORTEP diagram of trisalt **6.47** cation. (b) ORTEP diagram of trisalt **6.47** (cation and three anions).

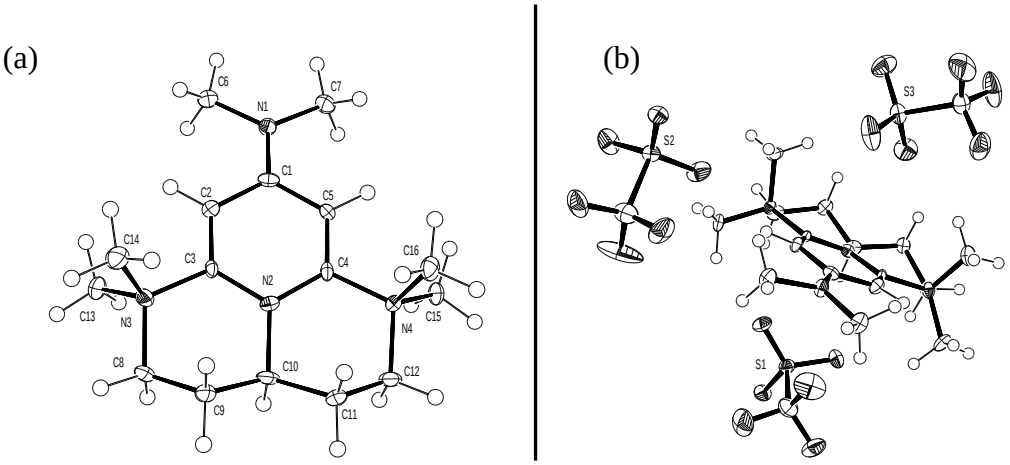

SCHEME 6.32: Resonance stabilisation of trisalt **6.47**.

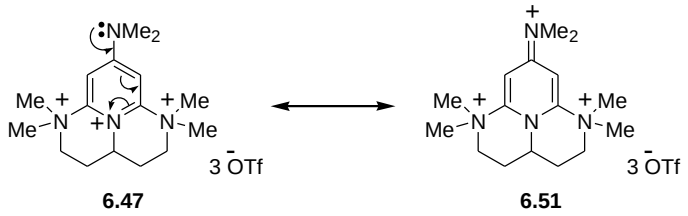

6.47 **6.51**

Scheme 6.33 shows a reactivity scale for the different superelectrophiles synthesised, with the reactivity of dimethyl sulfate in the methylation of triethylamine **5.28** arbitrarily set at 1.0. The disalts (**4.16**, **4.30**, **6.40** and **6.47**) have been scaled in terms of their relative reactivity in the methylation of triethylamine **5.28** compared to dimethyl sulfate. As can be seen, disalt **4.30** is the most reactive superelectrophile that has been synthesised, showing over 2 times the methylating ability of dimethyl sulfate.

A superelectrophilic trisalt based on dimethylaminopyridine has been synthesised and its reactivity has been determined in the methylation of nitrogen-nucleophiles.

The next stage of the project was to examine the reactivity of 2-DMAP disalt **4.16** with hydrogen and the synthesis of other types of superelectrophile.

SCHEME 6.33: Disalt electrophile scale.

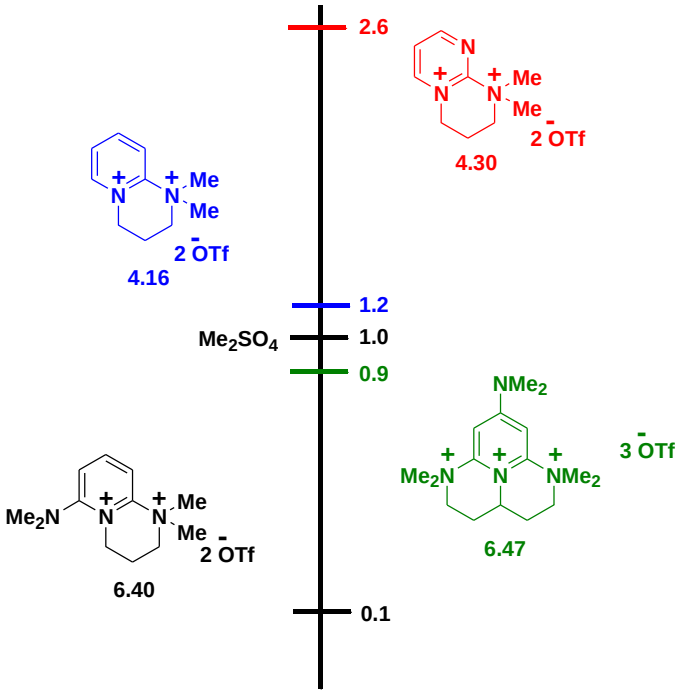

7 [Fe]-Hydrogenase

The concept of superelectrophilic activation has been generally limited to the activation of cations using superacids (Sections 2.1-2.3) or postulated as highly reactive intermediates in organic synthesis (Section 2.4). However, the concept of superelectrophilic activation has more recently been proposed as the mechanism for the reaction of a very unusual enzyme; the [Fe]-hydrogenase enzyme. This superelectrophilic enzymatic activation has particular relevance to the superelectrophile disalts reported in this thesis.

7.1 Introduction

Hydrogenases are enzymes that catalyse redox reactions with molecular hydrogen, either as a substrate or a product. The enzymes are found in aerobic and anaerobic bacteria, archaea and eucarya. All hydrogenases are metalloenzymes, the two most predominant are known as [NiFe]-hydrogenase (containing nickel and iron-sulfur clusters) and [FeFe]-hydrogenase (containing iron-sulfur clusters).[110]

A third type of hydrogenase was recently discovered that did not contain nickel or iron-sulfur clusters.[111] The [Fe]-hydrogenase (previously known as iron-sulfur-cluster free hydrogenase or H_2-forming methylenetetrahydromethanopterin dehydrogenase (Hmd)) is obtained from *methanogenic archaea* grown in nickel-limiting conditions. It catalyses the reversible reduction of N^5,N^{10}-methenyltetrahydromethanopterin ($CH{\equiv}H_4MPT^+$) **7.1** with H_2 to N^5,N^{10}-methylenetetrahydromethanopterin ($CH_2{=}H_4MPT$) **7.2** and a proton (Scheme 7.1) during the production of methane from CO_2 in *methanogenic archaea* ($\Delta G^{\circ\prime}$ = -5.5 kJmol^{-1}).[110] The [Fe]-hydrogenase catalyses reversible stereospecific hydride transfer from H_2 to **7.1** to the *pro-R* methylene hydrogen in **7.1** to give $CH_2{=}H_4MPT$ **7.2** by the reaction with C_{14a} in the imidazolinium ring of $CH{\equiv}H_4MPT^+$ **7.1**.[112] In the current climate, with worries about global warming (due to the presence of excess CO_2 in the atmosphere) and concerns over finite fossil fuel resources, requiring new sources of

fuel to be developed, the study of hydrogenases, especially the [Fe]-hydrogenase, is of particular importance.

SCHEME 7.1: Reaction catalysed by H_2-forming methylenetetrahydromethanopterin dehydrogenase.

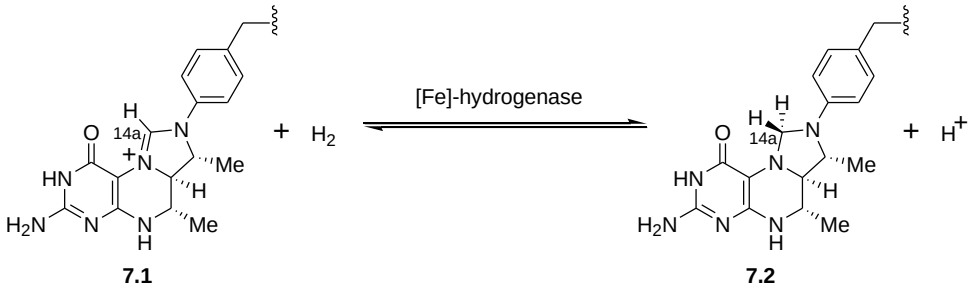

7.1 **7.2**

Initially, it was believed that H_2-forming methylenetetrahydromethanopterin dehydrogenase did not contain functional metal,[110] making it a unique, purely organic hydrogenase.[113] This discovery led to much excitement in the literature, with a variety of mechanistic proposals being forwarded. The proposal by Berkessel and Thauer[114] proved particularly interesting, as this served to develop the concept of superelectrophilic activation into the realm of enzymatic reactions, a concept which had previously been postulated only under superacid conditions. The enzyme was subsequently discovered to contain an iron cofactor essential for activity[115] and the enzyme crystal structure has been reported,[116,117] leading to a new range of mechanistic investigations and interest in this unusual hydrogenase. This review will examine the investigations carried out on the [Fe]-hydrogenase, from its initial discovery and analysis to the current opinions in the literature.

7.2 Intial Studies on H_2-Forming Methylenetetrahydromethanopterin Dehydrogenase

5,6,7,8-Tetrahydromethanopterin (H_4MPT) **7.3** serves as a carrier of C_1 fragments in the metabolism of *Methanogenic archaea*.[112] During the course of methanogenesis, a C_1 fragment is transferred to H_4MPT **7.3** at the oxidation level of formic acid and is subsequently reduced to the methyl oxidation level in a stepwise manner. During this process $CH{\equiv}H_4MPT^+$ **7.1** is converted to $CH_2{=}H_4$MPT **7.2** by the action of a hydrogenase, then named H_2-forming methylenetetrahydromethanopterin

dehydrogenase. In 1990, Thauer *et al.*[111] reported the hydrogenase activity found in *Methanobacterium thermoautotrophicum*, a thermophilic methanogenic archaebacterium that reduces CO_2 to CH_4. The hydrogenase activity was rapidly lost under aerobic conditions or in the presence of dithiothreitol (DTT) or mercaptoethanol.[111] Hmd is composed of only one type of subunit that has an apparent molecular mass of 43 kDa with a specific activity above 1000 U/mg.[111,118] Determination of the primary structure gave 37,788 Da as the actual mass of the polypeptide.[119]

SCHEME 7.2: 5,6,7,8-Tetrahydromethanopterin **7.3**.

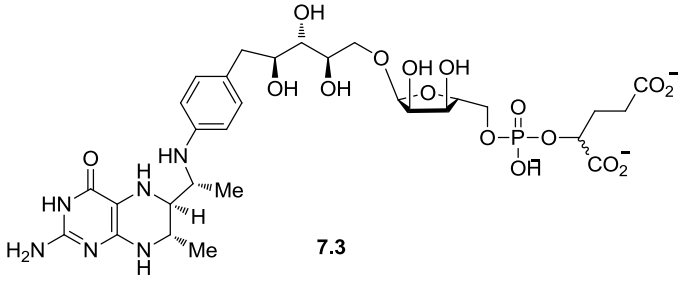

7.3

Both [NiFe]-hydrogenase and [FeFe]-hydrogenase mediate the reduction of one-electron acceptors (OEA) such as viologen dyes with hydrogen (Scheme 7.3).[110] In the absence of an electron-acceptor, the hydrogenases can catalyse the exchange between H^+ and H_2. Unusually, Hmd does not catalyse the reduction of viologen dyes and will catalyse the exchange between H^+ and H_2 only in the presence of $CH{\equiv}H_4MPT^+$ **7.1** or $CH_2{=}H_4MPT$ **7.2**.[112] Hmd was also unusual in that it appeared to contain no functional metal.[110,111] UV-visible spectroscopy showed no absorbance above 340 nm, indicating that Hmd wasn't an iron-sulfur protein or flavoprotein. In addition, analysis of non-heme iron showed < 0.4 mol iron per mol enzyme and ICP-MS and AAS analysis showed no nickel or transition metals (levels < 0.1 mol per mol enzyme). The only metal found in significant quantities was zinc, found to vary between 0.5-4 mol zinc per mol enzyme depending upon the enzyme culture. However, the zinc content did not correlate with the specific activity of the enzyme.[110] The effect of CO, CN^-, acetylene, nitrite, and azide as inhibitors was also investigated.[110] It was found that CO concentrations of 5 % and 50 % and 5 % of CN^- did not cause any significant loss in activity of the enzyme. Only a CN^-

concentration of 50 % caused a loss of activity below 50 %. Nitrite, azide and acetylene were not inhibitors under the conditions of the reaction.

SCHEME 7.3: OEA reduction by [NiFe]- and [FeFe]-hydrogenases.

Next, tritium exchange in the enzyme was examined.[110] When pure Hmd alone was used, no exchange between $^3H_2$ and ^1H_2O was observed at various *p*H values and temperatures. In the presence of CH≡H_4MPT$^+$ **7.1** or CH_2=H_4MPT **7.2**, exchange between $^3H_2$ and ^1H_2O was observed. Isolation of the products by HPLC showed that per mol of CH_2=H_4MPT **7.2** formed, 0.5 mol of ^3H was incorporated into the methylene group of CH_2=H_4MPT **7.2,** consistent with transfer of a single ^3H to the substrate from the $^3H_2$ and with the release of a corresponding 0.5 mol of ^3H into the aqueous medium. Similarly using ^3H-labelled CH_2=H_4MPT **2**, with the label in the CH_2 group, the CH≡H_4MPT$^+$ formed had only half the specific radioactivity of the labelled CH_2=H_4MPT **2**, again consistent with transfer of just one of the CH_2 hydrogens. Hmd did not catalyse the $^3H_2$/^1H_2O exchange in the absence of substrate CH≡H_4MPT$^+$ **7.1**.

Various hydrogen isotope studies have been conducted in order to probe the reaction between CH≡H_4MPT$^+$ **7.1** and dihydrogen in the presence of Hmd.

Schwörer *et al.*[120] examined the production of dihydrogen from CH_2=H_4MPT **7.2** using hydrogen isotopes. The purpose of these reactions was to determine if the reaction of CH≡H_4MPT$^+$ **7.1** with hydrogen occurred via hydride transfer. If this was the case, the dehydrogenation of CD_2=H_4MPT **7.4** in H_2O or the dehydrogenation of CH_2=H_4MPT **7.2** in D_2O would ideally produce only HD as a product, as only one of the hydrogen atoms (or deuterium atoms) could come from either substrate **7.2** or **7.4**.

The results showed that for CD_2=H_4MPT **7.4** in H_2O, HD and H_2 were produced, whereas for CH_2=H_4MPT **7.2** in D_2O only HD and D_2 were produced. The production of H_2 from CD_2=H_4MPT **7.4** in H_2O (or D_2 from CH_2=H_4MPT **7.2** in D_2O) was explained by the exchange between HD and the solvent, which was caused

by $CH{\equiv}H_4MPT^+$-dependent Hmd catalysis. A summary of the reactions is shown in Scheme 7.4.

SCHEME 7.4: Hydrogen isotope studies on the dehydrogenation of $CH_2{=}H_4MPT$ **7.2**.

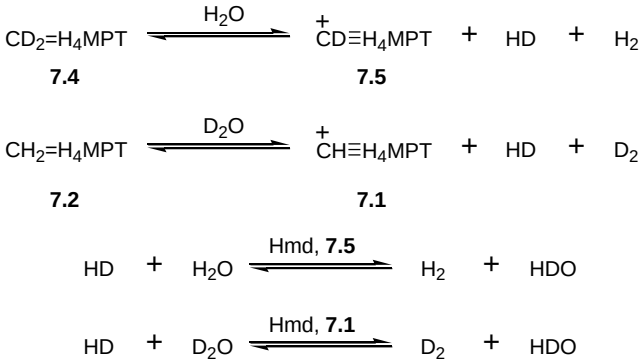

In the absence of $CH_2{=}H_4MPT$ **7.2** (or $CD_2{=}H_4MPT$ **7.4**), no exchange between H_2 and D_2O (or D_2 and H_2O) was observed, even when high concentrations of the enzyme were used. No generation of D_2 was observed when using $CD_2{=}H_4MPT$ **7.4** in H_2O and no generation of H_2 was observed when using $CH_2{=}H_4MPT$ **7.2** in D_2O. This indicated that only one of the hydrogens from $CH_2{=}H_4MPT$ **7.2** underwent reaction to form dihydrogen.

SCHEME 7.5: NMR-labelling studies showing stereochemistry of the reaction.

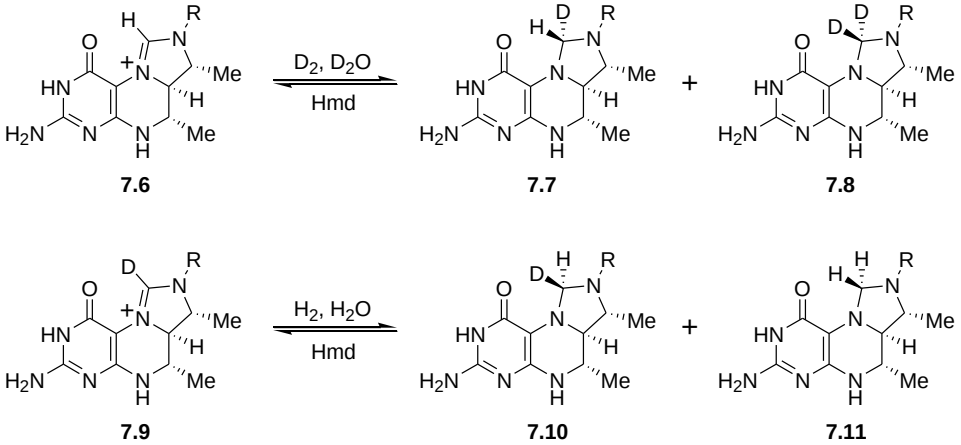

The stereochemical course of the reaction was determined by Schleucher *et al.*[112] using two-dimensional NMR spectroscopy. Reaction of $CH{\equiv}H_4MPT^+$ **7.6** with D_2 in D_2O led to formation of $CHD{=}H_4MPT$ **7.7** and $CD_2{=}H_4MPT$ **7.8** (Scheme 7.5).

Formation of **7.7** was due to deuteride abstraction from D_2 in the C_{14a} carbon to give labelled-**7.7**. It was found that for a solution of Hmd and $CH{\equiv}H_4MPT^+$ **7.6** in D_2O, the signal for the methenyl hydrogen gradually disappeared, indicating exchange of the proton with D^+ from D_2O. Due to this, formation of **7.8** in the reaction could be explained by H/D exchange of the methenyl H of **7.6** with D from D_2O, then reaction with D_2 to give $CD_2{=}H_4MPT$ **7.8** (Scheme 7.6). This side-reaction was not catalysed by the enzyme and increased with increasing *p*H. Correspondingly, reaction of $CD{\equiv}H_4MPT^+$ **7.9** with H_2 in H_2O led to formation of $CDH{=}H_4MPT$ **7.10** and $CH_2{=}H_4MPT$ **7.11** (Scheme 7.5). Subsequent NMR experiments confirmed that the hydride is transferred from H_2 (or D_2) rather than the solvent water. Determination of the absolute stereochemistry showed that hydride was transferred from hydrogen to take up the *pro-R* position of C_{14a} in $CH_2{=}H_4MPT$ **7.2**.

SCHEME 7.6: H/D exchange observed in $CH{\equiv}H_4MPT^+$ **7.6**.

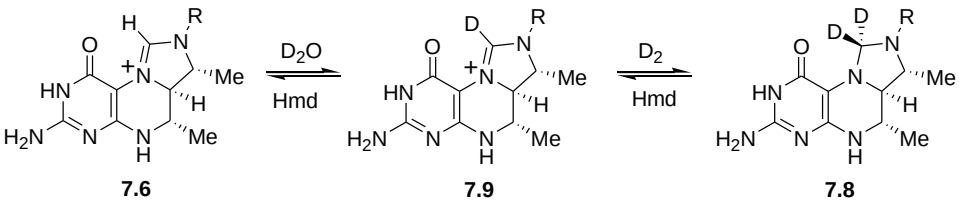

FIGURE 7.1: Representation of Hmd ultrafiltrate reaction.

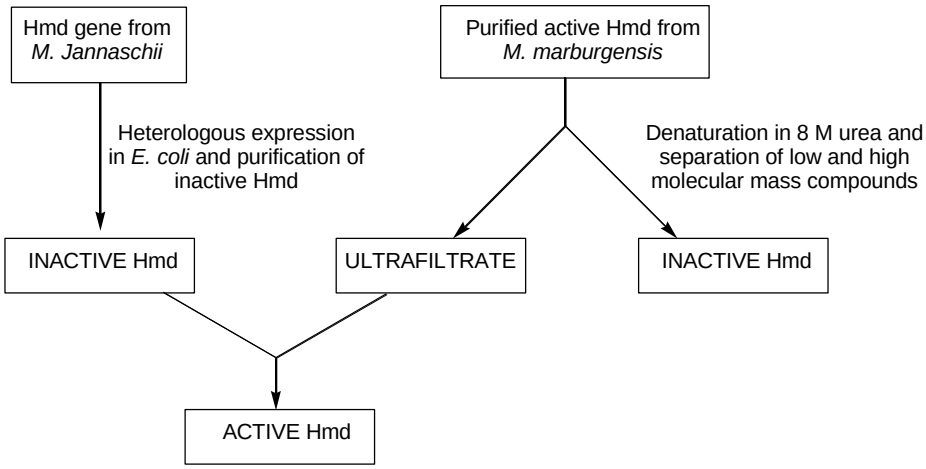

Thauer *et al*.[118] then showed the presence of a low molecular weight cofactor tightly bound to the enzyme containing no redox-active transition metal. Hmd was heterologously expressed from *Methanococcus jannaschii* and, surprisingly, showed no activity in the reduction of **7.1**. Hmd from *Methanothermobacter marburgensis*

was denatured in urea and the ultrafiltrate (components < 10 kDa molecular mass) was collected. When the heterologously produced Hmd in *M. jannaschii* was added to the ultrafiltrate from *M. marburgensis*, the combination showed activity in the reaction of **7.1** with hydrogen (Figure 7.1 shows a representation of the reaction performed). Similarly, Hmd heterologously expressed from *M. marburgensis* showed activity when added to the ultrafiltrate collected from *M. jannaschii*. Analysis of the ultrafiltrate showed components with a molecular mass below 1000 Da, shown to contain no nickel and only traces of iron and zinc by TXRF analysis (Total Reflection X-ray Fluorescence spectrometry).

7.3 Superelectrophilic Activation in Hmd

Although many activity studies and spectroscopic labelling studies had conclusively shown that Hmd catalysed the transfer of hydride from molecular hydrogen to $CH{\equiv}H_4MPT^+$ **7.1** to form $CH_2{=}H_4MPT$ **7.2**, the mechanistic details of the reaction still remained a mystery.

In 1995, Berkessel and Thauer[114] presented an intriguing mechanistic proposal for the reaction of Hmd based on superelectrophilic activation of alkanes.[46] The proposed mechanism is shown in Schemes 7.7 and 7.8. They proposed that protonation of $CH{\equiv}H_4MPT^+$ **7.6** in the enzyme active site would lead to formation of superelectrophilic dicationic species **7.12** (or **7.12′**). This, in turn, would increase the carbocationic character of C_{14a} in $CH{\equiv}H_4MPT^+$ **7.6**, allowing it to abstract hydride from molecular hydrogen to give $CH_2{=}H_4MPT$ **7.11** (Scheme 7.7). This proposal was based on the work of Olah *et al*.[46] on the activation of alkanes for hydride exchange in the presence of superacids.

According to their[114] proposal, when $CH{\equiv}H_4MPT^+$ **7.6** is in the enzyme active site, it can undergo protonation on either N^5 or N^{10} to give dication species **7.12**/**7.12′** (Scheme 7.7). Berkessel and Thauer[114] proposed that this protonation would be accompanied by a conformational change in the imidazolinium ring to give a distorted 5-membered ring such as **7.14**, with a pentacoordinated carbonium cation (Scheme 7.8). The antiperiplanar arrangement of the nitrogen lone pair of electrons to the C_{14a}-H bond in **7.14** would make it sufficiently reactive to abstract hydride from molecular hydrogen to give conformationally locked species **7.15**. Removal

from the enzyme active site frees the nitrogen lone pair of electrons to give reduced product **7.11**.

SCHEME 7.7: Superelectrophilic activation of CH≡H_4MPT$^+$ **7.6**.

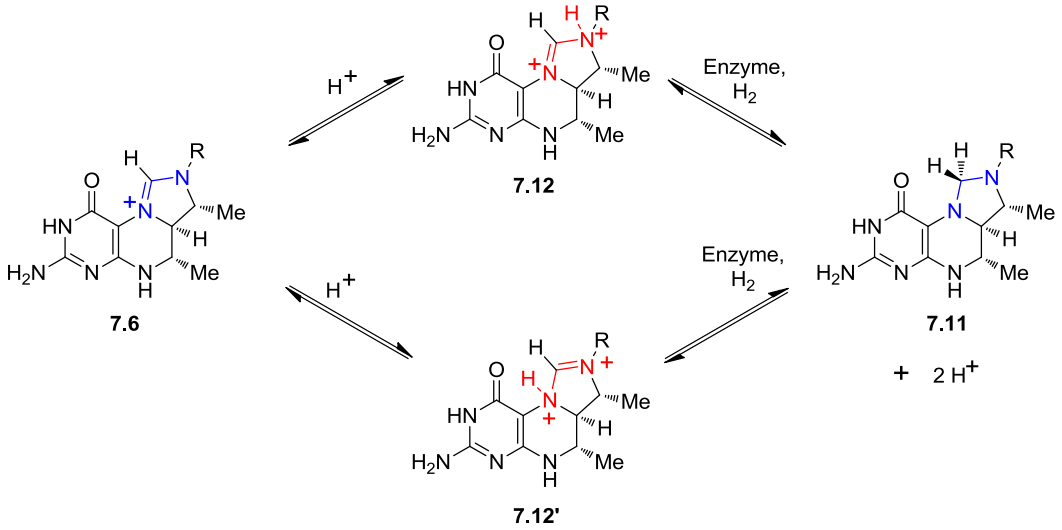

SCHEME 7.8: Schematic representation of superelectrophilic activation in Hmd.

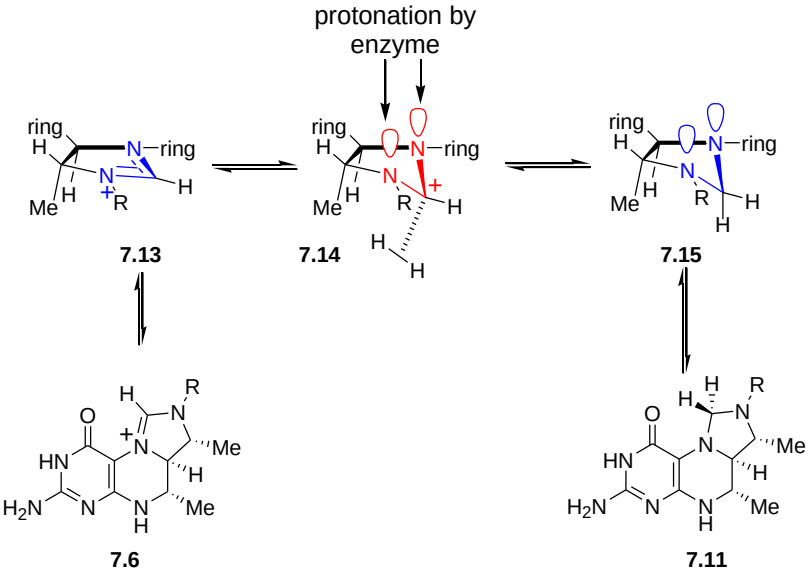

Berkessel and Thauer[114] compared the proposed mechanism to the analogous reaction observed in structurally-related orthoamides (Scheme 7.9). Upon treatment with acid (tetrafluoroboric acid at r.t. or HCl at 110 °C) perhydro-3a,6a,9a-triaza-phenalene **7.16** loses hydride to give guanidinium salt **7.17**. The unusual reactivity was explained by the interaction of the σ* orbital of the central C-H bond with the three antiperiplanar nitrogen electron lone pairs. This interaction weakens the C-H

bond, allowing it to be extracted to give guanidinium salt **7.17**. However, the reverse reaction, hydride abstraction from molecular H_2 by **7.17** to give **7.16** does not occur, unlike the reaction in Hmd where **7.2** is converted to **7.1**. In addition, H/D exchange is not observed in **7.16**, whereas CH_2=H_4MPT **7.2** can exchange the *pro-R* hydrogen with protons of solvent in the enzyme active site. Berkessel and Thauer proposed that conformational locking of **7.1** in the enzyme active site would allow the reaction with hydride due to decreased stabilisation of the imidazolidinium cation by tying up the stabilising nitrogen lone pair of electrons as well as exposing only the *pro-R* hydrogen of **7.2** to H/D exchange with the solvent, using a never before proposed superelectrophilic activation of CH≡H_4MPT$^+$ **7.1** in the enzyme active site.

SCHEME 7.9: Reaction of orthoamide **7.16** with acid.

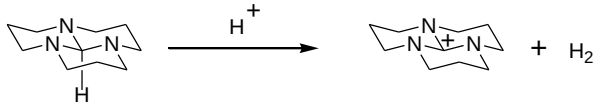

7.16 **7.17**

Thauer *et al*.[121] later examined the rate of dihydrogen production from the reaction of CD_2=H_4MPT **7.4** in H_2O, based on the previous proposal that the reaction occurs through a pentacoordinated carbonium cation such as **7.14**. Two mechanisms were proposed for the formation of H_2 in the reaction (Scheme 7.10).

SCHEME 7.10: Mechanisms of formation of H_2 by CD_2=H_4MPT **7.4**.

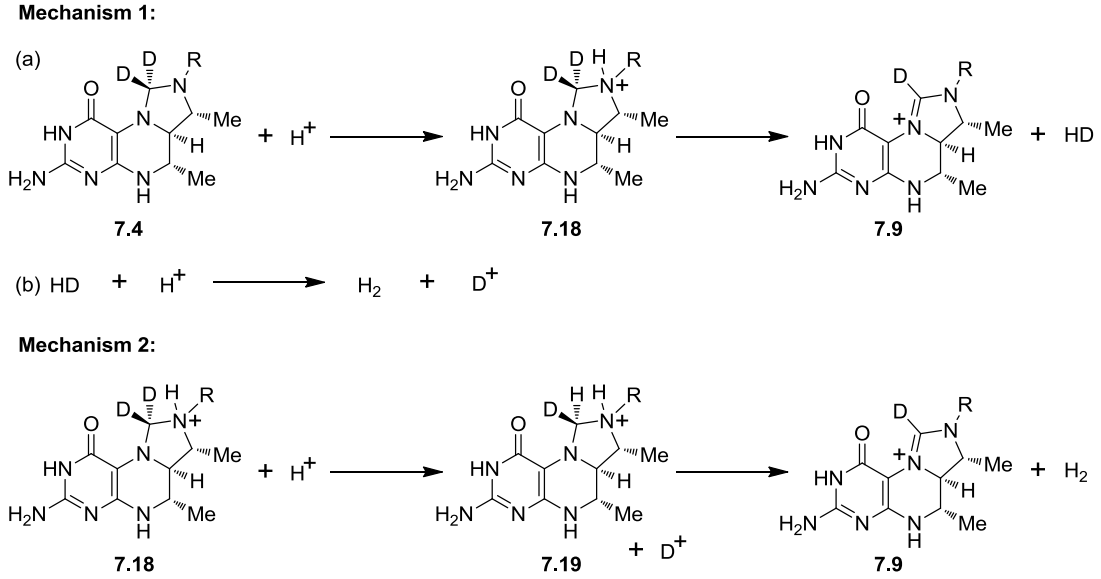

In mechanism 1, protonation of CD_2=H_4MPT **7.4** gives cation $[CD_2H$=$H_4MPT]^+$ **7.18**, which then loses HD to give $CD{\equiv}H_4MPT^+$ **7.9** (mechanism 1(a), Scheme 7.10). The HD produced can then undergo exchange with acid to give H_2 and D^+ (mechanism 1(b), Scheme 7.10). The second proposed mechanism again involves protonation of CD_2=H_4MPT **7.4** and gives cation $[CD_2H$=$H_4MPT]^+$ **7.18**. Instead of loss of HD, exchange of D^+ and H^+ occurs to give onium cation $[CH_2D$=$H_4MPT]^+$ **7.19**, with subsequent loss of H_2 to give $CD{\equiv}H_4MPT^+$ **7.9**. In mechanism 1, HD is formed as an intermediate in the reaction, whereas in mechanism 2, HD is not an intermediate in the reaction. Kinetic investigation of the mechanism could then discriminate between mechanisms 1 and 2.

They studied the kinetics of formation of H_2 and HD from CD_2=H_4MPT **7.4** in H_2O and the formation of HD and D_2 from CH_2=H_4MPT **7.2** in D_2O. They found that the rate of production of H_2 or D_2 was independent of the concentration of HD produced in either reaction. Based on this, the authors concluded that production of H_2 or D_2 would likely occur via mechanism 2 (Scheme 7.10), through a transition state intermediate CH_3=H_4MPT^+ which undergoes stereospecific exchanges with the protons of water.

After the proposal by Berkessel and Thauer,[114] various computational studies[122-124] were conducted on the feasibility of the reaction of amidinium ions with molecular hydrogen. Cioslowski and Boche examined the proposal that conformational changes in amidinium ions would promote reaction with H_2.[122] They calculated the energy for the reactions of amidinium cation **7.20** and bicyclic amidinium ion **7.22** in the reaction with H_2 to give reduced products **7.21** and **7.23** respectively (Scheme 7.11). Amidinium cation **7.20** was used to model $CH{\equiv}H_4MPT^+$ **7.1** in its "free" state, whereas bicyclic amidinium cation **7.22** was used to model the conformationally restricted $CH{\equiv}H_4MPT^+$ **7.1** proposed by Berkessel and Thauer. Both reactions were calculated as being highly endothermic; reduction of **7.20** with H_2 to form **7.21** gave a calculated energy change of 244 kcal/mol, whereas reduction of **7.22** with H_2 to give **7.23** was more favourable, but still endothermic, with a calculated energy change of 149 kcal/mol.

SCHEME 7.11: Theoretical reactions studied with amidinium cations.

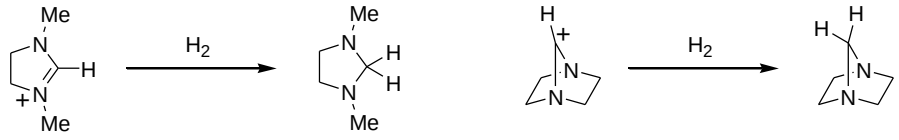

7.20 **7.21** **7.22** **7.23**

They then examined the effects of solvation of the reaction. When water was included in the calculations, reduction of **7.20** to **7.21** was still endothermic, though only by 33 kcal/mol, whereas reduction of **7.22** to **7.23** was exothermic by 57 kcal/mol. The presence of ammonia as a base for capturing the proton produced in the reaction was then examined (the ammonia was also solvated by water in the calculations). When ammonia was included, reaction to form **7.21** became endothermic by 4 kcal/mol, whereas reaction to form **7.23** became exothermic by 87 kcal/mol. These results are summarised in Table 7.1.

Table 7.1: Energy values calculated for reaction of amidinium cations **7.20** and **7.22** with H_2.

Reaction	**Solvation**	**Energy / kcal.mol^{-1}**
7.20→ 7.21	None	244
	H_2O	33
	NH_3/H_2O	4
7.22 → 7.23	None	149
	H_2O	-57
	NH_3/H_2O	-87

The authors stated that the proposal by Berkessel and Thauer[114] for activation of **7.1** by conformational distortion (possibly by superelectrophilic activation) was thermodynamically feasible, as shown by the calculated exothermic reaction when the substrates are solvated by water or a base is present. The endothermic energy calculated for planar amidinium cation **7.20** even in the presence of base showed that distortion of **7.1** may be necessary for hydride abstraction to occur.

Following this work, Teles *et al.*[123] reported *ab initio* studies on the reaction of **7.24** with H_2 to give **7.25** in the presence of different proton acceptors (Scheme 7.12).

Using water as a proton acceptor, they studied the effects of water being present as a single molecule, dimer, trimer or tetramer. The results (Table 7.2, entries 1-4) show that as additional water molecules are added, the reaction becomes thermodynamically more favourable, eventually becoming exothermic when a water tetramer is modelled (Table 2, entry 4). When amine is used as the base (ammonia, methylamine, dimethylamine or trimethylamine), the reaction becomes even more favourable (Table 7.2, entries 5-8), with methylamine calculated as being thermally neutral, similar to the thermoneutrality of Hmd ($\Delta G°' = -5.5$ kJmol^{-1}).

SCHEME 7.12: Reaction of amidinium cation **7.24** with H_2 in presence of base as proton acceptor.

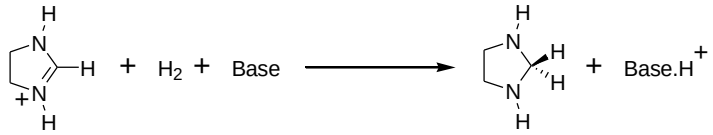

7.24 **7.25**

Table 7.2: Energies for reaction of **7.24** and H_2 in presence of base as proton acceptor.

Entry	**Base**	**Energy / kJmol^{-1}**
1	H_2O molecule	210
2	H_2O dimer	70
3	H_2O trimer	14
4	H_2O tetramer	-55
5	NH_3	37
6	$MeNH_2$	-8
7	Me_2NH	-39
8	Me_3N	-57

The authors concluded that the thermoneutrality of the enzymatic reaction could be reproduced by *ab initio* calculations if the higher basicity of bulk water was taken into account. Also, a low-energy pathway for reduction of amidinium cation **7.24** exists if an amine is used as a base. In this pathway distortion of the amidinium cation is not necessary. They predicted the presence of a basic nitrogen atom in the

enzyme's active site located on the *Re* side of reactive carbon atom C_{14a}, which would assist in the enzymatic reaction.

Just after the study reported by Teles *et al*.,[123] Scott *et al*. reported a similar study on the reaction of **7.20** with molecular hydrogen in the presence of a base.[124] The *ab initio* study showed that cleavage of molecular hydrogen could be achieved with a small energy barrier using the formate anion or ammonia as a base. In absence of a base, they calculated the activation barrier for conversion of **7.20** to **7.21** as 975 $kJmol^{-1}$. When solvated formate anion was used as the base, the barrier was lowered to 114 $kJmol^{-1}$ with an enthalpy of -6 $kJmol^{-1}$. With solvated ammonia as the base, the activation barrier was calculated at 140 $kJmol^{-1}$ with an enthalpy of 17 $kJmol^{-1}$. In addition, the calculated transition state for the reaction showed an antiperiplanar arrangement of the nitrogen lone pair of electrons with the forming C-H bond, which was thought to increase the reactivity of the imidazolidinium carbocation.[114]

The computational studies reported[122-124] explored the feasibility of hydride addition to amdinium salts but did not comment on the superelectrophilic actication of the amidinium salt by further protonation that had been proposed by Berkessel and Thauer.[114] Investigation into the mechanism of H_2-forming methylene-tetrahydromethanopterin dehydrogenase was attracting much attention in the literature as a purely organic hydrogenase. This interest however was about to intensify further, thanks to an important discovery that was to be reported.[115]

7.4 From Metal-Free to [Fe]-Hydrogenase

When Shima *et al*.[115] reexamined the spectral properties of the Hmd hydrogenase they made a startling discovery. They showed that Hmd was inactivated by UV-A/blue light irradiation, and from this determined that the "metal-free" hydrogenase did in fact contain an "active" iron cofactor.

Hmd was prepared under anaerobic conditions using an anaerobic chamber filled with 95 % N_2/5 % H_2. These preparations showed 1 ± 0.2 mol iron per mol Hmd monomer (determined by trapping the iron in a complex with absorption maximum at 563 nm, and measuring against an $FeCl_3$ calibration curve). The Hmd stored in the dark showed no loss in activity in contrast to samples exposed to white light, where

activity decreased to zero over 30 minutes. Tests using monochromatic light showed Hmd to be inactivated by UV-A (320-400 nm) and blue light (400-500 nm). In addition, experiments showed that iron-leaching increased linearly with decrease in Hmd activity when EDTA was present and that the inactive Hmd contained no iron. When EDTA was not present, light irradiation caused bleaching and inactivation of Hmd, but almost no iron was released from the enzyme. The authors suggested that this was the reason that the presence of "active" iron had not previously been observed in the enzyme, as previously prepared samples had not been stringently prepared in dark conditions.

Shima *et al*. also re-examined the effect of CO inhibition on Hmd.[115] Previous studies[110] had shown that Hmd was not inactivated by CO concentrations of 5 % or 50 %. At 100 % CO concentration, Hmd activity was inhibited by over 50 %. The CO concentration was ~100 X higher than that required to inhibit most [FeFe]-hydrogenases and ~10 X higher than for [NiFe]-hydrogenases, which was why the level had not been previously examined. The CO inhibition was shown to be reversible, and removal of CO resulted in a return in Hmd activity.

Studies on the cofactor alone showed a light sensitivity, with the cofactor being bleached, with resulting loss of iron, upon exposure to light. From these studies, Shima *et al*.[115] proposed that Hmd contained an iron-containing cofactor (also called the FeGP cofactor) that is not redox active and is necessary for the enzyme activity. With this important discovery, the H_2-forming methylenetetrahydromethanopterin dehydrogenase could no longer be considered as a purely organic hydrogenase and a great deal of research was conducted into determining the structure of this new iron active site and its importance in the hydrogenase activity.

Light- or heat-inactivation of the cofactor released iron and CO. Chemical analysis revealed 2.4 ± 0.2 mol of CO per mol Fe in the cofactor.[125] In addition, a relatively stable product of mass 542 Da could be isolated by HPLC and analysed. Structure elucidation on the stable product suggested a pyridone-type ligand consistent with **7.26** (Scheme 7.13).[125] The pyridone structure was supported by fluorescence spectroscopy on the inactivated cofactor.

SCHEME 7.13: Pyridone ligand isolated from Hmd cofactor.

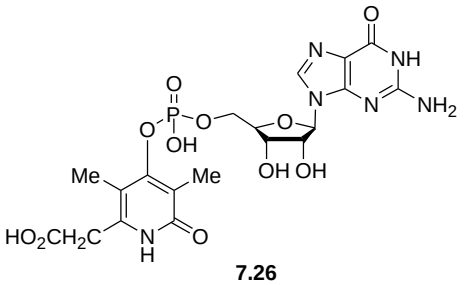

7.26

Next, Lyon *et al.*[126] examined the IR spectrum of Hmd in order to determine the ligands that were attached to the iron in the cofactor. IR analysis of the enzyme showed two absorption bands at 2011 and 1944 cm^{-1}, derived from the two intrinsic CO molecules bound to the iron atom in the cofactor. No change in the IR spectrum was observed when the enzyme's spectrum was measured under nitrogen, oxygen or hydrogen. Analysis of the intensity of the IR bands suggested the presence of an $Fe(CO)_2$ unit where the CO groups were present at an angle of 90°.

They then examined the IR spectra of CO-inhibited Hmd, CN^--inhibited Hmd and the spectrum of Hmd in the presence of **7.1** or **7.2**.

Incubation of Hmd under CO led to three CO bands (2074, 2020 and 1981 cm^{-1}) of similar intensity. Incubation under ^{13}CO resulted in three bands (2050, 1999 and 1980 cm^{-1}), one of which was determined as coming from ^{13}CO. The IR spectrum reverted back to the spectrum recorded for Hmd (two CO bands at 2011 and 1944 cm^{-1}) when the gas phase was replaced with argon, H_2, N_2 or air. The authors suggested that the CO-inhibited enzyme contains three CO units and that the extrinsic CO units will not replace the two intrinsic CO molecules under any incubation times or temperatures. In addition, the extrinsic CO is readily removed upon removal of CO from the gas phase, but the intrinsic CO ligands are not removed.

The CN^--inhibited Hmd contained three bands at 2091, 2020 and 1956 cm^{-1}. When $^{13}CN^-$ was used as the inhibiting reagent, three bands were observed at 2047, 2017 and 1956 cm^{-1}. Based on the shifts measured, the cyanide bands were assigned to 2091 and 2047 cm^{-1} for CN^- and $^{13}CN^-$ respectively. Calculations based on the spectrum intensities indicated that the two CO units were at 90° to one another.

Competition for inhibition binding between CO and CN^- showed the CN^--inhibited enzyme as the major product. This indicated that Hmd had a higher affinity for CN^- than for CO as a ligand.

Addition of **7.1** or **7.2** under the presence of argon or H_2 led to small changes in the IR spectrum of Hmd. The IR bands of the CO signals shifted slightly (from 1-7 cm^{-1}) and sharpening of the absorption bands occurred. The results suggested that $CH{\equiv}H_4MPT^+$ **7.1** binds close to or at the iron site in the cofactor, resulting in a slight higher frequency shift in the CO bands. The 20-30 % decrease in the width of the absorption bands indicated less vibration of the CO positions in space, consistent with a decrease in flexibility of the active-site pocket caused by binding of **7.1** to the iron centre or in close proximity to it. With the addition of H_2, the effects of **7.1** on the IR spectrum of Hmd were amplified. This could indicate that hydrogen may directly interact with the iron centre in the presence of **7.1**, although the authors could find no evidence of Fe-H or Fe-D stretches in the IR spectrum.

When the iron-containing cofactor was isolated and analysed, the CO bands were found to shift from 2011 and 1944 cm^{-1} to 2031 and 1972 cm^{-1}, indicative of decreased electron density in the iron centre or a change in the total number of ligands attached.

Based on the IR analysis of the CO ligands, Lyon *et al.*[126] concluded that the iron in the Hmd cofactor was co-ordinated to two CO molecules. From this they concluded that the iron present in Hmd is most likely to be Fe(II); coordination to three CO molecules in the CO-inhibited Hmd makes Fe(III) unlikely as iron (III) tricarbonyl complexes have not been reported. Fe(0) as the species is unlikely as iron (0) cyanide complexes are rare (but not unknown, $[Fe(CO)_4CN]^-$ has been reported[127]). Hmd was shown to be EPR silent,[126] which ruled out Fe(I) as the iron species. This makes Fe(II) the most probable species to be present in Hmd, but the results did not prove the oxidation state.

In order to gain insight into the electronic structure of iron in Hmd, Shima *et al.*[128] measured the Mössbauer spectra of ^{57}Fe-labelled Hmd prepared under dark conditions. The results showed the presence of a low-spin iron in a low oxidation state. Inhibition of the enzyme by CO or CN^- showed changes in the recorded Mössbauer spectrum, an indication that the inhibitors were bound to the iron site.

However, the addition of hydrogen and/or $CH{\equiv}H_4MPT^+$ **7.1** did not lead to any significant change in the Mössbauer spectrum. This would seem to indicate that H_2 or **7.1** bind near the iron in the enzyme, but are not direct ligands to the iron site, that when Hmd interacts with the substrates (H_2 and/or **7.1**), the electronic state of the iron doesn't change significantly.[128] This conclusion appears unlikely as even if **7.1** does not bind to the Fe centre, it would be expected that hydrogen would need to bind/interact with the Fe centre in order to become activated for heterolytic cleavage. Quantification of the Mössbauer signal intensities gave a calculated 1.14 ± 0.25 mol iron per mol protein monomer. Analysis of the magnetic properties of the three Hmd preparations (Hmd, CO-inhibited Hmd and CN^--inhibited Hmd) showed them to be diamagnetic with spin S = 0, consistent with Fe(II) or Fe(0) low-spin and not paramagnetic Fe(I) or Fe(III) low-spin. Based on the IR[126] and Mössbauer[128] studies, it appears likely that the iron present in Hmd is Fe(II), though this has not been conclusively proven.

7.5 The Crystal Structure Revealed

In 2006, Pilak *et al*.[129] reported the crystal structure of the apoenzyme of Hmd (the enzyme without the iron-containing cofactor present) from *M. jannaschii* and *M. kandleri* at 1.75 Å and 2.4 Å resolution respectively.

Hmd from *M. jannaschii* was found to consist of a homodimer with approximate dimensions of 90 Å X 50 Å X 40 Å, subdivided into a central globular unit attached to two peripheral units in a linear manner. Each peripheral unit corresponded to the N-terminal domain of one subunit and was composed of an α/β structure that belongs to the Rossmann fold protein family (Figure 7.2). The central globular unit was composed of the C-terminal segment of both subunits, each containing four α-helices that form an intertwined intersubunit helix bundle. The Hmd from *M. jannaschii* was present in a closed conformational state (Figure 7.3(a)), whereas the Hmd from *M. kandleri* was found to be in an open conformational state (Figure 7.3(b)). Within the crystal structure, the authors located a U-shaped electron density 13 Å long, located close to the bottom of the cleft. The electron density was found to be consistent with polyethyleneglycol, present in the crystallising solution. This was thought to indicate the presence of a channel for substrate delivery within the enzyme.

Figure 7.2: Crystal structure of Hmd apoenzyme of *M. jannaschii*. Reprinted from the *Journal of Molecular Biology*, *358,* O. Pilak *et al*., "The Crystal Structure of the Apoenzyme of the Iron-Sulphur Cluster-free Hydrogenase", 798-809, copyright **2006** with permission from Elsevier.

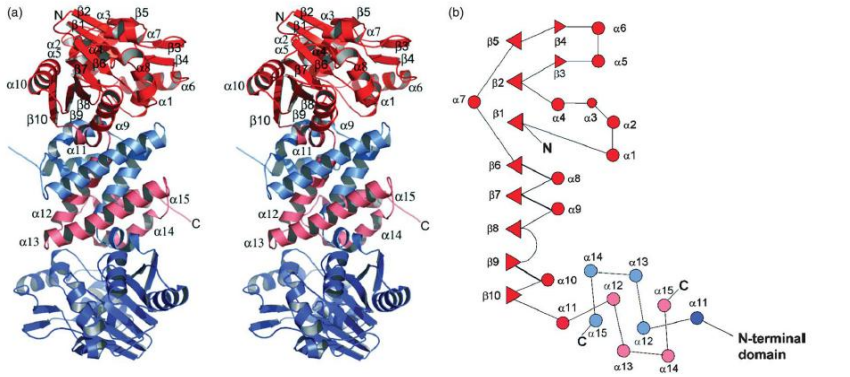

Figure 2. Structure of the iron–sulphur cluster-free hydrogenase (Hmd) apoenzyme from *Methanocaldococcus jannaschii*. (a) Ribbon diagram of the dimer in stereo. Hmd is composed of three globular units: two identical peripheral units consisting of a Rossmann fold like N-terminal segment of two subunits (coloured blue and red) and one central unit composed of the intertwined C-terminal segment of both subunits (presented in light colours). (b) Fold topology diagram of the dimer, which was calculated using the server Topology of Protein Structure (http://www.tops.leeds.ac.uk/) and modified.

Figure 7.3: (a) Closed conformational state of Hmd in *M. jannaschii*. (b) Open conformational state of Hmd in *M. kandleri*. The U-shaped electron density (see text) is shown in green. Reprinted from the *Journal of Molecular Biology*, *358*, O. Pilak *et al*., "The Crystal Structure of the Apoenzyme of the Iron-Sulphur Cluster-free Hydrogenase", 798-809, copyright **2006** with permission from Elsevier.

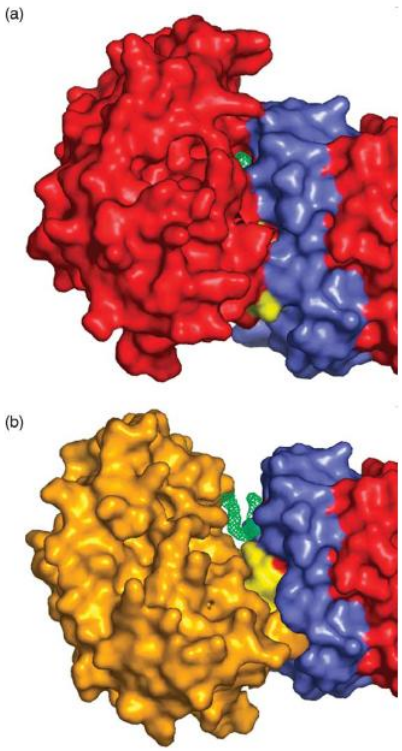

Activity measurements on Hmd reconstituted from *M. jannaschii* showed that for the three conserved cysteine residues (Cys10, Cys 176 and Cys250), only that at Cys176 was essential for enzyme activity.[129] Based on this, Cys176 was assigned as the iron-ligating sulfur ligand.

Figure 7.4: Model of the iron cofactor and substrate **7.2** in the presumed active site of Hmd in *M. jannaschii*. The model of the iron-containing cofactor is shown in yellow, the conformation of CH_2=H_4MPT **7.2** taken from the crystal structure of *M. extroquens*[130] is in grey and is unchanged. Reprinted from the *Journal of Molecular Biology*, *358*, O. Pilak *et al*., "The Crystal Structure of the Apoenzyme of the Iron-Sulphur Cluster-free Hydrogenase", 798-809, copyright **2006** with permission from Elsevier.

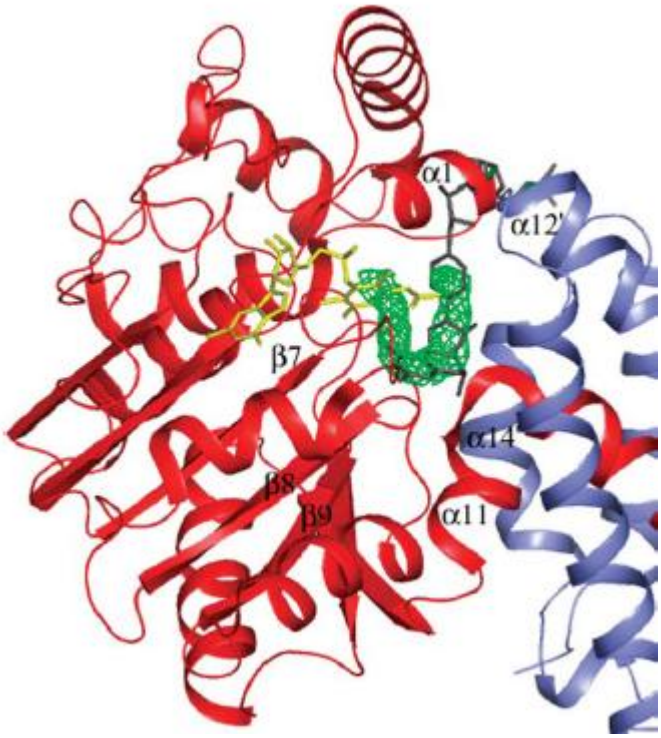

The authors modelled the iron active site and binding of CH_2=H_4MPT **7.2** in the enzyme based on the structure of the formaldehyde-activating enzyme of *M. extroquens* in a complex with CH_2=H_4MPT **7.2**.[130] They found that **7.2** sits in the iron active site at the base of the U-shaped electron density (Figure 7.4). In this position, the C_{14a} of **7.2** is ~6 Å from the assumed Cys176 ligated iron atom, with sufficient space for binding of molecular hydrogen. In this model, the phenyl ring

adjacent to the imidazolidine ring of **7.2** is ~4.5 Å from the pyridone ring of the cofactor ligand **7.26**, which the authors proposed could mean that the phenyl ring was present for binding or conformational purposes.

SCHEME 7.14: Geometry of the active site of Hmd.

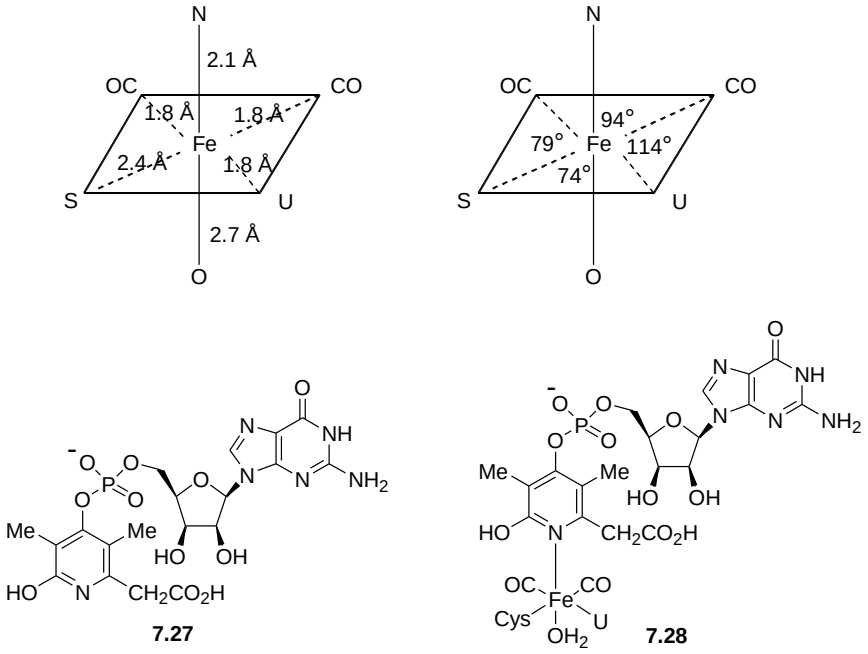

Shima *et al*.[116] were later able to obtain a crystal structure of the holoenzyme (the enzyme including the FeGP cofactor) of Hmd from *M. jannaschii* at 1.75 Å resolution. From this they were able to directly examine the ligands and their geometry in the iron active site of the cofactor (Scheme 7.14, Figure 7.5). The crystal structure showed that the FeGP cofactor was anchored to the enzyme by a guanosine monophosphate. Within the active site, the iron atom exists in a distorted octahedron ligation shell. One of the ligands is from the nitrogen of the pyridinol ligand **7.27** (Scheme 7.14), previously thought to be in the pyridone form **7.26**. The form of the ligand was changed based on the observed planarity of the pyridine ring of the ligand that was observed in the crystal structure. The carboxylate group in ligand **7.27** was disordered in the crystal structure, which led to a tentative determination of its orientation in the crystal structure. The other ligands on the iron were composed of two CO molecules at 90 ° to each other, consistent with previous studies,[126,128] a sulfur from the cysteine in Cys176, an unknown ligand (U in Scheme 7.14) that

could not be solved due to high levels of disorder and a solvent water molecule ('O' in Scheme 7.14).

The structure of the unknown ligand could not be determined from the electron density in the crystal structure. However, soaking the crystals in 3 mM cyanide led to a 1.6 X increase in the electron density at this site, suggesting that it could be the site of reversible cyanide inhibition.

Figure 7.5: Stereoview of electron density in Hmd crystal structure. From *Science* **2008**, *321*, 572-575. Reprinted with permission from AAAS.

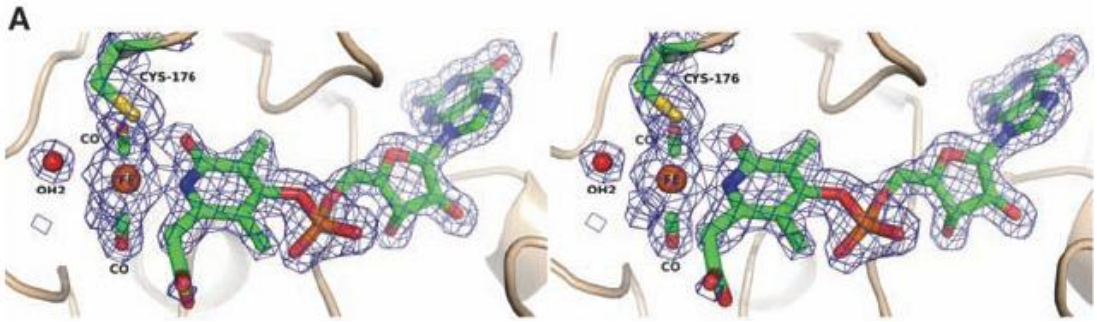

The ligand site below the nitrogen of **7.27** was shown to contain a water molecule. However, the distance between the oxygen atom of water and the iron atom was 2.7 Å, considered too far away to be a "proper" ligand to the iron.[116] The authors suggested that this could be the site of binding for H_2 or extrinsic CO in the CO-inhibited enzyme. The solvent molecule interacts with another solvent molecule, that in turn is linked to the carbonyl group of Cys250 (Figure 7.6).

Figure 7.6: Solvent interaction in the iron active site of Hmd. From *Science* **2008**, *321*, 572-575. Reprinted with permission from AAAS.

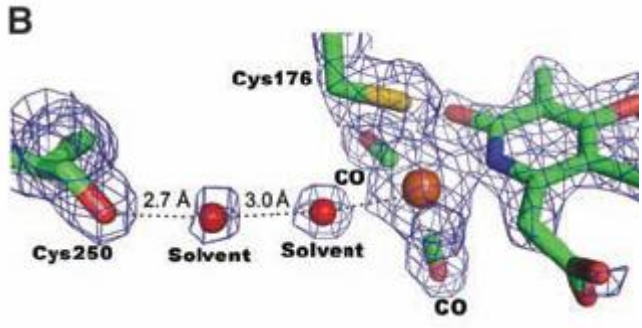

Shima *et al.*[116] suggested that the cleft between the peripheral and central units on the enzyme (Figure 7.2) could accommodate $CH{\equiv}H_4MPT^+$ **7.1**, with the C_{14a} atom being positioned sufficiently close to the iron centre without distortion of the polypeptide chain. However, they stated that the intersubunit cleft was too large for optimal $CH{\equiv}H_4MPT^+$ **7.1** adjustment, so that binding must be accompanied by an induced-fit movement in the enzyme.

The proposed mechanism for the reduction of $CH{\equiv}H_4MPT^+$ **7.1** to $CH_2{=}H_4MPT$ **7.2** is that the hydride accepting $CH{\equiv}H_4MPT^+$ **7.1** and Lewis acidic iron perform bifunctional catalysis to lower the pK_a of molecular hydrogen, allowing it to be heterolytically cleaved into hydride and a proton. Proton acceptors in the vicinity of the active site included Cys176 thiolate, the pyridinol N, O or CO and two histidines, His14 and His201. Along these lines, a His14 → Ala mutation greatly decreased the hydrogenase activity of Hmd, whereas a His201 → Ala mutation had little effect. This indicated the importance of His14 on Hmd activity, possible as a proton acceptor in the reaction.

SCHEME 7.15: FeGP cofactor geometry based on crystal structure of Cys176 mutated Hmd.

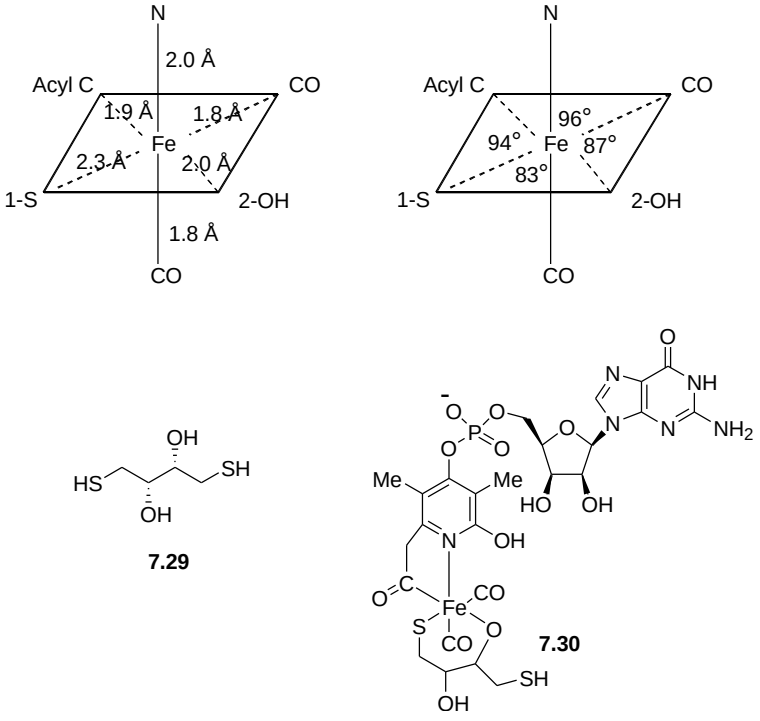

Based on the active site of the [Fe]-hydrogenase reported,[116] a mechanism[131] for hydride transfer to **7.1** and an active site model[132] were reported. These will be discussed in Section 7.6.

Hiromoto *et al.*[117] later revised the structure of the FeGP cofactor based on the crystal structure of a mutated Hmd enzyme. They reported the crystal structure of a holoenzyme of [Fe]-hydrogenase from *M. jannaschii* where Cys176 was mutated to alanine, and in the presence of dithiothreitol (DTT) **7.29**, at a resolution of 1.95 Å. Significant changes were observed in the iron ligands of the FeGP cofactor that had implications for the structure of the "wild-type" enzyme previously reported.[116] When DTT **7.29** was present, it displaced the binding of the sulfur of Cys176 and the unknown ligand with the 1S and 2-hydroxyl O atoms of DTT **7.29** (Scheme 7.15, Figure 7.7). More significantly, the pyridinol ligand **7.27** was found not only to bind to the iron through the ring nitrogen, but also through the acyl carbon of the "carboxylate" group. This resulted in a 180° rotation of the pyridinol ligand from the previously determined structure **7.28** (Scheme 7.14). As a result of this new acyl binding, the second intrinsic CO ligand is repositioned to the site previously occupied by a solvent molecule. ATR-IR analysis of the mutated enzyme before and after the crystal structure determination still showed the presence of two CO ligands with a calculated angle of 90 ° between them.

Figure 7.7: Stereoview of electron density in mutated Hmd (Cys176-Ala) crystal structure. Reprinted from *FEBS Letters*, *583*, T. Hiromoto *et al*., "The crystal structure of C176A mutated [Fe]-hydrogenase suggests an acyl-iron ligation in the active site iron complex", 585-590, copyright **2009** with permission from Elsevier.

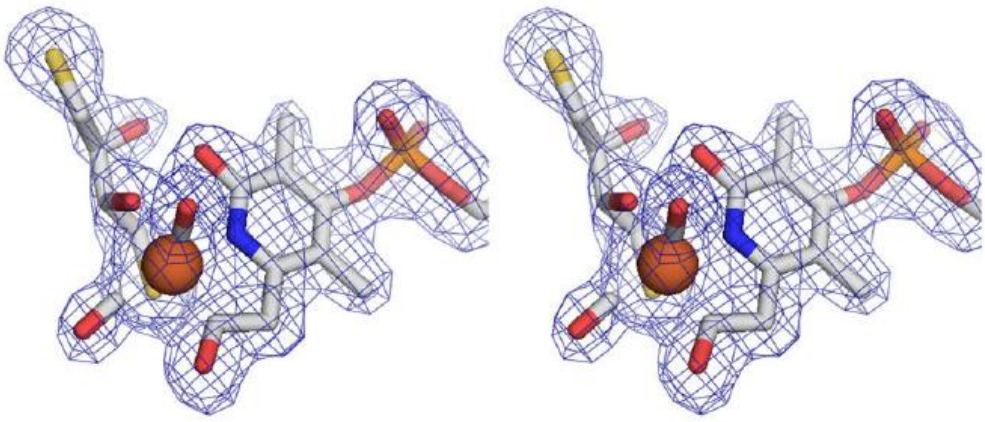

In the mutated enzyme, the hydroxyl group on the pyridinol ligand now interacted via a hydrogen bond to the imidazole group of His14. In addition, the oxygen of the acyl group of the pyridinol ligand was linked via a hydrogen bond to the amide group of Ala176.

Based on this new geometry, Hiromoto *et al.*[117] reexamined the previously reported[116] EXAFS data on the "wild-type" Hmd enzyme. Modifying the iron ligation to include the newly proposed bidentate ligation by the pyridinol ligand led to a better data fit upon re-refining. The authors stated that the "previous interpretation of the electron density was biased by the lack of imagination concerning the possibility of an acyl group as iron ligand and on the subsequent conclusion that the orientation of a negatively charged carboxylate group towards the rather unpolar protein interior is unlikely".[117] As a result of this, a new structure for the FeGP cofactor was proposed (Scheme 7.16, Figure 7.8). In this new structure, the authors state that the most probable site of the second intrinsic CO is that previously occupied by a solvent water molecule (Scheme 7.14). This was based on the crystal structure obtained for the Cys176-Ala mutated Hmd enzyme, but its position could not be identified on a structural basis from analysis of the crystal structure of the "wild-type" Hmd enzyme.

SCHEME 7.16: Revised crystal structure for "wild-type" Hmd.

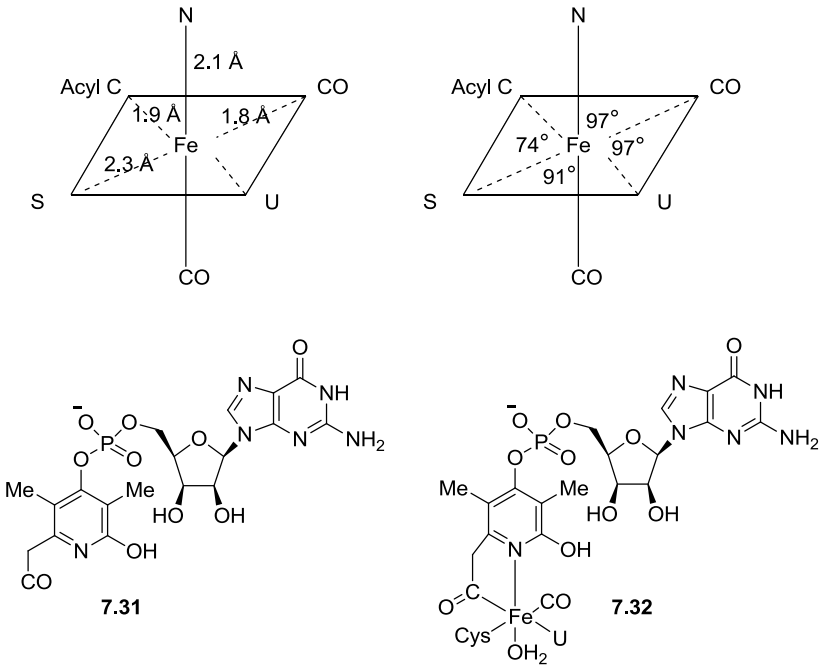

Based on all of the above studies it appears likely that the iron in the active site of the [Fe]-hydrogenase is ligated by the ring nitrogen and acyl carbon of pyridinol ligand **7.31**, two intrinsic CO molecules, the sulfur of Cys176 and an unknown ligand U. It is thought that both $CH{\equiv}H_4MPT^+$ **7.1** and H_2 can enter the active site via a channel in the protein and that the action of the cationic substrate **7.1** and Lewis acidic Fe heterolytically cleave molecular hydrogen, though the exact mechanism is not known. $CH{\equiv}H_4MPT^+$ **7.1** can be orientated close to the iron centre and even interact with the ligands of the iron, but it is not thought to bond directly to the iron centre during the reaction, although it has not been fully discounted. Mössbauer studies[128] on the iron centre showed no significant change on addition of **7.1** to the enzyme, however, no significant changes were observed on the addition of H_2, which makes the reliability of the conclusions questionable.

Figure 7.8: Reinterpretation of iron-ligation structure in [Fe]-hydrogenase. Reprinted from FEBS Letters, *583*, T. Hiromoto *et al*., "The crystal structure of C176A mutated [Fe]-hydrogenase suggests an acyl-iron ligation in the active site iron complex", 585-590, copyright **2009** with permission from Elsevier.

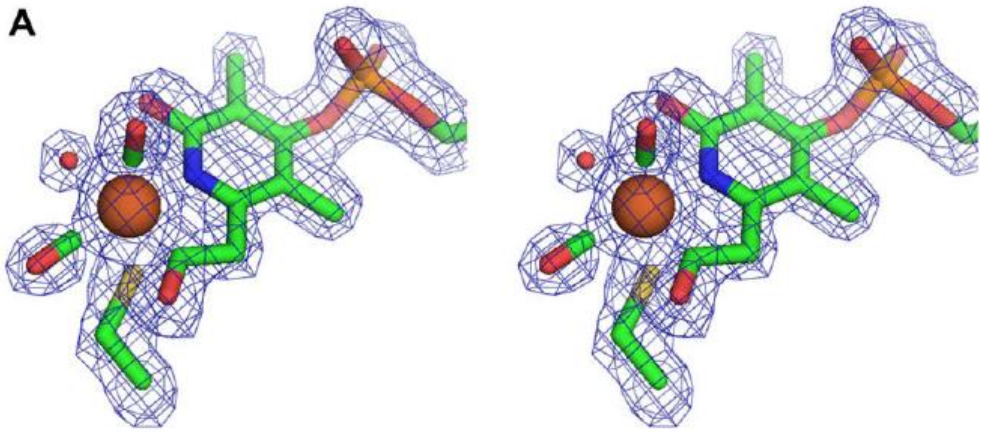

With the structure of [Fe]-hydrogenase determined and the geometry of the active site elucidated, the next stage in development will be obtaining a plausible mechanism for the reaction of $CH{\equiv}H_4MPT^+$ **7.1** with molecular hydrogen.

7.6 Mechanisms and Models

Since reporting of the crystal structure of Hmd, it was inevitable that much work would be conducted in order to try and understand the mechanism of reaction of this

unusual enzyme. As a result of this, a variety of mechanistic studies have been reported in an attempt to explain its unusual reactivity. In addition, a number of models of the proposed iron-active site have been synthesised. This section will briefly examine a few of these literature reports.

7.6.1 First Reported Crystal Structure

Yang and Hall[131] reported a trigger mechanism for the reaction of Hmd using density functional theory calculations. They used complex **7.33** (Scheme 7.17) as a model for the then-determined active-site **7.28**. Several differences in model **7.33** to the active site are apparent. The hydroxyl group in the model had been moved from the 2-position in the real group to the 3-position in order to prevent it from strongly interacting with the sulfur or CO groups bound to the iron. In addition, it was used in the pyridone form, rather than the less stable pyridinol form. Another significant change was inclusion of an oxygen bound to the iron in place of the unknown ligand, the oxygen coming from the carboxylate chain on the pyridone ring. The calculated IR values of the CO ligands in model **7.33** were 1957 and 2014 cm^{-1} (*cf.* 1944 and 2011 cm^{-1} in Hmd).[131]

SCHEME 7.17: Computational model for FeGP cofactor in Hmd.

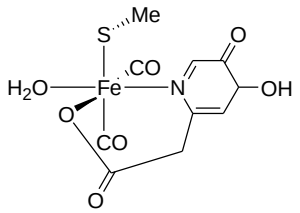

7.33

The calculated mechanism is shown in Scheme 7.18. In the absence of MPT **7.34**, the splitting of H_2 was calculated with a barrier of 69.7 kcal/mol. In the presence of MPT **7.34**, the activation barrier was decreased to 22.0 kcal/mol. The authors stated that the exchange of H_2/H^+ in the mechanism is strongly dependent on MPT **7.34** being present. Without it, H_2 splitting and the exchange of the proton with the protons of water will not occur. They stated that MPT **7.34** or H_2 could arrive in any order at the active site, but that both must be present for the reaction to occur.

SCHEME 7.18: Calculated mechanism of H_2 splitting by model **7.33**.[131] Energies are in kcal/mol.

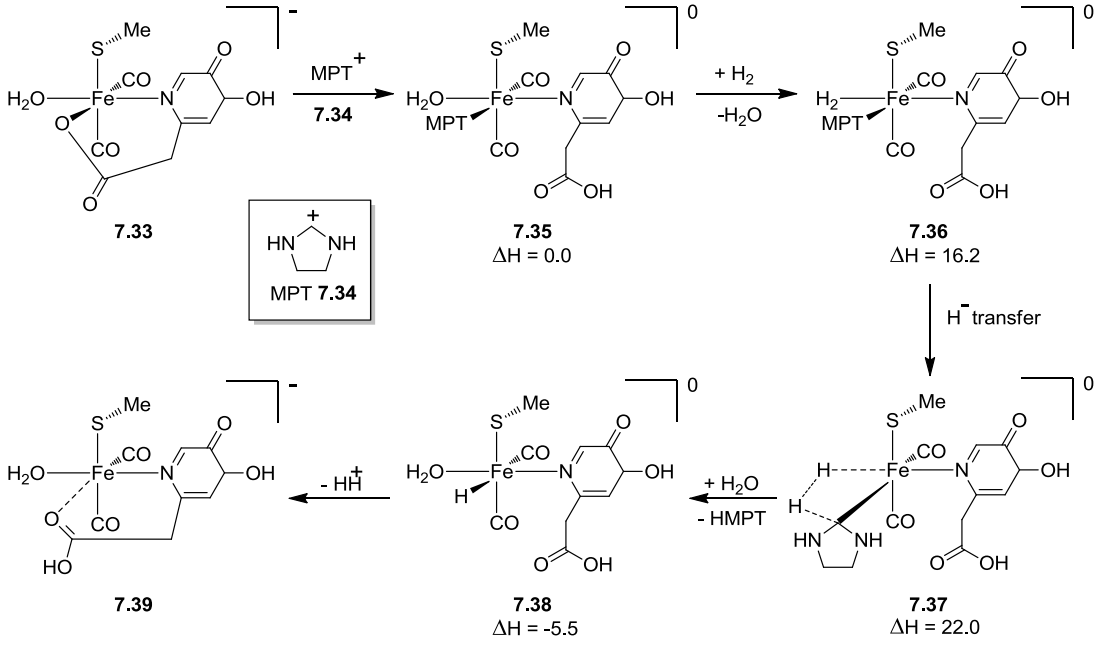

Royer *et al.*[132] reported the synthesis of ruthenium complex **7.40** as a model for the (then reported) active-site of Hmd. This model showed binding to the metal centre by the ring nitrogen in the pyridinol form (as shown by X-ray crystallography). Model **7.40** was able to dehydrogenate alcohol **1.150** to acetophenone **7.41** (Scheme 7.19).

SCHEME 7.19: Hmd active site model **7.40**.

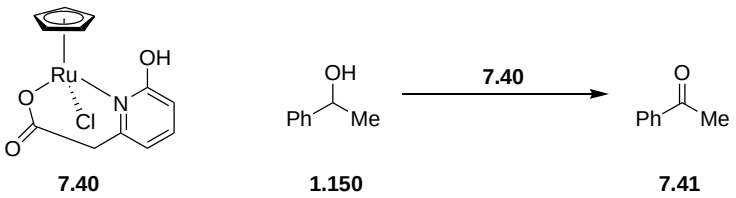

7.6.2 Most Recent Crystal Structure Models

With the reporting of a recalculated crystal structure of the active-site of the [Fe]-hydrogenase, further proposed mechanisms and active-site models have been reported in the literature.

Yang and Hall[133] once again reported a trigger mechanism for the newly re-determined active-site based on model **7.42** (Scheme 7.20).

SCHEME 7.20: Calculated active-site model **7.42**.

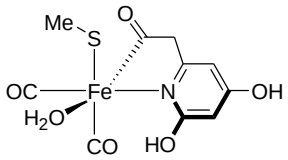

7.42

The calculated mechanism for the splitting of H_2 is shown in Scheme 7.21. A simplified version of the catalytic reaction between Ph-MPT$^+$ **7.51** and H_2 is shown in Scheme 7.22. It was calculated that exchange of H_2O with H_2 would occur to give complex **7.43** (calculated at 8.8 kcal/mol in water). The high energy of this exchange was attributed to the gas-phase calculations not taking into account the solvation by bulk water in the reaction. As a result of this, the authors claimed that the H_2O/H_2 exchange would likely be energetically neutral. Cleavage of H_2 would occur through transition state **7.44** (15.4 kcal/mol) to arrive at complex **7.45** (12.0 kcal/mol) containing a strong Fe-H-H-O bond. In this mechanism, the sulfur at Cys176, modelled here by MeSH, is essential for the hydrogen cleavage to occur.

SCHEME 7.21: Splitting of H_2 using model **7.42**.[133] Energies in kcal/mol.

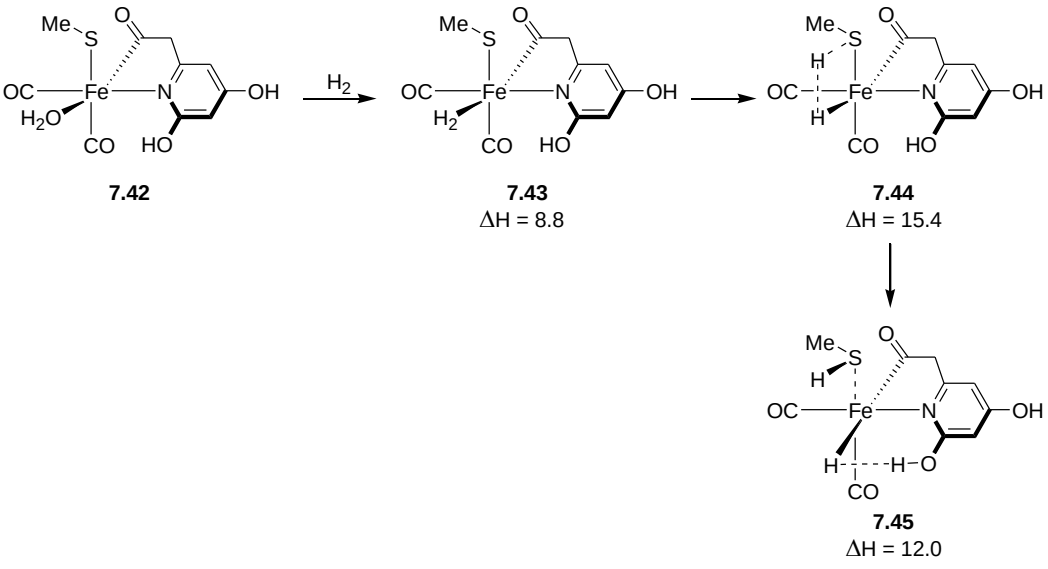

7.42

7.43
ΔH = 8.8

7.44
ΔH = 15.4

7.45
ΔH = 12.0

The authors proposed that complex **7.45** is the resting state of the enzyme. Evidence for this was from the calculated vibrational frequencies of the *cis* CO units at 2007 and 1949 cm^{-1} closely resembling those of the wild-type Hmd. Also, upon addition of H_2, the Mössbauer spectrum of the iron in Hmd does not change significantly.[128] The

authors proposed that complex **7.45** could be formed without significant alteration to the IR spectrum of Hmd.

Complex **7.45** reacts with Ph-MPT$^+$ **7.51** undergoing hydride abstraction through transition state **7.46** (15.6 kcal/mol) to intermediate **7.47** (11.3 kcal/mol). Ph-HMPT then detaches from the complex to be replaced by H_2, resulting in formation of more stable complex **7.48**. Proton loss from **7.48** could then occur from Cys176 (to give **7.50**, 2.1 kcal/mol) or from the pyridinol ligand (to give **7.49**, 0.1 kcal/mol). This is where the observed H_2O/H^+ exchange catalysed by Hmd and **7.1**/**7.2** occurs. Subsequent H_2 cleavage occurs in **7.49** or **7.50** to give complex **7.45** and the catalytic cycle continues.

SCHEME 7.22: Catalytic mechanism of reaction of Ph-MPT$^+$ with H_2.[133] Energies in kcal/mol.

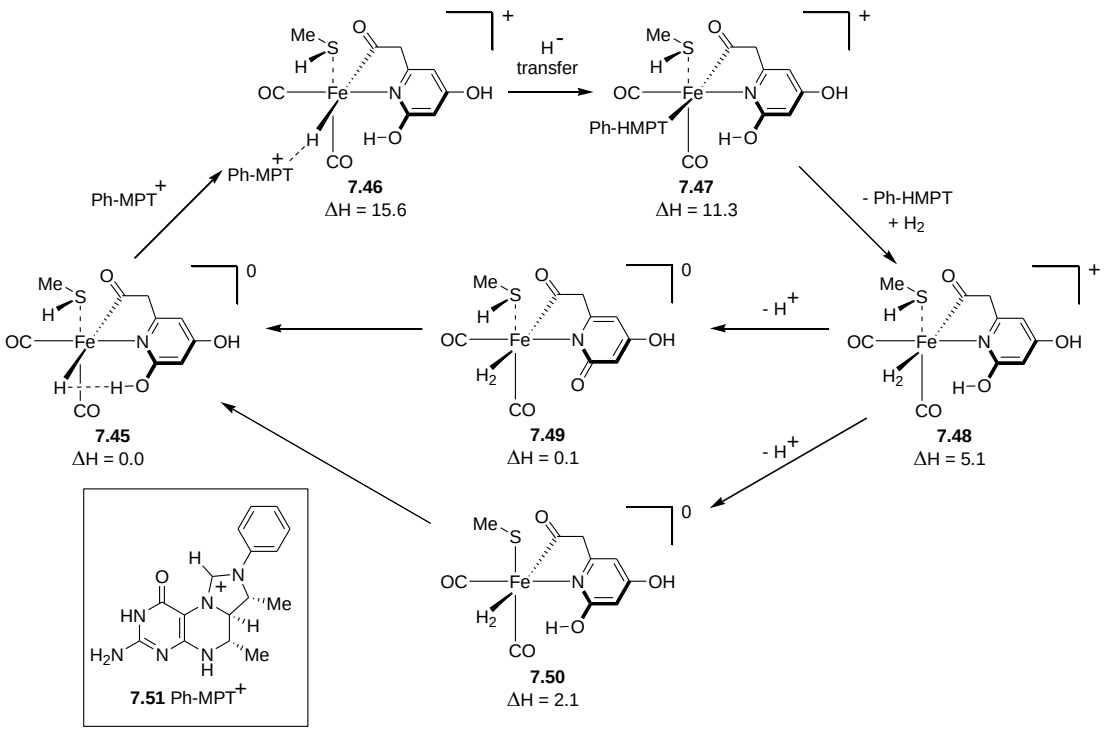

The authors stated that the model showed that the sulfur of Cys176 and the pyridine hydroxyl group were essential for the reaction to proceed, aiding in the splitting of H_2. It was also stated that in the absence of Ph-MPT$^+$ **7.51**, no H_2O/H^+ exchange (or similarly D_2O/H^+ exchange) would occur as the calculated deprotonation energies were too high (20-40 kcal/mol). The arrival of Ph-MPT$^+$ **7.51** triggers a breaking of

the strong Fe-H-H-O bond in **7.45**, allowing the transfer of hydride to occur with an energy barrier of 15.6 kcal/mol (excluding the energy of H_2 splitting as shown in Scheme 7.21).

The calculated deprotonation energies are shown in Table 7.1. As can be seen, the exothermic deprotonations occur in complexes **7.47** and **7.48**, which occur after the reaction with Ph-MPT$^+$ **7.51**. These calculations are consistent with the observed reactivity of Hmd, where exchange observed only in the presence of Hmd and CH≡H_4MPT$^+$ **7.1**/CH_2=H_4MPT **7.2**. However, it is unusual that the deprotonation of the sulfur of MeSH in complex **7.45** is calculated as being so endothermic (25 kca/mol). If complexed to the iron centre, a species such as R_2SH^+ would be expected to be easily deprotonated. If this was to occur, it would allow H^+/H_2O exchange in the absence of CH≡H_4MPT$^+$ **7.1**/CH_2=H_4MPT **7.2**, a reactivity that is not observed in Hmd.

TABLE 7.1: Calculated deprotonation energies of various complexes (Scheme 7.21 and 7.22).

Deprotonation	**ΔG / kcal/mol**
Pyridinol O in **7.43**	20
Pyridinol O in **7.45**	39
Cys176 S in **7.45**	25
Cys176 S in **7.47**	-9
Pyridinol O in **7.48**	-5
Thiol S in **7.48**	-3
Thiol S in **7.49**	23

A further development was reported by Shima *et al*.[134] They reported the crystal structure of a binary complex of Cys176-Ala-mutated [Fe]-hydrogenase with CH_2=H_4MPT **7.2** at 2.15 Å resolution. The results showed that CH_2=H_4MPT **7.2** fitted into the active-site cleft of [Fe]-hydrogenase (Figure 7.9). In the crystal structure obtained, the N_5 and N_{10} of the imidazolidine ring were found to be planar, rather than in the non-planar active form of the substrate. The authors stated that the non-planar active form could be induced by rotation of the phenyl ring adjacent to

the imidazolidine ring that could occur upon in the closed form of the enzyme. The authors stated that in the open-form of the enzyme crystallised, no carboxy group was present to protonate one of the nitrogens of $CH{\equiv}H_4MPT^+$ **7.1**. This protonation would be necessary for the superelectrophilic activation mechanism proposed previously (Scheme 7.7 and 7.8).

FIGURE 7.9: Active-site crystal structure of Cys176-Ala-mutated [Fe]-hydrogenase. S. Shima *et al*.: "The Crystal Structure of an [Fe]-Hydrogenase-Substrate Complex Reveals the Framework for H_2 Activation". *Angew. Chem. Int. Ed*. **2009**. *48*. 6457-6460.[134] Copyright Wiley-VCH Verlag GmbH & Co. KGaA. Reproduced with permission.

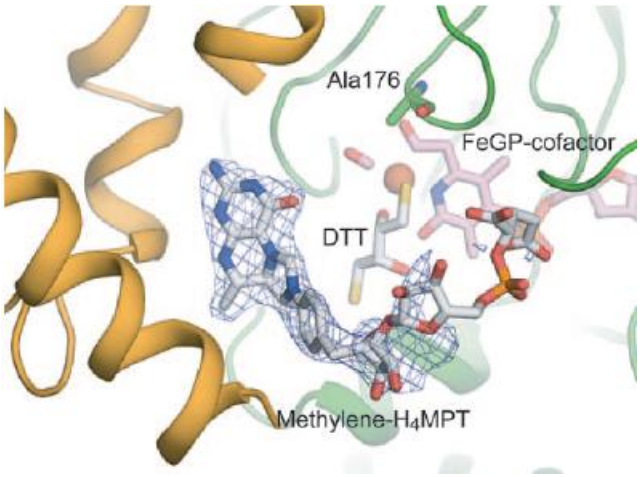

In the open form of the enzyme crystallised, it was found that the C_{14a} of $CH_2{=}H_4MPT$ **7.2** and iron of the active-site were separated by a distance of 9.3 Å, too far for hydride transfer.

Shima *et al*.[134] modelled the closed form of the enzyme with $CH_2{=}H_4MPT$ **7.2** present (Figure 7.10). In this model, the distance between C_{14a} of $CH_2{=}H_4MPT$ **7.2** and iron of the active-site decreased to only 3 Å. The model showed that the C_{14a} of $CH_2{=}H_4MPT$ **7.2** lay *trans* to the acyl carbon of the pyridinol ligand **7.31**, suggesting that the site of H_2 activation was in the position trans to the acyl carbon inhabited by the unknown ligand (U in **7.32**, Scheme 7.16).

FIGURE 7.10: A) Crystal structure representation of Cys176-Ala-mutated [Fe]-hydrogenase and CH_2=H_4MPT **7.2**. B) Modelled closed-form of enzyme with CH_2=H_4MPT **7.2** present. S. Shima *et al*.: "The Crystal Structure of an [Fe]-Hydrogenase-Substrate Complex Reveals the Framework for H_2 Activation". *Angew. Chem. Int. Ed*. **2009**. *48*. 6457-6460.[134] Copyright Wiley-VCH Verlag GmbH & Co. KGaA. Reproduced with permission.

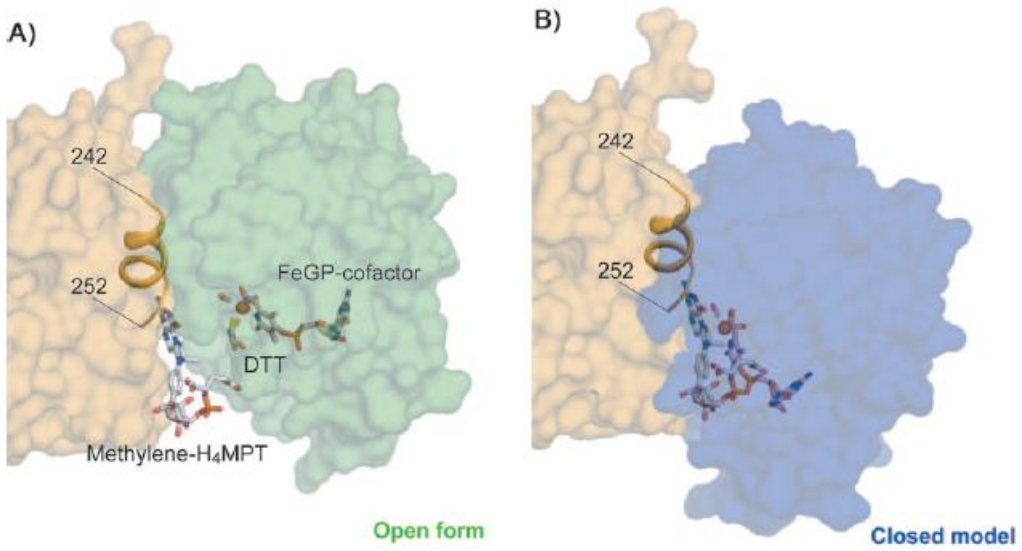

Based on the crystal structure, they proposed a catalytic mechanism based on an open/closed conformational transition (Scheme 7.23). The catalytic cycle is initiated by binding of CH≡H_4MPT$^+$ **7.1** to the open form of the enzyme (**7.52**, Scheme 7.23), causing the closure of the cleft to give the closed conformation (**7.53**, Scheme 7.23). This closure could induce conformational changes in CH≡H_4MPT$^+$ **7.1**, enhancing its carbocationic character. H_2 is then captured at the site of the unknown ligand, the proposed site of H_2-activation, binding side-on to the iron (7.54, Scheme 7.23). The H_2 molecule becomes polarised and can be heterolytically cleaved by the adjacent carbocation (C_{14a} of CH≡H_4MPT$^+$ **7.1**). The hydride is accepted by CH≡H_4MPT$^+$ **7.1** and the resulting proton is proposed to be taken by a base (either the Cys176 thiol or pyridinol oxygen). The results in formation of CH_2=H_4MPT **7.2** and a proton, which can undergo the exchange reactions detailed above.

SCHEME 7.23: Proposed catalytic mechanism for open/closed conformational transition.[134]

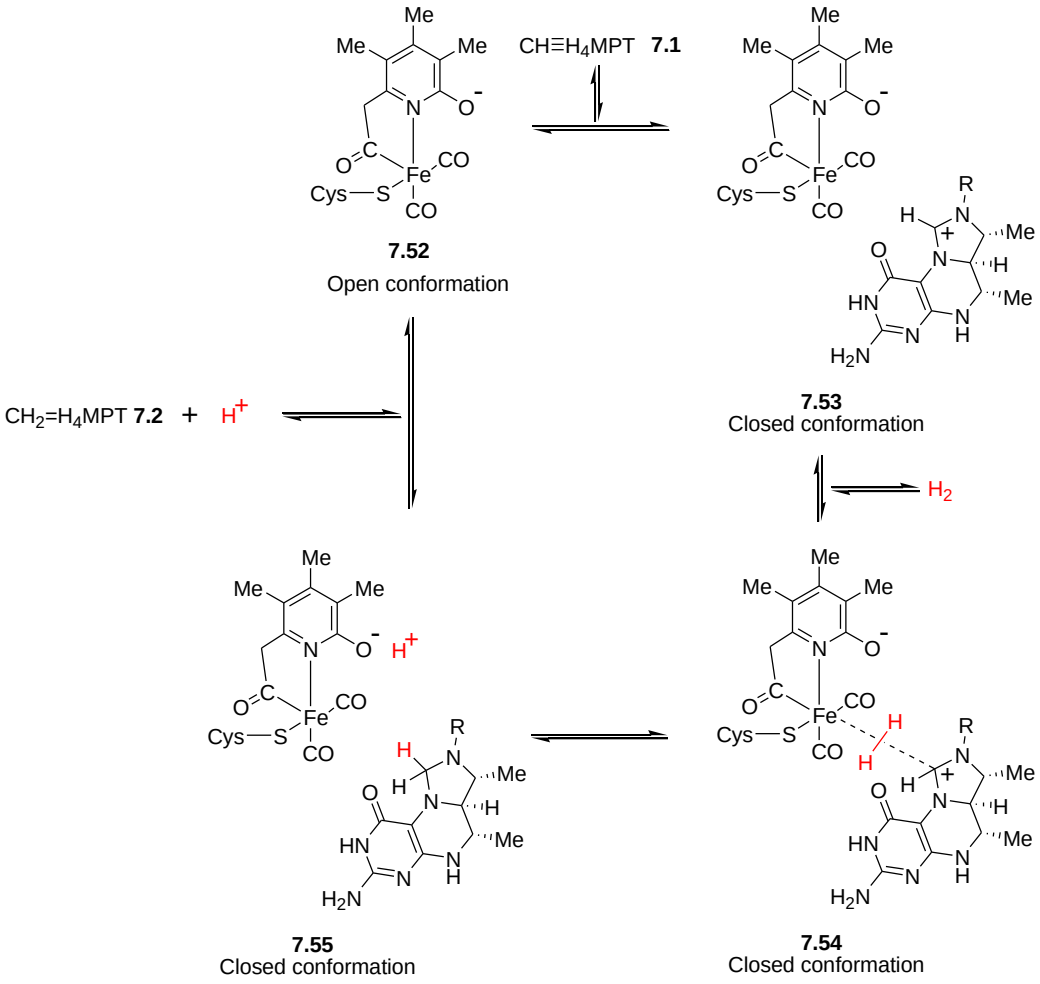

It was stated that no carboxy group was present to protonate one of the nitrogens of $CH{\equiv}H_4MPT^+$ **7.1**, however, in the modelled active-site **7.53**, it was also stated that the hydroxyl group of the pyridinol ring could interact with the N_{10} of $CH{\equiv}H_4MPT^+$ **7.1**, which the authors proposed could modify the properties of the pyridinol. The possibility of such an interaction enabling the superelectrophilic activation that has previously been proposed will be explored in a later section (Section 8.1).

A variety of models for the active site in the [Fe]-hydrogenase have also been synthesised. Hu *et al.*[135] prepared model **7.56**, incorporating a 2-pyridone ligand, while Popescu *et al.*[136] published the analogous complex **7.57** with a pyridine-2-thione in place of the 2-pyridone shortly afterwards. More recently, Hu's group[137] prepared complex **7.58**. With a pyridine, a thiolate, a *cis*-dicarbonyl and an acyl all

complexed to iron(II), this complex has a number of similarities to the FeGP cofactor.

The group of Pickett has also been active in preparation of model iron complexes. Their earlier work[138] reported the synthesis of *cis*-dicarbonyliron complex **7.59**, which had been useful in their study assigning iron(II) as the metal oxidation state in FeGP. In 2010, Pickett *et al.*[139] prepared the advanced analogue **7.60**, giving CO stretches in the IR spectrum at 2026 and 1958 cm^{-1} (compared to 2031 and 1972 cm^{-1} in the FeGP complex).

SCHEME 7.24: [Fe]-Hydrogenase active-site models reported.

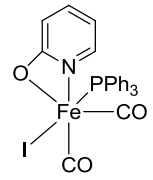

7.56

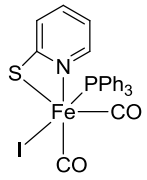

7.57

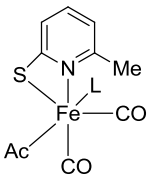

7.58

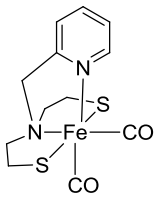

7.59

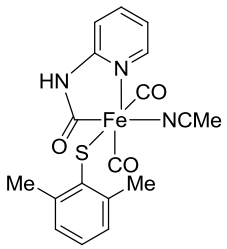

7.60

This review has examined some of the literature pertaining to the [Fe]-hydrogenase enzyme, an unusual hydrogenase with an interesting backstory. Though much work has been reported to understand the intriguing active-site of the enzyme and its mechanism of reaction, little work has been reported on the substrate of the enzyme, $CH{\equiv}H_4MPT^+$ **7.1**, and how activation of this substrate may contribute to the unusual reactivity observed with molecular hydrogen. The next chapter will look at work that has been conducted to examine the possibility of superelectrophilic activation occurring in [Fe]-hydrogenase.

8 [Fe]-Hydrogenase Model Reactions

8.1 Hydrogenation Reactions

A variety of mechanistic proposals and active-site models have been proposed for the [Fe]-hydrogenase. However, no models have been proposed for N^5,N^{10}-methenyl-tetrahydromethanopterin (CH≡H_4MPT$^+$) **7.1**, the substrate that reacts with hydrogen. The similarity between 2-DMAP disalt **4.16** and superelectrophilically activated N^5,N^{10}-methenyl-tetrahydromethanopterin **7.12**/**7.12′** (as proposed by Berkessel and Thauer[114]) was apparent (Scheme 8.1). Given the similar structures of **4.16** and **7.12**, the reactivity of 2-DMAP disalt **4.16** with hydrogen would provide an interesting model study for the reaction for superelectrophilic activation of **7.1**. Some differences between 2-DMAP disalt **4.16** and superelectrophilically-activated **7.12** do exist; the amidinium dication is part of a 6-membered ring in **4.16** and part of a 5-membered ring in **7.12**. Also, part of the amidinium dication in disalt **4.16** is also part of an aromatic ring, whereas the amidinium dication **7.12** is not.

SCHEME 8.1: Comparison of superelectrophile **4.16** and superelectrophile **7.12**.

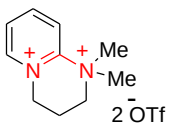

4.16

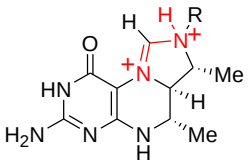

7.12

8.1.1 Hydrogenation Without a Catalyst

The first reactions attempted were the hydrogenation of **4.16** without a catalyst. If possible, this would provide powerful evidence for the superelectrophilic activation mechanism proposed by Berkessel and Thauer. The proposed reaction mechanisms

are shown in Scheme 8.2. In the first proposed mechanism, attack of hydride (from H_2) in the 2-position of **4.16** gives monocation salt **8.1**, with loss of aromaticity in the pyridine ring. Rearomatisation of the ring results in C-N bond cleavage to give pyridinium salt **8.3**. Protonation of pyridinium salt **8.3** with the proton from hydrogen gives new disalt species **8.4**. Obviously hydrogen would not normally act as a source of nucleophilic hydride; the proposed mechanism is meant to parallel the reactivity of $CH{\equiv}H_4MPT^+$ **7.1** in Hmd, which reacts with hydrogen to abstract a hydride. Alternatively, the second proposed mechanism involves addition of hydrogen across the C-N bond of disalt **4.16** to give intermediate **8.5**, which would break down to give pyridinium salt **8.4**.

SCHEME 8.2: Proposed mechanisms for hydrogenation of 2-DMAP disalt **4.16**.

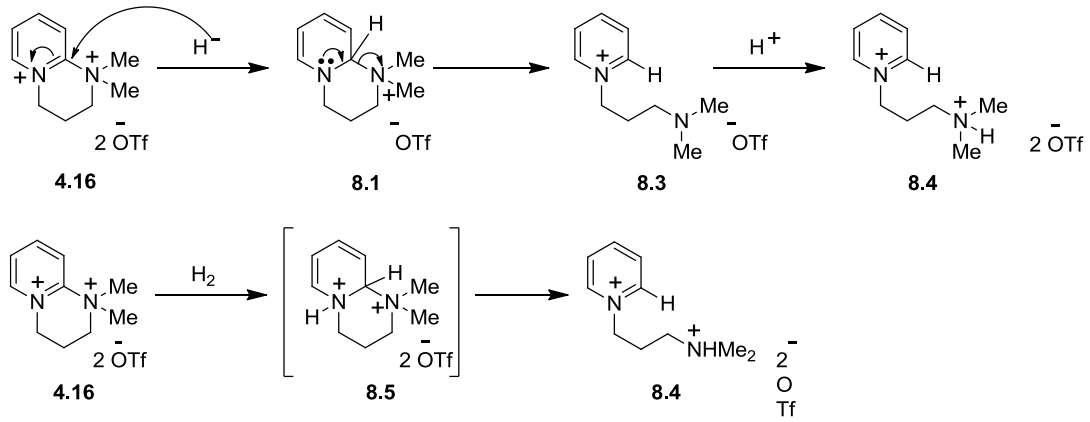

A dilute solution of 2-DMAP disalt **4.16** (0.002 mol.dm^{-3}) in acetonitrile was reacted with 50 atm hydrogen in the Parr hydrogenation vessel at r.t. for 5 days (Scheme 8.3). Unfortunately, no reaction of **4.16** with hydrogen was observed. The dilute solution was necessary as the dimensions of the hydrogenation apparatus required a large volume of solvent to be used. In order to use more concentrated solutions without using vast quantities of 2-DMAP disalt **4.16**, the volume of the vessel would need to be decreased. A nylon insert was machined to fit the hydrogenation vessel that functioned to decrease the volume of the vessel and to provide an inert surface. Use of this insert allowed higher concentration solutions to be used in the hydrogenation reaction. The hydrogenation reaction was repeated using a more concentrated solution (0.083 mol.dm^{-3}); however, no reaction of **4.16** with hydrogen was observed.

SCHEME 8.3: Attempted hydrogenation of **4.16** in absence of catalyst.

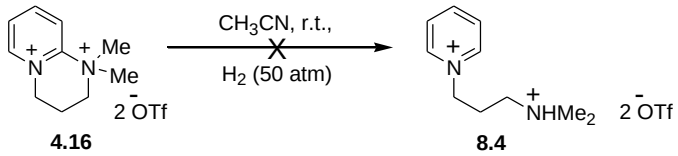

4.16 **8.4**

The lack of reaction between 2-DMAP disalt **4.16** with hydrogen in the absence of a catalyst is not suprising as the proposed first step involves removing the aromaticity of the pyridine ring, a process unlikely to be favourable.

8.1.2 Hydrogenation Using Palladium Catalyst

In order to determine the reactivity of 2-DMAP disalt **4.16** and hydrogen, the next step was to attempt hydrogenation in the presence of palladium on activated carbon. Hydrogenation of **4.16** with 10 mol% of palladium on activated carbon led to formation of 1-(3-dimethylaminopropyl)piperidinium trifluoromethanesulfonate **8.6** in 76 % yield (Scheme 8.4). Formation of piperidinium **8.6** was thought to occur through initial formation of pyridinium salt **8.3**, with subsequent hydrogenation of the pyridinium ring to give piperidine **8.7**. Protonation of the ring nitrogen gives product **8.6** (Scheme 8.4). This hydrogenation shows the potent reactivity of 2-DMAP disalt **4.16**, where complete hydrogenation of species **4.16** occurs under relatively mild conditions.

SCHEME 8.4: Hydrogenation of 2-DMAP disalt **4.16**.

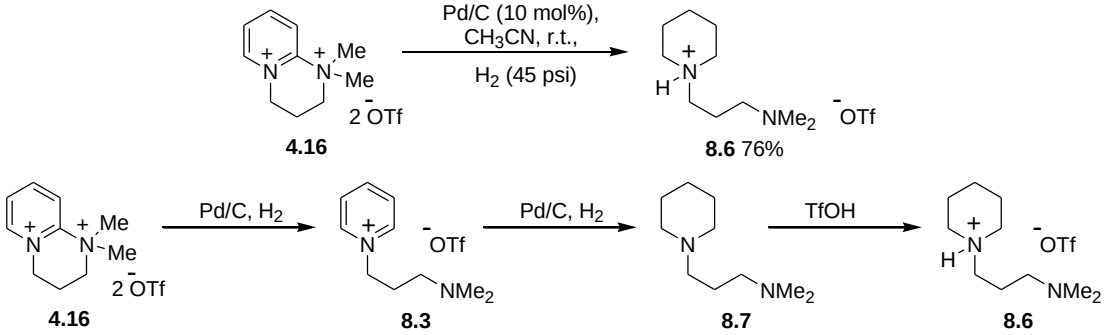

4.16 **8.6** 76%

4.16 **8.3** **8.7** **8.6**

In order to prevent complete hydrogenation, the catalyst loading was decreased to 1 mol%. After only 3 h, hydrogenation product **8.4** was isolated in excellent 99 % yield (Scheme 8.5). The formation of pyridinium salt **8.4** was thought to occur via one of the mechanisms shown in Scheme 8.2.

The reaction was repeated in D_2, with deuterated product **8.8** isolated in 99 % yield. Formation of the deuterated product was shown in the ^{1}H NMR spectrum by disappearance of one of the signals of one of the most downfield pair of aromatic protons. In addition, the methyl protons in **8.8** appeared as a singlet at $\delta_H(CD_3CN)$ 2.84 ppm compared to **8.4** which shows a doublet at $\delta_H(CD_3CN)$ 2.85 ppm (J(H,H)= 5.2 Hz). This showed that regiospecific hydrogenation occurred in disalt **4.16**, similar to the reactivity observed for CH≡H_4MPT$^+$ **7.1** with H_2 in the presence of Hmd.

SCHEME 8.5: Hydrogenation and deuteration of 2-DMAP disalt **4.16**.

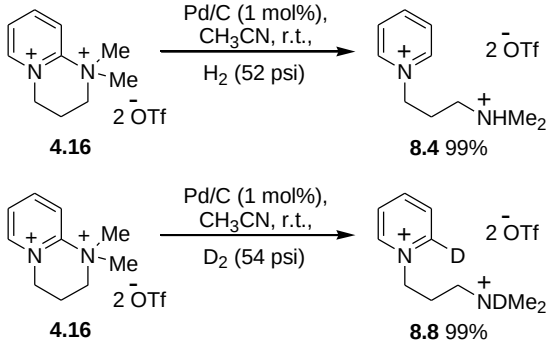

SCHEME 8.6: Reaction of **4.16** with hydride source.

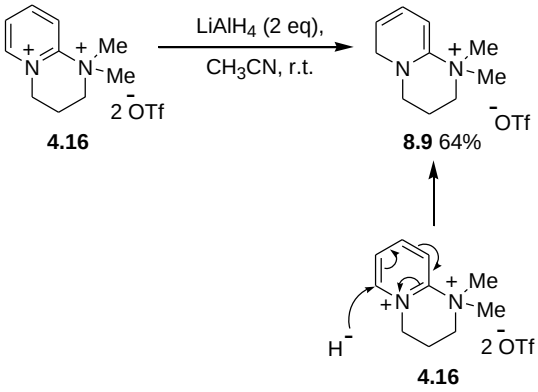

In order to determine if the reaction of hydride with a superelectrophile such as **4.16** (and, by inference, **7.12**) would lead to the desired product, 2-DMAP disalt **4.16** was reacted with a hydride source, namely lithium aluminium hydride (Scheme 8.6). However, reaction with hydride did not occur to give pyridinium salt **8.3**, but gave rise to 2-dihydropyridinium salt **8.9**, resulting from attack on the less-hindered 2-position of the pyridine ring. Salt **8.9** was subsequently isolated in 64 % yield. This result does not exclude hydride as the initial nucleophile in the reaction of H_2 with

disalt **4.16** to form salt **8.4**, as the catalyst may serve to direct the reaction to the superelectrophilic carbon, much as the iron atom in Hmd may direct the reaction of H_2 with **7.1** in the active-site.

The next step was to investigate whether the reaction of disalt **4.16** with hydrogen in the presence of a catalyst was due to the superelectrophilic nature of the substrate, or rather the action of the catalyst. For this, the hydrogenation reaction was repeated using monocation counterparts to 2-DMAP disalt **4.16**. Trimethylpyridin-2-ylammonium trifluoromethanesulfonate **1.169** and demethylated disalt product **4.22** were chosen as non-superelectrophilic equivalents to superelectrophile **4.16**. The substrates were chosen to represent (i) a quaternary nitrogen at the ring nitrogen and (ii) the dimethylamino group nitrogen of 2-DMAP **1.1**. Salt **4.22** was readily synthesised in 86 % yield (Scheme 8.7) by the reaction of **4.16** with triphenylphosphine **5.22** as described previously (Scheme 5.15).

SCHEME 8.7: Attempted hydrogenation of monocation salts **1.169** and **4.22**.

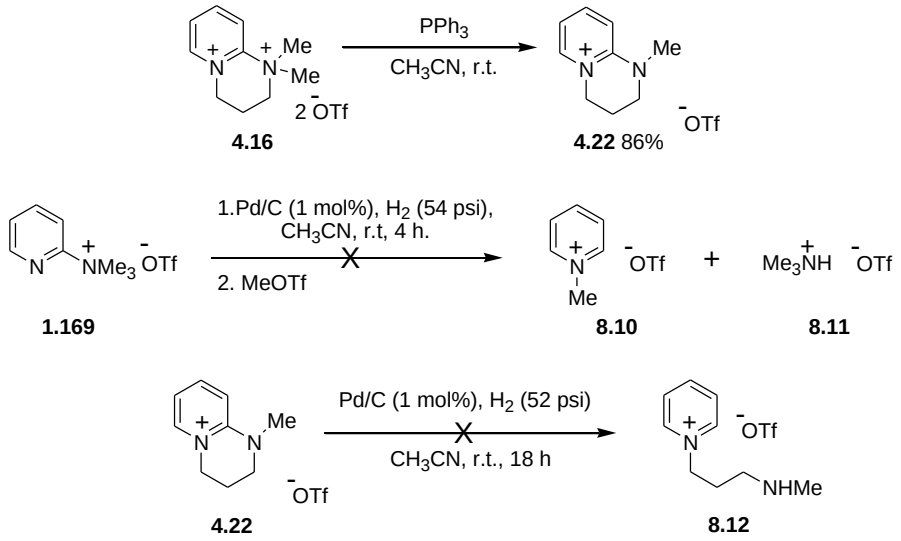

Reaction of 2-DMAP salt **1.169** with hydrogen in the presence of palladium on activated carbon showed no evidence of hydrogenation after 3 h. Methyl trifluoromethanesulfonate was added to the reaction mixture after hydrogenation and before work-up to aid in the isolation of the volatile products likely to be produced (pyridine and trimethylamine). No reaction was observed and salt **1.169** was recovered in 99 % yield. Similarly, no reaction of hydrogen with salt **4.22** in the

presence of palladium on activated carbon was observed, even after 18 h under hydrogen, with salt **4.22** being recovered in 100 % yield (Scheme 8.7).

The results show that the superelectrophilic activation of 2-DMAP disalt **4.16** is necessary for the reaction with hydrogen, as evidenced by no reaction occurring with monocationic salts **1.169** and **4.22** under the same conditions. As a result of the superelectrophilic activation, 2-DMAP disalt **4.16** can undergo regiospecific reaction with hydrogen in the 2-position to furnish pyridinium salt **8.4**, a reaction that shows parallels to the enzymatic superelectrophile activation previously proposed by Berkessel and Thauer (Scheme 7.7, reproduced below). The reactions detailed above show strong evidence that the mechanism proposed is plausible, as superelectrophilically activated amidine cations such as **4.16** (or **7.12**) display enhanced reactivity towards hydrogen compared to their monocationic equivalents (**1.169**/**4.22** and **7.6** respectively).

SCHEME 7.7: Superelectrophilic activation of CH≡H_4MPT$^+$ **7.6**.

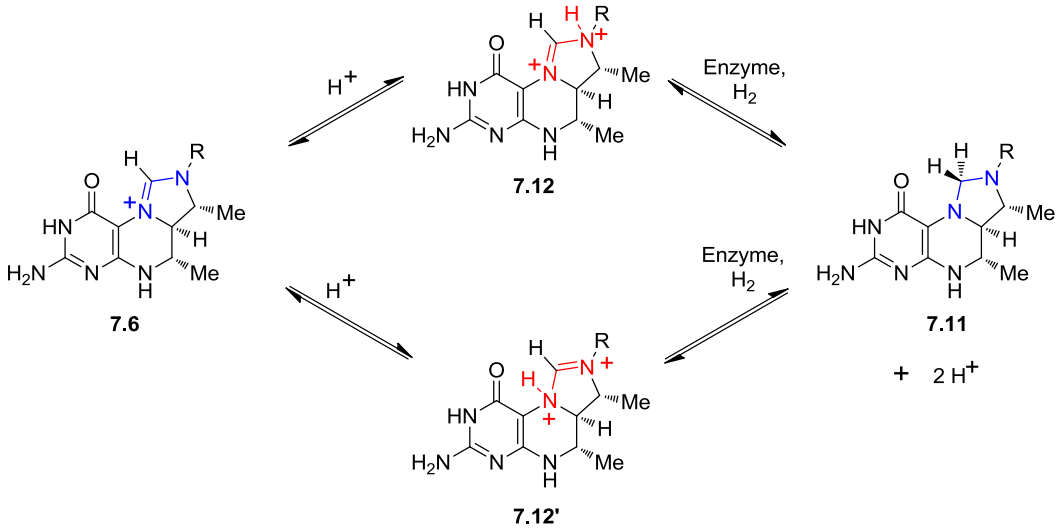

Based on the reactivity observed in 2-DMAP disalt **4.16** with hydrogen, the following mechanism was proposed for the catalytic mechanism of the [Fe]-hydrogenase (Scheme 8.8). The study by Shima *et al.*[134] on the co-crystallisation of Cys176-mutated [Fe]-hydrogenase and CH=H_4MPT **7.2** showed no site on the enzyme for protonation of **7.1** to allow for superelectrophilic activation. However, it was also proposed that the hydroxyl group in the pyridinol ligand could interact with

N_{10} of $CH{\equiv}H_4MPT^+$ **7.1**.[134] Based on these results, superelectrophilic activation of $CH{\equiv}H_4MPT^+$ **7.1** could be achieved by the hydroxyl group of the pyridinol ligand. In the proposed mechanism[140] (Scheme 8.8), the imidazolidinium substrate **8.14** is bound to the iron active-site by transfer of a proton (in red) to the oxygen of the pyridinol ligand to give complex **8.15**. Exchange of the water bound to the iron centre with hydrogen gives complex **8.16**.

SCHEME 8.8: Proposed mechanism for superelectrophilic activation of model substrate **8.14**.

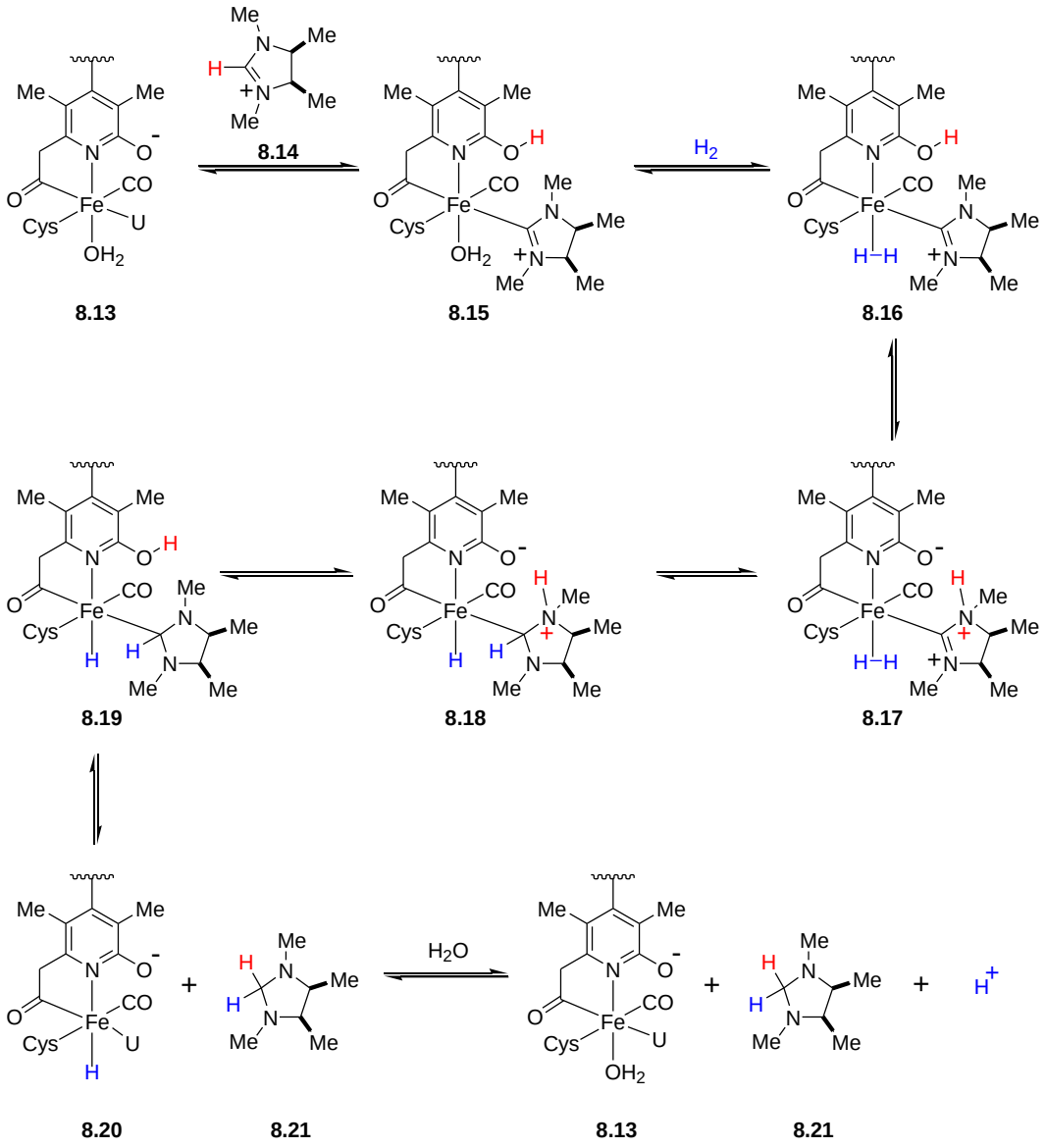

Superelectrophilic activation of model substrate **8.14** occurs via protonation of the nitrogen by the proton on the hydroxyl group in the pyridinol ligand to give

superelectrophilically-activated complex **8.17**. Transfer of hydride from H_2 to model substrate **8.14** gives the complex **8.18**. The original proton from substrate **8.14** (in red) is transferred from the nitrogen back to the hydroxyl group on the pyridinol ligand to give complex **8.19**. Detachment of the hydrogenation substrate occurs with concomitant transfer of the proton (in red) from the hydroxyl group back to the hydrogenation substrate to give reduced product **8.21** and complex **8.20**. The remaining proton (in blue) in complex **8.20** is then activated for transfer with the protons of water or with hydrogen as observed in [Fe]-hydrogenase.

In the proposed mechanism, the iminium proton of model substrate **8.14** is removed upon complexation to the iron in the active-site. This proton is trapped by the pyridinol oxygen in the ligand, preventing it from undergoing reaction with H_2O or H_2 in the enzyme. In addition, H_2 activation occurs *trans* to the nitrogen atom in the pyridinol ligand, ensuring that attack by hydride can only occur in the *pro-R* position, as observed in the enzyme. In the active-site model **8.13**, there are two positions available for binding of either model substrate **8.14** or hydrogen. The previously reported crystal structure study of Hmd has shown only one site for H_2 activation, with the second intrinsic CO molecule being position trans to the pyridinol ligand nitrogen atom in the Cys176-mutated [Fe]-hydrogenase (**7.30**, Scheme 7.15).[117] It was inferred that the second intrinsic CO would likely take the position of the water molecule ligand in the wild-type enzyme that was shown in the previously determined crystal structure[116] (**7.28**, Scheme 7.14). However, this electron density in the wild-type enzyme could not confirm this assumption.

SCHEME 8.9: Proposed superelectrophilic activation of model substrate **8.14** as complex **8.22**.

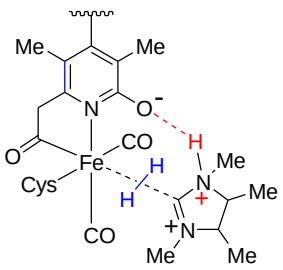

8.22

In order to examine the likelihood of this reaction mechanism, it was studied computationally using QM/MM simulations.[140] However, the calculations showed that binding of $CH{\equiv}H_4MPT^+$ **7.1** or model substrate **8.14** to the iron centre was sterically unfavourable. However, superelectrophilic activation of $CH{\equiv}H_4MPT^+$ **7.1** could still occur by protonation of N_{10} by the hydrogen of the hydroxyl group of the pyridinol ligand such as in Scheme 8.9, as it was shown by Shima *et al.*[134] that interaction of the hydroxyl group of the pyridinol ligand and N_{10} of $CH{\equiv}H_4MPT^+$ **7.1** was possible. However, this mechanism would also require computational analysis to see if it was valid.

8.2 Attempted Model Substrate Synthesis

2-DMAP disalt **4.16** is a pyridinium salt, which is different from the non-aromatic amidinium salts **7.12** and **7.12′** arising in the [Fe]-hydrogenase enzyme. It has been proposed that dications **7.12**/**7.12′** should be so electrophilic as to react with hydrogen in the absence of a catalyst.[114] This was not observed for dication **4.16**, which required a catalyst (albeit in low 1 mol% presence) to react with hydrogen, most likely to aid in the temporary sacrifice in aromaticity required to produce pyridinium salt **8.4**. It was proposed that synthesis of disalts **8.23** and **8.24** (Scheme 8.10) would provide access to dications that more closely resemble dications **7.12**/**7.12′**. Such disalts would not need to sacrifice aromaticity, so their reaction with hydrogen should be more favourable. Disalt **8.24** was chosen as the target for synthesis as disalt **8.23** contains a more strained 5-membered ring, making it more challenging to prepare (though if synthesised, its lesser stability may lead to enhanced reactivity making it a viable target in future studies).

SCHEME 8.10: Model substrates for dication **7.12**.

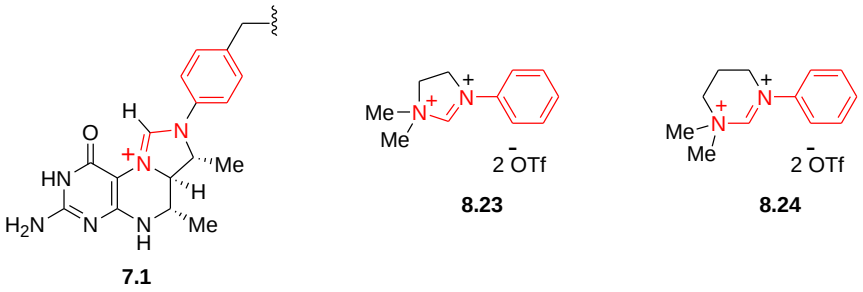

The retrosynthetic analysis for the synthesis of disalt **8.24** is shown in Scheme 8.11. Disalt **8.24** was envisioned to be formed via iminium triflate salt **8.25**. This was based on the work detailed in Section 2.4, where an iminium triflate salt in the presence of a tertiary amine base was suggested to give rise to a disalt species such as **2.70**. Iminium triflate **8.25** was proposed to be furnished from the reaction of amide **8.26** and Tf_2O. Amide **8.26** was to be synthesised from amine **8.27**, a product from the reduction of amide **8.28**, itself synthesised from methyl dimethylaminopropionate **8.29** and aniline **8.30**. Synthesis of a dication such as **8.24** would provide evidence for the formation of dications such as **2.70** that have been proposed as a superelectrophilic intermediate in a variety of synthetic transformations.

SCHEME 8.11: Retrosynthesis for disalt **8.24**.

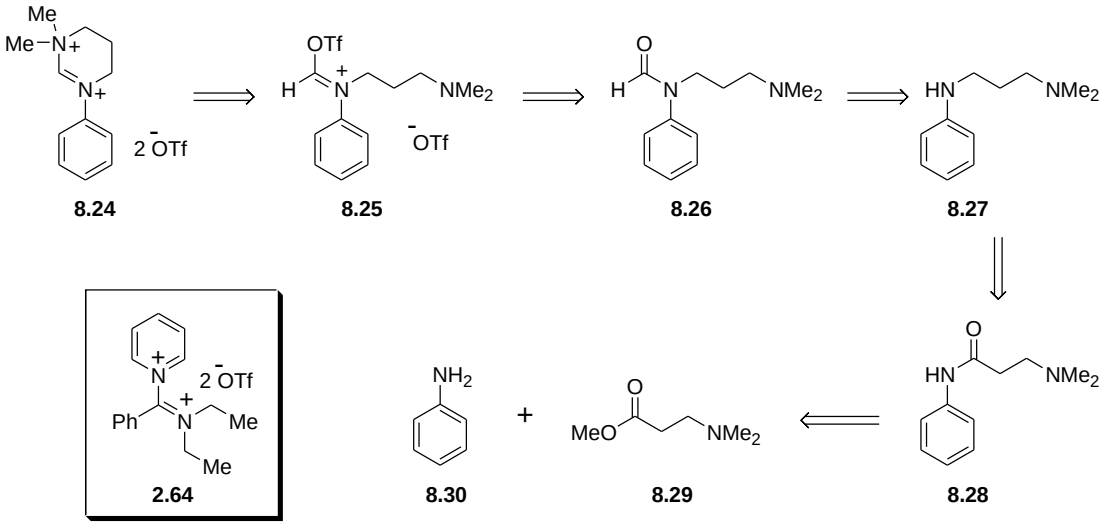

8.2.1 Synthesis of Amide Substrate

The first step in the synthesis of disalt **8.24** was the synthesis of amide **8.26**, which was to be reacted with Tf_2O. Amide **8.28** was synthesised from methyl dimethylaminopropionate **8.29** and aniline **8.30** using ethylmagnesium bromide as a base (Scheme 8.12).[141] Subsequent reduction with lithium aluminium hydride gave amine **8.27** in 97 % yield.

SCHEME 8.12: Synthesis of amine **8.27**.

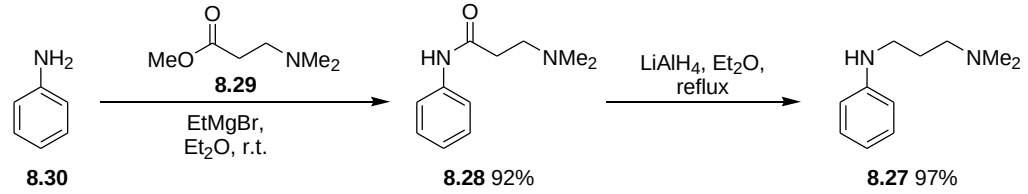

Reaction of amine **8.27** in refluxing ethyl formate **6.29** did not provide a route to amide **8.26** (Scheme 8.13). Synthesis of amide **8.26** was achieved using a protocol reported by Kitagawa *et al*.[142] involving oxalyl chloride and formic acid (Scheme 8.13). In a change to the reported synthetic procedure, 2 eq of the formylating reagent mixture (oxalyl chloride, formic acid, triethylamine and imidazole) was required for the reaction to proceed to completion, instead of the 1 eq reported. With amide substrate **8.26** obtained, the synthesis of disalt **8.24** could now be examined.

SCHEME 8.13: Synthesis of amide **8.26**.

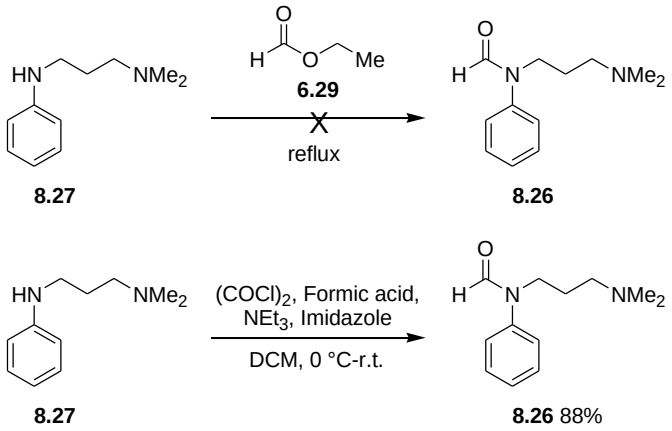

8.2.2 Attempted Disalt Synthesis

The first attempted synthesis of disalt **8.24** was based on the work of Charette *et al*. as detailed in Section 2.4.[56-61] A solution of amide **8.26** in dry DCM was added to a solution of Tf_2O in dry DCM at r.t. (Scheme 8.14). This resulted in the formation of an orange/brown solid. MS analysis of the reaction mixture showed peaks at *m*/*z* 221, 207 and 175. ^{1}H NMR analysis of the reaction mixture showed a complex mixture of products; a downfield methylene peak was observed at δ_H(d_6-DMSO) 4.19 ppm (t, *J*(H,H)= 6.0 Hz) and two singlets were observed at δ_H(d_6-DMSO) 8.22 and 8.43 ppm.

SCHEME 8.14: Attempted synthesis of disalt **8.23**.

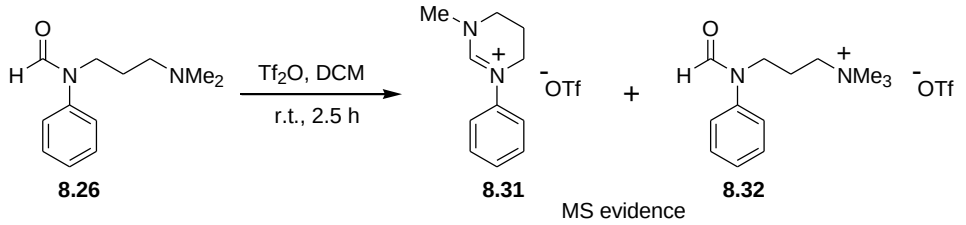

8.26 **8.31** **8.32**

The MS peak at *m*/*z* 207 was attributed to amide **8.26** $[M+H]^+$. The peaks at *m*/*z* 175 and 221 were thought to be due to monocation salts **8.31** and **8.32** respectively ($[M-OTf]^+$ in both cases). Formation of these products was thought to be due to formation of disalt **8.24** and subsequent reaction with another molecule of amide **8.26** (Scheme 8.15). Formation of products **8.31** and **8.32** was consistent with the observed ^{1}H NMR spectrum showing a downfield shift in all the relevant peaks. The products could not be isolated by recrystallisation or column chromatography.

SCHEME 8.15: Proposed mechanism for the formation of **8.31** and **8.32**.

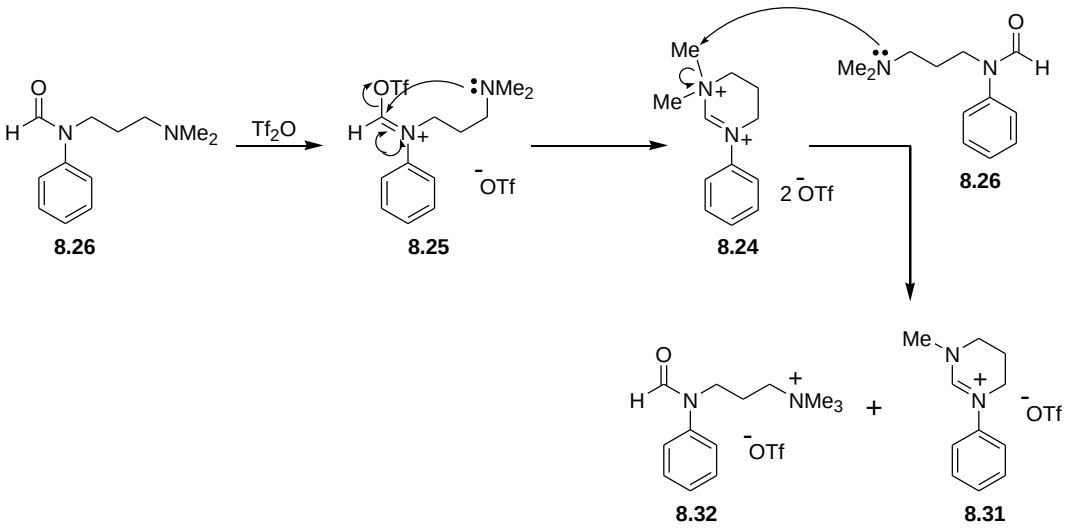

8.26 **8.25** **8.24** **8.26** **8.32** **8.31**

Formation of monocations **8.31** and **8.32** was attributed to fast addition of amide **8.25**, resulting in high a concentration of amide **8.25** in the reaction mixture causing the breakdown of disalt **8.24**. Slower addition of amide **8.26** (using a syringe pump) and decreasing the temperature of the reaction would hopefully prevent formation of monocation salts **8.31** and **8.32**. However, the reaction led to a complex mixture of products, identified by MS analysis to include monocation salts **8.31** and **8.32** (Scheme 8.16).

SCHEME 8.16: Attempted formation of disalt **8.24** at 0 °C.

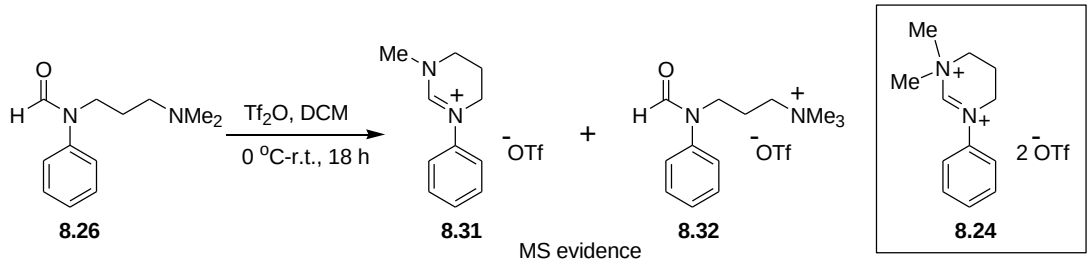

The reaction was then carried out using the same conditions for the formation of disalt **4.13**; neat at 0 °C (Scheme 8.17). ^{1}H NMR and MS analysis indicated formation of protonated amide **8.33**. This was indicated by downfield proton shifts in the methyl and methylene protons of amide **8.25**. In addition, a doublet was observed for the protons of the methyl groups at $\delta_{H}(CD_3CN)$ 2.80 (d, J(H,H)= 5.2 Hz). In addition, MS analysis showed a peak at m/z 207 $[M\text{-}OTf]^{+}$. The mechanism of formation of salt **8.33** was not known at the time, however, it was later identified that monocation **8.33** could be formed from the attack of water on disalt **8.23** (Scheme 8.17).

SCHEME 8.17: Attempted synthesis of disalt **8.24** using neat reaction conditions.

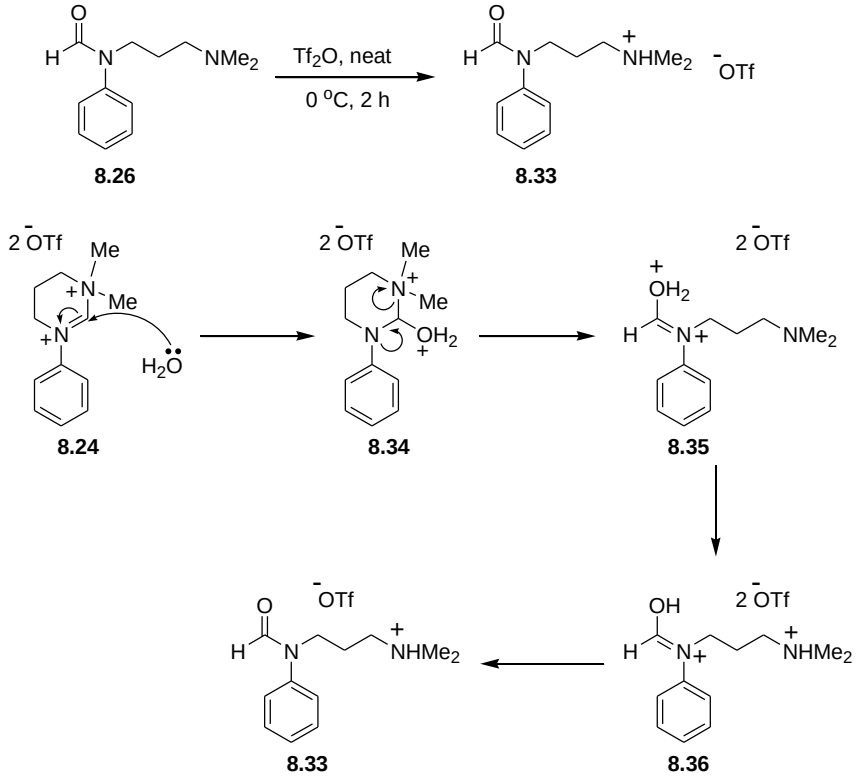

At this stage, the attempted synthesis of disalt **8.24** was suspended in order to investigate a more promising route towards the synthesis of dications such as **2.70**.

8.3 Pyridine-Amide Disalts

Dicationic systems arising from reaction of tertiary amides, Tf_2O and pyridine (or 2-chloropyridine **2.89** have been proposed as superelectrophile intermediates in a variety of reactions (Section 2.4). Such intermediates may display dramatically enhanced reactivity, which could be exploited for the reaction with unactivated substrates, e.g. Friedel-Crafts acylations of unactivated arenes.

An investigation was launched to determine if such dications could be synthesised and if so, could such highly reactive intermediates be isolated. A significant change would be to link the cations by a short chain. This would possibly help the reaction through intramolecular cyclisation, but would also force the pyridinium and iminium cations to be coplanar. Disalts such as **8.38** were envisioned as occurring from cyclisation of amide **8.37** (Scheme 8.18).

SCHEME 8.18: Proposed disalt **8.38** to be synthesised.

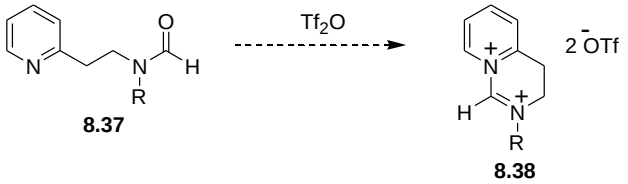

8.37 **8.38**

8.3.1 Amide Substrate Synthesis

The proposed substrate for the formation of a disalt is shown in Scheme 8.19. The tertiary amide **8.39** was chosen having a phenyl ring instead of a methyl group used in previously synthesised disalts **4.16** or **4.30**. The reason for this was that disalt **8.38** (R = Me[143]) could potentially undergo demethylation to give a non-superelectrophilic monocation. This would be less likely to occur with the bulkier phenyl group. In addition, the dication synthesised from amide **8.39** would bear closer resemblance to superelectrophilically activated $CH{\equiv}H_4MPT^+$ **7.1** than the corresponding methyl derivative.

SCHEME 8.19: Proposed synthesis of amide **8.39**.

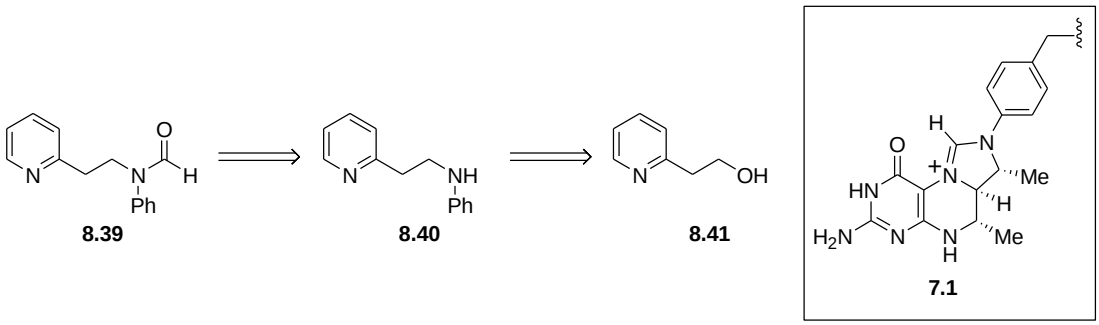

SCHEME 8.20: Synthesis of amine **8.40**.

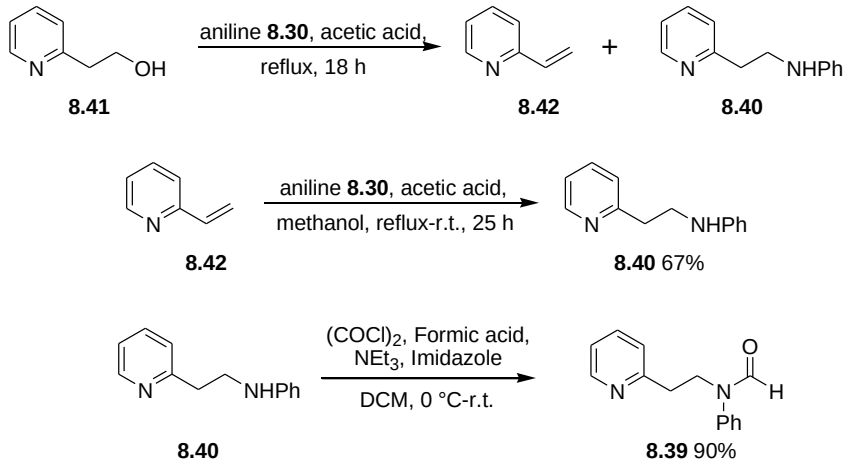

Synthesis of amine **8.40** was attempted using literature precedent[144] based on the reaction of alcohol **8.41** with aniline **8.30** and acetic acid (Scheme 8.20). After heating to reflux for 18 h, amine **8.40** was obtained as an inseparable mixture with 2-vinylpyridine **8.42**. The reaction mechanism is believed to occur through initial dehydration of 2-(2-hydroxylethyl)pyridine **8.41** to give 2-vinylpyridine **8.42** facilitated by the acid in the reaction mixture. Intermediate **8.42** then reacts with aniline **8.29** to give amine **8.40**. The slow reaction led to a mixture of **8.40** and **8.42**. In in effort to ensure complete conversion, the reaction was repeated using 2-vinylpyridine **8.42** instead of alcohol **8.41**, eliminating the first step in the reaction (Scheme 8.20).[145] This led to formation of phenyl(2-pyridin-2-ylethyl)amine **8.40** in 67 % yield. Formylation of amine **8.40** was readily achieved using the procedure of Kitagawa *et al.*[142] to give amide **8.39** in 90 % yield (Scheme 8.20).

SCHEME 8.21: Different conformations of amide **8.39**.

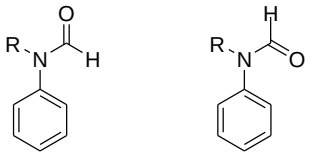

8.43a **8.43b**

The ^{1}H NMR spectrum of amide **8.39** showed a mixture of two rotamers. This was due to the two different conformations of the amide relative to the phenyl ring substituted on the nitrogen of the amide (Scheme 8.21). Of these two conformations, **8.43a** is the major conformer (~85:15 **8.43a**:**8.43b** by ^{1}H NMR). The two conformers are non-equivalent due to restricted rotation around the N-C bond of the amide,[146] giving rise to the different signals in the NMR spectrum.[147,148]

8.3.2 Disalt Synthesis

Addition of a solution of amide **8.39** in dry DCM to Tf_2O at 0 °C under argon, gave rise to a deep purple solution. The reaction mixture was transferred to the glovebox and the solvent was removed *in vacuo* to give a purple oil. ^{1}H NMR analysis showed a mixture of at least two products, with downfield signals at $\delta_H(CD_3CN)$ 4.07 (2H, t), 9.15 (1H, d) and 10.0 (1H, s) ppm being observed. In the glovebox, the reaction mixture gave rise to a deep purple solution in CD_3CN. Upon exposure to air, the solution rapidly lost its purple colour to give a yellow solution. Reexamination of the ^{1}H NMR spectrum showed that the downfield proton signals had disappeared. Based on these results, the signals were attributed to disalt **8.44**, which would be expected to show downfield proton signals due to the positive charge present in the molecule. MS analysis of the reaction mixture showed a major peak at *m*/*z* 227. This peak is consistent with either amide **8.39** $[M+H]^+$ or amide salt **8.45** $[M\text{-}OTf]^+$. The formation of amide salt **8.45** was more likely as comparison of the ^{1}H NMR spectrum of **8.39** (in CD_3CN) with the crude reaction mixture did not show a correlation between the two spectra.

SCHEME 8.22: Attempted synthesis of disalt **8.44**.

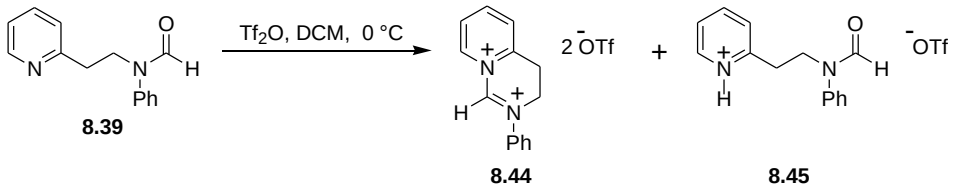

SCHEME 8.23: Mechanism for formation of disalt **8.44**.

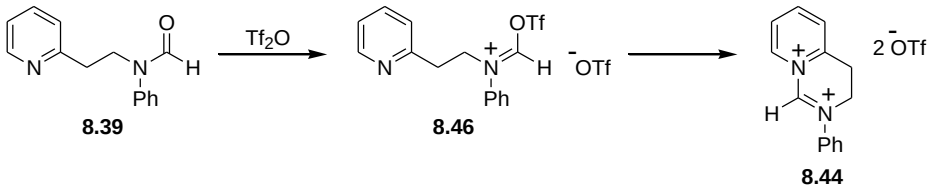

Formation of disalt **8.44** is likely to occur by the mechanism shown in Scheme 8.23. Reaction of amide **8.39** with Tf_2O gives rise to triflate salt **8.46**, which could undergo cyclisation to give disalt **8.44**. Formation of salt **8.45** was attributed to hydrolysis of disalt **8.44** in a similar mechanism to that described for disalt **8.23** (Scheme 8.17).

Various attempts were made to synthesise disalt **8.44** in a pure form, however, these attempts were unsuccessful. One interesting aspect of disalt **8.44** was the deep purple colour that was formed in solution. A vivid colouration is also observed in the formation of electron-donor species **3.5**, **3.20** and **3.40**. There was concern that the proton located on the carbon between the nitrogens could be so acidic that it could be easily removed by the triflate anion to form a carbene that could dimerise to give dimer species **8.47**. Such a carbene was proposed to form during the reaction of pyrimidinium disalt **2.138** (carbene **2.144**, Scheme 2.30). As MS analysis showed only a peak for hydrolysis product **8.45** and the ^{1}H NMR was too complex to rule out formation of **8.47**, a new disalt species was sought.

SCHEME 8.24: Structure of dimer species **8.47**.

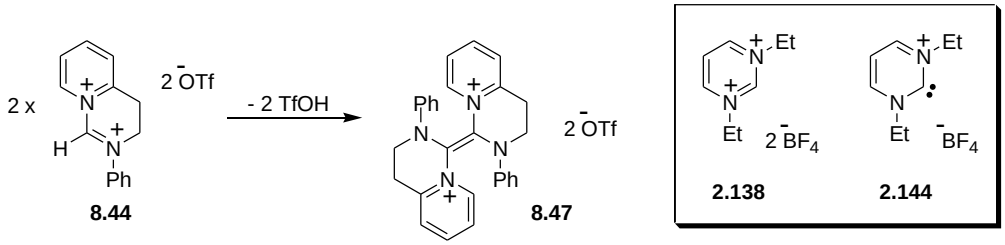

SCHEME 8.25: Synthesis of tertiary amide **8.48**.

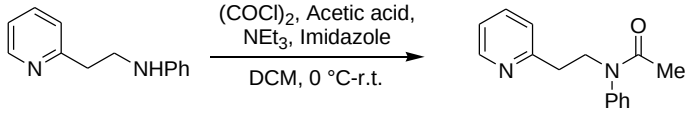

8.40 **8.48** 52%

The use of tertiary amide **8.48** as a substrate for synthesis of a disalt was next investigated. The introduction of a methyl group in place of the proton in **8.39** would prevent the formation of a dimer species if formation of this species from disalt **8.44** was possible. In addition, tertiary amide **8.48** may result in formation of a more stable disalt than from secondary amide **8.39**. Amide **8.48** was synthesised from the acetylation of amine **8.40** using the same procedure as detailed in Scheme 8.20 using acetic acid instead of formic acid (Scheme 8.27). Four equivalents of the acetylating reagent were required for complete conversion of amine **8.40** to the tertiary amide. Unlike secondary amide **8.39**, tertiary amide **8.48** only showed the presence of one isomer in the ^{1}H NMR spectrum.[147,148]

SCHEME 8.26: Attempted synthesis of disalt **8.49**.

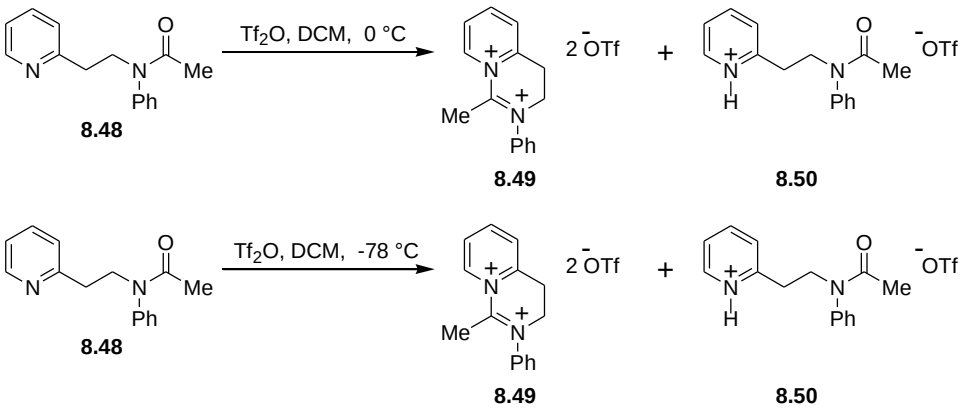

8.48 **8.49** **8.50**

8.48 **8.49** **8.50**

Slow addition of a solution of *N*-phenyl-*N*-(2-(pyridin-2-yl)ethyl)acetamide **8.48** in dry DCM to Tf_2O at 0 °C gave a red solution (Scheme 8.26). ^{1}H NMR analysis of the reaction mixture gave rise to two products, tentatively identified as disalt **8.49** and hydrolysis product **8.50** in a ratio of 1:1.5. MS analysis of the reaction mixture gave a peak at *m*/*z* 241 for hydrolysis product **8.50**. Again, exposure to air resulted in a disappearance of the downfield proton signals attributed to disalt **8.49**. Addition of dry diethyl ether to the reaction mixture gave rise to an orange precipitate. ^{1}H NMR analysis of the solid showed a mixture of **8.49** and **8.50**, this time in a ratio of 1.0:0.3.

Further recrystallisations from dry acetonitrile/diethyl ether were unable to fully purify disalt **8.49**, though they showed that hydrolysis product **8.50** could be removed.

The reaction was repeated at -78 °C to inhibit formation of hydrolysis product **8.50**. This time ^{1}H NMR analysis of the reaction mixture showed products **8.49** and **8.50** in a ratio of 9:1. Isolation of disalt **8.49** was being inhibited by formation of salt **8.50**, most likely due to the attack of adventitious water on disalt **8.49**.

In order to prevent this, all reagents and solutions in the reaction would need to be free of water. Trifluoromethanesulfonic anhydride was dried by distillation from phosphoric oxide and stored in the glovebox. Tertiary amide **8.48** was distilled under high vacuum and stored in the glovebox. Unfortunately, due to cooling of the reaction mixture and the syringe pump addition, the entire reaction could not be carried out in the glovebox. In order to prevent exposure to atmospheric water, the reaction solutions were prepared and sealed inside the glovebox, then transferred out of the glovebox for reaction. Using these protocols, a solution of amide **8.48** in dry DCM was added using a syringe pump (0.763 mL.h^{-1}) to a solution of dry Tf_2O in dry DCM at 0 °C. After the addition was complete, the reaction mixture was transferred to the glovebox, where the solvent was removed from the yellow solution. Recrystallisation from dry acetonitrile/DCM gave disalt **8.49** as a white solid in 42 % yield. Dry DCM was used for the recrystallisation rather than dry diethyl ether as in previous disalts. The reason for this was that, without heating the disalt, residual traces of diethyl ether could not be removed from pure disalt **8.49** before its decomposition. A larger-scale synthesis of disalt **8.49** allowed it to be isolated in improved 73 % yield (Scheme 8.27).

SCHEME 8.27: Successful synthesis of disalt **8.49**.

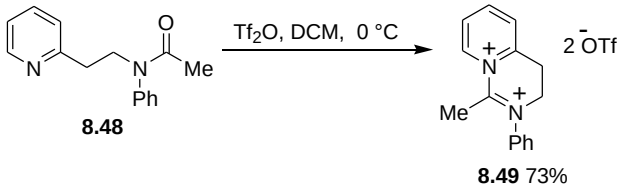

^{1}H (Figure 8.1) and ^{13}C NMR analysis of disalt **8.49** showed peaks consistent with its structure. However, since disalt **8.49** was too unstable for MS analysis (no facilities existed for MS analysis under an inert atmosphere) and X-ray quality crystals could not be grown, the presence of a dication could not be conclusively shown by one-dimensional NMR analysis. In order to show formation of disalt **8.49**, a nuclear Overhauser effect (NOE) difference spectrum was required.

FIGURE 8.1: ^{1}H NMR spectrum for disalt **8.49**. Spectrum taken in CD_3CN.

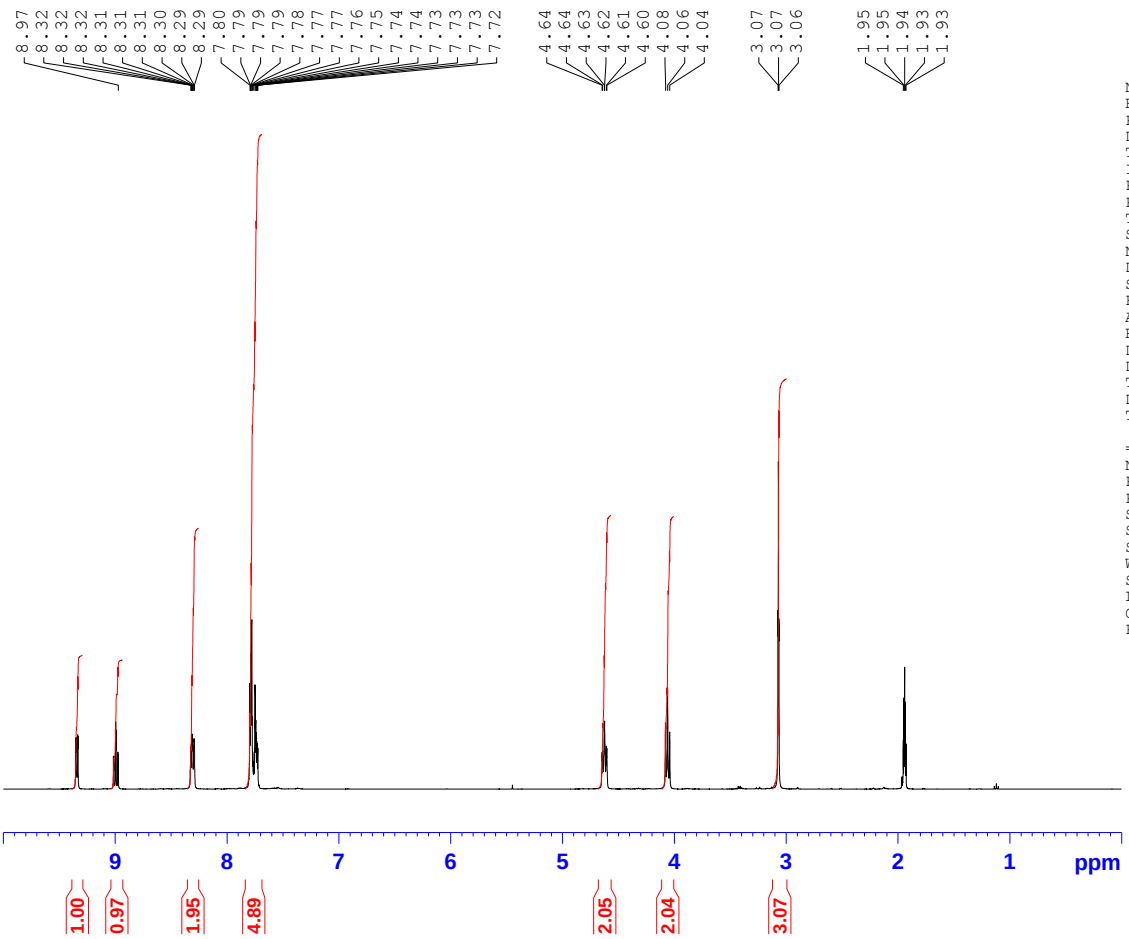

The interaction of one magnetic nucleus with another through the bonds of a molecule leads to spin-spin coupling, where the coupling constant (J) is affected by the geometrical arrangement of the intervening bonds. Magnetic nuclei can also interact through space, although this type of interaction does not lead to coupling. The interaction can only be shown by irradiation of one nucleus at its resonance frequency, which affects the signal of other nuclei (either decreasing the signal or

making it more intense). This is known as the nuclear Overhauser effect. The effect is generally only detectable over short distances (generally 2-4 Å). As a result of this, irradiation of one magnetic nucleus can result in signal enhancement of nuclei in close spacial proximity. In a normal ^{1}H NMR spectrum, this enhancement is usually in the range of 1-20 %, and so could go undetected in a normal spectrum.[149]

An NOE difference spectrum involves subtracting the normal ^{1}H NMR spectrum from the spectrum of the irradiated signal. The unaffected signals disappear, leaving only the enhanced peaks and the irradiated signal. Using the difference spectrum, nuclei in close spacial proximity to the irradiated signal can be determined.[149]

FIGURE 8.2: NOE difference spectrum for disalt **8.49**, *ortho*-proton irradiation. Spectrum taken in CD_3CN.

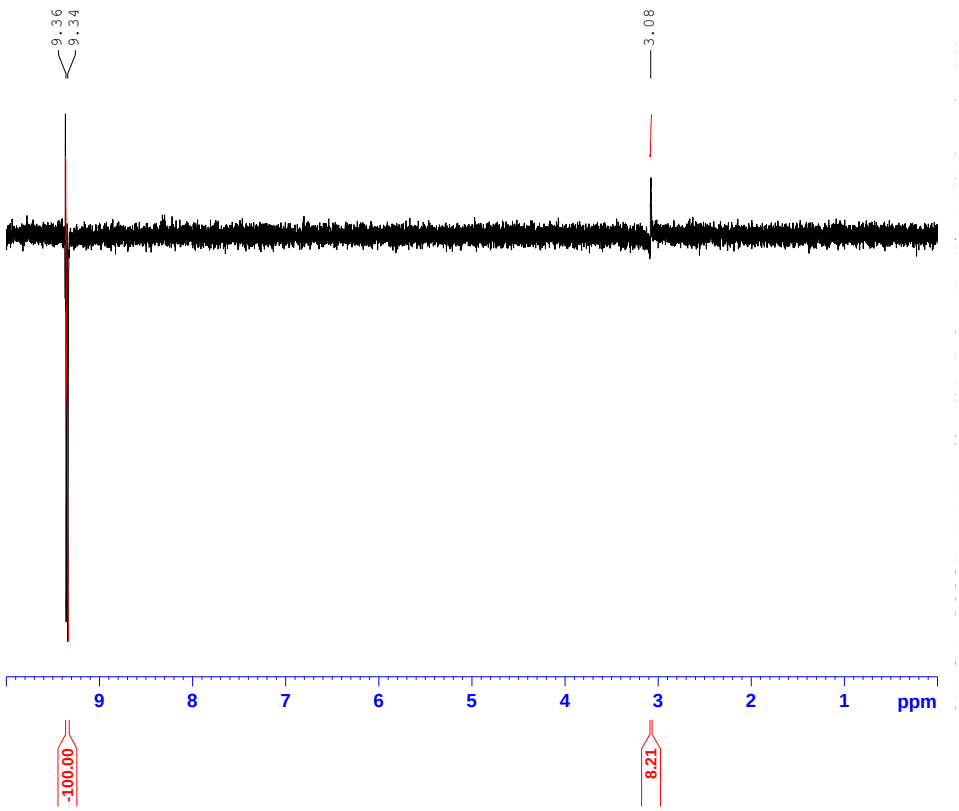

Irradiation of the proton signal of the *ortho*-proton of the pyridinium ring in disalt **8.49** resulted in an 8 % enhancement in the proton signal of the methyl group (Figure

8.2). Correspondingly, irradiation of the methyl protons of disalt **8.49** resulted in a 3 % enhancement of the *ortho*-proton of the pyridinium ring (Figure 8.3).

The NOE spectra show that disalt **8.49** has indeed been synthesised in the reaction, as indicated by the close spacial proximity of the pyridinium proton and methyl protons (Scheme 8.28, highlighted). A disalt species such as **8.51** could result in the downfield proton signals observed in the ^{1}H NMR spectrum (Figure 8.1). However, this species would not produce the observed NOE spectra due to the highlighted protons being too far apart (Scheme 8.28).

SCHEME 8.28: Highlighted protons in disalt **8.49** and **8.51**.

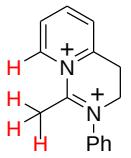

8.49

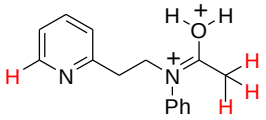

8.51

FIGURE 8.3: NOE difference spectrum for disalt **8.49**, methyl proton irradiation. Spectrum taken in CD_3CN.

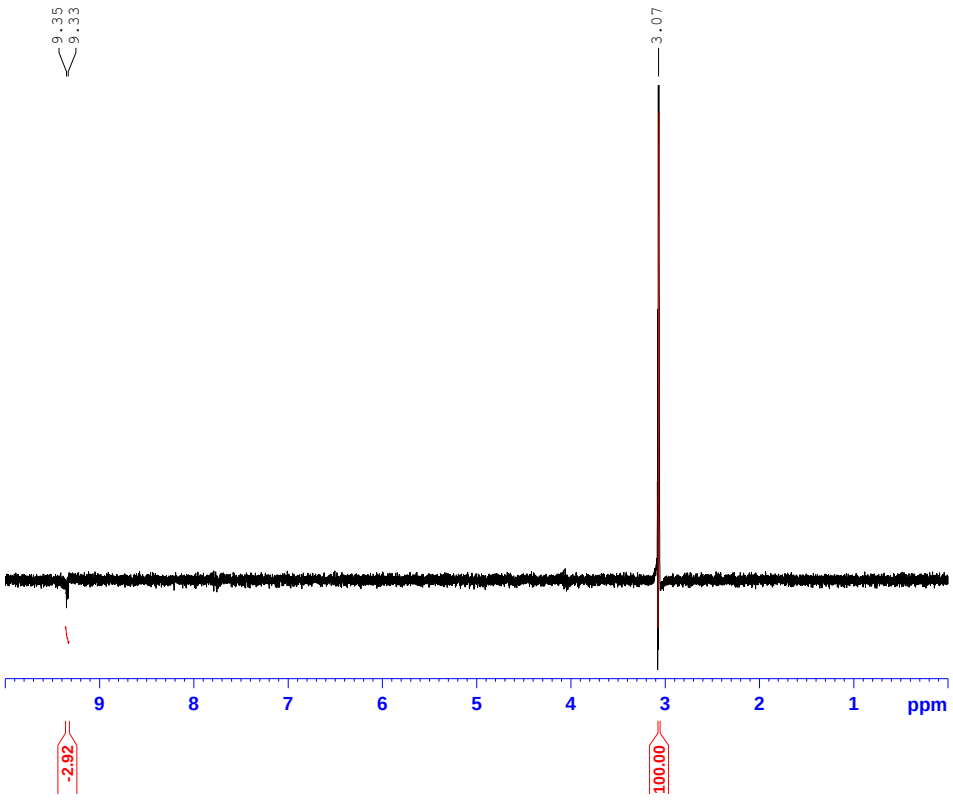

The filtrate from the recrystallisation was collected and the solvent was removed *in vacuo* to give protonated salt **8.50**, as shown by ^{1}H NMR, ^{13}C NMR and MS analysis. In order to confirm the formation of salt **8.50**, amide **8.48** was reacted with TFA to afford protonated salt **8.52** (Scheme 8.29). The ^{1}H NMR spectrum of **8.50** closely resembled the spectrum of **8.52** with one notable exception. The methyl signal in **8.50** was observed to be downfield compared to salt **8.52** (δ_H(CD_3CN) 2.26 and 1.79 ppm respectively). The reason for this discrepancy was not known, but may be due to the effect of the anionic counterion as this appears to be the only difference between the two compounds. Based on these results, it appears likely that salt **8.50** is the hydrolysis product of disalt **8.49**. The mechanism for formation of salt **8.50** (Scheme 8.29) is thought to occur in a similar fashion to that described in Scheme 8.17.

SCHEME 8.29: Protonation of amide **8.48** and hydrolysis of disalt **8.49**.

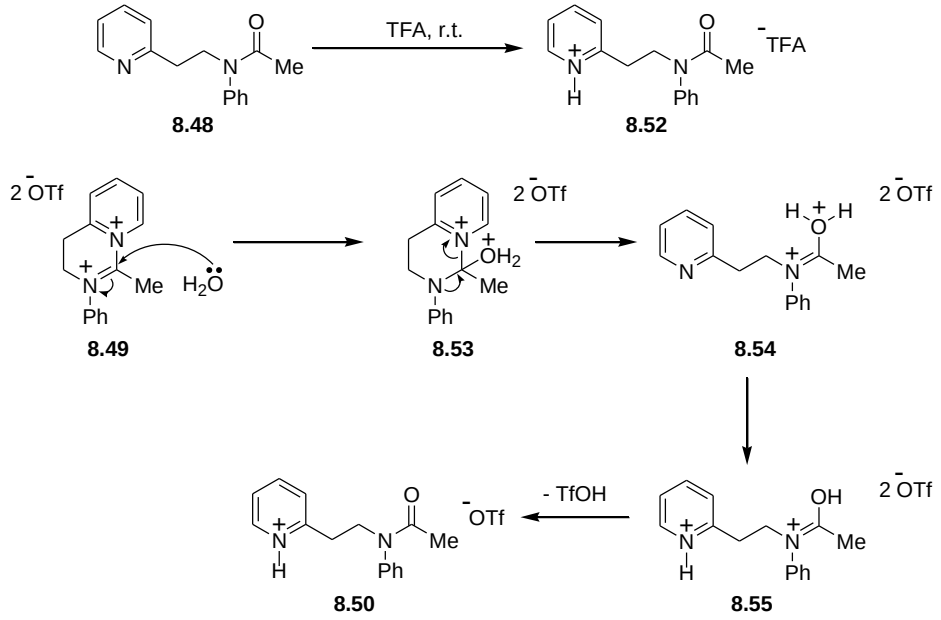

With disalt **8.49** synthesised, attention was once again turned to the synthesis of disalt **8.44**. Using the same protocols for the synthesis of disalt **8.49** (dried solutions prepared in glovebox and stringent low oxygen conditions), formyl disalt **8.44** was synthesised in 52 % yield in a small-scale reaction, and 82 % in a large-scale reaction (Scheme 8.30). The ^{1}H NMR spectrum (Figure 8.4) shows the correct peaks for disalt **8.44**.

FIGURE 8.4: ^{1}H NMR spectrum of disalt **8.44**. Spectrum taken in CD_3CN.

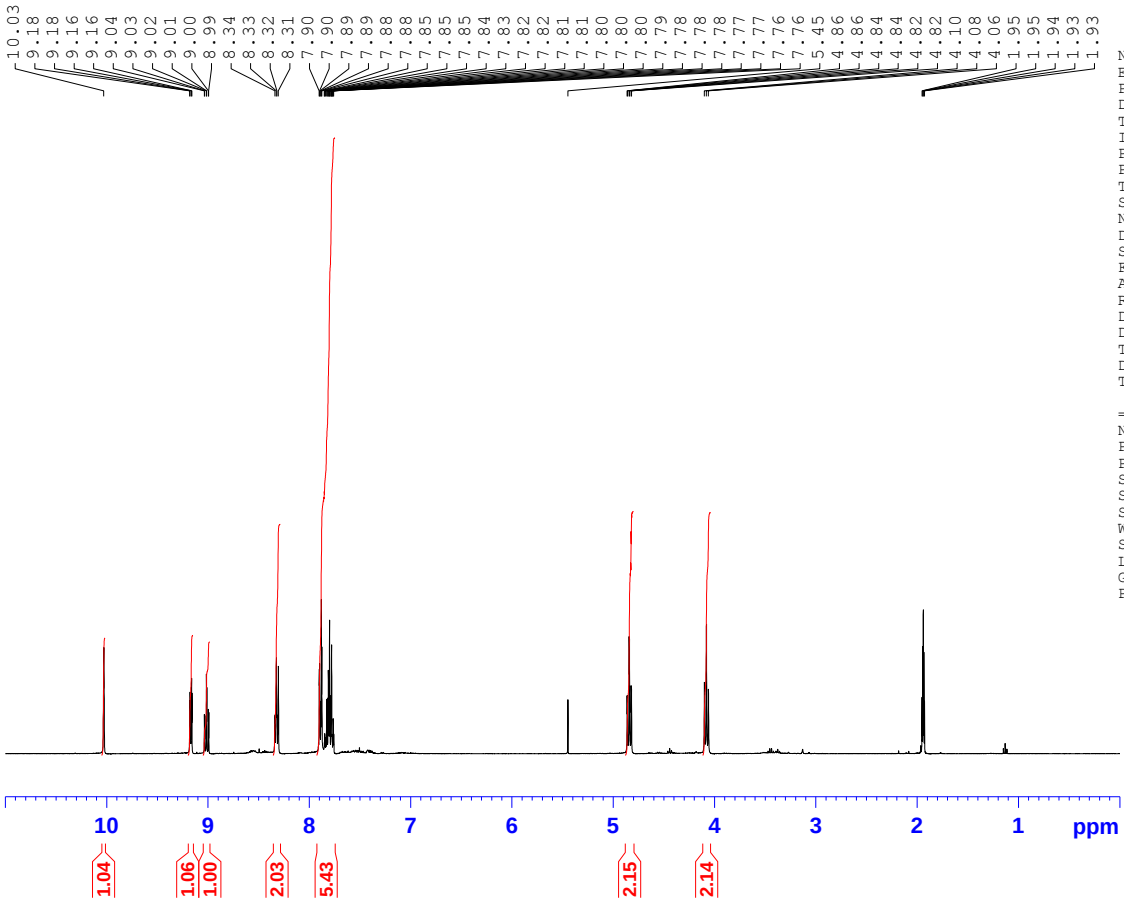

SCHEME 8.30: Synthesis of formyl disalt **8.44**.

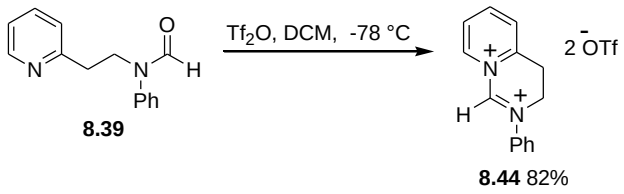

The NOE spectra (Figure 8.5 and 8.6) for disalt **8.44** also confirmed its formation; irradiation of the peak for the non-aromatic proton resulted in a 9 % enhancement of the *ortho*-proton of the pyridinium ring of disalt **8.44**. Conversely, irradiation of the *ortho*-proton of the pyridinium ring resulted in an 8 % enhancement of the non-aromatic proton of disalt **8.44**.

FIGURE 8.5: NOE difference spectrum for disalt **8.44**, non-aromatic proton irradiation. Spectrum taken in CD_3CN.

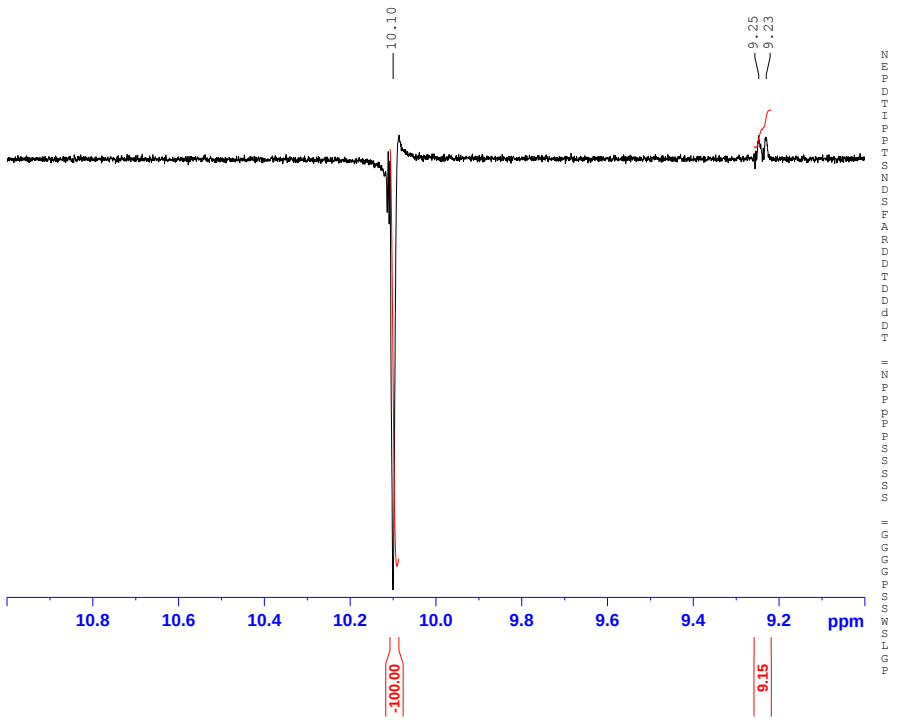

FIGURE 8.6: NOE difference spectrum for disalt **8.44**, *ortho*-aromatic proton irradiation. Spectrum taken in CD_3CN.

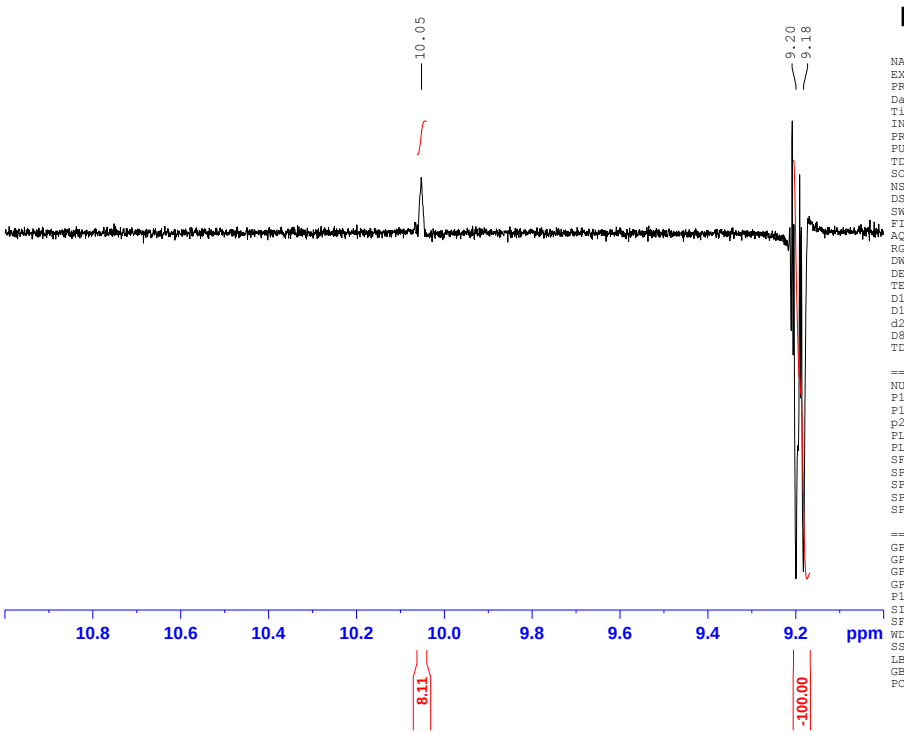

SCHEME 8.31: Hydrolysis of disalt **8.44**.

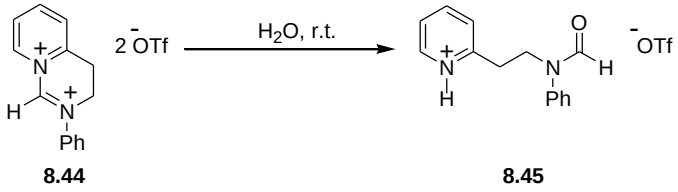

In order to determine the hydrolysis product of disalt **8.44**, the disalt was reacted with water (Scheme 8.31). ^{1}H NMR analysis of the products showed salt **8.45** as two different isomers (in a ratio of 10:1). The formation of hydrolysis product was likely to occur via a mechanism analogous to that shown in Scheme 8.29.

SCHEME 8.32: Synthesis of tertiary amine disalt **8.57**.

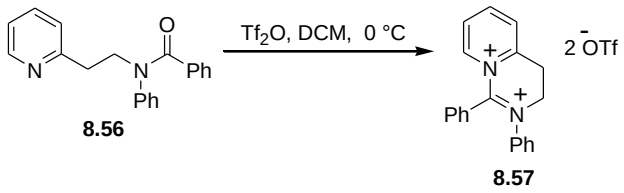

FIGURE 8.7: (a) ORTEP diagram of disalt **8.57** cation. (b) ORTEP diagram of disalt **8.57** cation (different angle).

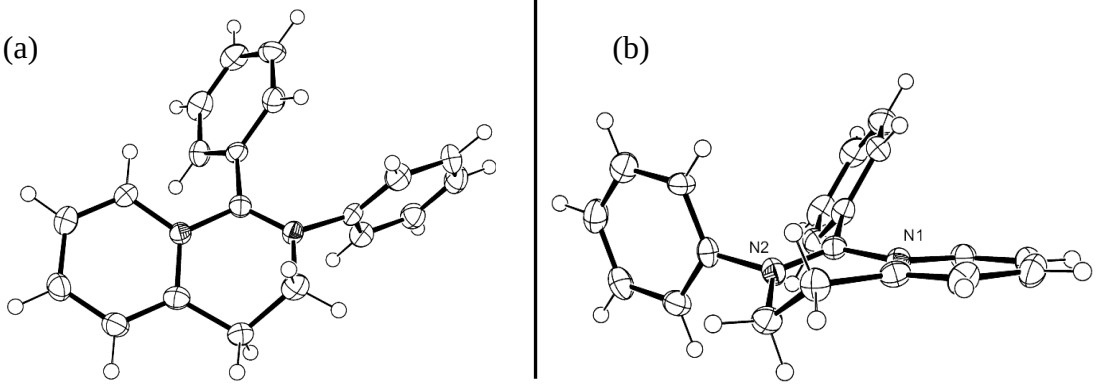

Further evidence for the formation of disalts **8.44** and **8.49** was subsequently obtained in an analogous study by a colleague in the research group.[150] Disalt **8.57** was synthesised from tertiary amine **8.56** (Scheme 8.32). ^{1}H and ^{13}C NMR spectra were obtained that were consistent with the proposed product. In addition, an X-ray crystal structure was obtained confirming the proposed structure (Figure 8.7). Given that the same synthetic protocol was used for the synthesis of disalts **8.44**, **8.49** and

8.57, it is reasonable to assume that disalts **8.44** and **8.49** share structural similarities with disalt **8.57**.

8.3.3 Hydrogenation Reactions

Disalt **8.44** has been synthesised as a potential model substrate for superelectrophilically-activated $CH{\equiv}H_4MPT^+$ **7.12**. It was hoped that disalt **8.44** would show sufficient reactivity to react with hydrogen in the absence of a catalyst. This provides some evidence for superelectrophilic activation occurring in [Fe]-hydrogenase.

SCHEME 8.33: Attempted hydrogenation of disalt **8.44**.

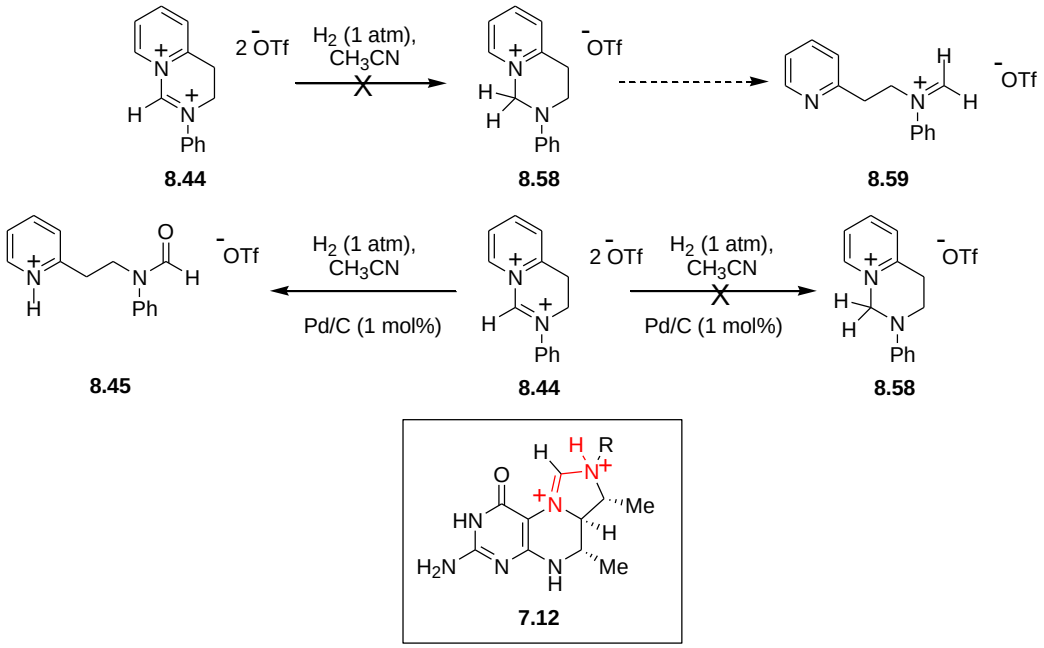

A solution of disalt **8.44** in acetonitrile was prepared in a low oxygen, low moisture glovebox in a reaction vessel fitted with a vacuum tap. The vessel was removed from the glovebox, evacuated using a vacuum pump and filled with H_2 (1 atm). The reaction mixture was stirred for 18 h, then transferred to the glovebox. ^{1}H NMR analysis of the reaction mixture showed only the hydrolysis product **8.45** (Scheme 8.33). The reaction was repeated in the presence of palladium on activated carbon (1 mol%) in an attempt to isolate the hydrogenation product for comparison. Unfortunately, ^{1}H NMR analysis of the reaction mixture showed only hydrolysis product **8.45** (Scheme 8.33).

SCHEME 8.34: Attempted hydrogenation of disalt **8.49**.

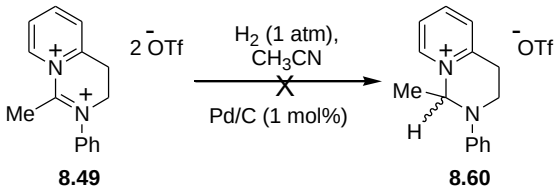

Hydrogenation of the more stable disalt **8.49** in the presence of palladium on activated carbon was also unsuccessful, producing only hydrolysis product **8.60** (Scheme 8.34).

SCHEME 8.35: Reaction of disalt **8.49** with lithium aluminium hydride.

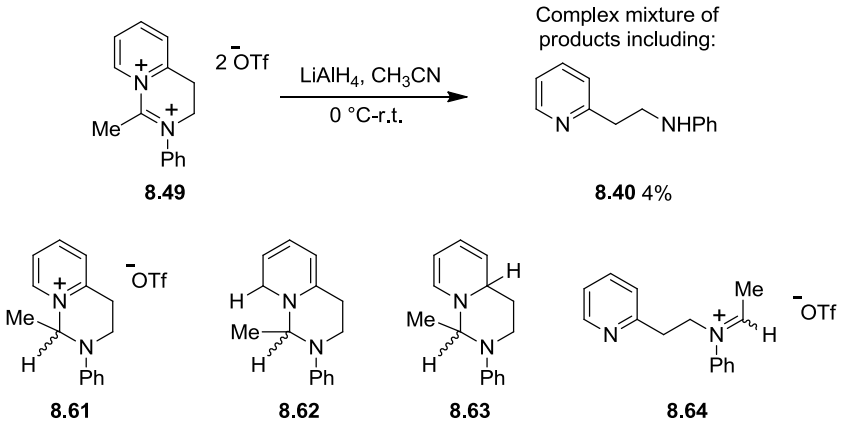

Acetyl disalt **8.49** was then reacted with lithium aluminium hydride in an attempt to determine if the reaction would occur regiospecifically to give product **8.61** or a product derived from this. The reaction proceeded further than expected to give a complex mixture of products (Scheme 8.35). A variety of doublets were observed in the region of $\delta_H(CD_3CN)$ 1.12-2.51 ppm (Figure 8.8). These signals were thought to be due to a methyl group coupled to a proton. At least 3 pairs of doublets of similar intensity were observed in the ^1H NMR spectrum. The peaks of similar intensity were attributed to the two possible diastereoisomers from the reaction of lithium aluminium hydride with disalt **8.49**. Possible products in the reaction (**8.61**-**8.64**) are shown in Scheme 8.35.

These products were thought to be due to the reaction of disalt **8.49** with lithium aluminium hydride in on the same carbon attached to the methyl group and reaction with the pyridinium ring, as in the case with 2-DMAP disalt **4.16** (Scheme 8.6). The

^{1}H NMR spectrum was too complex to accurately determine which (if any) of the products were formed. Column chromatography of the reaction mixture gave amine **8.40** in 4 % yield. Formation of amine **8.40** could result from the reaction with lithium aluminium hydride as shown in Scheme 8.36.

FIGURE 8.8: Selected ^{1}H NMR expansion of the reaction of disalt **8.49** with $LiAlH_4$. NMR in CD_3CN.

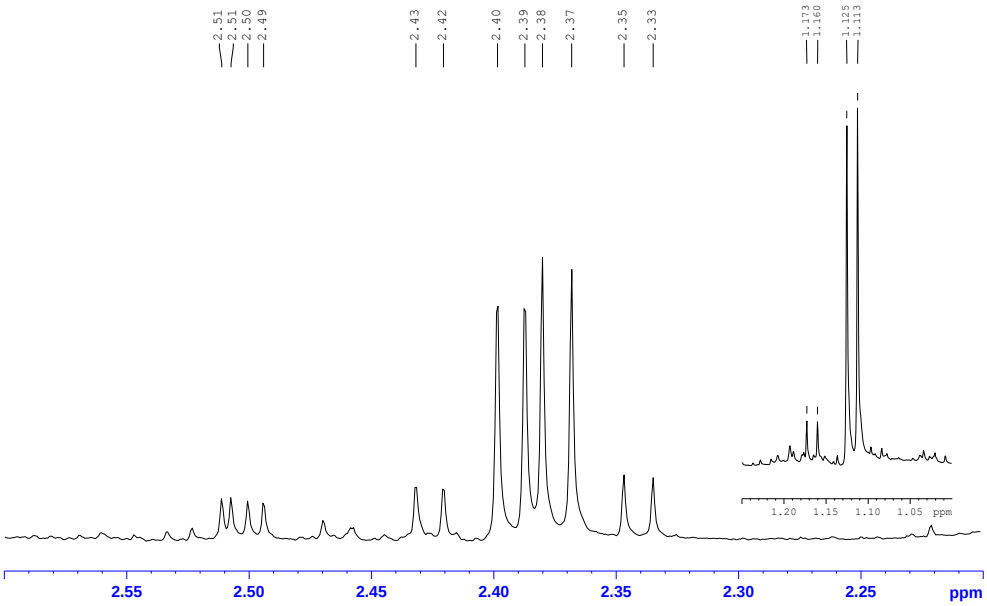

SCHEME 8.36: Possible reaction for formation of amine **8.40**.

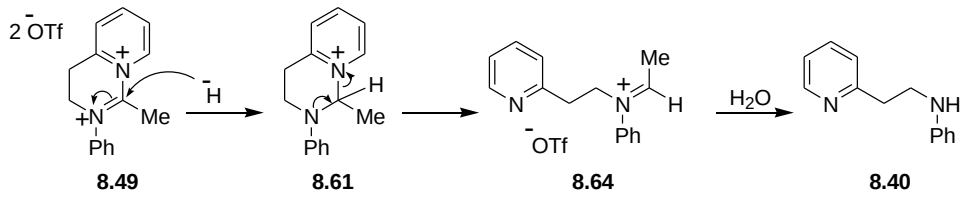

The enhanced reactivity of disalts **8.44** and **8.49** that we hoped to exploit actually served to hinder the hydrogenation of the superelectrophiles as a result of hydrolysis of the highly reactive disalts. Hydrogenation at higher pressure may provide a route to the synthesis of products such as **8.58**. However, the high pressure hydrogenation apparatus that was available does not allow for transfer of the disalt without exposure to air, resulting in immediate hydrolysis of the superelectrophile. If such apparatus became available for the preparation of hydrogenation solutions under an inert

atmosphere, hydrogenation of superelectrophile disalts **8.44** or **8.49** might be possible.

8.3.4 Acylation Reactions

It was thought that superelectrophile disalt **8.44** would allow for the acetylation of unactivated arenes. The proposed mechanism is shown in Scheme 8.37.

In order to determine if the proposed synthetic application was viable, the reaction with a more reactive substrate, anisole **8.68**, was investigated. Anisole **8.68** (1 eq) was reacted with disalt **8.44** in acetonitrile at r.t. (Scheme 8.38). After hydrolysis, the reaction gave rise to 4-methoxybenzaldehyde **8.69** in 31 % yield and amine **8.40** in 40 % yield.

SCHEME 8.37: Superelectrophilic acetylation of arenes.

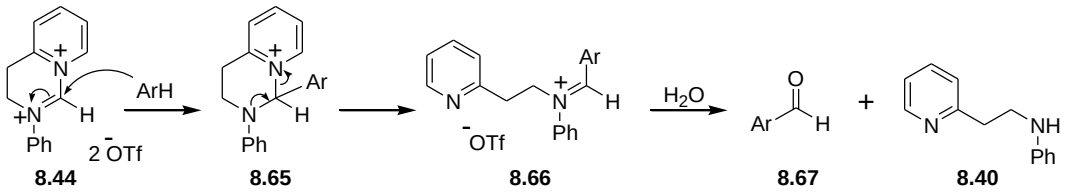

SCHEME 8.38: Reaction of formyl disalt **8.44** and anisole **8.68**.

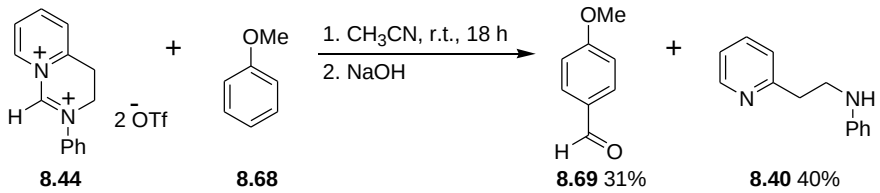

The proposed mechanism for the formation of the products is shown in Scheme 8.39. Attack by anisole **8.68** on disalt **8.44** results in formation of new disalt **8.70**, with subsequent ring cleavage to give iminium salt **8.71**. Hydrolysis of this iminium salt gives 4-methoxybenzaldehyde **8.69** and amine **8.40**.

Interestingly, formylation of anisole **8.68** only occurs in the *para*-position to give 4-methoxybenzaldehyde **8.69**, no *ortho*-formylation was observed (which would lead to disalt **8.72**). This regiospecific formylation is likely a result of the steric hindrance imposed by the phenyl ring on the non-aromatic ring nitrogen and/or the pyridinium

ring of disalt **8.44**. This steric hindrance prevents *ortho*-attack on the disalt, with the *para*-product being the only product observed.

SCHEME 8.39: Mechanism for the reaction of formyl disalt **8.44** and anisole **8.68**.

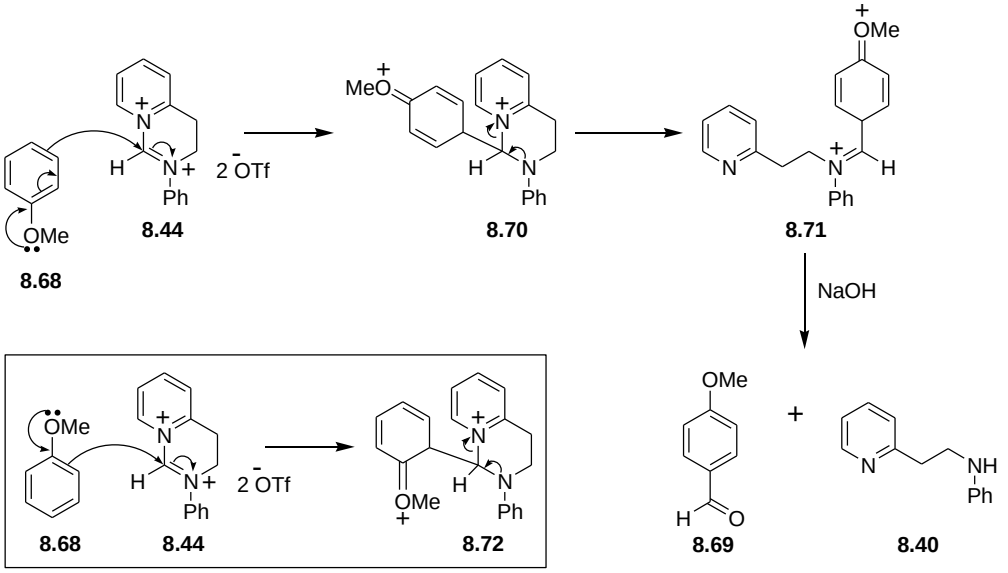

When 10 eq of anisole **8.68** was used, the yield of 4-methoxybenzaldehyde **8.69** was increased to 60 %, with amine **8.40** being isolated in 64 % yield (Scheme 8.40).

SCHEME 8.40: Reaciton of disalt **8.44** with an excess of anisole **8.68**.

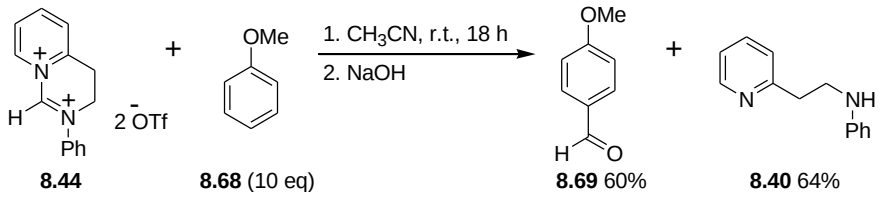

The formylation of anisole **8.68** with disalt **8.44** demonstrates the ability of this disalt as a formylating reagent. The scope of disalt **8.44** in the formylation of unactivated arenes is currently being investigated.[150]

8.4 Conclusions and Future Work

The reaction of 2-DMAP **1.1** and 1,3-diiodopropane **1.2** leads to the formation of 2-DMAP salts **1.4-1.6**, thought to arise from the formation of a dicationic superelectrophile intermediate. Using a more reactive bifunctional electrophile such

as ditriflate **4.15**, a variety of superelectrophile disalts were synthesised based on the 2-DMAP unit (Scheme 8.41).

SCHEME 8.41: Disalt superelectrophiles synthesised in this work.

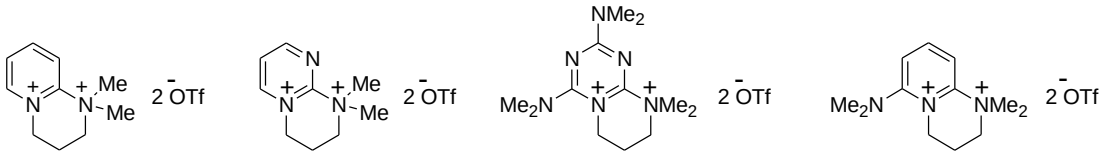

4.16 **4.30** **6.17** **6.40**

2-DMAP disalt **4.16** was shown to have enhanced reactivity over its monocationic counterparts **1.169** and **1.170** in the methylation of triphenylphosphine **5.26**. In the 1:1 competition reaction with dimethyl sulfate in the methylation of triethylamine **5.28**, 2-DMAP disalt **4.16** and 2-dimethylaminopyrimidine disalt **4.30** showed greater reactivity than dimethyl sulfate, with disalt **4.30** showing over 2.5 times the reactivity of dimethyl sulfate.

SCHEME 8.42: Hydrogenation of 2-DMAP disalt **4.16**.

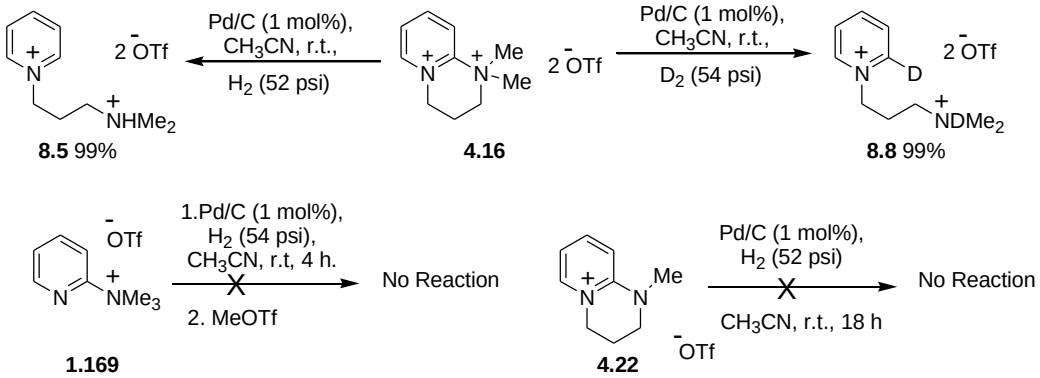

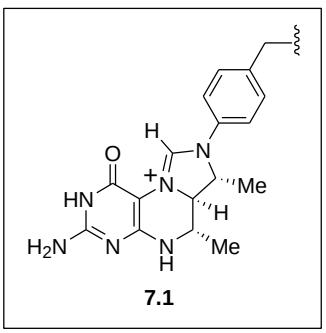

7.1

The reactivity of 2-DMAP disalt **4.16** towards hydrogenation was also examined. It was found that in the presence of palladium on activated carbon (1 mol%), disalt

4.16 underwent regiospecific hydrogenation (or deuteration) in the 2-position to give pyridinium disalt **8.5** (or **8.8** in the case of deuteration). In this case, 2-DMAP disalt **4.16** showed parallel reactivity to the substrate $CH{\equiv}H_4MPT^+$ **7.1** in the [Fe]-hydrogenase enzyme. This significantly enhanced reactivity over monocationic salts **1.169** and **4.22** provides evidence that superelectrophilic activation of $CH{\equiv}H_4MPT^+$ **7.1** in the enzyme active-site may contribute to the observed reaction of $CH{\equiv}H_4MPT^+$ **7.1** with hydrogen observed.

SCHEME 8.43: Superelectrophile trisalt **6.47** synthesised.

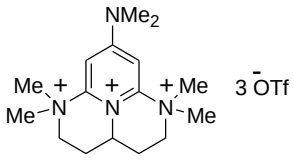

6.47

Superelectrophile trisalt **6.47** was also synthesised (Scheme 8.43). This trisalt showed slightly decreased reactivity compared to dimethyl sulfate in the methylation of triethylamine **5.24**. The high reactivity of the tricationic species was tempered by the dimethylamino group in the 4-position, which served to decrease the reactivity by delocalising the positive charge on the pyridinium ring nitrogen.

Amidine disalts **8.44** and **8.49** based on amides have also been synthesised (Scheme 8.44). Isolation of these superelectrophiles provides evidence of their formation as intermediates in a variety of reactions detailed in this work (Section 2.4). Disalt **8.44** was shown to be an effective reagent for the formylation of anisole **8.71** under mild conditions.

SCHEME 8.44: Amidine disalts **8.44** and **8.49**.

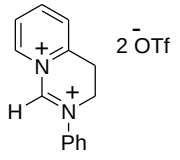

8.44

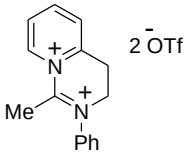

8.49

The work detailed here has reported first the identification of a superelectrophile disalt based on 2-DMAP **1.1**, then its subsequent isolation as well as the development

of a variety of superelectrophilic salts. Such superelectrophilic salts had only been previously observed in superacid media, or postulated as reaction intermediates in organic solvents. The synthesis and isolation of these superelectrophile disalts based on the 2-DMAP unit shows that highly reactive superelectrophiles can be obtained using standard laboratory conditions, which considerably widens the scope for synthesis and investigation of such species. There are several promising avenues for further development based upon the work detailed in this thesis, some of which will now be highlighted.

The synthesis and reactivity of disalts **4.16** and **4.30** as well as trisalt **6.46** has been described (Scheme 8.45). Disalt **4.30** showed the most potent reactivity in the methylation of nitrogen nucleophiles for all the superelectrophiles synthesised. The addition of electron-withdrawing groups on the pyrimidinium ring may serve to further enhance its already potent reactivity. As such the addition of a nitro group in the 4- or 5-position (to give **8.73** and **8.74** respectively) would hopefully increase the electrophilicity of such a disalt, increasing its reactivity (Scheme 8.46). In addition it would be advantageous to synthesise trisalt **6.3**. With the stabilising effect of the 4-dimethylamino group removed, it is hoped that the reactivity of disalt **6.3** would be significantly enhanced compared to trisalt **6.46**.

SCHEME 8.45: Superelectrophile salts synthesised.

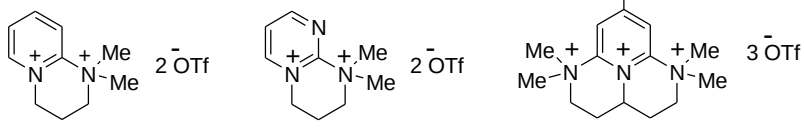

4.16 **4.30** **6.47**

SCHEME 8.46: Potential superelectrophiles for synthesis.

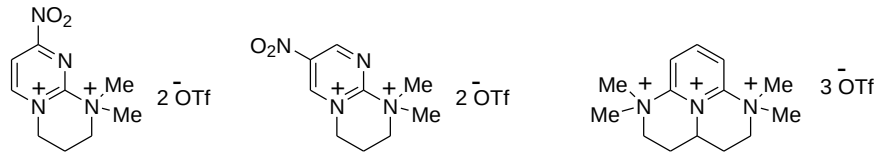

8.73 **8.74** **6.3**

2-DMAP disalt **4.16** has shown similar behaviour to $CH{\equiv}H_4MPT^+$ **7.1** in the [Fe]-hydrogenase enzyme. The hydrogenation requires the presence of palladium on activated carbon in low 1 mol% loading. The reactivity of 2-DMAP disalt **4.16** with

hydrogen in the presence of iron complexes would more closely mimic the enzyme system in [Fe]-hydrogenase. This iron complex could take the form of a simple iron (II) complex or a more complicated system involving a pyridinol ligand such as **7.31**.

SCHEME 8.47: Hmd substrate **7.1** and pyridinol ligand **7.31**.

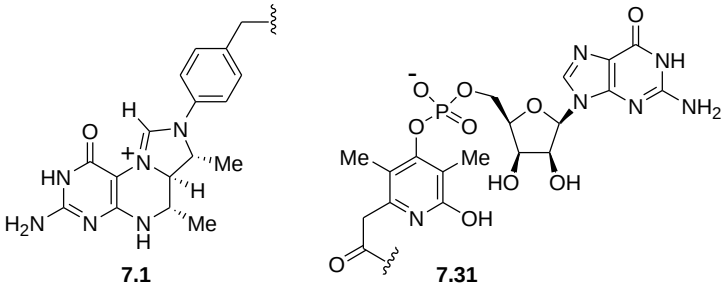

7.1 **7.31**

The successful synthesis and isolation of amidinium disalts **8.44** and **8.49** also opens up a new avenue of investigation. A variety of different tertiary amides could be synthesised to investigate the reactivity of such superelectrophiles (Scheme 8.48). Some of this work has already been instigated, resulting in the synthesis of unique amidinium disalt **8.57**.[150] The reactivity of formyl disalt **8.44** with unactivated arenes such as benzene and deactivated arenes such as chlorobenzene and nitrobenzene is also under investigation.[150]

SCHEME 8.48: Amidinium disalts to be synthesised.

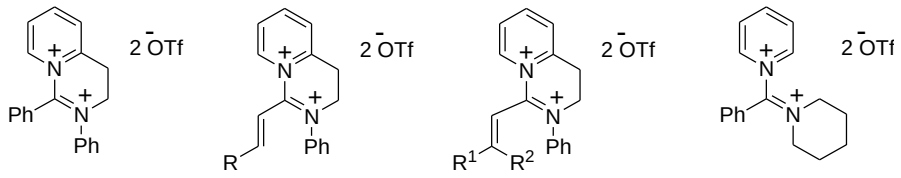

8.57 **8.75** **8.76** **8.77**

In addition, the formation of a carbene (such as **8.78**) from disalt **8.44** is under investigation (Scheme 8.49). Carbene **2.144** has been postulated as as an intermediate in the reaction of disalt **2.138** with acid (Scheme 2.21). A carbene formed from superelectrophile disalt **8.44** could show enhanced reactivity, such as H/D exchange with acid to form deuterated supereletrophile **8.79** or reaction with hydrogen to form pyridinium salt **8.58**.

Reaction of carbene **8.78** with hydrogen would show analogous reactivity to alkylaminocarbenes **8.80** and **8.82** reported by Bertrand *et al.*[151] (Scheme 8.50). Reaction of acyclic alkylaminocarbene **8.80** and cyclic alkylaminocarbene **8.82** with hydrogen in the absence of a catalyst led to formation of the dihydrogenated product **8.81** in 28 % yield and dehydrogenated product **8.83** in 32 % yield respectively. The diaminocarbene **8.84** and *N*-heterocyclic carbene **8.86** did not react with hydrogen (Scheme 8.50).

SCHEME 8.49: Potential formation of carbene from disalt **8.44**.

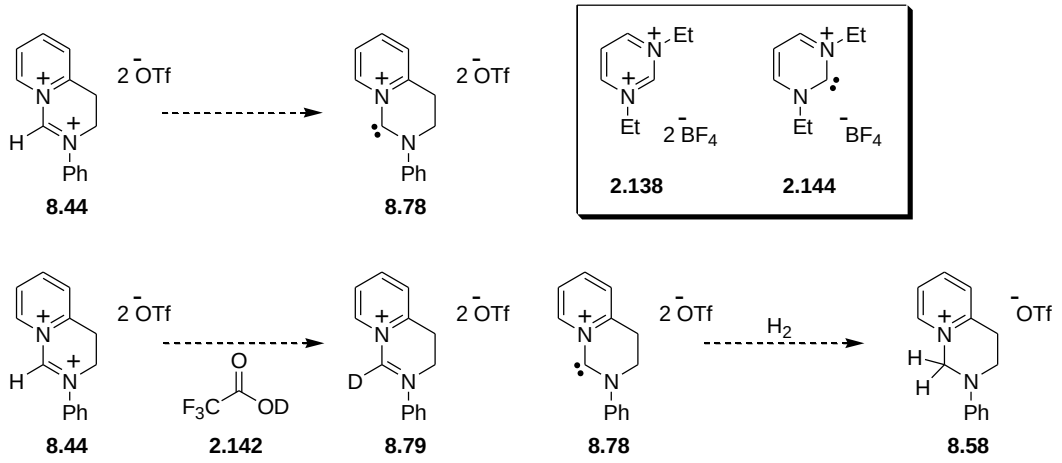

SCHEME 8.50: Hydrogenation of carbenes **8.80** and **8.82**.

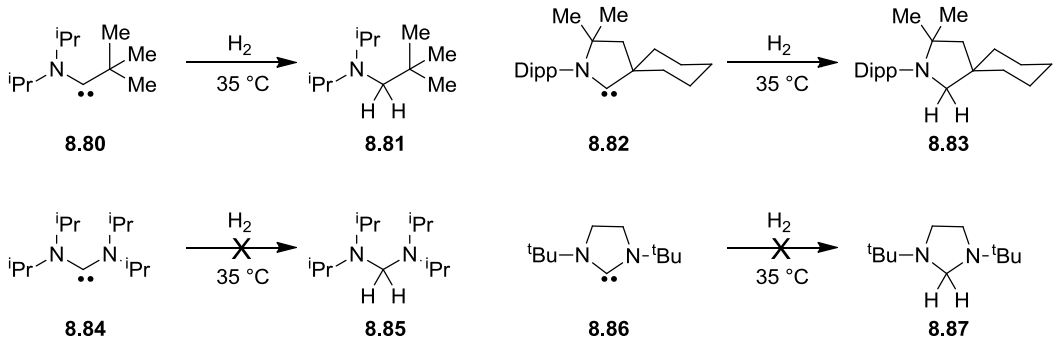

Disalt **8.44** bears a close resemblance to precursor salt **8.88** for carbene **8.82** (Scheme 8.51). In disalt **8.44**, the second quaternary nitrogen resembles the carbon in precursor salt **8.88**, meaning that carbene **8.78** could show the same reactivity as the carbenes synthesised by Bertrand *et al.*[151]

SCHEME 8.51: Proposed synthesis of carbene **8.78**.

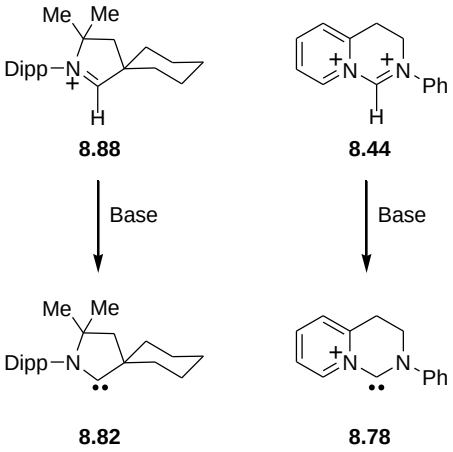

8.88 **8.44** **8.82** **8.78**

9 Experimental

9.1 General Methods

All reagents were purchased from Alfa Aesar, Aldrich or Fluorochem Ltd., with the exception of d_3-acetonitrile, which was purchased from Goss Scientific Instruments Ltd. d_3-Acetonitrile and acetonitrile were distilled from P_2O_5 (0.5-1.0 mol%) under argon. Tetrahydrofuran, dichloromethane, hexane, diethyl ether and toluene were dried and deoxygenated with a Pure-Solv 400 solvent purification system by Innovative Technology Inc., U.S.A. and the moisture content of the solvents was analysed using a Karl Fischer coulometer (METTLER TOLEDO DL39). The average water contents for the period August 2006-May 2010 were as follows; THF 5.66 ppm, DCM 2.23 ppm, hexane 1.85 ppm, diethyl ether 4.37 ppm, and toluene 1.27 ppm. All glassware was oven or flame-dried prior to use. Inert reactions were carried out under argon or nitrogen.

Infra-red spectra were recorded on Perkin Elmer Spectrum One FT-IR spectrometer. Proton NMR (^{1}H) and carbon NMR (^{13}C) spectra were recorded on a Bruker DPX400 spectrometer, Bruker AV400 spectrometer or Bruker DRX500 spectrometer. Using a JMOD sequence the ^{13}C NMR signals were assigned to CH_3, CH_2, CH and C. The NMR experiments were carried out in deuterochloroform ($CDCl_3$), d_6-dimethylsulfoxide or d_3-acetonitrile. The chemical shifts (δ) are quoted in parts per million (ppm). Multiplicities are abbreviated as s, singlet; d, doublet; t, triplet; q, quartet; m, multiplet for the ^{1}H NMR spectra. The coupling constants (J) are reported in Hertz (Hz). In cases, where superimposition of the signals of two, or more, isomers occurred, the signals have been reported as multiplets (m), unless the coupling constants of each isomer could be ascertained.

High and low resolution mass spectra were recorded at the EPSRC National Mass Spectrometry Service Centre, Swansea on a JLZX 102, VGZAB-E or at the Univeristy of Strathclyde on a JEOL JMS-AX505HA instrument.
All Gas Chromatography Mass Spectrometry (GC-MS) was performed on Thermo Finnigan PolarisQ Ion Trap Mass Spectrometer/Trace GC instrument with ZB-5 column (30 metres), at 1mL/min He gas flow rate and temperature range of 50 to 320 ^{o}C with an increment of 10 to 20 ^{o}C/min.

High performance liquid chromatography (HPLC) was performed using Gilson Model 302 pump, Gilson 802C manometric module, Milton Roy Spectrometer detector (λ = 254 nm) and a Kromasil Silica column (semi-preparative: 10 μm pore size, 100 Å particle size, 250 × 10.0 mm dimension) at a flow-rate of 4 mL/min or a Phenomenex Silica column (semi-preparative: 5 μm pore size, 100 Å particle size, 300 × 10.0 mm dimension) at a flowrate of 4 mL/min.

Melting points (mp) were carried out on Griffin melting point apparatus and are uncorrected.

Flash chromatography was performed using silica gel 60 (200-400 mesh). Thin layer chromatography (TLC) was performed using aluminium sheets of silica gel 60 F_{254} and was visualised under Mineralight UVGL-58 lamp (254 nm). The plates were developed with acidic methanolic vanillin solutions.

Glovebox experiments were carried out in an Innovative Technology Inc., System One glovebox under low oxygen, low moisture conditions (oxygen levels were maintained below 10 ppm, water levels were maintained below 10 ppm). Solvents and reagents to be used in glovebox experiments were dried and were degassed *in vacuo* for at least 5 min, then flooded with argon and the flasks were sealed. Reagents were then transferred to the glovebox port and the port was evacuated then flooded with nitrogen at least 8 times before transfer into the glovebox.

The IUPAC names of some compounds were obtained using ChemDraw Ultra version 7.0 or Beilstein's AutoNom Version 4.0 software.

Single crystal X-ray diffraction measurements were made on an Oxford Diffraction Gemini S instrument at 123 K. Final refinement was to convergence on F^2 and used the SHELXL-97 program.

9.2 Experimental for Chapter 4

EXPERIMENT 4.1: Reaction of 2-DMAP 1.1 and 1,3-Diiodopropane 1.2

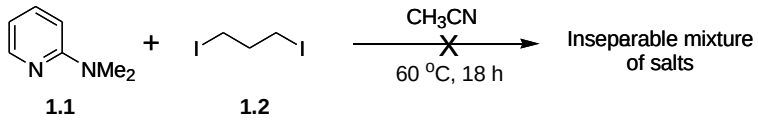

1,3-Diiodopropane **1.2** (0.12 mL, 1.0 mmol, 1.0 eq) was added to a solution of 2-DMAP **1.1** (0.25 mL, 2.0 mmol, 2.0 eq) in dry acetonitrile (10 mL) under argon. The reaction mixture was heated to 60 °C for 18 h. The solvent was removed *in vacuo*, and the residue was dissolved in diethyl ether (30 mL) and left to stir for 90 min. The solvent was decanted and the residual solvent was removed from the residue *in vacuo* to give an orange solid (0.026 g). Attempts to purify by recrystallisation were unsuccessful.

EXPERIMENT 4.2: Larger-Scale Reaction of 2-DMAP 1.1 and 1,3-Diiodopropane 1.2

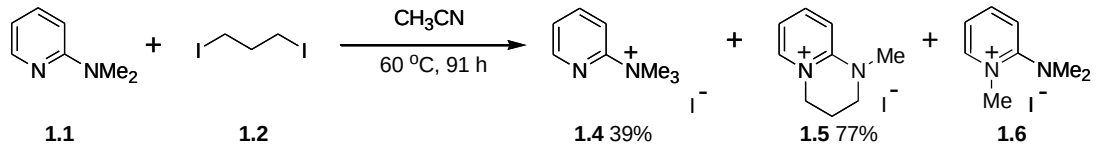

A solution of 2-DMAP **1.1** (0.62 mL, 5.0 mmol, 2.5 eq) and 1,3-diiodopropane **1.2** (0.23 mL, 2.0 mmol, 1.0 eq) in dry acetonitrile (5 mL) was heated at reflux for 2 days. The reaction mixture was cooled to r.t. and dry diethyl ether (5 mL) was added and the reaction mixture was stirred for 30 min, causing an orange solid to precipitate. Recrystallisation from dry acetonitrile/diethyl ether gave trimethylpyridin-2-ylammonium iodide **1.4** (0.207 g, 39 %) as a white solid. The filtrate was collected and the solvent removed *in vacuo*. Purification by column chromatography using silica gel (CH_3CN/DCM 1:3) gave 1-methyl-1,2,3,4-tetrahydropyrido[1,2-α]-pyrimidin-5-ylium iodode **1.5** (0.423 g, 77 %) as a hygroscopic yellow solid. 2-Dimethylamino-1-methylpyridinium iodide **1.6** could

not be isolated from the reaction mixture by recrystallisation, column chromatography using silica gel or by reverse-phase HPLC separation.

Trimethylpyridin-2-ylammonium iodide 1.4; mp 181-182 °C (lit.[37] 183-184 °C); ^{1}H NMR (400 MHz, d_6-DMSO) δ= 3.58 (9H, s, CH_3), 7.72 (1H, ddd, J(H,H)= 7.4, 4.8, 0.7 Hz, ArH), 8.08 (1H, dd, J(H,H)= 8.5, 0.7 Hz, ArH), 8.24 (1H, ddd, J(H,H)= 8.5, 7.4, 1.9 Hz, ArH), 8.68 (1H, ddd, J(H,H)= 4.8, 1.9, 0.7 Hz, ArH); ^{13}C NMR (100 MHz, d_6-DMSO) δ= 54.5 (CH_3), 115.2 (CH), 126.2 (CH), 141.0 (CH), 148.5 (CH), 156.6 (C); IR (KBr disc) $\tilde{\nu}$= 3055, 2988, 1596, 1442, 1265, 939, 739, 705; MS (ESI) 137 (100) $[M\text{-}I]^+$; HRMS: m/z calcd for $C_8H_{13}N_2$ $[M\text{-}I]^+$: 137.1073; found: 137.1072.

1-Methyl-1,2,3,4-tetrahydropyrido[1,2-α]pyrimidin-5-ylium iodode 1.5; mp 62-65 °C; ^{1}H NMR (400 MHz, d_6-DMSO) δ= 2.16 (2H, tt, J(H,H)= 6.0, 5.7 Hz, CH_2), 3.16 (3H, s, CH_3), 3.55 (2H, t, J(H,H)= 6.0 Hz, CH_2), 4.28 (2H, t, J(H,H)= 5.7 Hz, CH_2), 6.88 (1H, ddd, J(H,H)= 6.8, 6.7, 1.2 Hz, ArH), 7.23 (1H, d, J(H,H)= 9.2 Hz, ArH), 7.92 (1H, ddd, J(H,H)= 9.2, 7.1, 1.7 Hz, ArH), 8.02 (1H, dd, J(H,H)= 6.7, 1.2 Hz, ArH); ^{13}C NMR (100 MHz, d_6-DMSO) δ= 18.7 (CH_2), 38.7 (CH_3), 48.1 (CH_2), 50.7 (CH_2), 111.5 (CH), 112.5 (CH), 140.4 (CH), 142.1 (CH), 150.9 (C); IR (KBr disc) $\tilde{\nu}$= 3016, 2929, 2863, 1646, 1582, 1549, 1432, 1201, 1167, 1096, 1060, 1007, 758; MS (ESI) 149 (100) $[M\text{-}I]^+$. HRMS: m/z calcd for $C_9H_{13}N_2$ $[M\text{-}I]^+$: 149.1073; found: 149.1074.

EXPERIMENT 4.3: Reaction of 2-DMAP 1.1 with Iodomethane

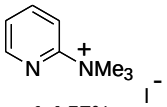

1.4 57%

2-DMAP **1.1** (1.24 mL, 10 mmol, 1.0 eq) and iodomethane (0.62 mL, 10 mmol, 1.0 eq) were added to dry acetonitrile (5 mL) under argon. The reaction mixture was heated to 60 °C and left to stir for 18 h. The solvent was removed *in vacuo*, and the residue was stirred in diethyl ether (25 mL) for 30 min. The superlatant was decanted and concentrated to give 2-DMAP **1.1** (0.304 g, 25%). The residual solvent was removed from the residue *in vacuo*. Recrystallisation from ethanol gave trimethylpyridin-2-ylammonium iodide **1.4** as a white solid (1.50 g, 57%). Data was consistent with that reported in experiment 4.2.

EXPERIMENT 4.4: Reaction of 2-DMAP 1.1 with Iodoethane

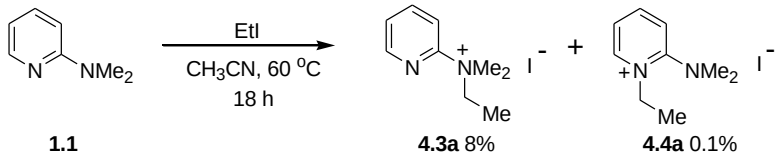

2-DMAP **1.1** (1.24 mL, 10 mmol, 1.0 eq) and iodoethane (0.62 mL, 10 mmol, 1.0 eq) were added to dry acetonitrile (5 mL) under argon. The reaction mixture was heated to 60 °C and left to stir for 18 h. The solvent was removed *in vacuo*, and the residue was stirred in diethyl ether (25 mL) for 30 min. The solvent was decanted and concentrated to give 2-DMAP **1.1** (0.919 g, 75%). The residual solvent was removed from the residue *in vacuo*, to give an off-white solid (0.410 g). ^{1}H NMR analysis showed the product to consist of a mixture of ethyldimethylpyridin-2-ylammonium iodide **4.3a** and 2-dimethylamino-1-ethylpyridinium iodide **4.4a** in a ratio of ~14:1 (by ^{1}H NMR). Recrystallisation from ethanol gave ethyldimethylpyridin-2-ylammonium iodide **4.3a** as a white solid (0.225 g, 8 %). Using reverse-phase HPLC chromatography of the reaction mixture with a solvent system of (10 % acetonitrile/0.1 % TFA/89.9 % water) with maximum loading of 5 mg/mL and a flowrate of 4 mL/min, the peak tail at RT 10 min 32 s to 16 min 30 s was collected and gave 2-dimethylamino-1-ethyl-pyridinium iodide **4.4a** (0.004 g) with some contamination by ethyldimethyl-pyridin-2-ylammonium iodide **4.3a**.

Ethyldimethylpyridin-2-ylammonium iodide 4.3a; mp 149-150 °C; ^{1}H NMR (400 MHz, d_6-DMSO) δ= 0.98 (3H, t, J(H,H)= 7.2 Hz, CH_3), 3.55 (6H, s, CH_3), 3.93 (2H, q, J(H,H)= 7.2 Hz, CH_2), 7.73 (1H, ddd, J(H,H)= 7.5, 4.7, 0.8 Hz, ArH), 8.04 (1H, dd, J(H,H)= 8.4, 0.8 Hz, ArH), 8.35 (1H, ddd, J(H,H)= 8.4, 7.5, 1.9 Hz, ArH), 8.69 (1H, dd, J(H,H)= 4.7, 1.9 Hz, ArH); ^{13}C NMR (100 MHz, d_6-DMSO) δ= 8.3 (CH_3), 51.5 (CH_3), 63.1 (CH_2), 116.9 (CH), 126.8 (CH), 141.7 (CH), 149.7 (CH), 155.4 (C); IR (KBr disc) $\tilde{\nu}$= 3001, 1618, 1595, 1575, 1477, 1442, 1402, 1166, 995, 169, 914, 806, 785, 566; MS (ESI) 151 (100) $[M\text{-}I]^+$; HRMS: *m/z* calcd for $C_9H_{15}N_2$ $[M\text{-}I]^+$: 151.1230; found: 151.1229.

2-Dimethylamino-1-ethylpyridinium iodide 4.4a; tentative identification: ^{1}H NMR (400 MHz, $CDCl_3$) δ= 1.65 (3H, t, J(H,H)= 6.3 Hz, CH_3), 3.19 (6H, s, CH_3), 4.54 (2H, q, J(H,H)= 6.3 Hz, CH_2), 7.32-7.39 (2H, m, ArH), 8.05-8.11 (1H, m, ArH), 8.35-8.45 (1H, m, ArH).

EXPERIMENT 4.5: Reaction of 2-DMAP 1.1 with 1-Iodopropane

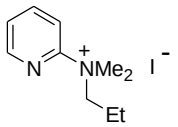

4.3b 3%

2-DMAP **1.1** (1.24 mL, 10 mmol, 1.0 eq) and 1-iodopropane (0.98 mL, 10 mmol, 1.0 eq) were added to dry acetonitrile (5 mL) under argon. The reaction mixture was heated to 60 °C and left to stir for 18 h. The solvent was removed *in vacuo*, and the residue was washed with diethyl ether (25 mL) and left to stir for 30 min. The solvent was decanted and concentrated to give 2-DMAP **1.1** (1.066 g, 87%). The residue was recrystallised from ethanol to give dimethylpropylpyridin-2-ylammonium iodide **4.3b** as a white solid (0.078 g, 3%); mp 127-128 °C; ^{1}H NMR (400 MHz, $CDCl_3$) δ= 0.99 (3H, t, *J*(H,H)= 7.3 Hz, CH_3), 1.46-1.51 (2H, m, CH_2), 3.95 (6H, s, CH_3), 4.28-4.33 (2H, m, CH_2), 7.55-7.58 (1H, m, ArH), 8.14 (1H, ddd, *J*(H,H)= 8.4, 7.5, 1.8 Hz, ArH), 8.46 (1H, dd, *J*(H,H)= 8.4, 1.6 Hz, ArH), 8.56 (1H, dd, *J*(H,H)= 4.6, 1.6 Hz, ArH); ^{13}C NMR (100 MHz, $CDCl_3$) δ= 10.1 (CH_3), 17.0 (CH_2), 53.5 (CH_3), 69.3 (CH_2), 117.6 (CH), 126.7 (CH), 142.0 (CH), 149.6 (CH), 155.3 (C); IR (KBr disc) $\tilde{\nu}$= 3011, 2958, 2873, 1593, 1574, 1474, 1430, 1155, 996, 947, 846, 797, 760, 747, 589; MS (ESI) 165 (100) $[M\text{-}I]^+$, 123 (10); MS (ESI) 165 (100) $[M\text{-}I]^+$, 123 (58); HRMS: *m*/*z* calcd for $C_{10}H_{17}N_2$ $[M\text{-}I]^+$: 165.1386; found: 165.1385.

EXPERIMENT 4.6: Reaction of 2-DMAP 1.1 and Benzyl Bromide 4.5

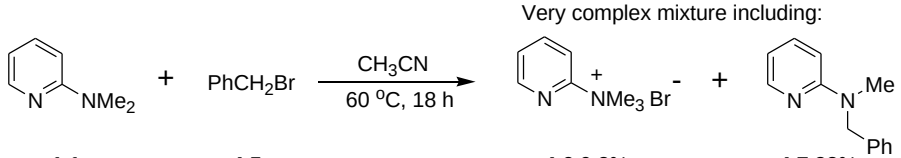

1.1 **4.5** **4.6** 0.3% **4.7** 23%

2-DMAP **1.1** (1.24 mL, 10 mmol, 1.0 eq) and benzyl bromide **4.5** (1.15 mL, 10 mmol, 1.0 eq) were added to dry acetonitrile (5 mL) under argon. The reaction mixture was heated to 60 °C and left to stir for 18 h. The solvent was removed *in vacuo*, and the residue was stirred in diethyl ether (25 mL) for 30 min. The solvent was decanted and concentrated to give a brown oil (0.647 g). The residual solvent was removed from the residue *in vacuo* to give a pale brown solid (2.444 g).

^{1}H NMR analysis of the solid showed a complex mixture of salts. Recrystallisation from warm ethanol gave trimethylpyridin-2-ylammonium bromide **4.6** as a white solid (0.007 g, 0.3 %). No other products were obtained from recrystallisation attempts. Separation through reverse-phase HPLC chromatography was attempted (10 % acetonitrile/0.1 % TFA/89.9 % water), but no separation of products was possible. 107 mg of the brown oil was separated using column chromatography using silica gel (EA/PE 1:9) to give benzylmethylpyridin-2-ylamine **4.7** as a yellow oil (0.076 g, 4 %, scaling up to ~0.460 g, 23% for complete organic fraction).

Trimethylpyridin-2-ylammonium bromide 4.6: mp 171-172 °C; ^{1}H NMR (400 MHz, $CDCl_3$) δ= 4.05 (9H, s, CH_3), 7.55 (1H, ddd, *J*(H,H)= 7.5, 4.6, 0.5 Hz, ArH), 8.13 (1H, ddd, *J*(H,H)= 8.3, 7.5, 1.9 Hz, ArH), 8.45 (1H, dd, *J*(H,H)= 4.6, 1.9 Hz, ArH), 8.60 (1H, dd, *J*(H,H)= 8.3, 0.5 Hz, ArH); ^{13}C NMR (100 MHz, $CDCl_3$) δ= 54.6 (CH_3), 115.8 (CH), 126.8 (CH), 141.8 (CH), 149.4 (CH), 157.5 (C); IR (KBr disc) $\tilde{\nu}$= 3080, 3011, 2943, 1598, 1574, 1471, 1431, 1401, 1147, 997, 944, 844, 786, 739, 552; MS (ESI) 137 (100) $[M\text{-}Br]^+$, 123 (57), 85 (19).

Benzylmethylpyridin-2-ylamine 4.7; ^{1}H NMR (400 MHz, $CDCl_3$) δ= 3.10 (3H, s, CH_3), 4.84 (2H, s, CH_2), 6.52 (1H, dd, *J*(H,H)= 8.6, 2.0 Hz, ArH), 6.60 (1H, ddd, *J*(H,H)= 7.0, 5.0, 0.7 Hz, ArH), 7.21-7.32 (5H, m, ArH), 7.45 (1H, ddd, *J*(H,H)= 8.6, 7.0, 2.0 Hz, ArH), 8.19 (1H, dd, *J*(H,H)= 5.0, 0.7 Hz, ArH); ^{13}C NMR (100 MHz, $CDCl_3$) δ= 36.7 (CH_3), 53.8 (CH_2), 106.2 (CH), 112.4 (CH), 127.4 (CH), 127.6 (CH), 129.1 (CH) 137.8 (CH), 139.1 (C), 148.5 (CH), 159.3 (C); GC-MS: RT 12.60 min, *m*/*z* 198 (47) $[M]^{+\bullet}$, 183 (100), 169 (56), 107 (96), 78 (92).

EXPERIMENT 4.7: Reaction of 2-DMAP 1.1 and Dimethyl Sulfate 4.8

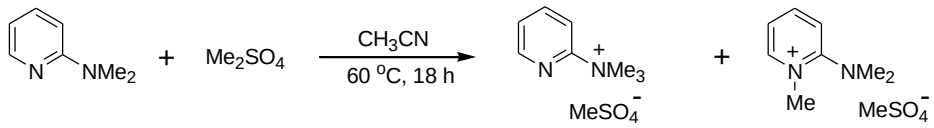

1.1 **4.8** **4.9** 38% **4.10**

2-DMAP **1.1** (1.24 mL, 10 mmol, 1.0 eq) and dimethyl sulfate **4.8** (0.95 mL, 10 mmol, 1.0 eq) were added to dry acetonitrile (5 mL) under argon. The reaction mixture was heated to 60 °C and left to stir for 18 h. The solvent was removed *in vacuo*, and the residue was stirred in diethyl ether (25 mL) for 30 min. The solvent was decanted and the residual solvent was removed from the residue *in vacuo*. ^{1}H

NMR analysis showed the product to consist of a mixture of trimethylpyridin-2-ylammonium methylsulfate **4.9** and 2-dimethylamino-1-methylpyridinium methylsulfate **4.10** in a ratio of 5:1 (by ^{1}H NMR). Recrystallisation from ethanol gave trimethylpyridin-2-ylammonium methylsulfate **4.9** (0.949 g, 38%) as a white solid. 2-Dimethylamino-1-methylpyridinium methylsulfate **4.10** could not be isolated from the reaction mixture.

Trimethylpyridin-2-ylammonium methylsulfate 4.9; mp 110-112 °C; ^{1}H NMR (400 MHz, d_6-DMSO) δ= 3.39 (3H, s, SO_4CH_3), 3.58 (9H, s, CH_3), 7.72 (1H, ddd, J(H,H)= 7.6, 4.8, 0.7 Hz, ArH), 8.09 (1H, dd, J(H,H)= 8.4, 0.7 Hz, ArH), 8.24 (1H, ddd, J(H,H)= 8.4, 7.6, 1.9 Hz, ArH), 8.67-8.68 (1H, m, ArH); ^{13}C NMR (100 MHz, d_6-DMSO) δ= 53.7 (CH_3), 55.4 (CH_3), 116.1 (CH), 127.1 (CH), 142.0 (CH), 149.5 (CH), 157.6 (C); IR (KBr disc) $\tilde{\nu}$= 3054, 2989, 1596, 1577, 1437, 1422, 1262, 1015, 896, 755; MS (ESI) 137 (100) $[M\text{-}MeSO_4]^+$; HRMS: m/z calcd for $C_8H_{13}N_2$ $[M\text{-}MeSO_4]^+$: 137.1073; found: 137.1072.

2-Dimethylamino-1-methylpyridinium methylsulfate 4.10 (not purified, taken from ^{1}H NMR of product mixture); ^{1}H NMR (400 MHz, d_6-DMSO) δ= 3.08 (6H, s, CH_3), 3.40 (3H, s, SO_4CH_3), 4.00 (3H, s, NCH_3), 7.29-7.33 (2H, m, ArH), 7.51-7.54 (1H, m, ArH), 8.14-8.18 (1H, m, ArH), 8.39-8.40 (1H, m, ArH).

EXPERIMENT 4.8: Attempted Reaction of 2-DMAP 1.1 and 1,3-*Bis*-(4-toluenesulfoxy)propane 4.12

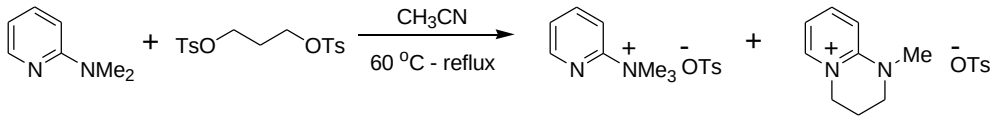

1.1 **4.12** **4.17** **4.18**

2-DMAP **1.1** (0.305 g, 2.5 mmol, 2.5 eq) and 1,3-*bis*-(4-toluenesulfoxy)propane **4.12** (0.378 g, 1 mmol, 1.0 eq) were added to dry acetonitrile (5 mL) under argon. The reaction mixture was heated to 60 °C and left to stir while being monitored by ^{1}H NMR spectroscopy. At 18 h, the temperature was increased to reflux. The heating was stopped at 139 h. No purification of the reaction mixture was attempted due to low conversion of starting material to products. A summary of the conversion of 2-DMAP **1.1** starting material to products is shown on the table below.

TABLE 4.2: Progress of reaction of 2-DMAP **1.1** and 1,3-*bis*-(4-toluene-sulfoxy)propane **4.12**.

Sampling time / h	T / °C	Wt. Sample removed / mg	Reaction mixture composition / % (Based on ^{1}H NMR (CD_3CN) integrations of given peaks)		
			1.1 (δ_H 6.56 ppm)	**4.18** (δ_H 6.85 ppm)	**4.17** (δ_H 8.65 ppm)
18	60	5	100	0	0
46.5	reflux	4	100	0	0
139	reflux	3	88	8	4

EXPERIMENT 4.9: Attempted Reaction of 2-DMAP 1.1 and 1,3-Diiodopropane 1.2 in the Presence of Silver Tetrafluoroborate

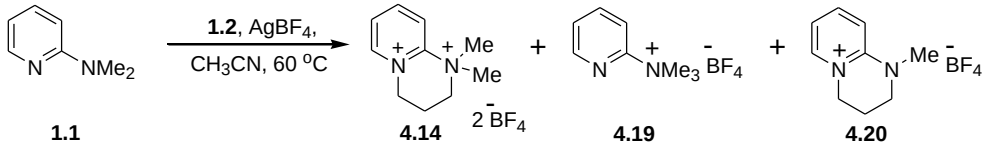

1,3-Diiodopropane **1.2** (0.296 g, 1.0 mmol, 1.0 eq) was added to a solution of 2-DMAP **1.1** (0.122 g, 1.0 mmol, 1.0 eq) and silver tetrafluoroborate (0.428 g, 2.2 mmol, 2.2 eq) in dry acetonitrile (5 mL) under argon. The reaction mixture was heated to 60 °C and left to stir for a period of 23 h, during which time the progress of the reaction was monitored by ^{1}H NMR spectroscopy. ^{1}H NMR monitoring of the reaction at 5 h showed the emergence of a compound with an aromatic multiplet at $\delta_H(CD_3CN)$ 8.74-8.79 ppm that was further downfield than the signals observed for trimethylpyridin-2-ylammonium iodide **1.4** and 1-methyl-1,2,3,4-tetrahydropyrido-[1,2-α]pyrimidin-5-ylium iodide **1.5** ($\delta_H(CD_3CN) \leq 8.6$ and ≤ 8.4 ppm respectively). ^{1}H NMR of the reaction mixture at 23 h showed no evidence of the signal at δ_H 8.74-8.79 ppm, but showed increased ratios of trimethylpyridin-2-ylammonium and 1-methyl-1,2,3,4-tetrahydropyrido[1,2-α]pyrimidin-5-ylium signals. The reaction products could not be separated from the reaction mixture. Trimethylpyridin-2-ylammonium tetrafluoroborate **4.19** and 1-methyl-1,2,3,4-tetrahydropyrido[1,2-α]pyrimidin-5-ylium tetrafluoroborate **4.20** were tentatively identified and showed ^{1}H NMR signals analogous to trimethylpyridin-2-ylammonium iodide **1.4** and 1-methyl-1,2,3,4-tetrahydropyrido[1,2-α]pyrimidin-5-ylium iodide **1.5**.

EXPERIMENT 4.10: ^{1}H NMR Monitoring of the Reaction of 2-DMAP 1.1 and 1,3-Diiodopropane 1.2 in the Presence of Silver Tetrafluoroborate

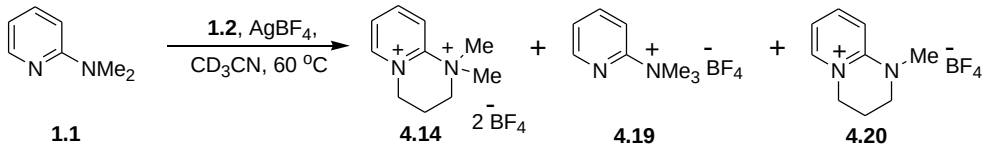

1.1 **4.14** **4.19** **4.20**

The reaction was carried out in a low oxygen, low moisture glovebox using the appropriate protocols detailed in the introduction. 1,3-Diiodopropane **1.2** (14.2 mg, 0.05 mmol, 1.0 eq), 2-DMAP **1.1** (5.8 mg, 0.05 mmol, 1.0 eq) and silver tetrafluoroborate (20.3 mg, 0.104 mmol, 2.2 eq) in dry d_3-acetonitrile (1 mL) were added to an oven-dried NMR tube and sealed with an NMR suba-seal cap. The cap was then wrapped in parafilm. The experiment was carried out on a Bruker AV400 spectrometer. The reaction mixture was held at 60 °C and a 2 min ^{1}H NMR scan was taken every 15 min over a period of 15 h. The reaction was monitored by comparison of the ^{1}H NMR ratios of the listed peaks with the residue of the non-deuterated acetonitrile peak at $\delta_H(CD_3CN)$ 1.94 ppm, which remained constant throughout the reaction.

TABLE 4.3: Reaction progress monitored by ^{1}H NMR.

NMR Experiment Number	**Reaction Time**	**Ratio[a] of δ_H 8.76 ppm (4.14)**	**Ratio[a] of δ_H 8.56 ppm (4.19)**
2	15 min	0.63	0.44
5	1 h 6 min	1.17	0.83
6	1 h 23 min	1.27	0.92
7	1 h 40 min	1.21	0.90
54	14 h 48 min	0.89	0.79

[a] Ratio with respect to the residue of the non-dueterated acetonitrile peak at $\delta_H(CD_3CN)$ 1.94 ppm taken as 1.000.

EXPERIMENT 4.11: Attempted Reaction of 2-DMAP 1.1 and 1,3-Diiodopropane 1.2 in the Presence of Silver Tetrafluoroborate

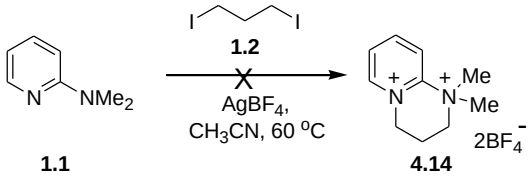

1.1 **4.14**

The reaction was carried out in a low oxygen, low moisture glovebox using the appropriate protocols detailed in the introduction. 1,3-Diiodopropane **1.2** (0.148 g, 0.5 mmol, 1.0 eq) was added to a solution of 2-DMAP **1.1** (0.061 g, 0.5 mmol, 1.0 eq) and silver tetrafluoroborate (0.214, 1.1 mmol, 2.2 eq) in dry acetonitrile (3 mL) and heated to 60 °C. A sample of the reaction mixture was removed at 1 h 23 min and was analysed using direct inject MS; *m*/*z* (ESI) 333, 191, 189, 181, 149, 137 and 123. Another sample of the reaction mixture removed at 1 h 23 min was stirred for 30 min in excess NaCl, then filtered. The sample was analysed using direct inject MS; *m*/*z* (ESI) 191, 189, 181, 163, 149, 137 and 123. LC-MS (C18 reverse-phase column using acetonitrile) of the sample was only able to separate 2-DMAP **1.1** from the mixture (RT 11.50-12.53 min; *m*/*z* (ESI) 123).

EXPERIMENT 4.12: 1,3-*Bis*-(trifluoromethanesulfonyloxy)propane 4.15[89]

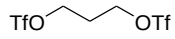

4.15 92%

1,3-Propanediol **4.21** (2.9 mL, 40.0 mmol, 1.0 eq) and pyridine (6.5 mL, 80 mmol, 2.0 eq) in dry DCM (20 mL) were added dropwise to a solution of trifluoromethanesulfonic anhydride (13.5 mL, 80.0 mmol, 2.0 eq) in dry DCM (100 mL) at –78 °C under argon. The reaction mixture was warmed to r.t. and stirred for 1 h to give a pink solution with a white precipitate. The reaction mixture was washed with distilled water (3 x 20 mL), dried over anhydrous Na_2SO_4 and filtered through silica gel (40 g). The silica gel was washed with DCM (50 mL) and combined with the first washing. The solvent was removed *in vacuo* to give 1,3-*bis*-(trifluoromethanesulfonyloxy)propane **4.15** (12.510 g, 92 %) as a red oil; ^{1}H NMR (400 MHz, $CDCl_3$) δ= 2.41 (2H, quintet, *J*(H,H)= 5.8 Hz, CH_2-CH_2-CH_2), 4.70 (4H, t, *J*(H,H)= 5.8 Hz, CH_2-OTf); ^{13}C NMR (100 MHz, $CDCl_3$) δ= 29.2 (CH_2), 71.5 (CH_2), 119.1

(q, *J*(C,F)= 322 Hz, CF_3); IR (thin film) $\tilde{\nu}$= 2991, 1417, 1248, 1207, 929, 854, 812, 735, 614, 581.

EXPERIMENT 4.13: Reaction of 2-DMAP 1.1 and 1,3-*Bis*-(trifluoromethane-sulfonyloxy)propane 4.15

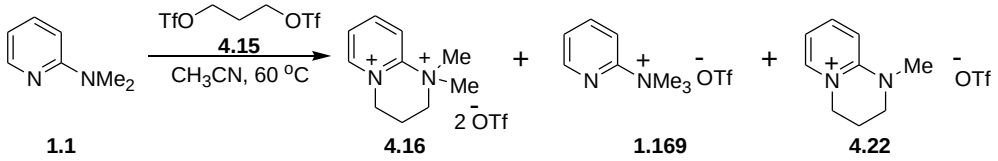

1.1 **4.16** **1.169** **4.22**

The reaction was carried out in a low oxygen, low moisture glovebox using the appropriate protocols detailed in the introduction. 1,3-*Bis*-(trifluoromethanesulfonyl-oxy)propane **4.15** (0.374 g, 1.0 mmol, 1.1 eq) was added to a solution of 2-DMAP **1.1** (0.122 g, 1.0 mmol, 1.0 eq) in dry acetonitrile (5 mL) and heated to 60 °C for 4 h while being monitored by ^{1}H NMR spectroscopy. The reaction was cooled to r.t. and the solvent was removed *in vacuo* leaving a viscous red oil. The reaction mixture was washed with dry diethyl ether (5 mL) and the ether layer was decanted from the reaction mixture. The residual solvent was removed from the residue *in vacuo*. ^{1}H NMR analysis of the reaction mixture showed a mixture of several products.

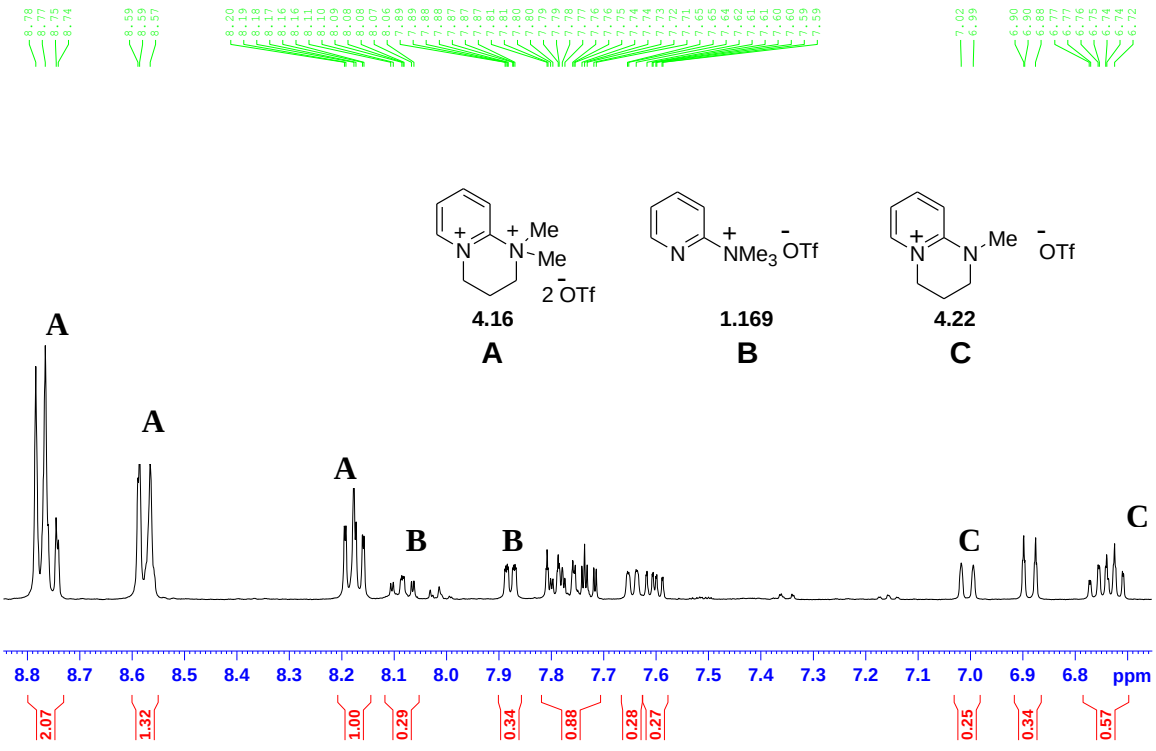

MS analysis of the red oil gave *m*/*z* 313, 149, 137, 123, 102 and 82 $[M]^{2+}$. These compounds were identified as 2-DMAP disalt species **4.16**, 1-methyl-1,2,3,4-tetra-hydropyrido[1,2-α]pyrimidin-5-ylium trifluoromethanesulfonate **4.22** and trimethyl-pyridin-2-ylammonium trifluoromethanesulfonate **1.169**. Separation of the products by recrystallisation from acetonitrile/diethyl ether was not possible.

EXPERIMENT 4.14: Synthesis of 2-DMAP Disalt Species 4.16

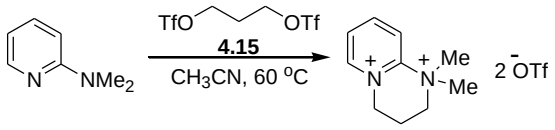

1.1 **4.16** 90%

The reaction was carried out in a low oxygen, low moisture glovebox using the appropriate protocols detailed in the introduction. 1,3-*Bis*-(trifluoromethanesulfonyl-oxy)propane **4.15** (0.255 g, 0.75 mmol, 1.5 eq) and 2-DMAP **1.1** (0.061 g, 0.5 mmol, 1.0 eq) were added to dry acetonitrile (5 mL) and heated to 60 °C for 4 h, the progress of the reaction being monitored by ^{1}H NMR spectroscopy. The reaction was cooled to r.t. and the solvent was removed *in vacuo*, leaving a viscous red oil. The reaction mixture was dissolved in dry acetonitrile (2 mL) and washed with dry diethyl ether (2 x 5 mL). The solvent was removed *in vacuo* to give 2-DMAP disalt **4.16** (0.209 g, 90%) as a red oil; ^{1}H NMR (400 MHz, CD_3CN) δ= 2.67 (2H, tt, *J*(H,H)= 6.2, 5.7 Hz, CH_2-C*H*$_2$-CH_2), 3.84 (6H, s, CH_3), 4.18 (2H, t, *J*(H,H)= 5.7 Hz, CH_2), 4.92 (2H, t, *J*(H,H)= 6.2 Hz, CH_2), 8.22 (1H, ddd *J*(H,H)= 7.5, 6.3, 1.1 Hz, ArH), 8.63 (1H, dd, *J*(H,H)= 8.2, 1.6 Hz, ArH), 8.79-8.83 (2H, m, ArH); ^{13}C NMR (100 MHz, CD_3CN) 17.7 (CH_2), 57.3 (CH_2), 60.8 (CH_3), 63.8 (CH_2), 122.9 (q, *J*(C,F)= 324 Hz, CF_3), 125.4 (CH), 131.6 (CH), 150.0 (CH), 152.3 (C), 152.5 (CH); MS (ESI) 313 (20) $[M\text{-}OTf]^{+}$, 181 (10), 163 (15), 149 (8), 123 (7), 82 (100) $[M\text{-}2OTf]^{2+}$.

EXPERIMENT 4.15: Attempted Large Scale Synthesis of 2-DMAP Disalt 4.16

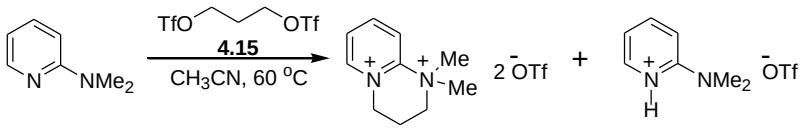

1.1 **4.16** **4.23**

The reaction was carried out in a low oxygen, low moisture glovebox using the appropriate protocols detailed in the introduction. 2-DMAP **1.1** (0.305 g, 2.5 mmol, 1.0 eq) in dry acetonitrile (1 mL) was added to a solution of 1,3-*bis*-(trifluoromethanesulfonyloxy)propane **4.15** (1.276 g, 3.75 mmol, 1.5 eq) in dry acetonitrile (14 mL) and heated to 60 °C for 23 h. ^{1}H NMR analysis of the reaction mixture showed 2-DMAP disalt species **4.16** and what was later identified as 2-dimethylaminopyridinium trifluoromethanesulfonate **4.23** in 1.0:0.9 ratio. The solvent was removed *in vacuo* and the residue was dissolved in dry acetonitrile (2 mL). Dry diethyl ether (5 mL) was added and the mixture was stirred for 1 h. The ether was decanted from the reaction mixture and the acetonitrile was removed *in vacuo*, ^{1}H NMR analysis of the reaction mixture showed 2-dimethylaminopyridinium trifluoromethanesulfonate **4.23** to be still present. The residue was dissolved in dry acetonitrile (3 mL) and washed with dry diethyl ether (3 x 15 mL). The solvent was removed *in vacuo* to give a red oil (1.041 g) shown by the ^{1}H NMR spectrum to contain 2-DMAP disalt **4.16**:protonated 2-DMAP **4.23** in ratio of 1.00:0.43. 2-DMAP disalt **4.16** could not be purified.

2-Dimethylaminopyridinium trifluoromethanesulfonate 4.23: ^{1}H NMR (400 MHz, $CDCl_3$) δ= 3.33 (6H, s, CH_3), 6.85 (1H, ddd, *J*(H,H)= 7.0, 6.3, 0.6 Hz, ArH), 7.01 (1H, dd, *J*(H,H)= 9.2, 0.6 Hz, ArH), 7.88 (1H, ddd, *J*(H,H)= 9.2, 7.0, 1.8 Hz, ArH), 8.02 (1H, ddd, *J*(H,H)= 6.3, 1.8, 0.6 Hz, ArH), 10.1 (1H, bs, NH); ^{13}C NMR (100 MHz, $CDCl_3$) δ= 39.5 (CH_3), 111.9 (CH), 112.4 (CH), 121.5 (q, *J*(C,F)= 322 Hz, CF_3), 137.6, 144.1 (CH), 153.1 (C); IR (thin film) $\tilde{\nu}$= 3501 (bs), 1652, 1624, 1552, 1251 (bs), 1168, 1168, 1030, 763, 640; MS (ESI) 123 (100) $[M\text{-}OTf]^{+}$.

Data for 2-DMAP disalt **4.16** were consistent with that reported in experiment 4.14.

EXPERIMENT 4.16: Temperature Dependence of the Formation of 2-DMAP Disalt 4.16

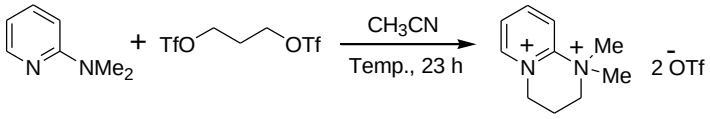

1.1 **4.15** **4.16**

2-DMAP **1.1** (0.305 g, 2.5 mmol, 1.0 eq) was added to a solution of 1,3-*bis*-(trifluoromethanesulfonyloxy)propane **4.15** (1.276 g, 3.75 mmol, 1.5 eq) in dry

acetonitrile (15 mL) at the required temperature and stirred for 24 h. For temperatures (-78)-0 °C, the temperature was held for 6 h, then allowed to warm to r.t. for the remainder of the experiment. Samples were removed at 4 h and 23 h for ^{1}H NMR analysis. After 23 h, the reaction was cooled to r.t. (if required) and the solvent was removed *in vacuo*. A ^{1}H NMR spectrum of the residue was obtained. The ratio of 2-DMAP disalt **4.16**:2-dimethylaminopyridinium trifluoromethanesulfonate **4.23** at each sampling is recorded in table 4.4.

TABLE 4.4: Ratio of **4.23** to **4.16** at different reaction temperatures.

Entry	**T / °C**	**Ratio of 4.23 in reaction mixture[a]**		
		4 h	**23 h**	**Post work-up**
1	60	0.78[b]	0.87	-
2	r.t.	0.64	0.79	0.68
3	0	0.79	0.80[c]	0.94[c]
4	-41	0.03	0.28[c]	0.30[c]
5	-78	0.05	0.32[c]	0.32[c]

[a] Ratio taken by ^{1}H NMR comparison of peak at δ_H(CD_3CN) 6.8 ppm for **4.23** in comparison to ratio of 1.00 taken for **4.16** for peak at δ_H(CD_3CN) 8.2 ppm. [b] Sampling taken at 5.5 h. [c] Sampling occurred when reaction mixture was at r.t.

EXPERIMENT 4.17: Isolation of 2-DMAP Disalt 4.16 at -41 °C

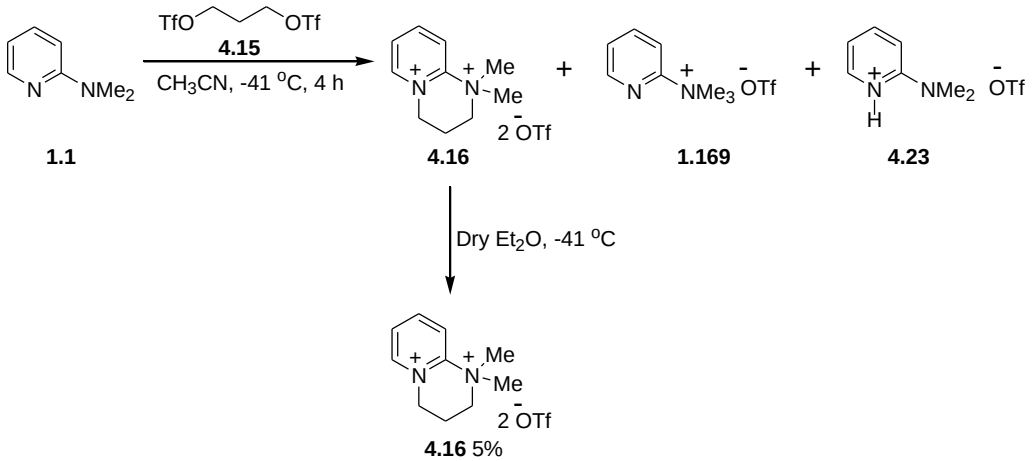

2-DMAP **1.1** (0.305 g, 2.5 mmol, 1.0 eq) was added to a solution of 1,3-*bis*-(trifluoromethanesulfonyloxy)propane **4.15** (0.850 g, 2.5 mmol, 1.5 eq) in dry acetonitrile (5 mL) at -41 °C under argon and stirred for 4 h. The entire reaction

mixture was transferred to a flask containing dry diethyl ether (~ 40 mL) at -41 °C, causing a white precipitate to form, which was identified as 2-DMAP disalt **4.16** (0.058 g, 5 %). Data for 2-DMAP disalt **4.16** were consistent with that reported in experiment 4.14.

EXPERIMENT 4.18: 2-DMAP Disalt 4.16

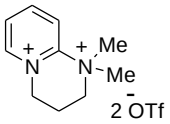

4.16 81%

2-DMAP **1.1** (0.31 mL, 2.5 mmol, 1.0 eq) was added dropwise to a tube containing 1,3-*bis*-(trifluoromethanesulfonyloxy)propane **4.15** (1.021 g, 3.0 mmol, 1.2 eq) at 0 ºC under argon. The reaction mixture was warmed to r.t. and stirred until solidification of the reaction mixture formed a yellow gel-like solid (approximately 5 min). The reaction mixture was washed with dry diethyl ether (2 x 30 mL) and the solvent was removed *in vacuo* to give a white powder (1.363 g), shown by ^{1}H NMR to contain 2-DMAP disalt **4.16**. The powder was recrystallised from dry acetonitrile/diethyl ether to give 2-DMAP disalt **4.16** (0.937 g, 81 %) as white crystals; mp 113-116 ºC; ^{1}H NMR (400 MHz, CD_3CN) δ= 2.67 (2H, tt, *J*(H,H)= 6.2, 5.7 Hz, CH_2-C*H*$_2$-CH_2), 3.84 (6H, s, CH_3), 4.18 (2H, t, *J*(H,H)= 5.7 Hz, CH_2), 4.92 (2H, t, *J*(H,H)= 6.2 Hz, CH_2), 8.22 (1H, ddd *J*(H,H)= 7.5, 6.3, 1.1 Hz, ArH), 8.63 (1H, dd, *J*(H,H)= 8.2, 1.6 Hz, ArH), 8.79-8.83 (2H, m, ArH); ^{13}C NMR (100 MHz, CD_3CN) 17.7 (CH_2), 57.3 (CH_2), 60.8 (CH_3), 63.8 (CH_2), 122.9 (q, *J*(C,F)= 324 Hz, CF_3), 125.4 (CH), 131.6 (CH), 150.0 (CH), 152.3 (C), 152.5 (CH); IR (KBr disc) $\tilde{\nu}$= 3136, 3102, 3080, 3050, 1638, 1591, 1519, 1488, 1452, 1256, 1228, 1155, 1033, 992, 962, 780, 636, 575, 519; MS (ESI) 313 (20) $[M\text{-}OTf]^+$, 181 (10), 163 (15), 149 (8), 123 (7), 82 (100) $[M\text{-}2OTf]^{2+}$; HRMS: *m*/*z* calcd for $C_{11}H_{16}F_3N_2O_3S$ $[M\text{-}OTf]^+$: 313.0828; found: 313.0826. Crystallographic data for 2-DMAP disalt **4.16** is given in Appendix 1.

EXPERIMENT 4.19: Attempted Large Scale Synthesis of 2-DMAP Disalt 4.16

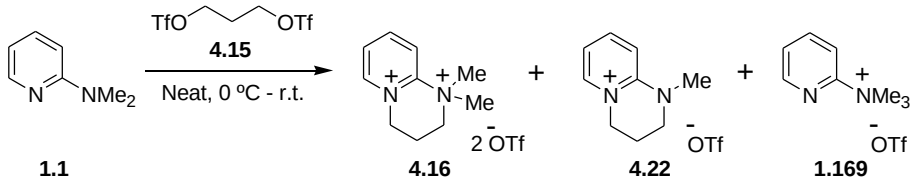

1.1 **4.16** **4.22** **1.169**

2-DMAP **1.1** (2.443 g, 20 mmol, 1.0 eq) was added dropwise to a flask containing 1,3-*bis*-(trifluoromethanesulfonyloxy)propane **4.15** (8.165 g, 24 mmol, 1.2 eq) at 0 °C under argon. The solution changed colour from colourless to green, then to black as the 2-DMAP **1.1** was added. The solution was stirred for 1 h at 0 °C, then warmed to r.t. and stirred for 1 h, then dry diethyl ether (20 mL) was added, but no white solid precipitated. Attempts to purify the 2-DMAP disalt **4.16** by recrystallisation from dry acetonitrile/diethyl ether were unsuccessful. ^{1}H NMR and MS analysis of the reaction mixture showed evidence of 2-DMAP disalt **4.16**, trimethylpyridin-2-ylammonium trifluoromethanesulfonate **1.169** and 1-methyl-1,2,3,4-tetrahydro-pyrido[1,2-α]-pyrimidin-5-ylium trifluoromethanesulfonate **4.22**. Data were consistent with that reported in experiment 4.18.

EXPERIMENT 4.20: Synthesis of 2-DMAP Disalt 4.16 using Syringe Pump

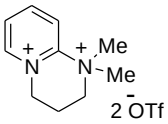

4.16 98%

2-DMAP **1.1** (2.48 mL, 20.0 mmol, 1.0 eq) was added using a syringe pump (1.27 mL.h^{-1}) to a flask containing 1,3-*bis*-(trifluoromethanesulfonyloxy)propane **4.15** (8.165 g, 24.0 mmol, 1.2 eq) at 0 ºC under argon. A white solid began to precipitate. After addition of half of the 2-DMAP **1.1**, dry diethyl ether (4 mL) was added to the reaction mixture to allow stirring to continue. After the addition of all the 2-DMAP **1.1**, the reaction mixture was stirred at 0 ºC for 1 h, then warmed to r.t. The resulting white powder was stirred in dry diethyl ether (30 mL) for 30 min, then collected and the solvent was removed *in vacuo*. The powder was recrystallised from dry acetonitrile/diethyl ether to give 2-DMAP disalt **4.16** (9.089 g, 98 %) as a white solid. Data were consistent with that reported in experiment 4.18.

EXPERIMENT 4.21: 2-Dimethylaminopyrimidine 4.31

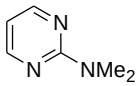

4.31 94%

Dimethylamine solution (40 % in water, 10.5 mL, 60 mmol, 3.0 eq) was added to a solution of 2-bromopyrimidine **4.32** (3.180 g, 20 mmol, 1.0 eq) in acetonitrile (60 mL) under argon and stirred for 18 h. The reaction mixture was filtered through a plug of potassium carbonate, which was then washed with acetonitrile (50 mL). The solvent was removed *in vacuo* to give 2-dimethylaminopyrimidine **4.31** (2.322 g, 94 %) as a colourless oil; ^{1}H NMR (500 MHz, $CDCl_3$) δ= 3.19 (6H, s, NCH_3) 6.45 (1H, t, *J*(H,H)= 4.5 Hz, ArH), 8.31 (2H, d, *J*(H,H)= 4.5 Hz, ArH); ^{13}C NMR (100 MHz, $CDCl_3$) δ= 37.2 (CH_3), 109.0 (CH), 157.7 (CH), 162.4 (C); IR (thin film) $\tilde{\nu}$= 2936, 2863, 2793, 1754, 1591, 1549, 1404, 1379, 1312, 1206, 1085, 988, 799, 638, 515; MS (CI) 124 (100) $[M+H]^+$, 114 (5), 110 (7), 58 (5), 52 (36), 46 (5) 44 (10); HRMS: *m*/*z* calcd for $C_6H_{10}N_3$ $[M+H]^+$: 124.0869; found: 124.0868.

EXPERIMENT 4.22: 2-Dimethylaminopyrimidine 4.31 from 2-Chloro-pyrimidine 4.33

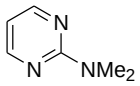

4.31 72%

Dimethylamine solution (2.0 M in THF, 12.5 mL, 25.0 mmol, 5.0 eq) was added to a flask containing 2-chloropyrimidine **4.33** (0.573 g, 5.0 mmol, 1.0 eq) cooled to 0 °C under argon. The reaction mixture was warmed to r.t. and stirred for 1 h, then heated to 50 °C and stirred for 18 h. The reaction mixture was cooled to r.t. and the solvent was removed *in vacuo*. The residue was dissolved in ethyl acetate (20 mL) and washed with sat. $NaHCO_3$ solution (20 mL). The organic layer was separated and the aqueous layer was re-extracted with ethyl acetate (20 mL). The combined organic layers were washed with brine (40 mL), dried over anhydrous Na_2SO_4 and the solvent was removed *in vacuo* to give 2-dimethylaminopyrimidine **4.31** (0.44 g, 72 %) as a colourless oil. Data were consistent with that reported in experiment 4.21.

EXPERIMENT 4.23: Attempted Synthesis of 2-Dimethylaminopyrimidine Disalt 4.30

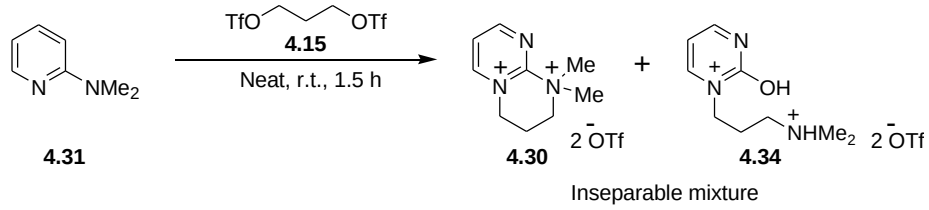

The reaction was carried out in a low oxygen, low moisture glovebox using the appropriate protocols detailed in the introduction. 2-Dimethylaminopyrimidine **4.31** (0.123 g, 1.0 mmol, 1.0 eq) was added dropwise to a tube containing 1,3-*bis*-(trifluoromethanesulfonyloxy)propane **4.15** (0.408 g, 1.2 mmol, 1.2 eq) at r.t. in the glovebox. The reaction mixture was stirred for 1.5 h, then dry diethyl ether (1 mL) was added and the reaction mixture was stirred for 30 min. The resulting orange precipitate was collected and the residual solvent was removed *in vacuo* to give an orange solid (0.26 g). ^{1}H NMR analysis of the solid showed a mixture of 2-dimethylaminopyrimidine disalt **4.30** and 1-(3-dimethylammoniumpropyl)-2-hydroxypyrimidinium trifluoromethanesulfonate **4.34** in a ratio of 4:1 (by ^{1}H NMR). The data were consistent with that reported in experiment 4.24 and 5.32.

EXPERIMENT 4.24: 2-Dimethylaminopyrimidine Disalt 4.30

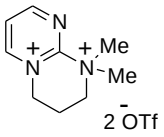

4.30 65%

The reaction was carried out in a low oxygen, low moisture glovebox using the appropriate protocols detailed in the introduction. 2-Dimethylaminopyrimidine **4.31** and 1,3-*bis*-(trifluoromethanesulfonyloxy)propane **4.15** were freshly distilled before the reaction. 2-Dimethylaminopyrimidine **4.31** (0.616 g, 5.0 mmol, 1.0 eq) was added dropwise to a tube containing 1,3-*bis*-(trifluoromethanesulfonyloxy)propane **4.15** (2.041 g, 6.0 mmol, 1.2 eq) in a glovebox. The reaction mixture was stirred for 1.5 h, then dry diethyl ether (1 mL) was added to the reaction mixture and stirred for a further 30 min causing an orange solid to precipitate. The solid was filtered and the solvent was removed *in vacuo*. Recrystallisation from dry acetonitrile/diethyl ether in

a glovebox gave 2-dimethylaminopyrimidine disalt **4.30** (1.508 g, 65 %) as an off-white solid; mp 160-163 ºC; ^{1}H NMR (500 MHz, CD_3CN) δ= 2.73 (2H, tt, *J*(H,H)= 6.3, 5.7 Hz, CH_2-C*H*$_2$-CH_2), 3.85 (6H, s, N-C*H*$_3$), 4.27 (2H, t, *J*(H,H)= 5.7 Hz, N-C*H*$_2$), 4.99 (2H, t, *J*(H,H)= 6.3 Hz, N-C*H*$_2$), 8.37 (1H, dd *J*(H,H)= 6.2, 4.8 Hz, ArH), 9.21 (1H, d, *J*(H,H)= 6.2, 1.9 Hz, ArH), 9.52 (1H, dd *J*(H,H)= 4.8, 1.9 Hz, ArH); ^{13}C NMR (125 MHz, CD_3CN) δ= 17.4 (CH_2), 57.6 (CH_2), 59.3(CH_3), 62.3 (CH_2), 122.0 (q, *J*(C,F)= 320 Hz, CF_3), 123.7 (CH), 154.2 (C), 157.9 (CH), 168.4 (CH); IR (KBr disc) $\tilde{\nu}$= 3167, 3114, 3083, 2985, 2935, 2879, 1749, 1634, 1599, 1565, 1495, 1479, 1443, 1376, 1259, 1155, 1031, 988, 902, 877, 837, 828, 771, 639, 575, 517; MS (ESI) 432 (38), 314 (100) [M-OTf] $^{+}$, 196 (38), 182 (13), 164 (46), 150 (26), 124 (17), 103 (31), 83 (54) $[M\text{-}2OTf]^{2+}$; HRMS: *m*/*z* calcd for $C_{10}H_{15}F_3N_3O_3S$ $[M\text{-}OTf]^{+}$: 314.0781; found: 314.0782. Crystallographic data for 2-dimethylaminopyrimidine disalt **4.30** is given in Appendix 2.

9.3 Experimental for Chapter 5

General Procedures for Chapter 5

Chlorobenzene was distilled from CaH_2 under vacuum. Triethylamine **5.28** and *N*,*N*-di-*iso*-propylamine **5.21** were distilled from CaH_2 under argon and vacuum respectively. Iodomethane was distilled from P_2O_5 under argon. Dimethyl sulfate was distilled from 4 Å molecular sieves under vacuum. All dried reagents were stored under 4 Å molecular sieves once distilled. All NMR kinetic experiments were carried out on a Bruker AV400 spectrometer at 300 K in CD_3CN with cyclooctatetraene **5.29** as an internal standard.

EXPERIMENT 5.1: Synthesis of 1,3-Dimethyl-1*H*-indole 3.58

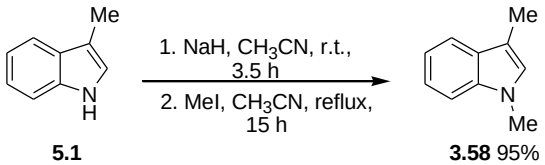

5.1 **3.58** 95%

Sodium hydride (60 % in oil, 0.120 g, 3.0 mmol, 3.0 eq) was washed with dry hexane (3 x 10 mL) and the solvent was removed under a flow of argon. The washed sodium hydride was cooled to 0 °C and dry acetonitrile (10 mL) and 3-methylindole **5.1** (0.131 g, 1.0 mmol, 1.0 eq) were added. The reaction mixture was warmed to r.t.

and stirred for 3.5 h. Iodomethane (0.07 mL, 1.1 mmol, 1.1 eq) was added dropwise and the reaction mixture was heated at reflux for 18 h. The reaction mixture was cooled to r.t. and the reaction was quenched with saturated NH_4Cl solution (5 mL) and left to stir for 30 min. The solvent was removed *in vacuo* and the residue was dissolved in diethyl ether (20 mL) and washed with water (20 mL). The water was re-extracted with diethyl ether (20 mL) and the combined ether layers were washed with water (1 x 50 mL), brine (3 x 50 mL), dried over anhydrous Na_2SO_4 and the solvent was removed *in vacuo* to give a 1,3-dimethyl-1*H*-indole **3.58** (0.138 g, 95 %) as a pale yellow oil; ^{1}H NMR (400 MHz, $CDCl_3$) δ= 2.42 (3H, s, CH_3), 3.79 (3H, s, CH_3), 6.86 (1H, s, ArH), 7.16 (1H, ddd, *J*(H,H)= 7.8, 6.8, 1.1 Hz, ArH), 7.25-7.34 (2H, m, ArH), 7.62 (1H, dd, *J*(H,H)= 7.8, 0.7 Hz, ArH); ^{13}C NMR (100 MHz, $CDCl_3$) δ= 9.2 (CH_3), 32.4 (CH_3), 109.5 (CH), 110.5 (C), 119.0 (CH), 119.5 (CH), 121.9 (CH), 127.1 (CH), 129.2 (C), 137.6 (C); GC-MS: RT 4.54 *m*/*z* 145 (83) $[M]^{+\bullet}$, 144 (100), 128 (15), 115 (17), 102 (22), 77 (23); HRMS: *m*/*z* calcd for $C_{10}H_{10}N_1$ $[M-H]^{+\bullet}$: 144.0808; found: 144.0807.

EXPERIMENT 5.2: Synthesis of 1,3-Dimethyl-1*H*-indole 3.58 from 1-Methylindole 3.57 and 2-DMAP Disalt 4.16

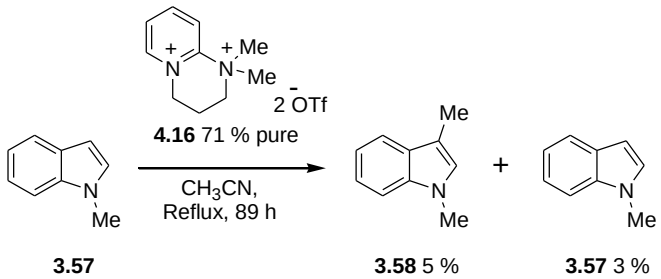

1-Methylindole **3.57** (0.059 g, 0.45 mmol, 1.0 eq) was added to a solution of 2-DMAP disalt **4.16** (71 % purity, 1.041 g, 2.25 mmol, 2.5 eq) in dry acetonitrile (8 mL) and heated at reflux for 89 h, the progress of the reaction being monitored by TLC. The reaction was cooled to r.t. and the solvent was removed *in vacuo*. The residue was dissolved in diethyl ether (20 mL) and washed with water (20 mL). The water was re-extracted with diethyl ether (2 x 10 mL) and the combined diethyl ether layers were washed with water (3 x 40 mL), brine (3 x 40 mL), dried over anhydrous Na_2SO_4 and the solvent was removed *in vacuo* to give a brown oil (31 mg). Separation by column chromatography using silica gel (EA/PE 1:9) gave a brown oil

(18 mg), which was shown to contain 1-methylindole **3.57** and 1,3-dimethyl-1*H*-indole **3.58** by GC-MS analysis. Purification using HPLC chromatography (EA/Hexane 1:200, flowrate 4 mL/min) gave 1-methylindole **3.57** as a colourless oil (RT 10.03-12.67 min; 0.002 g, 3 %) and 1,3-dimethyl-1*H*-indole **3.58** as a pale yellow oil (RT 8.53-10.03 min; 0.003 g, 5 %).

1-Methylindole 3.57; ^{1}H NMR (400 MHz, $CDCl_3$) δ= 3.86 (3H, s, NCH_3), 6.57 (1H, dd, *J*(H,H)= 3.1, 0.8 Hz, ArH), 7.11 (1H, d, *J*(H,H)= 3.1 Hz, ArH), 7.20 (1H, ddd, *J*(H,H)= 7.8, 7.0, 1.0 Hz, ArH), 7.31 (1H, ddd, *J*(H,H)= 8.2, 7.0, 1.0 Hz, ArH), 7.40 (1H, dd, *J*(H,H)= 8.2, 0.8 Hz, ArH), 7.71 (1H, ddd, *J*(H,H)= 7.8, 1.0, 0.8 Hz, ArH); ^{13}C NMR (100 MHz, $CDCl_3$) δ= 32.6 (CH_3), 101.2 (CH), 109.6 (CH), 119.7 (CH), 121.3 (CH), 122.0 (CH), 129.0 (C), 129.3 (CH), 137.3 (C); IR (thin film) $\tilde{\nu}$= 3054, 2943, 1614, 1513, 1463, 1330, 1317, 763, 740; GC-MS: RT 9.78 min, *m*/*z* 131 (100) $[M]^{+\bullet}$, 103 (10), 89 (8).

Data for 1,3-dimethyl-1*H*-indole **3.58** were consistent with that reported in experiment 5.1.

EXPERIMENT 5.3: Attempted One-pot Formation of Disalt Species 4.16 and Reaction with 1-Methylindole 3.57

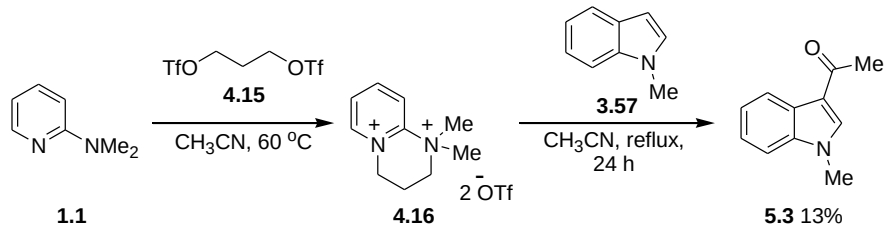

The reaction was carried out in a low oxygen, low moisture glovebox using the appropriate protocols detailed in the introduction. 2-DMAP **1.1** (0.061 g, 0.5 mmol, 1.0 eq) in dry acetonitrile (1 mL) was added to a solution of 1,3-*bis*(trifluoromethanesulfonyloxy)propane **4.15** (0.255 g, 0.75 mmol, 1.5 eq) in dry acetonitrile (4 mL) and heated at 60 °C for 4 h while being monitored by ^{1}H NMR spectroscopy. 1-Methylindole **3.57** (0.066 g, 0.5 mmol, 1.0 eq) in dry acetonitrile (1 mL) was added to the reaction mixture and the temperature was increased to reflux for 24 h. The reaction mixture was cooled to r.t. and the solvent was removed *in vacuo* to give a viscous red oil. The reaction mixture was removed from the glovebox and dissolved in diethyl ether (20 mL) and washed with water (20 mL). The water

was re-extracted with diethyl ether (2 x 10 mL) and the combined diethyl ether layers were washed with water (3 x 20 mL), brine (3 x 20 mL), dried over anhydrous Na_2SO_4 and the solvent was removed *in vacuo*. Purification by column chromatography using silica gel (EA/PE 1:4) gave 1-(1-methyl-1*H*-indol-3-yl)ethanone **5.3** (0.011 g, 13 %) as a brown solid; mp 100-102 °C (lit.[152] 103-104 °C); ^{1}H NMR (400 MHz, $CDCl_3$) δ= 2.57 (3H, s, CH_3), 3.89 (3H, s, C(O)CH_3), 7.33-7.35 (3H, m, ArH), 7.72 (1H, s, ArH), 8.38-8.40 (1H, m, ArH); ^{13}C NMR (100 MHz, $CDCl_3$) δ= 27.4 (CH_3), 33.3 (CH_3), 110.0 (CH), 117.4 (C), 123.0 (CH), 123.8 (CH), 126.7 (C), 136.4 (CH), 138.1 (C), 193.9 (C); IR (KBr disc) $\tilde{\nu}$= 3107, 3050, 2922, 2850, 1643, 1529, 1465, 1374, 1226, 1127, 1101, 929, 746; MS (EI) 173 (40) $[M]^{+\bullet}$, 158 (100), 130 (15), 105 (20), 77 (30), 43 (40); *m/z* calcd for $C_{11}H_{12}N_1O_1$ $[M+H]^+$: 174.0913; found: 174.0914.

EXPERIMENT 5.4: Determining the Stability of 1-Methylindole 3.57 in Acetonitrile

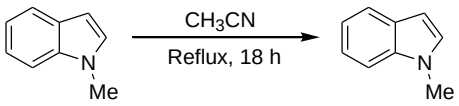

3.57 **3.57** 98%

A solution of 1-methylindole **3.57** (0.131 g, 1 mmol, 1.0 eq) in dry acetonitrile (10 mL) was heated at reflux under argon for 18 h. The reaction was cooled to r.t. and the solvent was removed *in vacuo* to recover 1-methylindole **3.57** (0.128 g, 98 %). Data were consistent with that reported in experiment 5.2.

EXPERIMENT 5.5: Iminium Salt 5.9

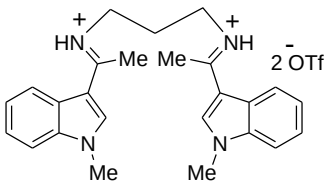

5.9 54%

1,3-*Bis*-(trifluoromethanesulfonyloxy)propane **4.15** (0.170 g, 0.5 mmol, 1.0 eq) was added to a solution of 1-methylindole **3.57** (0.066 g, 0.5 mmol, 1.0 eq) in dry acetonitrile (5 mL) and heated at reflux under argon for 18 h. The solvent was

removed *in vacuo* and the residue was recrystallised from dry acetonitrile/diethyl ether to give iminium salt **5.9** (0.723 g, 54 %) as a brown solid; mp 128-131 °C; ^{1}H NMR (400 MHz, d_6-DMSO) δ= 2.27-2.31 (2H, m, CH_2), 2.86 (6H, s, CH_3), 3.89-3.94 (10H, m, CH_3, CH_2), 7.38-7.45 (4H, m, ArH), 7.69 (2H, d, J(H,H)= 7.8 Hz, ArH), 8.07 (2H, d, J(H,H)= 8.0 Hz, ArH), 8.73 (2H, s, NCH), 10.34 (2H, bs, NH); ^{13}C NMR (100 MHz, d_6-DMSO) δ= 18.5 (CH_3), 27.5 (CH_2), 34.0 (CH_3), 43.8 (CH_2), 109.6 (C), 112.7 (CH), 121.3 (CH), 124.0 (CH), 124.1 (C), 125.0 (CH), 139.0 (C), 142.9 (CH), 174.3 (C); IR (KBr disc) $\tilde{\nu}$= 3580, 3365, 3111, 1619, 1537, 1469, 1360, 1263, 1145, 1029, 754, 638; MS (ESI) 535 (10) $[M\text{-}OTf]^+$, 385 (70), 213 (30), 193 (95), 127 (100), 107 (30); HRMS: *m*/*z* calcd for $C_{26}H_{30}F_3N_4O_3S_1$ $[M\text{-}OTf]^+$: 535.1985; found: 535.1991.

EXPERIMENT 5.6: Synthesis of 1-(1-methyl-1*H*-indol-3-yl)ethanone 5.3 from Iminium Salt 5.9

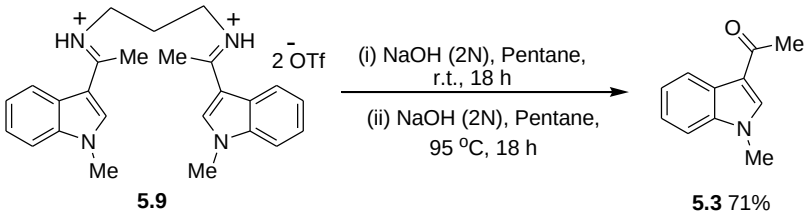

5.9 **5.3** 71%

NaOH solution (2N, 6 mL) was added to a solution of iminium salt **5.9** (0.064 g, 0.1 mmol, 1.0 eq) in pentane (3 mL) and stirred for 18 h. TLC (EA/PE 2:3) of the reaction mixture showed some formation of 1-(1-methyl-1*H*-indol-3-yl)ethanone **5.3**. The reaction mixture was heated at ~95 °C for 18 h. The reaction mixture was cooled to r.t. and diluted with diethyl ether (15 mL). The organic layer was separated from the aqueous layer, which was then re-extracted with diethyl ether (10 mL). The combined organic layers were washed with water (3 x 25 mL), brine (3 x 25 mL), dried over anhydrous Na_2SO_4 and the solvent was removed *in vacuo* to give 1-(1-methyl-1*H*-indol-3-yl)ethanone **5.3** (0.025 g, 71 %) as an off-white solid. Data for 1-(1-methyl-1*H*-indol-3-yl)ethanone **5.3** were consistent with that reported in experiment 5.3.

EXPERIMENT 5.7: Methylation of 1-Methylindole 3.57

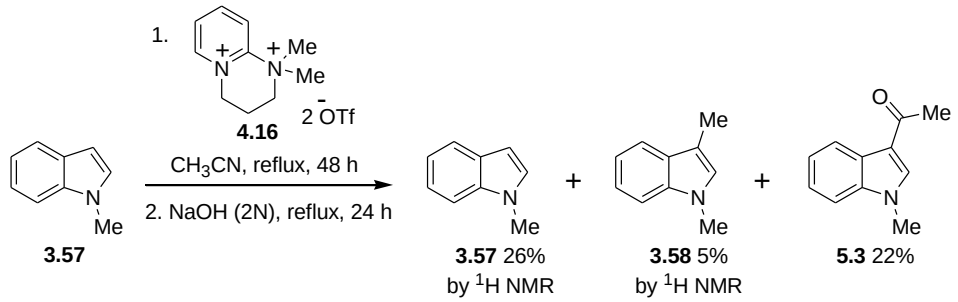

1-Methylindole **3.57** (0.066 g, 0.5 mmol, 1.0 eq) in dry acetonitrile (0.5 mL) was added to a solution of 2-DMAP disalt **4.16** (0.231 g, 0.5 mmol, 1.0 eq) in dry acetonitrile (2.5 mL) under argon. The reaction mixture was heated at reflux for 48 h. NaOH solution (2N, 3 mL) was added and the reaction mixture was refluxed for a further 24 h. The solvent was removed *in vacuo*. The residue was dissolved in diethyl ether (20 mL) and washed with water (20 mL). The water was re-extracted with diethyl ether (2 x 10 mL) and the combined ether layers were washed with water (20 mL), brine (20 mL), dried over anhydrous Na_2SO_4 and the solvent was removed *in vacuo* to give a brown oil (0.065 g). Column chromatography using silica gel (EA/PE 1:19) gave a mixture of 1-methylindole **3.57** and 1,3-dimethyl-1*H*-indole **3.58** as a red oil (0.021 g, 5:1 by ^{1}H NMR) that could not be separated and 1-(1-methyl-1*H*-indol-3-yl)ethanone **5.3** (0.087 g, 22 %) as a brown solid. Data were consistent with data reported for 1-methylindole **3.57** in experiment 5.4, 1,3-dimethyl-1*H*-indole **3.58** in experiment 5.2 and 1-(1-methyl-1*H*-indol-3-yl)ethanone **5.3** in experiment 5.3.

EXPERIMENT 5.8: Attempted Methylation of Acetonitrile using Disalt 4.16

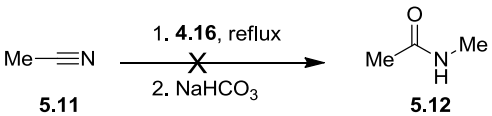

A solution of 2-DMAP disalt **4.16** 0.462 g, 1.0 mmol, 1.0 eq) in acetonitrile (0.5 mL, 10.0 mmol, 10.0 eq) was heated to reflux under argon for 18 h. Water (3 mL) and sat. $NaHCO_3$ solution (mL) were added and the reaction mixture was heated to reflux for a further 24 h. The reaction mixture was cooled to r.t. and diluted with diethyl ether (10 ml) and water (10 ml). The organic layer was separated, washed with brine (15

mL), dried over anhydrous Na_2SO_4 and the solvent was removed *in vacuo*. ^{1}H NMR analysis of the residue showed no evidence of amide **5.12**.

EXPERIMENT 5.9: Methylation of Benzonitrile 5.13 using Disalt 4.16

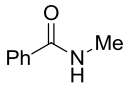

5.14 22%

A solution of 2-DMAP disalt **4.16** 0.462 g, 1.0 mmol, 1.0 eq) in benzonitrile **5.13** (0.5 mL, 5.0 mmol, 5.0 eq) was heated to reflux under argon for 18 h. Water (3 mL) and sat. $NaHCO_3$ solution (mL) were added and the reaction mixture was heated to reflux for a further 24 h. The reaction mixture was cooled to r.t. and diluted with diethyl ether (10 ml) and water (10 ml). The organic layer was separated, washed with brine (15 mL), dried over anhydrous Na_2SO_4 and the solvent was removed *in vacuo*. Purification by column chromatography using silica gel (EA/DCM 1:1) gave *N*-methylbenzamide **5.14** (0.023 g, 22 %) as a brown solid; ^{1}H NMR (400 MHz, $CDCl_3$) δ= 3.03 (3H, d, *J*(H,H)= 4.9 Hz, CH_3), 6.19 (1H, bs, NH), 7.41-7.52 (3H, m, ArH), 7.77 (1H, dd, *J*(H,H)= 7.0, 1.5 Hz, ArH); ^{13}C NMR (100 MHz, $CDCl_3$) δ= 27.1 (CH_3), 127.0 (CH), 128.8 (CH), 131.5 (CH), 134.9 (C), 168.5 (CO); IR (KBr disc) $\tilde{\nu}$= 3264, 3055, 1638, 1545, 1490, 1410, 1311, 1287, 1164, 872, 711, 696; MS (ESI) 136 (100) $[M+H]^+$, 105 (12); HRMS: *m*/*z* calcd for $C_8H_{10}N_1O_1$ $[M+H]^+$: 136.0757; found: 136.0756.

EXPERIMENT 5.10: Neat reaction of 2-DMAP Disalt 4.16 and 1-Methylindole 3.57

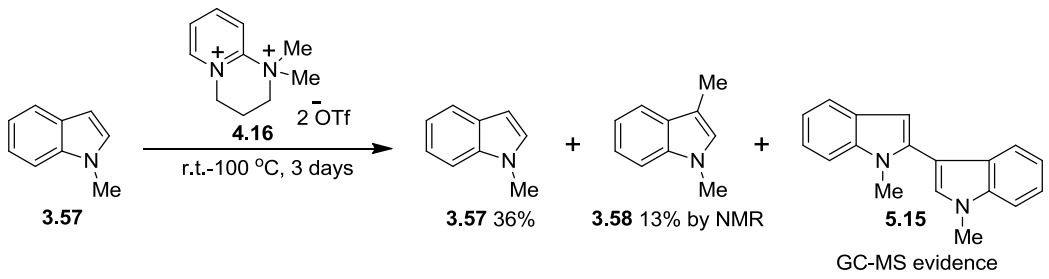

The reaction was carried out in a low oxygen, low moisture glovebox using the appropriate protocols detailed in the introduction. 2-DMAP disalt **4.16** (0.426 g, 1.0

mmol, 1.0 eq) was added to a flask containing 1-methylindole **3.57** (0.393 g, 3.0 mmol, 3.0 eq) and stirred at r.t. under argon for 18 h. ^{1}H NMR analysis of the reaction mixture showed no evidence of reaction. The temperature was increased to 60 °C for 24 h. Again, ^{1}H NMR analysis of the reaction mixture showed no evidence of reaction. The temperature was increased to 100 °C for 24 h, at which time ^{1}H NMR analysis of the reaction mixture showed evidence of reaction. The reaction mixture was dissolved in DCM (20 mL) and washed with water (20 mL). The water was re-extracted with DCM (2 x 10 mL) and the combined organic layers were washed with water (20 mL), brine (2 x 20 mL), dried over anhydrous Na_2SO_4 and the solvent was removed *in vacuo* to give an orange oil (0.459 g). GC-MS analysis of the mixture gave peaks corresponding to 1-methylindole **3.57**, 1,3-dimethyl-1*H*-indole **3.58** and 1-methylindole dimer species **5.15** respectively. No NMR evidence for 1-methylindole dimer **5.15** species was observed.

GM-MS: RT 9.70 min *m*/*z* (EI) 131 (100) [$M^{+\bullet}$], 130 (95); RT 10.38 min *m*/*z* (EI) 145 (55) [$M^{+\bullet}$], 144 (100); RT 16.93 min *m*/*z* (EI) 260 (100) [$M^{+\bullet}$], 245 (35), 207 (80), 144 (90).

Column chromatography using silica gel (EA/PE 3:97) gave 1-methylindole **3.57** (0.091 g, 23 % based on starting weight of 1-methylindole **3.57**) and an inseparable mixture of 1-methylindole **3.57** and 1,3-dimethyl-1*H*-indole **3.58** (0.073 g, 50 % based on **4.16**) in a ratio of 1.00:0.45 (by ^{1}H NMR). Data were consistent with data reported for 1-methylindole **3.57** in experiment 5.4 and 1,3-dimethyl-1*H*-indole **3.58** in experiment 5.2.

EXPERIMENT 5.11: Reactivity of 2-DMAP Disalt 4.16 in Chlorobenzene

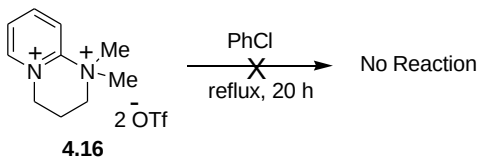

4.16

2-DMAP Disalt **4.16** (0.231 g, 0.5 mmol, 1.0 eq) was refluxed in chlorobenzene (5 mL) for 20 h. GC-MS analysis of the solution showed no evidence of reaction of the chlorobenzene; RT 5.93 min *m*/*z* (EI) 112 (100), [$M^{+\bullet}$], 77 (20).

EXPERIMENT 5.12: Reaction of 1-Methylindole 3.57 and 2-DMAP Disalt 4.16 in Chlorobenzene

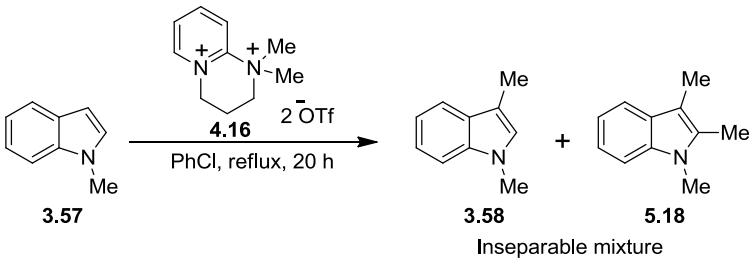

1-Methylindole **3.57** (0.131 g, 1.0 mmol, 1.0 eq) was added to a solution of 2-DMAP disalt **4.16** (0.462 g, 1.0 mmol, 1.0 eq) in distilled chlorobenzene (5 mL) under argon. The reaction mixture was heated at reflux for 20 h. The solvent was removed by column chromatography using silica gel, eluting with petroleum ether until no solvent remained. The reaction products were then eluted using EA/PE (1:20 – 1:4) to give an orange oil (0.006 g), as an inseparable mixture. Spectroscopic analysis showed a mixture of two major products, identified as 1,3-dimethyl-1*H*-indole **3.58** and 1,2,3-trimethyl-1*H*-indole **5.18** (in a ratio of ~3:1) by ^{1}H NMR and GC-MS analysis.

^{1}H NMR (400 MHz, $CDCl_3$) δ= 2.29 (3H, s, CH_3, **5.18**), 2.36 (3H, s, CH_3, **3.58**), 2.38 (3H, s, CH_3, **5.18**), 3.67 (3H, s, CH_3, **5.18**), 3.76 (3H, s, CH_3, **3.58**), 6.85 (1H, s, ArH, **3.58**), 7.08-7.32 (4H, m, ArH, **3.58** and **5.18**), 7.52 (1H, d, *J*(H,H)= 7.8 Hz, ArH, **5.18**), 7.60 (1H, d, *J*(H,H)= 7.9 Hz, ArH, **3.58**); GC-MS: RT 10.39 min *m*/*z* 145 (100) [$M^{+\bullet}$], 144 (90); RT 11.51 min *m*/*z* 159 (100) [$M^{+\bullet}$], 158 (70), 144 (20).

EXPERIMENT 5.13: Reaction of 2-DMAP Disalt 4.16 and *N*,*N*-Di-*iso*-propyl-ethylamine 5.21

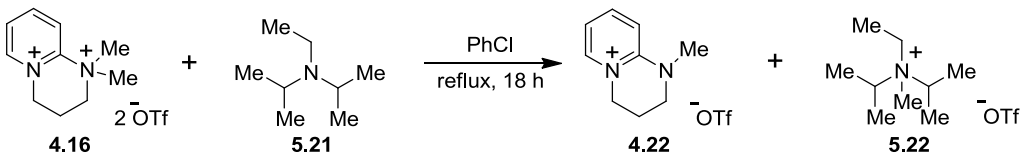

A solution of 2-DMAP disalt **4.16** (0.092 g, 0.2 mmol, 1.0 eq) and *N*,*N*-di-*iso*-propylethylamine **5.21** (0.026 g, 0.2 mmol, 1.0 eq) in distilled chlorobenzene (4 mL) was heated at reflux under argon for 18 h. The reaction mixture was cooled to r.t. and a sample was removed for MS analysis. The analysis showed peaks at *m*/*z* of 149,

144 and 130, consistent with formation of 1-methyl-1,2,3,4-tetrahydro-pyrido[1,2-α]pyrimidin-5-ylium trifluoromethanesulfonate **4.22**, ethyldi-iso-propyl-methyl-ammonium trifluoromethanesulfonate **5.22** and *N*,*N*-di-*iso*-propylethylamine **5.21** respectively. No isolation of the reaction products was attempted.

EXPERIMENT 5.14: Attempted Reaction of 2-DMAP Disalt 4.16 and 2,6-Di-*tert*-butylpyridine 5.23

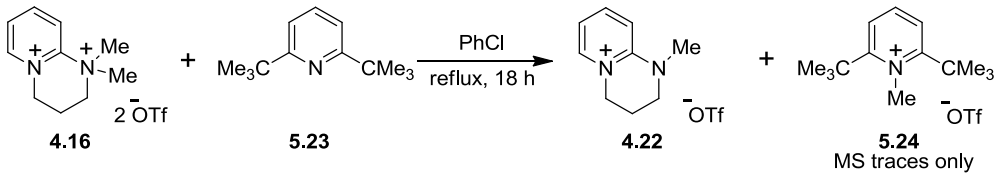

A solution of 2-DMAP disalt **4.16** (0.231 g, 0.5 mmol, 1.0 eq) and 2,6-di-*tert*-butylpyridine **5.23** (0.11 mL, 0.5 mmol, 1.0 eq) in distilled chlorobenzene (5 mL) was heated at reflux under argon for 18 h. MS analysis of the reaction mixture gave major peaks at *m*/*z* 192 and 149 for 2,6-di-tert-butylpyridine **5.23** and 1-methyl-1,2,3,4-tetrahydropyrido[1,2-α]pyrimidin-5-ylium **4.22**. A small peak at *m*/*z* 206 for 2,6-di-*tert*-butyl-1-methylpyridinium trifluoromethanesulfonate **5.24** were observed. The reaction mixture was cooled to r.t., diethyl ether (20 mL) was added and the reaction mixture was stirred for 30 min. The ether was decanted and the residue was collected. ^{1}H NMR analysis showed no evidence of 2,6-di-*tert*-butyl-1-methylpyridinium trifluoromethanesulfonate **5.24**, showing only 1-methyl-1,2,3,4-tetrahydropyrido[1,2-α]pyrimidin-5-ylium trifluoromethanesulfonate **4.22**.

EXPERIMENT 5.15: Methylation of 1-Methylindole 3.57 with 2,6-Di-*tert*-butylpyridine 5.23 Additive under Different Conditions

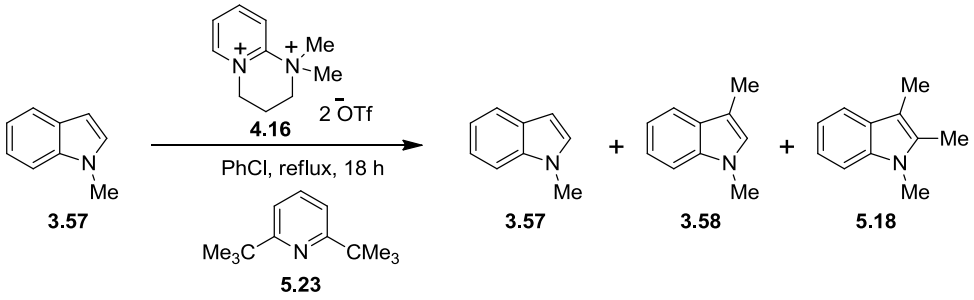

A solution of 2-DMAP disalt **4.16** (1.0-3.0 eq), 1-methylindole **3.57** (0.066 g, 0.5 mmol, 1.0 eq) and 2,6-di-*tert*-butylpyridine **5.23** (0.11 mL, 0.5 mmol, 1.0 eq) in distilled chlorobenzene (see Table 5.1 for volumes) was heated at reflux under argon for 18 h. The reaction mixture was cooled to r.t. Purification by column chromatography using silica gel (EA/PE 1:9) gave a mixture of 1-methylindole **3.57** and 1,3-dimethyl-1*H*-indole **3.58** (and 1,2,3-trimethyl-1*H*-indole **5.18** in some cases) as a colourless oil that could not be separated. Products were identified by ^{1}H NMR and GC-MS analysis and were consistent with that reported for 1-methylindole **3.57** in experiment 5.2, 1,3-dimethyl-1*H*-indole **3.58** in experiment 5.1 and 1,2,3-trimethyl-1*H*-indole **5.18** in experiment 5.10.

TABLE 5.1: Results for the reaction of 2-DMAP disalt **4.16** and 1-methylindole **3.57**.

Entry	**Eq of 4.16**	**Volume PhCl / mL**	**Mass Recovery Organics[a] / %**	**^{1}H NMR Ratios / %**		
				3.57[b]	**3.58[c]**	**5.18[d]**
1	1.0	5	88	70	30	-
2	3.0	20	82	42	49	9
3	3.0	15	72	39	54	7

[a] Yield based in 1-methylindole **3.57** as product. [b] ^{1}H NMR signal at $\delta_H(CDCl_3)$ 3.86 ppm used for ratio. [c] ^{1}H NMR signal at $\delta_H(CDCl_3)$ 3.79 ppm used for ratio. [d] ^{1}H NMR signal at $\delta_H(CDCl_3)$ 3.67 ppm used for ratio.

EXPERIMENT 5.16: Trimethylpyridin-2-ylammonium Trifluoromethane-sulfonate 1.169

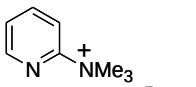

1.169 63%

Methyl trifluoromethanesulfonate (0.47 mL, 5.0 mmol, 1.0 eq) was added dropwise to a solution of 2-DMAP **1.1** (0.62 mL, 5.0 mmol, 1.0 eq) in dry DCM (1 mL) under argon at –78 °C. The reaction mixture was warmed to r.t. and stirred for 18 h. Dry toluene (2 mL) was added to the reaction mixture and stirred for 30 min. The toluene was decanted and the white solid was washed with toluene (2 mL). The white solid

was collected and the solvent was removed *in vacuo*. The reaction mixture was recrystallised from ethanol/diethyl ether to give trimethylpyridin-2-ylammonium trifluoromethanesulfonate **1.169** (0.906 g, 63 %) as white needles; mp 109-110 ºC; ^{1}H NMR (400 MHz, CD_3CN) δ= 3.58 (9H, s, CH_3), 7.72 (1H, ddd, *J*(H,H)= 7.3, 4.7, 1.0 Hz, ArH), 8.08 (1H, dd, *J*(H,H)= 8.5, 0.7 Hz, ArH), 8.23 (1H, ddd, *J*(H,H)= 8.5, 7.3, 1.8 Hz, ArH), 8.67 (1H, ddd, *J*(H,H)= 4.7, 1.8, 0.7, ArH); ^{13}C NMR (100 MHz, d_6-DMSO) δ= 54.5 (CH_3), 115.2 (CH), 120.7 (q, *J*(C,F)= 319 Hz, CF_3) 126.3 (CH), 141.1 (CH), 148.7 (CH), 156.8 (C); IR (KBr disc) $\tilde{\nu}$= 3128, 3076, 3042, 2973, 1600, 1576, 1497, 1474, 1439, 1265, 1165, 1029, 997, 847, 790, 745, 638, 574, 519; MS (ESI) 137 (100) $[M\text{-}OTf]^+$; HRMS: *m*/*z* calcd for $C_8H_{13}N_2$ $[M\text{-}OTf]^+$: 137.1073; found: 137.1075.

EXPERIMENT 5.17: 2-Bromo-1-methylpyridinium Trifluoromethanesulfonate 5.25

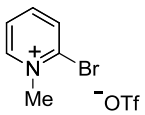

5.25 81%

Methyl trifluoromethanesulfonate (1.58 mL, 13.9 mmol, 1.1 eq) was added dropwise to a solution of 2-bromopyridine **1.171b** (1.21 mL, 12.7 mmol, 1.0 eq) in dry diethyl ether (10 mL) under argon at r.t. The reaction mixture was stirred for 1 h and the white precipitate formed was collected and the solvent was removed *in vacuo* to give 2-bromo-1-methylpyridinium trifluoromethanesulfonate **5.25** (3.29 g, 81 %) as a white solid; mp 164-166 ºC; ^{1}H NMR (400 MHz, CD_3CN) δ= 4.34 (3H, s, NCH_3), 7.97 (1H, ddd, *J*(H,H)= 8.1, 5.4, 1.8 Hz, ArH), 8.28-8.35 (2H, m, ArH), 8.83 (1H, dd, *J*(H,H)= 6.6, 0.9 Hz, ArH); ^{13}C NMR (100 MHz, CD_3CN) δ= 51.7 (CH_3), 122.2 (q, *J*(C,F)= 321 Hz, CF_3), 128.0 (CH), 135.1 (CH), 140.3 (C), 147.5 (CH), 149.5 (CH); IR (KBr disc) $\tilde{\nu}$= 3122, 3098, 3079, 2290, 1867, 1616, 1493, 1455, 1438, 1263, 1227, 1181, 1154, 1140, 1100, 1031, 801, 755, 691, 639, 573, 518; MS (ESI) 174 (95) $[M(^{81}Br)\text{-}OTf]^+$, 172 (100) $[M(^{79}Br)\text{-}OTf]^+$; HRMS: *m*/*z* calcd. for $C_6H_7Br_1N_1$ $[M(^{79}Br)\text{-}OTf]^+$: 171.9756; found: 171.9755.

EXPERIMENT 5.18: 2-Dimethylamino-1-methylpyridinium Trifluoromethanesulfonate 1.170

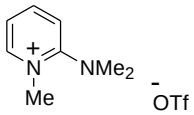

1.170 100%

Dimethylamine solution (40 % in water, 0.83 mL, 6.6 mmol, 2.2 eq) was added to a solution of 2-bromo-1-methylpyridinium trifluoromethanesulfonate **5.25** (0.966 g, 3.0 mmol, 1.0 eq) in acetonitrile (5 mL) and stirred at r.t. for 1 h. The reaction mixture was filtered through a plug of potassium carbonate, which was then washed with acetonitrile (20 mL). The solvent was removed *in vacuo* to give 2-dimethylamino-1-methylpyridinium trifluoromethanesulfonate **1.170** (0.856 g, 100 %) as a yellow oil**;** ^{1}H NMR (500 MHz, CD_3CN) δ= 3.08 (6H, s, CH_3), 3.94 (3H, s, CH_3), 7.19 (1H, dd, J(H,H)= 7.0, 6.8 Hz, ArH), 7.39 (1H, d, J(H,H)= 9.3 Hz, ArH), 8.03-8.08 (2H, m, ArH); ^{13}C NMR (125 MHz, d_6-DMSO) δ= 42.3 (CH_3), 44.5 (CH_3), 116.8 (CH), 118.0 (CH), 120.7 (q, J(C,F)= 323 Hz, CF_3), 143.5 (CH), 144.1 (CH), 158.9 (C); IR (thin film) $\tilde{\nu}$= 3574, 3100, 3078, 2966, 2923, 1640, 1576, 1538, 1435, 1264, 1225, 1153, 1031, 957, 777, 638, 573, 518; MS (ESI) 137 (100) $[M\text{-}OTf]^+$; HRMS: m/z calcd for $C_8H_{13}N_2$ $[M\text{-}OTf]^+$: 137.1075; found: 137.1075.

EXPERIMENT 5.19: Reaction of Pyridine Salts 1.169, 1.170 and 4.16 with Triphenylphosphine 5.26 in Acetonitrile.

In the typical procedure, a solution of pyridine salt (0.5 mmol, 1.0 eq) and triphenylphosphine **5.26** (0.131 g, 0.5 mmol, 1.0 eq) in dry acetonitrile (0.5 mL) was stirred at r.t. under argon for 18 h. Diethyl ether (2 mL) was added. The ether-soluble products were separated from the ether-insoluble products. The ether-insoluble products were purified by column chromatography using silica gel (CH_3CN/DCM 1:1) if necessary.

(a) Using the typical procedure, no reaction between trimethylpyridin-2-ylammonium trifluoromethanesulfonate **1.169** and triphenylphosphine **5.26** occurred. Trimethylpyridin-2-ylammonium trifluoromethanesulfonate **1.169** (0.138 g, 98 %)

was recovered as a white solid and triphenylphosphine **5.26** (0.138 g, 96 %) was recovered as a white solid. Data was consistent with trimethylpyridin-2-ylammonium trifluoromethanesulfonate **1.169** reported in experiment 5.14.

(b) Using the typical procedure, no reaction between 2-dimethylamino-1-methylpyridinium trifluoromethanesulfonate **1.170** and triphenylphosphine **5.26** occurred. 2-Dimethylamino-1-methylpyridinium trifluoromethanesulfonate **1.170** (0.121 g, 84 %) was recovered as a yellow oil and triphenylphosphine **5.26** (0.117 g, 90 %) was recovered as a white solid. Data were consistent with 2-dimethylamino-1-methylpyridinium trifluoromethanesulfonate **1.170** reported in experiment 5.22.

(c) Reaction of 2-DMAP Disalt **4.16** and Triphenylphosphine **5.26**

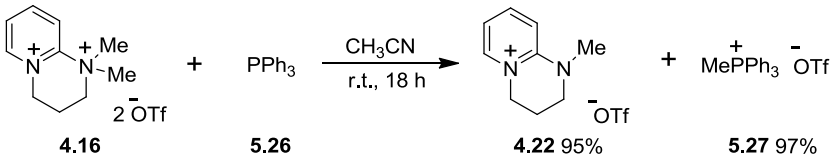

4.16 **5.26** **4.22** 95% **5.27** 97%

Reaction of 2-DMAP disalt **4.16** and triphenylphosphine **5.27** using the above general procedure gave methyltriphenylphosphonium trifluoromethanesulfonate **5.27** (0.208 g, 97 %) as a white solid and 1-methyl-1,2,3,4-tetrahydropyrido[1,2-α]-pyrimidin-5-ylium trifluoromethanesulfonate **4.22** (0.142 g, 95 %) as a white solid.

1-Methyl-1,2,3,4-tetrahydropyrido[1,2-α]pyrimidin-5-ylium trifluoromethanesulfonate 4.22; mp 58-61 ºC; ^{1}H NMR (400 MHz, d_6-DMSO) δ= 2.15 (2H, t, J(H,H)= 5.8 Hz, CH_2), 3.16 (3H, s, CH_3), 3.55 (2H, dd, J(H,H)= 5.8, 5.5 Hz, CH_2), 4.27 (2H, t, J(H,H)= 5.5 Hz, CH_2), 6.85 (1H, ddd, J(H,H)= 6.9, 6.8, 1.1 Hz, ArH), 7.19 (1H, dd, J(H,H)= 9.2, 1.6 Hz, ArH), 7.87 (1H, ddd, J(H,H)= 9.2, 6.9, 1.6 Hz, ArH), 7.97 (1H, dd, J(H,H)= 6.8, 1.1 Hz, ArH); ^{13}C NMR (100 MHz, d_6-DMSO) 18.8 (CH_2), 38.7 (CH_3), 48.1 (CH_2), 50.7 (CH_2), 111.6 (CH), 112.5 (CH), 120.7 (q, J(C,F)= 322 Hz, CF_3), 140.4 (CH), 142.1 (CH), 151.0 (C); IR (KBr disc) $\tilde{\nu}$= 3536, 3097, 3026, 2963, 2293, 1651, 1587, 1552, 1446, 1334, 1263, 1227, 1149, 1032, 881, 774, 757, 714, 639, 573, 517; MS (ESI) 149 (100) $[M\text{-}OTf]^+$, 121 (3); HRMS: m/z calcd for $C_9H_{13}N_2$ $[M\text{-}OTf]^+$: 149.1073; found: 149.1076.

Methyltriphenylphosphonium trifluoromethanesulfonate 5.27: mp 130-132 ºC (lit.[153] 138.5-140 ºC); ^{1}H NMR (400 MHz, d_6-DMSO) δ= 3.14 (3H, d, J(H,P)= 15

Hz, PCH_3), 7.73-7.78 (12H, m, ArH), 7.87-7.91 (3H, m, ArH); ^{13}C NMR (100 MHz, d_6-DMSO) δ= 7.1 (d, J(C,P)= 55.4 Hz, PCH_3), 120.1 (d, J(C,P)= 88.2 Hz, PC), 130.1 (d, J(C,P)= 12.7 Hz, CH), 133.2 (d, J(C,P)= 10.8 Hz, CH), 134.8 (d, J(C,P)= 3.0 Hz, CH); IR (KBr disc) $\tilde{\nu}$= 3065, 2990, 2917, 1589, 1486, 1440, 1560, 1224, 1151, 1117, 1030, 909, 784, 753, 744, 720, 690, 637, 572, 514, 501; MS (ESI) 277 (100) $[M\text{-}OTf]^+$; HRMS: *m*/*z* calcd for $C_{19}H_{18}P_1$ $[M\text{-}OTf]^+$: 277.1141; found: 277.1137.

EXPERIMENT 5.20: Reaction of Pyridine Salts 1.169, 1.170 and 4.16 with Triphenylphosphine 5.26 in Chlorobenzene

In the typical procedure, a solution of pyridine salt (0.5 mmol, 1.0 eq) and triphenylphosphine **5.26** (0.131 g, 0.5 mmol, 1.0 eq) in dry chlorobenzene (0.5 mL) was heated at reflux under argon for 18 h. The reaction was cooled to r.t. and diethyl ether (2 mL) was added. The ether-soluble products were separated from the ether-insoluble products. The ether-insoluble products were purified by column chromatography using silica gel (CH_3CN/DCM 1:1) if necessary. Any ether-soluble products were purified by column chromatography using silica gel (EA/PE 1:9) if necessary.

(a) Reaction of trimethylpyridin-2-ylammonium trifluoromethanesulfonate **1.169** and triphenylphosphine **5.26** using the above general procedure gave methyltriphenyl-phosphonium trifluoromethanesulfonate **5.27** (0.112 g, 52 %) as a white solid and trimethylpyridin-2-ylammonium trifluoromethanesulfonate **1.169** (0.041 g, 29 %) as a white solid. Purification of the ether-soluble products gave 2-DMAP **1.1** (0.005 g, 9 %) as a colourless oil and triphenylphosphine **5.26** (0.039 g, 29 %) as a white solid. Data were consistent with that reported for trimethylpyridin-2-ylammonium trifluoromethanesulfonate **1.169** reported in experiment 5.14 and methyltriphenyl-phosphonium trifluoromethanesulfonate **5.27** in experiment 5.23(c).

(b) Using the typical procedure, no reaction between 2-dimethylamino-1-methyl-pyridinium trifluoromethanesulfonate **1.170** and triphenylphosphine **5.26** occurred. Salt **1.170** (0.095 g, 67 %) was recovered as a yellow oil and triphenylphosphine **5.26** (0.131 g, 100 %) was recovered as a white solid. Data were consistent with that

reported for 2-dimethylamino-1-methylpyridinium trifluoromethanesulfonate **1.170** in experiment 5.22.

(c) Reaction of 2-DMAP disalt **4.16** and triphenylphosphine **5.26** using the above general procedure gave methyltriphenylphosphonium trifluoromethanesulfonate **5.27** (0.203 g, 95 %) as a white solid and 1-methyl-1,2,3,4-tetrahydropyrido[1,2-α]-pyrimidin-5-ylium trifluoromethanesulfonate **4.22** (0.137 g, 92 %) as a white solid. Data were consistent for 1-methyl-1,2,3,4-tetrahydropyrido[1,2-α]-pyrimidin-5-ylium trifluoromethanesulfonate **4.22** and methyltriphenylphosphonium trifluoro-methanesulfonate **5.27** reported in experiment 5.23(c).

EXPERIMENT 5.21: Procedure for Competitive Methylation Reactions

A solution of 2-DMAP disalt **4.16** (0.023 g, 0.05 mmol, 1.0 eq) [or disalt **4.30** (0.023 g, 0.05 mmol, 1.0 eq)], methylating reagent (0.05 mmol, 1.0 eq) and 1,3,5,7-cyclooctatetraene **5.29** (0.006 mL, 0.05 mmol, 1.0 eq) in CD_3CN (0.75 mL) was prepared in an oven-dried NMR tube. NMR ratios of the methyl protons for each methylating reagent were obtained relative to cyclooctatetraene **5.28** (set to 1.000). Triethylamine **5.28** (0.007 mL, 0.05 mmol, 1.0 eq) was added to the sealed NMR tube which was thoroughly shaken. After 5 min to ensure complete reaction, a second NMR spectrum was recorded. The NMR ratios of the methyl protons for each methylating reagent were again obtained, relative to cyclooctatetraene **5.29** (set to 1.000).

Entry	Disalt Used	Methylating Reagent (MR)	Starting		Finishing		Amount Remaining[a]	
			MR	Disalt	MR	Disalt	MR	Disalt
1	**4.16**[b]	MeI[c]	0.428	0.804	0.433	0.000	100	0
2	**4.16**[b]	Me_2SO_4[d]	0.796	0.768	0.470	0.470	59	53
3	**4.16**[b]	MeOTf[e]	0.274	0.841	0.000	0.794	0	94
4	**4.30**[f]	Me_2SO_4[d]	1.130	1.220	0.7883	0.286	70	23

[a] All proton signal integrations were taken relative to 1,3,5,7-cyclooctatetraene **5.29** $\delta_H(CD_3CN)$ 5.77 ppm set at 1.000. All experiments were carried out in CD_3CN. Amount remaining calculated from finishing proton integration as a percentage of starting proton integration. [b] Proton signal for Me groups at $\delta_H(CD_3CN)$ 3.84 ppm used. [c] Proton signal for Me group at $\delta_H(CD_3CN)$ 2.09 ppm used. [d] Proton signal for Me groups at $\delta_H(CD_3CN)$ 3.94 ppm used. [e] Proton signal for Me group at $\delta_H(CD_3CN)$ 4.27 ppm used. [f] Proton signal for Me groups at $\delta_H(CD_3CN)$ 3.85 ppm used.

EXPERIMENT 5.22: Kinetic Study on Reaction of 2-DMAP Disalt 4.16 and *N*,*N*-Di-iso-propylethylamine 5.21

A solution of 2-DMAP disalt **4.16** (0.023 g, 0.05 mmol, 1.0 eq) in CD_3CN (0.75 mL) was prepared in an oven-dried NMR tube in a glovebox. The NMR tube was sealed with an NMR tube suba seal cap and parafilm. The tube was removed from the glovebox and 1,3,5,7-cyclooctatetraene **5.29** (0.006 mL, 0.05 mmol, 1.0 eq) was injected into the solution and the tube was thoroughly shaken. An NMR spectrum of the initial concentration of disalt **4.16** was recorded at 300 K. *N*,*N*-Di-*iso*-propylethylamine **5.21** (0.009 mL, 0.05 mmol, 1.0 eq) was injected into the NMR tube and the tube was thoroughly shaken. A 16 scan proton spectrum was recorded at 300 K in order to obtain the receiver gain value for the kinetic run. Once obtained, a 16 scan proton spectrum was recorded at 300 K every 15 min for a period of 6 h. The progress of the reaction was monitored by comparing the integration values of the aromatic protons with 1,3,5,7-cyclooctatetraene **5.29**.

EXPERIMENT 5.23: 1-(3-Dimethylammoniumpropyl)-2-hydroxypyridinium Trifluoromethanesulfonate 5.32

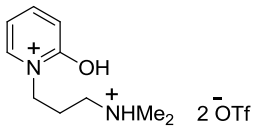

5.32 91%

2-DMAP disalt **4.16** (0.462 g, 1.0 mmol, 1.0 eq) was stirred in water (10 mL) at r.t. for 6 days. The solvent was removed *in vacuo* to give 1-(3-dimethyl-ammoniumpropyl)-2-hydroxypyridinium trifluoromethanesulfonate **5.32** (0.437 g, 91 %) as a white solid; mp 60-62 °C; ^{1}H NMR (400 MHz, CD_3CN) δ= 2.23-2.31 (2H, m, CH_2-CH_2-CH_2), 2.82 (6H, d, J(H,H)= 5.2 Hz, HN-CH_3), 3.14-3.19 (2H, m, N-CH_2), 4.36 (2H, t, J(H,H)= 7.2 Hz, N-CH_2), 7.35 (1H, ddd, J(H,H)= 7.4, 6.5, 1.1 Hz, ArH), 7.45 (1H, bs, NH or OH), 7.46 (1H, d, J(H,H)= 8.7 Hz, ArH), 8.15 (1H, dd, J(H,H)= 6.5, 1.6 Hz, ArH), 8.23 (1H, ddd, J(H,H)= 8.7, 7.4, 1.6 Hz, ArH); ^{13}C NMR (100 MHz, CD_3CN) δ= 24.9 (CH_2), 44.3 (CH_3), 51.6 (CH_2), 55.6 (CH_2), 116.3 (CH), 119.3 (CH), 142.4 (CH), 148.5 (CH), 161.3 (C); IR (KBr disc) $\tilde{\nu}$= 3501, 3100, 2793, 1646, 1596, 1524, 1476, 1278, 1250, 1030, 777, 639, 576, 518, 459; MS (ESI) 181 (100) $[M\text{-}H\text{-}2OTf]^+$, 149 (4), 136 (36); 108 (3). The product was too unstable to obtain a HRMS spectrum. Crystallographic data for 1-(3-dimethyl-ammoniumpropyl)-2-hydroxypyridinium trifluoromethanesulfonate **5.28** is given in Appendix 3.

EXPERIMENT 5.24: Dimethyl-[3-(oxo-2*H*-pyridin-1-yl)propyl]ammonium Trifluoromethanesulfonate 5.31

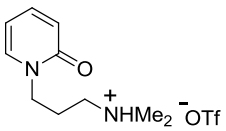

5.31

A solution of 1-(3-dimethylammoniumpropyl)-2-hydroxypyridinium trifluoro-methanesulfonate **5.32** in CD_3CN or d_6-DMSO, over several days or instantly respectively, was converted to dimethyl-[3-(2-oxo-2*H*-pyridin-1-yl)propyl]-ammonium trifluoromethanesulfonate **5.31**. The solvent was removed *in vacuo* for characterisation; ^{1}H NMR (400 MHz, d_6-DMSO) δ= 2.04 (2H, tt, J(H,H)= 9.0, 7.0

Hz, CH_2-C*H*$_2$-CH_2), 2.78 (6H, d, *J*(H,H)= 5.0 Hz, HN-C*H*$_3$), 3.03-3.08 (2H, m, N-C*H*$_2$), 3.93 (2H, t, *J*(H,H)= 7.0 Hz, N-C*H*$_2$), 6.28 (1H, ddd, *J*(H,H)= 6.7, 6.6, 1.4 Hz, 5-H), 6.43 (1H, dd, *J*(H,H)= 9.1, 1.4 Hz, 3-H), 7.45 (1H, ddd, *J*(H,H)= 9.1, 6.6, 2.1 Hz, 4-H), 7.68 (1H, dd, *J*(H,H)= 6.7, 2.1 Hz, 6-H), 9.21 (1H, bs, NH); ^{13}C NMR (100 MHz, d_6-DMSO) δ= 24.2 (CH_2), 42.4 (CH_3), 45.7 (CH_2), 54.2 (CH_2), 106.1 (CH), 119.6 (CH), 120.7 (q, *J*(C,F)= 322 Hz, CF_3), 139.0 (CH), 140.4 (CH), 161.8 (CO); IR (thin film) $\tilde{\nu}$= 3445 (bs), 2720, 1657, 1574, 1542, 1471, 1260, 1226, 1165, 1031, 1001, 827, 766, 641, 573, 518; MS (ESI) 215 (9), 192 (12), 181 (100) $[M\text{-}OTf]^+$, 149 (15), 136 (78), 85 (8); HRMS: *m*/*z* calcd for $C_{10}H_{17}N_2O_1$ $[M\text{-}OTf]^+$: 181.1335; found: 181.1332.

EXPERIMENT 5.25: 1-(2-Dimethylaminopropyl)-1*H*-pyridin-2-one 5.33

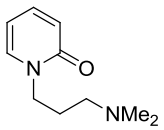

5.33 26%

2-DMAP disalt **4.16** (0.462 g, 1.0 mmol, 1.0 eq) was stirred in saturated NaOH solution (10 mL) for 18 h. The reaction mixture was extracted with diethyl ether (2 x 15 mL), and the ether was washed with brine (2 x 10 mL), dried over anhydrous Na_2SO_4 and the solvent was removed *in vacuo* to give 1-(2-dimethylaminopropyl)-1*H*-pyridin-2-one **5.33** (0.047 g, 26 %) as a brown oil; ^{1}H NMR (500 MHz, d_6-DMSO) δ= 1.79 (2H, tt, *J*(H,H)= 7.2, 7.1 Hz, CH_2), 2.24 (6H, s, NCH_3), 2.34 (2H, t, *J*(H,H)= 7.1 Hz, CH_2), 3.88 (2H, t, *J*(H,H)= 7.2 Hz, CH_2), 6.21 (1H, ddd, *J*(H,H)= 6.7, 6.6, 1.3 Hz, 5-H), 6.36 (1H, dd, *J*(H,H)= 9.1, 0.6 Hz, 3-H), 7.40 (1H, ddd, *J*(H,H)= 9.1, 6.6, 2.1 Hz, 4-H), 7.64 (1H, dd, *J*(H,H)= 6.7, 2.1 Hz, 6-H); ^{13}C NMR (125 MHz, d_6-DMSO) δ= 25.9 (CH_2), 44.3 (CH_3), 46.6 (CH_2), 55.4 (CH_2), 105.2 (CH), 119.6 (CH), 139.2 (CH), 139.8 (CH), 161.4 (CO); IR (thin film) $\tilde{\nu}$= 3460 (bs), 2945, 2863, 2824, 2780, 1652, 1575, 1539, 1469, 1255, 1226, 1162, 1031, 775, 640, 575, 519; MS (ESI) 181 (100) $[M+H]^+$, 149 (30), 136 (50), 121 (6); HRMS: *m*/*z* calcd for $C_{10}H_{17}N_2O_1$ $[M+H]^+$: 181.1335; found: 181.1332.

EXPERIMENT 5.26: Conversion of Dimethyl-(3-oxo-2*H*-pyridin-1-yl)propyl)-ammonium Trifluoromethanesulfonate 5.31 to 1-(2-Dimethylaminopropyl)-1*H*-pyridin-2-one 5.33

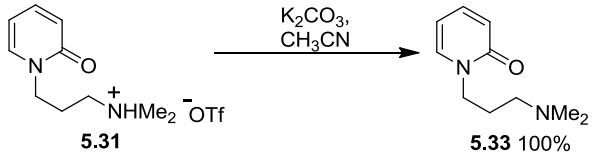

Potassium carbonate (0.138 g, 1.0 mmol, 2.0 eq) was added to a tube containing dimethyl-(3-oxo-2*H*-pyridin-1-yl)propyl)ammonium trifluoromethanesulfonate **5.31** (0.165 g, 0.5 mmol, 1.0 eq) in acetonitrile (0.5 mL). The reaction mixture was stirred for 1 h, then filtered, the residue was washed with acetonitrile (2 mL) and the solvent was removed *in vacuo* to give 1-(2-dimethylaminopropyl)-1*H*-pyridin-2-one **5.33** (0.089 g, 100 %) as a brown oil. Data were consistent with that reported in experiment 5.30.

EXPERIMENT 5.27: 1-(3-Dimethylammoniumpropyl)-2-hydroxypyrimidinium Trifluoromethanesulfonate 4.34

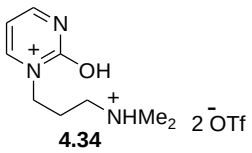

A sample of 2-dimethylaminopyrimidine disalt **4.30** was added to an ampule of d_6-DMSO, whereupon it was immediately converted to 1-(3-dimethylammonium-propyl)-2-hydroxypyrimidinium trifluoromethanesulfonate **4.34** as evidenced by analysis. The solvent was removed *in vacuo* for characterisation; ^{1}H NMR (400 MHz, d_6-DMSO) δ= 2.10 (2H, tt, J(H,H)= 7.6, 7.2 Hz, CH_2), 2.78 (6H, d, J(H,H)= 4.8 Hz, NCH_3), 3.10-3.15 (2H, m, CH_2), 4.07 (2H, t, J(H,H)= 7.2 Hz, CH_2), 6.91 (1H, dd, J(H,H)= 6.0, 6.0 Hz, ArH), 8.83 (2H, d, J(H,H)= 5.6 Hz, ArH), 9.25 (1H, bs, NH); ^{13}C NMR (100 MHz, d_6-DMSO) δ= 23.0 (CH_2), 42.4 (CH_3), 48.9 (CH_2), 53.8 (CH_2), 104.4 (CH), 120.7 (q, J(C,F)= 322 Hz, CF_3), 149.6 (C), 158.3 (CH), 160.6 (CH); IR (KBr disc) $\tilde{\nu}$= 3167, 3114, 3044, 2935, 2878, 1748, 1598, 1479, 1446, 1378, 1257, 1227, 1171, 1122, 1099, 1031, 805, 776, 759, 640, 574, 518; MS

(ESI) 182 (100) $[M\text{-}H\text{-}2OTf]^+$, 137 (14); HRMS: *m*/*z* calcd for $C_9H_{16}N_3O_1$ $[M\text{-}H\text{-}(2OTf)]^+$: 182.1288; found: 182.1290.

9.4 Experimental for Chapter 6

General Procedures for Chapter 6

Triethylamine **5.28** was distilled from CaH_2 under argon. Dimethyl sulfate was distilled from 4 Å molecular sieves under vacuum. All dried reagents were stored under 4 Å molecular sieves once distilled.

EXPERIMENT 6.1: Attempted Synthesis of 2-Bromo-1-methylpyridinium Iodide 6.7

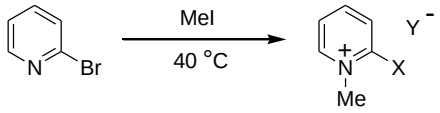

1.171b **6.7** X = I, Br; Y = I, Br

A mixture of 2-bromopyridine **1.171b** (0.95 mL, 10 mmol, 1.0 eq) and iodomethane (0.75 mL, 12 mmol, 1.2 eq) was heated at 40 °C in a sealed tube for 16 h. The reaction mixture was cooled to r.t. and dry diethyl ether (10 mL) was added and the mixture was stirred for 1.5 h. The resulting orange solid was collected and the solvent was removed *in vacuo* to give a mixture of salts (1.77 g, 59 % based on X = Br, Y = I) in a ratio of 1.0:0.8 for X = I:X = Br by ^{1}H NMR.

^{1}H NMR (400 MHz, d_6-DMSO) δ= 4.36 (3H, s, CH_3, X = Br), 4.40 (3H, s, CH_3, X = I), 8.05 (1H, ddd, *J*(H,H)= 7.5, 6.2, 1.5 Hz, ArH, X = I), 8.10-8.16 (2H, m, ArH, X = I and X = Br), 8.44 (1H, ddd, *J*(H,H)= 8.0, 7.8, 1.6 Hz, ArH, X = Br), 8.51 (1H, dd, *J*(H,H)= 8.2, 1.4 Hz, ArH, X = Br), 8.62 (1H, dd, *J*(H,H)= 8.0, 1.3 Hz, ArH, X= I), 9.23-9.26 (2H, m, ArH, X = I and X = Br); ^{13}C NMR (100 MHz, d_6-DMSO) δ= 50.3 (CH_3), 54.6 (CH_3), 124.7 (C), 126.5 (CH), 126.6 (CH), 133.4 (CH), 139.5 (C), 139.9 (CH), 144.2 (CH), 146.0 (CH), 148.0 (CH), 148.6 (CH).

EXPERIMENT 6.2: Attempted Synthesis of 1-Methyl-2-(methylpyridin-2-ylamino)pyridinium Iodide/Bromide

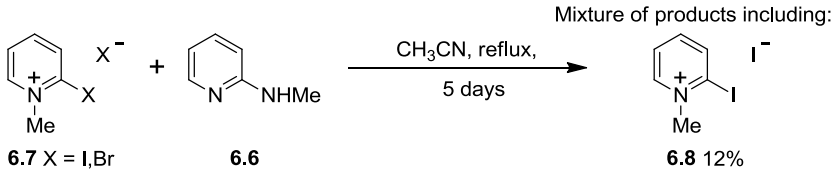

6.7 X = I,Br **6.6** **6.8** 12%

2-Methylaminopyridine **6.6** (0.119 g, 1.1 mmol, 1.1 eq) was added to a suspension of 2-bromo/2-iodo-1-methylpyridinium bromide/iodide **6.7** (0.300 g, ~1.0 mmol, ~ 1.0 eq) in dry acetonitrile (8 mL) and stirred at r.t. under argon. After 18 h, ^{1}H NMR analysis of the reaction mixture showed no reaction had occurred. The reaction mixture was heated at reflux for 5 days. The reaction mixture was filtered through a plug of potassium carbonate, which was then washed with acetonitrile (20 mL). The washings were combined and the solvent was removed *in vacuo*. The residue was washed with diethyl ether (10 mL) and the solvent was removed *in vacuo* to give an orange solid (0.184 g).

Recrystallisation from warm ethanol gave 2-iodo-1-methylpyridinium iodide **6.8** (0.041 g, 12 %) as an orange solid. No other products could be isolated by recrystallisation.

2-Iodo-1-methylpyridinium iodide 6.8; mp 190-191 °C; ^{1}H NMR (400 MHz, d_6-DMSO) δ= 4.40 (3H, s, CH_3), 8.07 (1H, ddd, J(H,H)= 7.7, 6.1, 1.6 Hz, ArH), 8.14 (1H, ddd, J(H,H)= 7.8, 7.7, 1.6 Hz, ArH), 8.66 (1H, dd, J(H,H)= 7.8, 1.5 Hz, ArH), 9.24 (1H, dd, J(H,H)= 6.1, 1.5 Hz, ArH); ^{13}C NMR (400 MHz, d_6-DMSO) δ= 54.6 (CH_3), 124.7 (C), 126.6 (CH), 139.9 (CH), 144.2 (CH), 146.0 (CH); IR (KBr disc) $\tilde{\nu}$= 3108, 3071, 3051, 3019, 2989, 1609, 1562, 1494, 1451, 1436, 1265, 1176, 1068, 776, 694; MS (ESI) 219 (100) $[M\text{-}I]^+$, 124 (35); MS (ESI, -ive) 127 (100) $[I]^-$; HRMS: m/z calcd for $C_6H_7I_1N_1$ $[M\text{-}I]^+$: 219.9618; found: 219.9619.

EXPERIMENT 6.3: Attempted Synthesis of 1-Methyl-2-(methylpyridin-2-ylamino)pyridinium Iodide/Bromide 6.7 by Palladium Coupling[98,99]

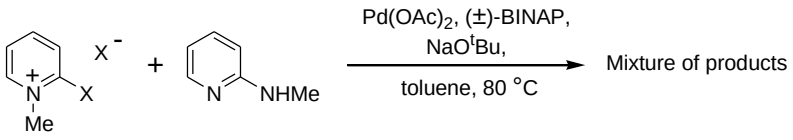

6.7 X = I,Br **6.6**

A suspension of (±)-BINAP (9.3 mg, 0.015 mmol, 15 mol%) in dry toluene (1 mL) was heated at 80 °C until the solid dissolved, then cooled to r.t. and $Pd(OAc)_2$ (2.2 mg, 0.01 mmol, 10 mol%) was added and the mixture was stirred at r.t. 2-Methylaminopyridine **6.6** (0.119 g, 1.2 mmol, 1.2 eq), sodium *tert*-butoxide (0.135 g, 1.4 mmol, 1.4 eq), 2-bromo/2-iodo-1-methylpyridinium bromide/iodide **6.7** (0.300 g, ~1.0 mmol, ~1.0 eq) and dry toluene (2 mL) were then added and the reaction mixture was heated at 80 °C under argon for 22 h. The reaction mixture was cooled to r.t. and the solvent was removed *in vacuo*. The residue was washed with diethyl ether (5 mL). ^{1}H NMR showed a complex mixture of products and MS analysis showed no peaks corresponding to the expected product. Attempts to purify by recrystallisation were unsuccessful. A counterion exchange was attempted to isolate the products; TFA (0.1 mL, 1.5 mmol, 1.5 eq) was added to silver (I) oxide (0.116 g, 0.5 mmol, 0.5 eq) in water (1.0 mL) under argon in a foil-covered flask. The reaction residue in water (1.0 mL) was added dropwise to the TFA/Ag_2O suspension and stirred for 1 h. No precipitate was observed to form. The solvent was removed *in vacuo*. Recrystallisation of the residue was unsuccessful.

EXPERIMENT 6.4 : 2-Chloro-1-methylpyridinium Trifluoromethanesulfonate 6.10[100]

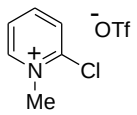

6.10 100%

Methyl trifluoromethanesulfonate (0.6 mL, 5.0 mmol, 1.0 eq) was added dropwise to a solution of 2-chloropyridine **6.9** (0.5 mL, 5.0 mmol, 1.0 eq) in dry DCM (1 mL) at -78 °C under argon. The reaction mixture was warmed to r.t. and stirred for 18 h under argon. Dry toluene (2 mL) was added to the reaction mixture and stirred for 30 min. The solvent was decanted and the residue was washed with dry toluene (2 mL). The solid was collected and the residual solvent was removed *in vacuo* to give 2-chloro-1-methylpyridinium trifluoromethanesulfonate **6.10** (1.38 g, 100 %) as a white solid; mp 156-158 °C (lit.[100] 162-164 °C); ^{1}H NMR (400 MHz, d_6-DMSO) δ= 4.32 (3H, s, CH_3), 8.09 (1H, ddd, J(H,H)= 7.7, 6.2, 1.3 Hz, ArH), 8.37 (1H, dd, J(H,H)= 8.2, 1.3 Hz, ArH), 8.59 (1H, ddd, J(H,H)= 8.2, 7.7, 1.5 Hz, ArH), 9.17 (1H,

dd, *J*(H,H)= 6.2, 1.5 Hz, ArH); ^{13}C NMR (100 MHz, d_6-DMSO) δ= 47.4 (CH_3), 126.1 (CH), 129.5 (CH), 139.9 (C), 147.0 (CH), 148.2 (CH); IR (KBr disc) $\tilde{\nu}$= 3126, 3100, 3061, 1619, 1571, 1497, 1457, 1448, 1264, 1227, 1183, 1160, 1144, 1031, 802, 715, 638, 574, 519; MS (ESI) 130 (40) [M(^{37}Cl)-OTf]$^+$, 128 (100) [M(^{35}Cl)-OTf]$^+$; HRMS: *m*/*z* calcd for $C_6H_7Cl_1N_1$ [M(^{35}Cl)-OTf]$^+$: 128.0262; found: 128.0263.

EXPERIMENT 6.5: Attempted Synthesis of 1-Methyl-2-(methylpyridin-2-ylamino)pyridinium Trifluoromethanesulfonate 6.4 Using 2-Chloro-1-methylpyridinium Trifluoromethanesulfonate 6.10

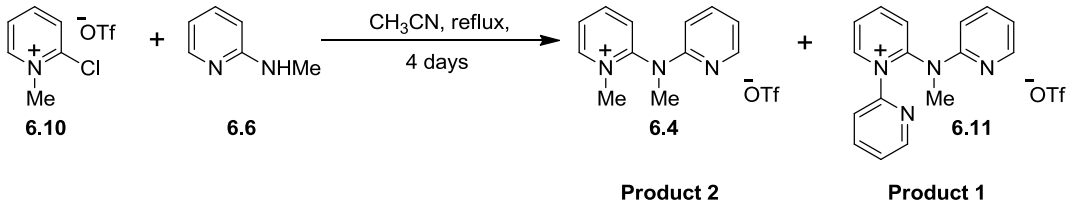

2-Chloro-1-methylpyridinium trifluoromethanesulfonate **6.10** (0.139 g, 0.5 mmol, 1.0 eq) was added to a flask containing 2-methylaminopyridine **6.6** (0.064 g, 0.6 mmol, 1.2 eq) in dry acetonitrile (5 mL) under argon and stirred at r.t. for 18 h. MS analysis of the reaction mixture showed no evidence of 1-methyl-2-(methylpyridin-2-ylamino)pyridinium **6.4** (*m*/*z* = 200). The reaction mixture was heated to reflux for 4 days. ^{1}H NMR analysis showed two major unidentified products. MS analysis of the reaction mixture showed peaks at *m*/*z* = 263, 200 and 128, consistent with **6.11**, **6.4** and **6.10** respectively. Selected ^{1}H NMR peaks are shown below;

Product 1: ^{1}H NMR (400 MHz, d_6-DMSO) δ= 4.33 (3H, s), 6.83 (1H, dd), 7.01 (1H, d), 8.37 (dd), 8.59 (1H, ddd), 9.17 (1H, dd).

Product 2: ^{1}H NMR (400 MHz, d_6-DMSO) δ= 3.96 (3H, s), 7.04 (1H, ddd), 7.17 (1H, d), 8.99 (1H, dd).

EXPERIMENT 5.6: Attempted Synthesis of 1-Methyl-2-(methylpyridin-2-ylamino)pyridinium Trifluoromethanesulfonate 6.4 Using Silver Tetrafluoroborate

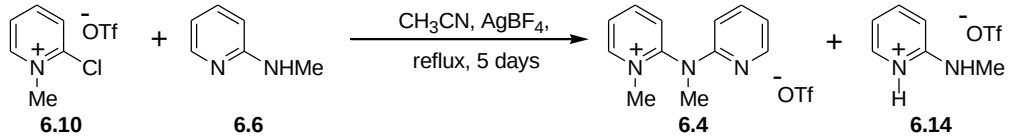

6.10 **6.6** **6.4** **6.14**

2-Chloro-1-methylpyridinium trifluoromethanesulfonate **6.10** (0.139 g, 0.5 mmol, 1.0 eq) was added to a solution of 2-methylaminopyridine **6.6** (0.064 g, 0.6 mmol, 1.2 eq) and silver tetrafluoroborate (0.195 g, 1.0 mmol, 2.0 eq) in dry acetonitrile (10 mL) under argon. The reaction mixture was heated at reflux for 6 days. ^{1}H NMR monitoring of the reaction showed 50 % conversion to 1-methyl-2-(methylpyridin-2-ylamino)pyridinium trifluoromethanesulfonate **6.4** after 5 days, with no further conversion occurring. The reaction mixture was filtered through a plug of potassium carbonate and the solvent was removed *in vacuo*. The residue was stirred in diethyl ether (10 mL) for 1 h. The ether was decanted and the solvent removed from the residue *in vacuo*. MS analysis of the residue showed *m*/*z* = 200, 128, 109, attributed to 1-methyl-2-(methylpyridin-2-ylamino)pyridinium **6.4**, 2-chloro-1-methyl-pyridinium **6.10** and protonated 2-methylaminopyridine **6.14** respectively. ^{1}H NMR signals were consistent with the three products, however, no isolation of the products by recrystallisation was successful.

EXPERIMENT 6.7: 1-Methyl-2-(methylpyridin-2-ylamino)pyridinium Trifluoromethanesulfonate 6.4

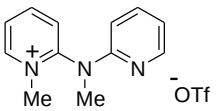

6.4 63%

A solution of 2-chloro-1-methylpyridinium trifluoromethanesulfonate **6.10** (0.139 g, 0.5 mmol, 1.0 eq), 2-methylaminopyridine **6.6** (0.064 g, 0.6 mmol, 1.2 eq), silver tetrafluoroborate (0.195 g, 1.0 mmol, 2.0 eq) and proton sponge (0.535 g, 2.5 mmol, 2.5 eq) in dry acetonitrile (10 mL) was heated at reflux under argon for 5 days. The reaction mixture was cooled to r.t. and filtered through a plug of potassium carbonate. The solvent was removed *in vacuo* and the residue was washed with diethyl ether. The ether-insoluble oil was collected and the solvent was removed *in*

vacuo to give 1-methyl-2-(methylpyridin-2-ylamino)pyridinium trifluoromethane-sulfonate **6.4** (0.110 g, 63 %) as a brown oil; ^{1}H NMR (400 MHz, CD_3CN) δ= 3.52 (3H, s, CH_3), 3.91 (3H, s, CH_3), 7.03 (1H, ddd, *J*(H,H)= 7.4, 5.0, 0.8 Hz, ArH), 7.09 (1H, dd, *J*(H,H)= 8.4, 0.8 Hz, ArH), 7.77 (1H, ddd, *J*(H,H)= 7.4, 6.3, 1.2 Hz, ArH), 7.83 (1H, ddd, *J*(H,H)= 8.4, 7.4, 1.9 Hz, ArH), 7.88 (1H, d, *J*(H,H)= 8.4 Hz, ArH), 8.11 (1H, ddd, *J*(H,H)= 5.0, 1.9, 0.8 Hz, ArH), 8.48 (1H, ddd, *J*(H,H)= 8.4, 7.4, 1.6 Hz, ArH), 8.59 (1H, dd, *J*(H,H)= 6.3, 1.2 Hz, ArH); ^{13}C NMR (100 MHz, CD_3CN) δ= 39.5 (CH_3), 45.4 (CH_3), 111.2 (CH), 119.1 (CH), 122.2 (q, *J*(C,F)= 321 Hz, CF_3), 124.9 (CH), 127.1 (CH), 140.4 (CH), 146.5 (CH), 148.2 (CH), 149.0 (CH), 157.0 (C), 157.6 (C); IR (thin film) $\tilde{\nu}$= 3565, 3097, 1634, 1594, 1578, 1518, 1475, 1435, 1356, 1263, 1225, 1157, 1031, 778, 639, 573, 518; MS (ESI) 200 (100) $[M\text{-}OTf]^+$, 184 (30), 169 (10); MS (ESI, -ve) 149 (100); HRMS: *m*/*z* calcd for $C_{12}H_{14}N_3$ $[M\text{-}OTf]^+$: 200.1182; found: 200.1180.

The reaction was repeated on a larger scale (3.0 mmol) to give 1-methyl-2-(methyl-pyridin-2-ylamino)pyridinium trifluoromethanesulfonate **6.4** (0.615 g, 59 %)

EXPERIMENT 6.8: Attempted Trication Synthesis

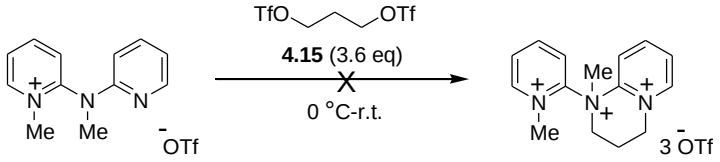

6.4 **6.1**

A solution of 1-methyl-2-(methylpyridin-2-ylamino)pyridinium trifluoromethane-sulfonate **6.4** (0.140 g, 0.4 mmol, 1.0 eq) in dry DCM (0.5 mL) was added dropwise to a tube containing 1,3-*bis*-(trifluoromethanesulfonyloxy)propane **4.15** (0.170 g, 0.5 mmol, 1.2 eq) at 0 °C under argon. After 1 h, the reaction mixture was warmed to r.t. and stirred for 18 h. MS analysis of the reaction mixture showed *m*/*z* of 200 for 1-methyl-2-(methylpyridin-2-ylamino)pyridinium trifluoromethanesulfonate **6.4** only. The reaction mixture was heated at reflux for 5 h. MS analysis of the reaction mixture showed *m*/*z* of 200 for 1-methyl-2-(methylpyridin-2-ylamino)pyridinium trifluoromethane-sulfonate **6.4** only. No formation of the trication was observed.

EXPERIMENT 6.9: *N,N,N',N',N'',N''*-Hexamethyl-[1,3,5]triazine-2,4,6-triamine 6.15[101]

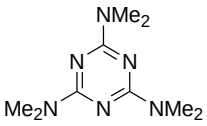

6.15 75%

Cyanuric chloride **6.16** (4.611 g, 25.0 mmol, 1.0 eq), dimethylamine solution (40 % in water, 17.5 mL, 100.0 mmol, 4.0 eq) and crushed 4 Å molecular sieves (0.01 g) were heated to 180 °C in a microwave oven for 5 min. The reaction mixture was dissolved in ethanol and filtered. The filtrate was collected and the solvent removed *in vacuo*. Purification by column chromatography using silica gel (EA/PE 2:3) gave *N*,*N*,*N*',*N*',*N*'',*N*''-hexamethyl-[1,3,5]triazine-2,4,6-triamine **6.15** (3.93 g, 75 %) as a white solid; mp 168-170 °C (lit.[154] 172-174 °C); ^{1}H NMR (400 MHz, $CDCl_3$) δ= 3.12 (18H, s, CH_3); ^{13}C NMR (100 MHz, $CDCl_3$) δ= 36.0 (CH_3), 165.7 (C); IR (KBr disc) $\tilde{\nu}$= 2924, 2864, 2785, 2481, 1528, 1390, 1301, 1211, 1051, 854, 806, 571, 477; MS (ESI) 211 (100) $[M+H]^+$, 52 (70); HRMS: *m*/*z* calcd for $C_9H_{19}N_6$ $[M+H]^+$: 211.1666; found: 211.1667.

EXPERIMENT 6.10: *N,N,N',N',N'',N''*-Hexamethyl-[1,3,5]triazine-2,4,6-triamine Disalt 6.17

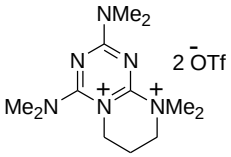

6.17 47%

N,*N*,*N*',*N*',*N*'',*N*''-hexamethyl-[1,3,5]triazine-2,4,6-triamine **6.15** (1.051 g, 5.0 mmol, 1.0 eq) was added over a period of 30 min to a flask containing 1,3-*bis*-(trifluoromethanesulfonyloxy)propane **4.15** (6.124 g, 18.0 mmol, 3.6 eq) at 0 °C and stirred for 1 h. The reaction mixture was warmed to r.t. and stirred for a further 1 h. Dry diethyl ether (10 mL) was added and the reaction mixture was stirred for 7 days. The solids were collected, washed with diethyl ether and the solvent was removed *in vacuo*. Recrystallisation from dry acetonitrile/diethyl ether gave disalt **6.17** (1.29 g, 47 %) as a white solid; mp 159-161 °C; ^{1}H NMR (400 MHz, CD_3CN) δ= 2.39 (2H,

tt, *J*(H,H)= 5.8, 5.7 Hz, CH_2), 3.24 (6H, s, CH_3), 3.28 (3H, s, CH_3), 3.31 (3H, s, CH_3), 3.65 (6H, s, CH_3), 4.08 (2H, t, *J*(H,H)= 5.7 Hz, CH_2), 4.14 (2H, t, *J*(H,H)= 5.8 Hz, CH_2); ^{13}C NMR (100 MHz, CD_3CN) δ= 19.3 (CH_2), 38.6 (CH_3), 38.7 (CH_3), 42.2 (CH_3), 52.3 (CH_2), 58.0 (CH_3), 63.9 (CH_2), 122.1 (q, *J*(C,F)= 320 Hz, CF_3), 158.4 (C), 159.7 (C), 160.1 (C); IR (KBr disc) $\tilde{\nu}$= 3068, 3038, 2989, 2945, 1749, 1665, 1644, 1578, 1493, 1409, 1285, 1260, 1154, 1031, 780, 638, 518; MS (ESI) 401 (100) $[M\text{-}OTf]^+$, 269 (23), 237 (15); HRMS: *m*/*z* calcd for $C_{13}H_{24}F_3N_6O_3S_1$ $[M\text{-}OTf]^+$: 401.1577; found: 401.1573.

EXPERIMENT 6.11: Attempted Hexacation 6.2 Synthesis

N,*N*,*N*',*N*',*N*'',*N*''-Hexamethyl-[1,3,5]triazine-2,4,6-triamine **6.15** (0.042 g, 0.2 mmol, 1.0 eq) was slowly added to a tube containing 1,3-*bis*-(trifluoromethane-sulfonyloxy)propane **4.15** (0.680 g, 2.0 mmol, 10.0 eq) and stirred at r.t. for 6 days. Dry diethyl ether (1 mL) was added and the reaction mixture was stirred for 30 min. The ether was decanted and the residual solvent was removed from the residue *in vacuo*. ^{1}H NMR analysis of the resulting residue gave a mixture of *N*,*N*,*N*',*N*',*N*'',*N*''-hexamethyl-[1,3,5]triazine-2,4,6-triamine **6.15** and disalt **6.17** in a ratio of 3:1. Data were consistent with that reported for *N*,*N*,*N*',*N*',*N*'',*N*''-hexamethyl-[1,3,5]triazine-2,4,6-triamine **6.15** in experiment 6.9 and disalt **6.17** reported in experiment 6.10.

EXPERIMENT 6.12: Attempted Hexacation 6.2 Synthesis

N,*N*,*N*',*N*',*N*'',*N*''-Hexamethyl-[1,3,5]triazine-2,4,6-triamine **6.15** (0.042 g, 0.2 mmol, 1.0 eq) was slowly added to a tube containing 1,3-*bis*-(trifluoromethane-sulfonyloxy)propane **4.15** (0.680 g, 2.0 mmol, 10.0 eq) at r.t., then heated at 60 °C for 18 h. The reaction mixture was cooled to r.t. and dry diethyl ether (1 mL) was added and the suspension was stirred for 30 min. The ether was decanted and the residual solvent was removed from the residue *in vacuo*. MS analysis of the resulting residue showed a major peak at *m*/*z* 237, attributed to demethylated disalt **6.18**.

EXPERIMENT 6.13: Attempted Hexacation 6.2 Synthesis

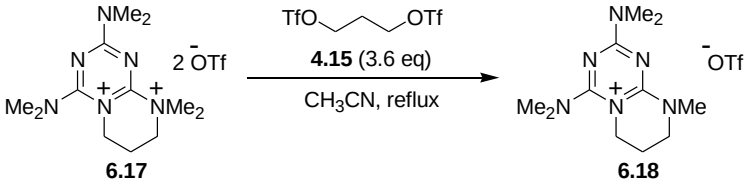

A solution of *N*,*N*,*N*',*N*',*N*'',*N*''-hexamethyl-[1,3,5]triazine-2,4,6-triamine disalt **6.16** (0.055 g, 0.1 mmol, 1.0 eq) and 1,3-*bis*-(trifluoromethanesulfonyloxy)propane **4.15** (0.170 g, 0.5 mmol, 5.0 eq) in dry acetonitrile (0.5 mL) was heated at reflux in a sealed tube for 18 h. The solvent was removed *in vacuo* to give a black oil. MS analysis of the oil showed *m*/*z* signals at 518, 368 and 237. The signals at *m*/*z* 518 and 368 could not be identified. The signal at *m*/*z* 237 was the largest in the spectrum and was attributed to demethylated disalt **6.18**. ^{1}H NMR analysis showed a complex mixture of products, with the most downfield triplet observed at $\delta_{H}(CD_3CN)$ 3.95 ppm, possibly due to a monocationic product, such as **6.18**.

EXPERIMENT 6.14: Attempted *N*,*N*,*N′*,*N′*-Tetramethylpyridine-2,6-diamine 6.18 Synthesis

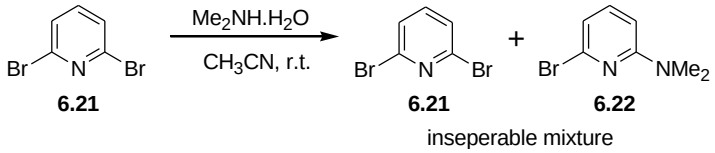

Dimethylamine solution (40 wt% in water, 3.5 mL, 20.0 mmol, 10.0 eq) was added to a solution of 2,6-dibromopyridine **6.21** (0.474 g, 2.0 mmol, 1.0 eq) in acetonitrile (10 mL) and heated at reflux under argon for 5 days. The reaction mixture was filtered through a plug of potassium carbonate and the solvent was removed *in vacuo* to give a brown solid (0.406 g), which was found to be a mixture of (6-bromopyridin-2-yl)dimethylamine **6.22** and 2,6-dibromopyridine **6.21** (1.0:0.2 respectively by ^{1}H NMR) that could not be separated by column chromatography. Data for (6-bromopyridin-2-yl)dimethylamine **6.22** were consistent with that reported in experiment 6.15.

EXPERIMENT 6.15: (6-Bromopyridin-2-yl)dimethylamine 6.22

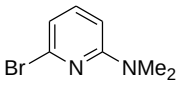

6.22 90%

Dimethylamine solution (40 wt% in water, 15 mL) was dropped onto potassium carbonate (30 g) to evolve dimethylamine gas, which was condensed into a tube containing 2,6-dibromopyridine **6.21** (1.184 g, 5.0 mmol, 1.0 eq) at -78 °C. The tube was sealed and warmed to r.t., then heated at 60 °C for 18 h. The tube was cooled to r.t. and the excess dimethylamine was allowed to evaporate. Purification by column chromatography using silica gel (EA/TEA/PE 2:1:97) gave (6-bromopyridin-2-yl)dimethylamine **6.22** (0.903 g, 90 %) as a brown oil; ^{1}H NMR (400 MHz, $CDCl_3$) δ= 3.07 (6H, s, CH_3), 6.39 (1H, d, *J*(H,H)= 8.4 Hz, ArH), 6.68 (1H, d, *J*(H,H)= 7.6 Hz, ArH), 7.25 (1H, dd, *J*(H,H)= 8.4, 7.6 Hz, ArH); ^{13}C NMR (100 MHz, $CDCl_3$) δ= 38.1 (CH_3), 104.0 (CH), 114.5 (CH), 139.3 (CH), 140.4 (C), 159.5 (C); IR (thin film) $\tilde{\nu}$= 3094, 2931, 2814, 1591, 1542, 1407, 1244, 1164, 1122, 975, 768, 659; MS (CI) 203 (100) [M(^{81}Br)+H]$^+$, 201 (100) [M(^{79}Br)+H]$^+$, 123 (80), 109 (65), 58 (60); HRMS: *m*/*z* calcd for $C_7H_{10}Br_1N_2$ [M(^{79}Br)+H]$^+$: 201.0022; found: 201.0021.

EXPERIMENT 6.16: *N*,*N*,*N′*,*N′*-Tetramethylpyridine-2,6-diamine 6.19[102]

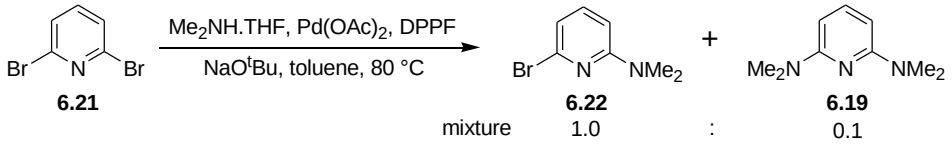

6.21 **6.22** **6.19**

mixture 1.0 : 0.1

A solution of 2,6-dibromopyridine **6.21** (0.5 g, 2.1 mmol, 1.0 eq), palladium (II) acetate (13.5 mg, 0.027 mmol, 1.3 mol%), DPPF (51.4 mg, 0.042 mmol, 2.0 mol%), sodium *tert*-butoxide (0.528 g, 5.5.mmol, 2.6 eq) and dimethylamine solution (2.0 M in THF, 2.3 mL, 4.6 mmol, 2.2 eq) in dry toluene (3 mL) under argon was heated at 80 °C in a sealed tube for 2 days. The reaction mixture was cooled to r.t. and dimethylamine solution (2.0 M in THF, 2.3 mL, 4.6 mmol, 2.2 eq) was added, then the reaction mixture was heated at 80 °C in a sealed tube for 5 days. ^{1}H NMR analysis of the reaction mixture showed a mixture of the mono-aminated **6.22** and diaminated product **6.19** in a ratio of 1.0:0.1. Data were consistent with that reported

for (6-bromopyridin-2-yl)dimethylamine **6.22** in experiment 6.15 and for *N*,*N*,*N*′,*N*′-tetramethylpyridine-2,6-diamine **6.19** in experiment 6.17.

EXPERIMENT 6.17: *N*,*N*,*N*,*N*′-Tetramethylpyridine-2,6-diamine 6.19

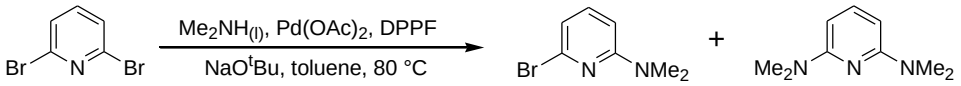

6.21 **6.22** 48% **6.19** 24%

Dimethylamine was condensed into a tube containing a solution of 2,6-dibromopyridine **6.21** (0.5 g, 2.1 mmol, 1.0 eq), palladium (II) acetate (13.5 mg, 0.027 mmol, 1.3 mol%), DPPF (51.4 mg, 0.042 g, 2.0 mol%) and sodium *tert*-butoxide (0.528 g, 5.5.mmol, 2.6 eq) in dry toluene (3 mL) under argon and was heated to 80 °C in a sealed tube for 4 days. The reaction mixture was cooled to r.t. and filtered through celite and the celite was washed with DCM (20 mL). The solvent was removed *in vacuo*. Purification by column chromatography using silica gel (TEA/toluene 1:99) gave *N*,*N*,*N*′,*N*′-tetramethylpyridine-2,6-diamine **6.19** (0.085 g, 24 %) as a hygroscopic brown solid and (6-bromopyridin-2-yl)dimethylamine **6.22** (0.201 g, 48 %) as a brown oil.

***N*,*N*,*N*′,*N*′-Tetramethylpyridine-2,6-diamine 6.19**; ^{1}H NMR (400 MHz, $CDCl_3$) δ= 3.07 (12H, s, CH_3), 5.85 (2H, d, J(H,H)= 8.0 Hz, ArH), 7.32 (1H, t, J(H,H)= 8.0 Hz, ArH); ^{13}C NMR (100 MHz, $CDCl_3$) δ= 38.0 (CH_3), 93.2 (CH), 138.7 (CH), 158.7 (C); IR (KBr disc) $\tilde{\nu}$= 3090, 2912, 2846, 2796, 1582, 1495, 1418, 1387, 1163, 1018, 764, 700, 520; MS (ESI) 166 (100) $[M+H]^+$, 151 (18), 136 (10); HRMS: *m*/*z* calcd for $C_9H_{16}N_3$ $[M+H]^+$: 166.1339; found: 166.1335.

Data for (6-bromopyridin-2-yl)dimethylamine **6.22** were consistent with that reported in experiment 6.15.

EXPERIMENT 6.18: *N*,*N*,*N*′, *N*′-Tetramethylpyridine-2,6-diamine 6.19

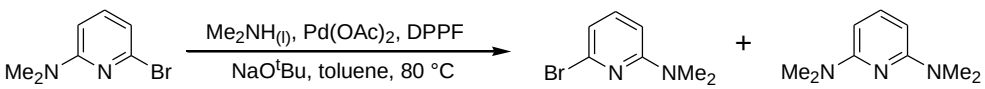

6.22 **6.22** 21% **6.19** 35%

Dimethylamine was condensed into a tube containing a solution of (6-bromopyridin-2-yl)dimethylamine **6.22** (0.422 g, 2.1 mmol, 1.0 eq), palladium (II) acetate (13.5

mg, 0.027 mmol, 1.3 mol%), DPPF (51.4 mg, 0.042 g, 2.0 mol%) and sodium *tert*-butoxide (0.528 g, 5.5.mmol, 2.6 eq) in dry toluene (5 mL) under argon and was heated at 80 °C in a sealed tube for 3 days. The reaction mixture was cooled to r.t. and filtered through celite and the celite was washed with DCM (20 mL). The solvent was removed *in vacuo*. Purification by column chromatography using silica gel (TEA/toluene 1:99) gave *N*,*N*,*N*′,*N*′-tetramethylpyridine-2,6-diamine **6.19** (0.121 g, 35 %) as a hygroscopic brown solid and (6-bromopyridin-2-yl)dimethylamine **6.22** (0.087 g, 21 %) as a brown oil. Data were consistent with that reported for (6-bromopyridin-2-yl)dimethylamine **6.22** in experiment 6.15 and for *N*,*N*,*N*′,*N*′-tetramethylpyridine-2,6-diamine **6.19** in experiment 6.17.

EXPERIMENT 6.19: *N*,*N*,*N*′,*N*′-Tetramethylpyridine-2,6-diamine 6.19

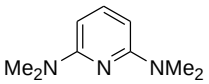

6.19 53%

A solution of 2,6-dibromopyridine **6.21** (5.92 g, 25 mmol, 1.0 eq) in dimethylamine solution (40 wt% in water, 12 mL) was heated at 120 °C in a microwave oven for 15 min. ^{1}H NMR analysis of the reaction mixture showed a mixture of *N*,*N*,*N*′,*N*′-tetramethylpyridine-2,6-diamine **6.19** and (6-bromopyridin-2-yl)dimethylamine **6.22**. The reaction mixture was heated at 150 °C in a microwave oven for a further 3.5 h. The reaction mixture was diluted with diethyl ether (40 mL) and water (40 mL). The ether layer was collected and the water layer was re-extracted with diethyl ether (2 x 40 mL). The combined ether layers were washed with water (100 mL) and brine (100 mL), dried over anhydrous Na_2SO_4 and the solvent was removed *in vacuo*. Purification by column chromatography using silica gel (TEA/toluene 1:99) gave *N*,*N*,*N*′,*N*′-tetramethylpyridine-2,6-diamine **6.19** (1.77 g, 53 %) as a hygroscopic brown solid. Data were consistent for *N*,*N*,*N*′,*N*′-tetramethylpyridine-2,6-diamine **6.19** in experiment 6.17.

EXPERIMENT 6.20: Attempted Pentane-1,3,5-triol 6.23 Synthesis[103]

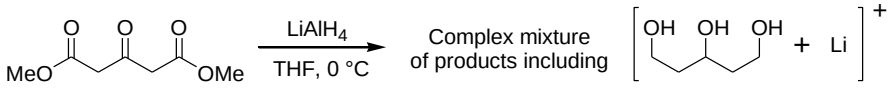

6.24 **6.25**

$LiAlH_4$ (2.66 g, 70 mmol, 2.1 eq) was added over 40 min to a solution of dimethyl-3-oxopentane-1,5-dioate **6.24** (4.8 mL, 33 mmol, 1.0 eq) in dry THF (50 mL) under argon and stirred at r.t. for 2 h. The reaction mixture was quenched with water (10 mL), then H_2SO_4 solution (2N, 20 mL) was added. The reaction mixture was filtered and the filtrate was collected and neutralised with ammonia solution (30 % in water). The reaction mixture was filtered, the filtrate was collected and the solvent was removed *in vacuo*. The residue was extracted with ethanol and the ethanol was removed *in vacuo* to give a viscous red oil (3.53 g). MS analysis of the reaction mixture showed peak at *m*/*z* 127, consistent with pentane-1,3,5-triol complexed to lithium $[M+Li]^+$. Attempted purification by Kugelrohr distillation was unsuccessful.

EXPERIMENT 6.21: 3-Hydroxypentanedioic acid dimethyl ester 6.26[105]

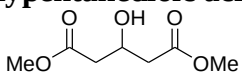

6.26 81%

Sodium borohydride (1.96 g, 52 mmol, 0.4 eq) was slowly added to a solution of dimethyl-3-oxopentane-1,5-dioate **6.24** (19 mL, 130 mmol, 1.0 eq) in methanol (130 mL) under argon at r.t. The reaction mixture was stirred for 3 h, then the solvent was removed *in vacuo*. The residue was dissolved in water (150 mL), then extracted with diethyl ether (3 x 100 mL). The combined organic layers were dried over anhydrous Na_2SO_4 and the solvent was removed *in vacuo* to give 3-hydroxypentanedioic acid dimethyl ester **6.26** (18.6 g, 81 %) as a colourless oil; ^1H NMR (400 MHz, $CDCl_3$) δ= 2.57 (4H, d, *J*(H,H)= 6.2 Hz, CH_2), 3.72 (s, 6H, OCH_3), 4.47 (1H, quintet, *J*(H,H)= 6.2 Hz, CH); ^{13}C NMR (100 MHz, $CDCl_3$) 40.6 (CH_2), 52.0 (CH_3), 64.9 (CH), 172.4 (C); IR (thin film) $\tilde{\nu}$= 3062, 3029, 2982, 2937, 2905, 1714, 1639, 1579, 1496, 1450, 1367, 1311, 1270, 1203, 1176, 1096, 1039, 980, 865, 768, 712, 685, 574, 484; MS (CI) 199 (36) $[M+Na]^+$, 194 (19), 177 (100) $[M+H]^+$, 145 (10), 127 (29); HRMS: *m*/*z* calcd for $C_7H_{13}O_5$ $[M+H]^+$: 177.0757; found: 177.0755.

EXPERIMENT 6.22: 3-(*Tert*-butyldimethylsilanyloxy)pentanedioic Acid Dimethyl Ester 6.27[104]

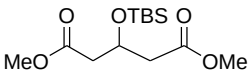

6.27 25%

A solution of *tert*-butyldimethylsilylchloride (13.1 g, 87 mmol, 1.2 eq) in dry DMF (15 mL) was added dropwise to a solution of 3-hydroxypentanedioic acid dimethyl ester **6.26** (12.9 g, 73 mmol, 1.0 eq) and imidazole (14.9 g, 219 mmol, 3.0 eq) in dry DMF (12 mL) at 0 °C under argon. The reaction mixture was warmed to r.t. and stirred for 18 h. The reaction mixture was diluted with water (100 mL) and extracted with diethyl ether (3 x 100 mL). The combined organic layers were washed with water (5 x 100 mL), brine (2 x 100 mL), dried over anhydrous Na_2SO_4 and the solvent was removed *in vacuo* to give 3-(*tert*-butyldimethylsilanyloxy)pentanedioic acid dimethyl ester **6.27** (5.23 g, 25 %) as a yellow oil; ^{1}H NMR (400 MHz, $CDCl_3$) δ= 0.07 (6H, s, $SiCH_3$), 0.85 (9H, s, CH_3), 2.57 (4H, dd, J(H,H)= 5.7, 1.0 Hz, CH_2), 3.68 (6H, s, CH_3), 4.56 (1H, quintet, J(H,H)= 6.2 Hz, CH); ^{13}C NMR (100 MHz, $CDCl_3$) δ= -4.8 (CH_3), 18.1 (C), 25.8 (CH_3), 42. 6 (CH_2), 51.8 (CH_3), 66.5 (CH), 171.6 (C); IR (thin film) $\tilde{\nu}$= 2955, 2931, 2889, 2858, 1743, 1473, 1464, 1438, 1257, 1201, 1150, 1091, 838, 779; MS (CI) 308 (60) $[M+NH_3]^+$, 291 (100) $[M+H]^+$, 259 (10); HRMS: *m*/*z* calcd for $C_{13}H_{27}O_5Si_1$ $[M+H]^+$: 291.1622; found: 291.1625.

EXPERIMENT 6.23: Attempted Reduction of 3-(*Tert*-butyldimethyl-silanyloxy)-pentanedioic Acid Dimethyl Ester 6.27

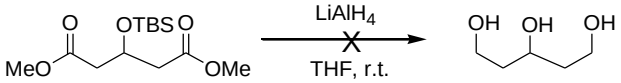

6.27 **6.23**

$LiAlH_4$ (1.20 g, 31.5 mmol, 2.1 eq) was added over 40 min to a solution of 3-(*tert*-butyldimethylsilanyloxy)pentanedioic acid dimethyl ester **6.27** (4.37 g, 15.0 mmol, 1.0 eq) in dry THF (25 mL) under argon and stirred at r.t. for 2 h. The reaction mixture was quenched with water (10 mL), then H_2SO_4 solution (2N, 20 mL) was added. The reaction mixture was filtered and the filtrate was collected and neutralised with ammonia solution (30 % in water). The reaction mixture was filtered, the filtrate was collected and the solvent was removed *in vacuo*. The residue was extracted with ethanol and the ethanol was removed *in vacuo* to give a viscous red oil (3.53 g). MS analysis of the reaction mixture showed peak at *m*/*z* 127, consistent with pentane-1,3,5-triol complexed to lithium $[M+Li]^+$. Attempted purification by Kugelrohr distillation was unsuccessful.

EXPERIMENT 6.24: Hepta-1,6-diene-4-ol 6.30[106]

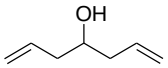

6.30 48%

A few drops of allyl bromide **6.28** were added to a suspension of magnesium turnings (2.55 g, 205 mmol, 2.1 eq) in THF (40 mL) and heated to initiate the reaction. A solution of allyl bromide **6.28** (9.1 mL, 105 mmol, 2.1 eq) and ethyl formate **6.29** (4.04 mL, 50 mmol, 1.0 eq) in THF (50 mL) was added dropwise at a rate to maintain autoreflux. After the addition, the reaction mixture was heated at reflux for 3 h, then cooled to 0 °C and HCl solution (2N) was added until the reaction mixture was acidic. The reaction mixture was diluted with water (20 mL) and the aqueous layer was separated. The aqueous layer was extracted with diethyl ether (2 x 40 mL). The combined ether layers were washed with water (50 mL), saturated $NaHCO_3$ (50 mL), brine (50 mL), dried over anhydrous Na_2SO_4, filtered through celite and the solvent was removed *in vacuo*. Purification by distillation (150-151 °C[106]) gave hepta-1,6-diene-4-ol **6.30** (2.70 g, 48 %) as a colourless oil; ^{1}H NMR (400 MHz, $CDCl_3$) δ= 1.75 (1H, bs, OH), 2.17-2.25 (2H, m, CH_2), 2.28-2.35 (2H, m, CH_2), 3.71-3.74 (1H, m, CH), 5.13-5.18 (4H, m, CH_2), 5.80-5.90 (2H, m, CH); ^{13}C NMR (100 MHz, $CDCl_3$) δ= 41.5 (CH_2), 70.0 (CH), 118.3 (CH_2), 134.9 (CH); IR (thin film) $\tilde{\nu}$= 3369, 3078, 2979, 2930, 1642, 1435, 1027, 997, 914.

EXPERIMENT 6.25: Attempted Pentane-1,3,5-tiol 6.23 synthesis[155]

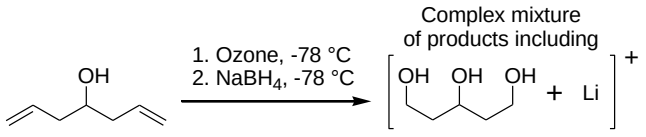

6.30 48% **6.25**

Ozone was bubbled through a solution of hepta-1,6-diene-4-ol **6.30** (2.24 g, 30 mmol, 1.0 eq) in dry methanol (100 mL) at -78 °C until a blue colour persisted in the reaction, indicating excess ozone and the end of the reaction. The reaction mixture was purged with oxygen until the blue colour disappeared. $NaBH_4$ (5.57 g, 160 mmol, 8.0 eq) was added to the reaction mixture at -78 °C, then allowed to warm to r.t. and stirred for 18 h. The reaction mixture was neutralised to *p*H 3 using conc.

HCl solution causing a white precipitate to form. The reaction mixture was filtered and the solvent was removed *in vacuo*. The residue was dissolved in methanol (100 mL) and the solvent was removed *in vacuo* to give an orange oil. ^{1}H NMR analysis showed a complex mixture of products. Purification by distillation was not successful.

EXPERIMENT 6.26: Pentane-1,3,5-triol 6.23[107]

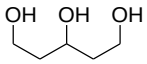

6.23 45% over 2 steps

Potassium hydroxide pellets (6.7 g, 120 mmol, 2.0 eq) were added slowly to a solution of 3-hydroxypentanedioic acid dimethyl ester **6.26** (10.6 g, 60 mmol, 1.0 eq) in methanol (30 mL) at 0 °C. The reaction mixture was warmed to r.t. and stirred for 2 h. The solvent was removed *in vacuo* and the residue was dissolved in water (100 mL). The solution was acidified to *p*H 2 using conc. HCl solution. The aqueous solution was extracted with ethyl acetate (3 x 200 mL). The combined organic layers were dried over anhydrous Na_2SO_4 and the solvent was removed *in vacuo* to give 3-hydroxypentanedioic acid **6.31** and pent-2-ene-1,5-dioic acid **6.32** as colourless oil (8.3 g, 85:15 by ^{1}H NMR) which was used without purification.

A solution of 3-hydroxypentanedioic acid **6.31** (85 % pure, 8.3 g, 56 mmol, 1.0 eq) in dry THF (50 mL) was added using a syringe pump (60.1 mL.h^{-1}) to a flask containing borane-dimethylsulfide complex (2.0 M in THF, 84 mL, 168 mmol, 3.0 eq) under argon at r.t. The reaction mixture was stirred for 18 h, then quenched with methanol and the solvent was removed *in vacuo*. The residue was twice washed with methanol (2 x 200 mL) and the solvent was removed *in vacuo*. The resulting oil was purified by column chromatography using silica gel (EtOH/DCM 1:4) to give pentane-1,3-5-triol **6.23** (3.06 g, 45 %) as a colourless oil; ^{1}H NMR (400 MHz, d_6-DMSO) δ= 1.42-1.56 (4H, m, CH_2), 3.46-3.51 (4H, m, CH_2), 3.62-3.70 (1H, m, CH), 4.26-4.30 (3H, m, OH); ^{13}C NMR (100 MHz, d_6-DMSO) 40.5 (CH_2), 58.2 (CH_2), 65.1 (CH); IR (thin film) $\tilde{\nu}$= 3338, 2944, 2885, 1420, 1339, 1207, 1061, 1006, 893; MS (ESI) 263 (35) $[2M+Na]^+$, 143 (46) $[M+Na]^+$, 121 (100) $[M+H]^+$; HRMS: *m*/*z* calcd for $C_5H_{13}O_3$ $[M+H]^+$: 121.0859; found: 121.0860.

EXPERIMENT 6.27: Trifluoromethanesulfonic Acid 3-Trifluoromethanesulfonyloxy-1-(2-trifluoromethanesulfonyloxyethyl)propyl Ester 6.20

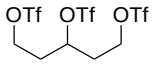

6.20 88%

A solution of pentane-1,3,5-triol **6.23** (1.20 g, 10 mmol, 1.0 eq) in pyridine (2.4 mL, 30 mmol, 3.0 eq) was added dropwise to a solution of trifluoromethanesulfonic anhydride (5.1 mL, 30 mmol, 3.0 eq) in dry DCM (60 mL) under argon at 0 °C. The reaction mixture was stirred at 0 °C for 4 h. The reaction mixture was washed with water (2 x 10 mL), dried over anhydrous Na_2SO_4 and the solvent was removed *in vacuo* to give trifluoromethanesulfonic acid 3-trifluoromethanesulfonyloxy-1-(2-trifluoromethanesulfonyloxyethyl)propyl ester **6.20** (4.52 g, 88 %) as a red/brown oil; ^{1}H NMR (400 MHz, $CDCl_3$) δ= 2.42 (4H, dt, J(H,H)= 6.0, 5.8 Hz, CH_2), 4.63-4.74 (4H, m, CH_2), 5.29 (1H, quintet, J(H,H)= 5.8 Hz, CH); ^{13}C NMR (100 MHz, $CDCl_3$) 34.5 (CH_2), 71. 0 (CH_2), 81.7 (CH), 118.5 (q, J(C,F)= 319 Hz, CF_3), 118.8 (q, J(C,F)= 320 Hz, CF_3); IR (thin film) $\tilde{\nu}$= 3470, 1416, 1247, 1208, 1144, 1031, 910, 808, 749, 615, 519, 463.

EXPERIMENT 6.28: (6-Dimethylaminopyridin-2-yl)trimethylammonium Iodide 6.29

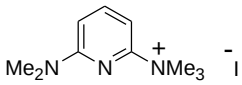

6.39 87 %

Iodomethane (0.03 mL, 0.5 mmol, 1.0 eq) was added to a solution of *N*,*N*,*N*′,*N*′-tetramethylpyridine-2,6-diamine **6.19** (0.083 g, 0.5 mmol, 1.0 eq) in acetonitrile (0.5 mL) at r.t. and stirred for 18 h. Dry diethyl ether (2 mL) was added and the reaction mixture was stirred for 30 min. The resulting pale blue precipitate was collected and washed with diethyl ether (10 mL), and the solvent was removed *in vacuo* to give (6-dimethylaminopyridin-2-yl)trimethylammonium iodide **6.39** (0.134 g, 87 %) as a pale blue solid; mp 190-192 °C; ^{1}H NMR (400 MHz, d_6-DMSO) δ= 3.08 (6H, s, NCH_3), 3.51 (9H, s, NCH_3), 6.85 (1H, d, J(H,H)= 8.4 Hz, ArH), 7.02 (1H, d, J(H,H)= 8.0 Hz, ArH), 7.80 (1H, dd, J(H,H)= 8.4, 8.0 Hz, ArH); ^{13}C NMR (100 MHz, d_6-DMSO) δ= 37.5 (CH_3), 54.0 (CH_3), 99.3 (CH), 107.8 (CH), 140.7 (CH),

155.1 (C), 157.4 (C); MS (ESI) 487 (82), 180 (100) $[M\text{-}I]^+$, 165 (22); HRMS: *m*/*z* calcd for $C_{10}H_{18}N_3$ $[M\text{-}I]^+$: 180.1495; found: 180.1492.

EXPERIMENT 6.29: *N*,*N*,*N*′,*N*′-Tetramethylpyridine-2,6-diamine Disalt 6.40

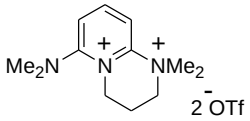

6.40 23%

A solution of *N*,*N*,*N*′,*N*′-tetramethylpyridine-2,6-diamine **6.19** (0.165 g, 1.0 mmol, 1.0 eq) in dry diethyl ether (1.0 mL) was added using a syringe pump (1.02 $mL.h^{-1}$) to a tube containing 1,3-*bis*-(trifluoromethanesulfonyloxy)propane **4.15** (0.408 g, 1.2 mmol, 1.2 eq) under argon at r.t. The reaction mixture was stirred for 1 h, causing formation of a pale purple/grey solid. Dry diethyl ether (2 mL) was added and the reaction mixture was stirred for 30 min. The resulting pink solid was collected. Recyrstallisation from dry acetonitrile/diethyl ether gave *N*,*N*,*N*′,*N*′-tetramethylpyridine-2,6-diamine disalt **6.40** (0.115 g, 23 %) as a white solid; mp 168-169 °C; ^{1}H NMR (400 MHz, CD_3CN) δ= 2.40 (2H, tt, *J*(H,H)= 6.0, 6.0 Hz, CH_2), 3.27 (6H, s, CH_3), 3.73 (6H, s, CH_3), 4.13 (2H, t, *J*(H,H)= 6.0 Hz, CH_2), 4.33 (2H, t, *J*(H,H)= 6.0 Hz, CH_2), 7.53 (1H, dd, *J*(H,H)= 9.3, 0.9 Hz, ArH), 7.64 (1H, dd, *J*(H,H)= 7.9, 0.8 Hz, ArH), 8.09 (1H, dd, *J*(H,H)= 9.3, 7.9 Hz, ArH); ^{13}C NMR (100 MHz, CD_3CN) δ= 20.5 (CH_2), 44.3 (CH_3), 54.1 (CH_2), 60.7 (CH_3), 66.1 (CH_2), 112.3 (CH), 120.9 (CH), 122.2 (q, *J*(C,F)= 321 Hz, CF_3), 143.4 (CH), 147.9 (C), 163.4 (C); MS (ESI) 356 (100) $[M\text{-}OTf]^+$; HRMS: *m*/*z* calcd for $C_{13}H_{21}F_3N_3O_3S_1$ $[M\text{-}OTf]^+$: 356.1250; found: 356.1245.

EXPERIMENT 6.30: *N*,*N*,*N*′,*N*′-Tetramethylpyridine-2,6-diamine Disalt 6.40 Competition Reaction

N,*N*,*N*′,*N*′-Tetramethylpyridine-2,6-diamine disalt **6.40** (0.025 g, 0.05 mmol, 1.0 eq) was reacted in competition with dimethyl sulfate as previously described (Experiment 5.21). The disalt methyl peak at $\delta_H(CD_3CN)$ = 3.73 ppm was used to determine the reactivity. After the reaction with triethylamine **5.28**, dimethyl sulfate

remained in 31 % and the disalt remained in 92 %, as determined by the ^{1}H NMR integrations of the methyl protons for disalt **6.40** and dimethyl sulfate.

Entry	Starting proton integration		Finishing proton integration		Remaining Compound[a]	
	Disalt[b]	Me_2SO_4[c]	Disalt[b]	Me_2SO_4[c]	Disalt	Me_2SO_4
1	0.7535	0.8229	0.6933	0.2543	92	31

[a] All proton signal integrations were taken relative to 1,3,5,7-cyclooctatetraene **5.29** $\delta_H(CD_3CN)$ 5.77 ppm set at 1.000. The experiment was carried out in CD_3CN. Amount remaining calculated from finishing proton integration as a percentage of starting proton integration. [b] Proton signal for Me groups at $\delta_H(CD_3CN)$ 3.73 ppm used. [c] Proton signal for Me groups at $\delta_H(CD_3CN)$ 3.94 ppm used.

EXPERIMENT 6.31: Attempted Trication 6.3 Synthesis in DCM

A solution of *N*,*N*,*N*′,*N*′-tetramethylpyridine-2,6-diamine **6.19** (0.083 g, 0.5 mmol, 1.0 eq) in dry DCM (1.0 mL) was added using a syringe pump (1.02 mL.h^{-1}) to a tube containing tritriflate **6.20** (0.310 g, 0.6 mmol, 1.2 eq) under argon at 0 °C. The reaction mixture was stirred at 0 °C for 1.5 h, then a sample was removed for ^{1}H NMR and MS analysis. ^{1}H NMR analysis showed downfield aromatic peaks at $\delta_H(CD_3CN)$ 8.72 and 8.54 ppm, as well as quintets at $\delta_H(CD_3CN)$ 5.21 and 5.36 ppm. MS analysis showed peaks at *m*/*z* 532, 382, 232 and 166. The reaction mixture was warmed to r.t. and left to stir for 16 h. ^{1}H NMR analysis of the reaction mixture showed no significant change in the ^{1}H NMR spectrum. No products could be isolated from the reaction mixture by recrystallisation.

EXPERIMENT 6.32: Attempted Trication 6.3 Synthesis Using Neat Reaction Conditions

The reaction was carried out in a low oxygen, low moisture glovebox using the appropriate protocols detailed in the introduction. *N*,*N*,*N*′,*N*′-Tetramethylpyridine-2,6-diamine **6.19** (0.083 g, 0.5 mmol, 1.0 eq) was slowly added over 20 min to a tube containing tritriflate **6.20** (0. 510g, 1.0 mmol, 2.0 eq) in the glovebox. The reaction mixture was stirred at r.t. until solidification occurred at ~2 h. Dry diethyl ether (2 mL) was added and the reaction mixture was stirred for 30 min. The resulting pale brown solid was collected. ^{1}H NMR and MS analysis showed a complex mixture of

products. Downfield aromatic peaks at $\delta_H(CD_3CN)$ 8.77 and 8.54 ppm were observed. MS analysis showed peaks at *m*/*z* 532, 382, 232 and 166. Attempts to purify the reaction mixture by recrystallisation from dry acetonitrile/diethyl ether were unsuccessful.

EXPERIMENT 6.33: Attempted Trication 6.3 Synthesis in Diethyl Ether

A solution of *N*,*N*,*N*′,*N*′-tetramethylpyridine-2,6-diamine **6.19** (0.041 g, 0.25 mmol, 1.0 eq) in dry diethyl ether (1.0 mL) was added using a syringe pump (2.03 $mL.h^{-1}$) to a tube containing tritriflate **6.20** (0.314 g, 0.26 mmol, 1.1 eq) under argon at r.t. The reaction mixture was stirred for 2 h, causing a white solid to precipitate, then transferred to a low oxygen, low moisture glovebox. The white solid was collected and the solvent was removed *in vacuo*. MS analysis showed a major peak at *m*/*z* 166, consistent with *N*,*N*,*N*′,*N*′-tetramethylpyridine-2,6-diamine **6.19** $[M+H]^+$. Recrystallisation from dry acetonitrile/diethyl ether was unsuccessful, causing formation of a brown oil.

EXPERIMENT 6.34: Attempted Trication 6.3 Synthesis in Diethyl Ether

A solution of *N*,*N*,*N*′,*N*′-tetramethylpyridine-2,6-diamine **6.19** (0.041 g, 0.25 mmol, 1.0 eq) in dry diethyl ether (1.0 mL) was added using a syringe pump (1.02 $mL.h^{-1}$) to a tube containing tritriflate **6.20** (0.314 g, 0.26 mmol, 1.1 eq) under argon at r.t. The reaction mixture was stirred for 18 h causing a white solid to precipitate, which slowly discoloured to a purple/brown solid. Dry diethyl ether (4 mL) was added and the reaction mixture was stirred for 1 h. The resulting precipitate was collected and the solvent was removed *in vacuo*. MS analysis showed peaks at *m*/*z* 532 and 166 only. Recrystallisation from dry acetonitrile/diethyl ether was unsuccessful, causing formation of a brown oil.

EXPERIMENT 6.35: Attempted Trication 6.3 Synthesis in Diethyl Ether, Featuring Slow Addition

A solution of *N*,*N*,*N*′,*N*′-tetramethylpyridine-2,6-diamine **6.19** (0.041 g, 0.25 mmol, 1.0 eq) in dry diethyl ether (1.0 mL) was added using a syringe pump (0.508 $mL.h^{-1}$) to a tube containing tritriflate **6.20** (0.387 g, 0.75 mmol, 3.0 eq) under argon at r.t. The reaction mixture was stirred for 18 h. The reaction mixture was transferred to a low oxygen, low moisture glovebox and dry diethyl ether was added (3 mL) and the reaction mixture was stirred for 30 min. MS analysis of the reaction mixture showed only a peak at *m*/*z* 166 for *N*,*N*,*N*′,*N*′-tetramethylpyridine-2,6-diamine **6.19** $[M+H]^+$.

EXPERIMENT 6.36: 2,6-Diiodo-4-(dimethylamino)pyridine 6.49[108]

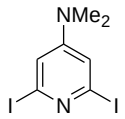

6.49 41%

Boron trifluoride diethyletherate (4.3 mL, 33.5 mmol, 1.1 eq) was added to a solution of 4-DMAP **1.8** (3.8 g, 30.5 mmol, 1.0 eq) in dry THF (200 mL) at 0 °C under argon. The reaction mixture was stirred at 0 °C for 30 min, then cooled to -78 °C.

n-Butyllithium (2.5 M in hexanes, 30.6 mL, 76.5 mmol, 2.5 eq) was added to a solution of di-*iso*-propylamine (11.0 mL, 76.5 mmol, 2.5 eq) in THF (150 mL) at 0 °C under argon. The solution was stirred at 0 °C for 30 min, then added to the flask containing the 4-DMAP-BF_3 adduct at -78 °C and the entire mixture was stirred for 30 min. A solution of iodine (20 g, 79.5 mmol, 2.6 eq) in THF (100 mL) was added to the reaction mixture, which was then warmed to r.t. and stirred under argon for 18 h. Saturated sodium thiosulfate solution (100 mL) was added to the reaction mixture and stirred for 30 min. The organic layer was separated and the aqueous layer was extracted with ethyl acetate (4 x 100 mL). The combined organic layers were washed with brine (100 mL), dried over anhydrous Na_2SO_4 and the solvent was removed *in vacuo*. Purification by column chromatography using silica gel (EA/PE 1:4) gave 2,6-diiodo-4-(dimethylamino)pyridine **6.49** (4.67 g, 41 %) as an off-white solid; mp 148-150 °C (lit.[108] 142-145 °C); ^{1}H NMR (500 MHz, $CDCl_3$) δ= 2.96 (6H, s, NCH_3), 6.88 (2H, s, ArH); ^{13}C NMR (125 MHz, $CDCl_3$) 39.2 (CH_3), 116.0 (C), 116.6 (CH),

155.1 (C); IR (KBr disc) $\tilde{\nu}$= 3105, 2920, 2798, 1574, 1495, 1426, 1389, 1282, 1226, 1152, 1077, 960, 820, 810, 723; MS (CI) 375 (100) $[M+H]^+$; HRMS: *m*/*z* calcd for $C_7H_9I_2N_2$ $[M+H]^+$: 374.8850; found: 374.8850.

EXPERIMENT 6.38: 2,4,6-*Tris*-(dimethylamino)pyridine 6.48[109]

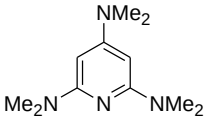

6.48 95%

Dimethylamine was condensed at -78 °C into a tube containing a solution of 2-(2-methylpropanoyl)cyclohexanone **6.50** (0.728 g, 4.3 mmol, 40 mol%), copper iodide (0.214 g, 1.7 mmol, 10 mol%), caesium carbonate (14 g, 42.8 mmol, 4.0 eq) and 2,6-diiodo-4-(dimethylamino)pyridine **6.49** (4.0 g, 10.7 mmol, 1.0 eq) in DMF (11 mL) under argon. The tube was sealed and the reaction mixture was warmed to 0 °C and stirred for 8 h. The reaction mixture was then warmed to r.t. and stirred for a further 10 h. The reaction mixture was filtered through celite, then anhydrous Na_2SO_4 and the solvent was removed *in vacuo*. Excess DMF was removed by distillation under vacuum. Purification by column chromatography using silica gel (EA/hexane 1:19) gave 2,4,6-*tris*-(dimethylamino)pyridine **6.48** (2.12 g, 95 %) as a brown solid; mp 90-101 ^oC; ^1H NMR (400 MHz, $CDCl_3$) δ= 2.91 (6H, s, NCH_3), 2.96 (12H, s, NCH_3), 5.20 (2H, s, ArH); ^{13}C NMR (125 MHz, $CDCl_3$) 38.3 (CH_3), 39.9 (CH_3), 79.6 (CH), 159.5 (C), 160.6 (C); IR (KBr disc) $\tilde{\nu}$= 3121, 2930, 2859, 2796, 1694, 1591, 1560, 1492, 1397, 1326, 1189, 1154, 1065, 1030, 770, 711, 641; MS (ESI) 209 (100) $[M+H]^+$; HRMS: *m*/*z* calcd for $C_{11}H_{21}N_4$ $[M+H]^+$: 209.1761; found: 209.1760.

EXPERIMENT 6.39: 2,4,6-*Tris*-(dimethylamino)pyridine Trisalt 6.47

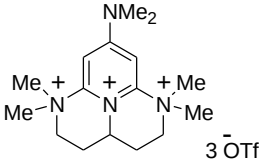

6.47 43%

A solution of 2,4,6-*tris*-(dimethylamino)pyridine **6.48** (0.104 g, 0.5 mmol, 1.0 eq) in dry diethyl ether (1.2 mL) was added using a syringe pump (1.27 $mL.h^{-1}$) to a tube

containing trifluoromethanesulfonic acid 3-trifluoromethanesulfonyloxy-1-(2-trifluoromethanesulfonyloxyethyl)propyl ester **6.20** (0.314 g, 0.6 mmol, 1.2 eq) under argon at r.t. The reaction mixture was transferred to a low oxygen, low moisture glovebox and stirred at r.t. for 18 h. Dry diethyl ether (2 mL) was added and the reaction mixture was stirred for 30 min. The off-white solid was collected and recrystallised from dry acetonitrile/diethyl ether to give 2,4,6-*tris*-(dimethyl-amino)pyridine trisalt **6.47** (0.156, 43 %) as a white solid; mp 190-192 °C (dec.); ^{1}H NMR (400 MHz, CD_3CN) 2.51-2.69 (4H, m, CH_2), 3.45 (6H, s, NCH_3), 3.79 (6H, s, NCH_3), 3.90 (6H, s, NCH_3), 4.05 (2H, dt, J(H,H)= 12.9, 4.0 Hz, CH_2); 4.17 (2H, ddd, J(H,H)= 12.7, 12.1, 3.8 Hz, CH_2), 4.65-4.73 (1H, m, CH), 7.30 (2H, s, ArH); ^{13}C NMR (100 MHz, CD_3CN) 24.2 (CH_2), 43.0 (CH_3), 60.1 (CH_3), 60.2 (CH), 61.4 (CH_3), 63.6 (CH_2), 106.4 (CH), 121.9 (q, J(C,F)= 321 Hz, CF_3), 151.2 (C), 158.4 (C); IR (KBr disc) $\tilde{\nu}$ = 3423, 3115, 3054, 3032, 2993, 1659, 1582, 1487, 1442, 1267, 1159, 1126, 1076, 1030, 941, 899, 888, 857, 849, 788, 758, 715, 640, 575, 518; MS (ESI) 1299 (13), 575 (100) $[M\text{-}OTf]^+$, 213 (80); HRMS: *m*/*z* calcd for $C_{18}H_{29}F_6N_4O_6S_2$ $[M\text{-}OTf]^+$: 575.1427; found: 575.1431. Crystallographic data for 2,4,6-*tris*-(dimethyl-amino)pyridine trisalt **6.47** is given in Appendix 4.

EXPERIMENT 6.40: 2,4,6-*Tris*-(dimethylamino)pyridine Trisalt 6.46 Competition Reaction

2,4,6-*Tris*-(dimethylamino)pyridine trisalt **6.47** (0.036 g, 0.05 mmol, 1.0 eq) was reacted in competition with dimethyl sulfate as previously described (Experiment 5.21). The trisalt aromatic peak at δ_H (CD_3CN) = 7.30 ppm was used to determine the reactivity. After the reaction with triethylamine **5.28**, the trisalt remained in 53 % yield as determined by the signal at δ_H (CD_3CN) 7.30 ppm for the aromatic protons of trisalt **6.47**.

Entry	Starting proton integration		Finishing proton integration		Remaining Compound[a]	
	Trisalt	Me_2SO_4	Trisalt	Me_2SO_4	Dication	Me_2SO_4
1	0.3477[b]	N.D.	0.1834[b]	N.D.	53	N.D.

[a] All proton signal integrations were taken relative to 1,3,5,7-cyclooctatetraene **5.29** $\delta_H(CD_3CN)$ 5.77 ppm set at 1.000. The experiment was carried out in CD_3CN. Amount remaining calculated from finishing proton integration as a percentage of starting proton integration. [b] Proton signal for aromatic hydrogen at $\delta_H(CD_3CN)$ 7.30 ppm used.

9.5 Experimental for Chapter 8

General Procedures for Chapter 8

Melting points obtained for disalts **8.44** and **8.49** were taken from sealed samples prepared inside a low oxygen, low moisture glovebox. Drying of *N*-phenyl-*N*-(2-(pyridin-2-yl)ethyl)formamide **8.39** was achieved by distillation under vacuum (176-179 °C at 0.5 mbar). Drying of *N*-phenyl-*N*-(2-(pyridin-2-yl)ethyl)acetamide **8.48** was achieved by distillation under vacuum (220-222 °C at 0.5 mbar). Trifluoromethanesulfonic anhydride was distilled from phosphorus pentoxide under argon and stored under 4 Å molecular sieves in a low oxygen, low moisture glovebox. Anisole **8.68** was distilled from $CaCl_2$ under argon (152-154 °C). Low pressure (< 60 psi) hydrogenation reactions were carried out on a Cook hydrogenation apparatus (Chas W. Cook and Sons, Ltd., Scientific apparatus makers, model 583-11-71-6) with a 700 mL reaction vessel using either hydrogen or deuterium (Boc gases). High pressure (50 atm) hydrogenation reactions were carried out on a Parr hydrogenation apparatus (Parr Instrument Company, Parr Compact Mini Reactor 5500) with a 600 mL reactor using hydrogen (Boc gases).

EXPERIMENT 8.1: Attempted Hydrogenation of 2-DMAP Disalt 4.16 in Absence of Catalyst

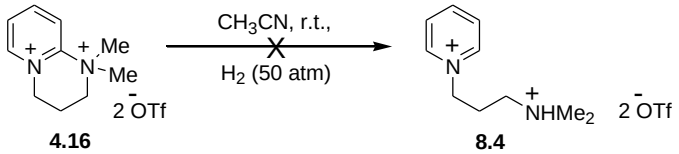

4.16 **8.4**

A solution of 2-DMAP disalt **4.16** (0.231 g, 0.5 mmol, 1.0 eq) in dry acetonitrile (250 mL) was transferred to the Parr hydrogenation vessel. The vessel was purged with hydrogen, then filled with hydrogen (50 atm). The reaction mixture was stirred

at r.t. for 5 days. The reaction mixture was collected and the solvent was removed *in vacuo*. ^{1}H NMR and MS analysis of the reaction mixture showed no evidence of hydrogenation of the 2-DMAP disalt **4.16**.

EXPERIMENT 8.2: Attempted Hydrogenation of 2-DMAP Disalt 4.16 in Absence of Catalyst Using Nylon Insert

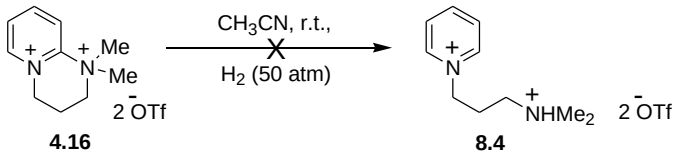

4.16 **8.4**

A solution of 2-DMAP disalt **4.16** (2.32 g, 5.0 mmol, 1.0 eq) in dry acetonitrile (60 mL) was added to the Parr hydrogenation vessel with the nylon insert fitted. The vessel was purged with hydrogen, then filled with hydrogen (50 atm) and the reaction mixture was stirred at r.t. for 4 days. ^{1}H NMR analysis of the reaction mixture showed no evidence of hydrogenation of the 2-DMAP disalt **4.16**.

EXPERIMENT 8.3: 1-(3-Dimethylaminopropyl)piperidinium Trifluoro-methanesulfonate 8.6

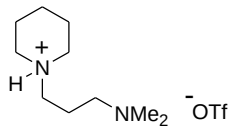

8.6 76%

A solution of 2-DMAP disalt **4.16** (0.462 g, 1.0 mmol, 1.0 eq) and palladium on activated carbon (10 wt% on activated carbon, 0.106 g, 10 mol% Pd) in dry acetonitrile (20 mL) was transferred to the Cook hydrogenation vessel. The vessel was evacuated using a vacuum pump, then filled with hydrogen (45 psi) and shaken for 18 h. The reaction mixture was returned to atmospheric pressure, then filtered through celite, which was washed with acetonitrile. The solvent was removed *in vacuo* to give a white solid. Purification by column chromatography using silica gel (CH_3CN/DCM 1:1) gave 1-(3-dimethylaminopropyl)piperidinium trifluoro-methanesulfonate **8.6** (0.243, 76 %) as white needles; mp 143-145 °C; ^{1}H NMR (500 MHz, d_6-DMSO) δ= 1.30-1.99 (6H, m, CH_2), 2.01 (2H, tt, J(H,H)= 6.5, 6.0 Hz, CH_2), 2.79 (6H, s, CH_3), 3.03-3.08 (4H, m, CH_2), 3.10-3.60 (4H, m, CH_2), 9.30 (1H,

s, NH); ^{13}C NMR (125 MHz, CD_3CN) δ= 20.4 (CH_2), 22.1 (CH_2), 23.8 (CH_2), 44.2 (CH_3), 54.6 (CH_2), 54.7 (CH_2), 55.7 (CH_2), 121.9 (q, J(C,F)= 321 Hz, CF_3); IR (KBr disc) $\tilde{\nu}$= 3065, 2973, 2809, 1485, 1443, 1291, 1244, 1225, 1158, 1030, 951, 758, 636, 575, 518; MS (ESI) 321 (15) $[M+H]^+$, 171 (100); HRMS: *m*/*z* calcd for $C_{11}H_{24}F_3N_2O_3S_1$ $[M+H]^+$: 321.1454; found: 321.1456.

EXPERIMENT 8.4: 1-(3-Dimethylpropylammonium)pyridinium Trifluoromethanesulfonate 8.4

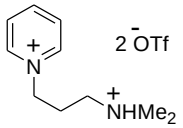

8.4 99%

A solution of 2-DMAP disalt **4.16** (0.462 g, 1.0 mmol, 1.0 eq) and palladium on activated carbon (10 wt% on activated carbon, 0.011 g, 0.01 mmol, 1 mol%) in dry acetonitrile (20 mL) was transferred to the Cook hydrogenation vessel. The vessel was evacuated using a vacuum pump and filled with hydrogen gas (52 psi). The reaction mixture was shaken for 3 h, then returned to atmospheric pressure. The reaction mixture was filtered through celite and the celite was rinsed with acetonitrile (20 mL). The acetonitrile layers were combined and the solvent was removed *in vacuo* to give 1-(3-dimethylpropylammonium)pyridinium trifluoromethanesulfonate **8.4** (0.458 g, 99 %) as a viscous brown oil; ^{1}H NMR (400 MHz, CD_3CN) δ= 2.36-2.44 (2H, m, CH_2), 2.85 (6H, d, J(H,H)= 5.2 Hz, NCH_3), 3.17-3.22 (2H, m, CH_2), 4.59 (2H, t, J(H,H)= 7.6 Hz, CH_2), 7.64 (1H, bs, NH), 8.08 (2H, t, J(H,H)= 7.1 Hz, ArH), 8.55 (1H, t, J(H,H)= 7.9 Hz, ArH), 8.74 (2H, d, J(H,H)= 5.8 Hz, ArH); ^{13}C NMR (100 MHz, CD_3CN) 27.0 (CH_2), 44.3 (CH_3), 55.2 (CH_2), 59.3 (CH_2), 122.0 (q, J(C,F)= 322 Hz, CF_3), 129.6 (CH), 145.8 (CH), 147.4 (CH); IR (thin film) $\tilde{\nu}$= 3511, 3140, 3072, 2792, 1638, 1492, 1258, 1227, 1163, 1030, 969, 776, 758, 686, 639, 575, 518; MS (ESI) 315 (52) $[M\text{-}OTf]^+$, 225 (4), 200 (7), 182 (3), 165 (100) $[M\text{-}H\text{-}2OTf]^+$; HRMS: *m*/*z* calcd for $C_{11}H_{18}F_3N_2O_3S$ $[M\text{-}OTf]^+$: 315.0985; found: 315.0985.

EXPERIMENT 8.5: Deuteration of 2-DMAP Disalt 4.16

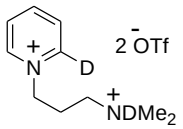

8.8 99%

A solution of 2-DMAP disalt **4.16** (0.462 g, 1.0 mmol, 1.0 eq) and palladium on activated carbon (10 wt% on activated carbon, 0.011 g, 0.01 mmol, 1 mol%) in dry acetonitrile (20 mL) was transferred to the Cook hydrogenation vessel. The vessel was evacuated using a vacuum pump and filled with deuterium gas (54 psi). The reaction mixture was shaken for 3 h, then returned to atmospheric pressure. The reaction mixture was filtered through celite and the celite was rinsed with acetonitrile (20 mL). The acetonitrile layers were combined and the solvent was removed *in vacuo* to give deuterated pyridinium salt **8.8** (0.458 g, 99 %) as a viscous brown oil; ^{1}H NMR (500 MHz, CD_3CN) δ= 2.38-2.44 (2H, m, CH_2), 2.84 (6H, s, NCH_3), 3.20 (2H, t, *J*(H,H)= 8.0 Hz, CH_2), 4.61 (2H, t, *J*(H,H)= 7.5 Hz, CH_2), 8.06-8.08 (2H, m, ArH), 8.55 (1H, ddd, *J*(H,H) = 7.9, 7.8, 0.9 Hz, ArH), 8.78 (1H, d, J(H,H) = 5.8 Hz, ArH); ^{13}C NMR (125 MHz, CD_3CN) δ= 27.0 (CH_2), 44.3 (CH_3), 55.2 (CH_2), 59.3 (CH_2), 122.0 (q, *J*(C,F) = 320 Hz, CF_3), 129.6 (CH/CD), 129.7 (CH/CD), 145.8 (CH), 147.4 (CH); IR (thin film) $\tilde{\nu}$= 3501, 3060, 2787, 2303, 1627, 1471, 1255, 1160, 1030, 803, 758, 638, 574, 517; MS (ESI) 488 (13) 316 (48) $[M\text{-}^{2}H\text{-}OTf+H]^{+}$, 185 (36), 166 (100) $[M\text{-}^{2}H\text{-}2OTf]^{+}$, 130 (16); HRMS: *m*/*z* calcd for $C_{11}H_{17}{}^{2}H_1O_3N_2F_3S$ $[M\text{-}^{2}H\text{-}OTf+H]^{+}$: 316.1048; found: 316.1050; *m*/*z* calcd for $C_{10}H_{16}{}^{2}H_1N_2$ $[M\text{-}^{2}H\text{-}2OTf]^{+}$: 166.1449; found: 166.1447. (Note that one deuterium atom is retained in the mass spectrometry sample).

EXPERIMENT 8.6: 1,1-Dimethyl-1,3,4,6-tetrahydro-2*H*-pyrido[1,2-*α*]pyrimidin-1-ium Trifluoromethanesulfonate 8.9

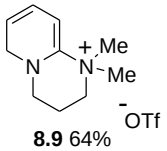

8.9 64%

Lithium aluminium hydride (0.076 g, 2.0 mmol, 2.0 eq) was added to a solution of 2-DMAP disalt **4.16** (0.462 g, 1.0 mmol, 1.0 eq) in dry acetonitrile (10 mL) and stirred

at r.t. under argon for 3 h. The reaction mixture was filtered through celite and the solvent was removed *in vacuo*. Purification by column chromatography using silica gel (CH_3CN/DCM 1:1) gave 1,1-dimethyl-1,3,4,6-tetrahydro-2*H*-pyrido[1,2-α]-pyrimidin-1-ium trifluoromethanesulfonate **8.9** (0.200 g, 64 %) as a pale orange solid; mp 110 ºC (dec.); ^{1}H NMR (400 MHz, d_6-DMSO) δ= 2.14 (2H, tt, *J*(H,H)= 5.9, Hz, CH_2), 3.00 (2H, t, *J*(H,H)= 5.9 Hz, CH_2), 3.36 (6H, s, NCH_3), 3.63 (2H, t, *J*(H,H)= 5.9 Hz, CH_2), 3.85 (2H, dd, *J*(H,H)= 4.2, 1.6 Hz, CH_2), 5.38 (1H, dt, *J*(H,H)= 8.9, 4.2 Hz, CH), 5.86 (1H, d, *J*(H,H)= 5.8 Hz, CH), 5.96-6.00 (1H, m, CH); ^{13}C NMR (100 MHz, d_6-DMSO) δ= 19.4 (CH_2), 48.8 (CH_2), 51.0 (CH_2), 52.3 (CH_3), 64.0 (CH_2), 99.1 (CH), 116.8 (CH), 120.7 (q, *J*(C,F)= 322 Hz, CF_3), 121.7 (CH), 147.1 (C); IR (KBr disc) $\tilde{\nu}$= 3060, 2926, 2857, 1654, 1590, 1488, 1471, 1413, 1293, 1252, 1174, 1049, 765, 733, 640, 515; MS (ESI) 479 (20), 165 (100) $[M\text{-}OTf]^+$; HRMS: *m*/*z* calcd for $C_{10}H_{17}N_2$ $[M\text{-}OTf]^+$: 165.1386; found: 165.1388.

EXPERIMENT 8.7: 1-Methyl-1,2,3,4-tetrahydropyrido[1,2-α]pyrimidin-5-ylium Trifluoromethanesulfonate 4.22

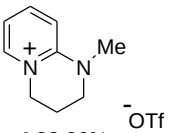

4.22 86%

Triphenylphosphine **5.22** (1.84 g, 7.0 mmol, 1.0 eq) was added to a solution of 2-DMAP disalt **4.16** (3.24 g, 7.0 mmol, 1.0 eq) in dry acetonitrile (10 mL) under argon and stirred at r.t. for 18 h. The solvent was removed *in vacuo*. Purification by column chromatography (CH_3CN/DCM 1:1) gave 1-methyl-1,2,3,4-tetrahydropyrido[1,2-α]pyrimidin-5-ylium trifluoromethanesulfonate **4.22** (1.785 g, 86 %) as a white solid.

EXPERIMENT 8.8: Attempted Hydrogenation of Trimethylpyridin-2-ylammonium Trifluoromethanesulfonate 1.169

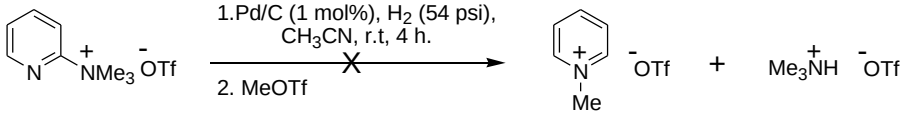

1.169 **8.10** **8.11**

A solution of trimethylpyridin-2-ylammonium trifluoromethanesulfonate **1.169** (0.284 g, 1.0 mmol, 1.0 eq) and palladium on activated carbon (10 wt% on activated carbon, 0.011 g, 0.01 mmol, 1 mol%) in dry acetonitrile (20 mL) was transferred to the Cook hydrogenation vessel. The vessel was evacuated using a vacuum pump and filled with hydrogen gas (54 psi). The reaction mixture was shaken for 3 h, and then returned to atmospheric pressure. Methyl trifluoromethanesulfonate (0.012 mL, 1.1 mmol, 1.1 eq) was added to the reaction mixture to methylate any pyridine that may have been formed during the reaction (and hence to facilitate its detection). The reaction mixture was filtered through celite and the celite was rinsed with acetonitrile (20 mL). The acetonitrile layers were combined and the solvent was removed *in vacuo*. The residue was washed with diethyl ether (2 x 10 mL) to remove any excess methyl trifluoromethanesulfonate and the residue was evaporated *in vacuo* to give recovered trimethylpyridin-2-ylammonium trifluoromethanesulfonate **1.169** (0.280 g, 99 %) as a white solid.

EXPERIMENT 8.9: Attempted Hydrogenation of 1-Methyl-1,2,3,4-tetra-hydropyrido[1,2-α]pyrimidin-5-ylium Trifluoromethanesulfonate 4.22

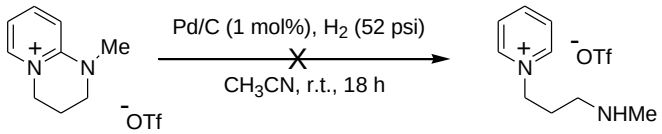

4.22 **8.12**

A solution of 1-methyl-1,2,3,4-tetrahydropyrido[1,2-α]pyrimidin-5-ylium trifluoro-methanesulfonate **4.22** (0.597 g, 2.0 mmol, 1.0 eq) and palladium on activated carbon (10 wt% on activated carbon, 21.2 mg, 1 mol%) in dry acetonitrile (20 mL) was added to the Cook hydrogenation apparatus. The vessel was evacuated using a vacuum pump, then filled with hydrogen (52 psi). The reaction mixture was shaken at r.t. ^{1}H NMR analysis of the reaction mixture after 4 h showed no reaction of the substrate with hydrogen. After 18 h, NMR analysis of the reaction mixture again showed no reaction. The reaction mixture was filtered through celite and the solvent was removed *in vacuo*. The residue was filtered through a pad of silica (CH_3CN/DCM 1:1) to give 1-methyl-1,2,3,4-tetrahydropyrido[1,2-α]pyrimidin-5-ylium trifluoro-methanesulfonate **4.22** (0.597 g, 100 %) as a white solid.

EXPERIMENT 8.10: 3-Dimethylamino-*N*-phenylpropionamide 8.28[141]

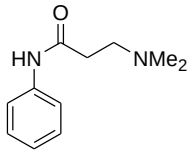

8.28 92%

Ethylmagnesium bromide (3.0 M in diethyl ether, 40 mL, 120 mmol, 4.0 eq) was added slowly to a solution of aniline **8.30** (10.9 mL, 120 mmol, 4.0 eq) in dry diethyl ether (40 mL). A solution of methyl 3-(dimethylamino)propionate **8.29** (4.3 mL, 30 mmol, 1.0 eq) in dry diethyl ether (40 mL) was added slowly under argon at r.t. The reaction mixture was heated to reflux for 30 min, then cooled to r.t. The reaction mixture was washed with HCl solution (2N, 100 mL). The aqueous layer was collected and made basic using potassium carbonate and then extracted with ethyl acetate (2 x 300 mL). The combined organic layers were dried over anhydrous Na_2SO_4 and the solvent was removed *in vacuo* to give a pale brown oil. Purification by column chromatography using silica gel (MeOH/DCM 1:4) gave 3-dimethylamino-*N*-phenylpropionamide **8.28** (5.31 g, 92 %) as a grey solid; mp 59-60 °C; ^{1}H NMR (400 MHz, $CDCl_3$) δ= 2.38 (6H, s, CH_3), 2.53 (2H, t, J(H,H)= 6.0 Hz, CH_2), 2.68 (2H, t, J(H,H)= 6.0 Hz, CH_2), 7.07 (1H, t, J(H,H)= 7.4 Hz, ArH), 7.31 (2H, dd, J(H,H)= 8.6, 7.4 Hz, ArH), 7.52 (2H, dd, J(H,H)= 8.6, 1.0 Hz, ArH); ^{13}C NMR (100 MHz, $CDCl_3$) δ= 33.6 (CH_2), 44.6 (CH_3), 55.3 (CH_2), 120.0 (CH), 124.8 (CH), 129.1 (CH), 138.9 (C), 170.8 (CO); IR (KBr disc) $\tilde{\nu}$= 3278, 3246, 3191, 3133, 3079, 3038, 2972, 2940, 2791, 2769, 1656, 1598, 1551, 1501, 1489, 1443, 1386, 1350, 1296, 1251, 1040, 1029, 972, 759, 694, 508; MS (ESI) 215 (20) $[M+Na]^+$, 193 (100) $[M+H]^+$; HRMS: *m*/*z* calcd for $C_{11}H_{17}O_1N_2$ $[M+H]^+$: 193.1335; found: 193.1333.

EXPERIMENT 8.11: *N*,*N*-Dimethyl-*N′*-phenylpropane-1,3-diamine 8.27

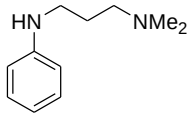

8.27 97%

A solution of 3-dimethylamino-*N*-phenylpropionamide **8.28** (1.92 g, 10.0 mmol, 1.0 eq) in dry diethyl ether (80 mL) was added at a rate to maintain autoreflux to a suspension of lithium aluminium hydride (0.474 g, 12.5 mmol, 1.25 eq) in dry diethyl ether (80 mL) under argon. Once addition was complete, the reaction mixture was heated to reflux for 20 h. The reaction mixture was quenched with ice water, then made strongly basic with NaOH solution (2N). The ether layer was collected and the aqueous layer was extracted with ethyl acetate (3 x 150 mL). The combined organic layers were dried over anhydrous Na_2SO_4 and the solvent was removed *in vacuo* to give *N*,*N*-dimethyl-*N*′-phenylpropane-1,3-diamine **8.27** (1.72 g, 97 %) as a brown oil; ^{1}H NMR (400 MHz, $CDCl_3$) δ= 1.79 (2H, tt, *J*(H,H)= 7.2, 6.4 Hz, CH_2), 2.25 (6H, s, CH_3), 2.40 (2H, t, *J*(H,H)= 7.2 Hz, CH_2), 3.19 (2H, t, *J*(H,H)= 6.4 Hz, CH_2), 4.26 (1H, bs, NH), 6.61 (2H, dd, *J*(H,H)= 8.5, 1.0 Hz, ArH), 6.69 (1H, dt, *J*(H,H)= 7.4, 1.0 Hz, ArH), 7.18 (2H, dd, *J*(H,H)= 8.5, 7.4 Hz, ArH); ^{13}C NMR (125 MHz, $CDCl_3$) δ= 27.2 (CH_2), 43.2 (CH_2), 45.8 (CH_3), 58.4 (CH_2), 113.0 (CH), 117.3 (CH), 129.4 (CH), 148.9 (C); IR (thin film) $\tilde{\nu}$= 3403, 3295, 3052, 3023, 2944, 2859, 2817, 2770, 1603, 1506, 1463, 1320, 1261, 1179, 1156, 1040, 866, 841, 748, 693, 509; MS (CI) 179 (100) $[M+H]^+$; HRMS: *m*/*z* calcd for $C_{11}H_{19}N_2$ $[M+H]^+$: 179.1543; found: 179.1541.

EXPERIMENT 8.12: Attempted Formylation of *N*,*N*-Dimethyl-*N*′-phenyl-propane-1,3-diamine 8.27

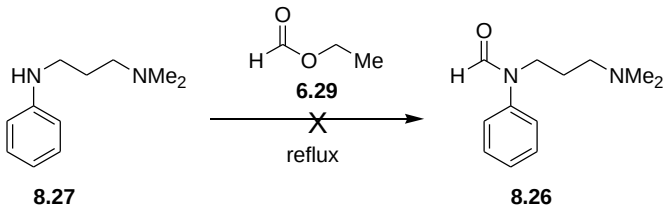

8.27 **8.26**

Ethyl formate **6.29** (0.65 mL, 8.0 mmol, 1.0 eq) was added dropwise to a flask containing *N*,*N*-dimethyl-*N*′-phenylpropane-1,3-diamine **8.27** (1.43 g, 8.0 mmol, 1.0 eq) under argon at 0 °C. The reaction mixture was warmed to r.t., then heated to reflux. After 18 h, ^{1}H NMR analysis of the reaction mixture showed no reaction.

EXPERIMENT 8.13: *N*-(3-Dimethylaminopropyl)-*N*-phenylformamide 8.26[142]

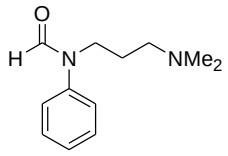

8.26 88%

A solution of oxalyl chloride (2.6 mL, 30 mmol, 1.0 eq) in dry DCM (17 mL) was added dropwise to a solution of imidazole (2.04 g, 30 mmol, 1.0 eq), triethylamine (8.4 mL, 60 mmol, 2.0 eq) and formic acid (1.13 mL, 30 mmol, 1.0 eq) in dry DCM (40 mL) at 0 °C under argon. The reaction mixture was warmed to r.t. and stirred for 15 min. A solution of *N*,*N*-dimethyl-*N*′-phenylpropane-1,3-diamine **8.27** (5.35 g, 30 mmol, 1.0 eq) in dry DCM (60 mL) was added and stirred at r.t. for 18 h. ^{1}H NMR analysis of the reaction mixture showed ~ 60 % conversion to product. A further 1 eq of the formylating reagent (prepared as described above) was added to the reaction mixture and stirred at r.t. for 1.5 h, where ^{1}H NMR analysis of the reaction mixture showed no starting material present. The reaction mixture was cooled to 0 °C and the precipitated imidazole chloride was removed by filtration. The filtrate was collected and the solvent was removed *in vacuo*. The residue was dissolved in ethyl acetate (200 mL) and washed with sat. potassium carbonate solution (2 x 200 mL), brine (200 mL), dried over anhydrous Na_2SO_4 and the solvent was removed *in vacuo* to give *N*-(3-dimethylaminopropyl)-*N*-phenylformamide **8.26** (5.44 g, 88 %) as a yellow oil; ^{1}H NMR (400 MHz, $CDCl_3$) (2 isomers in a ratio of 1.0:0.1) δ= 1.63 (2H, tt, *J*(H,H)= 6.9, 6.8 Hz, CH_2, minor isomer), 1.73 (2H, tt, *J*(H,H)= 7.3, 7.1 Hz, CH_2, major isomer), 2.17 (6H, s, CH_3, major isomer), 2.18 (6H, s, CH_3, minor isomer), 2.28 (4H, t (major isomer), *J*(H,H)= 7.1 Hz, CH_2, minor and major isomer), 3.75 (2H, t, *J*(H,H)= 6.9 Hz, CH_2, minor isomer), 3.87 (2H, t, *J*(H,H)= 7.3 Hz, CH_2, major isomer), 7.19 (3H, dd (major isomer), *J*(H,H)= 8.6, 1.3 Hz, ArH, minor and major isomer), 7.30 (3H, dt (major isomer), *J*(H,H)= 7.4, 1.2 Hz, ArH, minor and major isomer), 7.42 (3H, dd (major isomer), *J*(H,H)= 8.2, 7.5 Hz, ArH, minor and major isomer), 8.36 (1H, s, CH, minor isomer), 8.38 (1H, s, CH, major isomer); ^{13}C NMR (100 MHz, $CDCl_3$) (2 isomers) δ= 26.0 (CH_2, major isomer), 26.5 (CH_2, minor isomer), 43.4 (CH_2, major isomer), 45.5 (CH_3, major isomer), 47.7 (CH_2, minor isomer), 55.9 (CH_2, minor isomer), 57.0 (CH_2, major isomer), 124.2 (CH, major

isomer), 126.0 (CH, minor isomer), 126.9 (CH, major isomer), 127.0 (CH, minor isomer), 129.3 (CH, minor isomer), 129.7 (CH, major isomer), 138.5 (C, minor isomer), 141.1 (C, major isomer), 162.4 (CH, major isomer), 162.6 (CH, minor isomer),; MS (CI) 229 (15) $[M+Na]^+$, 207 (100) $[M+H]^+$, 162 (20); HRMS: *m*/*z* calcd for $C_{12}H_{19}N_2O_1$ $[M+H]^+$: 207.1492; found: 207.1492.

EXPERIMENT 8.14: Attempted Disalt 8.24 Formation in DCM at r.t.

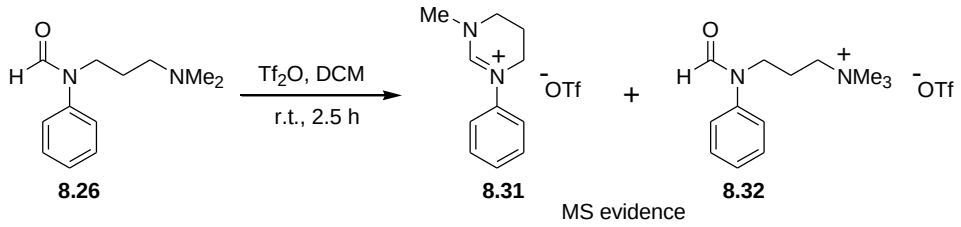

A solution of *N*-(3-dimethylaminopropyl)-*N*-phenylformamide **8.26** (0.413 g, 2.0 mmol, 1.0 eq) in dry DCM (0.5 mL) was added dropwise to a tube containing trifluoromethanesulfonic anhydride (0.27 mL, 2.4 mmol, 1.2 eq) in dry DCM (0.5 mL) under argon at r.t. This resulted in the formation of an orange/brown solid. After 2.5 h, a sample was removed for ^{1}H NMR and MS analysis. MS analysis of the reaction mixture showed peaks at *m*/*z* 221, 207 and 175, consistent with (3-(formylphenylamino)propyl)trimethylammonium trifluoromethanesulfonate **8.32**, *N*-(3-dimethylaminopropyl)-*N*-phenylformamide **8.26** and 3-methyl-1-3,4,5,6-tetrahydro-1-pyrimidinium trifluoromethanesulfonate **8.31**. ^{1}H NMR analysis showed a complex mixture of products with a downfield methylene proton signal at δ_H(d_6-DMSO) 4.19 ppm (t, *J*(H,H)= 6.0 Hz) and two singlets at δ_H(d_6-DMSO) 8.22 and 8.43 ppm.

EXPERIMENT 8.15: Attempted Disalt 8.24 Formation In Diethyl Ether at 0 °C

A solution of *N*-(3-dimethylaminopropyl)-*N*-phenylformamide **8.26** (0.103 g, 0.5 mmol, 1.0 eq) in dry diethyl ether (1.0 mL) was added using a syringe pump (0.254 $mL.h^{-1}$) to a tube containing trifluoromethanesulfonic anhydride (0.14 mL, 1.2 mmol, 2.4 eq) in dry diethyl ether (0.5 mL) under argon at 0 °C. After the addition was complete, the reaction was transferred to a low oxygen, low moisture glovebox and stirred at r.t. for 18 h. The excess liquid was removed from the reaction mixture and

the yellow solid was collected. MS analysis of the reaction mixture showed peaks at *m*/*z* 353, 235, 221, 175 and 162.

EXPERIMENT 8.16: Attempted Disalt 8.24 Formation Using Neat Conditions

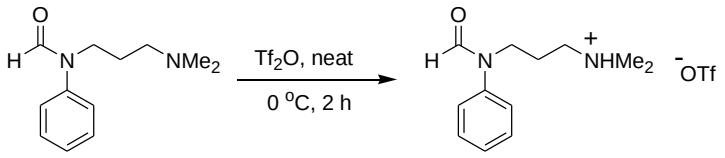

8.26 **8.33**

A solution of *N*-(3-dimethylaminopropyl)-*N*-phenylformamide **8.26** (0.103 g, 0.5 mmol, 1.0 eq) was added dropwise to a tube containing trifluoromethanesulfonic anhydride (0.14 mL, 1.2 mmol, 2.4 eq) under argon at 0 °C. The reaction mixture was stirred at 0 °C for 2 h, then warmed to r.t. and stirred for a further 18 h. The reaction mixture was washed with dry diethyl ether (2 mL) and analysed by ^{1}H NMR and MS analysis. ^{1}H NMR analysis showed what appeared to be (3-(formylphenylamino)-propyl)dimethylammonium trifluoromethanesulfonate **8.33** indicated by a downfield shift in the methyl and methylene protons; δ_H(CD_3CN, selected peaks) 2.80 (6H, d, *J*(H,H)= 5.2 Hz, CH_3), 3.06-3.11 (2H, m, CH_2), 3.92 (2H, t, *J*(H,H)= 6.7 Hz, CH_2). MS analysis was consistent, showing peaks at *m*/*z* 207 $[M\text{-}OTf]^+$ and 162.

EXPERIMENT 8.17: Attempted Synthesis of Phenyl(2-pyridin-2-ylethyl)amine 8.40[144]

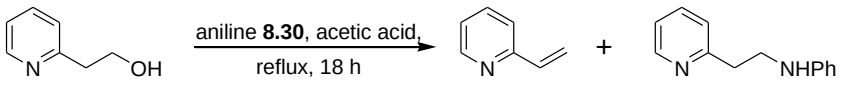

8.41 **8.42** **8.40**

A solution of 2-(2-hydroxyethyl)pyridine **8.41** (3.4 mL, 30 mmol, 1.0 eq) and aniline **8.30** (8.2 mL, 90 mmol, 3.0 eq) in glacial acetic acid (40 mL) was heated to reflux under argon for 3 days. The solvent was removed *in vacuo*, the residue was diluted with water (50 mL) and extracted with chloroform (4 x 20 mL). The aqueous layer was made alkaline with NaOH solution (2N) and extracted with chloroform (8 x 20 mL). The combined organic layers were dried over anhydrous Na_2SO_4 and the solvent was removed *in vacuo* to give a brown solid (0.37 g). ^{1}H NMR analysis

showed a mixture of 2-(2-hydroxyethyl)pyridine **8.41**, 2-vinylpyridine **8.42** and phenyl(2-pyridin-2-ylethyl)amine **8.40**. The products could not be separated by column chromatography using silica gel.

EXPERIMENT 8.18: Phenyl(2-pyridin-2-ylethyl)amine 8.40[145]

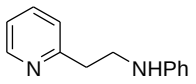

8.40 67%

A solution of 2-vinylpyridine **8.42** (21.6 mL, 200 mmol, 1.0 eq), aniline **8.30** (18.2 mL, 200 mmol, 1.0 eq) and glacial acetic acid (11.4 mL, 200 mmol, 1.0 eq) in methanol (55 mL) was heated at reflux under argon for 8 h, then cooled to r.t. and stirred at r.t. for 17 h. The methanol was removed by distillation. The residue was poured over ice and made very basic with NaOH solution (2N). The aqueous layer was extracted with ether (3 x 100 mL) and the combined organic layers were washed with brine (200 mL), dried over anhydrous Na_2SO_4 and the solvent was removed at atmospheric pressure. Purification by distillation under vacuum gave *N*-(2-(pyridin-2-yl)ethyl)benzenamine **8.40** (26.7 g, 67 %) as a yellow oil, forming an off-white solid upon cooling; mp 41-43 °C (lit.[145] 40.6-41.5 °C); ^{1}H NMR (400 MHz, $CDCl_3$) δ= 3.13 (2H, t, *J*(H,H)= 6.7 Hz, CH_2), 3.56 (2H, t, *J*(H,H)= 6.7 Hz, CH_2), 6.66 (2H, d, *J*(H,H)= 8.7 Hz, ArH), 6.71 (1H, dd, *J*(H,H)= 7.4 Hz, ArH), 7.16-7.22 (4H, m, ArH), 7.65 (1H, ddd, *J*(H,H)= 7.8, 7.4, 1.9 Hz, ArH), 8.57-8.58 (1H, m, ArH); ^{13}C NMR (100 MHz, $CDCl_3$) δ= 37.5 (CH_2), 43.5 (CH_2), 122.9 (CH), 117.2 (CH), 121.5 (CH), 123.3 (CH), 129.2 (CH), 136.5 (CH), 148.2 (C), 149.4 (CH), 159.8 (C); IR (thin film) $\tilde{\nu}$= 3655, 3022, 1591, 1498, 1474, 1435, 1326, 1266, 1177, 1150, 1093, 1071, 1050, 997, 988, 746, 694, 502; MS (CI) 199 (100) $[M+H]^+$; HRMS: *m*/*z* calcd for $C_{13}H_{15}N_2$ $[M+H]^+$: 199.1230; found: 199.1229.

EXPERIMENT 8.19: *N*-Phenyl-*N*-(2-(pyridin-2-yl)ethyl)formamide 8.39[142]

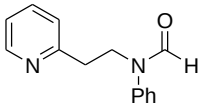

8.39 90%

Oxalyl chloride (7.0 mL, 80 mmol, 2.0 eq) was added dropwise to a solution of imidazole (5.44 g, 80 mmol, 2.0 eq), triethylamine (22.4 mL, 160 mmol, 4.0 eq) and formic acid (3.0 mL, 80 mmol, 2.0 eq) in dry DCM (100 mL) at 0 °C under argon. The reaction mixture was stirred for 30 min at 0 °C, then warmed to r.t. A solution of phenyl(2-pyridin-2-ylethyl)amine **8.40** (7.93 g, 40 mmol, 1.0 eq) in dry DCM (50 mL) was added and the reaction mixture was stirred at r.t. for 18 h. The solvent was removed *in vacuo*. The residue was dissolved in ethyl acetate (200 mL) and washed with saturated potassium carbonate solution (3 x 200 mL) and brine (200 mL), dried over anhydrous Na_2SO_4 and the solvent was removed *in vacuo* to give *N*-phenyl-*N*-(2-(pyridin-2-yl)ethyl)formamide **8.39** (8.15 g, 90 %) as a colourless oil; ^{1}H NMR (400 MHz, $CDCl_3$) [2 isomers in ratio of 1.0:0.3] δ= 2.96 (2H, t, *J*(H,H)= 6.7 Hz, CH_2, minor isomer), 3.09 (2H, t, *J*(H,H)= 7.7 Hz, CH_2, major isomer), 4.18 (2H, t, *J*(H,H)= 6.7 Hz, CH_2, minor isomer), 4.23 (2H, t, *J*(H,H)= 7.7 Hz, CH_2), 7.03-7.19 (8H, m, ArH, minor and major isomer), 7.25-7.40 (6H, m, ArH, minor and major isomer), 7.56-7.63 (2H, m, ArH, minor and major isomer), 8.18 (1H, s, CH, minor isomer), 8.38 (1H, s, CH, major isomer), 8.50 (1H, dd, *J*(H,H)= 3.9, 0.8 Hz, ArH, major isomer), 8.59 (1H, m, ArH, minor isomer); ^{13}C NMR (100 MHz, $CDCl_3$) [2 isomers] δ= 36.4 (CH_2, major isomer), 37.0 (CH_2, minor isomer), 45.5 (CH_2, major isomer), 49.5 (CH_2, minor isomer), 121.8 (CH, major isomer), 122.1 (CH, minor isomer), 123.7 (CH, major isomer), 124.5 (CH, major isomer), 126.3 (CH, minor isomer), 127.0 (CH, major isomer), 127.3 (CH, minor isomer), 129.5 (CH, minor isomer), 129.8 (CH, major isomer), 136.6 (CH, major isomer), 136.8 (CH, minor isomer), 141.1 (C, major isomer), 149.6 (CH, major isomer), 149.9 (CH, min), 157.8 (C, minor isomer), 158.7 (C, major isomer), 162.6 (CH, major isomer), 162.7 (CH, minor isomer); IR (thin film) $\tilde{\nu}$= 3331, 3064, 3011, 2938, 2875, 1683, 1595, 1497, 1475, 1436, 1360, 1176, 764, 699, 674, 543, 511; MS (CI) 475 (90) $[2M+Na]^+$, 249 (80) $[M+Na]^+$, 227 (100) $[M+H]^+$, 199 (30); HRMS: *m/z* calcd for $C_{14}H_{15}N_2O_1$ $[M+H]^+$: 227.1179; found: 227.1176.

EXPERIMENT 8.20: Attempted Disalt 8.44 Formation at 0 °C

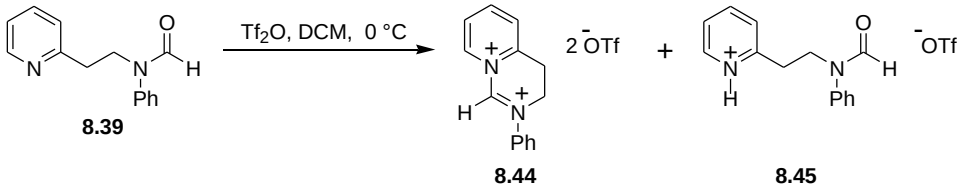

A solution of *N*-phenyl-*N*-(2-(pyridin-2-yl)ethyl)formamide **8.39** (0.113 g, 0.5 mmol, 1.0 eq) in dry DCM (0.5 mL) was added using a syringe pump (0.254 mL.h^{-1}) to a tube containing trifluoromethanesulfonic anhydride (0.1 mL, 0.6 mmol, 1.2 eq) at 0 °C under argon. After the addition (~ 2 h), the reaction mixture was stirred at 0 °C for a further 1 h, then warmed to r.t. and transferred to a low oxygen, low moisture glovebox. The solvent was decanted and the residual solvent was removed from the residue *in vacuo* to give a purple oil. ^{1}H NMR analysis showed a mixture of at least two major products. Downfield signals were observed at δ_H(CD_3CN) 4.07 (2H, t), 4.85 (2H, t), 9.15 (1H, d) and 10.0 (1H, s) thought to be due to disalt **8.44**. MS analysis showed a major peak at *m*/*z* 227, consistent with hydrolysed product **8.45** [M-OTf]$^+$. In air, a purple solution of the reaction mixture was found to rapidly change colour to give an orange solution. ^{1}H NMR analysis of this solution showed no evidence of the downfield proton signals detailed above, indicating the absence of disalt **8.44**.

EXPERIMENT 8.21: *N*-Phenyl-*N*-(2-(pyridin-2-yl)ethyl)acetamide 8.48[142]

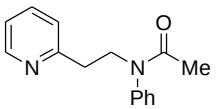

8.48 52%

Oxalyl chloride (10.4 mL, 120 mmol, 4.0 eq) was added dropwise to a solution of imidazole (8.16 g, 120 mmol, 4.0 eq), triethylamine (33.4 mL, 240 mmol, 8.0 eq) and acetic acid (7.0 mL, 120 mmol, 4.0 eq) in dry DCM (200 mL) at 0 °C under argon. The reaction mixture was stirred for 30 min at 0 °C, then warmed to r.t. A solution of phenyl(2-pyridin-2-ylethyl)amine **8.40** (5.95 g, 30 mmol, 1.0 eq) in dry DCM (60 mL) was added and the reaction mixture was stirred at r.t. for 18 h. The solvent was removed *in vacuo*. The residue was dissolved in ethyl acetate (200 mL) and washed with saturated potassium carbonate solution (3 x 200 mL) and brine (200 mL), dried

over anhydrous Na_2SO_4 and the solvent was removed *in vacuo*. Purification by column chromatography using silica gel (100 % ethyl acetate) gave *N*-phenyl-*N*-(2-(pyridin-2-yl)ethyl)acetamide **8.48** (3.78 g, 52 %) as a colourless oil; ^{1}H NMR (400 MHz, $CDCl_3$) δ= 1.82 (3H, s, CH_3), 3.06 (2H, t, *J*(H,H)= 7.8 Hz, CH_2), 4.09 (2H, t, *J*(H,H)= 7.8 Hz, CH_2), 7.07-7.10 (3H, m, ArH), 7.23 (1H, d, *J*(H,H)= 7.8 Hz, ArH), 7.30-7.39 (3H, m, ArH), 7.58 (1H, ddd, *J*(H,H)= 7.7, 7.6, 1.8 Hz, ArH), 8.45 (1H, d, *J*(H,H)= 4.5 Hz, ArH); ^{13}C NMR (100 MHz, $CDCl_3$) δ= 23.0 (CH_3), 36.6 (CH_2), 49.3 (CH_2), 121.6 (CH), 123.6 (CH), 128.0 (CH), 128.3 (CH), 129.8 (CH), 136.6 (CH), 143.3 (C), 149.4 (CH), 159.2 (C), 170.5 (CO); IR (thin film) $\tilde{\nu}$= 3515, 3062, 3009, 2934, 1655, 1595, 1496, 1435, 1396, 1299, 773, 702, 558; MS (CI) 503 (100) $[2M+Na]^+$, 263 (86), $[M+Na]^+$, 241 (90) $[M+H]^+$, 199 (10); HRMS: *m/z* calcd for $C_{15}H_{17}N_2O_1$ $[M+H]^+$: 241.1335; found: 241.1335.

EXPERIMENT 8.22: Attempted Disalt 8.49 Formation in DCM

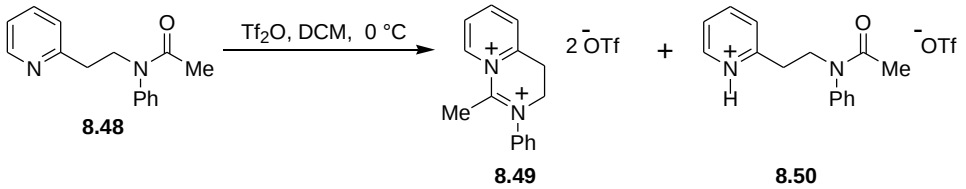

A solution of *N*-phenyl-*N*-(2-(pyridin-2-yl)ethyl)acetamide **8.48** (0.120 g, 0.5 mmol, 1.0 eq) in dry DCM (0.5 mL) was added using a syringe pump (0.254 mL.h^{-1}) to a tube containing trifluoromethanesulfonic anhydride (0.1 mL, 0.6 mmol, 1.2 eq) at 0 °C under argon. After the addition (~ 2 h), the reaction mixture was stirred at 0 °C for a further 1 h, giving a red solution, then warmed to r.t. and transferred to a low oxygen, low moisture glovebox. The reaction mixture was stirred at r.t. for 18 h. The solvent was removed *in vacuo* to give a viscous red oil. ^{1}H NMR analysis of the oil showed a mixture of two products, thought to be *N*-phenyl-*N*-(2-(pyridin-2-yl)ethyl)acetamide disalt **8.49** and the hydrolysis product **8.50** (in a ratio of 1:1.5 by ^{1}H NMR), as shown be the downfield shift in proton signals compared to *N*-phenyl-*N*-(2-(pyridin-2-yl)ethyl)acetamide **8.40**. MS analysis of the oil gave a signal at *m/z* 241 for *N*-phenyl-*N*-(2-(pyridin-2-yl)ethyl)acetamide **8.40** $[M+H]^+$ only. Recrystallisation from dry acetonitrile/diethyl ether gave an orange/red solid. ^{1}H NMR analysis showed an increase in proton signals attributed to *N*-phenyl-*N*-(2-

(pyridin-2-yl)ethyl)acetamide disalt **8.49**, a ratio of 1:0.3 by NMR. Exposing the NMR sample to air resulted in the disappearance of the downfield proton signals attributed to the *N*-phenyl-*N*-(2-(pyridin-2-yl)ethyl)acetamide disalt **8.49**. ^{1}H NMR data were consistent with that reported for *N*-phenyl-*N*-(2-(pyridin-2-yl)ethyl)acetamide disalt **8.49** and hydrolysis product **8.50** reported in experiment 8.24.

EXPERIMENT 8.23: Attempted Disalt 8.49 Formation at -78 °C

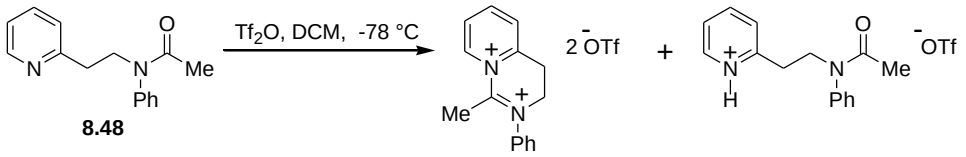

8.48 **8.49** **8.50**

A solution of *N*-phenyl-*N*-(2-(pyridin-2-yl)ethyl)acetamide **8.48** (0.120 g, 0.5 mmol, 1.0 eq) in dry DCM (0.5 mL) was added using a syringe pump (0.254 mL.h^{-1}) to a tube containing trifluoromethanesulfonic anhydride (0.1 mL, 0.6 mmol, 1.2 eq) at -78 °C under argon. After the addition (~2 h), the reaction mixture was stirred at -78 °C for a further 1 h, giving a yellow slurry. Dry diethyl ether (2 mL) was added and the reaction mixture was warmed to r.t., forming a red solution, and transferred to a low oxygen, low moisture glovebox. The solvent was removed *in vacuo* to give a red oil. Recrystallisation from dry acetonitrile/diethyl ether gave a brown solid. ^{1}H NMR analysis showed the disalt species in ~90 % purity. Further recrystallisation attempts were unsuccessful in purifying the disalt. ^{1}H NMR data were consistent with that reported for *N*-phenyl-*N*-(2-(pyridin-2-yl)ethyl)acetamide disalt **8.49** and hydrolysis product **8.50** reported in experiment 8.24.

EXPERIMENT 8.24: *N*-Phenyl-*N*-(2-(pyridin-2-yl)ethyl)acetamide Disalt 8.49

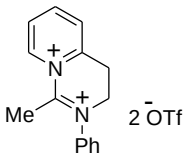

8.49 73%

A solution of *N*-phenyl-*N*-(2-(pyridin-2-yl)ethyl)acetamide **8.48** (1.20 g, 5.0 mmol, 1.0 eq) in dry DCM (5 mL) was prepared in a low oxygen, low moisture glovebox.

The solution was transferred to a syringe, which was then sealed under nitrogen. A solution of trifluoromethanesulfonic anhydride (1.0 mL, 6.0 mmol, 1.2 eq) in dry DCM (5 mL) was also prepared in a low oxygen, low moisture glovebox. The solution was transfered to a flask, which was then sealed under nitrogen. The two solutions were removed from the glovebox. The solution of *N*-phenyl-*N*-(2-(pyridin-2-yl)ethyl)acetamide **8.48** in dry DCM was added using a syringe pump (1.78 $mL.h^{-1}$) to the solution of trifluoromethanesulfonic anhydride in dry DCM at –78 °C under nitrogen. After the addition (~3 h), the reaction mixture was stirred for 1 h at –78 °C, then warmed to r.t. The reaction mixture was transfered to a low oxygen, low moisture glovebox and the resulting precipitate was collected. The pink solid was washed with dry DCM (10 mL), then recrystalllised from dry acetonitrile/DCM to give *N*-(2-(pyridin-2-yl)ethyl)acetamide disalt **8.49** (1.91 g, 73 %) as a white solid; mp 194-197 °C (dec.); ^{1}H NMR (400 MHz, CD_3CN) δ_H = 3.07 (3H, t, *J*(H,H)= 1.6 Hz, CH_3), 4.06 (2H, t, *J*(H,H)= 7.6 Hz, CH_2), 4.63 (2H, tt, *J*(H,H)= 7.6, 1.6 Hz, CH_2), 7.72-7.80 (5H, m, ArH), 8.29-8.32 (2H, m, ArH), 8.99 (1H, ddd, *J*(H,H)= 7.9, 7.8, 1.3 Hz, ArH), 9.35 (1H, dd, *J*(H,H)= 7.2, 1.3 Hz, ArH); ^{13}C NMR (100 MHz, CD_3CN) δ_C = 23.5 (CH_3), 26.5 (CH_2), 52.9 (CH_2), 121.9 (q, *J*(C,F)= 319 Hz, CF_3), 124.8 (CH), 128.7 (CH), 130.1 (CH), 132.3 (CH), 133.8 (CH), 141.4 (C), 145.4 (CH), 154.3 (C), 156.6 (CH), 171.1 (C). The disalt was too unstable for MS, HRMS or IR analysis.

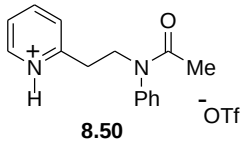

8.50

The recrystallisation filtrate was collected and the solvent was removed *in vacuo* to give 2-(2-(acetylphenylamino)ethyl)pyridinium trifluoromethanesulfonate **8.50** as a red oil; ^{1}H NMR (400 MHz, CD_3CN) δ= 2.26 (3H, s, CH_3), 3.42 (2H, t, *J*(H,H)= 7.5 Hz, CH_2), 4.36 (2H, t, *J*(H,H)= 7.5 Hz, CH_2), 7.38-7.40 (2H, m, ArH), 7.58-7.60 (3H, m, ArH), 7.87-7.92 (2H, m, ArH), 8.46 (1H, ddd, *J*(H,H)= 8.0, 7.9, 1.6 Hz, ArH), 8.58 (1H, dd, *J*(H,H)= 6.7, 5.9 Hz, ArH), 13.64 (1H, bs, NH); ^{13}C NMR (125 MHz, CD_3CN) δ= 22.1 (CH_3), 32.9 (CH_2), 49.7 (CH_2), 121.9 (q, *J*(C,F)= 318 Hz, CF_3), 126.6 (CH), 128.5 (CH), 129.2 (CH), 130.3 (CH), 131.3 (CH), 142.1 (C), 142.3

(CH), 148.1 (CH), 155.2 (C), 175.6 (CO); IR (thin film) $\tilde{\nu}$= 3453, 3281, 3075, 2973, 2921, 1635, 1625, 1547, 1497, 1475, 1287, 1244, 1168, 1029, 770, 702, 639, 517; MS (ESI) 241 (100) $[M\text{-}OTf]^+$; HRMS: *m/z* calcd for $C_{15}H_{17}N_2O_1$ $[M\text{-}OTf]^+$: 241.1335; found: 241.1331.

EXPERIMENT 8.25: Reaction of *N*-Phenyl-*N*-(2-(pyridin-2-yl)ethyl)acetamide 8.48 With TFA

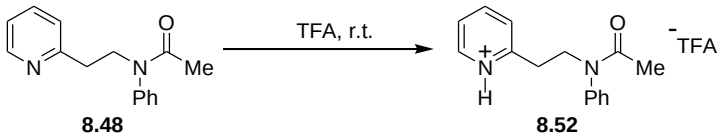

8.48 **8.52**

A sample of *N*-phenyl-*N*-(2-(pyridin-2-yl)ethyl)acetamide **8.48** was stirred in TFA. The solvent was removed *in vacuo* to give 2-(2-(acetylphenylamino)ethyl)pyridinium trifluoroacetate **8.52** as a brown oil; ^{1}H NMR (400 MHz, CD_3CN) δ= 1.79 (3H, s, CH_3), 3.33 (2H, t, *J*(H,H)= 6.3 Hz, CH_2), 4.16 (2H, t, *J*(H,H)= 6.3 Hz, CH_2), 7.26 (2H, d, *J*(H,H)= 7.2 Hz, ArH), 7.40-7.49 (3H, m, ArH), 7.82-7.87 (2H, m, ArH), 8.41 (1H, ddd, *J*(H,H)= 8.0, 7.8, 1.1 Hz, ArH), 8.62 (1H, d, *J*(H,H)= 5.8 Hz, ArH), 12.95 (1H, bs, NH); ^{13}C NMR (100 MHz, CD_3CN) δ= 22.7 (CH_3), 33.5 (CH_2), 48.8 (CH_2), 116.9 (q, *J*(C,F)= 307 Hz, CF_3), 126.4 (CH), 128.9 (CH), 129.1 (CH), 129.6 (CH), 131.0 (CH), 142.3 (CH), 143.3 (C), 147.5 (CH), 156.0 (C), 160.1 (q, *J*(C,F)= 39 Hz, *C*OCF_3), 173.6 (C); IR (thin film) $\tilde{\nu}$= 3395, 3070, 2696, 1779, 1653, 1595, 1497, 1408, 1306, 1173, 772, 703, 625; MS (ESI) 503 (35) $[2M+Na]^+$, 241 (100) $[M\text{-}TFA]^+$; HRMS: *m/z* calcd for $C_{15}H_{17}O_1N_2$ $[M\text{-}TFA]^+$: 241.1335; found: 241.1337.

EXPERIMENT 8.26: Attempted Disalt 8.44 Formation at -78 °C

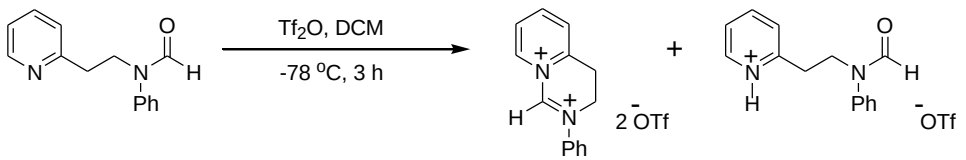

8.40 **8.44** 90% pure **8.45**

A solution of *N*-phenyl-*N*-(2-(pyridin-2-yl)ethyl)formamide **8.40** (0.113 g, 0.5 mmol, 1.0 eq) in dry DCM (0.5 mL) was added using a syringe pump (0.254 $mL.h^{-1}$) to a tube containing trifluoromethanesulfonic anhydride (0.1 mL, 0.6 mmol, 1.2 eq) at -

78 °C under argon. After the addition (~2 h), the reaction mixture was stirred at -78 °C for a further 1 h, then warmed to r.t. and transferred to a low oxygen, low moisture glovebox. The solvent was decanted and the residue was washed with dry diethyl ether (2 mL). The ether was decanted and the residual solvent removed from the residue *in vacuo* to give a pale brown solid. ^{1}H NMR analysis showed the *N*-phenyl-*N*-(2-(pyridin-2-yl)ethyl)formamide disalt **8.44** in ~90 % purity. Recrystallisation from dry acetonitrile/diethyl ether was unsuccessful in purifying the disalt. ^{1}H NMR data were consistent with that reported for *N*-phenyl-*N*-(2-(pyridin-2-yl)ethyl)formamide disalt **8.44** in experiment 8.27 and hydrolysis product **8.45** reported in experiment 8.29.

EXPERIMENT 8.27: *N*-Phenyl-*N*-(2-(pyridin-2-yl)ethyl)formamide Disalt 8.44

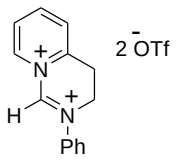

8.44 52%

A solution of *N*-phenyl-*N*-(2-(pyridin-2-yl)ethyl)formamide **8.40** (0.113 g, 0.5 mmol, 1.0 eq) in dry DCM (0.5 mL) was prepared in a low oxygen, low moisture glovebox. The solution was transferred to a syringe, which was then sealed under nitrogen. A solution of dry trifluoromethanesulfonic anhydride (0.1 mL, 0.6 mmol, 1.2 eq) in dry DCM (0.5 mL) was also prepared in a low oxygen, low moisture glovebox. The solution was transferred to a tube, which was then sealed under nitrogen. The two solutions were removed from the glovebox. The solution of *N*-phenyl-*N*-(2-(pyridin-2-yl)ethyl)formamide **8.40** in dry DCM was added using a syringe pump (0.254 $mL.h^{-1}$) to the solution of trifluoromethanesulfonic anhydride in dry DCM at –78 °C under nitrogen. After the addition (~2 h), the reaction mixture was stirred for 1 h at –78 °C, then warmed to r.t. The tube was transferred to a low oxygen, low moisture glovebox and the solvent was decanted. The residue was washed with dry DCM (2.0 mL) and the solvent was removed *in vacuo* to give *N*-(2-(pyridin-2-yl)ethyl)formamide disalt **8.44** (0.132 g, 52 %) as an off-white solid; mp 124 °C (dec.); ^{1}H NMR (400 MHz, CD_3CN) δ_H = 4.08 (2H, t, *J*(H,H)= 7.9 Hz, CH_2), 4.84 (2H, td, *J*(H,H)= 7.9, 1.4 Hz, CH_2), 7.76- 7.90 (5H, m, ArH), 8.31-8.34 (2H, m,

ArH), 9.02 (1H, ddd, *J*(H,H)= 8.0, 7.9, 1.5 Hz, ArH), 9.17 (1H, dd, *J*(H,H)= 6.9, 1.4 Hz, ArH), 10.03 (1H, s, CH); ^{13}C NMR (125 MHz, CD_3CN) δ_C = 26.2 (CH_2), 50.6 (CH_2), 122.4 (q, *J*(C,F)= 320 Hz, CF_3), 124.5 (CH), 129.7 (CH), 130.9 (CH), 132.5 (CH), 135.3 (CH), 140.6 (C), 148.1 (CH), 152.6 (C), 158.1 (CH), 158.4 (CH). The disalt was too unstable for MS, HRMS or IR analysis.

EXPERIMENT 8.28: *N*-Phenyl-*N*-(2-(pyridin-2-yl)ethyl)formamide Disalt 8.44, Larger Scale

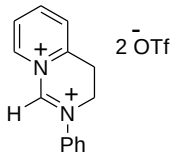

8.44 82%

A solution of *N*-phenyl-*N*-(2-(pyridin-2-yl)ethyl)formamide **8.40** (1.13 g, 5.0 mmol, 1.0 eq) in dry DCM (5 mL) was prepared in a low oxygen, low moisture glovebox. The solution was transferred to a syringe, which was then sealed under nitrogen. A solution of dry trifluoromethanesulfonic anhydride (1.0 mL, 6.0 mmol, 1.2 eq) in dry DCM (5 mL) was also prepared in a low oxygen, low moisture glovebox. The solution was transferred to a flask, which was then sealed under nitrogen. The two solutions were removed from the glovebox. The solution of *N*-phenyl-*N*-(2-(pyridin-2-yl)ethyl)formamide **8.40** in dry DCM was added using a syringe pump (1.78 $mL.h^{-1}$) to the solution of trifluoromethanesulfonic anhydride in dry DCM at –78 °C under nitrogen. After the additon (~3 h), the reaction mixture was stirred for 1 h at –78 °C, then warmed to r.t. The reaction mxiture was transferred to a low oxygen, low moisture glovebox and the resulting precipitate was collected. The precipitate was washed with dry DCM (10 mL) and the solvent was removed *in vacuo* to give *N*-(2-(pyridin-2-yl)ethyl)formamide disalt **8.44** (2.08 g, 82 %) as an off-white solid. Data were consistent with that reported for *N*-phenyl-*N*-(2-(pyridin-2-yl)ethyl)formamide disalt **8.44** in experiment 8.27.

EXPERIMENT 8.29: Reaction of *N*-Phenyl-*N*-(2-(pyridin-2-yl)ethyl)formamide Disalt 8.44 With Water

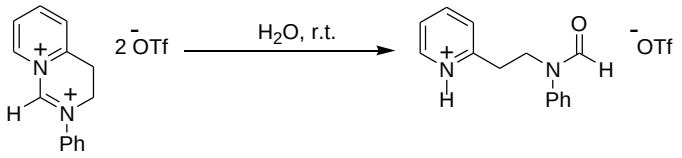

8.44 **8.45**

A tube containing *N*-phenyl-*N*-(2-(pyridin-2-yl)ethyl)formamide disalt **8.44** (0.2 mmol) was prepared in a low oxygen, low moisture glovebox. The sealed tube was removed from the glovebox and water (1.0 mL) was added. The reaction mixture was stirred at r.t. under argon for 4 h. The solvent was removed *in vacuo* to give 2-(2-(formylphenylamino)ethyl)pyridinium trifluoromethanesulfonate **8.45** as a red oil as a mixture of two isomers; ^{1}H NMR (400 MHz, CD_3CN) [2 isomers 1.0:0.1] δ= 3.32 (2H, t, J(H,H)= 6.6 Hz, CH_2, major isomer), 3.56 (2H, t, J(H,H)= 7.5 Hz, CH_2, minor isomer), 4.29 (2H, t, J(H,H)= 6.6 Hz, CH_2, major isomer), 7.24-7.28 (2H, m, ArH, major isomer), 7.34-7.38 (1H, m, ArH, major isomer), 7.42-7.48 (4H, m, ArH, minor and major isomer), 7.56-7.58 (3H, m, ArH, minor isomer), 7.83-7.86 (2H, m, ArH, major isomer), 7.92-7.98 (2H, m, ArH, minor isomer), 8.32 (1H, s, CH, major isomer), 8.44 (1H, ddd, J(H,H)= 8.0, 6.6, 1.6 Hz, ArH, major isomer), 8.47 (1H, s, CH, minor isomer), 8.55 (2H, ddd (major isomer), J(H,H)= 8.3, 6.6, 1.6 Hz, ArH, minor and major isomer), 8.62-8.67 (1H, m, ArH, minor isomer); ^{13}C NMR (125MHz, CD_3CN) [2 isomers] δ= 30.8 (CH_2, major isomer), 33.2 (CH_2, minor isomer), 44.5 (CH_2, major isomer), 50.7 (CH_2, minor isomer), 121.8 (q, J(C,F)= 318 Hz, CF_3), 123.4 (CH, major isomer), 125.2 (CH, minor isomer), 126.6 (CH, minor isomer), 127.5 (CH, major isomer), 128.2 (CH, major isomer), 129.4 (CH, minor isomer), 130.4 (CH, minor isomer), 130.7 (CH, major isomer), 130.9 (CH, minor isomer), 131.5 (CH, major isomer), 136.3 (C, major isomer), 141.2 (C, minor isomer), 142.3 (CH, major isomer), 142.9 (CH, minor isomer), 148.0 (CH, minor isomer), 148.7 (CH, major isomer), 152.6 (C, major isomer), 155.4 (C, minor isomer), 164.2 (CH, major isomer); MS (ESI) 227 (100) $[M\text{-}OTf]^+$; *m*/*z* calcd for $C_{14}H_{15}O_1N_2$ $[M\text{-}OTf]^+$: 227.1179; found: 227.1776.

EXPERIMENT 8.30: Attempted Hydrogenation of *N*-Phenyl-*N*-(2-(pyridin-2-yl)ethyl)formamide Disalt 8.44

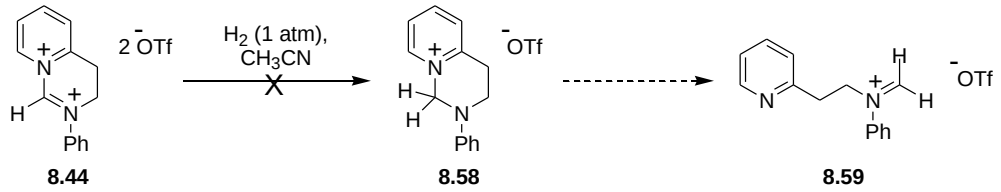

8.44 **8.58** **8.59**

A solution of *N*-phenyl-*N*-(2-(pyridin-2-yl)ethyl)formamide disalt **8.44** (0.117 g, 0.2 mmol, 1.0 eq) in dry acetonitrile (5 mL) was prepared in a low oxygen, low moisture glovebox in a flask fitted with a tap. The sealed reaction flask was removed from the glovebox and the reaction mixture was evacuated using a vacuum pump. The reaction mixture was filled with hydrogen (1 atm) and stirred at r.t. for 18 h. The solvent was removed *in vacuo*. ^{1}H NMR and MS analysis showed only the product of hydrolysis of the *N*-phenyl-*N*-(2-(pyridin-2-yl)ethyl)formamide disalt **8.44**, consistent with data reported in experiment 8.29.

EXPERIMENT 8.31: Attempted Hydrogenation of *N*-Phenyl-*N*-(2-(pyridin-2-yl)ethyl)formamide Disalt 8.44

A solution of *N*-phenyl-*N*-(2-(pyridin-2-yl)ethyl)formamide disalt **8.44** (0.254 g, 0.5 mmol, 1.0 eq) in dry acetonitrile (10 mL) was prepared in a low oxygen, low moisture glovebox in a flask fitted with a tap. The sealed reaction flask was removed from the glovebox and the reaction mixture was evacuated using a vacuum pump. The reaction mixture was filled with hydrogen (1 atm) and stirred at r.t. for 18 h. The reaction mixture was evacuated using a vacuum pump and transferred to a low oxygen, low moisture glovebox. The solvent was removed *in vacuo*. ^{1}H NMR and MS analysis showed only the product of hydrolysis of the *N*-phenyl-*N*-(2-(pyridin-2-yl)ethyl)formamide disalt **8.44,** consistent with data reported in experiment 8.29.

EXPERIMENT 8.32: Attempted Hydrogenation *N*-Phenyl-*N*-(2-(pyridin-2-yl)ethyl)formamide Disalt 8.44 Using Catalyst

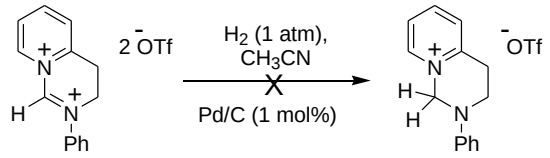

8.44 **8.58**

A solution of *N*-phenyl-*N*-(2-(pyridin-2-yl)ethyl)formamide disalt **8.44** (0.254 g, 0.5 mmol, 1.0 eq) in dry acetonitrile (10 mL) was prepared in a low oxygen, low moisture glovebox. The solution was transferred into a syringe, which was sealed and removed from the glovebox. The solution was injected into a dry flask containing palladium on activated carbon (10 wt% on activated carbon 0.005 g, 0.005 mmol, 1 mol%) under argon. The reaction mixture was evacuated using a vacuum pump. The reaction mixture was filled with hydrogen (1 atm) and stirred at r.t. for 18 h. The reaction mixture was evacuated using a vacuum pump and transferred to a low oxygen, low moisture glovebox. The solvent was removed *in vacuo*. ^{1}H NMR and MS analysis showed only the product of hydrolysis of the *N*-phenyl-*N*-(2-(pyridin-2-yl)ethyl)formamide disalt **8.44**, consistent with data reported in experiment 8.29.

EXPERIMENT 8.33: Attempted Hydrogenation *N*-Phenyl-*N*-(2-(pyridin-2-yl)ethyl)acetamide Disalt 8.49 Using Catalyst

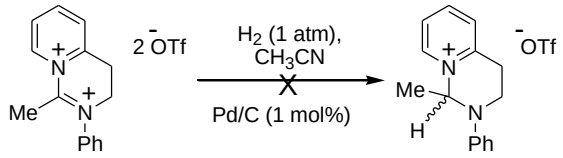

8.49 **8.60**

A solution of *N*-phenyl-*N*-(2-(pyridin-2-yl)ethyl)acetamide disalt **8.49** (0.261 g, 0.5 mmol, 1.0 eq) in dry acetonitrile (10 mL) was prepared in a low oxygen, low moisture glovebox. The solution was transferred into a syringe, which was sealed and removed from the glovebox. The solution was injected into a dry flask containing palladium on activated carbon (0.005 g, 0.005 mmol, 1 mol%) under argon. The reaction mixture was evacuated using a vacuum pump. The reaction mixture was filled with hydrogen (1 atm) and stirred at r.t. for 2 days. The reaction

mixture was evacuated using a vacuum pump and transferred to a low oxygen, low moisture glovebox. The solvent was removed *in vacuo*. ^{1}H NMR and MS analysis showed only the product of hydrolysis of the *N*-phenyl-*N*-(2-(pyridin-2-yl)ethyl)acetamide disalt **8.49**, consistent with data reported in experiment 8.24.

EXPERIMENT 8.34: Reaction of *N*-Phenyl-*N*-(2-(pyridin-2-yl)ethyl)acetamide Disalt 8.49 With Lithium Aluminium Hydride

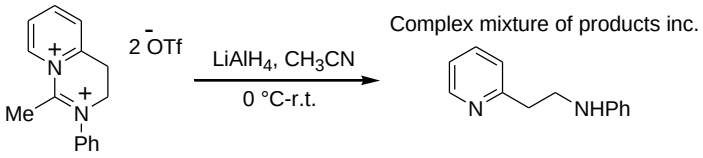

8.49 **8.40** 4%

A solution of *N*-phenyl-*N*-(2-(pyridin-2-yl)ethyl)acetamide disalt **8.49** (0.261 g, 0.5 mmol, 1.0 eq) in dry acetonitrile (10 mL) was prepared in a low oxygen, low moisture glovebox. The solution was transferred into a syringe, which was sealed and removed from the glovebox. The solution was injected into a dry flask containing lithium aluminium hydride (0.038 g, 1.0 mmol, 2.0 eq) at 0 °C under argon. The reaction mixture was stirred at 0 °C for 5 min, then warmed to r.t. and stirred for 2.5 h. The reaction mixture was transferred to a low oxygen, low moisture glovebox. The reaction mixture was filtered through celite and the solvent was removed *in vacuo* to give a viscous red oil. ^{1}H NMR analysis of the oil showed a very complex mixture of products. Several doublet signals were observed in the region of δ_H(CD_3CN) 1.11-1.17 and 2.34-2.51 ppm.

^{1}H NMR (500 MHz, CD_3CN) δ= 1.12 (d, *J*(H,H)= 6.4 Hz), 1.15 (d, *J*(H,H)= 6.4 Hz), 2.35 (d, *J*(H,H)= 6.0 Hz), 2.38 (d, *J*(H,H)= 6.0 Hz), 2.40 (d, *J*(H,H)= 5.6 Hz), 2.43 (d, *J*(H,H)= 5.6 Hz), 2.50 (d, *J*(H,H)= 5.3 Hz), 2.51 (d, *J*(H,H)= 5.3 Hz).

Purification by column chromatography using silica gel (CH_3CN/DCM 1:4) gave only *N*-(2-(pyridin-2-yl)ethyl)benzenamine **8.40** (0.004 g, 4 %) as a yellow oil, consistent with data reported in experiment 8.18.

EXPERIMENT 8.35: Reaction of *N*-Phenyl-*N*-(2-(pyridin-2-yl)ethyl)formamide Disalt 8.44 With Anisole 8.68

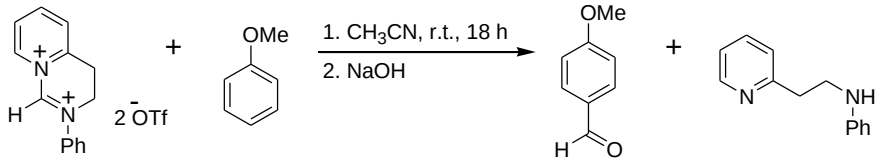

8.44 **8.68** **8.69** 31% **8.40** 40%

A solution of *N*-phenyl-*N*-(2-(pyridin-2-yl)ethyl)formamide disalt **8.44** (0.508 g, 1.0 mmol, 1.0 eq) and anisole **8.68** (0.11 mL, 1.0 mmol, 1.0 eq) in dry acetonitrile (2 mL) was prepared in a low oxygen, low moisture glovebox. The reaction mixture was removed from the glovebox and stirred at r.t. under argon for 18 h. NaOH solution (2N, 1 mL) was added to the reaction mixture, which was stirred for 1 h. The solvent was removed *in vacuo* and the residue was dissolved in DCM (30 mL) and water (30 mL). The organic layer was separated and the aqueous layer was re-extracted with DCM (30 mL). The combined organic layers were washed with brine (50 mL), dried over anhydrous Na_2SO_4 and the solvent was removed *in vacuo*. Purification by column chromatography using silica gel (EA/PE 1:4-1:0) gave 4-methoxybenzaldehyde **8.69** (0.042 g, 31 %) as a green oil and phenyl(2-pyridin-2-ylethyl)amine **8.40** (0.080 g, 40 %) as a yellow oil.

4-Methoxybenzaldehyde 8.69; ^{1}H NMR (400 MHz, $CDCl_3$) δ= 3.90 (3H, s, CH_3), 7.02 (2H, d, *J*(H,H)= 8.8 Hz, ArH), 7.85 (2H, d, *J*(H,H)= 8.8 Hz, ArH), 9.90 (1H, s, CH); ^{13}C NMR (100 MHz, $CDCl_3$) δ= 55.8 (CH_3), 144.5 (CH), 130.2 (C), 132.2 (CH), 164.8 (C), 191.0 (CH); IR (thin film) $\tilde{\nu}$= 3010, 2958, 2935, 2841, 2740, 1683, 1600, 1578, 1511, 1461, 1427, 1316, 1261, 1216, 1161, 1109, 1026, 834, 643, 607, 597; GC-MS: RT 7.35 *m*/*z* 136 (70) $[M]^{+\bullet}$, 135 (100), 107 (10), 92 (20), 77 (30); HRMS: *m*/*z* calcd for $C_8H_7O_2$ $[M-H]^{+\bullet}$: 135.0441; found: 135.0440.

Data for phenyl(2-pyridin-2-ylethyl)amine **8.40** were consistent with that reported in experiment 8.18.

EXPERIMENT 8.36: Reaction of *N*-Phenyl-*N*-(2-(pyridin-2-yl)ethyl)formamide Disalt 8.44 With Anisole 8.68

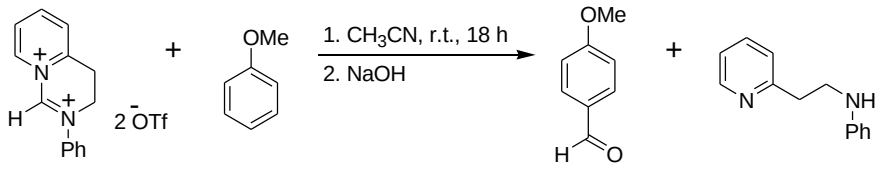

8.44 **8.68** (10 eq) **8.69** 60% **8.40** 64%

A solution of *N*-phenyl-*N*-(2-(pyridin-2-yl)ethyl)formamide disalt **8.44** (0.254 g, 0.5 mmol, 1.0 eq) and anisole **8.68** (0.54 mL, 5.0 mmol, 10.0 eq) in dry acetonitrile (2 mL) was prepared in a low oxygen, low moisture glovebox. The reaction mixture was removed from the glovebox and stirred at r.t. under argon for 18 h. The solvent was removed *in vacuo*. The residue was dissolved in DCM (5 mL) and NaOH solution (2N, 5 mL) was added to the reaction mixture, which was stirred for 1 h. The organic layer was separated and the aqueous layer was re-extracted with DCM (30 mL). The combined organic layers were washed with brine (50 mL), dried over anhydrous Na_2SO_4 and the solvent was removed *in vacuo*. Purification by column chromatography using silica gel (EA/PE 1:4-1:0) gave 4-methoxybenzaldehyde **8.69** (0.041 g, 60 %) as a green oil and phenyl(2-pyridin-2-ylethyl)amine **8.40** (0.063 g, 64 %) as a yellow oil.

Data were consistent with that reported for phenyl(2-pyridin-2-ylethyl)amine **8.40** in experiment 8.18 and for 4-methoxybenzaldehyde **8.69** experiment 8.35.

10 References

[1] Litvinenko, L. M.; Kirichenko, A. I. *Dokl. Akad. Nauk.* **1967**, *176*, 97.

[2] Hassner, A. *Encyclopaedia of Reagents for Organic Synthesis, Vol. 3*; Ed. Paquette, L. A., Wiley, New York, **1995**, 2022-2024.

[3] Grondal, C. *Synlett* **2003**, *10*, 1568-1569.

[4] Steglich, W.; Höfle, G. *Angew. Chem. Int. Ed*. **1969**, *8*, 981.

[5] Mugura, R.; Scriven, E. F. V. *Aldrichimica Acta* **2003**, *36*, 21-27.

[6] Hassner, A.; Krepski, L. R.; Alexanian, V. *Tetrahedron* **1978**, *34*, 2069-2076.

[7] Höfle, G.; Steglich, W.; Vorbrüggen, H. *Angew. Chem. Int. Ed. Engl*. **1978**, *17*, 569-583.

[8] Heinrich, M. R.; Klisa, H. S.; Mayr, H.; Steglich, W. *Angew. Chem. Int. Ed*. **2003**, *42*, 4826-4828.

[9] Mayr, H.; Bug, T.; Gotta, M. F.; Hering, N.; Irrgang, B.; Janker, B.; Kempf, B.; Loos, R.; Ofial, A. R.; Remennikov, G.; Schimmel, H. *J. Am. Chem. Soc*. **2001**, *123*, 9500-9512.

[10] Singh, S.; Das, G.; Singh, O. V.; Han, H. *Org. Lett*. **2007**, *9*, 401-404.

[11] Forsythe, P.; Frampton, R.; Johnson, C. D.; Katritzky, A. R. *J. Chem. Soc., Perkin Trans. 2* **1972**, 671-673.

[12] Spivey, A. C.; Arseniyadis, S. *Angew. Chem. Int. Ed*. **2004**, *43*, 5436-5441.

[13] Sammakia, T.; Hurley, T. B. *J. Org. Chem*. **1999**, *64*, 4652-4664.

[14] Kattnig, E.; Albert, M. *Org. Lett*. **2004**, *6*, 945-948.

[15] Xu, S.; Held, I.; Kempf, B.; Mayr, H.; Steglich, W.; Zipse, H. *Chem. Eur. J*. **2005**, *11*, 4751-4757.

[16] B3LYP/6-31G(d) level of theory for mechanism and B3LYP/6-311+G-(d,p)//B3LYP/6-31(d) level of theory for enthalpies.

[17] Lutz, V.; Glatthaar, J.; Würtele, C.; Serafin, M.; Hausmann, H.; Schreiner, P. R. *Chem. Eur. J*. **2009**, *15*, 8548-8557.

[18] Markey, M. D.; Kelly, T. R. *Tetrahedron*, **2008**, *64*, 8381-8388.

[19] Rezugi, F.; El Gaied, M. M. *Tetrahedron Lett*. **1998**, *39*, 5965-5966.

[20] Shi, M.; Li, C.-Q.; Jiang, J.-K. *Chem. Commum.* **2001**, 833-834.

[21] McMurray, J. S.; Dyckes, D. F. *J. Org. Chem*. **1985**, *50*, 1112-1115.

[22] Hernandez, D.; Chaudhary, S. K.; Cox, R. H.; Porter, J. *Tetrahedron Lett*. **1981**, *22*, 1491-1494.

[23] Chaudhary, S. K.; Hernandez, O. *Tetrahedron Lett*. **1979**, *20*, 99-102.

[24] Schirrmacher, R.; Wängler, B.; Schirrmacher, E.; August, T.; Rösch, F. *Synthesis* **2002**, 538-542.

[25] Wurz, R. P. *Chem. Rev*. **2007**, *107*, 5570-5595.

[26] Vedejs, E.; Chen, X. *J. Am. Chem. Soc*. **1996**, *118*, 1809-1810.

[27] Kawabata, T.; Nagato, M.; Takasu, K.; Fuji, K. *J. Am. Chem. Soc*. **1997**, *119*, 3169-3170.

[28] Ó Dálaigh, C.; Hynes, S. J.; Maher, D. J.; Connon, S. J. *Org. Biomol. Chem*. **2005**, *3*, 981-984.

[29] Ó Dálaigh, C.; Stephen, S. J. ; O'Brien, J. E.; McCabe, T.; Maher, D. J.; Watson, G. W.; Connon, S. *J. Org. Biomol. Chem*. **2006**, *4*, 2785-2793.

[30] Spivey, A. C.; Fekner, T.; Adams, H. *Tetrahedron Lett*. **1998**, *39*, 8919-8922.

[31] Spivey, A. C.; Fekner, T.; Spey, S. E. *J. Org. Chem*. **2000**, *65*, 3154-3159.

[32] Spivey, A. C.; Zhu, F.; Mitchell, M. B.; Davey, S. G.; Jarvest, R. L. *J. Org. Chem*. **2003**, *68*, 7379-7385.

[33] Spivey, A. C.; Leese, D. P.; Zhu, F.; Davey, S. G.; Jarvest, R. L. *Tetrahedron* **2004**, *60*, 4513-4525.

[34] Ruble, J. C.; Fu, G. C. *J. Org. Chem*. **1996**, *61*, 7230-7231.

[35] Ruble, J. C.; Latham, H. A.; Fu, G. C. *J. Am. Chem. Soc*. **1997**, *119*, 1492-1493.

[36] Tao, B.; Ruble, J. C.; Hoic, D. A.; Fu, G. C. *J. Am. Chem. Soc*. **1999**, *121*, 5091-5092.

[37] Tschitschibabin, A. E.; Konowalowa, R. A. *Ber. Deutsch. Chem. Ges*. **1926**, *59*, 2055-2058.

[38] Frampton, R.; Johnson, C. D.; Katritzky, A. R. *Liebigs Ann. Chem*. **1971**, *749*, 12-15.

[39] Barbieri, G.; Benassi, R.; Grandi, R.; Pagoni, U. M.; Ferdinando, T. *Org. Mag. Res*. **1979**, *12*, 159-162.

[40] Spartan® 5.0, Wavefunction Inc., Irvine, California, USA.

[41] Ab initio and density functional approaches can provide a good account of equilibrium geometries of molecules incorporating main group elements according to the Spartan® 5.0 User's Guide. Our selection between these was not deemed particularly critical; the requirement was based upon obtaining reasonable and accessible results (in terms of time required given the power of our PCs) as a first estimate, for our molecules. It was recognised from the start that more accurate determinations could be carried out by specialist computational chemists, if and when a more rigorous quantitative approach is required.

[42] Dolci, L.; Dollé, F.; Jubeau, S.; Vaufrey, F. *J. Labelled Cpd. Radiopharm*. **1999**, *42*, 975-985.

[43] Karramkam, M.; Hinnen, F.; Vaufrey, F.; Dollé, F. *J. Labelled Cpd. Radiopharm*. **2003**, *46*, 979-992.

[44] Olah, G. A. *Angew. Chem. Int. Ed. Engl*. **1993**, *32*, 767-788.

[45] Olah, G. A.; Klumpp, D. A. *Superelectrophiles and their Chemistry* **2008**, Wiley-Interscience, New Jersey.

[46] Olah, G. A. ; Germain, A. ; Lin, H. C.; Forsyth, D. A. *J. Am. Chem. Soc*. **1975**, *97*, 2928-2929.

[47] Olah, G. A. ; Klumpp, D. A. *Acc. Chem. Res*. **2004**, *37*, 211-220.

[48] Brouwer, D. M.; Kiffin, A. A. *Recl. Trav. Chim. Pays-Bas* **1973**, *92*, 689-697.

[49] Olah, G. A.; Surya-Prakash, G. K.; Barzaghi, M.; Lammertsma, K.; Schleyer, P. V. R.; Pople, J. A. *J. Am. Chem. Soc*. **1986**, *108*, 1032-1035.

[50] Olah, G. A.; DeMember, J. R.; Mo, Y. K.; Svoboda, J. J.; Schilling, P.; Olah, J. A. *J. Am. Chem. Soc*. **1974**, *96*, 884-892.

[51] Hogeveen, H.; Kwant, P. W. *Tetrahedron Lett*. **1973**, *19*, 1665-1670.

[52] Lammertsma, K.; Barzaghi, M.; Olah, G. A.; Pople, J. A.; Schleyer, P. V. R., Simonetta, M. *J. Am. Chem. Soc*. **1983**, *105*, 5258-5263.

[53] Ohwada, T.; Yamagata, N.; Shudo, K. *J. Am. Chem. Soc*. **1991**, *113*, 1364-1373.

[54] Yato, M.; Ohwada, T.; Shudo, K. *J. Am. Chem. Soc*. **1991**, *113*, 691-692.

[55] Yokoyama, A.; Ohwada, T.; Shudo, K. *J. Org. Chem*. **1999**, *64*, 611-617.

[56] Charette, A. B.; Chua, P. *Tetrahedron Lett*. **1997**, *38*, 8499-8502.

[57] Charette, A. B.; Chua, P. *J. Org. Chem*. **1998**, *63*, 908-909.

[58] Charette, A. B.; Chua, P. *Synlett* **1998**, 163-165.

[59] Charette, A. B.; Chua, P. *Tetrahedron Lett*. **1998**, *39*, 245-248.

[60] Charette, A. B.; Grenon, M.; Lemire, A.; Pourashraf, M.; Martel, J. *J. Am. Chem. Soc*. **2001**, *123*, 11829-11830.

[61] Charette, A. B.; Grenon, M. *Can. J. Chem*. **2001**, *79*, 1694-1703.

[62] Falmagne, J.-B.; Escudero, J.; Taleb-Sahraoui, S.; Ghosez, L. *Angew. Chem. Int. Ed. Engl.* **1981**, *20*, 878-880.

[63] Thomas, E. W. *Synthesis* **1993**, 767-768.

[64] Movassaghi, M.; Hill, M. D. *J. Am. Chem. Soc*. **2006**, *128*, 14254-14255.

[65] Movassaghi, M.; Hill, M. D. *J. Am. Chem. Soc*. **2006**, *128*, 4592-4593.

[66] Medley, J. W.; Movassaghi, M. *J. Org. Chem*. **2009**, *74*, 1341-1344.

[67] Cui, S.-L.; Wang, J.; Wang, Y.-G. *J. Am. Chem. Soc*. **2008**, *130*, 13526-13527.

[68] Banwell, M. G.; Bissett, B. D.; Busato, S.; Cowden, C. J.; Hockless, D. C. R.; Holman, J. W.; Read, R. W.; Wu, A. W. *J. Chem. Soc., Chem. Commun*. **1995**, 2551-2553.

[69] Summers, L. A.; Dickeson, J. E. *Chem. Commun*. **1967**, 1183.

[70] Dickeson, J. E.; Eckhard, I. E.; Fielden, R.; Summers, L. A. *J. Chem. Soc., Perkin Trans. 1* **1973**, 1973-1975.

[71] Pokorny, D. J.; Paudler, W. W. *Can. J. Chem*. **1973**, *51*, 476-481.

[72] Curphey, T. J. *J. Am. Chem. Soc*. **1965**, *89*, 2063-2064.

[73] Curphey, T. J.; Prasad, K. S. *J. Org. Chem*. **1972**, *37*, 2259-2266.

[74] Katritzky, A. R.; Lewis, J.; Nie, P.-L. *J. Chem. Soc., Perkin Trans. 1* **1979**, 442-445.

[75] Weiss, R.; Roth, R. *Synthesis* **1987**, 870-873.

[76] Murphy, J. A.; Khan, T. A.; Zhou, S. Z.; Thomson, D. W.; Mahesh, M. *Angew. Chem. Int. Ed*. **2005**, *44*, 1356-1360.

[77] Garnier, J. *Development and Study In the Field of Neutral Organic Electron Donors*, Ph.D. 9 month report, University of Strathclyde, Glasgow **2006**.

[78] Imamoto, T. *Comprehensive Organic Synthesis Col. 8*, Ed. Frost, B. M., Pergamon, Oxford **1991**, 795-797.

[79] Peters, D. G. *Organic Electrochemistry*, Ed. Lund, H.; Hammerich, O., Marcel Dekker, New York **1991**, 354.

[80] Hook, J. M.; Mander, L. N. *Nat. Prod. Rep*. **1986**, *3*, 35-85.

[81] Hollowood, C. J.; Ley, S. V. *Org. Biomol. Chem*. **2003**, *1*, 3197-3207.

[82] Schoenebeck, F.; Murphy, J. A.; Zhou, S. Z.; Uenoyama, Y.; Miclo, Y.; Tuttle, T. *J. Am. Chem. Soc*. **2007**, *129*, 13368-13369.

[83] Murphy, J. A.; Zhou, S. Z.; Thomson, D. W.; Schoenebeck, F.; Mahesh, M.; Park, S. R.; Tuttle, T.; Berlouis, L. E. A. *Angew. Chem. Int. Ed*. **2007**, *46*, 5178-5183.

[84] Murphy, J. A.; Garnier, J.; Park, S. R.; Schoenebeck, F.; Zhou, S. Z.; Turner, A. T. *Org. Lett*. **2008**, *10*, 1227-1230.

[85] Cutulic, S. P. Y.; Murphy, J. A.; Farwaha, H.; Zhou, S. Z.; Chrystal, E. *Synlett* **2008**, *14*, 2132-2136.

[86] Cutulic, S. P. Y.; Findlay, N. J.; Zhou, S. Z.; Chrystal, E. J. T.; Murphy, J. A. *J. Org. Chem*. **2009**, *74*, 8713-8718.

[87] Zhou, S. Z. *Unpublished work*, University of Strathclyde **2006**.

[88] Williams, D. H.; Fleming, I. *Spectroscopic Methods in Organic Chemistry*, *5th Edition*, McGraw-Hill Publishing Company, London **1995**, 70-75.

[89] Alder, R. W.; Ellis, D. D.; Gleiter, R.; Harris, C. J.; Large, H.; Orpen, A. G.; Read, D.; Taylor, P. N. *J. Chem. Soc., Perkin Trans. 1* **1998**, 1657-1668.

[90] Williams, D. H.; Fleming, I. *Spectroscopic Methods in Organic Chemistry*, *5th Edition*, McGraw-Hill Publishing Company, London **1995**, 145, Table 3.6.

[91] Booth, B. L.; Jibodu, K. O.; Fernanda, M,; Proenca, J. R. P. *J. Chem. Soc., Perkin Trans. 1* **1983**, 1067-1073.

[92] This work was carried out in tandem with work conducted by Gibson, K. F.

[93] Results not reported here.

[94] Brown, H. C.; Grayson, M. *J. Am. Chem. Soc*. **1953**, *75*, 6285-6292.

[95] Anslyn, E. V.; Dougherty, D. A. *Modern Physical Organic Chemistry*, University Science Books, Sausalito, California **2006**, 382-389.

[96] Castejon, H.; Wiberg, K. B. *J. Am. Chem. Soc*. **1999**, *121*, 2139-2146.

[97] 1-Methyl-2-pyridone: ^{1}H NMR ($CDCl_3$) δ= 3.54 (3H, s, CH_3), 6.17 (1H, ddd, *J*(H,H)= 8.1, 6.6, 1.4 Hz, H-5), 6.54 (1H, dd, *J*(H,H)= 9.7, 1.4 Hz, H-3), 7.34 (1H, ddd, *J*(H,H)= 9.7, 6.6, 2.2 Hz, H-4), 7.35 (1H, dd, *J*(H,H)= 8.1, 2.2 Hz, H-6); ^{13}C NMR ($CDCl_3$) δ= 34.7 (CH_3), 105.8 (CH), 120.2 (CH), 138.8 (CH), 139.7 (CH), 162.9 (CO); Shiina, I.; Kawakita, Y. *Tetrahedron Lett*. **2003**, *44*, 1951-1955.

[98] Xiao, Y.; Malhotra, S. V. *J. Organometallic Chem*. **2005**, *690*, 3609-3613.

[99] Wolfe, J. P.; Buchwald, S. L. *J. Org. Chem*. **2000**, *65*, 1144-1157.

[100] Folmer, J. J.; Acero, C.; Thai, D. L.; Rapoport, H. *J. Org. Chem*. **1998**, *63*, 8170-8182.

[101] Arya, K.; Dandia, A. *Bioorg. Med. Chem*., **2007**, *17*, 3298-3304.

[102] Subat, M.; König, B. *Synthesis*, **2001**, *12*, 1818-1825.

[103] Viscontini, M.; Ebnöther, C. *Helv. Chim. Acta*. **1951**, *13*, 116-118.

[104] Mori, K.; Ikunaka, M. *Tetrahedron* **1987**, *43*, 45-58.

[105] Aucagne, V.; Berná, J.; Crowley, J. D.; Goldup, S. M.; Hänni, K. D.; Leigh, D. A.; Lusby, P. J.; Ronaldson, V. E.; Slawin, A. M. Z.; Viterisi, A.; Walker, D. B. *J. Am. Chem. Soc*. **2007**, *129*, 11950-11963.

[106] Parks, B. W.; Gilbertson, R. D.; Domaille, D. W.; Hutchison, J. E. *J. Org. Chem*. **2006**, *71*, 9622-9627.

[107] Roydhouse, M. D. *Multicationic Superelectrophilic Species*, Postdoctoral Report **2009**.

[108] Aucagne, V.; Berná, J.; Crowley, J. D.; Goldup, S. M.; Hänne, K. D.; Leigh, D. A.; Lusby, P. J.; Ronaldson, V. E.; Slawin, A. M. Z.; Viterisi, A.; Walker, D. B. *J. Am. Chem. Soc*. **2007**, *129*, 11950-11963.

[109] Shafir, A.; Buchwald, S. L. *J. Am. Chem. Soc.* **2006**, *128*, 8742-8743.

[110] Zirngibl, C.; Van Dongen, W.; Schwörer, B.; Von Bünau, R.; Richter, M.; Klein, A.; Thauer, R. K. *Eur. J. Biochem*. **1992**, *208*, 511-520.

[111] Zirngibl, C.; Hedderich, R.; Thauer, R. K. *FEBS Lett*. **1990**, *261*, 112-116.

[112] Schleucher, J.; Griesinger, C.; Schwörer, B.; Thauer, R. K.; *Biochemistry* **1994**, *33*, 3986-3993.

[113] Thauer, R. K.; Klein, A. R.; Hartmann, G. C. *Chem. Rev*. **1996**, *96*, 3031-3042.

[114] Berkessel, A.; Thauer, R. K. *Angew. Chem. Int. Ed. Engl*. **1995**, *34*, 2247-2250.

[115] Lyon, E. J.; Shima, S.; Buurman, F.; Chowdhuri, S.; Batschauer, A.; Steinback, K.; Thauer, R. K. *Eur. J. Biochem*. **2004**, *271*, 195-204.

[116] Shima, S.; Pilak, O.; Vogt, S.; Schick, M.; Stagni, M. S.; Meyer-Klaucke, W.; Warkentin, E.; Thauer, R. K.; ErmLer, U. *Science* **2008**, *321*, 572-575.

[117] Hiromoto, T.; Ataka, K.; Pilak, O.; Vogt, S.; Stagni, M. S.; Meyer-Klaucke, W.; Warkentin, E.; Thauer, R. K.; Shima, S.; ErmLer, U. *FEBS Lett*. **2009**, *583*, 585-590.

[118] Buurman, G.; Shima, S.; Thauer, R. K.; *FEBS Lett*. **2000**, *485*, 200-204.

[119] von Bünau, R.; Zirngibl, C.; Thauer, R. K.; Klein A. *Eur. J. Biochem.* **1991**, *202*, 1205.

[120] Schwörer, B.; Fernandez, V. M.; Zirngibl, C.; Thauer, R. K. *Eur. J. Biochem*. **1993**, *212*, 255-261.

[121] Klein, A. R.; Fernandez, V. M.; Thauer, R. K. *FEBS Lett*. **1995**, *368*, 203-206.

[122] Cioslowski, J.; Boche, G. *Angew. Chem. Int. Ed. Engl*. **1997**, *36*, 107-109.

[123] Teles, J. H.; Brode, S.; Berkessel, A. *J. Am. Chem. Soc*. **1998**, *120*, 1345-1346.

[124] Scott, A. P.; Golding, B. T.; Radom, L. *New J. Chem*. **1998**, 1171-1173.

[125] Shima, S.; Lyon, E. J.; Sordel-Klippert, M.; Kauβ, M.; Kahnt, J.; Thauer, R. K.; Steinbach, K.; Xie, X.; Verdier, L.; Griesinger, C. *Angew. Chem. Int. Ed*. **2004**, *43*, 2547-2551.

[126] Lyon, E. J.; Shima, S.; Boecher, R.; Thauer, R. K.; Grevels, F.-W.; Bill, E.; Roseboom, W.; Albracht, S. P. J. *J. Am. Chem. Soc*. **2004**, *126*, 14239-14248.

[127] Goldfield, S. A.; Raymond, K. N. *Inorg. Chem*. **1974**, *13*, 770-775.

[128] Shima, S.; Lyon, E. J.; Thauer, R. K.; Mienert, B.; Bill, E. *J. Am. Chem. Soc*. **2005**, *127*, 10430-10435.

[129] Pilak, O.; Mamat, B.; Vogt, S.; Hagemeier, C. H.; Thauer, R. K.; Shima, S.; Vonrhein, C.; Warkentin,E.; ErmLer, U. *J. Mol. Biol*. **2006**, *358*, 798-809.

[130] Acharya, P.; Goenrich, M.; Hagemeier, C. H.; Semmer, U.; Vorholt, J. A.; Thauer, R. K.; ErmLer, U. *J. Biol. Chem*. **2005**, *280*, 13712-13719.

[131] Yang, X.; Hall, M. B. *J. Am. Chem. Soc*. **2008**, *130*, 14036-14037.

[132] Royer, A. M.; Rauchfuss, T. B.; Wilson, S. R. *Inorg. Chem*. **2008**, *47*, 395-397.

[133] Yang, X.; Hall, M. B. *J. Am. Chem. Soc*. **2009**, *131*, 10901-10908.

[134] Hiromoto, T.; Warkentin, E.; Moll, J.; ErmLer, U.; Shima, S. *Angew. Chem. Int. Ed*. **2009**, *48*, 6457-6460.

[135] Obrist, B. V.; Chen, D.; Ahrens, A.; Schünemann, V.; Scopelliti, R.; Hu, X. *Inorg. Chem*. **2009**, *48*, 3514-3516.

[136] Li, B.; Liu, T.; Popescu, C. V.; Bilko, A.; Darensbourg, M. Y. *Inorg. Chem*. **2009**, *48*, 11283-11289.

[137] Chen, D.; Scopelliti, R.; Hu, X. *J. Am. Chem. Soc*. **2010**, *132*, 928-929.

[138] Wang, X.; Li, Z.; Zeng, X.; Luo, Q.; Evans, D. J.; Pickett, C. J.; Liu, X. *Chem. Commun*. **2008**, 3555-3557.

[139] Turrell, P. J.; Wright, J. A.; Peck, J. M. T.; Oganesyan, V. S.; Pickett, C. J. *Angew. Chem. Int. Ed*. **2010**, *49*, in press. We thank Prof. Pickett for early private communication of these results.

[140] Morrell, T. E.; Tuttle, T. *Determining the Mechanism of the Fe-Hydrogenase Enzyme Using a QM/MM Simulations* **2009**, unpublished work.

[141] Reich, H. E.; Levine, R. *J. Am. Chem. Soc*. **1955**, *77*, 5434-5436.

[142] Kitagawa, T.; Ito, J.; Tsutsui, C. *Chem. Pharm. Bull*. **1994**, *42*, 1931-1934.

[143] Synthesis of disalts such as **8.38** (R = Me) were investigated by Godin, R. P. and Findlay, N.

[144] Ivanov, I. C.; Karagisov, S. K.; Sulay, P. B. *Arch. Pharm.* **1989**, 322, 181-182.

[145] Reich, H. E.; Levine, R. *J. Am. Chem. Soc*. **1955**, *77*, 5434-5436.

[146] Clayden, J.; Greeves, N.; Warren, S.; Wothers, P. *Organic Chemistry*, Oxford University Press, Oxford **2004**, 247.

[147] Bourn, A. J. R.; Gillies, D. G.; Randall, E. W. *Tetrahedron* **1966**, *22*, 1825-1829.

[148] Curran, D. P.; Liu, H. *J.Chem. Soc., Perkin Trans. 1* **1994**, 1377-1393.

[149] Williams, D. H.; Fleming, I. *Spectroscopic Methods in Organic Chemistry, 5th Edition*, McGraw-Hill Publishing Company, London **1995**, 112-115.

[150] Scullion, C. Unpublished work, 1st year PhD, **2010**. Crystallograpic data for disalt **8.57** is given in Appendix 5.

[151] Frey, G. D.; Lavallo, V.; Donnadieu, B.; Scholler, W. W.; Bertrand, G. *Science* **2007**, *316*, 439-441.

[152] Ryang, H.-S.; Sakurai, H. *J. Chem. Soc., Perkin Trans. 1* **1975**, 1590-1594.

[153] Lewis, E. S.; McLaughlin, M. L.; Douglas, T. A. *J. Am. Chem. Soc*. **1985**, *107*, 6668-6673.

[154] Kaiser, D. W.; Thurston, J. T.; Dudley, J. R.; Schaefer, F. C.; Hechenbleikner, I.; Holm-Hansen, D. *J. Am. Chem. Soc*. **1951**, 73, 2984-2986.

[155] Wender, P. A.; Baryza, J. L.; Bennett, C. E.; Bi, F. C.; Brenner, S. E.; Clarke, M. O.; Horan, J. C.; Kan, C.; Lacôte, E.; Lippa, B.; Nell, P. G.; Turner, T. M. *J. Am. Chem. Soc*. **2002**, *124*, 13648-13649.